SECOND EDITION OF
ROCK ENGINEERING of UNDERGROUND COAL MINING

J. Nielen van der Merwe

Bernard J. Madden

SECOND EDITION OF
ROCK ENGINEERING FOR UNDERGROUND COAL MINING

SAIMM PUBLICATIONS

THE MONOGRAPH SERIES

Ml   **Lognormal-De Wijsian Geostatistics for Ore Evaluation**
(2nd ed 1981) D.G. Krige

M2   **An Introduction to Geostatistical Methods of Mineral Evaluation**
(2nd ed 1981) J.-M.M. Rendu

M3   **Principles of Flotation**
(1982) (3rd imp. 1986) Edited by R.P. King

M4   **Increased Underground Extraction of Coal**
(1982) Edited by C.J. Fauconnier and R.W.O. Kersten

M5   **Rock Mechanics in Mining Practice**
(1983) (3rd imp. 1986) Edited by S. Budavari

M6   **Assay and Analytical Practice in the South African Mining Industry**
(1986) W.C. Lenahan and R. de L. Murray-Smith

M7   **The Extractive Metallurgy of Gold in South Africa,**
2 volumes (1987) Edited by G.G Stanley

M8   **Mineral and Metal Extraction — An Overview**
(1994) L.C. Woollacott and R.H. Eric

M9   **Rock Fracture and Rockbursts—an illustrative study**
(1997) Edited by W.D. Ortlepp

THE SPECIAL PUBLICATIONS SERIES

SPI   **Proceedings, Underground Transport Symposium**
(1986) Edited by R.C.R. Edgar

SP2   **Backfill in South African Mines** (1988)

SP3   **Treatment and Re-use of Water in the Minerals Industry** (1989)

SP4   **COREX Symposium 1990**
(1990) Edited by H.M.W. Delport and P.J. Holaschke

SP5   **Measurement, Control, and Optimization in Mineral Processing**
(1994) Edited by H.W. Glen

SP6   **Handbook on Hard-rock Strata Control**
(1994) A.J.S. Spearing

SP7   **Rock Engineering for underground coal mining**
(2002) J. Nielen van der Merwe and Bernard J. Madden

SUPPLEMENT TO THE SAIMM *JOURNAL*

The Metals and Minerals Industry in South Africa - Part 1 (1989)
Edited by H.W. Glen

THE SYMPOSIUM SERIES

S1 **Mathematical Statistics and Computer Applications in Ore Valuation** (1966)
S2 **Planning Open Pit Mines** (1970) (4th imp.) Edited by P.W.J. van Rensburg
S3 **Application of Computer Methods in the Mineral Industry** (APCOM 1973) Edited by M.D.G. Salamon
S4 **Infacon 1974** Edited by H.W. Glen
S5 **Proceedings of the 12th CMMI Congress** 2 volumes (1982) Edited by H.W. Glen
S6 **Rockbursts and Seismicity in Mines** (1984) Edited by N.C. Gay and E.H. Wainwright
S7 **The Planning and Operation of Open Pit and Strip Mines** (1986) Edited by J.P. Deetlefs
S8 **GOLD 100: Proceedings of the International Conference on Gold (1986)**
    Volume 1: Gold Mining Technology Edited by H. Wagner and R.P. King
    Volume 2: Extractive Metallurgy of Gold Edited by C.E. Fivaz and R.P. King
    Volume 3: Industrial Uses of Gold Edited by G. Gafner and R.P. King
S9 **APCOM 87: Proceedings of the Twentieth International Symposium on the Application of Computers and Mathematics in the Mineral Industries (1987)**
    Volume 1: Mining Edited by L. Wade, R.W.O. Kersten and J.R. Cutland
    Volume 2: Metallurgy Edited by R.P. King and I.J. Barker
    Volume 3: Geostatistics Edited by I.C. Lemmer, H. Schaum and F.A.G.M. Camisani-Calzolari
S10 **International Deep Mining Conference (1990)**
    Volume 1: Innovations in Metallurgical Plant Edited by G.A. Brown and P. Smith
    and
    Application of Materials Engineering in the Mining Industry Edited by B. Metcalfe
    Volume 2: Technical Challenges in Deep Level Mining Edited by D.A.J. Ross-Watt and P.D.K. Robinson
S11 **Infacon 6 (Incorporating Incsac) (1992)** Edited by H.W. Glen
S12 **Massmin 92** Edited by H.W. Glen (out of print)
S13 **Minefill 93** Edited by H.W. Glen
S14 **XVth CMMI Congress Publications (1994)**
    Volume 1: Mining Edited by H.W. Glen
    Volume 2: Metals Technology and Extractive Metallurgy (1994) Edited by H.W. Glen
S15 **Surface Mining 1996** Edited by H.W. Glen
S16 **Hidden Wealth** (1996) Edited by H.W. Glen
S17 **Heavy Minerals 1997** Edited by R.E. Robinson
S18 **The 8th International Platinum Symposium (1998)**
S19 **Mining in Africa '98**
S20 **Extraction Metallurgy Africa '98**
S21 **Sixth International Symposium for Rock Fragmentation by Blasting (1999)**
S22 **Metallurgy Africa '99**
S23 **Heavy Minerals 1999** Edited by R.G. Stimson
S24 **Tunnels under Pressure** Technical Editor T.R. Stacey
S25 **Mine Hoisting 2000**
S26 **Coal–The Future (2000)**
S27 **The Fifth International Symposium on Rockburst and Seismicity in Mines (RaSim 5) (2001)**
S28 **6th International Symposium on Mine Mechanization and Automation (2001)**
S29 **XIV International Coal Preparation Congress and Exhibition**
S30 **Surface Mining 2002—Modern Developments for the New Millennium**
S31 **IFSA 2002, Industrial Fluidization South Africa**
S31A **APCOM 2003—Application of Computers and Operations Research in the Minerals Industries**
S32 **ISSA/Chamber of Mines Conference—Mines and Quarries: Prevention of Occupational Injury and Disease**
S33 **ISRM—Technology Roadmap for Rock Mechanics**
S34 **Heavy Minerals Conference 2003**
S35 **Safety in Mines Research Institutes (2003)**
S36 **VII International Conference on Molten Slags, Fluxes & Salts (2004)**
    Tenth International Ferroalloys Congress INFACONX 2004
S37 **Deep and high stress mining 2004**
S38 **'Platinum adding value' 2004**
S39 **Base Metals—Southern Africa's response to changing global base metals market dynamics 2005**
S40 **Strategic versus Tactical approaches in mining 2005**
S41 **Best practices in rock engineering SARES 2005**
S42 **IFSA 2005 (Mintek)**
S43 **Southern African Pyrometallurgy 2006 International Conference**
S44 **Stability of rock slopes in open pit mining and civil engineering situations**
S45 **'Platinum Surges Ahead' 2006**
S46 **Hydraulic Transport of Solids - Hydrotransport 17 (2007)**
S47 **Fourth Southern African Base Metals Conference 'Africa's base metals resurgence'**
S48 **Heavy Minerals Conference, 2007**
S49 **Cave Mining Conference, 2007**
S50 **International Symposium on Lead and Zinc processing – Lead & Zinc 2008**
S51 **Surface Mining 2008**
S52 **Platinum in transformation 2008**
S53 **IFSA 2008**
S54 **Hydrometallurgy Conference 2009**
S55 **Shotcrete for Africa 2009**
S56 **Base Metals Conference 2009**
S57 **Heavy Minerals Conference, 2009**
S58 **Hard Rock Safe—Safety Conference 2009**
S59 **Sampling and Blending 2009**
S60 **World Gold 2009 Conference**
S61 **Physical Beneficiation 2010 Conference**

The papers in this volume have been for the most part prepared from files supplied by the authors,
with additional typesetting and formatting by The Southern African Institute of Mining and Metallurgy.

SECOND EDITION OF

ROCK ENGINEERING FOR UNDERGROUND COAL MINING

A Practical Guide for Supervisors at all levels,
Mine Planners and Students

J. Nielen van der Merwe

Professor Rock Engineering, Department of Mining Engineering,
University of the Witwatersrand

and

Bernard J. Madden

G-Ro, Geotechnical Services (Pty) Ltd.

ABOUT THE AUTHORS

Prof. J. Nielen van der Merwe, Pr. Eng., has almost 30 years' experience of practical rock engineering on mines; consulting, researching and, recently, teaching. His initial rock engineering work was done on the deep level gold mines, after which he became involved with platinum, chrome, asbestos, etc. His coal rock engineering experience was gained on mines in the Vaal Basin, KwaZulu-Natal, the Highveld and Witbank. He has published more than 40 papers in several countries of the world and is a past president of The South African National Institute of Rock Engineering. He was the initiator and first President of the International Interest Group on Mining Rock Engineering and is President Elect of the International Society for Rock Mechanics. He is currently Head of the Department of Mining Engineering at the University of Pretoria.

Dr Bernard J. Madden has worked in research and consulting to the mining industry, particularly in underground coal mining, in Australia and South Africa for the past 20 years. He has worked for the research institutions of the Chamber of Mines Research Organization (COMRO), CSIR Miningtek, and ACIRL, and currently operates a consultancy to the mining industry. He has published over 30 papers.

Bernard Madden and Nielen van der Merwe

ABOUT THE INSTITUTE

The Southern African Institute of Mining and Metallurgy is a dynamic organization attending to the professional needs of its members since its inception in 1894. There are approximately 3 800 members and the Institute's membership continues to grow.

A key service by the Institute to its members, is the promotion of the transfer of technology and scientific knowledge, relevant to the sustainable development of the minerals and metals section of the South African economy and its stakeholders.

PREFACE

This second edition of the book contains certain extensions to the first edition: firstly, to stay abreast of developments in the field of underground coal mining rock engineering and, secondly, to satisfy the needs of the industry in the current milieu.

For the immediate future, the challenge for South African mines will be to extend the lives of mines in the Witbank coalfield as far as possible. This requires safe secondary mining of old and often small pillars at shallow depth, which were not intended for further mining at the time of their development. A chapter on shallow mining has therefore been added as have methods to deal with time-related scaling of pillars.

The appendices have been reviewed and more worked examples, to further explain the various methodologies, have been added. Where it was attempted with the first edition to simplify the mathematics as far as possible by substituting certain constants with acceptable numbers, the more correct fundamental equations have now been retained in parallel to the simplified ones.

Finally, a few minor corrections were made to the script of the first edition; the need for this is inevitable, no matter how carefully a script is checked prior to publication.

The work took longer than Bernard and I anticipated as there was less time available for it than we expected. This is a sign of the times, professional people being busier than ever before. It also indicates the seriousness with which mine owners and operators now approach rock-related stability issues on the mines.

We hope that this second edition will contribute in some small way to the safe and profitable operation of our coal mines.

Nielen van der Merwe
May 2010

Contents

Contents (continued)

Contents (continued)

Contents (continued)

Chapter 1

Fundamentals

Introduction

It is necessary for those using this book to have some fundamental understanding of the basics of rock engineering. In this chapter, the basics will be explained in a simplified manner while the formal scientific treatment can be found in Appendix A. Some mathematics have to be used, but the more complex equations will be avoided. Another important element of the chapter is to define some of the terms that are used in the rest of the book.

To avoid confusion later, it is necessary to provide this material first. There will be very few unfamiliar terms. The most obvious challenge will be to avoid confusing common terms used in the scientific context with different meanings in daily use.

The contents of the chapter have been carefully selected to include only those aspects that are important for understanding the material in the rest of the book. It should therefore not be seen as a comprehensive guide to fundamental rock mechanics. Entire books have been devoted to that subject. The interested reader is referred to the bibliography at the end of Appendix A.

The equations that are supplied in this chapter are mostly of a generic nature, which means that they can be used with any system of units. However, in the light of the practical intent of the material, units that are commonly used in South African coal mining are supplied with the equations. It is important to note that in doing this, the user has to be careful in supplying input to the equations that are of the same order of magnitude as the end unit. For instance, if Mega-units are used, all the input also has to be supplied in Mega-units.

Rock mechanics and rock engineering

The science of rock mechanics is relatively new as a separate branch of the study of mechanics. While it has always existed, it has only been formally recognized since the 1960s. It has been defined as the study of the reaction of the rock mass to changes made therein by man.

While *rock mechanics* is a field of study, or a science, the application thereof is *rock engineering*. Rock mechanics is basic and generic. Rock engineering has several specialist facets, covering the spectrum from deep level gold mine applications in Welkom to dam foundations in China. Seen in the broad context, mining rock engineering covers an estimated twenty per cent of the total.

Mining rock engineering can also be sub-divided into a number of smaller divisions, like deep tabular hard rock, shallow hard rock, massive mining, surface mining, shallow soft rock, etc. Coal mining falls into the last-mentioned class, i.e. shallow soft rock. It is not alone in this class, sharing the berth with other minerals like rock salt or gypsum.

An important reason for having these sub-divisions is that the application of the fundamentals is a function of, amongst other things, the mining method and the rate of mining. Not all coal mining falls into the shallow class. Some European coal mines, for instance, are much deeper. The application of rock engineering for those mines requires understanding of different aspects than for shallow mines and vice versa. One should therefore be careful when attempting to apply methods developed for the deep coal mines to a shallow environment.

The main thrust of this book will be on shallow underground coal mines. In this context, shallow means down to approximately 350 metres deep. Beyond that depth, the basics remain the same, but the style and the focus of the applications are different. The different nature of the problems require a different approach to that presented in this book. Coal mining in South Africa, Australia and North America is sufficiently similar with regard to physical parameters and mining equipment to be classified jointly.

First level of fundamentals

In this section, the very basic concepts like mass, force, weight, density, etc., will be explained. While many of them can be used interchangeably in everyday use, they have specific meanings in science and cannot be interchanged.

Mass

Every object in the universe has mass—it is a description of the quantity of matter in an object. It is independent of gravity. An object's mass will be the same in outer space as it is on the Earth. It is denoted by the symbol *'m'* and is measured in *grams*, abbreviated as *'g'*. One gram is the quantity of matter contained in one cubic centimetre of water. In this book, the unit *kilogram* (*kg*—one thousand grams) will be used most of the time. Anything in science that is independent of direction is called a scalar. Mass is a scalar.

Force

Force is that which is required to accelerate an object that has mass. In this context, 'accelerate' means to cause it to move faster or slower (a negative acceleration) or to change direction. The symbol *'F'* is used for force and it is measured in *Newtons*, for which the symbol *'N'* is used. In this book, *kilo-Newtons* (*kN*—one thousand Newtons) will be used most often for support applications and *Mega-Newtons* (*MN*—one million Newtons or one thousand kilo-Newtons) for rock forces. One Newton is the force that is required to accelerate a mass of one kilogram by one metre per second. Mathematically,

$$F = ma \quad \text{kN} \tag{1}$$

or, Force equals mass times acceleration. Note that as acceleration has direction, so has force. Force is thus a vector.

Weight

Weight is a special case of force. It is the force with which the Earth attempts to accelerate an object toward its centre. The acceleration in this case is the so-called gravitational acceleration, *'g'*. Therefore,

$$W = mg \tag{2}$$

The exact value of *g* is a function of the distance of the point of measurement from the centre of the Earth—the further away, the smaller *g* becomes. At sea level it is slightly greater than at the top of a mountain. The generally accepted value of *g* is 9,81 m/s^2.

One should be clear on the difference between weight and mass. In everyday usage a person's weight may be 80 kg. In the scientific context, however, the weight of a person with a mass of 80 kg is 784,8 N.

Density

Density describes the concentration of mass. It basically says how much mass is contained in a unit volume. The basic unit is grams per cubic centimetre, or *g/cm³*. In mining the unit kilogram per cubic metre (*kg/m³*) is usually used. Density is denoted by the symbol *'ρ'*.

Stress

As density describes the concentration of mass, stress describes the concentration of force. It is measured in units of force per area, or *N/m²*. One *N/m²* is commonly known as one *Pascal (Pa)*. In mining, the commonly used units are *kilo-Pascal* (kPa) or *Mega-Pascal (MPa)*—one thousand Pascals or one million Pascals respectively.

There are two major types of stress. If the stress acts perpendicularly—or normally—to the surface under consideration, it is known as a *normal stress*, see Figure 1, and denoted by the symbol σ. If the effect of a stress is to compress an object on which it acts, it is called a *compressive normal stress*. The opposite is called a *tensile normal stress*.

Note that in mining, the common convention is to denote a compressive force or stress as positive and the tensile ones as negative. In other branches of engineering and in the pure sciences, the opposite convention is followed.

If stress acts parallel to the surface, it is known as a *shear stress* and is denoted by the symbol τ. Therefore,

$$\sigma = \frac{F}{A_n} \quad \text{kPa (or MPa)} \tag{3}$$

and

$$\tau = \frac{F}{A_p} \quad \text{kPa (or MPa)} \tag{4}$$

where A_n = area normal to direction of force, and
A_p = area parallel to direction of force.

Strain

Strain is the amount by which an object has become longer or shorter (or thinner or thicker) relative to its original size and shape, see Figure 2. The symbol used for strain is ε, and it has no dimensions. In mining, though, the magnitudes of changes are small and it is convenient to express them in terms of millistrains, *mm/m* being the most common mode of expression. Mathematically,

$$\varepsilon = \frac{\Delta l}{l} \quad \text{mm/m} \tag{5}$$

where l = original length and
Δl = change in length.

Second level of fundamentals

In this short section, some of the inter-relationships between the basic fundamentals are examined in a simplified manner.

Normal Force

Area

Normal

Shear Force

Area
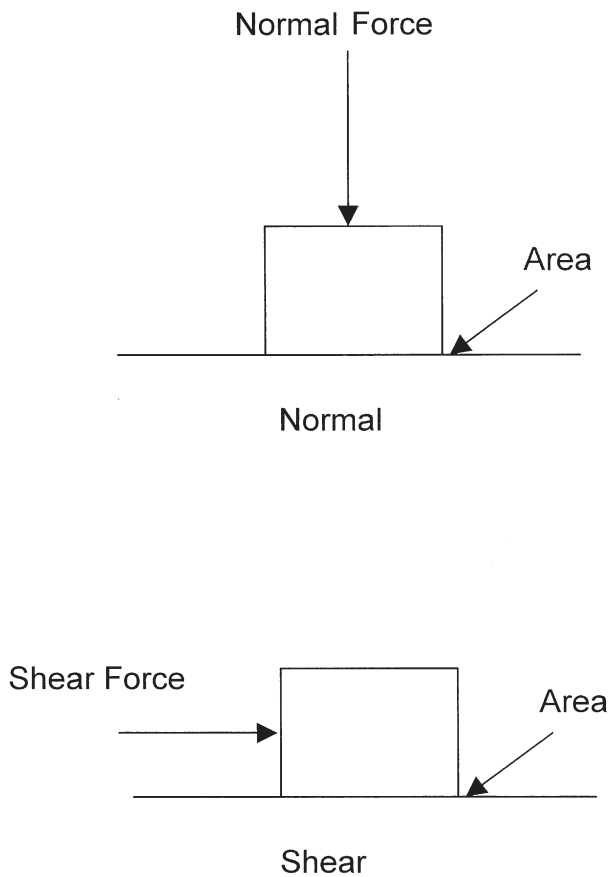
Shear

Figure 1. Illustration of the principles of normal and shear stress

F

F

Δl

l

F

F
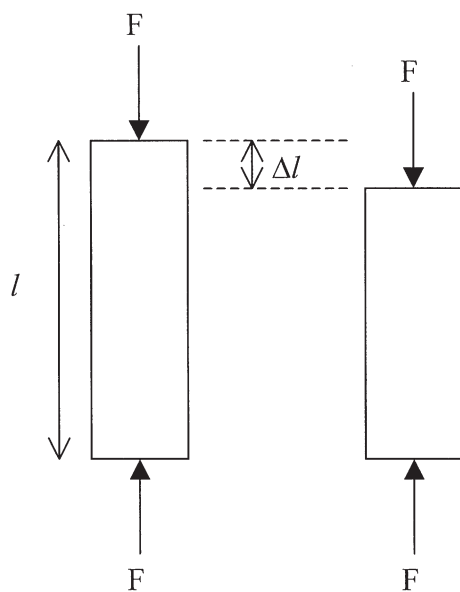
Figure 2. Strain is the amount of deformation relative to the original dimension of an object

Young's Modulus

When force or stress is applied to an object that cannot move, the object reacts by deforming. The

amount of deformation is dependent on the magnitude of the applied force and on the characteristics of the material. If the material is of such a nature that it returns to its original shape when the force is removed, it is classified as elastic. Most rock types can be considered as elastic materials at small strains.

Furthermore, if there is a constant relationship between the magnitude of the applied force and the amount of deformation, the material is sub-classified as *linear* elastic. Again, most rock types fall into this sub-class at small strains.

The ratio between the applied stress and the resultant strain is known as the *Young's Modulus* or *Modulus of Elasticity*, denoted by the symbol *'E'*. The greater the modulus, the stiffer the material. This means that the stiffer the material, the greater the stress required to result in any given magnitude of strain. The modulus of elasticity is mathematically expressed as,

$$E = \frac{\sigma}{\varepsilon} \qquad GPa \qquad [6]$$

As strain is dimensionless, the units of *E* are the same as the units of stress. However, due to the high magnitudes, it is usually more convenient to express *E* in terms of *Giga-Pascals* (*GPa*—one billion *Pascals* or one thousand *Mega-Pascals*).

Although rock can be described as linearly elastic, it is not infinitely so. When the stress reaches a certain level, rock fails. Small rock specimens fail violently and that behaviour is described as *brittle*. Most rock types in the coal environment can thus be described as *brittle linearly elastic materials*. This concept, and the principle of different stiffness, is illustrated in Figure 3.

Material 'X'

C

D

Stress

Material 'Y'

B

A

Strain
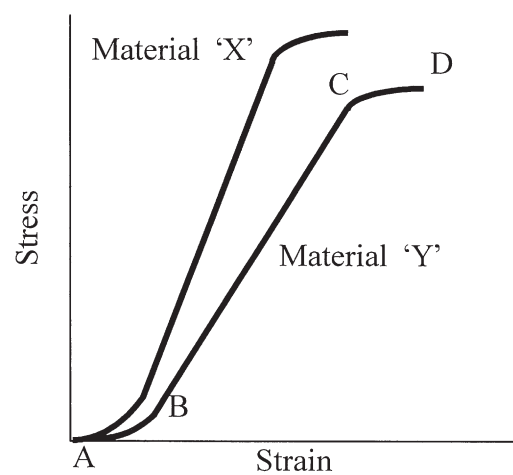
Figure 3. Concept of linear elasticity

In Figure 3, the initial stiffness of the two materials is low, shown as the zone A-B. This is because most rocks contain micro fractures that close before the material itself starts deforming. Once the deformation of the consolidated material begins, the curves become steeper. The zones B-C are the linear elastic zones of the two materials. At points C, the behaviour becomes non-linear. Point C is called the Elastic Limit of the materials. Failure occurs at points D on the curves, where it reaches Ultimate Strength. It is customary to design roof support using the Elastic Limit and not the Ultimate Strength of the material.

The elastic portion of material X's curve has a steeper slope than that of material Y. Material X is the stiffer of the two materials.

Poisson's ratio

When a compressive force is applied to an object in a particular direction, it shortens in that direction. However, if the object is unconstrained, it also expands laterally, see Figure 4. One force will thus result in two strains, one in the longitudinal direction and a second one in the lateral direction. The ratio between these two strains is constant, and is called the *Poisson's Ratio*, denoted by the symbol *v*. It has no dimensions. Simply,

$$v = \frac{\varepsilon_t}{\varepsilon_l} \qquad\qquad [7]$$
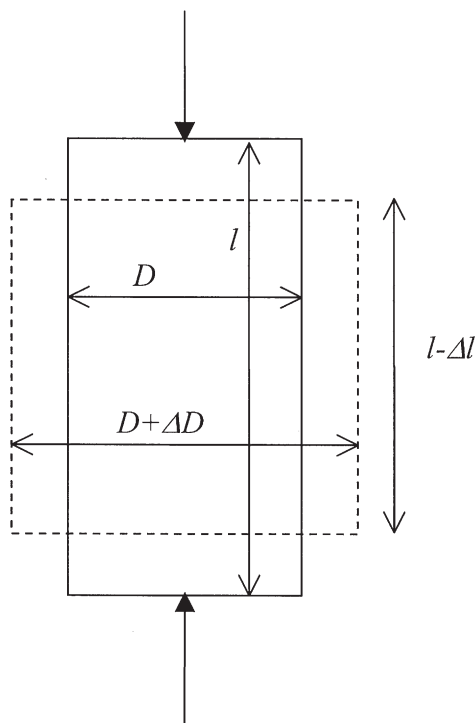
Figure 4. The normal force applied to the specimen results in axial shortening and transverse expansion

where ε_t = lateral strain and
ε_l = longitudinal strain.

Energy

Energy can be simply defined as the product of force and the distance of displacement, resulting from the application of the force. The basic unit is the *Joule*, being the amount of energy expended when a force of one *Newton* results in displacement of one *metre*. In mining terms, the unit *Mega-Joule* is generally used. An interesting application of energy considerations is the evaluation of the amount of violence accompanying pillar failure. This is discussed in more detail in Appendix C: Pillars.

An aspect that requires discussion here is the refinement that the area underneath a Force-Displacement curve is the amount of energy that was required to result in the deformation shown in the curve, as in the example in Figure 5.

In Figure 5, the stiffer material, X, stores more energy after it has been deformed than material Y. This means that when it fails, it has more energy available and it can be expected that the fragments after failure will be displaced further than the fragments from material Y, indicating more violent failure in X.

There are several different forms of energy and one form can be transformed to another. For instance, an object that has been lifted to a higher position has more *potential energy* than before. When it is dropped, it falls and the *potential energy* is translated into *kinetic energy*. When it hits the floor, the *kinetic energy* is transformed into *deformation energy, heat energy* and *sound energy*. If the object is deformed beyond its limits, it can shatter and the *deformation energy* can again become *kinetic energy,* etc. Note that energy cannot be created or destroyed—it can only be changed from one form to another.

In the consideration of mining stability, *kinetic energy* and *deformation energy* are the important forms.

Stability

Stability can be defined in several ways. In the pure scientific context it is not necessarily the absence of movement—uniform movement can also be seen as stable movement or displacement. It is possible to distinguish between violent and stable pillar failure— well designed crush pillars are examples of stable failure. However, in order to simplify matters, stability in the context of this book will refer to the situation where all forces are in equilibrium or balance and no movement or failure occurs. The term 'stable failure' is often used in rock engineering. In this book, the
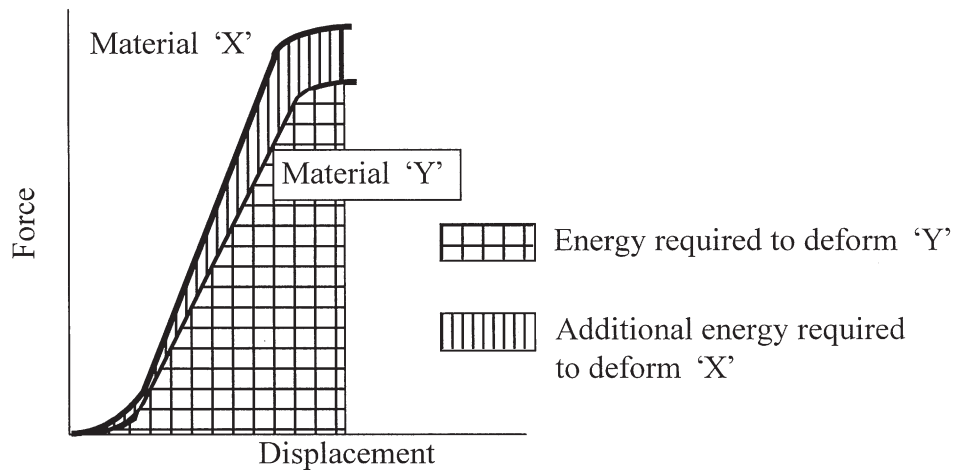
Figure 5. The areas underneath the curves indicate the amounts of energy expended in the deformation of the two objects

term 'non-violent' failure will be used. It refers to the situation where the failure does not occur so rapidly that flight is the only option out of a dangerous situation.

Beam behaviour

Sufficient attention has now been paid to the very basic fundamentals and the discussion can move on to one or two other derived fundamental matters. There are several gaps in the discussion up to this point, and readers are referred to the bibliography in Appendix A for a more complete treatment of the fundamentals.

The coal mining environment is characterized by stratified or layered geological units. These behave like plates, and the behaviour of plates can be simplified to that of beams under most circumstances. When the length of a plate is significantly greater than its width, its behaviour approaches that of a beam. In this discussion, beam behaviour will be considered but readers should be aware of the limitations: when the thickness of a geological unit approaches its width, or if the width of a unit approaches its length, it is more accurate to consider plate behaviour.

There are several different types of beams. It is the intention with this chapter to supply only the

Figure 6. Simplified diagram showing the positions of maximum tensile and compressive stresses in a clamped beam

knowledge that is necessary to understand the following chapters (mainly the chapter on roof support) rather than to provide a comprehensive fundamental treatment, and consequently only two types of beams will be discussed, namely clamped beams and cantilevers.

Clamped beams

An unjointed roof acts like a clamped beam in its simplest form.

The most important visual, or measurable, characteristic of a clamped beam is that it sags. The amount of sag is greatest in the centre and it approaches zero at the edges.

The *invisible* aspect is that purely by virtue of having an unsupported span, a beam has a unique stress distribution. If the generated stresses exceed the strength of the beam, it will fail. A simplified stress distribution in a clamped beam is shown in Figure 6.

The maximum stresses induced in the beam occur at the edges. At the bottom of the beam the stresses are compressive and they are tensile at the top. Note that the tensile stress at the centre bottom of the beam is half of the magnitude of tensile stress at the top. Rock is weaker in tension than in compression, and failure of the beam is thus more likely to begin at the top, at the two edges. In the case of a mine roof, this part of the beam is not visible and therefore the onset of tensile failure cannot be seen. This topic will be expanded in the chapter on roof support.

The magnitude of the maximum tensile stress is:

$$\sigma_t = \frac{\gamma L^2}{2t} \qquad \text{kPa (or MPa)} \qquad [8]$$

where γ = unit weight of beam
 t = thickness of beam
 L = length of unsupported span.

The maximum deflection of the beam occurs at the centre, and its magnitude is calculated by:

$$\eta = \frac{\gamma L^4}{32 E t^2} \qquad \text{mm} \qquad\qquad [9]$$

where

E = Young's Modulus of material.

In both of the equations, the parameter that has the single most important contribution, is the length of the unsupported span. The induced stress is directly proportional to the square of the length. The amount of sag is proportional to the fourth power of the length. In other words, if the span is doubled the stress will increase by a factor four, while the sag will increase sixteen-fold. It is also interesting to note that the magnitude of the stress is independent of E, and thus of the type of the material.

Cantilever beam

When the continuity of a clamped beam is broken, for instance by a joint in the roof, the magnitudes of sag and stress as calculated with Equations [8] and [9] are no longer valid.

The free end of the beam is now stress free, but the stresses at the clamped edge are still there.

Figure 7 is an illustration of a cantilever.

The magnitude of the maximum stress is:
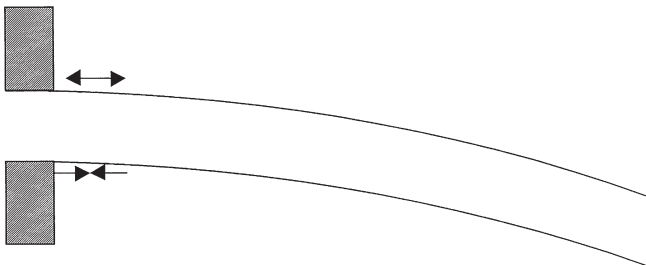
Figure 7. A cantilever beam

$$\sigma_t = \frac{3\gamma L^2}{t} \qquad \text{kPa (or MPa)} \qquad [10]$$

Comparison of Equations [8] and [10] shows that in a cantilever beam, the magnitude of the tensile stress increases six-fold. The practical implication of this is that the mere presence of a joint in the roof immediately results in six times the tensile stress, again at a point at the top of the beam that is not visible.

Friction

The study of objects sliding over one another immediately raises the matter of friction. In the mining environment, friction plays a major role in the efficiency of roof support anchors, be it resin or mechanical anchors, and in the sliding of roof layers over one another in a laminated roof.

Friction is the force that resists sliding. Its magnitude depends on only three basic parameters, namely: the magnitude of normal force acting on the sliding plane, the cohesion acting on the plane and the friction coefficient between the two surfaces. Figure 8 is a simple illustration of the friction effect.

The magnitude of the shear stress required to overcome friction can be calculated by:

$$\tau = C + \sigma_n \tan \phi, \qquad \text{kPa (or MPa)} \qquad [11]$$

where $\tan \phi$ = friction coefficient
ϕ = friction angle
σ_n = normal stress
C = Cohesion between objects.

In the case of roof layers sliding over one another, the cohesion and friction coefficient are given by nature. However, the resistance to sliding can be increased by increasing the normal force on the interfaces. In practice this is achieved by pre-stressing roof bolts, as shown in Figure 9.

Figure 8. Simplified diagram illustrating the stresses that play a role in friction
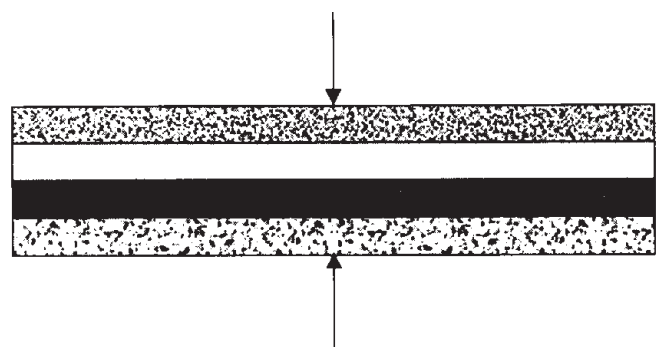
Figure 9. Prestressed roof anchors result in a normal force on the roof layers, increasing their resistance to sliding
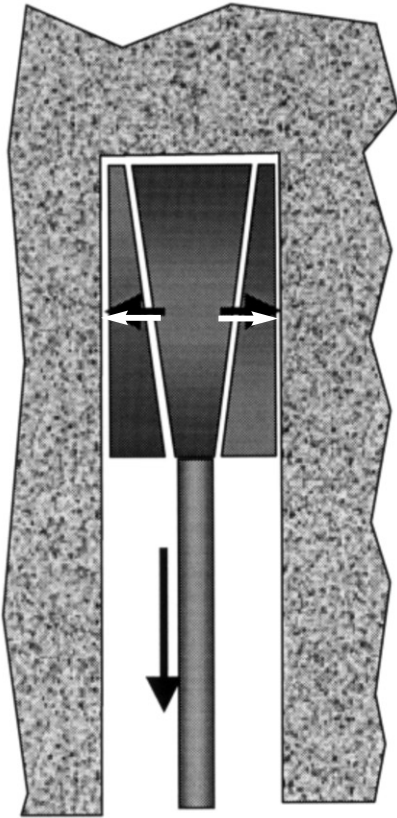
Figure 10. Another example of the use of the friction effect in mining: as the central barrel of a roofbolt is pulled down, it forces the wedges out toward the rock interface, thereby increasing the normal stress and thus the frictional resistance

The resistance to sliding of a roof bolt anchor can also be controlled, as shown in Figure 10. With a mechanical anchor, the normal force is increased by the expansion of the anchor and the friction coefficient is increased by the configuration of the ripple marks on the anchor. There is no cohesion.

With resin anchors, the cohesion is very low and the normal force is non-existent. Resistance to sliding is achieved by the friction coefficient of the resin-rock interface, which is enhanced by the intimate contact between the resin and the rock. The contact area is much greater than with a mechanical anchor and this has the effect of increasing the force that resists sliding. As will be shown in Chapter 3 on roof support, this contact area, and consequently the resisting force, can be increased by expanding both the length and the diameter of the borehole.

The coarser the resin filler, the greater the frictional resistance, but, the more difficult it becomes to insert a bolt through the resin.

State of stress in the coal mining environment

Under the first six headings of this chapter, we briefly investigated how materials behave when they are subjected to loads and deformations. The next matter that needs to be looked at is the underground state of stress.

The first important principle is that mining does not create stress. It merely re-arranges the stresses that were always there. An increase in load in one place will always be balanced precisely by a decrease in load somewhere else. The exact manner of the re-distribution of stress depends on exactly how mining is done. In very broad terms, the magnitude of the changes caused by mining depends on the extent of mining. If the extent of mining is limited to bord-and-pillar mining, the stress changes are also minimized. If high extraction mining is done, we experience the full extent of stress re-distribution.

In essence, the remaining chapters of this book will revolve around the nature and the magnitude of the stress re-distributions. It will be shown that stability problems are caused as much by increases in stress as by decreases. Mining tends to unbalance the natural forces that have been in balance for geological time. Nature always tends toward balance, and, when we create disturbances, nature will react by striving to reach a new balance. The study of this reaction is called the science of rock mechanics.

The virgin stress condition is three dimensional. It is simplified by being considered in three main directions, namely one vertical and two orthogonal to each other in the horizontal direction. The mathematical complications of analysing the three-dimensional state of stress and stress changes will be avoided in the main part of the book—that is the field of the rock engineering specialist. However, it remains important to take note of the principles that are involved.

The magnitude of the virgin stress is governed by four main parameters, namely the weight of the overlying material, the desire of the loaded rock to expand, historical stresses that are locked into the rock (called tectonic stresses) and the continual movement of the Earth's crust.

Weight of the overlying material

This is the main source of load on the coal horizon. Therefore, the deeper the coal, the higher the load. Also, the higher the density of the overlying rocks, the greater the load. This latter aspect becomes important when mining under thick dolerites, as dolerite is about twenty per cent more dense than the normal sedimentary rock types.

The following very simple equation is used to calculate the virgin vertical stress on the coal horizon:

$$\sigma_v = 0.025(H - D) + 0.03D \qquad \text{MPa} \qquad [12]$$

where

$H =$ depth to the floor of the seam in metres

$D =$ combined thickness of all the dolerite sills in the overburden.

At mining depths of 100 to 200 metres, the virgin vertical stress is in the range of 2,5 to 5 MPa.

Desire to expand

When rock is compressed in one direction, it will shorten in the direction of the applied load and expand in the direction normal to that load. In the case of confined rock, the lateral expansion—in this case, horizontal—cannot take place. The arrested expansion results in the generation of stress in the horizontal direction. This is called the Poisson effect (after the Poisson ratio) that is the driving force behind this category of stress.

The Poisson effect results in a horizontal stress that is equal to the vertical multiplied by the Poisson ratio of the rock, which is in the range of 0,2 to 0,3. From this effect, it is thus clear that a relatively small horizontal stress is the result. It is evident from underground observation and limited stress measurements that the horizontal stress is much greater than this and logically, there have to be other contributors to the horizontal stress.

Tectonic stresses

Over geological time, the Earth was subjected to a multitude of changes. According to theory, the now solid earth started as a gas cloud, which later liquefied and eventually turned into a solid mass as it cooled down. Following that, there were severe changes in weather patterns, volcanic eruptions, squeezing that resulted in huge mountain ranges, etc. All of these were accompanied by varying degrees of stress changes. In some cases, these stresses are still locked into the rock mass. Their magnitudes cannot be estimated by simple calculations, because nobody knows the full extent of change that occurred in any one area of the crust of the Earth.

Movement of the Earth's crust

It is estimated (close to the point of being proven beyond any doubt) that the core of the Earth is still liquid. The solid crust that we know is not a homogeneous mass, but consists of a number of plates that continue to move, to this day. A number of large plates have already been identified and their movements are monitored.

Horizontal movement can only be caused by horizontal force and this horizontal stress in the rock is another contributor to the virgin state of stress in the rock. The magnitude of the horizontal stress is not simple to measure or estimate.

Due to the unsettled nature of forces in the Earth's crust, faults and slips abound. Some faults are the result of forces that were spent in causing the Earth to move, while in other cases the movement was incomplete and some force remains. It is thus not strange to expect a different stress situation in the vicinity of faults.

The same can be said for dykes. One can only imagine the magnitude of force that was necessary to displace rock to allow a dyke to intrude. That amount of displacement resulted in compression of the rock, implying that elevated levels of stress still exist in the vicinity of dykes. This, of course, is in addition to the fact that the tremendous heat of the molten lava altered the rock in the vicinity—strengthening it in some cases but weakening it in most.

The basic fact is that the horizontal stress is greater than can be caused by the Poisson effect alone, but its cause is open to speculation and its magnitude possible but expensive to measure.

Changes in rock stresses are often measured by a number of methods, but the *absolute magnitude* is a different matter. The basic method is usually to drill a hole and then glue a strain gauge to the end of the hole. The rock with the attached strain gauge is then overcored. The amount of relaxation is then measured, and the stress that was active on the rock to compress it in the first place is calculated. One of the practical difficulties with this type of measurement, especially at shallow depth, is that the amount of relaxation is very small and often within the error range of the strain gauges. The type of glue is also important and it is necessary to obtain very accurate laboratory determinations of the Young's modulus of the rock, which is itself given to at least some measure of variation. It is thus necessary to do a great number of measurements.

Mechanical properties of the rock

The majority of rocks that are affected by coal mining are of sedimentary origin, being sandstones, shales, mudstones and siltstones in different proportions. In comparison to the metamorphosed sedimentary rocks of the gold mining environment, these rock types can be described as weak and soft, meaning they are characterized by lower ultimate strength and smaller magnitudes of Young's Modulus.

From a stability viewpoint, there is not a significant amount of difference between a deep gold mine and a

shallow coal mine. For instance, at a depth of 200 m in a coal mine, the virgin stress is 5 MPa while it is 54 MPa in a gold mine at 2 000 m depth. The Uniaxial Compressive Strength (UCS) of coal in the laboratory is in the region of 20 to 40 MPa while the UCS of quartzite is around 200 to 250 MPa. The ratio of virgin stress to UCS for that coal mine is about 0.125 to 0.25 and for the gold mine it is about 0.22 to 0.27. While the coal mine environment is subjected to much lower stress levels, it is also characterized by a much weaker rock environment. The ratio of stress to strength for the two environments is similar.

Mention has to be made of the difference between mechanical properties determined in a laboratory and the *in situ* mass properties of a rock material. In the laboratory, small samples without obvious defects are tested to obtain a characteristic strength for that particular material type. In nature, the same material in bulk is characterized by discontinuities such as slips, joints, faults, etc. The unit strength obtained in a laboratory is thus the maximum strength that the material can ever have—in nature it is invariably much weaker.

Rock strength in tension is typically 1/8 to 1/12 of that in compression. The Uniaxial Tensile Strength (UTS) of laminated sedimentary strata can be very low perpendicular to bedding, particularly if micaceous layers are present on the bedding planes.

In situ strength determinations can be done. It is, for instance, often done for civil excavations like dam foundations. However, it is very expensive and even then only valid for the particular area where the test was carried out, and often a single set of joints a few metres away into the unseen rock can invalidate the results immediately. For a mine it is simply not practical to do this.

In mining, rock engineers are more prone to determine the essential *in situ* characteristics by means of inexpensive back analysis. The methods are usually very simple, requiring rudimentary measurements of displacements followed by back calculations to determine what the properties must have been to conform to the observed displacements. Those properties are then used for future calculations, mainly as input into complex stress analysis programs.

Table I summarizes some of the important mechanical properties of rocks. These are general

Table I
Laboratory determined mechanical properties of some rock types

Rock type	UCS (MPa)	UTS (MPa)	Shear strength (MPa)	Young's Modulus (GPa)	Density (kg/m³)
Sandstone	75	5	15	13	2 480
Shale	75	5	7	15	2 480
Siltstone	70	6	8	1	2 480
Mudstone	40	5	8	7	2 480
Dolerite	190	14	20	100	3 000
Coal	25	5	8	5	1 500

South African laboratory results and should not be used as input into programs for rock mass behaviour analysis. However, they are useful for comparative purposes. For instance, note the differences between the dolerite and the other materials. The dolerite is both heavier and significantly stronger and stiffer than the other rock types.

The Table is also useful to demonstrate the differences between laboratory and *in situ* rock properties. Coal, for instance, has an average laboratory strength of around 25 MPa, while the *in situ* strength has been found to be in the range of 5.2 MPa with underground testing of large specimens and between 4.0 and 7.2 MPa with statistical back analysis. Also, while the dolerite material is shown to be very strong, in nature it is known to be densely jointed. The properties of the discontinuities, rather than those of the intact rock material, govern the bulk behaviour.

Rock mechanics is often called an 'inexact science'. Strictly speaking, the statement is not correct. The science is exact; the problem lies in the variability of the rock properties, which lends a degree of uncertainty to the input. It is as unwise to rely totally on laboratory input into rock engineering calculations, as it is to reject calculations on the basis of uncertain input. The difference between a good and a mediocre rock engineer lies in the judgement applies to the input and the same applies to the evaluation of the results of a calculation.

Setting up and running a numerical model is to some extent a mechanical action. The engineering skill is in the interpretation of the output. However, the most dangerous rock engineering action of all is to guess the output without having analysed the problem.

Chapter 2

Geotechnical classification

Introduction

This chapter is a practical guide, aimed at the rock engineer or geologist who wants to perform rock characterization or classification underground. It describes a number of classification systems with worked examples.

The coal deposits of the Main Karoo Basin have been sub-divided into different coalfields, based on differences in coal qualities, numbers and thickness of coal seams and geography. The major coalfields are described by Fauconnier and Kersten (1982).

The geology of the overburden and, in particular, the immediate strata surrounding a coal seam, are of prime importance to the design layout and support requirements of a successful mining operation. The immediate roof strata determines support requirements and maximum spans, and will influence equipment selection and mining method, particularly for high or secondary extraction. Likewise, a weak floor or one with a propensity to swell, will impact on the type of mining equipment and on pillar design. The behaviour of the overburden must be taken into account in the design and layout of high extraction mining systems in order to anticipate problems, especially difficulties associated with strata that will not cave readily.

The geologist plays an important role in describing exploration borehole core for determining coal quality during feasibility investigations. It is the exploration geologist who typically provides the first technical description of the overburden and the strata in the immediate vicinity of the coal seam. The geologist's log is often used to make assumptions as to the likely behaviour of the roof and floor strata during mining. This may result in misunderstandings because the geologist describes the physical nature of the various lithologies whereas the mining engineer needs to know how the strata will behave mechanically and how they will react to exposure to air and moisture.

The rock engineer classifies strata according to its mechanical behaviour rather than in classic geological terms. However, many of the geological descriptions regarding the characteristics of a layer are pertinent. For example, the description of cross-bedding, micaeous layers or fissile beds can indicate potential failure planes. Structural information regarding faults, dykes and the associated burnt coal all indicate potential instability that must be investigated.

Geophysical logs of exploration holes can also indicate the individual strata characteristics. Sonic logs have shown a correlation with rock strength and Young's Modulus while neutron logs are useful for lithological interpretations, McNally (1987). Geophysical logging has been used for the interpretation of roof in poor ground. Figure 1 shows a Gamma-Gamma log with the weaker layers having the higher readings. However, these techniques need to be further developed for use in rock engineering.

Rock mass classification

Classification of the rock mass into groups where similar support systems are required for stability, or where an indication of the behaviour of the strata can be obtained, is beneficial for the mining operator. It is also useful for the development of hazard plans, whereby the information obtained from the exploration drill core is reproduced to inform mining operators of potential immediate roof conditions that may require changes to the support pattern. This may be in the form of reduced cut-out distance or width of cut of a continuous miner or the need for different support types.

A detailed summary of several classification systems is given by Hoek, *et al.* (1997). Most of the classification systems were developed for civil engineering tunnelling and aim to determine the stand-up time before support is required, as well as the type of support that should be used for a given rock mass class. Most of the rock mass classification systems are not pertinent to coal mining because they do not provide for the layered geology and geologic structure typical of coal mine strata. The Karoo sediments form only a small section of most of these systems. They need to be further sub-divided to become useful in coal mining. The rock mass classifications have their place, particularly in rock excavations such as shafts, inclines and raises. These important excavations require stability over an
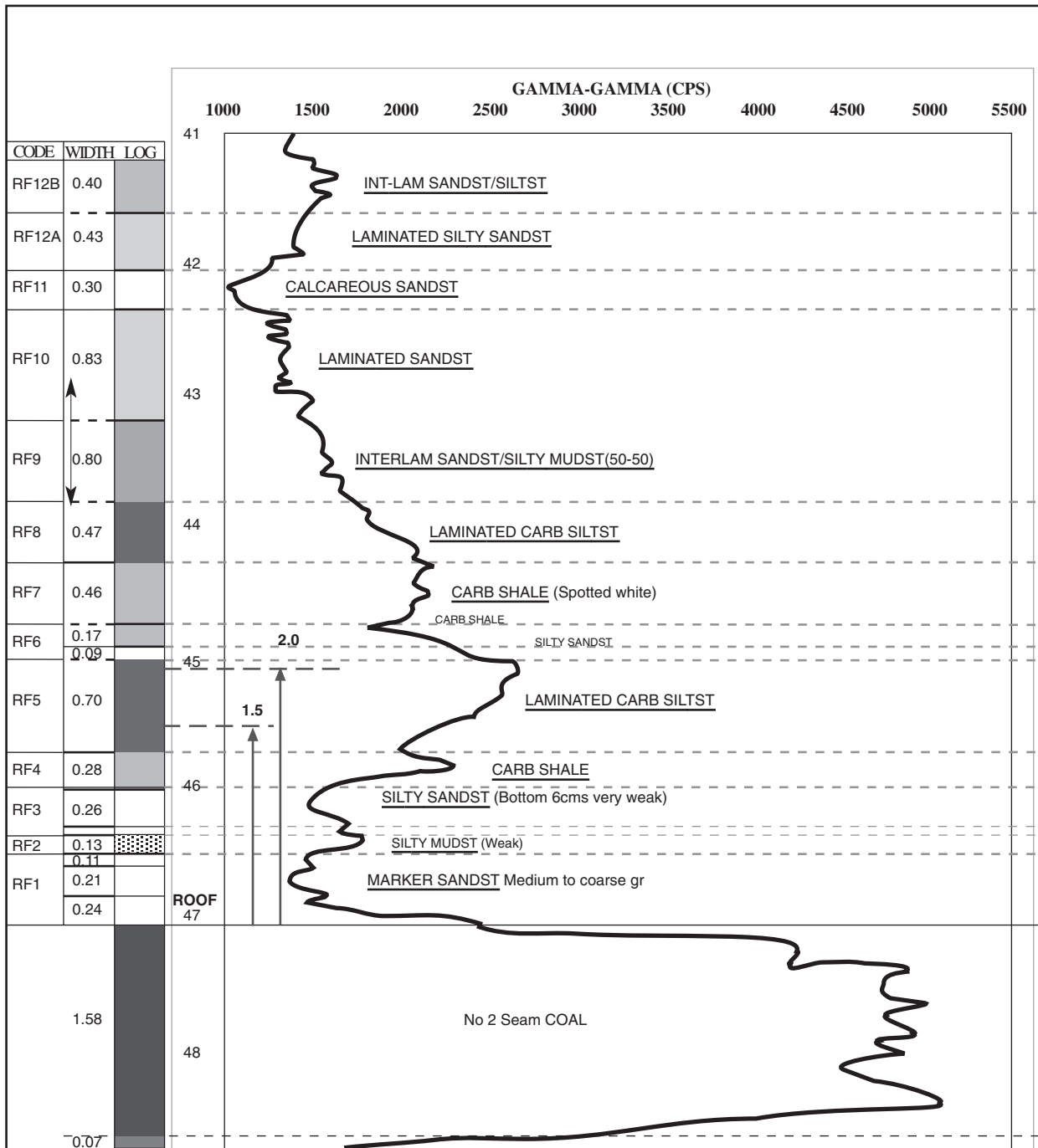
Figure 1. Geological log and geophysical gamma-gamma log indicating rock characteristics

extended period of time and therefore the support systems could be similar to those required in civil engineering.

Several of the classifications use index tests to gain an estimate of the characteristics of the rock mass. The need for simple index tests have developed due to the extensive time required to conduct laboratory testing as well as the costs involved. Another problem is the non-representative nature of the laboratory tests where only a small portion of the rock mass is tested. Considering the large volume of rock contained in

drill core, the necessity of a simple system whereby potential problems could be highlighted, arose. One of the first of these was the Rock Quality Designation (RQD) where an estimate of the blocky nature of the strata is obtained. RQD is defined as the length of core in excess of 100 mm divided by the total length of a particular strata unit expressed as a percentage, and is used in several of the rock mass rating systems. However, the skill of the drill operator can influence the RQD result.

The strength of the rock is usually stated in terms of

Uniaxial Compressive Strength (UCS). The UCS is a laboratory strength test of a rock sample; with length at least 1,5 times the diameter. The Point Load Test was developed to estimate the UCS of core by testing core in the field. A hand-operated pump is used to record the load taken to break the core. The load is then multiplied by a factor to obtain the estimated UCS. As the usual procedure is to test the core parallel to the bedding plane, the results in typical coal bearing strata are often not a close estimate of the UCS determined directly from laboratory specimens. In addition, the Point Load Test in coal strata suffers from two drawbacks: although quick in relation to laboratory testing, it is slow considering the testing of tens or hundreds of metres of core, and it has to be carried out on certain minimum lengths of core, meaning that it cannot be applied to highly fractured units.

Slake Durability and swell tests provide an estimate into the likely impact of clay minerals and water on the behaviour of the strata and are particularly important as indicators of floor conditions. Simple immersion tests can be conducted whereby discs or cylinders of core are placed in water for a period of 24 hours and visual observation of the core estimates the degradation of the sample. Highly susceptible material will begin to disintegrate immediately upon immersion, while other layers may crack over a longer time period. The immersion test can indicate if the more costly tests are required. Buddery and Oldroyd (1992) discussed index tests for South African coal measure strata including Duncan Swell, Slake Durability and Impact Splitting of drill core.

Duncan swell test

The Duncan swell test measures the unconfined swelling strain in one or more directions when a sample of rock is immersed in water. When testing borehole cores from coal measures strata it is only necessary to measure the swelling strain perpendicular to the laminations since, in rocks liable to swell, that swelling will greatly exceed that in other directions.

Samples are not prepared but are chosen with their ends approximately parallel. This reduces the costs and time involved and, above all, allows the testing of weak samples that would otherwise break up during machining.

The test procedure requires that swelling displacement should continue to be recorded until it reaches a constant level or passes a peak. This can be extremely time consuming and, for practical purposes, is not necessary. For the vast majority of specimens, 90% or more of their final swell will have taken place by the time 30 minutes have elapsed. For this reason a 30 minute swelling strain is determined.

The swelling strain, S_{30}, is calculated as follows:

$$S_{30} = \frac{d_{30}}{L} \times 100\%. \qquad [1]$$

where: d_{30} = swelling displacement after 30 minutes,
L = initial length of the sample.

At the end of the test the sample is immediately removed from the water. It is then assigned a rating from 1–6 according to its condition. A rating of 1 is assigned to an undisturbed sample and a rating of 6 to a totally degraded one. The swell index of the sample is then determined by multiplying the swelling strain by the condition rating.

Slake durability test

This test assesses the resistance offered by a rock sample to weakening and disintegration when subjected to two standard cycles of drying and wetting. The slaking fluid used in all instances is water. The International Standard calls for a representative sample comprising ten rock lumps, each weighing 40 to 60 g. The size of core typically used means that 40 to 60 g lumps can only be obtained from the more competent rock types. If only these rocks are tested then the results would be biased towards good floor conditions. For this reason the lump requirement has been modified to 20 to 30 g unprepared lumps. The drying periods have been shortened from 2 to 6 hours to 0.5 to 2 hours in order to speed up the procedure and because the lumps are smaller.

The slake durability index (second cycle), I_{d2}, is calculated as follows:

$$I_{d2} = \frac{C}{A} \times 100\% \qquad [2]$$

where: A = dry mass prior to testing (g)
C = dry mass after two slaking cycles (g).

Conventionally, a high swell index implies a poor rock, conversely a high slake durability index implies a good rock. To avoid confusion Buddery and Oldroyd (1992) present the slake durability index as $100 - I_{d2}$. Both floor indices therefore increase as expected floor conditions get worse. Table I shows the floor rating for the swell and slake durability index.

Table I
Swelling and slake durability floor classification

Rating	Description	Swell index	Slake durability index
A	Good	<1	<14
B	Moderate	1–3	14.1–26
C	Poor	3.1–15	26.1–36
D	Very poor	>15	>36.1

There is not always complete correlation between the two indices. In these circumstances the index suggesting poorer floor conditions dictates the rating.

Impact splitting index

Roof failure in South African coal mines is predominantly governed by the frequency of laminations or bedding planes and therefore an indication of the potential for opening along these features is ideally required from borehole core.

An impact splitting test was developed whereby a constant impact is applied to every 20 mm of drill core by dropping a 1.5 kg chisel from a pre-determined height according to core diameter, for example, 100 mm onto TNW core (60 mm diameter) Buddery and Oldroyd (1992). When designing for roof support 2.0 m of the immediate roof is tested. The strata is divided into geotechnical units which may differ from geological units. The units are tested and the mean fracture spacing for each is obtained. The impact splitter causes weak or poorly cemented bedding planes and laminations to open, thus giving an indication of the likely *in situ* behaviour when subjected to bending stresses, in some instances compounded by blasting.

Using Equations [3] or [4], an individual roof rating for each unit is determined.

$$For\ fs \le 5 \quad rating = 4\,fs \qquad [3]$$

$$For\ fs > 5 \quad rating = 2\,fs + 10 \qquad [4]$$

Where fs = fracture spacing in cm.

Where coal forms the immediate roof, the unit rating is multiplied with a coal correction factor of 1.5625.

An example of Impact Splitting is given in Table II where the units were selected and the initial fracturing and final fracturing after impact splitting were obtained.

Table II
Example of unit rating from impact splitting test

Depth (m)	Thickness (cm)	Lithology	Initial	Final	fs	Rating	Coal correction factor
125.78	33	M	3	11	3.00	12.00	
126.24	46	M	5	20	2.30	9.20	
126.74	50	F/S	9	25	2.00	8.00	
127.12	38	F/S	6	28	1.36	5.43	
127.80	68	C	6	15	4.53	28.33	1.5625
128.38	58	C	4	22	2.64	16.48	1.5625
128.97	59	C	3	18	3.28	20.49	1.5625
129.64	67	C	5	20	3.35	20.94	1.5625
130.29	65	C	4	20	3.25	20.31	1.5625
130.66	37	CBD	3	16	2.31	9.25	
131.27	61	C	4	15	4.07	25.42	1.5625
131.66	39	C	3	12	3.25	20.31	1.5625
132.35	69	F/S	4	22	3.14	12.55	

The immediate roof unit will have a greater influence on the roof behaviour, and consequently the unit ratings are weighted according to their position in the roof by using the following equation:

$$Weighted\ rating = unit\ rating \times 2\,(2 - h)\,t \qquad [5]$$

Where h = mean unit height above the roof (m)
    t = thickness of unit (m).

The weighted ratings for all units are added to give a final roof rating.

If a coal layer was left in the roof in the above example so that the immediate roof was at 127.8 m, the calculated weighted rating of 76 (rounded number) is obtained, see Table III.

Table III
Calculated weighted rating immediate roof at 127.8 m

Depth (m)	Thickness (m)	Unit rating	Mean height (m)	Weighted rating
126.24	0.46	9.20	1.79	1.78
126.74	0.50	8.00	1.31	5.52
127.12	0.38	5.43	0.87	4.66
127.80	0.68	28.33	0.34	63.97
			Total	75.92
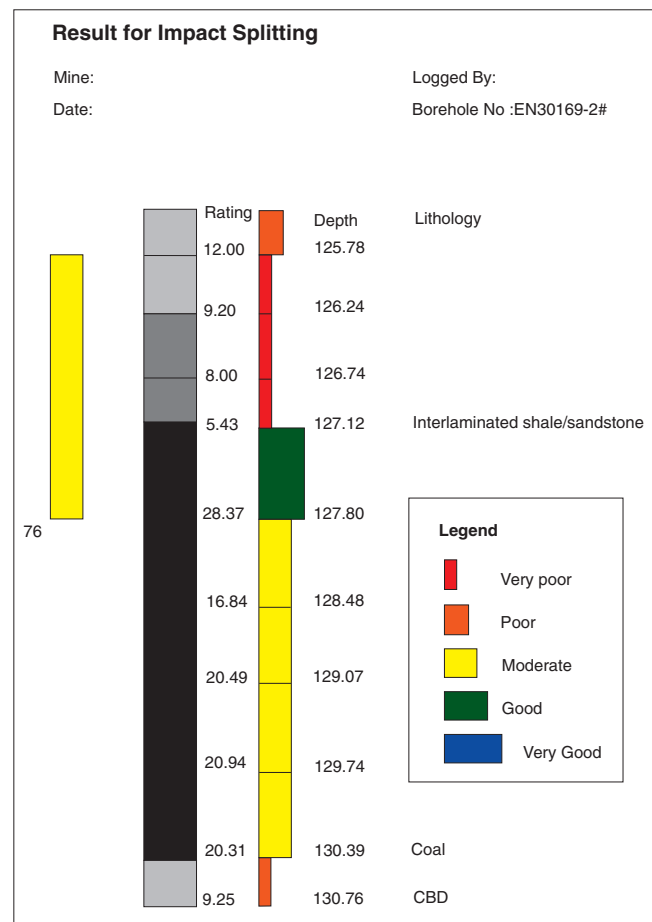
Figure 2. Graphical log of the impact splitting result for the example in Table III

Table IV
Unit rating and coal roof classification system

Unit rating	Rock class	Roof rating
<10	Very poor	<39
11–17	Poor	40–69
18–27	Moderate	70–99
28–32	Good	100–129
>32	Very good	>130

Table V
General guide for support and rock classification

Roof rating	Bord width (m)	Example of support
Very good	6.5	1.2 m × 16 mm point anchor, 5 bolts intersection only
Good	6.0	1.2 m × 16 mm point anchor, 5 bolts intersection, 2 bolts per row, rows 2.0 m apart
Moderate	5.5	1.5 m × 16 mm full column, 9 bolts per intersection, 3 bolts per row with rows 1.5 m apart
Poor	5.0	1.8 m 20 mm full column, 16 bolts per intersection, 4 bolts per row with rows 1.0 m apart, possibly with W-straps
Very poor	<5.0	Specialized support, e.g. combination of cable anchors, trusses, shotcrete, W-straps, etc.

Figure 2 shows the graphical log of the impact splitting result for the example in Table III.

Table IV shows the unit and roof ratings in relation to the rock classification.

A general guide for the support type is given in Table V. However, each situation should be assessed by a rock engineer on a site-specific basis.

The minerology of the layers should also be examined. Extensive roof falls can occur in an apparent massive sandstone if the matrix between the sand particles is in fact a clay mineral. The original visual observation that the rock is a sandstone, and therefore considered to be competent, should be tested by simple field tests.

Physical risk and performance rating

Oldroyd and Lattlia (1999) of the Ingwe Rock Engineering Department developed simple rating forms to classify the adherence to mine standards and physical conditions at mines. The underground physical rating form is based on; the type of mining, geological conditions and mining support. Three risk categories are determined from the physical risk rating: 'Good', 'Moderate' and 'Special Areas'. Production personnel conduct the physical rating on a regular basis, determining the type and density of support and the cutout distance of a continuous miner.

Should the rating category of Special Area apply, the mine overseer confirms the rating and issues changes to the support system. A rock engineer visits the section and confirms or gives advice regarding the support system. Should a further rating show that the conditions have improved, the declassifying of a Special Area is approved by the Section Manager.

Adherence to Mine Standards and Procedures is determined by carrying out the Section Performance Rating.

The rating system considers the following:

- Fall of ground statistics over a six-month period
- Adherence to the support requirements for slips, brows and temporary support
- Quality of installation
- Adherence to standards and designed dimensions
- Erection of barricades
- Last bolt indicators
- Whether or not people go under unsupported roof and
- Quality of barring loose rock from the roof or sidewalls.

This system is an excellent practical method for the face personnel to determine changes in strata conditions. Adaptation of the rating form has been done for mines other than Ingwe Collieries and has gained popularity with mine management.

The Ingwe Rating requires the mining personnel, usually the Shift Overseer, to rate the physical risk and performance of the section, with the back-up of the rock engineering department. The Ingwe Physical Risk Rating system is shown in Figure 3. The Section Performance Rating system has been adapted for general use and an example is shown in Figure 4.

The following example is given to demonstrate the use of the rating system:

A colliery mining the No. 1 Seam has had problems with roof stability in the past due to the nature of the immediate roof. The immediate roof consists of about 0.3 m of sandstone, overlain by 0.3 m of coal and in excess of 2.0 m of shale. The thickness of the sandstone varies from about 0.1 m to 0.5 m and the shale layer deteriorates if exposed. The support pattern adopted is 1.5 m long, 16 mm diameter, full column resin rebar roofbolts installed four in a row and 2.0 m between rows. A bord width of 6.5 m is required.

The Physical Risk rating, Figure 3, shows that no falls occur in the section. However, due to the type of roof, 'shale/sandstone', the 'thin 60–200 mm' bedding in both the sandstone and coal layers and the 'Poor' nature of the roof, the roof was rated at the middle of the 'Moderate' classification range. Should conditions deteriorate a reduction in the spacing of the support would be applied or the general support could be altered as per Table V.

COLLIERY: _____ SEAM: _____ SECTION: _____ DATE: _____

RISK RATING: <40 Good area   41 to 60 Moderate   >60 Special Area

Mining method	Chequer board 14	Stone development 12	Top coaling 10	Bottom coaling 8	CM bord & pillar 4	Conv. bord & pillar **X** 2	2
Roof lithology	Shale 10	Shale/sandstone **X** 8	Coal/shale 4	Mudstone 2	>0,5 m coal 2	Sandstone 0	8
Roof condition	Very poor 20	Poor **X** 14	Moderate 10	Good 5	Very good 0	Variable 14	14
Discontinuities	Dyke/fault 20	Slips <5 m apart 18	Slips 5–10 m apart 12	Slips 10–20 m apart 8	Slips >20 m apart **X** 4	No slips 0	4
Discontinuities: Influence	Severe 20	Very strong 16	Strong 12	Moderate 8	Slight **X** 4	Nil 0	4
Geological conditions	Severe weathering Wet roof 12	Slight weathering Wet roof 12	Seam dip >5° or false roof **X** 10	Fossil logs 8	Floor/roof rolls 4	Good 0	10
Mining height	> 5.5 m 12	4.5–5.5 m 8	3.5–4.5 m 6	2.5–3.5 m 4	2.0–2.5 m **X** 2	< 2.0 m 0	2
Systematic support	None 6	Intersection only 4	2.5 m grid 3	2 m grid 2	1.5 m grid **X** 1	1 m grid 0	1
General	Shallow workings <25 m; Multi-seam parting <4 m 10	Shallow workings 25–40 m; multi-seam parting 4–12 m 4	Multi-seam parting >12 m 2	Slips in pillars, high frequency 10	Slips in pillars, medium frequency 4	Slips in pillars, low frequency **X** 2	2
Advance per month	>1400 12	1200–1400 9	1000–1200 6	800–1000 4	600–800 **X** 2	<600 0	2
						TOTAL	49

Received by: _____ Designation: _____ Time: _____ Date: _____

Summary of changed conditions: _____

Remedial action taken: _____

Remarks: _____

Figure 3. Underground section physical risk rating showing an example of possible values (designated by X) and the total

COLLIERY: _____ SEAM: _____ SECTION: _____ DATE: _____

VISITED BY: _____ BOLT TYPE: _____ MINING METHOD: _____

FOG stats (Previous 6 months)	Fatal - 20	Reportable -10	Lost/shift -2	D/S / incident 0	None 5 **X**	5
Temporary support	Not used at all -5	Occasionally used 0	In good condition, installed correctly and always in place **X** 5			5
Slip support	Poor, 3 slips not detected or bolted -15	1 Slip not detected or bolted -3	Good. all slips supported according to COP **X** 10			10
Brow support	2 Brows not supported -10	Incorrect spacing -5	Bolt length correct for depth of brow and all brows correctly supported according to COP **X** 5			5
Support spacing	Out of specification >15% -10	Out of specification 10–15% of planned **X** -5	Spacing 5–10% of planned 0	Spacing 0–5% of planned 10		-5
Road width control	Individual bord > Max., >15% design **X** -15	Average bord 10–15% -5	Average Bord 5–10% 0	On design width 0–5% 10		-15
Intersection cutting	Diagonal deviation >10% **X** -15	Diagonal deviation 5–10% -5	0–5% 5	Correct length 10		-15
Support of intersections	Seen to be cutting into unsupported intersections -10	All intersections supported before being cut **X** 10				10
Bolt installation	Crimps not broken. Plates loose. Broken bolts not replaced.- 15	Protruding thread length variable 0	Most defective or damaged bolts replaced and all installations to standard **X** 10			10
Additional support (where required)	Not installed -5	Partially installed -3	Extra bolts in enlarged intersections 3	Always installed **X** 5		5
People under unsupported roof	People seen to be working under unsupported roof -15	People inferred to be working under unsupported roof-5	Clear evidence that people are not working under unsupported roof **X** 10			
Barring	Roof and sidewalls not barred -15	Roof barred OK, but sidewalls (overhangs) poor 0	General standard of barring very good **X** 10			10
Points in Table are a guide only, adjust as required (If not satisfied with performance award 5/10)					TOTAL	35

SECTION PERFORMANCE RATING:
  80–100   VERY GOOD
  61–79   GOOD
  41–60   MODERATE
  0–40   POOR
  >0   VERY POOR

TOTAL RATING	35
Classification	Poor

Recommendations/Action plan: _____ Overmining bords and intersections _____

        Bolt spacing too wide

Figure 4. Performance rating showing values (designated by X) and the total

Table VI
Section physical risk and support standards

Section physical rating	Support
Good	Standard support rules
Moderate	Reduce cutout distance, narrow bord, minor modifications to support spacing, length of bolt
Special area	As per colliery's Rockfall Code of Practice, input from rock engineer

The section performance with regard to the adherence to mine standards appears to be 'good', as no accidents have been recorded due to falls of ground in the previous six-month period. In addition, an inspection of the section showed that the temporary support was being used during the visit and that all slips and brows had been supported according to the manager's support rules. Additional bolts had been installed where required, barring of the roof and sidewalls were of a high standard and people were not working under unsupported roof.

A competent person records the bolt spacing as falls between bolts have occurred in the past. In addition, the bord width and intersection diagonals are also recorded due to the potential for roof falls. The bolt spacing, bord and diagonal widths are plotted on frequency diagrams, Figures 5–7 on a monthly basis. This information is used in the performance rating in Figure 4.

A rating of -5 is given for support spacing as the spacing was 14% over specification, allowing a 0.1 m tolerance. Then, 29 of the 125 bolt spacing between rows were over the required 2.0 m maximum. A rating of -15 was given for the bord width as over 15% of the bord widths exceeded 6.6 m (allowing a tolerance of 0.1 m) and also because the maximum bord width, according to the 'Code of Practice to Prevent Rockfall Accidents', states that the maximum bord width allowable is 7.0 m. The acceptable diagonal distance of 10.2 m was found from the bord width (6.5 m) times 1.4 (for the diagonal distance) plus a tolerance. Thus 6.5 x 1.4 = 9.1 m + 1.1 m = 10.2 m. As 25 per cent of the diagonals exceeded 10.2 m a rating of -15 is applied.

A performance rating of 35 was given to the section due to overmining of the bord width and intersections, as well as the excessive distance between bolts. At first inspection, the section appeared to adhere to the manager's rules and design, but by measuring the main parameters the overmining of the section was detected. Usually the surveyor supplies the manager with the monthly statistics, including the average bord width. Figure 6 shows that the average bord width can mask wide roadways where there is potential for a fall of ground.

Shafts and inclines

The Impact Splitting Index has also been used to determine the classification of strata in incline shafts from boreholes. Once the strata has been exposed other rock mass classifications can be used to assess the conditions.

Figure 8 shows sandstone exposed in an incline mined through a fault to access the coal seam. The sandstone is competent but several joints result in a blocky rock mass. Barton's Q System (1993) was used to classify the rock and provide a comparison with the selected support system.

The Q Index is given by:

$$Q = \frac{RQD}{J_n} \times \frac{J_r}{J_a} \times \frac{J_w}{SRF} \qquad [6]$$

Where RQD is the Rock Quality Designation,

J_n = Joint Set Number

J_r = Joint Roughness Number

J_a = Joint Alteration Number

J_w = Joint Water Reduction Factor

SRF = Stress Reduction Factor.

Table VII shows the values for the input parameters while Figure 9 shows examples of the Joint Roughness, J_r.

Values for the sandstone exposed in the incline are shown in the example of the Q ratings in Figure 10. The input values are visually estimated by a range taken from positions within the exposed layer. For example, the RQD of the sandstone is estimated to be high given the thickness of the bedding exposed and despite there being some thin layers that may result in core less than 100 mm in length. Two dominant joint sets occur in the rock mass as well as the bedding plane. However, a fourth set is present, although to a lesser extent. The major joint in Figure 8 is not taken into account in the number of joints as it is an atypical single feature which would be individually supported according to the support requirements for joints and slips.

The joints are 'planar and smooth' (Figure 9) and are 'tightly healed with impermeable filling'. The area was dry. Stress Reduction Factor of 1.0 was used as the depth to the incline is approximately 180 m below surface which is in 'medium stress, favourable stress condition' with the ratio σ_c/σ_1 in the range 10–200. The virgin stress at this depth is 4.5 MPa and the UCS of the sandstone approximately 100 MPa.

Figure 10 shows the field sheet, after Barton (1993), with the typical range obtained from the rock mass shown in Figure 8 with the Q values obtained varying from 5.8 to 14.8, while the mean Q value was 8.8.

Section 1
ROOFBOLT SPACINGS
DATE: 17/1/2000

	1.4	1.5	1.6	1.7	1.8	1.9	2	2.1	2.2	2.3	2.4	2.5	2.6
In spec - 42.4%	1	6	5	9	15	17							
On spec - 34.4%							43						
Out spec - 23.2%								12	6	5	3	1	2

DISTANCES

☐ In spec - 42.4% ■ On spec - 34.4% ☐ Out spec - 23.2%
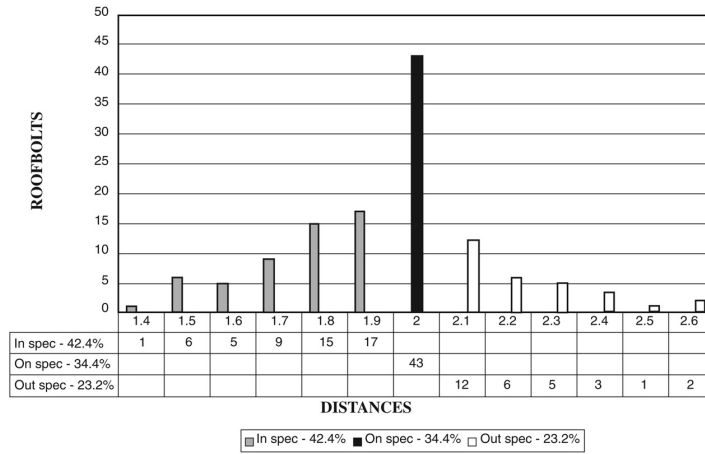
Figure 5. Bolt spacing between rows

January-10

Herewith the analysis of Bord Widths as measured by the Survey Department for Safety factor purposes

Panel No:	DECLINE EAST1 S5	Section:	1
Mine Overseer:	HUGO BURGER		
Measurements between Splits	0	to	FACE

Exception Report		
Percentage widths less than 7.0 meters	72	94.7%
Percentage widths exceeding or equal to 7.0 meters	4	5.3%

Summary	
Number of bord widths measured	76
Average bord widths for period	6.73
Planned bord widths	6.8
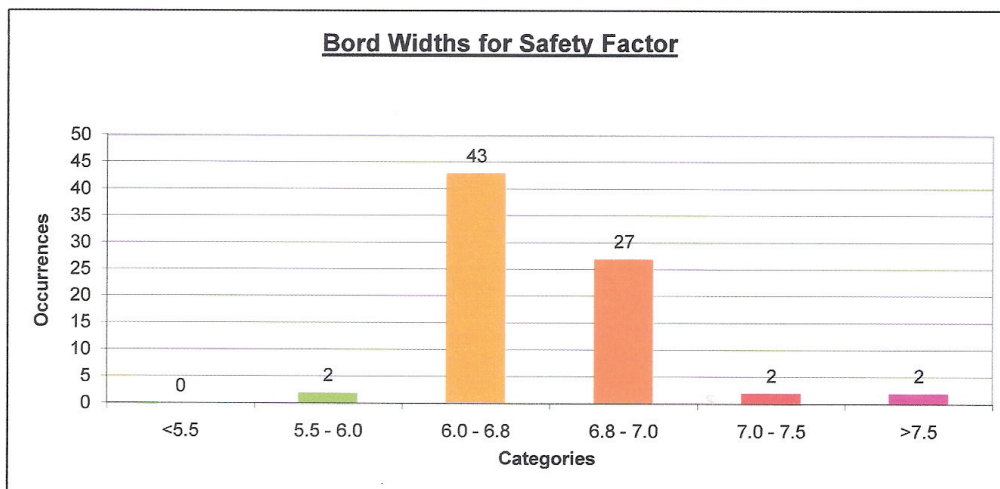
Figure 6. Bord width vs frequency

ROCK ENGINEERING FOR UNDERGROUND COAL MINING

January-10

Herewith an analysis of Intersection Areas measured by the Survey Department

Panel No:	DECLINE EAST1 S5	Section:	1
Mine Overseer:	HUGO BURGER		
Measurements between Splits	0	to	FACE

Exception Report	
Number of areas between 14 and 23 m²	89.5%
Number of areas in excess of 23 m²	10.5%

Summary	
Number of Intersections measured	19
Average Intersection Area for period	20.49

Remarks:
Intersections that are greater than 23 m²

Intersections

Figure 7. Diagonal intersection distance
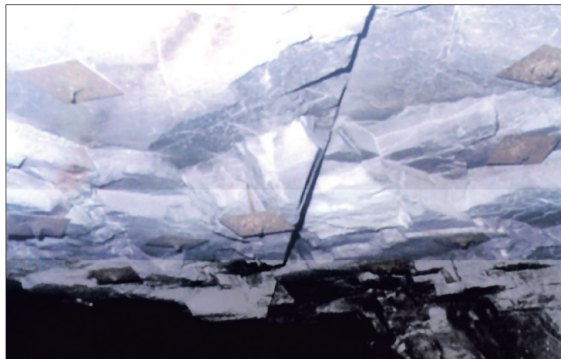
Figure 8. Sandstone layers in incline shaft

Table VIII contains the Excavation Support Ratio (ESR) values for different types of excavations according to Barton. An ESR value of 1.6–2.0 was used, as the incline will be required for the exploitation of a block of ground with an estimated life expectancy of several years. An 8.0 m wide incline is required, as the conveyor belt and the transport road are to be together within the incline. Thus the Span-to-ESR ratio is between 4.0–5.0 (8/1.6 or 8/2).

A Q value of 8.8, from Figure 10, puts the rock mass into rock class C 'Fair' but close to class B 'Good' (Figure 11). Plotting the Span-to-ESR value of 5.0 against Q on the support chart, Figure 11, indicates that 'systematic bolting' is suggested, although the rating is close to the 'spot bolting' and 'unsupported' classes. Considering the blocky nature of the sandstone exposed in the 8.0 wide roadway, the combination of systematic support together with spot bolting for individual blocks is required. The length of

the bolt selected was 1.5 m, based on the thickness of the bed exposed and while point anchor anchorage could have been applied, full column anchorage was selected because of the time the decline was to be exposed.

Coal roof classification

The CMRR, or Coal Mine Roof Rating, was developed by Molinda and Mark (1994) of NIOSH (formerly the USBM) in the USA, as a tool to quantify geological information for use in coal mines. It has found extensive use in the USA and to a lesser extent in Australian collieries. The system has been tried in South Africa and preliminary results are encouraging.

The strata in the Physical Risk Rating was rated according to the CMRR. Figure 12 shows the field data sheet for the immediate roof from the No. 1 Seam classified in Figure 3. The CMRR Tables IX–XIII, were used to obtain values for the sandstone, coal and shale layers and these values were used in the Unit Rating (UR) calculation sheet, Figure 13. These were multiplied by the unit thickness within the bolting horizon and applying CMRR Tables XIV–XVII, the overall CMRR rating of 37.1 was obtained, see Figure 14.

The Immersion Test data sheet is shown in Figure 15 and should be applied to the unit in the immediate roof or an upper layer if exposed to water.

The CMRR has been applied to exploration drill core. However, the method is dependent on point load testing and as stated previously, the results of testing bedding parallel to the bedding, then applying a factor to obtain the UCS strength is questionable. A combination of the Impact Splitting Index test procedure combined with the CMRR for drill core may hold potential.

Table VII
Q-system input parameters

1 Rock quality designation		RQD
A	Very poor	0–25
B	Poor	25–50
C	Fair	50–75
D	Good	75–90
E	Excellent	90–100

Note: i) Where RQD is reported or measured as ≤ 10 (including 0), a
nominal value of 10 is used to evaluate Q
ii) RQD intervals of 5 i.e .100, 95, 90 are sufficiently accurate

2 Joint set number		J_n
A	Massive, no or few joints	0.5–1.0
B	One joint set	2
C	One joint set plus random joints	3
D	Two joint sets	4
E	Two joint sets plus random joints	6
F	Three joint sets	9
G	Three joint sets plus random joints	12
H	Four or more joint sets, random, heavily jointed, 'sugar cube' etc.	15
J	Crushed rock, earthlike	20

Note: (i) For intersections use $(3.0 \times J_n)$
(ii) For portals use $2.0 \times J_n$

3 Joint roughness number		J_r
(a) Rockwall contact and (b) rockwall contact before 10 cm shear		
A	Discontinuous joints	4
B	Rough or irregular, undulating	3
C	Smooth undulating	2
D	Slickensliding undulating	1.5
E	Rough irregular planar	1.5
F	Smooth planar	1.0
G	Slickenslide planar	0.5

Note: (i) Descriptions refer to small-scale features and intermediate-scale
features, in that order

(b) No rockwall contact when sheared		
H	Zone containing clay minerals thick enough to prevent rockwall contact	1.0
J	Sandy, gravelly or crushed zone thick enough to prevent rockwall contact	1.0

Note: (i) Add 1.0 if the mean spacing of the relevant joint set is greater
than 3.0 m
(ii) $J_r = 0.5$ can be used for planar slickenslide joints having
lineations, provided the lineations are orientated for
minimum strength

4 Joint Alteration number		φ_r approx	J_a
(a) Rockwall contact (no mineral fillings, coatings only)			
A	Tightly healed, hard, non-softening, impermeable filling, .ie. quartz	-	0.7 5
B	Unaltered joint walls, surface staining only	25–35	1.0
C	Slighly altered joint walls, non-softening mineral coatings, sandy particles, clay-free disintegrated rock	25–35	2.0
D	Silty or sandy-clay coatings, small clay fraction (non-softening)	20–25	3.0
E	Softening or low friction clay mineral coatings, kaolinite or mica, chlorite, talc, gypsum, graphite, small quantities of swelling clays	8–16	4.0
(b) Rockwall contact before 10 cm shear (thin mineral fillings)			
F	Sandy particles, clay free disintegrated rock	25–30	4.0
G	Strongly over-consolidated non-softening clay mineral fillings (continuous but <5 mm thickness)	16–24	6.0
H	Medium or low over-consolidated softening clay mineral fillings (continuous but <5 mm thickness)	12–16	8.0
J	Swelling clay fillings i.e. montmorillonite (continuous but <5 mm thickness). J_n value depends on % of swelling clay-sized particles and access to water	6–12	8–12
(c) No rockwall contact when sheared (thick mineral fillings)			
K L M	Zones or bands of disintegrated or crushed rock and clay (see G, H, J, for description of clay condition)	6–24	6,8 or 8–12
N	Zones or bands of silty or sandy-clay, small clay fraction (non-softening)	-	5.0
O P R	Thick, continuous zones or bands of clay (see G, H, J, for description of clay condition)	6–24	10, 13 or 13–20

5 Joint water reduction factor		Water pressure (kg/cm³)	J_w
A	Dry excavation or minor flow < 5 l/min locally	<1	1.0
B	Medium inflow or pressure occasional outwash of joint fillings	1–2.5	0.66
C	Large inflow or high pressure in competent rock with unfilled joints	2.5–10	0.5
D	Large inflow or high pressure considerable outwash of joint fillings	2.5–10	0.33
E	Exceptionally high inflow or water pressure at blasting, decaying with time	>10	0.2–0.1
F	Exceptionally high inflow or water pressure continuing without noticeable decay	>10	0.1–0.05

Note: (i) Factors C to F are crude estimates. Increase J_w if drainage
measures are installed.
(ii) Special problems caused by ice formations are not considered

Table VII
Q system input parameters (continue)

6 Stress reduction factor		SRF
(a) Weakness zones intersecting excavation which may cause loosening of rock mass when tunnel is excavated		
A	Multiple occurrences of weakness zones containing clay or chemically disintegrated rock, very loose surrounding rock (any depth)	10
B	Single weakness zones containing clay or chemically disintegrated rock (depth of excavation ≤ 50 m)	5
C	Single weakness zones containing clay or disintegrated rock (depth of excavation > 50 m)	2.5
D	Multiple shear zones in competent rock (clay-free), loose surrounding rock (any depth)	7.5
E	Single shear zones in competent rock (clay-free) (depth of excavation ≤ 50 m)	5.0
F	Single shear zones in competent rock (clay-free) (depth of excavation > 50 m)	2.5
G	Loose, open joints, heavily jointed or 'sugar cube', etc. (any depth)	5.0

Note: (i) Reduce these values of SRF by 25–50% if the relevant shear zones only influence but do not intersect the excavation

(b) Component rock, rock stress problems		σ_c/σ_1	σ/σ_c	SRF
H	Low stress, near surface, open joints	>200	<0.01	2.5
J	Medium stress, favourable stress conditions	200–10	0.01–0.3	1
K	High stress, very tight structure. Usually favourable to stability, may be unfavourable to wall stability	10–5	0.3–0.4	0.5–2
L	Moderate slabbing after > 1 hour in massive rock	5–3	0.5–0.65	5–50
M	Slabbing and rock burst after a few minutes in massive rock	3–2	0.65–1	50–200
N	Heavy rock burst (strainburst and immediate dynamic deformations in massive rock	<2	>1	200–400

Note: (i) For strongly anisotropic virgin stress field (measured): when $5 \leq \sigma_1/\sigma_3 \leq 10$, reduce σ_c to 0.75 σ_c. When $\sigma_1/\sigma_3 > 10$, reduce σ_c to 0.5 σ_c, where σ_c = unconfined compression strength, σ_1 and σ_3 are the major and minor principal stresses, and σ_L = maximum tangential stress (estimated from elastic theory).
(ii) Few case records available where depth of crown below surface is less than span width. Suggest SRF increase from 2.5 to 5 for such cases (see H)

(c) Squeezing rock: plastic flow of incompetent rock under the influence of high rock pressure		σ_6/σ_1	SRF
O	Mild squeezing rock pressure	1–5	5–10
P	Heavy squeezing rock pressure	>5	10–20

Note: (iv) Cases of squeezing rock may occur for depth $H > 350 Q^{1/3}$ (Singh et al., 1992). Rock mass compression strength can be estimated from $q = 7 \gamma Q^{1/3}$ (MPa) where γ = rock density in gm/cc (Singh, 1993)

(d) Swelling rock: chemical swelling activity depending on presence of water		SRF
R	Mild swelling rock pressure	5–10
S	Heavy swelling rock pressure	10–15

Subscripts refer to block size (cm)	J
I rough	4
I smooth	3
I slickensided — Stepped	2
IV rough	3
V smooth	2
VI slickensided — Undulating	1.5
VII rough	1.5
VIII smooth	1.0
IX slickensided — Planar	0.5

Figure 9. Example of joint roughness, J_r

Elevation or depth zone:

Q (typical range) = 14.8–5.83	Q (mean) = 8.83
$(\dfrac{80\text{–}100}{15\text{–}9})$ x $(\dfrac{1.0}{0.75\text{–}1.0})$ x $(\dfrac{1.0}{10})$	$(\dfrac{95}{12})$ x $(\dfrac{1.0}{0.9})$ x $(\dfrac{1.0}{1.0})$

B L O C K

Very Poor	Poor	Fair	Good	Excellent

0   10   20   30   40   50   60   70   80   90   100   100

RQD %

Core pieces ≧ 10 cm

S I Z E S

Earth	Four		Three		Two		One		None

20   15   12   9   6   4   3   2   1   0.5

J_n

Number of joint sets

T A N (Φ_r)

Fills	Planar	Undulating	Dsc

1.0   0.5   1.0   1.5   1.5   2   3   4

J_a

Joint roughness —least favourable

T A N (Φ_p)

Thick Fills	Thin Fills	Costed	Unfilled	Heal

20   13   12   10   8   6   5   12   8   6   4   4   3   2   1   0.75

J_a

Joint alteration —least favourable

A C T I V I T Y

Exc. Inflows	High Pressure	Wet	Dry

.05   .10   .20   .33   .50   .66   1

J_w

Joint water pressure

S T R E S S

Squeeze	Swell	Faults	Stress/Strength

20   15   10   5   20   15   10   5   10   7.5   5   2.5   100 50   20   10   5   2   0.5 1.0 2.5

SRF

Stress reduction factor

Figure 10. Field sheet of rock mass shown in Figure 8

Table VIII
Summary of recommended *ESR* values for selecting safety level

Type of excavation		*ESR*
A	Temporary mine openings, etc.	2–5
B	Permanent mine openings, water tunnels for hydropower (exclude high pressure penstocks), pilot tunnels, drifts and headings for large openings, surge chambers	1.6–2.0
C	Storage caverns, water treatment plants, minor road and railway tunnels, access tunnels	1.2–1.3
D	Power stations, major road and railway tunnels, civil defence chambers, portals, intersections	0.9–1.1
E	Underground nuclear power stations, railway stations, sports and public facilities, factories, major gas pipeline tunnels	0.5–0.8

Figure 11. Support system and *Q*-rating. The abbreviations in the Figure have the following meanings: *CCA* = cast concrete lining, *RRS* = reinforced ribs of shotcrete, *B* = bolts, *Sfr* = fibre-reinforced shotcrete, *sb* = spot bolts and *S* = un-reinforced shotcrete

UNIT						UNIT DISCONTINUITIES							
Unit No.	Unit Thickness	Strip Log	Description	Strength	Moisture Sensitivity	Disco I.D.	Description	Cohesion	Rough-ness	Spacing	Persistance Lateral/Vert	Orientation Strike	Dip
3	2.0		*Shale*	2	4	A.	*Slip*	4	2	2	1		45°
						B.	*Bedding*	3	3	3	4		*Horizontal*
						C.							
			CONTACT		*Sharp*								
2	0.3		*Coal*	3	1	A.	*Bedding*	3	3	4	4		*Horizontal*
						B.	*Slip*	4	3	1	4		
						C.							
			CONTACT		*Sharp*								
1	0.3		*Sandstone*	1	1	A.	*Bedding*	3	3	5	4		*Horizontal*
						B.							
						C.							
		1	Rebounds	Not Sensitive		1	Strong (>7**)		Jagged	>1.8 m	0.09 m	N.	Horizon
		2	Pits	Slightly Sensitive		2	Moderate (4–7)		Wavy	0.6–1.8 m	0.9–3 m	NE.	Subhorizon
		3	Dents	Moderate Sensitive		3	Weak (1–3)		Planar	20–60 cm	3.9 m	E.	45°
		4	Craters	Severely Sensitive		4	Slicken-sided (0)			6.20 cm	>9 m	SE.	Subvert.
		5	Molds			5				<5 cm		S.	Vert.

Rebounds >103 MPa Pits 103–65 MPa Dents 65–21 MPa Craters 21–7 MPa Molds <7 MPa

Groundwater (inflow/10 m of entry lenght) (Circle) L/min
Dry 0 — 1   Heavy Drip 10–50 — 4
Damp 0–5 — 2   Flowing >50 — 5
Light Drip 5–10 — 3

Describe condition in vicinity of fall (circle one)
1. Good   3. Heavy
2. Scaly   4. Failed

**Hammer blows necessary to split bedding with 9-cm (3.5 in) chisel
COMMENTS: (Roof support, etc.)

Figure 12. Example of CMRR rating for immediate roof strata from Figure 3

Table IX
Cohesion–roughness rating

Roughness	(1) Strong cohesion	(2) Moderate cohesion	(3) Weak cohesion	(4) Slickened
(1) Jagged	35	29	24	10
(2) Wavy	35	27	20	10
(3) Planar	35	25	16	10

Note: If a unit has no bedding or discontinuities, then apply test to the intact rock. Strong cohesion implies that the discontinuities have no weakening effect on the rock

Table X
Spacing–persistence rating

Persistence m	(1) > 1.8 m	(2) 0.6–1.8 m	(3) 20–61 cm	(4) 6–20 cm	(5) < 6 cm
(1) 0–0.9	35	30	24	17	9
(2) 0.9–3	32	27	21	15	9
(3) 3 to 9	30	25	20	13	9
(4) > 9	30	25	20	13	9

Note: If unit has no bedding or discontinuities, then enter 35. If cohesion is strong, enter 35.

Table XI
Multiple discontinuity set adjustment

Two lowest individual discontinuity ratings both lower than:	Adjustment
30	−5
40	−4
50	−2

Table XII
Strength rating

	Strength, MPa	Rating
(1)	> 103	30
(2)	55 to 103	22
(3)	21 to 55	15
(4)	7–21	10
(5)	< 7	5

Table XIII
Moisture sensitivity rating

	Moisture sensitivity	Rating
(1)	Not sensitive	0
(2)	Slightly sensitive	−3
(3)	Moderately sensitive	−10
(4)	Severely sensitive	−25

Note: Apply only when unit forms immediate roof or water is leaking through bolted interval

UNIT RATING (UR)
Calculation Sheet

Mine Name _____ **Date:** _____

Location _____ **Data collected by:** _____

1) Calculate the individual discontinuity rating

Unit	**1 Sandstone**			**2 Coal**			**3 Shale**		
	Discontinuity			*Discontinuity*			*Discontinuity*		
	Set 1	Set 2	Set 3	Set 1	Set 2	Set 3	Set 1	Set 2	Set 3
Cohesion-Roughness (Table IX)	**20**			**16**	**10**		**10**	**16**	
	+	+	+	+	+	+	+	+	+
Spacing-Persistence (Table X)	**13**			**13**	**30**		**25**	**9**	
Individual Discontinuity Ratings	**33**			**29**	**40**		**35**	**25**	

	Unit	**1**	**2**	**3**
(2)	Enter the lowest of the individual discontinuity ratings	**33**	**29**	**25**
		+	+	+
(3)	If there is more than one discontinuity set, enter the multiple discontinuity adjustment from Table XI, otherwise enter 0.	**0**	**-4**	**-4**
		+	+	+
(4)	Calculate the unit strength Table XII	**30**	**15**	**15**
		+	+	+
(5)	Calculate the unit moisture sensitivity, Table XIII, (this applies only to Unit 1, or if upper unit is exposed to water)	**0**	**0**	**-10**
	Unit rating	**63**	**40**	**26**

Figure 13. Example of CMRR rating

Table XIV
Strong bed adjustment

Thickness	Strong bed difference							
	5–9	10–14	15–19	20–24	25–29	30–34	35–40	> 40
0.3–0.6	0	2	4	5	7	8	9	10
0.6–0.9	2	4	7	9	12	14	17	20
0.9–1.2	3	5	10	14	18	21	25	30
>1.	4	8	13	18	23	28	34	40

Note: The strong bed adjustments should be reduced to account for the weight of the weaker rock suspended from it as follows

Thickness of weaker rock, m	Multiply strong bed adjustment by
0–0.9	1.0
0.9–1.8	0.7
> 1.2	0.3

Table XV
Unit contacts adjustment

Number of major contacts	Adjustment
0	0
1–2	−2
3–4	−4
> 4	−5

Note: Apply only if unit contacts are significant planes of weakness (persistent, low cohension)

Table XVI
Groundwater adjustment

Condition	Adjustment
Dry	0
Damp	−2
Light drip	−4
Heavy drip	−7
Flowing	−10

ROOF RATING (CMRR)
Calculation Sheet

Mine Name _____ Date: _____
Location _____ Data collected by: _____

(1) Calculate the weighted average of the unit ratings (RR_w)

	UR		**Unit Thickness (m)**		

Unit 1 Sandstone | 63 | X | 0.3 | = | 18.9

+

Unit 2 Coal | 40 | X | 0.3 | = | 12.0

+

Unit 3 Shale | 26 | X | 0.9 | = | 23.4

+

Unit 4 | ____ | X | ____ | = | ____

RR_w

Bolted Interval (BI) (m) | 1.5 | = | 54.3 | 36.2

(2) Calculate Strong Bed Difference (SBD) Largest (UR) = 63

(SB) | 63 | − | 36.2 | RR_w | = | 26.8 | (SBD)

(RR_w) | 36.2

+

(3) Calculate the strong bed adjustment — Table 14 | 4.9

+

(4) Calculate the unit contact adjustment — Table 15 | -2

+

(5) Calculate the groundwater adjustment — Table 16 | 0

+

(6) Calculate the surcharge adjustment — Table 17 | -2

CMRR Final Rating | 37.1

Figure 14. CMRR rating for roof rated in Figure 8

Table XVII
Surcharge adjustment

Condition	Adjustment
Upper units approximately equal in strength to bolted interval Upper units significantly weaker than bolted interval	0 −2 to−5

IMMERSION TEST

Mine Name _____ Date: _____
Unit No. _____ Tested by: _____

Sample description (lithology, bedding, etc.)

Immersion		Breakability	
Observation	Rating	Observation	Rating
Appearance in water			
Clear = 0		No change = 0	
Misty = -2		Small change = -3	
Cloudy = -5		Large change = -10	
Talus formation			
None = 0			
Minor = -2			
Major = -5			
Cracking of sample			
None = 0			
Minor random = -2			
Major preferred orientation = -5			
Specimen breakdown = -15			
Total =			

Procedure for immersion test

1. *Select sample (s) ≈ hand-sized*
2. *Test for hand breakability*
3. *Rinse specimen (to remove surface dirt, dust etc.*
4. *Immerse in water for 24 hours*
5. *Observe and rate water appearance, talus formation and cracking of sample*
        Sum rating for immersion test index
6. *Re-test for hand breakability*
        Determine breakability index
7. *Use the larger negative value of the immersion test Index or the breakability index as the weatherability rating*

Figure 15. Immersion test form

Roof and sidewall stability

Introduction

In any underground situation, the two most common dangers are accumulations of dangerous gases and falls of roof. Roof stability is jeopardized by a number of different mechanisms and successful roof control can be obtained only if the mechanism is understood and identified correctly. Perhaps the major difficulty in applying successful roof control measures is to identify changes in the roof composition and to react in the correct manner.

Usually, the stress environment is not as variable as the roof composition. In a constant stress environment, roof behaviour will vary as the geology varies and different effects will be observed in different positions. The most important variables are the thickness of lithological units in the roof and the unexpected appearance of discontinuities such as slips and dykes.

In the context of this chapter, the colloquial term 'slip' will be used for all non-intrusive discontinuities and 'dyke' will be used for all igneous intrusions.

Following detailed measurements of roof movements, it was shown by Canbulat and van der Merwe (2000) that coal mine roof behaviour can be approximated by beam behaviour. This is consequently the model that was chosen for this chapter. Real roof is made up of real rock, which is known to be imperfect. However, as was shown by measurement, the difference between using the much more complex methods to determine roof behaviour and using the simplified approach used in this book, is very small. It is considered to be better to use a simple method to perform ball-park calculations than to use no method at all because it is too difficult to use.

Pre-mining state of stress

Before mining commences, the rock environment is subjected to stress. The vertical component is caused by the weight of the overlying rock and is easily calculated. The horizontal component, however, has an uncertain origin and cannot be calculated as easily. It is often expressed as a multiple of the vertical stress, referred to as the k-ratio. At depths in excess of say 1 000 m, the k-ratio has been found by measurement to be in the region of 0.5 to 1.0. At shallow depth, the ratio is much higher, ranging from around 1.0 to as high as 6.0, while in isolated areas it has been found to be as high as 12. It is usually about 2.0.

The use of the concept of the k-ratio at shallow depth is questionable and often misleading, because in general the stress magnitudes are low. Often a high k-ratio does not necessarily imply that the absolute stress levels are high enough to cause undue problems. Very often, it sounds much more dramatic than it is. It is also highly variable and does not appear to be a function of the vertical stress. However, it is so firmly embedded in everyday use that horizontal stress will probably continue to be tagged as a ratio of the vertical stress.

Consider that at a depth of 2 000 m the addition of 5 MPa horizontal stress will increase the k-ratio from 0.5 to 0.59, which is within the accepted range of a 'normal' stress regime. The same addition at a depth of 50 m will push the ratio up to more than 5. In deep-level rock engineering terms, a k-ratio of 5 sounds disastrous—at 50 m it merely means a total horizontal stress of about 6 MPa, which is still well below the compressive strength of most rock types.

Nonetheless, the horizontal component of stress at shallow depth is greater than that which can be explained by the Poisson effect (i.e. the rock under vertical compression attempts to expand laterally—because it is confined, stresses are generated). There are several theories to explain the origin of this horizontal stress.

A popular theory in the USA and Australia is that the stresses are generated by plate tectonics. Therefore, the stresses are generated by the continental plates pushing against one another. In South Africa, this theory is not widely accepted, as the coal mining region is remote from any known plate contact points.

A second theory holds that in geological time, the region was covered by more than 1 000 m of lava. At

that time, the vertical stress was much higher than today and consequently the horizontal stress was also. The overlying lava has since been eroded and the vertical stress relaxed, while the horizontal stress remained 'locked in.' The locking in mechanism has not been fully explained.

It is much more plausible that dyke intrusions generated the high horizontal stresses during the process of forcing the rock mass apart to create routes for themselves. The same can be said of faults, but this does not explain the occurrences of high horizontal stress in areas free of such discontinuities. The majority of horizontal stress effects, however, are observed in the vicinities of discontinuities, mainly dykes.

It is also possible that the earth is still shrinking as the molten mass deeper down gradually cools down. The solid crust is thus being contracted and squeezed in the process.

None of the theories is without shortcomings. The most accurate statement that can be made about the origin of the horizontal stress is that it is uncertain. In the absence of a plausible theoretical explanation of the phenomenon, mathematical predictions of the stress magnitude cannot be made and, where it is believed to be a problem, the horizontal stress should be measured.

Effects of creating a roadway on the stress environment

As stated in Chapter 1, mining does not create stresses; it merely redistributes the existing ones. Exactly how the stresses are redistributed depends on several factors, mainly the shape of the roadway and the pre-mining state of stress.

The very basic consideration is that where the roadways are created no stresses perpendicular to the skin of the roadway can exist. There is then a concentration of stresses around the edges of the roadway. All the stresses acting perpendicular to the skin are reduced to zero whereas all the ones parallel to the skin are magnified. This means that in the roof, the horizontal stress is magnified whereas the vertical stress is zero. In the ribsides, the horizontal stress becomes zero and the vertical stress is magnified. This is shown in Figure 1.

The magnitude of the amplification is not uniform around the edges. There is a higher concentration in the corners, as shown in Figure 2. In a homogeneous environment the severity of the stress concentration in the corners depends on two factors, namely the

sharpness of the corner and the orientation of the principal stresses.

The rounder the corner, the less severe the stress concentration. However, a stress concentration factor of about 5 can be accepted as the maximum for most coal mining situations. The concentration factor is a maximum (about 6) when the ratio of vertical to horizontal stress is equal to 1.0. For all other stress ratios (greater or less than 1.0) it is less than that.

It was explained in Chapter 1 that there are several components of stress. In the corner, where the difference between the stress perpendicular to the skin and the stress parallel to the skin are the greatest, the shear stress will also reach maximum levels. The magnitude of the shear stress there is half of the
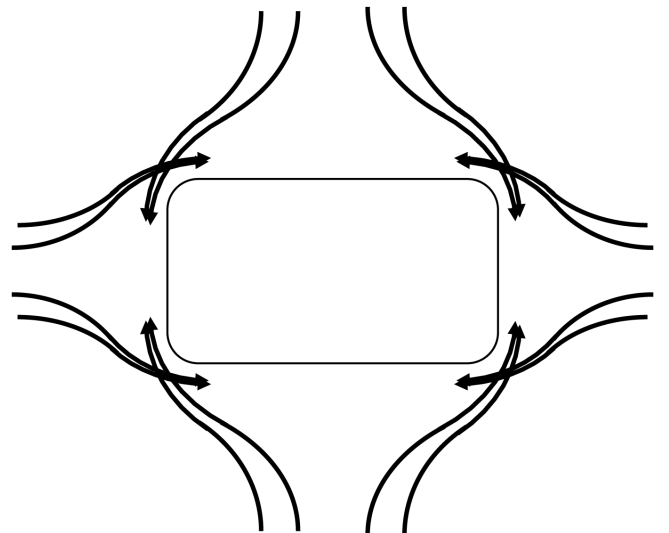

Figure 1. Vertical section through a roadway, showing that stresses are redistributed when an opening is created
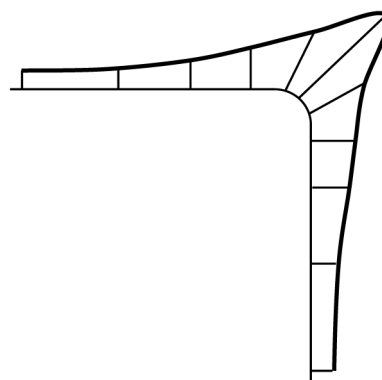

Figure 2. Detail of the corner of a roadway, showing the stress concentration. The further the dark line from the edge, the higher the induced stress at the skin of the roadway

magnitude of the normal stress.

The shear strength of most rocks is around a quarter to a tenth of their compressive strength. This means that the most likely position of stress related failure will be in the corners, and that the most likely mode of failure will be shear. This is often seen underground as guttering, like the example shown in Figure 3. Note that guttering is not necessarily an indication of high horizontal stress. There are other indications of high horizontal stress, as will be discussed later.

The next important parameter is the orientation of the principal stresses. If they are perfectly vertical and horizontal, the stress concentration 'bubble' around the roadway will be symmetrical, as shown in Figure 4. However, if they are off vertical/horizontal, a lopsidedness will be introduced into the distribution.

This means that under the conditions of a tilted stress orientation in the vertical plane, guttering is more likely to occur on one side of the roadway than the other; the side on which it occurs is an indication of the orientation of the principal stresses in the vertical plane.

The discussion so far relates only to the influence of the external stress environment on the roof and ribsides of a roadway. The roof itself is still subject to gravity.

A coal mine roof is usually laminated and can be considered as consisting of a number of plates. The plate consideration can be further simplified to that of a beam, an assumption that is valid provided the length of a roadway is more than about twice the width. The beam simplification is also a safe one because it represents the worst case.

As discussed in Chapter 1, a roof beam is subjected to horizontal tensile stresses at the centre of the roadway, at the bottom side of the beam and also at the edges of the roadway on the upper side of the beam. Horizontal compressive stresses develop in the corners at the bottom of the beam and in the centre of the beam on its upper side, as shown in Figure 5. The maximum shear stresses occur at the beam edges.

The magnitudes of the induced stresses depend primarily on the thickness of the beams (the thinner the beams, the higher the stresses) and on the road widths (the wider the roads, the higher the stresses). The road width is the most important controllable variable, as the stress increases are directly proportional to the square of the road width. The deflections are directly proportional to the fourth power of the width of the roadway. Thus, if the road width doubles, the stresses increase fourfold and the roof sag by a factor of sixteen.

Once the roof beam has started bending, the horizontal stress is magnified in the upper corner of the roadway. The magnitude of the increase is a function of the roof sag and the beam thickness. The greater the sag, and the thinner the beam, the higher the stress.

Stresses are additive. The stress experienced by the roof rocks are thus the total of the stress increase caused by the stress magnification that is due merely to the existence of the roadway and the stresses induced by the bending of the roof beam.
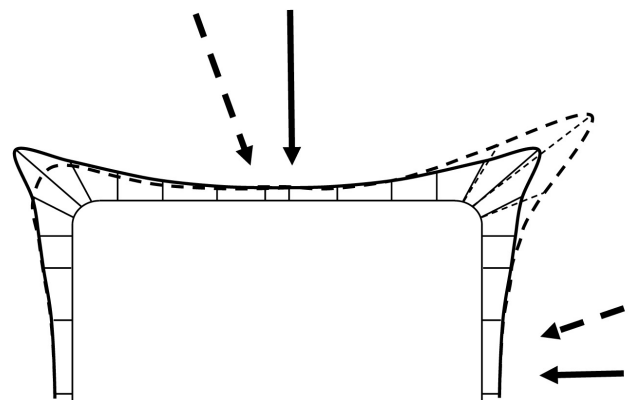

Figure 3. Illustration of mild guttering, as is sometimes seen in South Africa

Figure 4. If the principal stress orientation is off vertical, the stress concentrations in the corners of the roadway will be asymmetrical

At a depth of 100 m below surface with a horizontal stress equal to twice the vertical, the stress in the upper corners of the roof, due to the existence of the roadway, is around 25 MPa. Add to that the compressive stress caused purely by the bending of the beam—about 2 MPa for a 7 m wide roadway with a 10 cm thick roof beam—and about 15 MPa as additional stress due to the moment caused by the horizontal stress and the roof sag of say 10 mm, then the total of 47 MPa could lead to failure in the form of guttering. This example also illustrates the interaction between support and the generation of stress—if roof sag can be prevented altogether in this example, the stress generated reduces by almost half to only 25 MPa. At this stress level, guttering is unlikely to appear.

This example is given to show that guttering can appear without the existence of abnormally high horizontal stresses.

Failure modes of the roof

A coal mine roof may fail in a number of different modes. Whatever the mode, however, failure results when the forces exerted on the roof exceeds the strength of the roof rocks. There are therefore always two basic parameters that have to be examined when failure is considered: the forces and the strength of the material.

With regard to the forces in the roof, it is important to consider the overall situation and not to single out one component. As shown in the previous section, the stress situation in the roof is a complex combination of factors. Some of those factors are given, such as the
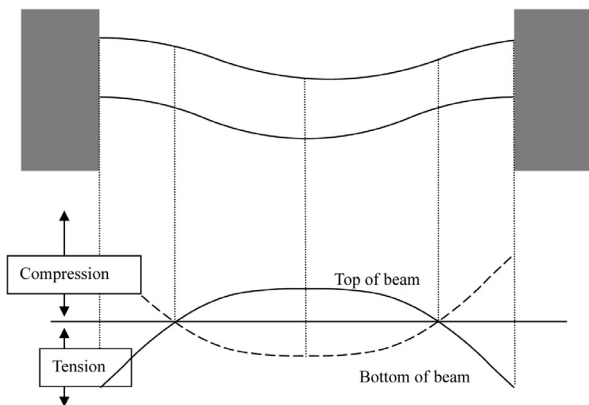
Figure 5. Induced stresses in a roof beam, due to bending of the beam. These stresses are in addition to those caused merely by the creation of an opening in the rock

pre-mining state of stress and the roof composition. Others can be controlled, such as the road width and the installation of artificial support. The direction of drivage can be controlled to some extent, although there are often constraints imposed by the shape of the mine and the positions and directions of dykes and faults.

The other half of the failure equation, the strength of the roof, is equally complex. Firstly, the rock strength is not the same for all stress situations. For instance, rock is strong in compression but significantly weaker in tension and shear, refer to the table in Chapter 1. Furthermore, being a natural material, rock is given to tremendous variation in properties. Specifically in the case of a coal mine roof, the physical thickness of the lithological units also influences the overall roof stability. In general, there is much more variation in the given geological parameters, such as the strengths and thickness of roof units, than in the stress situation.

The last observation could often lead to incorrect interpretation of the cause of roof instability. For instance, signs of horizontal stress damage may appear sporadically in the same area, which could lead to the conclusion that so-called 'stress pockets' are present. The real cause of the problem may be varying thickness or strength of the lithological units in the roof while the stress may be constant.

More information on different failure modes and how to prevent these is contained in Chapter 11: Monitoring.

Effects of discontinuities

In addition to weakening the rock structure, discontinuities change the mechanical behaviour of the rock structure making up the roof. In essence, they have the effect of amplifying the negative consequences of the situations described in the preceding paragraphs. For instance, if a joint is present in the roof strata, the beam stress concentrations mentioned previously are magnified by a factor of six. This increases the probability of roof failure considerably.

It should be no surprise then that a slip is present in the majority of roof falls. Successful roof control measures on any mine should include training on the hazards of discontinuities and methods to recognize and treat them immediately.

There are a number of proven methods to support discontinuities. One method is to install additional

bolts to intersect the plane of the discontinuities. The disadvantage of this method is that the inclination of the discontinuity has to be known—this is often very difficult to determine, as often only the bottom trace is visible. If the slip is also visible in the coal, the inclination can be measured there. The distance between the bolts and the slip must be such that the bolt intersects the slip.

Another method is to install bolts on either side of the slip, connected by short lengths of W-strap or metal strips. The bolt through the slip is a stiffer system and will permit less movement. The W-strap option is softer (will thus permit some displacement) but it has the advantage of being more successful in cases where the inclination is difficult to determine or if multiple slips are present.

Controllable parameters

The issues covered in the foregoing sections refer to the given parameters. The rock quality, state of stress, and the presence of discontinuities are given and cannot be changed. To prevent unplanned collapses, the controllable parameters have to be used in such a way as to counter the negative aspects of the given situation. The three main controllable parameters are road width, time of support installation (linked to the cutout distance), and the characteristics of the support system. They will be briefly discussed in the following sections.

Road width

The amount of roof sag is proportional to the fourth power of road width. This means that if the road width is doubled, the amount of sag will increase sixteen times.

It is well known that decreasing the road width is the first step to be taken when bad roof is encountered, and this explains why. It also explains why road width control is essential in high extraction mining, why intersections are prone to roof falls, and why uncontrolled cutting away of the corners at intersections is dangerous.

In an intersection, the diagonal distance is 1.4 times the road width. This means that the roof sag is potentially 3.8 times as great. If only one metre is cut off one corner of a pillar, the 3.8 factor increases to 5.8. To make matters worse, if a holing is made into an unsupported intersection, the increase in width is a sudden event and the roof experiences the sudden

increase in sag as a shock. It is like the difference between slowly squeezing a lump of rock in a vice grip and hitting it with a hammer. The result is shattering.

Road width control is vital for another very important reason. In several situations the supports that are installed are intended only to suspend the weak material underneath the more competent layers above (like sandstone), and not to support the main sandstone beam itself. In the absence of special supports like long anchors, the stability of the sandstone beam is controlled by one parameter, and one only, and that is road width.

On several mines, road widths are controlled by reporting average road widths on a monthly basis. While this is better than no control at all, it is far from ideal. The problem is that the average figure hides the small percentage of areas that are cut too wide. The average may be within the prescribed limit on a mine, creating the false impression that all is well.

In most cases, the majority of the exposed roof area is surprisingly stable. The secret of a successful support strategy is to prevent the unstable minority from falling. There are statistical procedures to describe the distribution of road widths, but perhaps the most practical way of concentrating on the outliers is to report road widths by means of a histogram, like the example shown in Figure 6. The diagram was created with the aid of a readily available spreadsheet program.

Time

As yet, the effects of time on roof behaviour cannot be quantified mathematically. From limited work done in laminated shale/sandstone type roofs and thick mudstone units, it appears that the majority of the deflections occur soon after the roof has been exposed and that roof behaviour is controlled to a larger extent by face advance than by time.

From the stage that the face advance away from the last line of bolts is equal to the road width, the rate of deflection decreases rapidly with further advance. This means that especially in adverse conditions, bolts should be installed very close to the face if they are to have the maximum effect. Note that this means that if it is necessary to increase the cutout distance, it can be done by limiting the road width, provided that the ventilation requirements are met.

If a particular road is left unsupported for any length of time, further deflection will continue, albeit at a

reduced rate. The more time goes by, the more the roof bends, and the bigger the hidden micro cracks grow. The bigger they become, the more air and moisture will seep in, draining the rock's strength, causing it to bend even more, etc. It is a vicious circle.

It gets to the stage where it is too late to support. The cracks are there, just waiting for the slightest disturbance. What is the trigger? Sometimes the late installation of support is the disturbing force. If the roof survives that, the second possible trigger is the disturbance caused by high extraction mining.

Sometimes the causes of roof falls in stooping cannot be established. Maybe there are no joints, no slips, and the bolts are well installed—yet there was a fall. Often what is called a 'danger inherent to mining' is a man-made danger, created months ago by not having installed support soon enough during development.

Roof support is not a separate operation in mining. It is an integral part of the act of mining. If the roofbolter breaks down, mining should cease. An excavation that cannot be supported must not be made. This should be borne in mind at the end of the shift, and before weekends.

The term 'soon enough' in the context of roof support, cannot easily be quantified. It depends on the material in the roof. Some roofs, like the weak mudstone in the Vaal Basin's No. 3 Seam, should be supported within no more than, say, two hours after exposure. In other cases, where the roof is, for instance, a strong sandstone, this period can be stretched to, say, half a shift.

Apart from the physical effects of not supporting a roof quickly, there is the consideration that the longer an exposed roof is left unsupported, the greater the probability that someone will be underneath it before it can be supported. If it has to be supported, it is as well to do it as quickly as possible.

Distribution of Road Widths

Figure 6. Distribution of road widths, indicating the 'problem zone' that will be hidden if only the average road width is reported

Support provision

The support provision loop begins with the identification of the most likely mechanism of roof falls in any area. The second step is to design a suitable support system, taking cognisance of the geological and stress conditions, the equipment that is available to install the supports, the support materials that are available and the level of training of the workforce. If any new element is to be introduced into the chain, it has to be accompanied by proper training.

The design procedures are covered in detail in Appendix B. However, it is pertinent to mention the basic design procedure at this stage. The first step is to determine the load on the system, including gravity and, if present, the effects of higher than normal horizontal stress. Next, the system has to be able to withstand the imposed loads. This is achieved by balancing the length, diameter, and the spacing of the tendons.

It is important to first fix the spacing of the tendons, and then the lengths. The reason for this is that a load calculation on its own may result in a system that is able to withstand the loads imposed on it from a force balance point of view, but it will not necessarily create a stable beam. Neither will it be able to prevent the small but potentially lethal falls between bolts.

In cases where high horizontal stress is the cause of roof instability, or where an artificial beam is to be created, it is essential to concentrate on the stiffness of the support system. The design procedure for this is also dealt with in Appendix B.

The third step is to install the supports. It is vital that a proper procedure for this be laid down and that the necessary discipline is maintained.

The fourth step is monitoring, which consists of four main elements. The applicability of the system as designed must be monitored on an ongoing basis, which includes taking cognisance of changes in the geological conditions. The quality of the installations has to be monitored daily—this is an important function of supervisors. The quality of the support materials has to be checked to ensure that it conforms to the requirements of the designed system. Lastly, the integrity of the support over time has to be checked, bearing in mind that steel corrodes. The monitoring issues are discussed in more detail in Chapter 11: Monitoring.
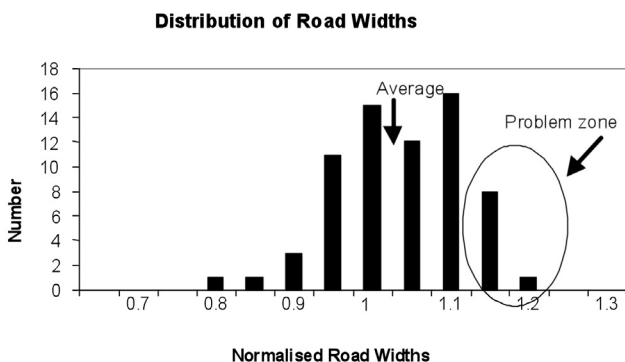
ROCK ENGINEERING FOR UNDERGROUND COAL MINING

Leaving coal in the roof

The beneficial effects of leaving a layer of coal in the roof for roof stability is well known. Why does it work?

Reference to Table 1 in Chapter 1 will show that coal is substantially weaker in compression than the rock types commonly found in the roof. As explained earlier in this chapter, compressive strength is not a good indicator of likely roof stability because the roof does not fail in compression. Yet, even in tension and shear, coal is no stronger than, for instance, shale or mudstone.

There are two reasons why coal in the roof has a stabilizing effect. Firstly, it acts as a seal against weathering. Secondly, provided it is not itself jointed, it provides a continuous beam underneath a jointed rock mass. If the overlying rock mass is jointed, the strength of the material is of little consequence as failure is dominated by the joints. The principle is explained in Figure 7, showing the effect of a timber lintel on the stability of bricks over a door opening in a brick wall. The timber is weaker than the bricks, yet it prevents the bricks—which can be likened to a jointed roof rock mass—from collapsing, because it is continuous.

Figure 8 demonstrates another very important principle of roof support. The photograph is of the same building as the one in Figure 7, but now with a concrete lintel across the roof opening. The concrete is stiffer than the timber and it has an obvious limiting effect on the displacement of the overlying bricks.

Different support systems

Requirements

Previously, the main consideration when comparing different support systems was whether the support was 'active' or 'passive'. Active support is installed with pre-tension, whereas passive support generates reaction only once the rock mass starts moving.

Recently, the concept of stiffness has received more attention. Stiff support limits rock movement to the absolute minimum (technically, it has a high modulus, deforming very little when loads are applied to it), while soft support allows movement to take place, although the system does not fail immediately. Stiff systems also supply constraint to rock expansion and shearing due to high horizontal stress.

In deep level mining, where the forces in the rock are in the practical sense irresistible, yielding support is required. In the majority of coal mining environments where the stresses are relatively low, the dangerous damage is done when roof layers are allowed to move. To prevent movement, stiff support is required.

In addition to restricting movement, the support tendons also have to be strong enough to suspend the roof layers. Therefore the steel has to have a certain minimum strength and the anchor portion must meet certain minimum requirements. Exactly how strong these elements should be is variable, depending on the thickness of the roof to be suspended, spacing of tendons, etc.

Very often, where friable roof such as mudstone exists, area cover becomes an important issue. This can be supplied by wiremesh, headboards, W-straps, etc.

Figure 7. Stabilising effect of a timber lintel on bricks across a door opening

Figure 8 Enhanced stabilizing effect of a concrete lintel on bricks across a door opening

Characteristics of commonly used systems

Successful support requires that the right system be used for the existing conditions. Therefore, some knowledge of the characteristics of the commonly available systems is necessary. Coal mine roofs in South Africa vary considerably, and there is no single 'best' system. The best system is the one that performs to requirements in any given situation.

Mechanical anchors

A mechanical anchor consists of a steel tendon with an expandable shell that is inserted into the hole. When the bolt is rotated, the shell expands. Once the shell is fully expanded, the bolt is tensioned either by tightening a nut against the washer at the free end, or by further rotation of the bolt in the case of fixed head bolts.

Because of the long free length of the steel tendon, mechanical anchor bolts can stretch when load is applied. It is therefore soft support, even though it is active by virtue of its pre-tension. In most coal mine roof types, the anchors start slipping at anything between 30 and 70 kN.

They are relatively cheap, and easy and quick to install. However, frittering of the roof underneath the washer, slippage of the anchor or even vibrations cause them to lose pre-tension quickly. On certain mines, corrosion is also a problem.

Mechanical anchors are ideal for short-term purposes where speed is important, such as during stooping or even short bord and pillar panels. They are also suitable for suspending massive (unlaminated) roof layers.

Mechanical anchors should be avoided in long-term applications such as main development, wet areas and thick, weak roof situations where beams have to be created.

Point anchor resin

Resin installations are discussed in more detail later in this chapter. In principle, however, the same remarks as for mechanical anchors apply. The only difference between mechanical anchors and resin point anchors is that the expandable shell of the former is replaced by a resin anchor. It is also soft active support, the same as a mechanical anchor.

Resin point anchors require more time and care to install than mechanicals. The only real advantage is that the anchor resistance can be increased by making

the anchor longer. A second advantage is that the changeover to full-column resin support, should it be required by changing conditions, is less troublesome because operators will already be trained in resin installations.

Resin should be avoided in friable or burnt coal ribsides because the unstable holes make resin mixing difficult.

Full-column resin

Because the steel is friction bound to the rock over its entire length, full-column installations allow very little displacement to take place once they are installed and are therefore stiff. Furthermore, they fill the entire volume of the hole and thereby restrict lateral movement between different layers. The significance of this fact is explained in Appendix B.

If resin of uniform speed is used in the entire hole, the tensioning effect is restricted to the very bottom layers where the resin bonding is often less than perfect, and the support is therefore passive. However, if a fast anchor portion is used in combination with a slower setting column filler (the dual resin system), tensioning is done before the slow set resin gels and the result is stiff active support.

Full-column resin support is relatively expensive and requires care to install properly—operators have to be well trained.

Full-column installations can be used almost anywhere. They are ideal for any long-term requirement such as main development, underground workshops, etc, and are essential in beam building situations (e.g. thick, weak roof). They are also ideal for the support of laminated roofs. The passive nature of single resin type installations can be overcome by installing bolts close to the face, before layer separation occurs.

In burnt coal or very friable ribsides the resin mixing operation is often suspect because the holes tend to fritter inside, and therefore resin should be avoided in favour of split sets.

Split sets

A split set is a hollow tube with a slit along its entire length. It is forced into a hole with a slightly smaller diameter than the tube itself. Like a full-column resin installation, it is friction bonded to the entire length of the hole and can be classified as 'stiffish'. Because it cannot be tensioned, it is passive.

Note, however, that under normal conditions the

frictional resistance of a split set is significantly lower than that of resin. While it offers some resistance to lateral displacement between layers, the tube is collapsible and thus the lateral resistance is also lower than in the case of full-column resin.

Split sets are quick and easy to install (provided compressed air and jackhammers are available) but are expensive. Because of their large surface contact area, they corrode quickly. They should be avoided in long-term excavations and the support of massive roofs. In split set applications, control over hole diameters is crucial.

However, they are the ideal ribside support for burnt coal and, for instance, to mould wiremesh to hollows in roofs and ribsides prior to shotcreting. For the latter application, they must be used in conjunction with stronger tendons. They may also be used as short-term support for thinly laminated roofs underneath stronger beams.

Roof trusses and cable trusses

A cable truss is a variation of the older steel roof truss, shown in Figure 9. The steel roof truss consists of grouted anchor elements installed at 45° in the corners of roadways. These are connected by lateral bars, which are tensioned. In a cable truss, the round bar steel of the steel roof truss is replaced by cable.

Because of the lateral tension, trusses provide clamping forces across joint surfaces in the roof (although the magnitudes of the forces are questionable). The anchor elements play an important role in the operation of a roof truss, as they traverse the area of maximum lateral displacement between roof layers. A further benefit of trusses is that they form a basket in which to contain roof rocks, and that they are anchored over the ribsides, thus outside the potential failure area.

Trusses are excellent supports across major joints, and as regional support in highly jointed areas. They have to be installed across joints, not parallel to them. They are of little use in spanning across hollows where the roof has already collapsed, except perhaps to create a basket to contain, rather than prevent, further roof falls. Where trusses span across hollows, it is common practice to fill the gap between the truss and the roof with timber, empty drums, etc. Note that timber can seldom be regarded as good long-term support, because of its tendency to decay.
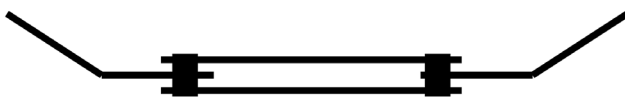
W-straps

W-straps, schematically shown in Figure 10, are steel plates with a 30 cm width and any length with an elongated 'w' cross-section. They are provided with holes to fit over roofbolts, and are bolted to the roof.

In very friable or highly jointed ground, W-straps provide essential area cover. Where roof beams are to be created, they perform a vital function by increasing the stiffness of the whole system and by providing artificial tensile strength to the roof. Woven and weaker weld mesh straps can also be used. They are more blast resistant and allow bolts to be placed more easily. Rod straps are superior to both W-straps and weld mesh straps.

Wiremesh and shotcrete

Wiremesh and shotcrete are predominantly used in very weak, friable conditions like burnt coal or in densely populated long-term excavations like shaft stations and underground workshops.

The mesh serves as areal cover, and, as such, it needs tensile strength. The mesh strands should be 4–6 mm thick and the squares should be at least 75 mm wide if shotcrete is to be applied. The mesh should be firmly anchored by means of, say 1.8 m cement grouted rebar, supplemented by split sets or shotcrete pins to mould it into the hollows, so that it is flush with the rock surface. Fibre can be added to the shotcrete to serve the same function as wiremesh.

The shotcrete isolates the rock from the atmosphere and protects the mesh against corrosion. Its other vital function is to strengthen the skin of the rock mass, not as much by its own strength as by penetrating into cracks and thereby inhibiting sliding of the blocks.

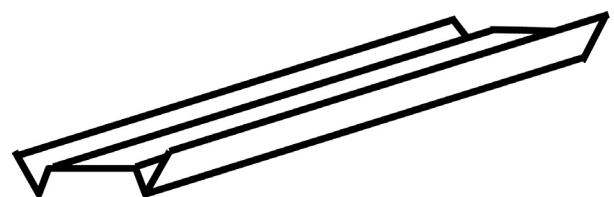It is essential to spray the shotcrete on the rock

Figure 9. Simplified diagram of a roof truss

Figure 10. Schematic diagram of a W-strap

surface, which requires the mesh to be flush with the rock and to have sufficiently large openings in order not to clog up during the spraying operation. Care must also be taken to get as much of the shotcrete as possible into cracks in the rock. For most applications, a thickness of 50 to 75 mm is sufficient.

As an alternative to wiremeshing in conjunction with shotcrete, different types of fibres can be added to the shotcrete. Steel and several synthetic fibres have been used.

Steel sets and arches

Steel sets and arches are very rarely used in South African coal mining, and then mainly in extremely poor conditions such as in badly burnt coal around dykes or through fault zones. They are also sometimes used to resupport major fall areas, in which case some form of cavity filler such as expanding light weight cements or even empty drums are often used. Steel sets and arches are expensive and time consuming to install.

Wooden or fibre glass dowels

Timber or fibreglass dowels are often used as ribside support where steel is not suitable, for instance in longwalls or where stooping is contemplated. They are grouted into holes with either pumpable, or cartridge cementituous grouts. Dowels are very effective to prevent longwall face deterioration in cases where the face has to stand for extended periods.

Chemical injection

The practice of injecting chemical binders into the rock is not common in South Africa, although notable successes have been achieved on the few occasions where it was applied. The method is to drill holes into the rock and then to install packers to prevent the material flowing out of the hole. The grout is then pumped into the rock behind the packer. Silica based grouts and polyurethane have been used successfully, the latter having the advantage of developing its own internal pressure and forcing itself into very fine cracks.

The usual practice is to first consolidate the skin of the rock mass by pumping into short holes, say 5 m long. This is a low-pressure operation to prevent forcing rock into the excavation. Pumping continues until the material starts oozing out of cracks in the rock. Once the skin has been consolidated, longer holes are drilled and injection is done deeper.

This technique has been very successfully employed in rescuing longwalls after major face breaks. The sooner it is done, the better it performs. It is an expensive method, but the cost of the material should be weighed up against the advantage of starting the face-up sooner.

Polyurethane is prohibited in South Africa and other countries as a surface spray. In South Africa, it has been approved as an injection material, but mines are reluctant to use it due to the toxic fumes resulting from it in case of a fire.

System selection

As a very general guide, the foregoing discussion is summarized in the two tables to follow. Table I
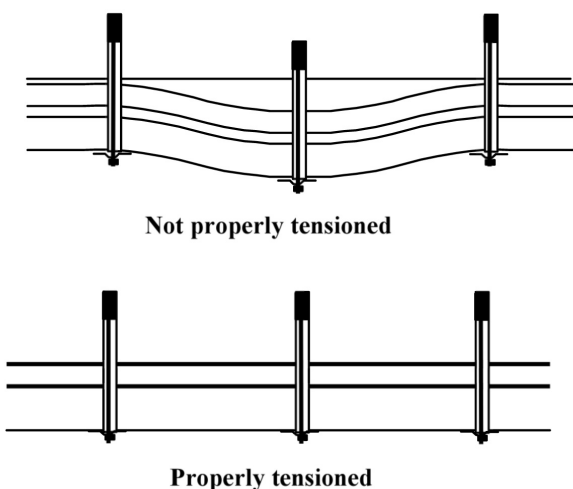
Figure 11. Point anchor installations, whether resin point anchor or mechanical, have to be tensioned to be effective
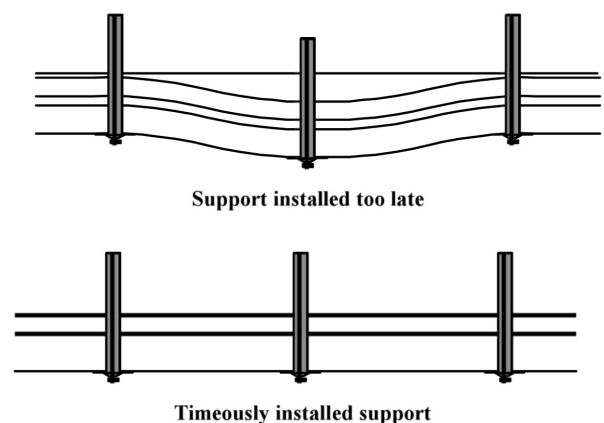

Figure 12. Full column resin support that is installed too late is as inefficient as untensioned point anchors

summarizes the characteristics of the different support systems and indicates their main areas of applicability. Table II lists some of the more commonly encountered ground conditions, and indicates which support systems are best suited to them.

Resin bolt support systems

The emphasis in this chapter is on resin bolt systems, being by far the most popular system employed on South African coal mines. Brief mention will be made of other systems as well.

No man-made support can ever correct the force redistribution caused by mining. At the very best, one can control the disturbance to the extent that damage is prevented. Support merely delays the inevitable. Given enough time, the roof will collapse, but the better it is supported the longer it will last.

There is no single correct formula for roof support. It has to be site specific: the effects of the stress changes are governed by the rock characteristics, and a successful support system must consider this. This section will therefore concentrate on the essential common principles, leaving specific designs to the specialists.

A simple roofbolt performs several functions, depending on whether it is a mechanical anchor, resin point anchor, or full column resin anchor.

A mechanical anchor and resin point anchor suspend weak rock onto stronger rock, provided that the anchor is situated in the stronger rock. If properly pre-tensioned, it pulls laminated layers together, thereby increasing the friction between them and so restricting movement—see Figure 11. The latter effect is valid only for as long as the pre-tension remains which in a mechanical or resin point anchor is not very long.

A full-column resin anchor also serves the suspension function and it restricts movement between layers, but by a different method. It fills the hole with steel and resin, and so prevents movement—see Figure 12. It is less dependent on pre-tension, but there are two 'ifs' attached.

Firstly, if the support is installed too late, layer separation will already have occurred and the effort is largely wasted. Secondly, the mouth of the hole seldom, if ever, has properly mixed resin because the mouth often fritters and is reamed during the drilling process. To cater for the bottom layers (the most dangerous ones) it is thus important for full-column resin installations to be pre-tensioned.

An excellent system is the dual full-column resin. A single fast capsule is installed in the top of the hole, followed by slow capsules. The resin is mixed and tensioned as soon as the fast capsule has gelled, and before the slow capsules start gelling. The end result is a properly pre-tensioned full column installation, with the pre-tension locked in.

The main benefit of full-column resin systems over the other systems is the fact that they are significantly stiffer. However, as stated, there are a number of important prerequisites that have to be met in order to realize this benefit.

Positions of bolts

In a laminated roof, the laminations can bend only if they are free to slide over one another. If the sliding can be stopped, the bending will be inhibited. The greatest amount of sliding takes place, not in the centre, but at the edges of the roadway—see Figure 13. Therefore, the most valuable bolts are the ones at the edges of the roadways, not the centre.

Of course, the centre bolts are also necessary. The reason is that the laminations, especially the thin ones, will still bend between the bolts. If the bolt spacing is too wide, this can result in failure of the roof between bolts.

What happens between laminations in a laminated roof, happens inside the weak material in a weak, less obviously laminated roof. Hence, the side bolts are also critical under those conditions.

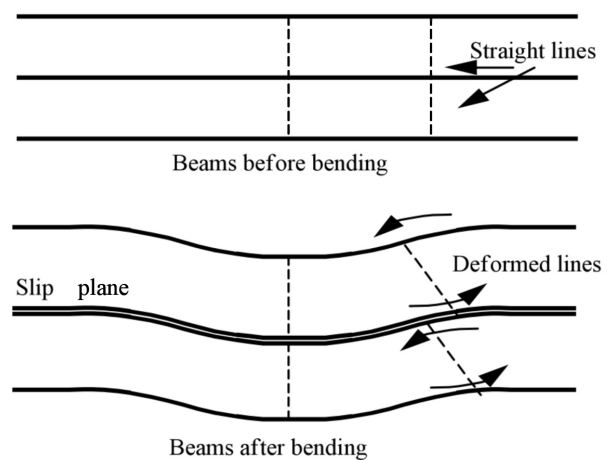It is important for side bolts to be installed first.

Figure 13. Horizontal displacements in the roof caused by bending of the beams. Note that the maximum horizontal displacement occurs at the edges of the beams, not at the centre. Preventing the horizontal slip will prevent bending of the beams

Table I
Summary of support element characteristics

System	Active/ passive	Stiff/ soft	Corrosion resistance	Ease of installation	Pull-out resistance	Where to use	Where to avoid	Relative cost
Mechanical anchors	Active	Soft	Medium	Good	Medium	Short term Unlaminated roof Medium to light load	Long term Laminated roof Burnt coal ribside	Cheap
Resin point anchor	Active	Soft	Medium	Medium, requires training	Very good	Short term Unlaminated roof Medium to heavy load	Long term Laminated roof Burnt coal ribside	Cheap
Full column resin (single resin type)	Passive	Stiff	Good	Medium, requires training	Very good	Long term Laminated roof Heavy load Thick weak roof Close to face	Burnt coal ribside	Expensive
Full column resin (slow/fast combination)	Active	Stiff	Good	Medium, requires training	Very good	Long term Laminated roof Heavy load Beam building Thick weak roof High horizontal stress	Burnt coal ribside	Expensive
Split set	Passive	Stiffish	Poor	Good	Poor	Burnt coal ribsides Wiremesh fill-in Thin laminated layers Short term Light load	Long term Heavy load Thick layers	Expensive
Trusses	Active	Stiffish (cable trusses soft)	Good	Cumbersome	Very good	Jointed areas Major joints, faults	- - -	Very Expensive
W-straps	- - -	Stiff	Medium	Cumbersome	- - -	Jointed areas Friable roof Beam building High horizontal stress	- - -	Expensive
Wooden dowels	Passive	Stiff but weak	Excellent	Easy	Poor	Longwall faces ribsides in stooping	Roof	Cheap
Fibreglass dowels	Passive	Stiff	Excellent	Easy	Good	Longwall faces ribsides in stooping	- - -	Expensive
Wiremesh and shotcrete	Passive	Stiff if well installed	Good	Cumbersome	- - -	Burnt coal Jointed areas Friable roof Long term, densely populated areas	- - -	Expensive
Chemical injection	Passive	Stiff	Excellent	Cumbersome	- - -	Longwall face break Pre-support in very weak, jointed conditions	- - -	Very expensive

Length of bolts

Suspension function

Roof support by suspension is done in the case where the roof consists of a layer of weak, or laminated, material overlain by a self-supporting layer such as a thick sandstone. The roof is then stabilized by suspending the weak material onto the stronger layer.

It is important to realize that in this case, the bolts do nothing to support the strong beam. The stability of the stronger beam is governed only by the road width. The bolts merely suspend the weaker layers underneath it, as shown in Figure 14.
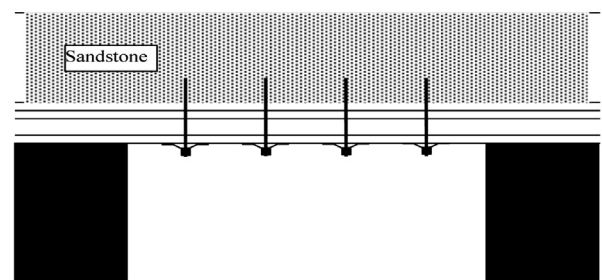
Figure 14. The laminated material underneath the sandstone is suspended onto the self-supporting beam

Table II
Support system suitability chart

Roof description	Suitability rating		
	Good	Medium	Poor
Sandstone, occasional false roof	Mechanical Resin point anchor	Split set	Full-column resin bolts (cost)
Sandstone underlain by thin layer of laminated material	Short full-column resin bolts	Resin point anchor Split set (short term)	Mechanical
Thick layer of laminated material	Full-column resin bolts (slow/fast combination) Angled bolts	Resin point anchor Full-column resin bolts (single resin type)	Split set Mechanical anchor
Thick layer of weak material	Full-column resin bolts (slow/fast combination) Angled bolts Trusses	Full-column resin bolts (single resin type)	Resin point anchor Mechanical split sets
High horizontal stress	Full-column resin W-straps Long anchors	Resin point anchor	Mechanical anchor
Burnt coal ribsides	Split sets Wiremesh and shotcrete	Dowels	Any resin anchor Mechanical

With resin bolts, the longer the resin portion in the hole, the stronger the anchor. The bolt length must thus be greater than the thickness of the laminations, with enough left over to have a strong enough anchor to suspend the laminations, see Figure 15.

The required strength of the anchor depends on the spacing of the bolts and the thickness of the laminated layer. Therefore, the thicker the laminated layer and the greater the spacing, the longer the bolts must be.

Beam building

For the beam building function, the bolts must be longer than the thickness of the beam to be created.
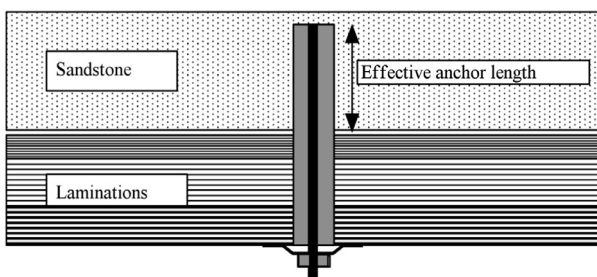
**Figure 15. In suspension-type roof support, the effective length of a resin anchor is the portion of the bolt in the strong roof layer, sandstone in this case. The longer the effective anchor, the more weight the bolt can suspend.
In these illustrations, the term 'sandstone' refers to any strong roof unit**

This thickness depends on road width, horizontal stress, etc.

The basic philosophy in this case is that the bolts are used to create a stable beam by preventing lateral sliding of the laminae. This can be achieved only if the bolts are installed before any bed separation occurs. Obviously, full- column resin is required for this function. In theory, the same can be achieved by installing pre-tensioned mechanical or resin point anchors, but because these lose tension, the beam building function is lost very soon.

The calculations to determine the optimum spacing and bolt length are done by specialists using the procedures described in Appendix B. What is important here is the adherence to those parameters, which are linked. Stretching the bolt spacing has two serious consequences: firstly, the laminations between the bolts can sag and then break, and secondly, the anchor may be overloaded and then fail.

Installation of a normal resin anchor

There are several serious misconceptions about resin installations, which could all lead to failures of the system. In order to motivate the correct procedures, it is important to understand how a resin bolt works. The system is made up of three elements, namely the resin, the bolt and the hole.

Resin

A resin capsule consists of two parts, namely the resin (which is usually coloured black) and the catalyst (which is usually white or light grey). They are separated by a membrane in the capsule—see Figure 16.

After the hole has been drilled, the resin capsules are inserted into the hole. Then the resin bar is pushed home and spun.

During this phase, the membrane separating the resin from the catalyst is broken and the two components are mixed. They have to be properly mixed, and thus it is important to adhere to the stipulated mixing time. For a fast resin, this is usually 5 to10 seconds.

What follows next is the so-called holding time, which is the crucial phase in resin installation. Due to the catalyst, heat is generated and consequently the short molecules in the resin start joining up to form long chains. The bonding process is driven by heat. In the beginning, these chains are weak and easily broken. If broken during this phase, they cannot recover and the resin will not develop to full strength.

It is therefore of the utmost importance not to disturb the bolt during the holding time. For a fast resin, this period is 10 to 30 seconds long. Once the holding time is over, the bolt is tensioned and the installation is complete.

There are a number of important points about the resin itself. Firstly, the holding time depends not only on the type of resin being used, but also on the temperature. The colder it is, the longer the holding time, and vice versa.

Never store resin capsules on the motor of the roofbolter. They will heat up, and the resin will start gelling before its time. In winter, resin should not be stored outside and then used immediately. When the temperature drops below 4°C, the resin will be unstable for up to 24 hours. Sections, which work close to the shaft, should increase the holding time in winter, to compensate for the lower temperatures.

Never use old resin. Check the expiry date on the box, and if it is old, have it replaced.

Check the resin from time to time. Cut open a capsule, squeeze out about a third of the contents, mix it by hand and then prod it lightly to feel when it gels. This is a simple but effective test.

Spin-to-stall installation

A recent tendency on certain mines is to spin the resin through the curing phase until the crimp arrangement on the nut fails and the nut is tightened, thus not allowing a waiting period. In this case, a very fast resin is used. In this application, the resin bond is weakened, but there still is sufficient frictional resistance to afford efficient support. Note that this type of application may require a denser support spacing to compensate for the weakened bonds. The spin-to-stall application should be approached with great caution and should be implemented only following a comprehensive test programme.

This is a new development that has the potential to overcome several common bolt installation problems. However, in the light of the importance of effective roof support, more work is required on this method and the resins that are used before it can be commonly used.

The bolt

There are a number of different types of bolts available. They all consist of a body, a threaded portion, a nut and a washer.

The body

The body must be rough, such as rebar. The reason for the roughness is to mix the resin properly and to prevent the bolt pulling out of the resin. There are several different types of bolts available, all with different designs to mix the resin more efficiently. Some have slightly oval bodies to enhance mixing; others have patterns that are designed especially to push the resin back into the hole during mixing. The best bolt for any given situation should be found by underground testing. It is preferable to crop the end of the bar to ensure that it pierces the resin capsules.
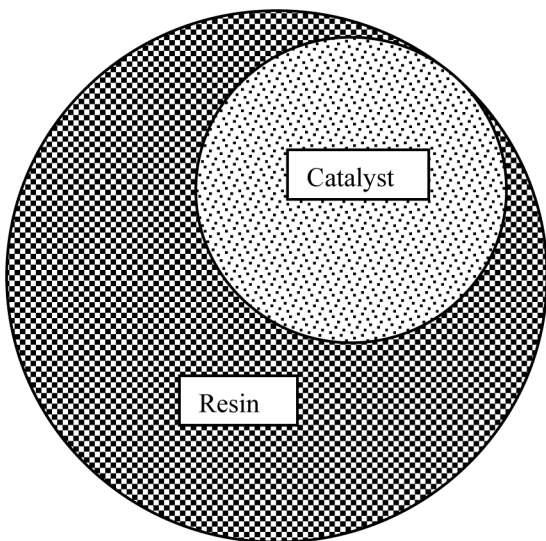
Figure 16. Cross-section through a resin capsule. The bulk of the resin portion is actually an inert filler
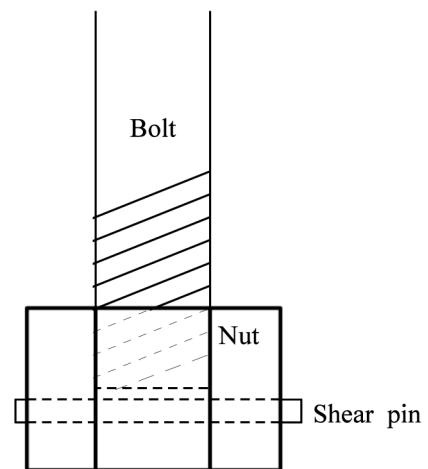

Figure 17. The shear pin nut

The thread

The thread must be smooth and regular, so as not to inhibit movement of the nut. In general, rolled threads are preferred to cut threads, as they are more consistent and smoother. The roughness is usually peeled off and the thread is then rolled onto the smoothed portion of the bolt. An uneven thread can interfere with the nut's action during mixing, resulting in over or under mixing of the resin.

The nut

The nut is usually either a crimp nut or a shear pin nut. The crimp nut has a deformed thread that breaks at a predetermined torque. The shear pin nut has a small hole drilled through it, into which a steel pin is inserted—see Figure 17. The steel pin also breaks at a predetermined torque.

The way in which the system operates is that the crimp or shear pin is strong enough to allow resin mixing because when the nut is rotated, the whole bolt rotates inside the hole. Once the resin has set, the nut is again rotated. By this time, there is much more resistance to rotation of the steel. The crimp or shear pin breaks, the nut moves up the thread and the bolt is tensioned.

In practice, problems are often encountered with the nuts. The crimp or shear pin may be either too strong or too weak. If it is too strong, it breaks the bolt or damages the thread during tensioning. If too weak, the

nut will start moving up the thread during the mixing phase and the resin will not be properly mixed. Figure 18 shows a problem that has been encountered with shear pins, where the remainder of the pin after failure was caught between the nut and the bolt.

A system, which overcomes these problems, is the nib bolt, a system that originated in France in the 1970s. The nut is screwed onto the bolt, and then the thread on the bolt is nibbed behind the nut—see Figure 19. For mixing, the bolt is rotated anticlockwise. The nut moves down the thread and rotates the bolt when it locks against the nib. Tensioning is done clockwise, and the nut moves up the thread without restriction.

To implement this system, it may be necessary to adapt the roofbolter for bidirectional rotation. In most cases, this merely requires unblocking the anticlockwise hydraulic circuit. It is also sometimes necessary to prevent the chuck of the roofbolter unscrewing itself during the anti-clockwise rotation. Wherever nib bolts have been implemented, dramatic improvements in support installation quality has been seen.

The crimp should fail at about 50 to 70 Nm torque. Full-column installations (with a single resin type) should be torqued to about 150 Nm and point anchor installations and dual resin full column systems at 210–250 Nm.

The washer

The washer is either dome shaped or ribbed. Its function is to clamp the lower laminations onto the roof. If the roof continually breaks right next to the
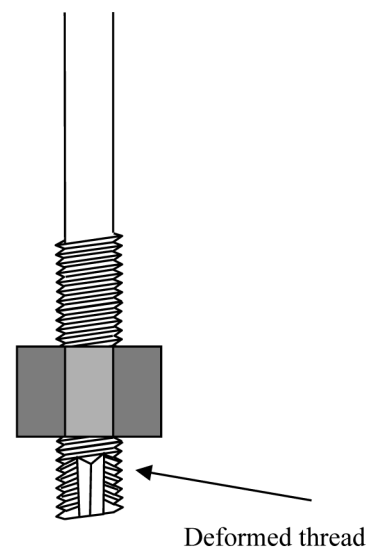

Figure 18. The remainder of the shear pin can be seen between the nut that has been cut away and the bolt. Note how the thread has been destroyed. This problem has three negative consequences: firstly, the bolt could not be properly tensioned; secondly, the excessive torque caused micro fractures in the steel body of the bolt; and thirdly, the thread/nut contact distance is greatly reduced

Deformed thread

Figure 19. The 'nib bolt'

washer or the washer pulls into the roof, it indicates that the stress that the washer exerts on the roof is too high. Rather solve the problem by using a bigger washer than decreasing the tension on the bolt, which should be about 50 kN. In heavily jointed roof, wiremesh or headboards usually perform better than bigger washers do, due to the greater areal coverage.

Under adverse roof conditions, or where bolts are inclined, it is important to use domed washers with spherical seat nuts. This ensures load application along the true direction of the bolt and avoids damage to the bolt due to bending.

The hole

The hole is very often overlooked as being part of the support system, yet it can be the cause of system failures.

The hole has to be of the right length. If it is too short, the anchor in the sandstone will be too short and thus not strong enough. If it is too long, some of the resin will be pushed into the back of the hole and be wasted. Worse than that, there is now less resin available as anchor and consequently the anchor will, again, be too weak. The loss of anchor length is about double the amount of overdrill—see Figure 20.
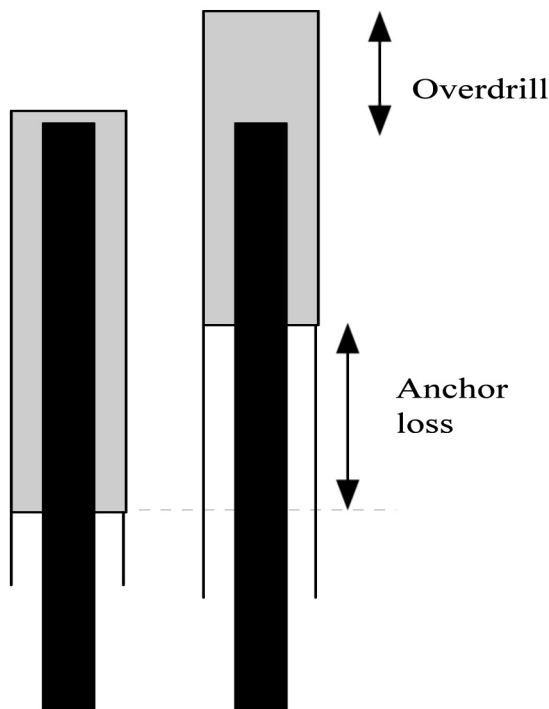
Figure 20. The anchor loss due to overdrill is often about twice the length of overdrill

The same happens when the wrong drill bits are used and the hole is too wide. Because there is now more volume between the steel and the rock, the anchor length will be shorter. If the hole is too narrow, there will be areas in the hole where there is no resin between the steel and the rock. Tests have shown that the ideal is for the hole diameter to be 6 to 8 mm greater than the steel diameter for granular resins and 3 to 6 mm for smoother resins.

The size of the annulus is of prime importance for the prevention of sliding of the roof layers. It the bolt installation is done correctly, the first defence against sliding is the resin's resistance to compression. The thicker the body of the resin, i.e. the greater the annulus, the more the resin can compress. To get a feel for exactly how critical this issue is, consider the following example:

A 0.25 m thick sandstone layer in the roof of a 7 m wide roadway can deflect about 4 mm at its centre before it fails. With that magnitude of deflection, the amount of horizontal sliding is less than 1.3 mm. Thus, to prevent failure of the roof beam, the amount of sliding that has to be prevented by the bolt installation is less than 1.3 mm. This example emphasizes the importance of using as stiff a system as possible in adverse roof conditions, especially in high horizontal stress conditions.

Cable anchors

Long cable anchor supports are becoming increasingly popular in South African coal mines. In contrast to resins, there are no recognized, industry wide, standards for the quality of materials or installation methods. There is no practically usable tool to determine the quality of grouting.

The recommended installation procedure is to install the bolts with a point anchor (which can be resin or a spring triggered mechanical anchor) and then to pre-tension to 50% of the breaking load of the tendon. Cement grout is then pumped into the annulus through a short tube. When cement comes out of the breather tube, which goes right to the back of the hole, the hole is filled.

In general, the mechanical anchor is preferred to the theoretically superior resin anchor. In practice, proper resin mixing is seldom achieved for a number of reasons. One reason is the flexibility of the cable, another the wider holes—one often finds contractors using the mine's standard resin capsules suitable for use in 25 mm or 28 mm holes in 32 mm or 35 mm

cable anchor holes. It is difficult to control resin mixing in a hole that may be 4 m to 8 m long.

There are two indirect ways of checking the grout in a hole. The first is visual observation of the bleeder tubes. Ideally, they should be filled with cement, and even if subsequent blasting dislodged the cement in the tubes, there will be traces of cement on the insides.

The second method is a pull test. If the hole is grouted, the load during the test will increase rapidly with virtually no stretching of the cable. If the cable stretches, the hole is not grouted. The disadvantage of the pull test is that it indicates only the virtual absence of any grout at all—in a half grouted hole the grout will be in the bottom of the hole and the cable will not stretch, creating the false impression of a fully grouted hole.

Tension should ideally be checked visually by installing reliable load indicators on the cables. There are good, relatively inexpensive, indicators available on the market.

The best way of ensuring good installations is to select a reputable contractor for the work and to have good supervision during installation. Inspections should include visual observations of the breather tubes, the load indicators, as well as pull tests. The tensioning apparatus should also be checked.

In addition, the back areas (and even refuse bins) should be checked for discarded lengths of cable cut-offs or plastic tubing, which could be breather tube cut-offs. The load indicators should be inspected prior to installation for any sign of tampering, and serious questions should be asked if a vice grip is found in the sections.

Joint support

Joints, slips and faults have the same effect on stability and will all be treated as joints in this chapter.

The effect of joints on roof stability has already been pointed out. Just to repeat the crucial information, a roof with one joint is six times more likely to fail than an unjointed roof. The longer it is left unattended, the more likely it is to fail and the more dangerous even the support operation becomes.

Even before discussing where and how long the bolts should be, it is pertinent to look at what should happen when a joint is found.

Pre-support procedure

The first step is often the most difficult one, namely to find the joint. Not all joints are patently obvious; some merely appear as a thin line, sometimes with a layer of whitish material inside. Do not just examine the roof; also, check the ribsides. It is often easier to find a joint in the sides than on the roof, especially at high mining heights.

Do not have the attitude of looking whether there are joints. Rather assume that the joints are there, and it is up to you to find them. Once found, determine a joints direction. Follow the joint; joints sometimes turn or are displaced by other joints.

Then determine the joints dip and dip direction. Never, not even for examination purposes, stand underneath its weak side. Immediately install temporary supports underneath its weak side. Then check for the smoothness of the joint surface.

Use the following guide to estimate exactly how dangerous the situation is:

Smoothness: the smoother, the more dangerous.

Direction: the more closely parallel to the roadway, the more dangerous.

Dip: the shallower the dip, the more dangerous, but any joint with a dip of more than $10°$ off the vertical is likely to fail. Be careful of trusting a vertical joint. They are sometimes curved. The rib- sides usually display more information on the nature of a joint than the roof.

Position: the longer the exposed weak side of a roof with a joint, the more dangerous the situation. Be extremely careful of a joint close to the ribside, with the weak side over the roadway, as shown in Figure 21.
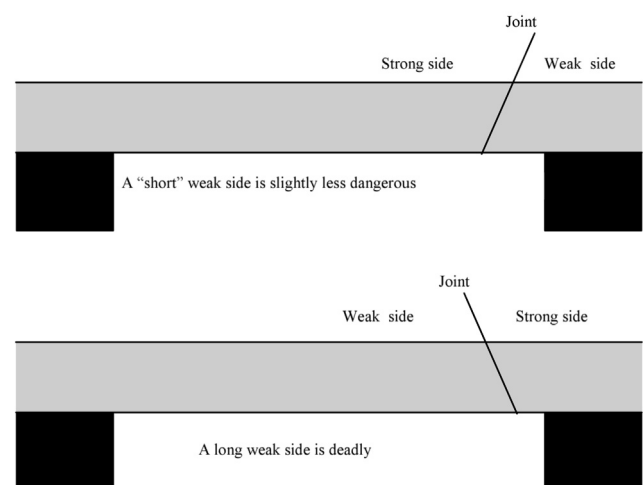

Figure 21. The combined effect of dip and position of a joint on the degree of danger it poses

Joint support pattern

The only effective bolts for a joint are the ones that intersect the joint plane—see Figure 22. The whole idea of bolting a joint is to clamp the rock on either side of it together again, to fix the flaw that nature puts in our way.

To achieve this, check the dip again, make a sketch on the ribside. Make sure that the distance of installing the bolts from the joint is small enough for the bolt to intersect the joint plane.

Draw a horizontal line through the joint exposure in the ribside—see Figure 23. Pretend that is the roof. Now take a bolt and move it backwards and forwards along the line to find the position where about a third to half of the bolt goes through the joint plane. Now measure the distance of the bolt to the joint along the horizontal line—that is how far from the joint the bolts must be installed.

This procedure for determining the bolt positions will not always work, for instance where joints are very steeply dipping. In addition, where joints are very shallow dipping, the procedure may indicate a distance that is too far from the joint, creating a dangerous feather edge. Therefore, moderate the distance for those extreme cases: for very steep joints install bolts 0.5 m from the joint and for very shallow dipping ones, a maximum of 1.5 m.

The next step is to mark off the holes and install the bolts 1 m apart along the joint. Install two lines of bolts, one on either side of the joint, with the bolts opposite one another. The bolts should be installed in pairs, each member on opposite sides of the joint. Where vertical, or very steeply dipping joints occur, W-straps should be provided across the joint, as shown in Figure 24. If the dip of the joint cannot be determined, assume it to be vertical and treat it as such.

The short W-strap is additional support for situations

Figure 24. Plan view of suggested method for supporting with W-straps a joint of which the dip is very steep or difficult to ascertain

Ineffective   Effective   Ineffective
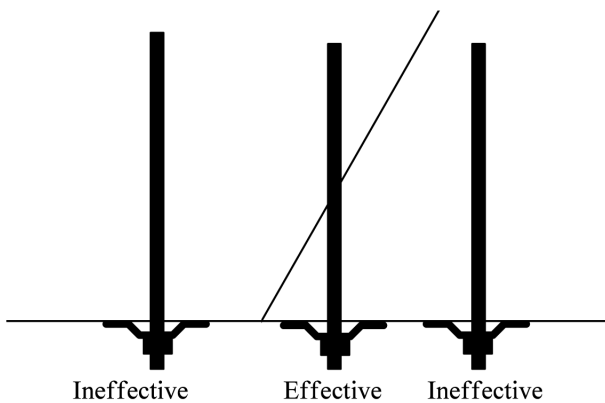
Figure 22. Bolts that do not intersect the joint plane have no supporting effect on the joint
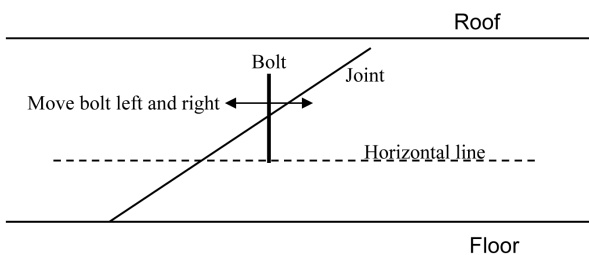
Figure 23. Method to find the best position to install bolts to support a joint
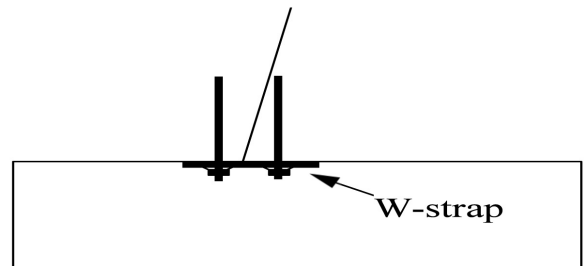
Figure 25. Cross-section through the roof, showing the effect of W-straps on the support of a very steeply dipping joint. Where bolts do not intersect the joint, the W-strap is the only link between the strong and weak sides

where the bolts intersect the joint plane. In situations where the bolts do not intersect, W-straps are the only supports, as shown in Figure 25.

For short-term purposes, short conveyor belt strips can also be used. Timber tapes have also been used. Over the longer term they decay, and therefore long-term support should be proper steel W-straps.

Heavily jointed areas

The previous two sections dealt with the situation where one or maybe more widely spaced isolated joints occur. In areas where the joint density is more severe, say spacing less than half the road width, a strategic approach is called for.

Firstly, investigate the possibility of stepping the section to avoid the jointed zone. If that is not feasible, at least drop the non-essential roadways or splits until conditions improve. Reduce road widths to the bare minimum, especially the ones parallel to the joints. Stepping the splits to reduce the intersection sizes by having 3-way intersections has been done, but this doubles the number of intersections. If the mining discipline is less than 100%, this method will double the size of the problem.

Change the mining sequence by cutting in a maximum of 6 m single drum. Then install temporary supports and inspect. If joints are found, support them before mining the step. Then mine the step and support before mining the next cut.

In roadheader sections, restrict the advance to 3 m before support is installed. Call in a specialist to investigate the roof support system. Be prepared for the fact that additional support such as cable trusses, W-straps, long anchors, wiremesh, etc. may be required.

Support of very weak roof

Much of the discussion in this chapter involved one common situation, namely, a relatively thin layer of laminated material overlain by a thicker, competent layer. The competent layer could be a sandstone or a well-cemented laminated sequence. While this is a treacherous situation, it is not too difficult to deal with, provided the right steps are taken. The biggest danger is injury to people, the roof falls seldom being big enough to damage equipment or seriously disrupt production.

In other cases, the situation is different. Where the entire roof is weak, which can mean either consisting of a very thick laminated layer or a weak material such as mudstone, the support mechanism has to perform a different function. An artificial beam has to be created by making use of roofbolts and W-straps, trusses or cable trusses.

There are two basic ways of approaching the problem. One is to determine the typical height and shape of roof falls by observation and then to design a support system that performs like a basket, i.e. assume that the roof will fail and then merely suspend it in place. The other approach is to strengthen the roof to the extent where it will not fail in the first place.

Weight suspension

When a support system is inadequate, roof falls will occur. They supply valuable information to enable one to improve the system. The most important information to be gathered is the height of the falls, road widths, and the pattern, i.e. whether they tend to occur more in one direction than another. The following is a brief description of the design principle—the details are contained in Appendix B.

The width and height of the falls can be used to determine the weight per linear metre, which is to be supported. The required resistance of the support system can then be calculated. Once that is known, the length of the anchors can be determined. The length of anchor is simply the required total resistance divided by the resistance per metre of the anchors (which is determined by pull tests underground).

The next step is to calculate the number and length of bolts to be used. These two considerations are interdependent: one can use either a small number of long bolts or a greater number of shorter bolts. The total combined anchor lengths into the competent material must just be the same. At this stage of the design, the steel strength must also be considered.

Very often, meaningful savings can be achieved by installing inclined bolts, making sure that the bolts are inclined over the solid ribsides—see Figure 26. Of course, area cover in the form of wiremesh and/or W-straps must also be provided. This design approach may not be the most sophisticated, but it will cater for roof falls irrespective of what the mechanism of failure is.

Beam creation

One mechanism of roof failure occurs when its shear resistance in a horizontal direction is too low to prevent slipping. The roof then bends, which causes horizontal tensile stresses to develop, mainly at the edges but also in the centre of the beam. The philosophy behind beam
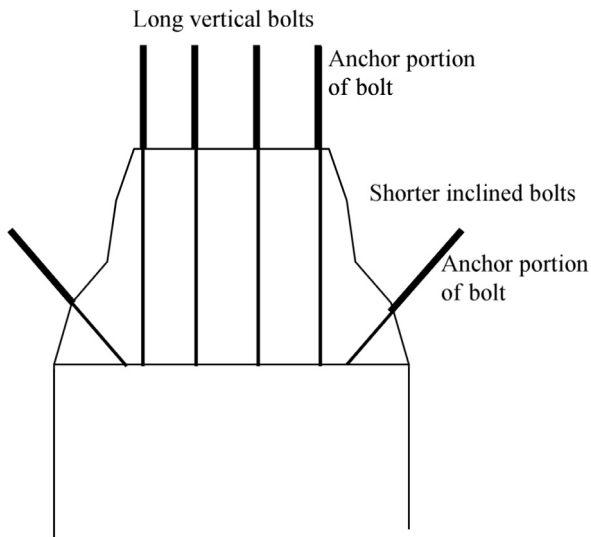
Figure 26. The benefit of inclined bolts. The same amount of anchorage can be obtained with shorter inclined bolts, as with longer vertical bolts

creation is to provide artificial shear strength to the roof material by installing vertical bolts of specified characteristics in the correct positions. Applying pre-tension to the bolts will place the beam in compression in the vertical direction, which will further enhance the resistance to horizontal sliding. It provides vertical confinement to prevent thin layers sliding over one another.

Usually, W-straps are added to increase area cover and to provide artificial tensile strength and stiffness to the roof material. For the beam creation function, W-straps are superior to wiremesh because they are stiffer, and it is of paramount importance to prevent any roof deflection from taking place. It is therefore also even more important to install bolts close to the face, before deflection has started taking place. In addition to the W-straps, wiremesh should also be used to provide areal cover.

The scientific principles in Appendix B can be used to design a first order system, which has to be refined based on underground observations. Rock is so variable that it is only by coincidence that the first design will be the correct one. This type of system has to be developed on site, and in the developmental process underground monitoring has to be done.

The most valuable contributions of the practical person underground during the development of this sort of system are co-operation with the specialists and observation. The specialist can visit the observation sites only at certain times. He will notice changes, like snapshots taken at specific times. What happened in

between can only be described by the person who is there all the time.

Monitoring mainly consists of measurement of roof movement. This is done by installing either simple telltales or magnetic anchors at specific positions into a hole in the roof, and then to determine their displacement with a probe stuck into the hole. This supplies information on where the displacements take place and how much displacement occurs. By monitoring the displacements over time, one can also judge how effective the support system is, and predict whether or not the roof is likely to collapse—see Chapter 10: Monitoring, for more details.

The extensometer observations described above can be supplemented by petroscope observations and instrumented roofbolts. The petroscope is a probe that is inserted into a borehole, which allows one to see cracks and bedding separation. An instrumented roofbolt supplies information on the load that develops at different positions on the body of the bolt.

Of course, visual observations of the area are very important. These should be done photographically to ensure objectivity. It is inevitable that during the course of monitoring there will be some interference with the normal production work of a section. This may be due to site preparation, installation of instruments and taking readings. Such exercises should thus be well planned and communicated to ensure minimal disruption and the best possible co-operation.

Supporting the competent layer

It has often been remarked so far that one general case is that the competent layer is self-supporting and that the normal roof support is aimed at suspending the laminated material underneath it. This may not always be the case, especially with the newer generation continuous miners, which cannot cut narrow road widths productively.

Where the wider roadways coincide with a thinner competent layer in the roof, the beam is likely to fail. Under those conditions, the options are either to mine the area with equipment that is more suitable to narrower road widths, or to support the competent layer with long anchors.

When considering supporting the sandstone beam, the sequence of rock types above the sandstone has to be borne in mind. Often it includes at least one coal seam, which is likely to fail in sympathy with the sandstone. Therefore, the design has to cater for the

ROCK ENGINEERING FOR UNDERGROUND COAL MINING

entire roof sequence up to the sandstones above the coal seam. Much longer bolts and a denser pattern than normally encountered will therefore have to be used. Merely installing more bolts of the usual length used for suspension will not solve the problem. An example of such a design is provided in Appendix B.

Inspecting and making safe

Sounding the roof is always a good practice, provided the roof has been visually checked and no obvious loose slabs or joints were found. Loose roof should always be barred down from a safe position under supported roof.

Look carefully before barring. Be particularly careful of a joint that may cause the barred roof to slide back as it comes loose. Always be at least 1.5 m laterally away from the roof that is being barred.

Do not neglect the ribsides. Sound them, too, because accidents have occurred where joints run just inside the pillar. Remember that pillar sides are highly stressed and that if joints are present, they can easily become unstable.

Ribside support

Very few ribsides require systematic support. However, where joints occur in the roof, one should be particularly suspicious of ribsides. The worst ribside joints are the ones that run at about the same height for a long distance, and dip into the roadway, as shown in Figure 27. Once those have been exposed for, say, the length of a split, there is little hope left of supporting them safely.

The problem is that during drilling into the ribside, it could become dislodged. Prop it up as well as possible, using angled mine poles stuck into hitches cut in the floor, or support with slings installed around the corners, but only if this happens to be in a road which cannot be barricaded off permanently. Otherwise barricade off and abandon permanently.

The only really safe treatment for a joint of this nature is to support it in small lengths as it is exposed during development. Continuous miner operators and shuttle car drivers should be aware of the dangers associated with this type of joint, and must be encouraged to find them.

Another dangerous type of situation that often arises is where ribside joints occur on the corners of pillars, as shown in Figure 28. Depending on their height, etc, they should be barred down, knocked down with the drum of the CM or supported with slings. Unless they can be stabilized before the time, drilling into them for bolting is dangerous.

Breaker line supports

The purpose of breaker line supports in pillar extraction is to prevent the roof collapsing from the goaf side into roadways. The ideal breaker line forms a
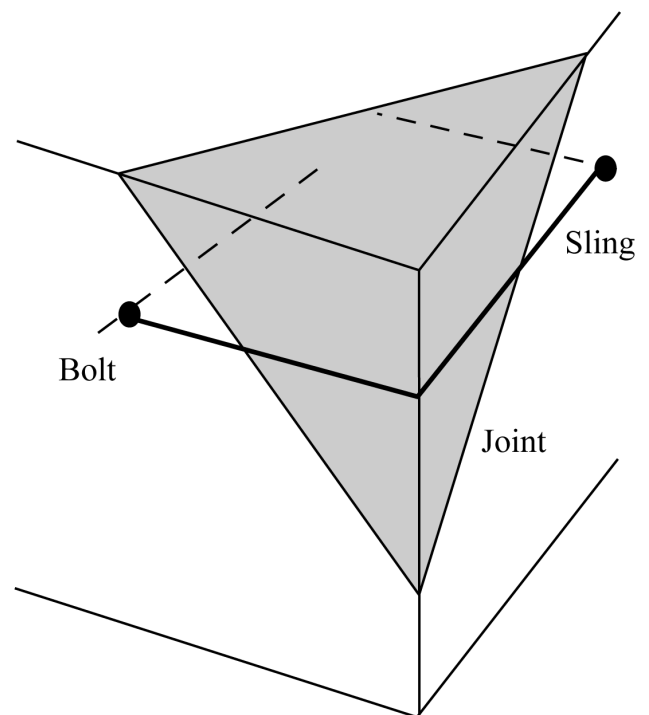

Figure 27. Schematic view of proposed support prior to bolting for a joint in the ribside. The best treatment for joints of this nature is to support them in small lengths as they are exposed, or to abandon the roadway permanently, if possible

Figure 28. Dangerous ribside joint on a pillar corner
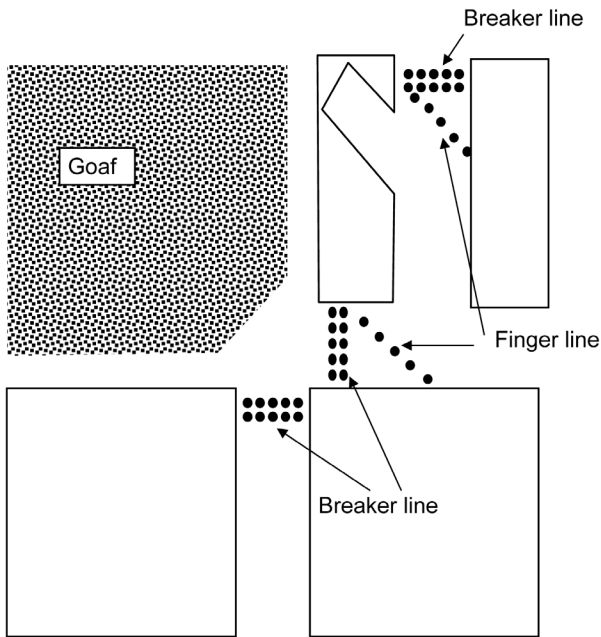
Figure 29. Commonly used pattern for mine pole breaker lines

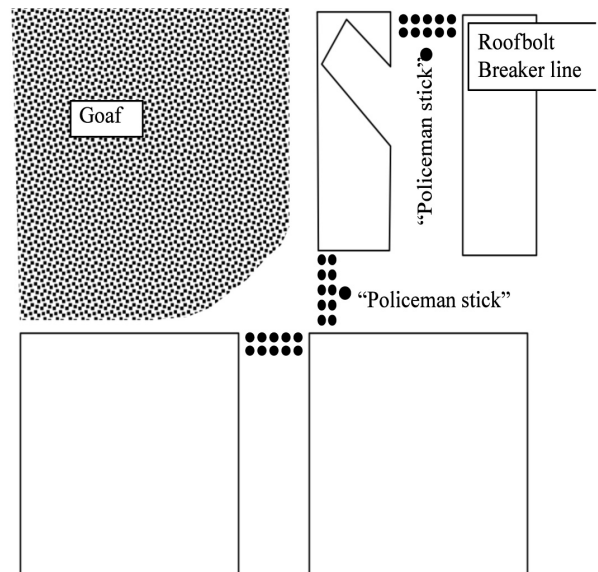**Figure 30. Roofbolt breaker lines and the 'policeman stick'. Roofbolt breaker lines should be installed during panel development**

sharp edge across the roadway, causing the roof to break off on the goaf side, hence the name. To perform this function, a breaker line must be stiff and strong enough, and the individual elements, be they mine poles or bolts, must be spaced close enough together.

There are three basic types of breaker lines: mine poles, roofbolts and mobile hydraulic prop systems. The exact configurations vary as local conditions require. The following are very broad guidelines.

Mine pole breaker lines

A common type of arrangement for a mine pole breaker line is shown in Figure 29. It usually consists of a double line of mine poles spaced 1 m apart supplemented by a finger line running diagonally across the roadway. Breaker lines and finger lines have to be cut the right length and must be firmly wedged against the roof. It is customary for breaker lines to be installed a short distance from the pillar edges, to prevent the mine poles being knocked over by rocks sliding out of the goaf.

The disadvantages of mine pole breaker lines are that they are labour intensive to transport and install, cumbersome to install properly (especially at high mining heights), and require people to work at the goaf edge during their installation. Where mining heights are in excess of 3.5 m, it even becomes difficult to get mine poles of the right length.

On the positive side, they have been shown to be effective over several decades of mining and have the advantage of warning of impeding roof failure by making cracking noises and showing obvious signs of increased load. To the experienced miner, timber talks.

Roofbolt breaker lines

Roofbolt breaker lines perform the same function as timber breaker lines. They usually consist of a double line of full column resin grouted bolts across the roadway, spaced at 1 m—see Figure 30.

Roofbolt breaker lines come into their own in relatively strong strata, being particularly successful in areas where a strong sandstone beam overlies laminated material. They are often the only economical solution at high mining heights.

It is important for the roofbolts to be long enough to penetrate into the sandstone beam. They must be full-column resin bonded for stiffness, and should ideally be installed during development, i.e. before the stooping induced movements start taking place.

The major disadvantage of roofbolt breaker lines is that they give less warning of changing conditions. This problem is usually overcome by installing a single timber prop in the centre of the roadway, the so-called policeman stick.

The advantages of roofbolt breaker lines are that they are easier to install, can be installed during development (which is safer than working at the goaf

edge), are not affected by mining height, and require less labour. If pre-installed, their installation does not hamper the process of pillar extraction.

Mobile breaker lines

A mobile breaker line consists of a set of four hydraulic props in a frame. It resembles a longwall shield with a flat steel roof, mounted on cat tracks. The units are remote controlled, and are used in pairs, parked side by side in the roadway, see Figure 31. Being mobile, they are moved forward after each cut into a pillar, following the continuous miner.

The advantages of mobile breaker lines are that the loads they generate can be adjusted to suit specific roof conditions, they are always close to the continuous miner, and are safe to operate and low on labour requirements.

The disadvantages are that they require a relatively obstruction-free floor, high capital outlay, their use increases the number of units in a section that require maintenance, and they may break down. The varying load cycles they impart on the roof have been seen to cause especially jointed roof to fall, and in instances where they are not moved forward timeously, may themselves be covered by goaf collapse.

Although they were developed in South Africa for

Figure 31. Placement of mobile breaker lines during stoping

the Middelbult Colliery, they are not used locally, mainly due to the high capital cost. Their popularity appears to be increasing in Australia and the USA.

Probabilistic design methods

Up until now, the discussion was of a deterministic nature, i.e. it is assumed that all the design input parameters are constant. It is well known that this is not the case: both the elements making up the load on the system (i.e. the thickness of the layers to be supported, density, etc.) as well as the elements making up the resistance to failure (resin strength, bolt strength, rock tensile strength, etc.) are subject to variability.

The variability is catered for by incorporating a safety factor. The concept of safety factor, however, is nebulous: no-one can say how much safer a system with a safety factor of 1.8 is than one with safety factor of say 1.5.

If the variabilities of the elements making up the system are known, then the probability of failure can be quantified. This aspect is dealt with only at the end of this chapter because probability-based design is not yet common practice in mining, but the authors feel that this represents a more realistic way to deal with roof instability and hope that the concept will find application in the future. It is thus considered more than worthy of inclusion.

Conceptually, the variability of the load on the system can be described by a distribution characterized by a mean and standard deviation rather than just a single number, the average. The smaller the standard deviation, the less the variability. The same can be done for the resistance to failure of the system.

When these two distributions are then plotted on the same scale, the area of overlap between the two represents the probability of failure, see Figure 32. In the area of overlap, the load is greater than the resistance and failure will occur.

Note that the quotient of the means of the two distributions in fact represents the safety factor. Depending on the standard deviations, the same safety factor can have different implications for stability. For instance, if the standard deviation of the resistance distribution increases, the probability of failure will also increase even though the safety factor, based purely on the means of the distributions, remains the same, see Figure 33.

This demonstrates the main advantage of the concept of the probability of failure. There is a much clearer picture of the relative stability of a system.
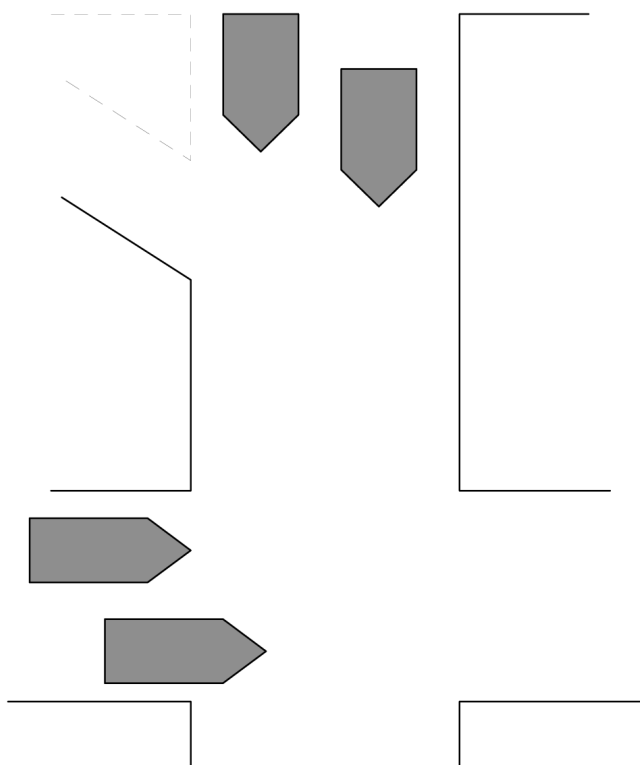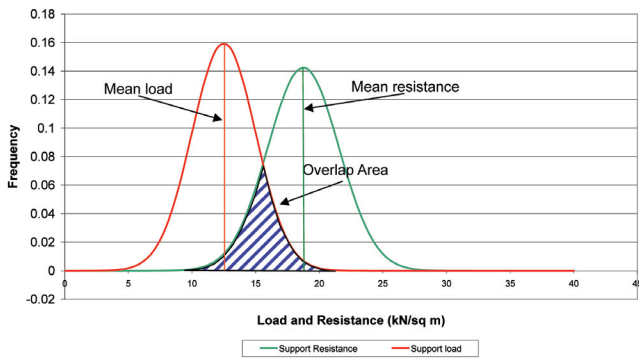
Figure 32. Load and resistance frequency distributions

If the means and standard deviations of the two distributions are known, then the area of overlap of the distributions is relatively simple, see Appendix B, for details.

Consider the following example:

A weak layer, 0.5 m thick, needs to be supported. This results in a load density of 12.5 kN/m². It was found that a support system comprising 0.7 m resin anchors at a spacing of 1.63 m would be sufficient. The support density of the system is then 18.75 kN/m².

The safety factor of the system is 1.5, which is usually considered to be adequate.

Now bring in variability. Say the standard deviation of the thickness of the weak layer is 0.1 m (i.e. 85% of the weak layer is between 0.4 m and 0.6 m thick). This will translate directly to the load on the system, which will vary by the same percentage (20%). This means that the standard deviation of the load will be 2.5 kN/m².

Say further that only one of the variables making up the resistance, the shear strength of the resin bond, varies by 25% while all the other variables (hole

length, steel diameter, etc.) remain constant. This means that the support resistance will also vary by 25%, i.e. the standard deviation will be 4.7 kN/m².

It is then found, using the procedures outlined in Appendix B, that the probability of failure is 0.12, or 12 %.

If now the standard deviation of the support resistance can be reduced by half, say by applying more consistent installation or merely switching to a more consistent resin product, then the standard deviation of the support resistance will also reduce by 50% to 2.35 kN/m². It is then found that the probability of failure reduces to 3.4%, less than a third of the previous value.

This means that without increasing the safety factor, the probability of failure can be substantially reduced merely by reducing the variability of the resin.

Alternatively, if the resin shear strength cannot be made more consistent, it will be necessary to increase the safety factor to 1.8 to achieve the same probability of failure as with the more consistent shear strength. This will come at a cost.

Similar examples can be developed to demonstrate the impact of the other variables in the system. The numbers in the example are not totally out of the realistic range, and indicate that at the commonly accepted safety factor of 1.5 as in the example, some failures are bound to occur. The failures are not due to inferior design, but due to variability.

The most important point to note, however, is that improvement can be achieved by limiting the variability inherent in the support elements without increasing the safety factor. This essentially comes down to tighter quality control, both over the quality of the product and the installation procedures.
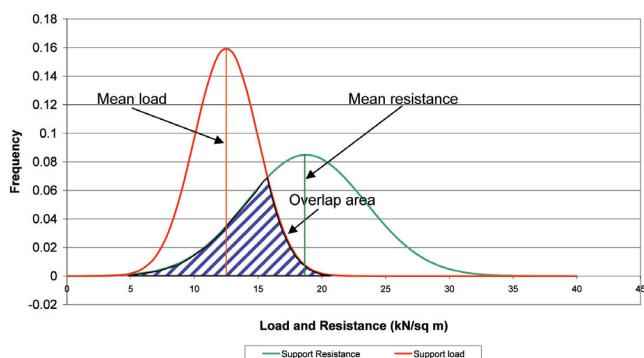

Figure 33. Effect of increased standard deviation on the probability of failure. Note the increase in overlap area between the two curves as compared to Figure 32
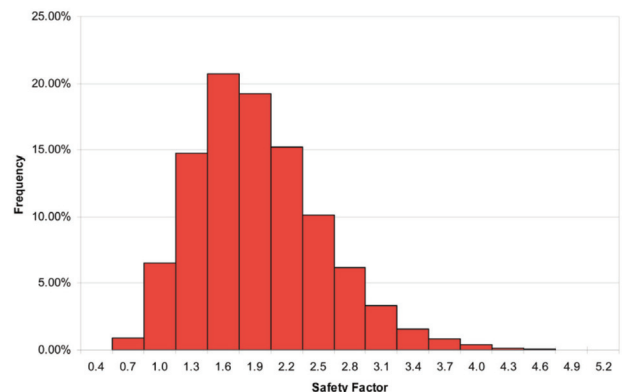

Figure 34. Distribution of safety factors resulting from Monte Carlo simulation of a great number of combinations of variables

ROCK ENGINEERING FOR UNDERGROUND COAL MINING

Table III
Variability of some factors that influence roof stability

Parameter	Number of samples	Minimum	Maximum	Average
Height of roof softening (m)	93	0.2	1.6	0.7
Bord widths (m)	129	5.3	7.5	6.5
Thickness of immediate layer (m)	43	0.1	1.6	0.8
Thickness of upper coal layer (m)	43	1.5	3.3	2.5
Bond strength (kN/mm)	46	0.2	0.6	0.4
Bolt tensioning (kN)	145	0	32	16.4
Bolt spacing (m)	217	1.3	3	2
Roofbolt ultimate strength (KN)	209	119.3	137.8	129.3
Unit weight of immediate layer (MN/m^3)	99	1382.8	2214.4	1835.3
Unit weight of upper coal layer (MN/m^3)	154	1380.9	1669.7	1530.1
Coal tensile strength (MPa)	40	0.4	1.8	1

In order to fully implement a probabilistic design system, additional information is required. The load, for instance, is a function of mainly the thickness of the layer to be supported and the density of the roof rock— these variabilities can be found by simple measurement.

The resistance part of the equation is subject to more variability, the main variables being the following:

- Resin/rock interface shear strength
- Hole diameter
- Steel diameter
- Hole length
- Road width
- Bolt spacing
- Roofbolter toque setting
- Nut and thread consistency
- Density of roof rock.

Canbulat and Van der Merwe (2009) measured some of the variables in one section at a mine in the Witbank coalfield and the results, demonstrating the extent of the variability, are summarized in Table III.

Table IV
Proposed limits of acceptable failure probabilities, after Canbulat and van der Merwe (2009)

Roof class	Consequence	Design probability of failure	Example
1	Moderately serious	5%	Short-term requirement (< 1 year), personnel access partially restricted
2	Serious	1%	Medium-term requirement (1–5 years) personnel access partially restricted
3	Very serious	0.3%	Long-term requirement (> 5 years) no personnel access restrictions

It is clear from the table that a design based purely on the averages is likely to result at least in some under design. Just the thickness of the immediate roof layer, for instance, can be less than half of the average value in several areas.

Handling all the variables simultaneously in a spreadsheet or with a calculator is not practically possible. However, Canbulat and Van der Merwe (2009) describe a statistical procedure that can be used. It is essentially based on the Monte Carlo technique, where several thousand possible combinations of the variables are randomly selected for the calculation of safety factors. The distribution of the safety factors resulting from the individual calculations, like the example in Figure 34, then supplies a realistic view of the probability of failure.

One of the deterrents to the application of a probability of failure is the decision about what can be considered an acceptable maximum limit. There can never be a zero probability.

A suggestion made by Canbulat and Van der Merwe (2009) is contained in Table IV, based on examples of acceptable failure probabilities in open cast mines and civil engineering slopes.

Other ways of finding an acceptable limit would to equate it to the probability of pillar failure at a safety factor of 1.6, which is 0.17%. It may perhaps be more feasible to back calculate the probability of failure of a number of existing roof support systems on a selection of mines, and to use that as a starting point.

In the meanwhile, however, the probabilities of failure of support systems can be quantified using existing and relatively simple procedures. This is recommended as the design method of the future.

Pillar design

Introduction

Coal pillar design is of primary importance for the safe, economic extraction of a valuable national resource. It is often determined by the strategy of the mining company or the philosophy of the mine manager. The basic choice is whether to opt for maximum extraction on the advance, thereby leaving permanent coal pillars, or maximum overall extraction of the coal reserves, where larger pillars are deliberately formed with the intention of extracting them at a later date. As a mine nears the end of its life there are economic and social pressures to extend the life of the mine for as long as is technically and economically feasible. Consequently, areas designed only for primary extraction and showing no signs of stress or deterioration are often reappraised to determine if they are suitable for some form of secondary extraction.

Often a pillar designed for maximum extraction on the advance is performing its intended task by not showing signs of load, but would not be able to carry the additional loads resulting from secondary extraction. However, continued research and practical experimentation have advanced the knowledge of rock engineering so that pillars formed under previous design methodologies can be re-evaluated in an effort to obtain maximum extraction of previously mined pillars. These latest developments can also be utilized by mine planners, managers and rock engineers in designing new panels.

Basic mining methods

The basic method of mining depends on a number factors, such as: seam thickness, selected mining height, depth of workings, number of economic seams, thickness of the parting between seams, overburden characteristics, immediate roof and floor conditions, type of equipment available, and market requirements. Prior to designing the layout, the extent of the mineable reserves must be known, together with the strata characteristics. In particular, the presence of a dominant stratum, such as a thick dolerite sill, may influence the pillar layout philosophy due to the potential additional loading of the pillars during secondary pillar extraction.

The general design will consist of determining the maximum depth of the panel together with the maximum selected mining height at that point. The selection of the bord width will depend on the mining equipment to be used and the likely stability of the immediate strata, taking into account the required roof support. The pillar dimensions will depend on the design philosophy, as shown in Tables I to III.

History of pillar design

Initially pillar dimensions and road widths were based on experience obtained through trial and error. Some of the errors committed had disastrous consequences in terms of loss of life, equipment, and coal reserves. Research efforts worldwide therefore have concentrated on the development of effective design procedures that can be used by collieries.

At the start of the twentieth century this more rational approach to the determination of coal pillar strength began with the testing of coal specimens in the laboratory. While general trends were quickly established (such as a decrease in the specimen strength with increasing height and size, and an increase in

Table I
Advantages and disadvantages of designing for primary mining only

Advantages	Disadvantages
Higher extraction on advance	Lower overall percentage extraction of reserves
Pillar stability long term Minimal surface effects at medium to great depth	Reduced life of mine. At shallow depths may cause sinkholes
Minimal effect on underground water aquifers	
Potentially cheaper mining method, roofbolting primary support only	

Table II
Advantages and disadvantages of partial extraction design

Advantages	Disadvantages
Increased extraction compared to primary mining only	At shallow depth may cause surface effects
Lower support cost, compared to total extraction	Lower primary extraction; this may affect productivity
Lower safety risk compared to total extraction	High retreat rate with small centres may cause problems with belt and pipe retreat
Reduced effect on surface compared to total extraction	Potential longer-term surface effects, sinkholes
Reduced effect on aquifers compared to total extraction	Risk of sudden collapse if not correctly designed

Table III
Advantages and disadvantages of pillar extraction

Advantages	Disadvantages
Greatest extraction of reserves	Surface effects, short to long term
Subsidence occurs at known time	Affects surface water and aquifers
Life of mine extended	Higher capital costs, if additional equipment such as mobile breaker lines is used

strength with increasing width), the wide scatter of results made the extrapolation of strength results to full size pillars extremely difficult. In order to overcome the limitations of the laboratory tests, testing of large *in situ* samples was initiated during the late 1930s when *in situ* tests were performed in the USA. These experiments had the advantage of being conducted in the underground environment and yielded valuable information about the stress-strain behaviour of coal pillars. However, these tests were time consuming, expensive and did not overcome the problem of extrapolation of results to full size pillars.

Research in South Africa

Research into coal pillar strength in South Africa gained momentum after the Coalbrook disaster in January 1960 in which 437 miners lost their lives.

The feasibility of conducting large-scale *in situ* tests in South Africa was investigated by Hoek (1966) at the Wolvekrans Section, Witbank Colliery in the No. 4 Seam. Continuing from this report, a substantial *in situ* testing programme was conducted over an eight-year period by the Chamber of Mines Research Organisation and the CSIR with 91 *in situ* tests being conducted. These were summarized by Bieniawski and van Heerden (1975). Bieniawski and Mulligan (1967)

concluded that there would be no increase in the strength of a sample beyond a 5.0 foot cube.

Concurrent with the CSIR testing programme, *in situ* tests were conducted by Cook *et al.* (1971) and Wagner (1974). A major finding of this work was the realization that the centre portion of a pillar was capable of withstanding extremely high stresses, even when the pillar had been compressed beyond its maximum resistance, which is traditionally regarded as the strength of the pillar. Other important findings were that the strength of circumferential portions of a pillar was virtually independent of the sample width-to-height ratio, whereas the strength of its centre increases with an increasing width-to-height ratio, Wagner (1974). While the modulus of elasticity was found to be a true material property and independent of geometry, the post-failure modulus was markedly affected by width-to-height ratio, which indicated that the post-failure behaviour of a pillar is a structural (or system) property and not an inherent material property.

The *in situ* testing of coal resulted in increased knowledge of the behaviour of coal pillars, particularly as far as the stress-strain behaviour is concerned. However, as with the laboratory investigations, a wide scatter of results was obtained. In addition, *in situ* experiments were limited by the capacity of the loading system applied to the pillar and proved to be time consuming, elaborate and expensive.

With material of highly variable and difficult to determine properties, such as rock, it is difficult to accurately establish either the real strength or the real load. This is particularly true of coal and coal measures strata. The values for strength and load must be regarded as estimations, which can be subject to error.

Oravecz (1973) investigated the load on coal pillars by field measurement, analytical analysis and use of an electrical resistance analogue. He concluded, on the basis of theoretical work and experimental investigation, that at the low levels of stress, as well as small displacements that occur in stable bord and pillar workings of coal mines, the theory of elasticity applies to coal measures strata. This was a significant conclusion for the future development of coal mining rock engineering in South Africa, although there are occasions where it may be taken too far and the effects of discontinuities are overlooked.

Salomon and Munro

In South Africa, an intensive investigation into the strength of coal pillars was initiated through the

statistical analysis of 98 intact and 27 collapsed pillar geometries by Salamon and Munro (1967) using a probabilistic approach.

Load is calculated using the modified cover load or Tributary Area Theory, where each individual pillar is assumed to carry the weight of the overburden immediately above it. This assumption applies where the pillars are of uniform size and the panel width is larger than the depth to the seam. The majority of bord and pillar panels in South African collieries fulfil these conditions.

Load on a square pillar is calculated from:

$$Load = \frac{25HC^2}{w^2} \text{ kPa} \qquad [1]$$

where H is the depth to the floor of the workings,

          C is the pillar centre distance and

          w is the pillar width.

In Equation [1], the number '25' is the unit weight of the overburden strata in kN/m^3, provided it consists of sedimentary rock types. Where a denser dolerite sill of thickness T is present in the overburden, the formula should be adjusted to the following:

$$Load = \frac{[25(H-T)+30T]C^2}{w^2} \qquad [1a]$$

Equation [1a] is the full form of the load equation. For simplicity, however, the form of the expression given by Equation [1] will be used in this and subsequent chapters.

Strength is taken to mean the strength of a coal pillar as opposed to the strength of a coal specimen. The strength of a pillar is said to depend not only on the material strength, but also on the pillar's volume and shape. The shape effect is a result of constraints imposed on the pillar through friction or cohesion by the roof and floor.

The formula for strength takes the form:

$$Strength = kw^{\alpha} h^{\beta} \text{ kPa} \qquad [2]$$

Salamon's analysis gave values of $k = 7\,176$ kPa, $\alpha = 0.46$ and $\beta = -0.66$.

Substituting these values for the constants in Equation [2] yields the following well-known coal pillar strength formula of Salamon and Munro (1967):

$$Strength = 7176 \frac{w^{0.46}}{h^{0.66}} \text{ kPa} \qquad [3]$$

Note that Equation [3] is valid only for square pillars. If rectangular pillars are used, an equivalent width, w_e, is to be used instead of the pillar width, w. Wagner

(1980) suggested that w_e be calculated by

$$w_e = \frac{4A}{c} \text{ m} \qquad [4]$$

Where A is the pillar area and c is the pillar circumference. Note that this adjustment is valid only for the calculation of pillar strength. For the calculation of pillar load, the real dimensions should be used, in the following formula:

$$Load = \frac{25HC_1C_2}{w_1w_2} \text{ kPa} \qquad [5]$$

Salamon (1967) emphasizes that the pillar strength formula is essentially empirical and should not be extended beyond the range of data that were used to derive it. Furthermore, the assumption in the formula of one average strength for all coal-seams is recognized as a limitation. However, a major advantage of the statistical methodology used by Salamon is the prediction of the probability of a stable geometry as shown in Table IV.

Safety factor is defined by:

$$Safety\ Factor = \frac{Strength}{Load} \qquad [6]$$

Equations [1], [3] and [6] can be combined into a single expression for the safety factor (SF), as follows:

$$SF = 288 \frac{w^{2.46}}{HC^2 h^{0.66}} \qquad [7]$$

Salamon (1967) thought it reasonable to suppose that the majority of mining engineers had arrived at an acceptable compromise between safety and economic mining, with the optimum safety factor lying in the range where 50 per cent of the stable cases are most densely concentrated. This occurs between safety factors of 1.3 and 1.9 with the mean being 1.6. This is the value used for the design of production pillars in South African bord and pillar workings.

Figure 1 is a curve showing the probability of failure as a function of the safety factor. It shows that at a safety factor of 1.0 there is a 50% probability of having a stable layout and that beyond a safety factor of 1.6 there is no further significant improvement in the expectation of stability.

Madden (1991) states that since the introduction of the Salamon pillar design formula, 38 pillar collapses have been recorded (1966 to 1988). Two significant features are evident from the analysis of the original and additional collapsed pillar cases. These are: pillars

mined at shallow depths, less than 40 m, have collapsed even with high designed safety factors, and pillar collapse is limited to low pillar width to mining height ratios less than 3.75. Of the 38 cases, for which the time period was known, 26 per cent of the collapse occurred within the first year, while 50 per cent occurred within four years of mining.

Madden (1991) suggests that, at depths of less than 40 m, pillar widths should preferably be greater than 5.0 m, the width-to-height ratio should be in excess of 2.0 and the percentage extraction be less than 75 per cent. In addition, a safety factor of more than 1.6 should be maintained.

Bieniawski

At about the same time as Salamon and Munro's statistical work on the determination of coal pillar strength was being carried out, Bieniawski continued attempts to derive the strength from tests on coal specimens. He soon realized that the tests on small specimens in a laboratory was not sufficient and then concentrated on testing larger specimens underground. His work, reported in Bieniawski (1992), resulted in a linear formula as opposed to the power formula of Salamon and Munro. It has the following form:

$$Strength = 4300 \left(0.64 + 0.36 \frac{w}{h} \right) \text{ kPa} \qquad [8]$$

This formula has not been widely applied in South Africa but gained wider acceptance in the USA and later in Australia. In the formula, the constant representing the coal strength (4 300 kPa) was based

Figure 1. Probability of failure as a function of safety factor

on *in situ* tests as opposed to Salamon and Munro's statistically derived value.

Linear formula for coal pillar strength

Using a different statistical approach to that adopted by Salamon and Munro, van der Merwe (2003) re-analysed the data gathered by them, using an updated data base, which included pillar failures up to 2005. The approach was to optimize the formula from the point of view of decreasing the size of the overlap area between the failed and stable populations of pillars. The basic reasoning was that the perfect formula would result in no overlap between those populations and that consequently the smaller the overlap area, the more effective the formula. The resultant formula had a 12% reduction of the overlap area as compared to the one by Salamon and Munro, which can be interpreted as a 12% improvement of efficiency. It is in the form:

$$Strength = 3500 \frac{w}{h} \text{ kPa} \qquad [9]$$

This formula has the following characteristics:
- The constant representing the strength of the coal material, 3 500 kPa, is lower than the one used by Salamon and Munro, which was 7 176 kPa.
- This new constant is closer to the 4 300 kPa obtained by Bieniawski in direct tests.
- The exponents of *w* and *h* are unity, indicating a linear relationship when comparing the strength increase with increasing ratio of *w/h*, see Figure 2.
- The new formula predicts greater strength than the Salamon and Munro formula for pillars with *w/h* greater than 2.5 and lower strength for smaller pillars. This is in accordance with the observed trend that smaller pillars are more likely to fail, even with higher safety factors obtained with the Salamon and Munro formula.
- The probability of failure as a function of safety

Table IV

Safety factor, probability of a stable geometry, and number of pillars likely to collapse out of one million pillars formed

Safety factor	Probability of a stable geometry	No. of pillar collapses in one million
2.1	0.999999	<1
2.0	0.999994	6
1.9	0.999974	26
1.8	0.999894	106
1.7	0.999586	414
1.6	0.998468	1 532
1.5	0.9947	5 300
1.4	0.9830	17 000
1.3	0.9508	49 200
1.2	0.8748	125 200
1.1	0.7259	274 100
1.0	0.5000	500 000
0.9	0.2534	746 000
0.8	0.0799	920 100
0.7	0.0066	993 400
0.6	0.0060	999 400

ROCK ENGINEERING FOR UNDERGROUND COAL MINING

factor is for all practical purposes the same as that obtained with the Salamon and Munro formula, implying that the new formula can be used without affecting the risk of failure. The probability of failure, shown in Table V and Figure 1, is therefore also valid for the linear strength formula.

The load is still calculated using the Tributary Area Theory, implying that the single formula for the safety factor when using the van der Merwe strength formula is:

$$SF = 140 \frac{w^3}{hH(w+B)^2} \qquad [10]$$

Design of squat pillars

Salamon and Oravecz (1976) consider the strength formula to be conservative when the width-to-height ratio exceeds five or six, and regard a pillar with a width-to-height ratio of 10 as being virtually indestructible. Salamon (1982) extended his pillar strength formula (Equation [2]) to take cognizance of the increasing ability of a pillar to carry loads with increasing width-to-height ratio.

Laboratory tests on sandstone specimens were analysed by Wagner and Madden (1984), to examine the suitability of the new formula, known as the squat-pillar formula, to predict the strength increase with increasing width-to-height ratios. The squat-pillar formula was found to fit the laboratory results well, and although these laboratory results cannot be related directly to coal pillars because of the difference in the material, scale, and time taken to test the samples, the general trend can be assumed to be similar.

The strength of a pillar given by the squat-pillar formula is

$$\sigma_s = k \frac{R_o^b}{V^a} \left\{ \frac{b}{\varepsilon} \left[\left(\frac{R}{R_o} \right)^\varepsilon - 1 \right] + 1 \right\} \qquad [11]$$

where R_o is the critical width-to-height ratio
   R is the pillar width to mining height ratio
   ε is the rate of strength increase
   a is a constant 0.0667
   b is a constant 0.5933
   V is pillar volume ($w_1 \, w_2 \, h$).

Salamon and Wagner (1985) suggest that the squat-pillar formula could be used with the critical width-to-height ratio (R_o) taken as 5.0 and that ε could be taken as 2.5, although a realistic estimate was more difficult

for the latter. The assumption of 5.0 for R_o was based on the fact that no pillar with a width-to height ratio of more than 3.75 was at the time known to have collapsed in South Africa. Field investigations into the performance of squat pillars have been conducted at Longridge, Hlobane and Piet Retief collieries.

Substituting the values for the constants indicated above in Equation [11], results in the following simplified version of the formula for the strength of a squat pillar:

$$Strength = \frac{0.0786}{V^{0.0667}} \left\{ R^{2.5} + 181.6 \right\} \text{ MPa} \quad \text{kPa} \qquad [12]$$

Note that the only criterion for using the squat-pillar formula is that the ratio of $w/h > 5$. There is, for instance, no depth limitation.

Comparison of different strength formulae

The Bieniawski formula, which was never as extensively used in South Africa as in the USA, consistently predicts lower strength at all width-to-height ratios than the other two. The van der Merwe formula predicts lower strength for small pillars and higher strength for larger pillars when compared to the Salmon and Munro formula, see Figure 2. Note that in Figure 2, the squat-pillar formula was used instead of the Salamon and Munro formula for width-to-height ratios greater than 5.0.

The practical difference between the different formulae is reflected by the percentages extraction obtained. Figure 3 compares the percentage extraction obtained by using each of the formulae for the depth range of 70 to 160 m. It is apparent that the differences become more pronounced with increasing depth, the greatest extraction being obtained with the van der Merwe formula. For this example, a mining height of 3 m, bord width of 6 m and safety factor of 1.6 were chosen.

Correction for parallelogram shaped pillars

Where continuous haulage systems are used, it is difficult to mine with square turn-offs. Instead, 60° or 70° angles are more common, resulting in parallelogram shaped pillars, as shown in Figure 4. Figure 4 also explains the symbols that are used in Equations [13] to [17].

The first correction that is required is the unadjusted pillar width, w. The reason for this adjustment is that misunderstanding could arise because the mined road width (B), from the point of view of the underground operator, differs from the bord width used for

calculation purposes as indicated in Figure 4.

The unadjusted pillar width is:

$$w = C - \frac{B}{Sin\alpha} \quad \text{m} \qquad [13]$$

Then, the pillar width should also be adjusted according to the principle suggested by Wagner (1980). The equivalent width, w_{ep}, for a parallelogram pillar with unequal side lengths then becomes:

$$w_{ep} = \frac{2w_1 w_2 Sin\alpha}{w_1 + w_2} \quad \text{m} \qquad [14]$$

or where the pillar sides are equal,

$$w_{ep} = w Sin\alpha \quad \text{m} \qquad [15]$$

Similarly, the pillar load formula in the case of unequal dimensions has to be adjusted to

$$Load_p = \frac{25HC_1 C_2}{\left[C_1 - \frac{B}{Sin\alpha} \right]\left[C_2 - \frac{B}{Sin\alpha} \right]} \quad \text{kPa} \qquad [16]$$

or, for equal dimensions,

Figure 2. Comparison of pillar strength predictions using different strength formulae
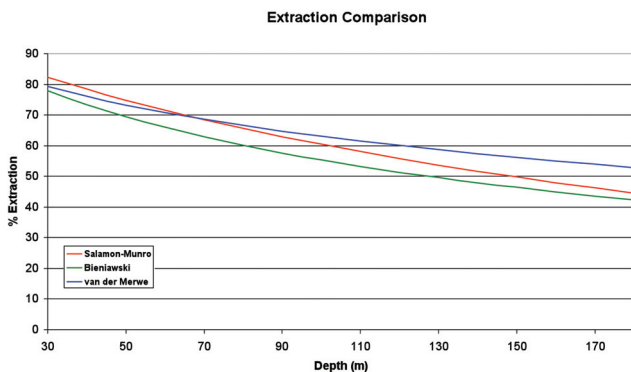
Figure 3. Comparison of percentage extraction obtained using different strength formulae
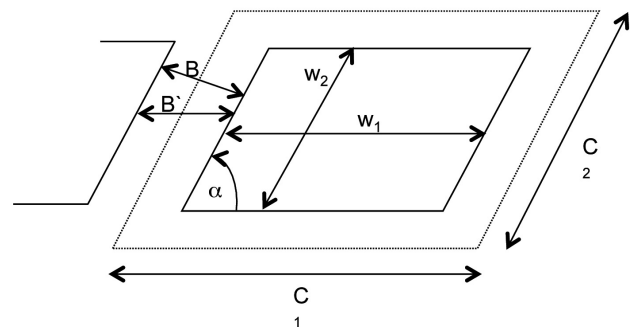
$$Load_p = \frac{25HC^2}{\left[C - \frac{B}{Sin\alpha} \right]^2} \quad \text{kPa} \qquad [17]$$

It is important to note that equivalent pillar width, w_{ep}, cannot be used for the load calculation.

Correction for continuous miners

Because the Salamon and Munro pillar design formula is based on the designed mining dimensions of workings, which were mined by the drill-and-blast method, the formula for pillar strength indirectly takes into account the weakening effect of blast damage. Therefore, the effective width of a pillar designed according to the Salamon and Munro formula, but mined by a continuous miner, must be greater, by an amount approaching twice the depth of the blast zone, than that of a pillar formed by drill and blast.

The depth of blast damage into the side of a pillar has been quantified as being between 0.25 and 0.3 m, Madden (1989). The effect on the safety factor of a pillar formed by a continuous miner can be estimated on the assumption that effective pillar width increases by twice the depth of the fractured zone, over that of a pillar mined by drill and blast methods. If the nominal pillar width, w, results in a safety factor, then the safety factor of bord-and-pillar workings developed by means of a continuous miner, η, can be calculated from the following expression, Wagner and Madden (1984):

$$\eta = \eta_o \left(1 + \frac{2\Delta w_o}{w} \right)^{2.46} \qquad [18]$$

when using the Salamon and Munro strength formula, while it is

$$\eta = \eta_o \left(1 + \frac{2\Delta w_o}{w} \right)^{3} \qquad [18a]$$

Figure 4. Explanations of the symbols used in the discussion of the strength of parallelogram shaped pillars

ROCK ENGINEERING FOR UNDERGROUND COAL MINING

when using the van der Merwe formula, where w_o is the blast damage width (typically taken to be 0.3 m), w is the pillar width and η_o is the drill and blast safety factor.

This means that for pillars developed by continuous miners, the single equation for the calculation of safety factors when using the Salamon and Munro strength formula (see Equation [7]) can be written as

$$SF_{CM} = 288 \frac{w^{2.46}}{HC^2 h^{0.66}} \left(1 + \frac{0.6}{w}\right)^{2.46} \qquad [19]$$

When using the van der Merwe strength formula, the single formula can be written as

$$SF_{CM} = 140 \frac{w^3}{HC^2 h} \left(1 + \frac{0.6}{w}\right)^3 \qquad [19a]$$

It is important to note that for a pillar formed by a continuous miner, there is a fixed increase in pillar width by the extent of the blast-damage zone, and not a fixed increase in safety factor.

The benefit in terms of increased extraction from the use of continuous miners occurs with pillars greater in width than 5.0 m and at depths of less than 175 m. Small pillar widths are sensitive to overmining so a minimum dimension has been suggested. At the depth of about 175 m the onset of stress induced slabbing of the pillar sidewalls can occur.

Barrier pillar strength

Esterhuizen (1993) investigated barrier pillar design. Barrier pillars are required, among other functions, to prevent the possible collapse of underground coal workings in one area from spreading to adjacent workings. They should thus be able to resist increased loads imposed on them. A study showed that barrier pillars, which were as wide as the adjacent panel pillars, were able to arrest a collapse.

The load on barrier pillars was found to depend largely on the behaviour of the overlying strata. Where no collapse has taken place, the barrier pillars are at a lower stress level than the adjacent pillars in the workings. If the width of barriers is designed to be a constant multiple of the adjacent panel pillars they will be subject to approximately constant stresses. Thus the barrier width was suggested to be equal to the in-panel pillar width.

Effects of discontinuities on strength

Major discontinuities occurring in the coal-seam were considered the reason for five pillar collapses that occurred in the Klip River Basin. In these cases the discontinuities were smooth, slickensided, and continuous over tens of metres and occurred in two to three different orientations within a pillar. These cases failed soon after mining despite high safety factors and high pillar width-to-height ratios.

Esterhuizen (1995) suggests that considerable variations in the large-scale strength of coal are likely to exist due to variations in the intensity of discontinuities in the different coal-seams, which in South Africa varies from massive unjointed coal to highly jointed coal. The application of standard rock classification techniques supports this contention. Numerical model studies show that the reduction in the strength of coal pillars due to the presence of a given density and orientation of jointing is not constant for all width-to-height ratios but the effect of jointing becomes less pronounced as the width-to-height ratio increases.

Figure 5 illustrates the effects of discontinuities on pillar stability.

Collapses since 1966

The database on which Salamon and Munro performed the analyses to derive their coal pillar strength formula, was created in 1965. Since then, a number of additional collapses have occurred. These were studied on two occasions, by Madden and Canbulat in 1997 and by van der Merwe in 2006.

Collapses decribed by Madden and Canbulat (1997)

In 1996 a complete review of the back analysis of collapsed pillar cases was undertaken, Madden and

Figure 5. The effects of discontinuities on pillar stability

Canbulat (1997). The first coal pillar collapse was recorded in South Africa in 1904 and Salamon found 50 cases up to 1967. However, only 27 of these were used due to either unreliable information or because of weak roof conditions at shallow depth. In Salamon's cases the coal pillar was the weakest element with a strong roof and floor. Madden (1991) found that 38 pillar collapse cases had occurred since 1967, but excluded 21 cases where weak roof or coal deterioration was thought to have contributed to the collapse. Again the coal pillar was the weakest element and all cases had competent roof and floor. From 1988 to 1996 an additional 23 pillar collapses have occurred.

In an attempt to develop an understanding of the effect of the floor and roof strata, and other influencing factors, Madden and Canbulat (1996) plotted all collapses where reliable information existed concerning the pillar design geometries.

Figure 6 shows the frequency of the collapsed pillar cases versus their designed safety factor. The categories indicated in Figure 6 are as broad as possible. Several observations can be made from this figure. Firstly, pillar collapses have occurred with very high, up to 5.6, designed safety factors. In fact, 35 of the 90 pillar collapses have occurred with safety factors in excess of a designed value of 1.6. Secondly, the majority of the collapsed pillar cases occurred in Salamon's original empirical range and have a designed safety factor of less than 1.6. In eight cases the pillars stood for between 30 and 50 years at designed safety factors of between 0.91 and 1.37 before failing.

It should be noted that the majority of coal produced underground in South Africa comes from the Witbank and Highveld coalfields. In these coalfields Salamon's strength formula is performing well in the design of stable pillar systems. However, coal is produced underground in a variety of other coalfields with varying conditions. Examination of the collapsed cases with designed safety factors higher than 1.6 suggest that they can be broadly grouped into geographic areas.

Of the 90 collapsed cases, in terms of frequency versus the pillar width to mining height ratio, 25 cases occurred with width-to-height ratios in excess of 3.5. However, the majority of these occurred in the Vaal and Klip River basins. An important observation is that no collapses have occurred in the squat pillar range where the pillar width to mining height ratio exceeds five. The squat pillar formula has been in use for over 10 years in at least 15 collieries throughout South Africa.

Whereas the majority of cases involve between 50 and 200 pillars, several large collapses have occurred. In the Coalbrook Colliery disaster in 1960, an estimated 4 000 pillars collapsed in about 15 minutes, with the total number of collapsed pillars thought to be about 7 700.

Collapses described by van der Merwe (2006)

The purpose of the work performed in 2006 was to establish an official database of failed and stable pillar cases for South Africa. The work was performed under the auspices of SIMRAC.
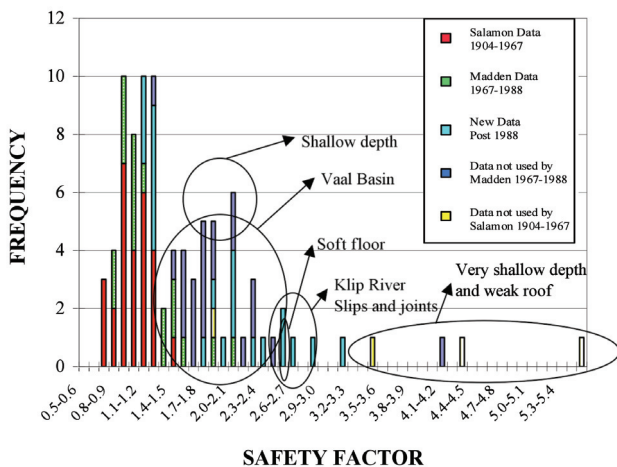

Figure 6. Histogram of pillar collapses, after Madden and Canbulat (1997)

Table V
Summary of dimenions of failed pillar cases

	Combined data-base (m)	Old database (m)	New collapses (m)
Depth			
Maximum	205.0	193.2	205.0
Minimum	19.0	21.3	19.0
Average	71.5	71.5	71.5
Pillar width			
Maximum	17.0	15.9	17.0
Minimum	3.2	3.4	3.2
Average	7.6	6.7	8.0
Mining height			
Maximum	6.2	5.5	6.2
Minimum	1.4	1.4	1.4
Average	3.6	3.8	3.4
Bord width			
Maximum	8.5	8.5	6.7
Minimum	4.8	5.5	4.8
Average	6.2	6.7	5.9
Width-to-height ratio			
Maximum	4.3	3.5	4.3
Minimum	0.9	0.9	1.0
Average	2.3	1.8	2.5

ROCK ENGINEERING FOR UNDERGROUND COAL MINING

The new database contained 75 cases of failed pillars, almost three times the number available to Salamon and Munro in 1965. While there were similarities in the dimensions of the cases in the two databases, there were also a number of important differences.

Table V indicates that whereas the mining depth has remained essentially the same, the latter failures are characterized by slightly wider pillars, slightly lower mining height, narrower bords and higher width-to-height ratio.

The percentage extraction of the failed cases decreased slightly, from an average 76.2% to 68.3%.

The most significant finding was that the safety factors of the failed cases increased dramatically, no matter which formula is used to calculate the pillar strength. Table VI contains a summary of the safety factors of the failed pillar cases.

Note that the safety factors shown in the table reflect the safety factors at the time of mining, and not at the time of failure.

Another very interesting shift was observed in the ages of the pillars at the time of failure, see Table VII.

It is seen that the average lifespans of the pillars increased from 8.2 years to 21.3 years. It can now be concluded that the post 1965 pillar collapses occurred after a longer time with pillars that were initially mined at higher safety factors. This highlights the need to address the issue of pillar strength deterioration over time. This chapter addresses the issue of pillar scaling over time later.

Coal pillar strength in the Vaal Basin

A disproportionate number of pillar collapses occurred in the Vaal Basin, mainly at the Coalbrook, Cornelia and Sigma collieries. These failures were analysed by van der Merwe (1993) who found that the distribution of failures did not conform to the probability distribution of failures and safety factors shown in Table V. Although the Vaal Basin was well known for its weak roof, the primary mechanism of failure was seen to be failure of the pillars as opposed to failure of the roof or floor.

Van der Merwe concluded that the failure distribution could become similar to that found by Salamon and Munro by downgrading the constant representing the coal strength in the formula to 4 500 kPa, as opposed to 7 176 kPa. Therefore, the strength formula for coal pillars in the Vaal Basin is

$$Strength = 4500\frac{w^{0.46}}{h^{0.66}} \text{ kPa} \qquad [20]$$

and the combined safety factor formula for that coalfield then becomes:

$$SF = 180\frac{w^{2.46}}{HC^2h^{0.66}} \qquad [21]$$

Predicting the lifespan of pillars

Van der Merwe (2003a) analysed pillar collapses in different coal-seams and areas of South Africa. He

Figure 7. Severe scaling of a pillar in the Vaal Basin. Note that the roof is still intact

Table VI
Summary of safety factors of failed pillar cases

	Combined database	Old database	New collapses
Salamon and Munro strength formula (1967)			
Maximum	4.2	1.5	4.2
Minimum	0.7	0.7	0.9
Average	1.5	1.0	1.7
Van der Merwe linear strength formula (2003)			
Maximum	4.2	1.3	4.2
Minimum	0.5	0.5	0.6
Average	1.4	0.9	1.8

Table VII

Lifespans of pillars at the time of failure

	Combined data-base	Old data base	New failures
Maximum	52.0	32.0	52.0
Minimum	0.0	0.0	1.0
Average	16.4	8.2	21.3

Table VIII

Values for *m* and *x*

	m-Value	*x*-Value
Vaal Basin, Klip River and South Rand	1.3888	0.804
Witbank No 2 and 4 Seams	0.1624	0.8135

found that the majority of pillars collapsed by a process of progressive scaling, such as shown in Figures 7 and 8. As the pillar continues to scale, it becomes progressively smaller and its load bearing capacity is reduced while its load increases. Eventually, it reaches the stage where it has to fail. By inspection of the database, he postulated that the lowest value of safety factor that a pillar can tolerate, was 0.4. He then calculated the distances that pillars in the database of failed pillars had to scale before they reached the minimum value. Using that distance and the known life of the pillars, he was able to indirectly deduce the rate at which pillars scaled.

The distance a pillar has to scale in order to reach the minimum safety factor, S_m, is

$$d_c = w - \left[0,00714 S_m HhC^2\right]^{0,333} \qquad [22]$$

The rate of scaling, R, for $S_m = 0.4$, was found to be

$$R = m\left[\frac{h}{T}\right]^x \text{ m/yr} \qquad [23]$$

where T = the time since creating the pillar; m and x are dimensionless constants.

The predicted life of the pillar is then

$$T_L = \left[\frac{d}{mh^x}\right]^{\frac{1}{1-x}} \text{ years} \qquad [24]$$

Different values for m and x were found for different areas and coalseams of the country, shown in Table VIII.

Using Equations [20] to [22], the lifespans of pillars in the failed database were predicted and the predictions compared to the known lifespans of those pillars. The results of the comparison are shown in Figure 9.

Subsequent direct measurement, described by van der Merwe (2004), confirmed the scaling rates previously found indirectly. The direct measurements conformed to the deduced ones with a level of certainty of 80%.

It has to be noted that not all pillars will fail due to scaling. The database of intact pillars had predicted

Figure 8. Illustration of time dependent pillar scaling. The two photographs were taken in the same coalseam, a few kilometres apart. The pillar in the upper photograph was about three months old, the one in the bottom photograph about ninety years
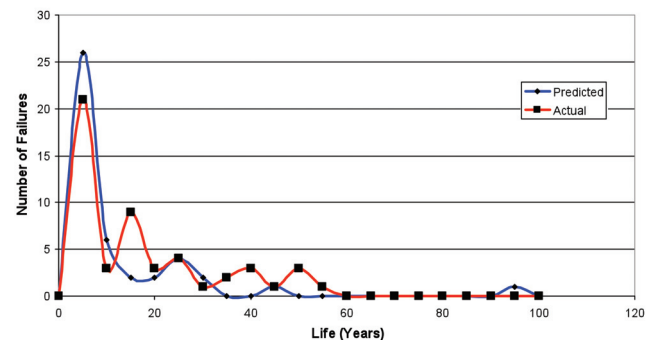
Figure 9. Comparison of the frequencies of predicted and observed pillar lifespans

lives extending to several millennia. The scaling debris from the pillars will build up against the pillar sides, eventually offering sufficient resistance in the majority of cases to prevent any further scaling.

Other mechanisms of pillar failure

The strength of a coal pillar is a function of numerous parameters including: seam strength, geometry, discontinuities, the contact conditions with the roof and floor, weathering of the coal- seam, time, loading rate, geology, the material characteristics of the roof and floor strata, as well as the mining method employed. It has been seen that many of the collapses of bord and pillar workings can be clearly attributed to causes that indicate that the pillar was not the weakest element. Also, pillars that were stable initially may fail over time as the pillar material and the environment are susceptible to weathering.

For example, in the collapsed cases from the Klip River Coalfield, it is likely that the mechanism of failure was dominated by the orientation and properties of the discontinuities, which are not specifically accounted for in the empirical strength formula, rather than the nominal seam strength.

There is, of course, some interaction between these elements. These interactions are complex and not amenable to analytic solution, especially in jointed country rock and pillars. These problems can be analysed with the aid of computer software.

Three main mechanisms of pillar system failure have been identified, namely roof failure, floor failure, and failure of the pillar material. Failure of the pillar material by weathering and progressive scaling is saliently included in the empirical methods of determining pillar strength.

Roof failure

Where roof failure occurs, the pillar height increases and the pillar strength is reduced. In severe cases, this can result in pillar failure, although the rubble from the roof has some strengthening effect on the pillars through the lateral confinement it supplies.

Top or bottom coaling can also accelerate pillar failure, especially in cases where jointing is present in the pillars. The higher the mining height, the greater the probability that joints may daylight in the pillar sides, which could accelerate the failure process—see Figure 10.

If the height of the pillars in a panel increase by an amount Δh, the new safety factor, $SF^{/}$, in the case of the Salamon and Munro strength formula, can be calculated by:

$$SF^{/} = SF\left(\frac{h}{h + \Delta h}\right)^{0,66} \tag{25}$$

In the case of the van der Merwe strength formula, the adjustment is

$$SF^{/} = SF\left(\frac{h}{h + \Delta h}\right) \tag{25a}$$

Floor failure

Where the floor material is weaker than the roof or the pillars, the pillars may punch into the floor. If the floor material exhibits plastic behaviour, the material may be displaced laterally underneath the pillars and the friction between this material and the pillars can induce
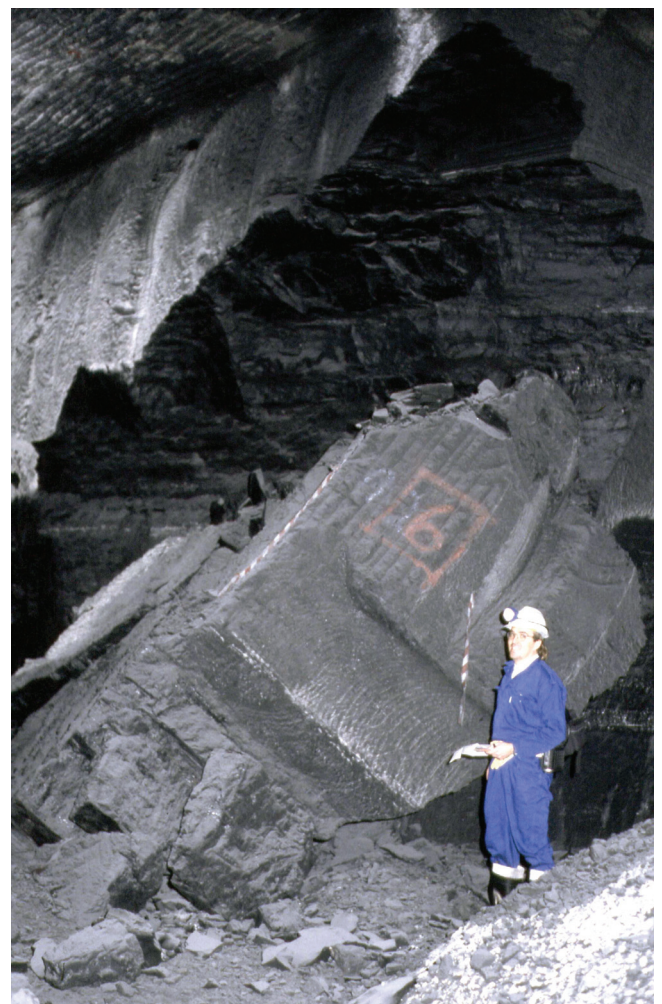

Figure 10. Accelerated pillar deterioration caused by roof coaling in an area where the pillars were jointed

sufficient tension in the pillars to result in tensile failure. Figure 11 shows tensile cracks in a pillar that had punched into the floor. Floor failure is illustrated by an example in Appendix C: Pillar Design.

Progressive scaling

When pillar widths are reduced by scaling, the safety factors are reduced by a double mechanism: the pillar stress increases and the strength is reduced. If a pillar with width w scales and the pillar width is reduced by Δw, the new safety factor in the case of the Salamon and Munro strength formula, $SF^{//}$, is:

$$SF^{//} = SF\left(\frac{w - \Delta w}{w}\right)^{2.46} \qquad [26]$$

In the case of the van der Merwe strength formula, the equivalent expression is

$$SF^{//} = SF\left(\frac{w - \Delta w}{w}\right)^{3} \qquad [26a]$$
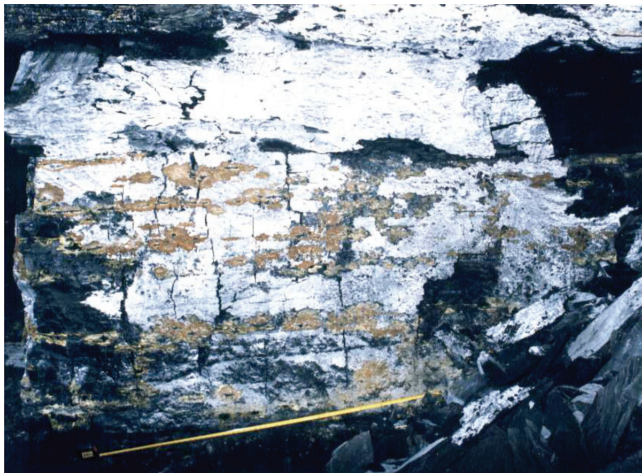
Figure 11. Tension cracks in a pillar that was being torn apart by soft floor material flowing out from underneath the pillar

Figure 12. View inside a panel where the pillars had failed

Using Equations [25] and [26] it is seen that if a pillar's height increases by 10%, the safety factor reduces by 6% using the Salamon and Munro strength formula and by 10% if using the van der Merwe formula. If the width is reduced by 10%, the safety factor decreases by respectively 23% or 27%. No matter which formula is used, changing the pillar width has a much more serious effect on pillar stability than changing the pillar height.

It is believed that pillars seldom fail to the extent that the mined void is closed completely. In this regard, there are only a small number of observations to confirm this statement, as it is seldom possible to gain entry into panels where the pillars have failed. In the majority of cases, pillars fail only after the entry routes to them have been sealed, or otherwise abandoned. However, Figure 12 shows a case where pillars had failed in an instance where it was possible to gain entry into the panel. The mining height in that particular case was reduced from around 4 m to about 2 m. The figure indicates that after failure, there still were openings. Note that the rubble from adjoining pillars had built up to a height of approximately a metre in the centre of the roadway before failure was arrested.

Underground fire

In abandoned mines, flooding of the workings may, over time, weaken the floor material and even the pillars themselves, especially where the clay content of the coal is high. Another potential hazard in shallow abandoned mines is that the coal could combust spontaneously and that the pillars may be destroyed by fire. This mechanism is known to be prevalent in the old shallow mined areas surrounding Witbank, of

Figure 13. View through a crack from the surface of a coal fire underground

ROCK ENGINEERING FOR UNDERGROUND COAL MINING

which an example is shown in Figure 13.

This mechanism is unlikely to occur at depth in excess of 40 m, as fire needs oxygen to sustain it and sinkholes providing access to the surface (and thus oxygen) do not normally occur at depths of more than 40 m.

Prevention of pillar failure

The most popular methods to prevent pillar failure all rely on providing lateral constraint to the pillars. This can be achieved in a number of ways, ranging from wiremeshing, see Figure 14, to backfilling.

In burnt coal, wiremeshing is often supplemented by shotcreting. Where this is done, care should be taken to use wide aperture mesh (greater than 100 mm) and to fit the mesh snugly to the rock surface. Otherwise, the shotcrete may build up on the mesh without making contact with the rock surface.

For short-term purposes, wiremesh has been replaced by discarded conveyor belt strips, see Figure 15. At

Figure 14. Wire mesh and oslo-straps installed

Figure 15. Conveyor belt wrapping around a pillar

Sigma colliery this proved very successful and economical.

Backfilling is effective but relatively expensive. At Sigma Colliery it was done on a large scale to prevent pillar failure underneath a main road. Where the underground panels are still accessible, filling could be properly controlled. Timber retaining walls with drainage holes were constructed in the panels at intervals of 400 m to 500 m.

Waste ash from the power station was pumped directly from the ash pump station to the underground via boreholes. The run-off water was collected in underground dams and re-circulated.

Where the underground panels were inaccessible, the filling was more difficult to control. Filling was then done to refusal. The ash was allowed to settle, usually over a period of two to three weeks, and water was then pumped out using pumps on surface.

No cement or other additives were added to the ash. It was found that after a few weeks, the ash usually had shear strengths in excess of 10 kPa, while it was found by Ryder (1994) that a shear strength of only 1 kPa would be sufficient to arrest failure.

On other occasions, excess fine coal was also used as a filling material. The coal was mixed with water and a small percentage of cement in concrete mixing trucks. The fine coal filling was as effective as the ash, with the advantage that less run-off water had to be handled. Figure 16 is an illustration of the fine coal filling operation at Sigma Colliery.

Role of the overburden

Traditionally, in South Africa, pillar stability is viewed as being a function of the pillar strength. The other half

Figure 16. Filling with fine coal at Sigma Colliery. Note the scaling debris from the pillars on the floor and the largely intact roof

of the equation, the load acting on the pillar, is dismissed by the worst-case assumption that the full overburden load is transferred to the pillars—this is the so-called Tributary Area Theory (TAT).

Strictly speaking, this is not the case. Numerical analyses have shown that in normal layouts where panels are separated by inter panel pillars, the inter panel pillars also bear some of the load and that the smaller the pillars, the larger the proportion of load that is borne by the larger and stiffer inter panel pillars. The load acting on the pillars inside the panel is thus somewhat less than indicated by the TAT. The magnitude of load that is actually borne by the pillars depends on the following:

- Panel width—the wider the panel for any given depth, the larger the proportion of load on the pillars
- Overburden stiffness—the stiffer the overburden, the smaller the proportion of load on the pillars
- Percent extraction—the higher the percent extraction, the smaller the proportion of load on the pillars.

Figure 17 is an example of a situation where there is minimal load acting on a pillar. The obviously undersized small pillar in the photograph had been standing for more than ninety years when the photograph was taken. Clearly, there is almost no load acting on it, the load being borne by the surrounding larger pillars. The small pillar is also protected by the stiff roof.

On a larger scale, it has on occasion been observed that pillars on a specific mine scale much less than in similar situations on other mines or regions. This phenomenon has led to the dangerous conclusion that pillars in a specific region or mine are stronger than predicted by the strength formulae. For failure to occur, both the overburden and the pillars have to fail. If the overburden does not fail, it will deflect to a certain degree and nothing further will happen. The pillars will not fail.

However, the problem is that over time, nature will take its course and a joint in the strong overburden layer may decay or become lubricated by water, resulting in loss of strength and then failure. Then, failure will be sudden and dramatic.

At the time when the overburden fails, the full overburden load is suddenly transferred to the pillars and then the TAT is valid. Following the route to assume that the full overburden load is acting on the pillars all the time is thus not as conservative as it sounds, as at the time of overburden failure, the full load is indeed acting on the pillars.

Holistic approach to pillar system design

The empirical approach to pillar design is limited to the cases where the pillar is the weakest element in the system comprising the roof, the pillar, and the floor. When designing pillar geometries, a holistic approach would be preferable. This should consider the stability of the floor, the pillar and the roof, within the overall loading environment, including all relevant parameters for each component.

There is scope for the creation of generic guidelines for a pillar system design procedure. This concept is illustrated in Figure 18. A proposed full design
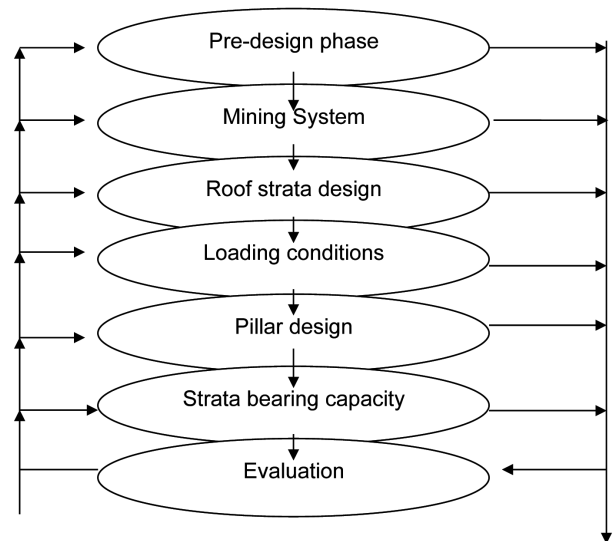

Figure 17. Example of a small pillar that has not failed because the load acting on it is less than the TAT load

Figure 18. Schematic of a system based approach to pillar design

ROCK ENGINEERING FOR UNDERGROUND COAL MINING

procedure is illustrated from the pre-mining phase to the detailed phases concurrent with production. In the flow chart, the 'Pillar Design' box currently incorporates adaptations for mining method, shallow working guidelines and the provision for the squat-pillar formula depending on pillar geometry. However, for a design procedure that can reliably provide stable pillar systems across a wide spectrum of conditions, consideration of all the interrelated components illustrated is essential.

Most of the coal-seams currently mined in South Africa are approximately horizontal. However, the effect of dip on the strength of the pillar cannot be ignored once the dip exceeds about 6^0 or 1 in 10. Another factor that must be considered is the characteristics of the floor material.

Oldroyd *et al.* (1997) reported slake durability test results showing 38.7 to 84.4% loss of mass for floor material in areas where pillar collapse had occurred. It is not certain whether the weak floor initiates pillar failure or pillar failure causes floor punching. The latter can be explained by the increased stress beneath the pillar caused by the shrinking of the pillar as it scales. Work done by Wagner (1974) on *in situ* pillar testing showed that as a pillar fails the central core

becomes more highly loaded, which may be sufficient to cause the pillar to punch into the floor. Alternatively stable pillars may begin to punch into the floor and as they do so, the edges scale and the pillar is pulled apart as the floor lifts, which may also cause failure.

It is likely that both mechanisms occur and it will not be easy to determine which is the dominant cause of pillar failure where weak floor is found. The fact that weak floors have been indicated as the cause of pillar failure requires that the rock engineer and mining profession take this factor into account when designing pillars. This applies particularly where stable pillars are required over the long term such as beneath surface structures or in stooping sections where high loads are placed on the pillars and equipment may be trapped if failure occurs.

Three cases of pillar failure, thought to be associated with weak floor, were analysed by Oldroyd *et al.* (1997). The relationship between average pillar stress acting on the pillar and the ratio of pillar width to thickness of weak floor was proposed as a possible design criterion based on the failed cases. This aspect is expanded on in Appendix C: Pillars.

Pillar extraction

Introduction

Maximizing extraction from coal reserves is a process that involves the principles of rock mechanics in combination with the mining operation and possible consequences of management decisions. For example, leaving panels mined on pillars formed to support the overburden for the long term can result in lower percentage extraction of the available reserves.

The utilization of the coal reserve with the bord and pillar mining method in the depth range of 80 m to 200 m is typically in the range of 60% to 40%. Some relief is provided by using the van der Merwe (2003), or the squat-pillar formula, for pillar design, as opposed to the Salamon and Munro (1967) formula.

However, significant increases in reserve utilization can come about only by deploying an alternative mining philosophy, aimed at removing all the coal. It is explained in Chapter 1: Fundamentals, that mining cannot create stress, it merely redistributes the stresses that are in the earth before mining begins. The magnitude of the redistribution is proportional to the magnitude of the change that mining creates. Bord and pillar mining causes the least change and consequently has the least impact on the redistribution. By contrast, high extraction methods involve the maximum change and thus result in the maximum stress redistribution.

There are essentially two high extraction methods: longwalling, dealt with in Chapter 6, and pillar extraction. Where conditions permit, longwalling is the preferred method. However, the high frequency of occurrence of dolerite intrusions in South Africa and the high capital costs involved in longwalling very often distract from its attractiveness.

The most popular high extraction method in South Africa is thus pillar extraction. There are several variations of the method, as for instance described comprehensively by Beukes (1990). More recently, the NEVID method, developed by Sasol Coal, has also been applied with great success. In this chapter, however, the focus will be on the more generic issues, dealing with principles rather than specifics.

Broadly speaking, pillar extraction involves developing pillars on the advance that are larger than the minimum size required for bord and pillar mining, to cater for the stress increase during pillar removal. Those pillars are then extracted on the retreat. Development and extraction can be done using either drill and blast methods or the more popular continuous miner methods, or a combination of the two.

If pillars are specifically created with the purpose of extracting them later, they can be designed optimally. In this way, productivity during the advance phase can be optimized. Very often, however, the economics of mining necessitates that pillars that were not designed for high extraction are often considered for extraction at a later stage. This happens frequently towards the end of the life of a mine or even a coalfield. While this is not a desirable situation, it is a reality and needs to be addressed. This aspect will also be discussed in this chapter.

Rock mechanics principles relevant to pillar extraction

The stress history of pillars in pillar extraction is the same as the stress history in the case of longwalling, dealt with in Chapter 6: Longwalling.

In the most basic view, there is no fundamental difference between the stress change caused by bord and pillar mining and that caused by pillar extraction. There are, however, orders of magnitude differences in the absolute magnitudes of the changes. The changes caused by high extraction are those of bord and pillar mining, magnified several times. Consider that the mining span in bord and pillar mining is of the order of six to eight metres; in pillar extraction, that span is increased to more than a hundred metres. The effects of the change are likewise magnified. In bord and pillar mining, the span is limited to that which will not result in failure; in pillar extraction, failure cannot be avoided and thus has to be controlled.

It is necessary to consider both the macro and the micro changes that occur as a result of high extraction mining. In the macro sense, the environment is affected by, for instance, changes in the groundwater regime and subsidence. The underground extraction occurs at a specific point, where the microenvironment has to be considered. While third parties are affected by the consequences of the macro changes, the safety of the underground worker depends on the effects of the stress changes in the microenvironment. The manager has to deal with the entire spectrum.

Stress changes

When pillars are removed, the vertical stresses are relaxed and can become tensile. The extent of the tensile zone is a function of the ratio of mining depth, *H*, to the panel span, *W*.

It was shown by Wagner (1996) that at great depths, the *H/W* ratio is large, resulting in small tensile zones. For this reason extensive caving in gold mines does not occur due the limited tensile stress distribution. This changes at shallow depth where tensile stresses extend to the surface, Figure 1. As rock is weak in tension, caving readily occurs. At depths equal to the span, about 35 per cent of the overburden rock is in tension.

In the absence of very competent strata layers in the overburden, such as a dolerite sill, the overburden will usually fail, resulting in subsidence. If there is a strong layer, the failure process could be arrested and subsidence would be minimized. However, there will be a negative effect underground as the inter panel pillars as well as the pillars that are being extracted will be subjected to higher loads.
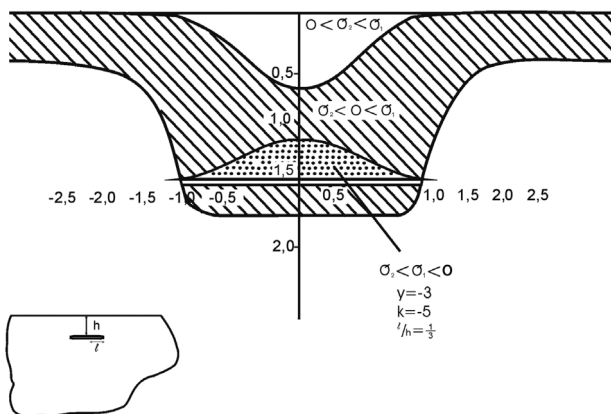
Figure 1. Tensile zones above and beneath an isolated panel at shallow depth, after Wagner (1996)

Underground, the stresses on the pillars initially increase as the mining span increases. In the absence of a strong layer, the overburden will fail at a certain stage. At that point, there will be a stress relief and the stresses will stabilize at this lower level.

If there is a strong layer, the stresses will continue to increase until the face advance equals the panel span. From that point onwards, the rate of increase will be reduced, and eventually stabilized, when the face advance equals about twice the panel width.

Critical panel width

Whether to allow the overburden to fail, or not, is a management decision. From an underground mining point of view, it is often desirable to allow failure to take place. This will minimize the stresses on the pillars that are being removed. However, groundwater ingress will also be maximized. To prevent having to handle large volumes of water underground and to minimize the magnitude of change to the environment, it is sometimes better to prevent overburden failure. This can be achieved primarily by restricting the panel span. The calculation of the required span to break the overburden strata can be made from the following:

In the case of incompetent strata

$$L_c = 2H \tan\phi \qquad [1]$$

where $L_c =$ the critical mining span,
     $H =$ depth of mining below surface and
     $\phi =$ goaf angle; in the absence of more exact site-specific data, can be taken as 15° off the vertical.

Figure 2 shows the relationship between the depth of mining, overburden type and critical mining span for the situation where a very strong layer such as dolerite is absent in the overburden. The composition of the overburden, like the ratio of strong sandstones to weak shales, affects the goaf angle and thereby controls the critical span.

In the case of very strong strata such as a dolerite sill

The critical width at which dolerite failure can be expected, can be estimated from the following, van der Merwe (1995):

$$L_c = 2T\sqrt{k_s + \frac{\beta}{D}} + 2(H-D)\tan\phi \qquad [2]$$

with

                            ROCK ENGINEERING FOR UNDERGROUND COAL MINING

$$\beta = \frac{1.53}{\gamma_m} - 0.8 \qquad [3]$$

and

$$\gamma_m = 0.025\frac{D-T}{D} + 0.03\frac{T}{D} \qquad [4]$$

where: k_s = ratio of horizontal to vertical virgin stress
H = mining depth
D = depth of dolerite base
T = thickness of dolerite
ϕ = goaf angle (measured off the vertical)

It should be noted that the most uncertain mining conditions would be experienced when the panel width is in the critical span range. Super critical or well below critical spans are preferred as unpredictable conditions can occur around the critical span. Therefore, to ensure that the overburden does not fail, the critical span as calculated should be reduced by 10%. If the intention is to ensure failure, 10% should be added to the critical span.

The extraction safety factor

From the foregoing discussion it should be clear that in the course of pillar extraction, the pillars are subjected to varying magnitudes of stress. The stress magnitude is mainly a function of the status of the overburden, i.e. failed or intact, the panel width, face advance and depth of mining. The conventional safety factor calculation as discussed in Chapter 4: Pillar Design, takes into account only the intact overburden weight
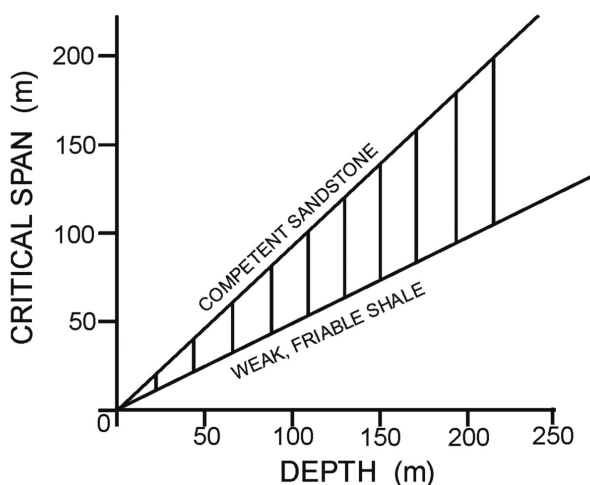
Figure 2. Relationship between critical span and depth for competent and weak strata

and does not cater for the stress increase during pillar extraction. The safety factor so calculated is thus not valid in the pillar extraction operation.

For that reason, van der Merwe (1995) introduced the notion of the extraction safety Factor (ESF). It essentially uses the usual strength calculation in combination with the increased pillar loads during pillar extraction to calculate a safety factor.

$$ESF = \frac{Pillar\ strength}{Real\ pillar\ load\ during\ extraction} \qquad [5]$$

As the load increases during face advance, so the safety factor decreases. The progression of the safety factor with advancing face is conceptually shown in Figure 3. The critical safety factor is the one at the point when the stress is a maximum, i.e. just before the overburden fails. It was seen that as long as this value of the ESF > 1.1, problems due to pillar overloading are unlikely.

In the situation where the overburden does not fail, a higher ESF is required, in the range of 1.3 to 1.4. The reason for having a higher ESF is that in the former case, the minimum ESF is valid only for a short period, whereas in the case of an intact overburden, the entire panel will be extracted under high stress conditions.

There is no direct correlation between the normal safety factor and the ESF. The ESF depends on the additional load that is a function of site-specific factors such as the position and thickness of the dolerite sill or other very strong layers, if present. Pillar loads should be determined using numerical modelling techniques, as described in Chapter 9: Modelling.

Pillar and system stiffness

In the situations where pillar remnant failure is possible, as in partial high extraction methods, the mode of failure is important. At Coalbrook, for instance, the pillar failure was violent. It is estimated that over 4 000 pillars failed in a matter of minutes. By contrast, van der Merwe (1999) describes a case where, at Welgedacht Colliery, the pillar failure took place gradually.

The difference between violent and stable failure is governed by the stiffness of the pillars and the loading system, or the environment in which the pillars are located.

The stiffness of intact coal is a true material property and has been found to be approximately 3.5 to 4.0 GPa. By contrast, the post-peak stiffness of a pillar depends on the pillar geometry. The mode of failure, violent or
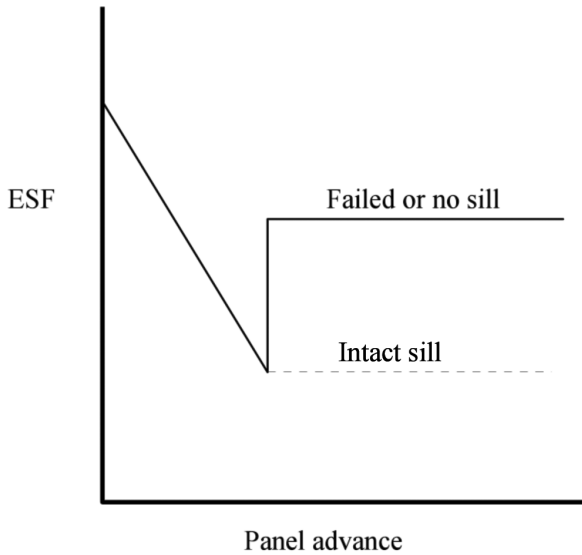
Figure 3. Conceptual variation of the extraction safety factor (ESF) with advancing face

controlled, depends on the post-peak slope of the pillar's load/deformation characteristic and that of the system.

Stiffness, λ, is the ratio of force to deformation (F/ε),

$$\lambda = \frac{EA}{h} \quad [6]$$

In the case of the post-peak stiffness the geometry of the pillar, (w/h), influences the post-peak stiffness. The greater the w/h ratio, the greater the post-peak stiffness.

For stability $\lambda_m > \lambda_c < 0$, where λ_m is the post-peak failure slope of the pillars and λ_c is the critical system stiffness for a panel of pillars. The critical system stiffness reduces with the number of pillars in a panel.

Post-peak stiffness has been obtained by the back analysis of *in situ* coal pillar tests and laboratory tests by different researchers:

$$\lambda_m = 1.861\left(\frac{w}{h}\right)^{-0.931} \text{GPa} \quad \text{(after Van Heerden, 1975)} \quad [7]$$

$$\lambda_m = 1.033\left(\frac{w}{h}\right)^{-1.159} \text{GPa} \quad \text{(after Wagner)} \quad [8]$$

$$Ep = \frac{0.562\,w}{h} - 2.293 \text{ GPa} \quad \text{(Van der Merwe from} \quad [9]$$
van Heerden's data (1998)

$$-\frac{Ep}{E} = 0.23\left|\frac{5}{(\frac{w}{h})} - 1\right| \quad \begin{array}{l}\text{Normalized post - peak}\\ \text{modulus after Ryder and}\\ \text{Ozbay (1990)}\end{array} \quad [10]$$

In Equations [6] to [10], Ep = post-peak modulus, E

=Young's Modulus, w = pillar width and h = pillar height.

Based on the Salamon and Oravecz (1976) concept of local system stiffness, violent failure can occur if there is more energy released from the system than is required by the pillar for continued deformation. This condition is met if the system stiffness is greater (for clarity: smaller negative value of the force-deformation curve) than the post-peak stiffness of the pillar, see Figure 4. Conversely, to prevent violent failure, the pillar post-peak stiffness has to be greater than the system stiffness.

In typical South African conditions of shallow depth with a relatively stiff overburden, the maximum elastic deflection of the overburden over a typical panel width of 130 m to 250 m is insufficient to allow typical pillars of 2.5 m to 5 m height to fail if the overburden remains continuous. For instance, the maximum elastic deflection of a 20 m thick sandstone beam over a panel span of 150 m, is approximately 12 mm. At greater deflections, the tensile stress generated in the beam
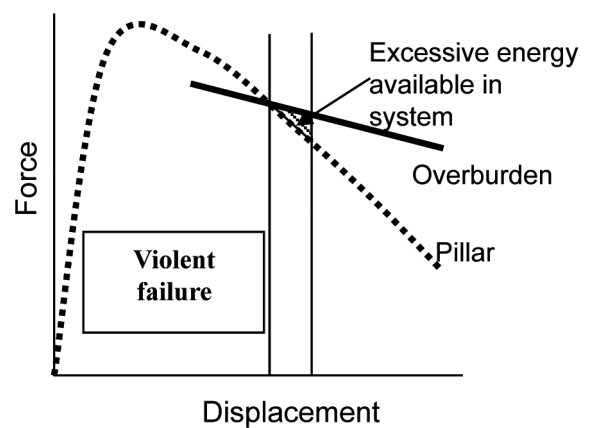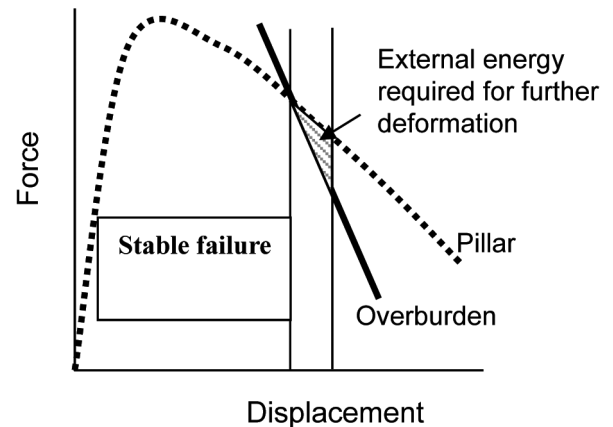
Figure 4. The concept of local system stiffness, after Salamon and Oravecz (1976)

ROCK ENGINEERING FOR UNDERGROUND COAL MINING

will exceed the tensile strength of sandstone. If that deflection is transferred to a 3 m high pillar, the pillar strain is 4.0 mm/m. At that strain, the stress in coal material with a modulus of 3.5 GPa is 14 MPa. While that may result in damage to the pillar, the pillar will not be destroyed because the roof cannot deflect further. The failure process in this case is driven by the sandstone in the overburden, which cannot deflect any further without failing itself.

For the destruction of pillars in most situations, it is therefore a prerequisite that the overburden layers also have to fail. Under those conditions, the problem reduces to that of a dead weight resting on the pillars. In other words, the system stiffness reduces to zero.

This implies that in order for violent failure to be prevented, the post-peak stifness of the pillars has to be positive. This condition is met if the post-peak modulus of the pillars is zero, or greater than zero. Therefore, from Equation [9],

$$E_p > 0, \ or \ \frac{0.562 \, w}{h} - 2.293 > 0 \qquad [11]$$

This condition is met if the prefailure ratio of *w/h* > 4.08. This corresponds with the suggestion of Ryder and Ozbay (1990) that pillars with a width to height ratio of 5.0 can fail only in a stable manner.

It should be noted that pillar failure is not restricted to the failure of pillar snooks or the remnants left by partial high extraction methods. Pillar runs ahead of the extraction area have also been known to occur, as at Welgedacht Colliery, see Chapter 9: Modelling.

The foregoing discussions raise a number of important points relative to pillar extraction:

- When a pillar is split, the stress on the fenders increases because the load bearing area is smaller.

- Also, the stiffness of the fenders is less than that of the pillar prior to being split, because the *w/h* ratio is less.
- Therefore, the probability of the pillar failing in the first place, and failing violently in the second place, is higher.
- The system stiffness depends on the number of pillars in a panel—the wider the panel, the softer the system and the greater the possibility of violent failure;
- System stiffness is reduced by non-continuity of the overburden – faults and dykes therefore reduce the system stiffness and increase the probability of violent failure.

Direction of stooping

One of the important success factors of stooping is consistency. Variations in the stooping angle, direction and rate of advance should be reduced to the minimum.

Stooping angle

The stooping angle is primarily a function of the mining equipment that is used. With drill and blast methods, which is no longer considered a safe stooping method, an angled stooping line was preferred. The reason for this is that in drill and blast, it was necessary to have a number of faces that were being worked simultaneously to cater for the cycle of operations. The angled line means that the span between the unmined pillars and the solid inter panel pillar is reduced, thereby reducing the stresses on the pillars. Also, any particular pillar is partially protected by the other pillars being extracted next to it, as shown in Figure 5.

With continuous miners (CMs) a straight line is usually preferred, although there have been notable exceptions such as at Usutu and Ermelo Collieries
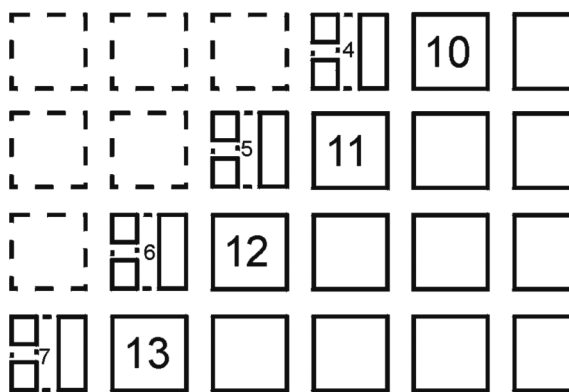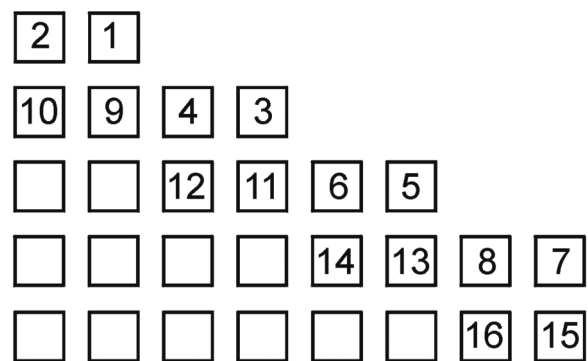

Figure 5. A 45° stooping line

Figure 6. A 30° stooping line

where 30° and 45° lines were preferred, see Figure 6. With CMs, an entire pillar is extracted before moving on to the next one. With a straight line the shuttle car tramming distances are a minimum.

Stooping direction

The general principle in determining stooping direction is to always mine toward the closest solid. Therefore, where adjacent panels are being stooped, it is best to stoop from the previously stooped panel back towards the unmined panel, shown in Figure 7. Wherever possible, stooping between two goafed panels should be avoided. Where it cannot be avoided, it is marginally better to stoop from the oldest panel towards the youngest one.

Another less desirable practice is to stoop a dog-leg panel, shown in Figure 8. Where it is unavoidable, two lines of pillars (or sufficient lines to leave a barrier of 50 m wide) should be left as shown in the sketch. Under adverse roof conditions, it is better to stoop the left-hand section in the figure before moving to the longer panel. In good conditions, and provided the pillars are large enough, the upper part of the long panel (shown as 'A' in Figure 8) can be stooped up to

the position of the dog-leg. The dog-leg can then be stooped before stooping in the long panel resumes. The latter option is better from an operational point of view because of the simpler conveyor belt configuration, whereas the former option is better from a ground control viewpoint because it is more continuous.

Negative consequences of changing the stooping direction

During the process of extracting a pillar, additional load is distributed to the surrounding unmined pillars. These cause micro fractures to develop in the roof and the surrounding pillars.

The micro fractures follow the same pattern as the stress contours. If the direction of stooping is changed, the directions of the stress contours will also change, implying that a new set of micro fractures, criss-crossing the ones that already exist, will develop—see Figure 9.

During the process of extracting a pillar that is intersected by two different sets of micro fractures, the fractures will open up during the load cycle. This means that both the fender and the roof will be considerably weakened. This could cause the fender, a snook or the roof to fail prematurely.
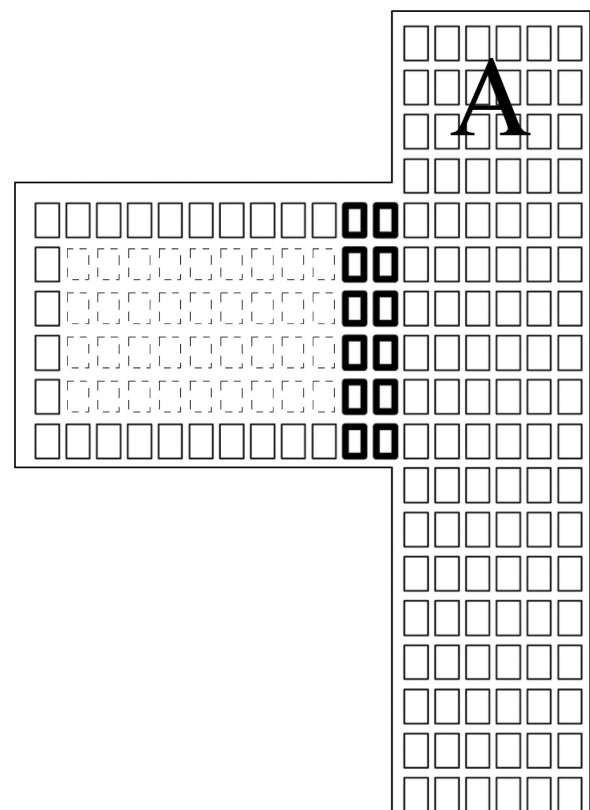

Figure 7. The stooping direction should always be from the old goaf towards the unmined ground

Figure 8. Stooping a dog-leg panel

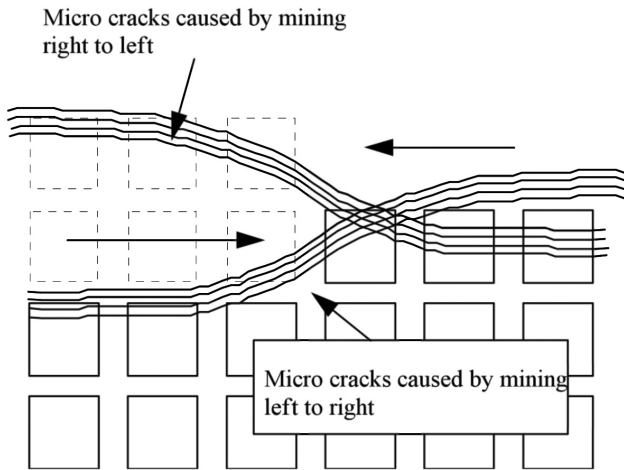ROCK ENGINEERING FOR UNDERGROUND COAL MINING

Figure 9. Criss-crossing cracks caused by changing direction. The diagram is conceptual and shows only two sets of fractures, to illustrate the principle

The second argument against changing the direction of stooping relates to time. For argument's sake, if stooping is always done from left to right, then the time lapse between first exposing a pillar to the goaf and then mining the pillar, is always the time it takes to extract one line of pillars. If, however, the sequence is changed, say left to right for one line and then right to left for the next, then the time lapse between exposing the far left-hand pillar to the goaf and extracting it, is the time it takes to extract two lines of pillars—see Figure 10.

Consistantly mining left to right means that the bold pillar is mined as number 6 after being exposed to the

Changing the direction of mining means that the bold pillar is now mined as number 10 after being exposed to the goaf.
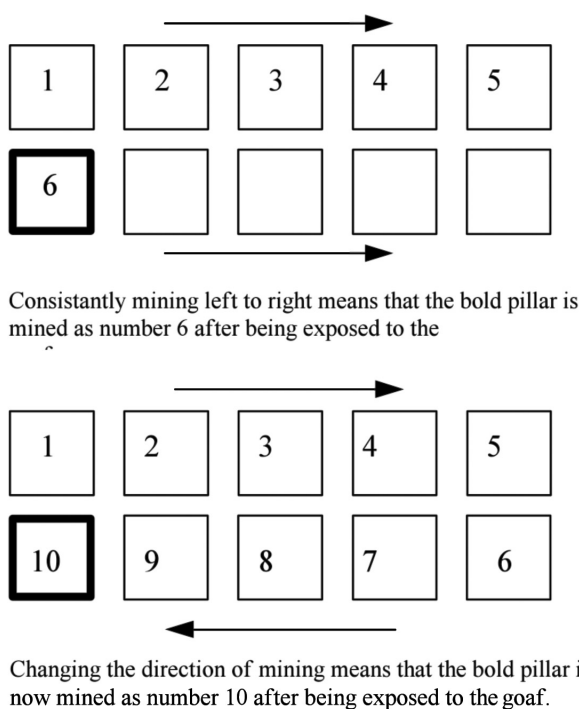
Figure 10. The negative effects on time of exposure to the goaf caused by changing the direction of stooping

Failure is time dependent and the fractures now have twice the time to develop and start opening up. The pillars on the left are now subjected to two aggravating factors, namely a long time and two different sets of fractures. Somewhere along the line a problem has to arise.

The role of snooks in stooping

Previously, the golden stooping rule was to remove all pillars completely. Reality dictates that it is seldom, if ever, achievable. Snooks, or even whole pillars, will be left behind for any one of several very valid reasons, such as adverse jointing conditions, uneven or weak floor, water ingress, etc. While very high extraction ratios are sometimes claimed for stooping, it seldom exceeds 70% in reality.

The more recent view requires the opposite: well-designed snooks have to be left. The underlying philosophy is that if coal is going to be lost, then utilize it to protect the microenvironment. The sizes and positions of the snooks are the key to the success of the system. Basically, they are intended to stabilize the micro-environment without upsetting the balance in the macro environment.

The ideal stooping panel can be divided into three zones: the stooped area, where unconditional snook failure must occur, the working area, where temporary
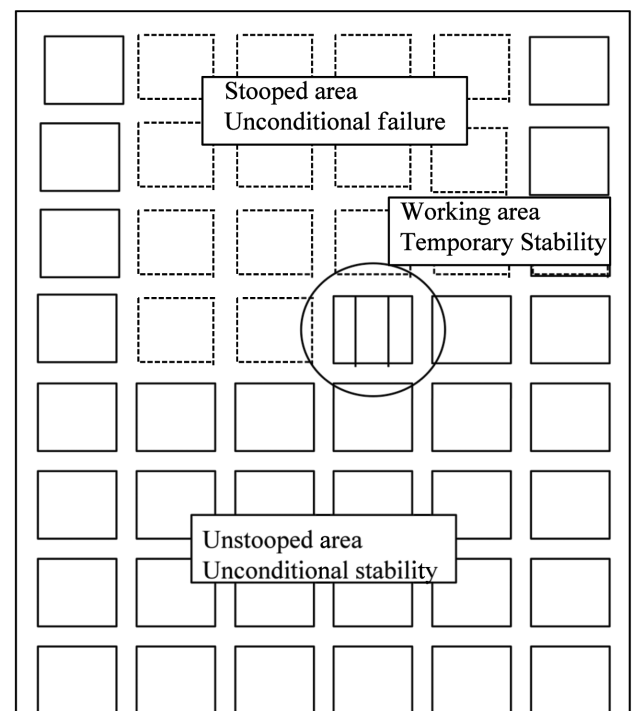

Figure 11. The three stability zones of the ideal stooping panel
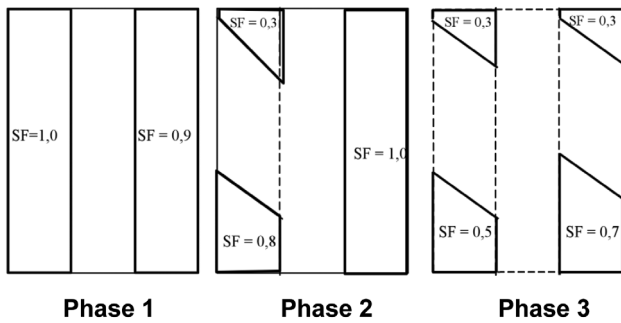
Figure 12. The three phases of mining a pillar showing the approximate safety factors of the snooks, with the loads calculated by numerical modelling

stability is required; and the unstooped area, where pillars have to be unconditionally stable—see Figure 11. To achieve the stability requirements, the pillars have to be of the right size prior to stooping and the stooping sequence has to be right.

The fundamental rock characteristic that is used for the system is that although stress change occurs immediately as a cut is made in a pillar, the failure process is time dependent. Stooping works in the time lapse between stress change and fracturing.

Snook sizes

Experience has shown that with a competent sandstone roof, snooks with a safety factor of 1 (with the loads calculated by means of pseudo three-dimensional boundary element programs) will be stable for a period of a few days. At 0.8 to 0.6 they will remain stable for a few hours, while at 0.4 or less they will fail almost

immediately. The roof characteristics play a dominant role in the failure of snooks. A stiff sandstone roof can cantilever for at least some distance for some time, say 10 to 15 m for an hour or more, which means that a snook is not necessarily fully loaded immediately.

The following example is valid for a mining depth of around 120 m. Once a pillar has been split, the safety factors of the two fenders (measuring say 6 m by 12 m) are about 1.0 to 0.9—see Figure 12. Upon extracting the fender closest to the goaf, the safety factor of the furthest snook (area say 4 m²) is about 0.3. The fact that it may fail very quickly is largely immaterial because by the time it has been formed, the continuous miner should be in the process of moving away from it. The snook closest to the solid should be marginally bigger. This should leave the continuous miner sufficient time to tram out of the split and around to the second fender.

The goaf side snook of the second fender should again be small, around 4 m², to have a safety factor of around 0.3. The final snook, i.e. the one on the second fender closest to the unmined pillars, should be the largest of the four, say about 10 m² with a safety factor of about 0.7.

Figure 13 shows examples of the fenders and snooks during extraction.

As mining progresses further away from these snooks, the load on them builds up, their safety factors decrease and eventually they fail. The ideal situation is for only the first line of snooks next to the unmined pillars to be visible. The ones further back should all have failed—see Figure 14. Figure 15 is an underground view of a well-designed snook system.

Figure 13. The fender on the left has a safety factor of around 1.0 and can be expected to be stable for a few days. The snook on the right has a very low safety factor, in the region of 0.3, and is failing. Note that in this case, the strong overhanging roof can protect the snook until the roof beam fails
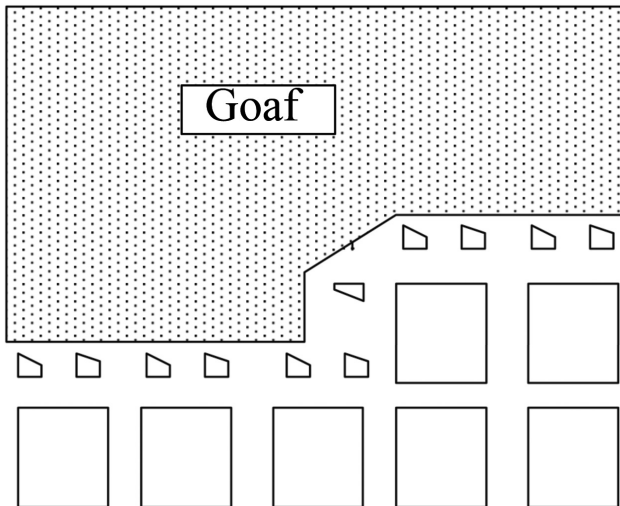
ROCK ENGINEERING FOR UNDERGROUND COAL MINING

Figure 14. The ideal stooping situation with only the first line of snooks visible, the ones further back all having failed

Figure 15. View of a well-designed snook system. The photograph was taken behind the last line of unmined pillars, just off the picture on the right. Note the line of snooks that are still standing, while the area behind them has goafed
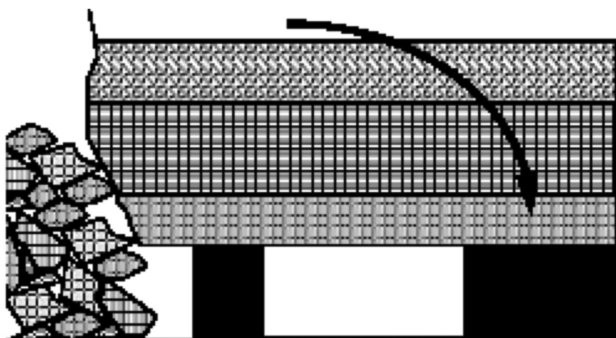

Figure 16. An unfailed snook causing increased stress on the unmined pillars

Note that the quoted dimensions in this section are ballpark figures, valid for a 3 m high mined seam at 150 m depth and should be adapted for panel width, mining depth, mining height, etc. The exact dimensions should be determined by using the procedures described earlier in this chapter or by a specialist using a three-dimensional stress analysis program, such as LAMODEL in the case of more complex geometries.

Once a snook has been created, the load on it will increase as the pillars adjacent to it are mined. The increased loads decrease the safety factors and this means that snooks in the mined area are more likely to fail due to two factors: increased loads and longer time.

Negative consequences of snooks that are too large

If snooks are too large they will not fail, even in the mined area. This is especially true if extensive roof falls around the snooks occur before they fail. The rubble provides at least some confinement to the snook, increasing its strength.

The problem caused by leaving an unfailed snook or pillar in the goaf is that it could prevent goaf development by supporting the roof—see Figure 16. Figure 17 is an underground view of a stooping area where the goaf is hanging up due to the presence of snooks that are too large. If the goaf does not develop, the weight of the overburden is distributed to the abutments. The increased stress on the pillars being mined will pose its own problems, which very often results in either another large snook having to be left or premature collapse. Either way, the ultimate result is premature collapse sometime or another.

Sizing of snooks using fundamental procedures

By their nature, snooks exist in the vicinity of larger, intact pillars where they are protected to at least some extent by the overhang of the roof. Very often, as long as the roof remains intact, the snooks will not be fully loaded, but will fail once the overhanging roof beam fails. This is a mutually supportive situation, as the snooks themselves contribute to the stability of the roof.

The contribution of the snook to the roof stability arises from the positive moment it supplies to the roof, considered as a beam with uniform loading and a with a point support underneath, see Figure 18.

Figure 17. Panoramic view of a goaf hanging up due to oversize snooks

Consider the situation where the total thickness of the overhanging roof beam is T and the pillar centre distance, or in this case the width of the roof beam, is b. According to van der Merwe (2005), the load on the snook as long as the snook is intact, F_{xi}, is given by

$$F_{xi} = \frac{3q}{2}\left(\frac{1}{2}\frac{a_h^2}{a_x} - \frac{1}{3}a_h + \frac{1}{12}a_x \right), \text{MN} \qquad [12]$$

where: $q =$ uniformly distributed load on roof
beam $= bpgT$

$a_h =$ total length of overhang

$a_x =$ distance of snook to edge of closest solid pillar

If the snook is situated at the furthest edge of the overhang, i.e. $a_x = a_h$, then

$$F_{xi} = \frac{3qa_h}{8}, \text{MN} \qquad [13]$$
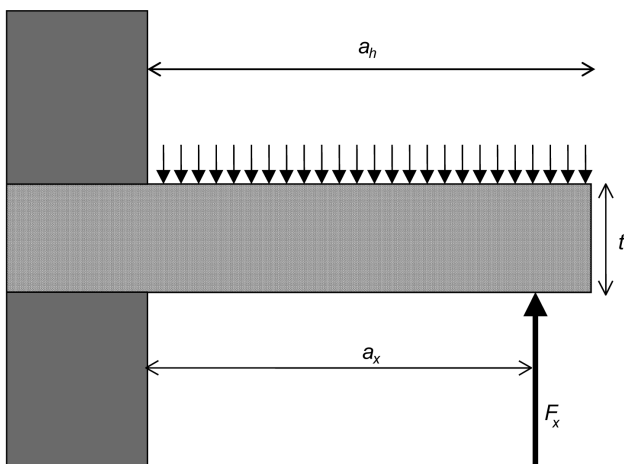
Figure 18. Conceptual view of the force diagram illustrating the contribution of a snook to the stability of the immediate roof. The immediate roof beam is shown here as a uniformly loaded cantilever while the snook is a point support underneath

The snook, however, has an upper limit to its strength, given by:

$$F_{xm} = 3.5\frac{w^3}{h}, \text{MN (Note that the units} \qquad [14]$$

are those of force, not stress)

where w is the snook width and h is the snook height.

If $F_{xi} > F_{xm}$, the snook will fail and then the reaction force becomes zero.

The fibre stress in the roof beam at the edge of the solid pillar depends on the moment supplied by two forces, namely the loading on the beam, which will result in a tensile stress, and the reaction force of the snook, which will result in a compressive stress.

According to van der Merwe (2005), the single expression for the stress (where compressive stresses are positive) is given by:

$$\sigma_{si} = \frac{q}{3bt}\left[\frac{a_h^2}{2} + \frac{a_x^2}{4} - a_h a_x \right] \text{MPa} \qquad [15]$$

as long as the snook is intact. Once it fails, the stress is given by:

$$\sigma_{sf} = -\frac{3a_h^2 q}{bt} \text{MPa} \qquad [16]$$

This procedure can be used to determine snook sizes that will be intact in the immediate vicinty of the closest unstooped pillar, but that will fail once stooping progresses to the next line of pillars. It is illustrated by a worked example in Appendix D: Pillar Extraction.

Direction of splitting

There are several variations of pillar extraction, see Beukes (1990). The exact method depends on factors such as the equipment that is used, roof conditions,

ROCK ENGINEERING FOR UNDERGROUND COAL MINING

seam thickness, sizes of the pillars, and panel width. In cases where a pillar is initially split at right angles to the roadway, the splitting direction is important.

A pillar should be split parallel or perpendicularly to the line of advance. Pillars should always be split in the direction of the overall advance, i.e. into the main goaf and not parallel to it. The reason for this is that the main fractures in the pillar develop parallel to the goaf, see Figure 19. If a pillar is split parallel to the main goaf, it means that the whole fender closest to the goaf will be weakened by the fractures.

If, on the other hand, splitting is correctly done, only the parts of the fenders closest to the goaf will be damaged. This latter situation is less serious because now the damaged portion is furthest away from the CM operator, and at least some of it will be left as a snook anyway. The fractures will then assist in crushing the end snook, which is beneficial.

It is not essential to split a pillar at exactly 90°. While this is the ideal, it has to be balanced against the speed of extracting a pillar, which is of great importance. If a pillar can be extracted more quickly by splitting at say 80°, it should be tolerated. It remains important, however, to split through the central core of the pillar so as to leave two equally sized fenders. This remark must not be taken to mean that pillars can be split diagonally across corners, which should be done only under very special conditions such as shallow workings, very strong roof, etc.

The major objection to splitting a pillar diagonally under weak roof conditions is that it increases the size of the intersection and could result in roof falls, trapping the miner inside the pillar. However, if roof conditions permit, the 45° split can be done much more quickly as it requires less intricate continuous miner manoeuvring.
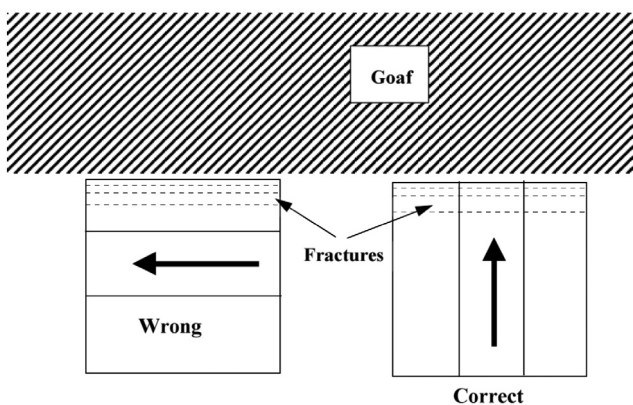
Sequence of fender extraction

As with the direction of the initial pillar split, the sequence of fender extraction is a function of several variables. There are no hard and fast rules, but at least one principle is generally applicable: always mine toward the largest solid. The further away from the nearest solid a pillar is, the higher its load because it gets less assistance in load bearing. Also, the smaller the pillar, the higher its stress.

For instance, in extracting a fender, starting nearest to the solid and mining towards the goaf means that two factors combine to increase the stress on the snook. As it gets smaller, it also gets further away from the solid.

Doing it the other way around, i.e. starting at the furthest point and mining towards the solid, means that as the snook gets smaller, its centre moves closer to the solid. Although the snook itself does not get physically moved towards the solid, at least its free end (the one facing the goaf) is closer to the solid each time a cut is made—see Figure 20 as an illustration of this principle in the case where a pillar is split perpendicularly to the roadway.

Where rectangular pillars are left, they should preferably be orientated with their long axes parallel to the goaf, as shown in Figure 21. In this way, they are split more than once, again into the goaf. The advantage of this is that the splits are shorter, as opposed to splitting along the long axes of the pillars.

Figure 19. Pillars should be split in a direction perpendicular to the main goaf line, not parallel to it
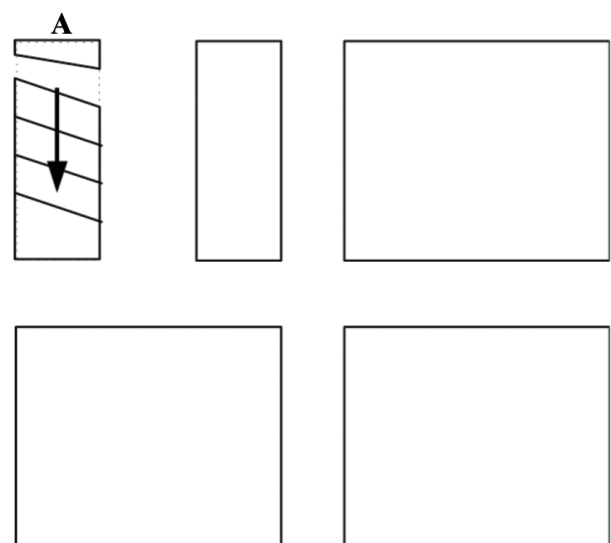

Figure 20. The fact that the fender gets progressively smaller as mining progresses, is offset somewhat by the fact that it gets closer to the solid pillar. The snook at A is in the process of failing and does not count as solid

Splitting along the long axis increases the risk of instability. It is important that the splits should not be predeveloped, i.e. each fender should be extracted immediately after the split has been completed. The reason for this is not to leave the fenders with low safety factors standing for an extended period before they are mined.

The general principle of mining towards the solid also applies to extracting a pillar using drill and blast. Figure 22 is an example of the sequence of pillar extraction of a 25 m wide pillar with drill and blast. The reason for the non-sequential way of mining is to cater for the mining cycle in drill and blast operations.

Support during stooping (see also Chapter 3: Roof support)

Historically, the only specific roof support in coal
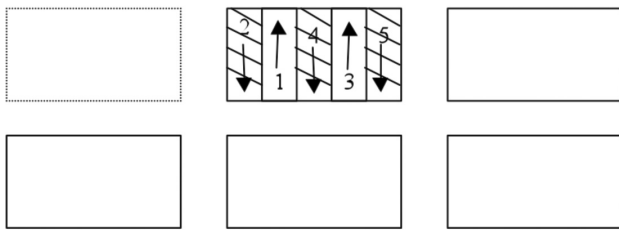
Figure 21. Sequence of extracting a rectangular pillar
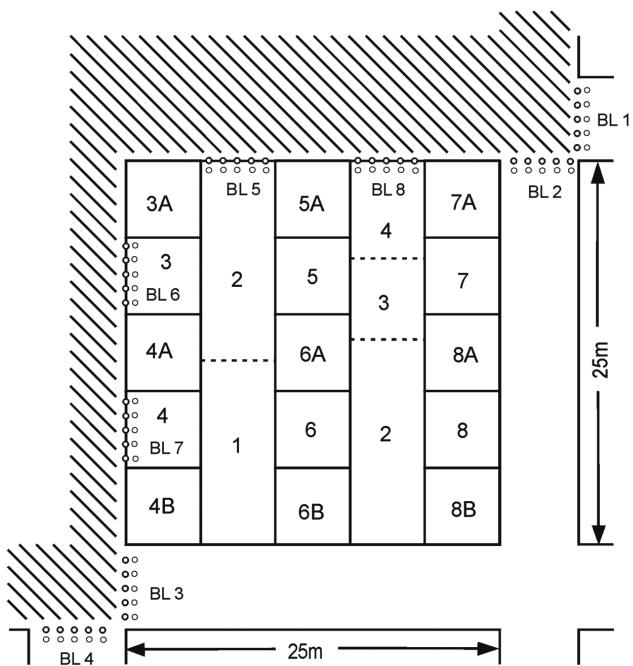
Figure 22. Conventional drill and blast sequence of extraction of a 25 m pillar

mining that has been required in terms of the regulations, is that a double line of props, spaced not more than one metre apart, shall be placed between the workings and the goaf, not more than one metre from the solid pillar edge. In the past, timber props were almost exclusively used.

Timber breakerlines

The vast majority of breakerlines consist of timber props. Little use has been made to date of hydraulic props, mainly due to the mass of the long props in high seams and the possibility of losing these in the goaf, which would prove very costly. While alternatives to timber props are now being used, they are often supplemented by at least one timber prop—called a 'policeman prop'—because of the audible and visual warning signs they exhibit prior to failure.

Mobile mechanical breakerlines

The use of mobile mechanical breakerlines, which was pioneered in South Africa, has gained ground worldwide in pillar and rib pillar extraction. The main problem with these breakerlines is the high initial capital cost and the need for an even floor for them to operate on. They were pioneered by the Sasol Company to replace timber props at high mining heights. Figure 23 shows timber props at high mining heights.

In Australia mobile breakerlines are used in increasing numbers in both rib pillar and pillar extraction. The common method is for three breakerlines to be used in conjunction with a remote controlled continuous miner. The miner lifts both left

Figure 23. A timber breakerline installed in a pillar extraction section at high mining height. The effectiveness of such a breakerline is questionable

and right in front of the breakerlines. This system has been developed to reduce the support required on primary development and to maintain the miner in the extraction of ribs, which is the most productive. The introduction of this method has resulted in not only safer conditions but also in greater percentage extraction due to operators being less exposed to the effect of the goaf. The latter results in fewer problems with goaf hang-up, which improves working conditions and increases productivity.

Roofbolt breakerlines

Roofbolt breakerlines, MacGosh *et al.* (1989) are being used successfully on South African collieries with both competent roof strata and laminated, incompetent roof strata. An example is shown in Figure 24. Although roofbolt breakerlines differ from the other two types mentioned, as they function according to the beam formation theory, they have been successful to date in preventing the goaf from extending into the working area in the collieries where they are used.

Figure 24. A roofbolt breakerline before the goaf (top picture) and the same one after the goaf (bottom picture). The chevron tape hanging from the roof indicates the positions of the roofbolts. Note the 'policeman sticks' in the upper picture

The main advantages of roofbolt breakerlines are:
• Low cost compared to alternatives
• Can be installed during the development phase, meaning that people are not exposed to the goaf during installation, as with standing props
• No disruption to the mining activities
• Independent of mining height, while timber props have to be thicker the longer they are.

Determining pillar sizes for stooping

Determining pillar sizes for stooping is a complex matter, depending on several variables. The extraction safety factor concept caters only for the minimum pillar size to prevent pillar collapse during stooping. It takes cognizance of the overburden characteristics and panel width, but it does not take account of the other factors such as the equipment that is to be used and the need for speedy extraction of pillars.

With narrow drum width CMs (nominally 3 m wide cutting drums) it is preferable to mine pillars with dimensions in multiples of 3, such as 18 m wide pillars. Pillar widths are then determined by performing a calculation (such as the ESF procedure) to determine the minimum width and then adding to that minimum size to arrive at a pillar that suits the equipment. For consistency of the method of pillar extraction, some mines prefer to design a pillar that will suit the worst conditions and then to implement that size on the mine as a whole.

It is not only the width of the cutting drum that needs to be taken into account when designing a practical pillar size, but also the length of the CM. The length of the machine will determine the ease with which it can turn in any given road width. It is, for instance, unrealistic to expect a long CM to perform a 90° cut into a pillar with a road width of only 6 m. The best pillar size is arrived at by good communication between the rock engineering specialist and his production colleagues on a mine.

Figure 25 illustrates the interaction between the factors that have to be taken into account when designing pillars for stooping.

Rate of extraction

The pillar size and panel width have bearing on the rate of extraction of pillars. It is important to optimize this rate. As explained previously, successful pillar extraction depends on utilizing the time between stress change and the onset of fracturing. This can be termed

dynamic stability, implying that stability is maintained as long as the operation remains dynamic.

However, large, intact snooks or even entire pillars should not be left unmined to maintain a given rate of advance. The negative effects of doing that far outweigh the positive effects. If there is good reason not to extract a pillar to the required (i.e. designed) extent, attempts should be made to destroy it.

Far too often, leaving an intact snook results in overloading of the next pillar to be mined. This either results in collapse of the pillar during extraction or damage to the roof, necessitating another large snook to be left, or even an entire pillar to be skipped. This is a vicious circle that can result only in failure. If conditions necessitate a pillar to be skipped, it is often good practice to leave an entire line of pillars (or two lines, depending on the magnitude of the load) and to start over.

The panel width has to be designed taking cognizance of the desired width either to result in overburden failure or to protect it, coupled to the rate at which the pillars can be extracted. The wider the panel, the longer the shuttle car tramming routes become and consequently the slower the rate of extraction will be. This will seldom decrease the rate to the extent that instability will occur, but it has to be considered, especially in cases where the rate cannot be increased by adding more shuttle cars to the operation.

The other alternative to increase the rate of extraction, which should be approached with caution, is to extract pillars with double header sections. The
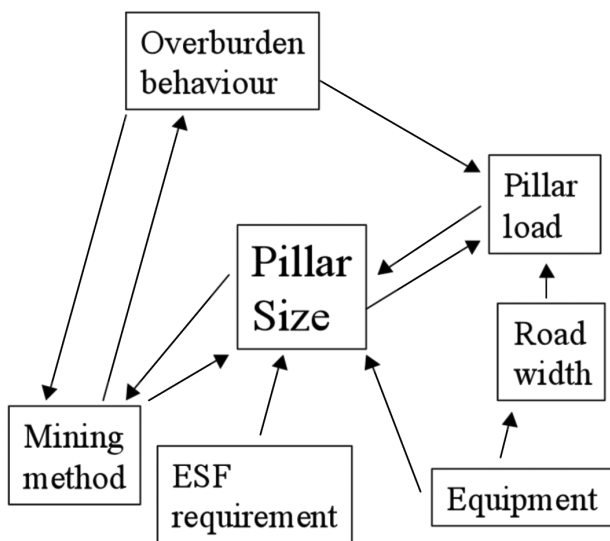
risk in this type of operation is that it is difficult to maintain the correct sequence between two CMs. If it has to be done, it is important to maintain the relative positions between the machines, as shown in Figure 26. Problems arise when one of the two machines breaks down or when one crew simply performs better than the other one. Instead of allowing the better crew to mine away from their colleagues, the situation should be rectified by reallocating the number of pillars to be mined by the respective crews, even if only temporarily.

For instance, when mining from left to right, the left-hand section should lead by one line of pillars. If there is no lead, the left-hand section will end up trying to extract a pillar that has been isolated when it reaches the centre of the panel. If the lead is more than one line of pillars, the final pillar the left-hand section has to mine in the centre of the panel will be overloaded. Either way, the centre pillar will be difficult to extract and will be skipped more often than not. This unmined pillar in the centre of the panel will have the same detrimental effect as an oversized snook.

The same basic argument holds for the converse situation, when mining from right to left.

Mining left to right
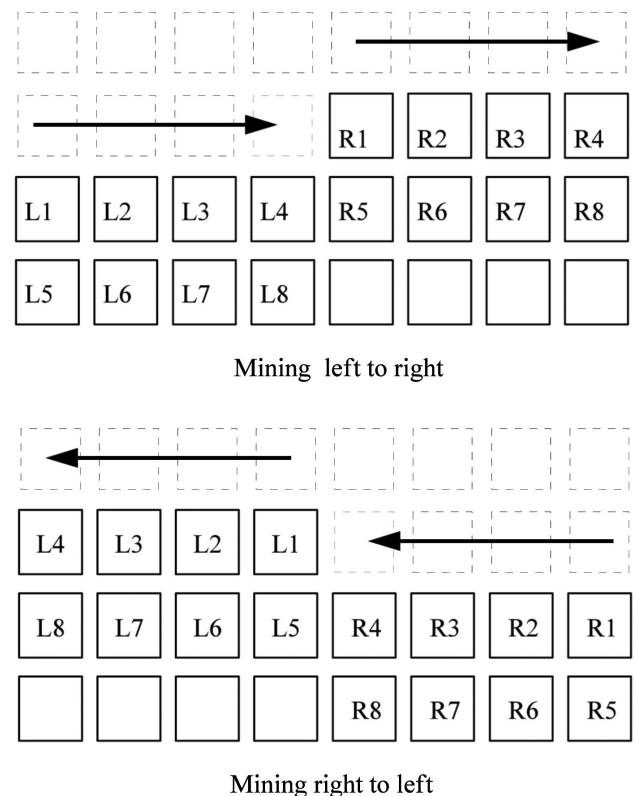

Mining right to left

Figure 26. Correct sequence for stooping with a double header section. The prefix 'R' indicates pillars to be mined by the section on the right-hand side and 'L' the left-hand section

Figure 25. Interaction between the factors that have an impact on pillar sizes for stooping

Influence of the face advance on the stress regime

As explained earlier and in Chapter 6: Longwalling, high extraction mining is characterized by a varying stress environment. Initially, the pillar stress is at the same low level as during development. As the face advances, the overall stress increases until the major goaf occurs. At that time, there is a decrease in stress. If the overburden remains intact, as when there is a strong layer such as a thick dolerite sill in the overburden, the stress will stabilize at the higher level. This stress history is conceptually shown in Figure 27.

Against this background, each pillar that is extracted has its own stress cycle as the pillar gets progressively smaller. The three main phases of stress, the building-up phase, the transition phase and the stable phase, each has its own consequences underground.

The build-up phase

Each successive pillar is subjected to a higher stress than the previous one. During this phase, say the first 100–150 m of the panel, one should be aware that the stress is going to increase and that joints are going to behave progressively worse. Ribsides are going to spall progressively more. The vice is getting tighter all the time.
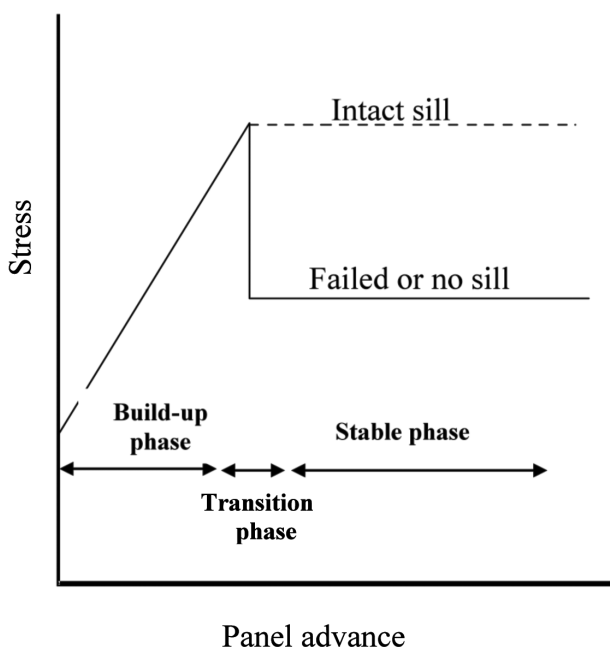
Figure 27. Conceptual variation in the stress on the front line of pillars with an advancing face

The transition phase

The intermediate or transition phase (when the first real goaf falls) is perhaps more serious. Pillar extraction ventilation is much more dependent on ventilation stopings than longwalling, and the windblast can have a far more serious effect on ventilation. It is during, and just before, this occurrence that the stress reaches maximum levels and consequently this is the time when things can go wrong. Several continuous miners have been buried just about at the time when the advance is equal to the mining depth (or, for that matter, to the panel width).

Immediately after the goaf has come down, the stress is relieved to some extent. This is also the time when fractures which were formed during the maximum stress period will open up due to the relaxation. The clamping effect is now somewhat less. The roof may be less noisy but the joints will fail with less warning.

The stable phase

During this phase, things should start stabilizing. The stress levels will be more consistent. The bad news is that, if the panel is too narrow to let the overburden fail, the stress reduction due to the goaf collapse will not occur. There are more cases than one on record where a conventionally calculated safety factor of over two was insufficient to permit stooping, all because of the high stress caused by the intact overburden. At the other end of the scale, carefully planned and executed stooping with safety factors below 1.5 has been successful where the overburden has failed.

During this phase, stress build-ups will occur periodically as the overburden hangs up from time to time.

Partial pillar extraction

In order to protect the overburden where wide panels are to be stooped, partial pillar extraction has been carried out. It has also been done in high coal-seams, where the pillar stresses generated by more complete stooping could result in excessive sidewall spalling.

There are currently two popular methods of partial pillar extraction, namely, chequerboard extraction and pillar splitting. In general, the design of partial pillar extraction requires a sound understanding of the concept of stiffness.

Chequerboard stooping

Chequerboard extraction with a continuous miner has

been used and has been found to be superior to conventional pillar extraction in many ways, Oldroyd and van Rooyen (1999). In particular, it results in higher productivity and reduced costs. Figure 28 shows an example of this method as developed for good roof conditions. Every other pillar is almost entirely removed. Only three small snooks are left and no breakerlines or fingerlines are set. A few mine poles are set mainly as policemen. Large open spans are created during mining and the method is suited to very competent roofs. In some areas where pillar widths are sufficiently wide, every other pillar is removed and an additional cut is taken across the corner of the remaining pillar. If correctly done this allows the pillar to support the overburden and thus prevent goafing.

The obvious danger in chequerboard stooping is uncontrolled violent collapse of the pillars remaining in the back area. Due to the stress increase, failure of those pillars cannot be prevented, except by leaving unacceptably large pillars. The failure mode can be controlled by balancing the stiffness of the pillars and the loading system.

Neither of these two parameters is easily determined. However, estimates can be made and analyses carried out, as shown earlier in this chapter. While the methods to determine the post-peak stiffness of coal pillars vary to some extent, there is consensus that at width-to-height ratios greater than 4.08 to 5.0, the post-peak slope of the load/deformation characteristic is zero and that at greater width-to-height ratios, it becomes positive.

As the loading system can have only a negative slope, at worst becoming zero if the overburden fails completely, the pillars can fail only in a stable fashion when width-to-height ratios are greater than 5.0.

There are indications from the test results analysed by Ozbay and from observations at ZAC and Emaswati Collieries (Oldroyd and Buddery 1988) that post-peak
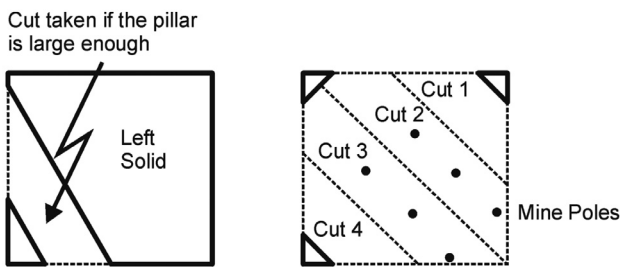
stiffness for coal pillars may well turn positive at width-to-height ratios below 5.0. This corresponds to van der Merwe's (1998b) conclusion that the stiffness becomes zero at a width-to-height ratio of 4.08. This would be very significant for yield pillar design and would enable safe yield pillar designs at lower width-to-height ratios.

Local stiffness can be determined in an elastic medium by using any of the two-dimensional computer models and is simply defined as force divided by displacement.

It was shown by Oldroyd and Latilla (1999) that at a certain stage, failed pillars resume their load bearing capacity, shown in Figure 29. In this case, over a metre of closure was required to achieve a situation where movement ceased. In the process the roof separated along joints and faults, thus behaving inelastically.

Cost savings achieved with continuous miner, chequerboard mining are achieved largely through the reduction in the quantity of timber props used and the labour required to install these. Oldroyd (1999) states that an 80% reduction in timber prop finger and breakerlines has been achieved in the chequerboard method. The labour requirement for installing timber in a chequerboard stooping section drops from five in stooping to three. Productivity in chequerboard panels has been shown to be around 12% greater than in normal stooping sections.

It can be argued that the productivity and safety gains come at the expense of reduced percentage extraction, but this is not necessarily the case. Taken at face value, the differences in percentage extraction measured over two pillars is 56.3% with chequerboard compared to 98.3% with stooping. However, it is well known that additional losses occur in stooping when portions of pillar, whole pillars or even rows of pillars are left behind for various reasons.

Figure 28. An example of checkerboard mining with a continuous miner
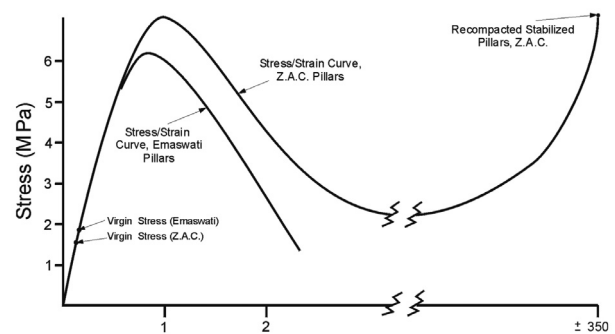

Figure 29. *In situ* stress-stain curve, after Oldroyd and Latilla (1999)

Most of these are associated with poor roof and potential goaf overruns. For these reasons secondary percentage extraction in stooping is at best 75% and more likely 70% or lower. It has been estimated to be as low as 60%. In chequerboard mining unplanned losses of pillars, due to potential goaf overruns, are unlikely and the planned percentage extraction is more likely to be achieved. Nonetheless, some losses are inevitable and a secondary extraction figure of 50% of the pillars is more likely. There is thus not a major difference in the overall extraction ratios that can be achieved.

Pillar splitting

At high mining heights, in excess of 4 m, stooping can be dangerous due to the increased risk of sidewall spalling. To overcome this problem, certain mines have started splitting pillars instead of stooping. This system entails mining a single or double cut through a pillar, leaving large remnants behind, as shown in Figure 30.

In broad terms the percentage of coal that is left behind does not differ from that in chequerboard stooping and consequently the pillar loads are more or less the same. However, the shapes of the pillars are different. In pillar splitting it is much more difficult to maintain a satisfactory w/h ratio of the pillar remnants in order to satisfy the stiffness requirement.

For example, consider the case where 20 m square pillars are mined with 6 m bords at a mining height of 4 m and depth of 150 m. The safety factor prior to secondary mining is 1.8.
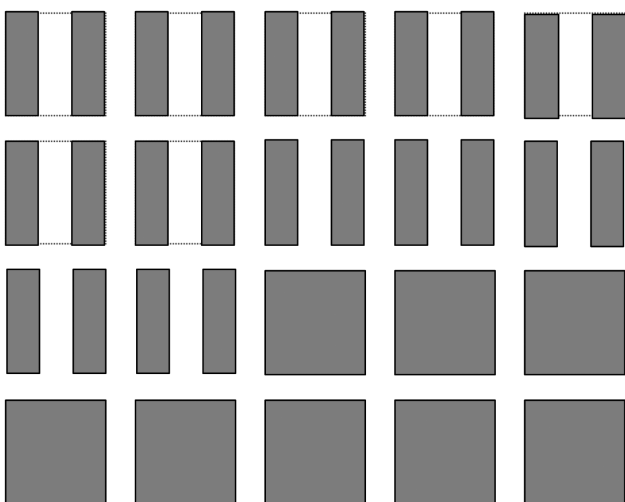

Figure 30. Diagram illustrating the concept of pillar splitting

After chequerboarding, the safety factor decreases to 0.9 (the pillar stresses double but the strengths remain the same), which implies that failure can be expected. However, the w/h ratio of the pillars is 5.0 and therefore the failure can be expected to be non-violent. This will be the case even if the system stiffness is zero, which is the worst situation.

If the same pillars are split by a 6 m wide cut through the centre, the safety factors of the remnants decrease to less than 0.9 (the pillar stresses double and the strengths are reduced) and failure is more likely than with chequerboard stooping. However, in this case the w/h ratio of the remnants is only 1.75. This is well below the minimum requirement to prevent violent failure, and thus violent failure is likely to occur.

The only condition under which violent failure can be prevented in this example is if the loading system is stiffer than the post-peak stiffness of the pillars. Using Equation [9], the post-peak stiffness of the pillars is approximately –1.3 GPa. The stiffness of the loading system is very difficult to determine and therefore this situation cannot be easily evaluated in a quantifiable manner. The designer has no option but to rely on guesswork.

It is known that the system stiffness is influenced mainly by the overburden characteristics and the panel width. An environment with thick sandstone layers is stiffer that one with softer shale layers. The only control parameter underground is to restrict the panel width.

A false sense of security may prevail if pillar splitting is done with a restricted panel span underneath thick sandstone or other strong beds. The overburden may be able to bridge the panel and restrict the extent to which the pillars are compressed. The pillars underground will then apparently stabilize, creating the false impression that they are able to support the overburden. This situation will reverse suddenly and dramatically the moment an unseen weakness in the overburden, such as a joint zone or a slip, is present. The pillars will then fail violently without any warning signs.

Pillar splitting is a risky operation and should be avoided if the w/h ratio of the post split pillars is less than about 4.0. To achieve this, it will be necessary to leave very large pillars on the advance and everything will probably be simplified significantly by optimizing the extraction ratio on the advance and leaving matters at that.

If splitting has to be done, the situation can be controlled to some extent by limiting the panel width

and further controlling the mined span by leaving lines of pillars unmined. However, this method needs to be meticulously engineered and should not be embarked on lightly.

The NEVID method

A partial pillar extraction method that has become popular in recent times is the NEVID method, named after its developers, Neels Joubert and David Postma who were both with Sasol Mining at the time. From a rock engineering viewpoint, it is essentially a variant of pillar splitting as the pillars are not extracted completely.

Great care was taken to ensure maximum stability in the development of the sequence of extraction, taking cognizance also of the positions of cable handlers and miners to place them outside the areas likely to collapse. The sequence of cutting is shown in Figure 31.

The sequence is such that only one large intersection is created per pillar, namely that between Cuts 4 and 5 (also Cuts 7 and 8 for the next two pillars) on Figure 31. However, that is the final cut in the sequence between two pillars and little time is spent in that area.

The initial design, incorporating the important aspects of the sizes of the snooks, was based on local knowledge and sound judgement. The dimensions obtained are thus valid only for specific conditions and application elsewhere will need adaptation.

The basic principles applicable to stooping remain valid for this method as well, i.e. the snooks have to be stable initially but they have to fail eventually. The design process described earlier in this chapter and also the modelling procedures described in Chapter 9 should be followed when making adjustments.

It is common practice to leave one or more lines of pillars in place as stopper lines, as safeguards against pillar overruns. The number of pillars and their spacing should be determined by modelling, taking care not to space them so closely together that overburden failure is prevented.
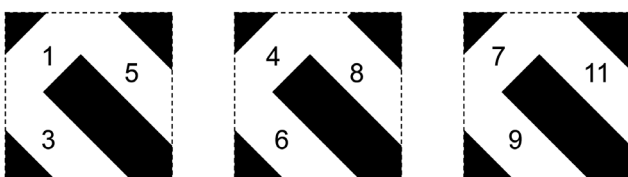
Evaluating old pillars for extraction (see also Chapter 8: Shallow workings)

Towards the end of the life of a mine there is often a possibility of extracting pillars that were not designed for extraction. Even if they were, extraction of old pillars should not be carried out before a detailed investigation has been done.

Over time, the pillars may have become weakened due to weathering. Almost invariably, there would have been scaling and the roads would be wider and the pillars smaller than at the time of mining. The older the pillars, the worse the ageing effects would be, see Figure 32.

In situ inspection of the workings is an essential part of the investigation. The roof stability should be evaluated, as it is likely that the supports would have lost efficiency over time. The floor should be checked for signs of floor heave, as shown in Figure 33, as moisture over a long period could weaken the floor.

The pillar dimensions should be checked. In most cases it will not be possible to do a direct comparison of 'as mined' and current safety factors, so a statistical approach is called for. The road width should be measured at at least 200 spots in a panel and a distribution curve should be constructed, as shown in Figure 34. This should be compared with a similar curve taken from the survey records, which should still be available, except perhaps in the case of very old mines.
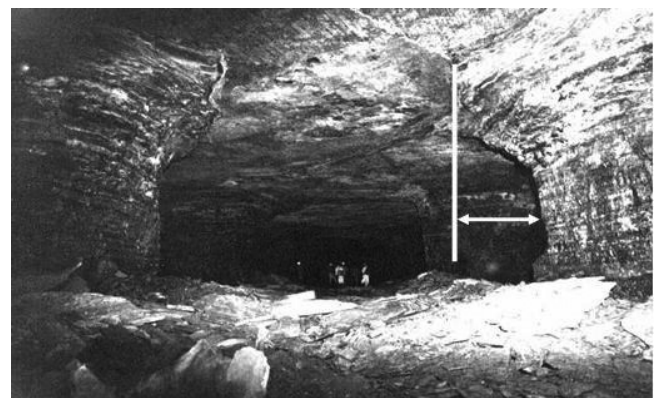

Figure 32. View of pillars that are approximately 100 years old. Note the extent of scaling that had taken place over time

Figure 31. The sequence of cutting for the NEVID method

The difference between the distributions can be used to get a feel for the extent to which the pillars have been weakened. The scatter should also be taken into account, by comparing the standard deviations of the two populations. The new dimensions should then be used in the calculation of the ESF.

If at all possible, it is better to obtain the amount of pillar scaling that has taken place by direct measurement. This is not always possible, as it becomes increasingly difficult to determine the original ribside positions as sections get older. The reason for this is that cases have occurred where the 'new' roadway widths are smaller than the original ones, casting doubt on the integrity of the original measurements.

Essentially the same precautions as for normal stooping operations should be observed, but they should be tightened up, bearing in mind that one is probably dealing with weaker than normal coal pillars. There is unfortunately no satisfactory laboratory method to determine the strength of coal pillars. The difference in the distributions of road widths is very important in this respect as it offers at least some feel for the weakening of the pillars.

In the case of very old, shallow mines, one should be particularly careful. The pillars will be much smaller than normal and the panels would be wide. Therefore the system stiffness will be low, increasing the risk of violent pillar failure. If inter panel pillars are absent, consideration should be given to filling selected lines of pillars with ash or other suitable material to create artificial barriers. Individual pillars can also be strengthened by strapping with wiremesh or discarded conveyor belt, as shown in Figure 35, but the effects of doing this, while known to be beneficial, are difficult to quantify. At shallow depth snooks are less likely to fail, and attempts should be made to destroy them.

If stooping is to be carried out, it should begin in an area where the overburden is most likely to fail, for instance by retreating away from a major discontinuity or an existing goaf. Once it has failed, the overburden usually continues to fail more easily than initially. The reason for this (refer to Chapter 1: Fundamentals) is that the overburden beams change from being clamped beams to cantilevers once the first failure has occurred.

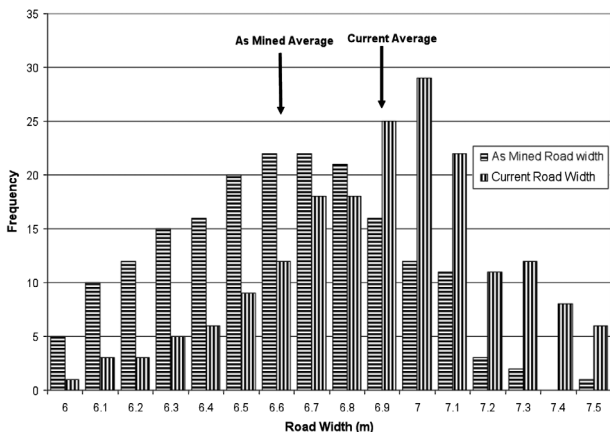**Figure 33. Example of floor heave in old workings**

Figure 34. Comparison of 'as mined' and current road widths

Figure 35. An old pillar that has been stabilized by wrapping with discarded conveyor belting

General remarks

The most stable mining method is properly designed bord and pillar mining, which is also the least desirable from a reserve utilization point of view. Beyond that, the potential for instability increases as the reserve utilization is improved by using high extraction mining methods. However, instability does not necessarily occur as a result of increased extraction. What is required for increased extraction without increasing the risk to people or property to unacceptable levels, is proper design of the workings.

Extracting pillars, either totally or partially, without taking cognizance of the overall environment and implementing sound rock engineering principles is uncontrolled stooping. Uncontrolled stooping is reckless. It can lead to unnecessary damage to property or injury to people.

In general, pillar extraction means moving closer to the point of instability than mining with bord and pillar methods. However, it is not done blindly; the miner has the advantage of prior knowledge of ground conditions, gained during the advance phase of pillar development. This knowledge should be used to supplement the science that is described in this book.

Increased extraction of coal need not come at the expense of stability. It should come after detailed investigation and implementation of proper designs based on sound judgement and the application of engineering principles within an acceptable risk framework.

Longwalling

Introduction

In this chapter, the term 'longwalling' means mechanical mining under the protection of shields. It thus includes shortwalling, which is done with the same equipment but shorter face lengths. Where a normal longwall face length is of the order of 200 m, shortwall face lengths are in the region of 50 to 100 m. The rock mechanics of a shortwall is similar to that of a longwall, but often under the conditions of an overburden that has not failed through to surface.

Longwalling in South Africa has met with mixed fortunes. Few would doubt its benefits as a mining method under favourable conditions; fewer would dispute its problems under unfavourable conditions. Conditions in this context refer more to the macro geology than to micro ground conditions. Dykes are fairly common occurrences in the South African coalfields and while there are a number of methods of dealing with dykes in a longwall, they are expensive and they slow mining down. The occasional dyke does not present a serious problem, but where the frequency increases, a more flexible mining method is called for.

As with pillar extraction, the rock mechanics of longwalling in South Africa is dominated by the status (i.e. failed or intact) of the dolerite sill or another strong layer where it is present. The sill is an igneous intrusion in an otherwise sedimentary environment. The dolerite material is significantly stronger and stiffer than the surrounding rock types. It often has the capability to bridge over panels of common mining dimensions.

Where this happens, significantly higher vertical loads result than in cases where it has failed or where it is absent. These increased loads are borne on the face, and inter panel pillars, with a number of advantages and disadvantages to mining.

However, it is important to note that the loads do not result from the sill, but from the fact that the sill prevents failure of the overburden. Therefore, the same effects will result from any other geological or mining condition that does not result in overburden failure. There are, for instance, areas where at least one—and often more—of the overburden layers is a thick, massive sandstone that can also bridge a panel and thereby cause the same high stress levels that are associated with an intact dolerite sill.

Failure of the sill has been studied and there are methods whereby its status can be predicted. The same cannot be said for the massive sandstone situation. The reason for this is that it is virtually impossible to judge the condition (massive or jointed) of sandstone from vertical exploration boreholes, while the presence of dolerite in a borehole is self-evident. More often than not, one becomes aware of the presence of a massive sandstone only after mining has started in a particular geotechnical area.

This chapter is primarily devoted to the rock engineering of working retreat longwalls. Other important matters such as shield design and choice of equipment are more specialized, being vitally important at the stage when consideration is given to the purchase of a longwall. For those purposes, readers are referred to the bibliography.

It should also be noted that the discussion to follow is restricted to the common South African situation, where the depth of mining is 200 m or less and face lengths are up to 300 m.

Stress history of a longwall panel

As a longwall face mines away from the start-up position, it is characterized by increasing vertical stress. The stress continues to increase until either one of two things happens, the overburden goafs completely, or the face advance equals about one and a half times the panel width. When the overburden fails completely, there is a sudden decrease in stress—however, if the overburden hangs up and the face advance is greater than the panel width, the stress merely stabilizes at the high level.

The reasons for the stress history are explained in

Figures 1 and 2. At the initial stages of mining, falls occur in the back area. These are minor falls, often referred to as the small goaf, extending some distance into the roof, depending on the roof geology. The bulk of the roof initially hangs up, and it is this weight that is transferred to the face and the inter panel pillars.

It is only when the overburden fails completely—when the major goaf occurs—that its weight is transferred to the goaf, relieving the loads on the face and the inter panel pillars. The development of the goaf and the subsequent surface subsidence are covered in Chapter 10: Subsidence.

Complete failure of the overburden may be prevented by two mechanisms: firstly, there could be an intact dolerite sill (or other strong layer), or secondly, the mining span may be too narrow for the mining depth to result in total failure. The goaf edges are not vertical, but inclined over the goaf. Thus, the higher the goaf, the narrower its top. It is possible for the span at the top of the goaf to become too narrow to allow failure of the overburden layer immediately above it. This mechanism is the larger-scale equivalent of a roof fall that has 'wedged out'.

In South Africa, it is common for the major goaf to occur at a face advance of approximately 150 m to 200 m where there is no dolerite, although there are no hard and fast rules for this.

A conceptual figure of stress history with increasing face advance is shown in Figure 3. In this figure, the sudden stress drop at point A occurs when the overburden fails. The stabilization at point B occurs under the conditions where the overburden is prevented from failing by, for instance, the presence of an intact dolerite sill. The stress peaks shown as points C, are due to sporadic goaf overhangs.

Inter panel pillar design and longwall development

In retreat longwalling, inter panel pillars are primarily provided to protect the gate roads while they also serve as gas and water barriers. Inter panel pillars are designed according to their function and the loads expected to be imposed on them. There are several basic options, ranging from solid pillars to chain pillars, to bearing pillars with crush pillars, to crush pillars only.

If pillars are to serve as gas and water barriers as well as to stabilize the gate roads, solid pillars have been used, but they require double the amount of development as one panel's maingate cannot become the next panel's tailgate. If successive panels are to progress up dip so that water runs back into the old panels and gas does not present a problem, chain pillars are usually used.

The sizes of the pillars can be determined using two-dimensional numerical models for situations where the sill is not expected to fail. Figure 4 illustrates the basic principle to be used. Once the load has been calculated, the width can be determined to result in a safety factor of not less than 1.4 using an appropriate pillar strength formula; see Chapter 4: Pillars.

For final design, the load should be determined by suitable pseudo three-dimensional numerical modeling; see Chapter 9: Modelling. If the overburden fails completely, the load situation is different. The pillars then bear the load of the overburden directly above them plus the overhang, which has been determined from subsidence studies to be approximately 15° off the vertical, inclined over the goaf. There are a number of numerical codes that can be used for this purpose.
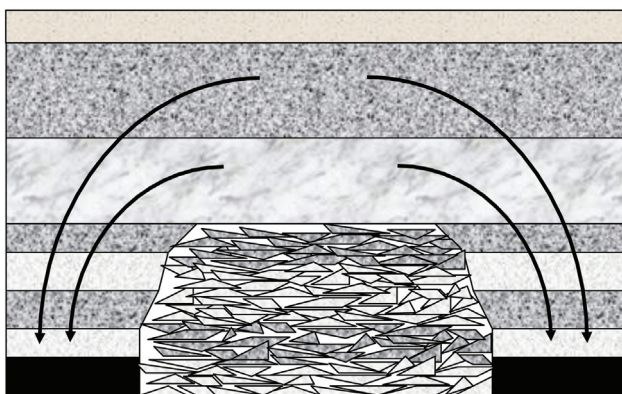

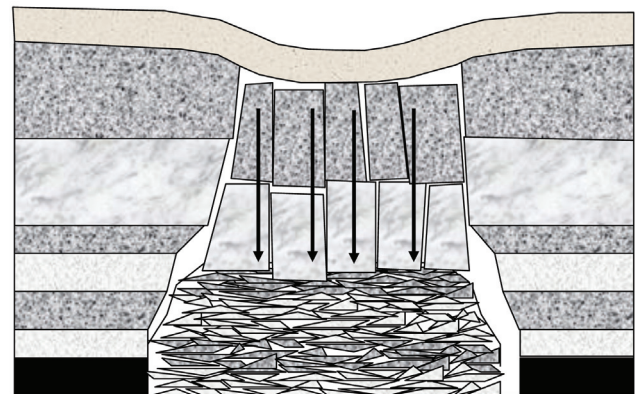**Figure 1. The weight of the bridging overburden is transferred to the abutments**

Figure 2. Once the overburden has failed, its load is transferred to the goaf. The abutments are now stress relieved
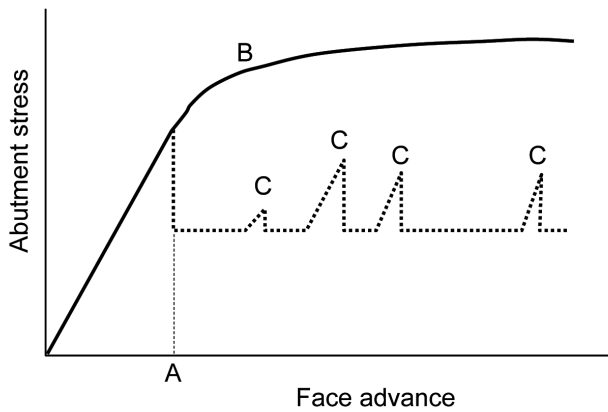
ROCK ENGINEERING FOR UNDERGROUND COAL MINING

Figure 3. Conceptual curves of stress as a function of face advance. The solid line indicates the situation where the overburden remains intact and the broken line indicates the stress levels for an overburden that fails when the face advance is equal to 'A'
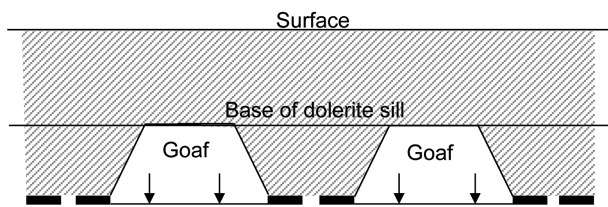

Figure 4. Explanation of the loading system on inter panel pillars for a longwall without a complete goaf, such as where an intact dolerite sill is present. The shaded area represents the area supported by the pillars

Even in cases where the overburden fails, the pillars at the beginning of the panel will be subjected to high loads. It is common for those pillars to be longer than the ones beyond the position where failure is expected, see Figure 5.

In longwall development, there has to be a balance between reserve utilization and rate of advance. The most successful longwall mines tend to be the ones where utilization is sacrificed for the sake of speedy advance. If the aim is rate of advance, roadways will be as narrow as possible, which will improve (or at least not compromise) the stability of the roadways during longwall production. Ventilation requirements and regulations differ from country to country and area to area and this often overrides other considerations in longwall development design. In South Africa, three road development is common although there have been instances of two road development.

For situations that are characterized by weak roof, yield pillars have been designed in conjunction with larger bearing pillars, see Figure 6. The mechanism
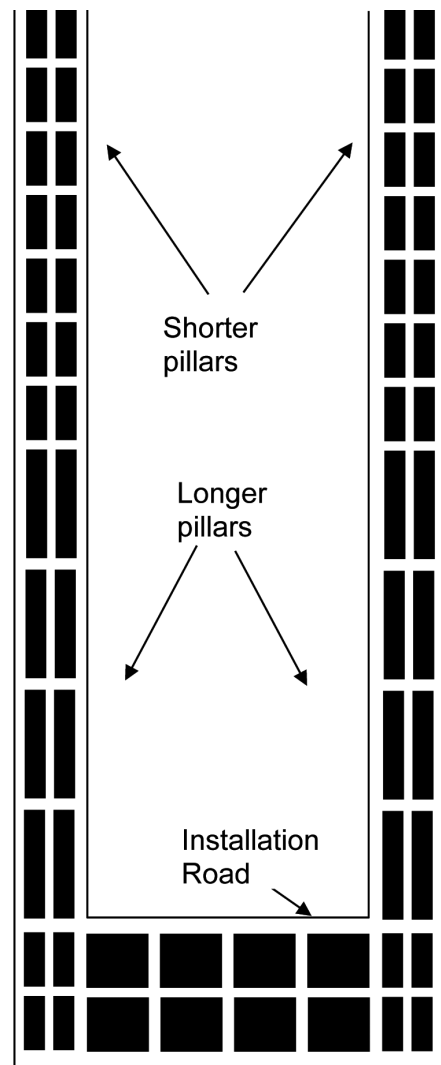

Figure 5. Sketch of the installation end of a developed longwall. Note the longer pillars at the beginning end of the longwall, as has been done in South Africa

then is that the yield pillars allow roof deflection to take place, preventing shear failure of the roof against the pillar edges. This is common practice in areas with weak roof in the USA, although there seems to be a tendency for crush pillars to be implemented in areas with good roof as well.

Where a number of adjacent longwall panels are mined, it is not uncommon for gateroad conditions to deteriorate progressively. This phenomenon is more evident in cases where the overburden does not fail totally, as it is caused by the progressive load increase as the mined area increases. This is similar to the mechanism of load increase in bord and pillar mining, on a larger scale.

The first panel in a series is usually mined without undue problems. In the second panel, tailgate problems begin to appear and by the time the third panel is

mined, serious falls are not uncommon in the tailgate. It is therefore sound practice to either increase the inter panel pillar widths for successive panels or to improve the roof support.

It is counterproductive to save money on roof support in longwall development. In longwalling, the tons produced per bolt installed is at least ten times that of bord and pillar mining, and to jeopordize production from a R100 million investment for the sake of a R20 roofbolt is not sound practice.

Mining inter panel pillars

In order to improve coal reserve utilization, the inter panel pillars are sometimes either partially or completely mined during the longwalling operation. Total removal is not always a good option, as it usually requires artificial support to have been installed on the maingate side of the previous panel to prevent the goaf flushing onto the face and removal is also detrimental for ventilation.

Partial mining has often been carried out, like the example shown in Figure 7. In that example, one of the two chain pillars is mined completely and the other one left intact. The splits are developed at 60° to prevent the entire length of the split being exposed by the longwall.

On fewer occasions, the one pillar in three road development has been mined completely, with the major portion of the remaining pillar, as shown in Figure 8. In the latter example, blind cutting on the tailgate side required modification of the equipment. The remaining pillar was designed to crush out for reasons of surface subsidence control. The size of the pillar remnant was critical in this case, as it had to be stable on the face, yet crush a short distance behind the face, before it could be strengthened by the confining effect of the goaf on either side. Numerical modelling coupled with observations in stooping sections on the same mine was extensively used in the design

procedure. In the end, a 6 m wide crush pillar was left. The depth of mining was 120 m, the panel was 212 m wide, the mining height was 3 m and there was no dolerite in the overburden.

The main disadvantage of mining the inter panel pillars is the risk of instability, in the splits and intersections, ahead of the face. This risk can be minimized by installing timbers or other supports in those areas, as shown in Figure 9. On occasion, turned around shields have been used ahead of the face in the tailgate as well, although this option requires a strong and even floor.

There is a case on record where small inter panel pillars had to be mined, again for reasons of subsidence control. The small pillars could not be left *in situ* with the risk of subsequent failure and thus unexpected subsidence at a later stage. On that occasion, the entries were filled with an ash mixture that had approximately the same strength as coal. This was done to counter the risk of failure of the small pillars ahead of the face.

The pillars were then mined together with the ash, as shown in Figure 10. The ash filling was not done to the roof in order to allow ventilation flow. Short timbers were installed on top of the ash for roof control.

Panel orientation and face shape

Panel orientation is a function of at least three considerations. These are the shape of the mine property that determine the overall layout, the directions of the major jointing, dykes and faults, and the direction of the maximum horizontal stress. The first consideration unfortunately often overrides the others.
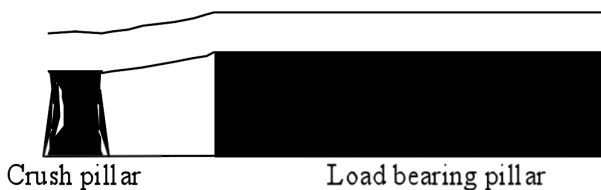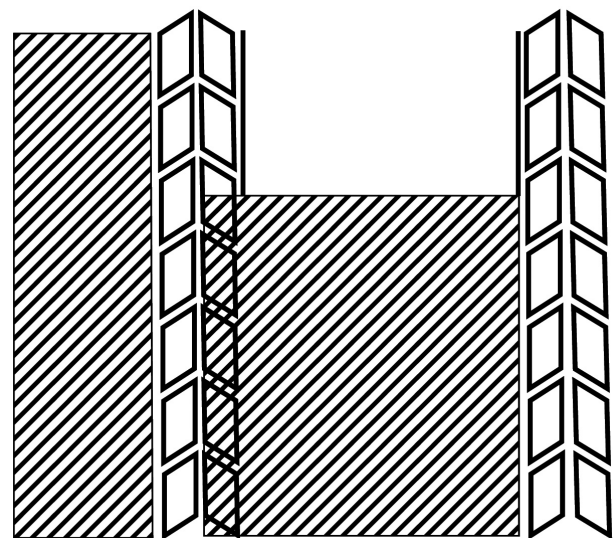

Figure 6. Conceptualized cross-section of a yield pillar. The large pillar to the right is the load-bearing pillar while the small crush pillar on the left provides yieldable roof support, preventing shear failure against the pillar edges

Figure 7. Complete mining of one inter panel pillar

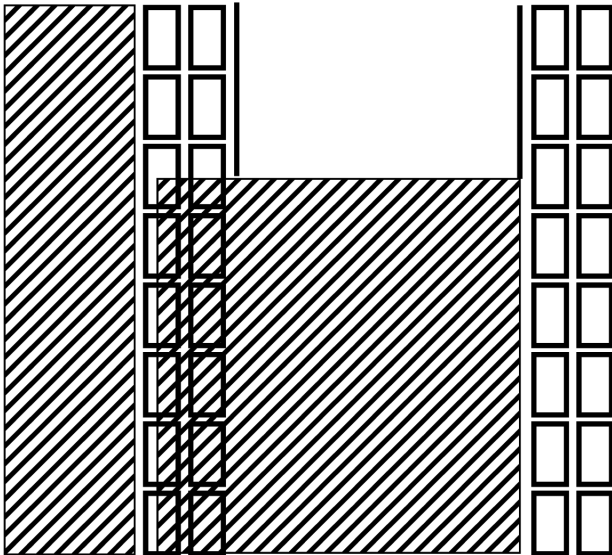ROCK ENGINEERING FOR UNDERGROUND COAL MINING

Figure 8. Complete extraction of one inter panel pillar and partial extraction of the other one

Figure 9. Timber supports in a split ahead of a longwall face where the inter panel pillars are mined

If possible, the panels should be laid out with the length slightly off the direction of the maximum horizontal stress. In this way, horizontal stress induced falls of roof in the gate roads are minimized. The arresting effects of the horizontal stress on goaf development are likewise minimized.

Often, the major joints will be orientated parallel to the maximum horizontal stress. If the panel is thus orientated slightly off that direction, it means that the face will intersect the joints at an oblique angle. This is the desired situation, shown in Figure 11.

It is desirable to have the face as straight as possible, but this is not always easy in practice. The best

Figure 10. A view of the ash fill that was mined through by longwalling. The ash was placed to stabilize the inter panel pillars that were too small for mining without being reinforced

practical face shape is a very slight concave, with the centre not more than 3 to 4 m ahead of the edges, see Figure 12. With this shape, the toes of the shields will be slightly splayed. With a convex shape, the toes of the shields will tend to lock, which could result in a steel bound face.

Where more densely jointed zones are expected, with the joints running in the same direction as the face, the face should be swung slightly to avoid intersecting the joints parallel to the face. There is a limit to the extent to which this can be done, as mining an angled face uses up shield length in the face, reducing the cover in tailgate.

Face breaks

Face breaks occur when the roof collapses ahead of the shields. Face breaks, like the example in Figure 13, are more serious from a lost production viewpoint than continuous miner burials, simply because of a longwall's high rate of production when working, and the idle capital investment when not working. It is therefore imperative to prevent face breaks as far as possible and to recover the face as quickly as possible when they do occur.

The most important preventative measures are to have the best face orientation under the prevailing conditions and to have the correct face shape. The third preventative step is less obvious, namely, to maintain all the equipment in good running order. For instance, operating a face with shield leg pressures that are too low is looking for trouble, as is having shields with non-uniform roof pressure.

It has all too often been seen that a face break is preceded by an unplanned stoppage of more than a day. One possible explanation for this is that during a prolonged standing time, the transient high stress zone ahead of the face remains in the same place for long enough to allow fractures to develop there.

Rock failure is time dependent. One way to minimize rock damage is to have the high stress zone move through the rock mass as quickly as possible, which can be achieved only by moving the face as quickly as possible. Wherever it remains stationary, it has the opportunity to enlarge the rock fractures. When mining resumes, the damage has already been done and the face merely mines into the pre-existing fracture, see Figure 14. A regular rate of face advance is perhaps one of the most important strata control aspects of longwalling.

Under severe conditions, rock stabilization ahead of the face is sometimes achieved by chemical injection. In countries such as Germany, it has been used on a routine basis, but in South Africa, it has been used only in emergencies. Polyurethane has been used although it lost favour due to the toxic nature of its by-products when it burns. In South Africa, it is still approved for the purposes of rock injection although it has been banned for use as an insulating material or any other use in the open. It has since been replaced by other chemicals (mainly silicone based ones), which, although safer to use, are not quite as effective for rock
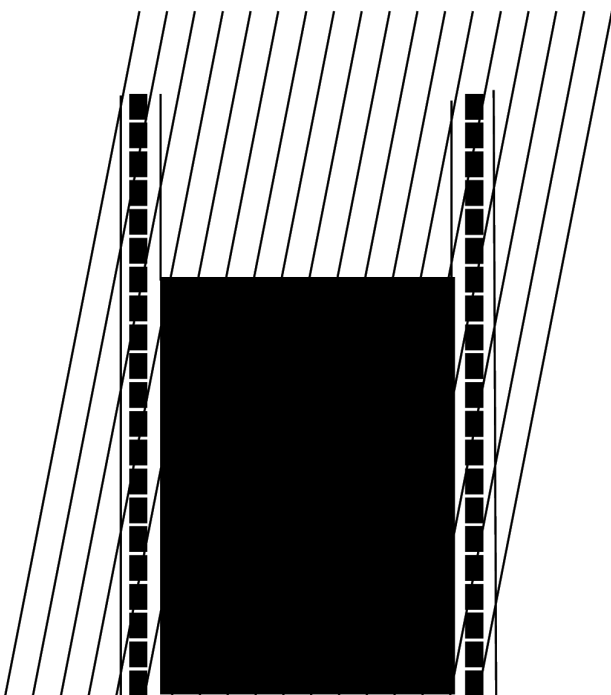

Figure 11. The ideal panel orientation, with the face intersecting the major joints obliquely

Figure 13. One of the less pleasant aspects of longwalling: a face break
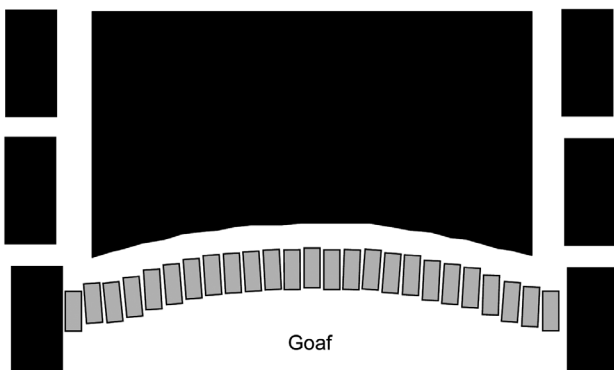

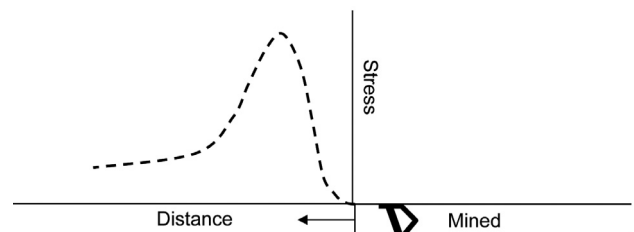**Figure 12. Greatly exaggerated view of the ideal face shape, with the centre slightly ahead of the edges**

Figure 14. The stress distribution ahead of a longwall face. The zone of increased stress can extend as far as 30 to 50 m ahead of the face

ROCK ENGINEERING FOR UNDERGROUND COAL MINING

binding. Figure 15 is an example of a face that was recovered using polyurethane.

Where rock injection has been correctly applied, it has been effective in reducing the time taken to recover a face. It is relatively expensive, but when balanced against the revenue of saving time to get a face back to production, the cost is not an important consideration.

When using injection, it is important to stabilize an area that is wider than the area that is seen to be unstable. If this is not done, it will probably not be effective and the money would have been spent without getting any benefit. It is better to spend a bit more money and get the full benefit.

The method to be used, shown in Figure 16, is to drill short holes, 2 to 3 metres deep, into the rock and to inject through non-return valves, placed inside the holes, until the injected material is seen to come out of cracks. This is done to form a skin for further rounds of injection. The process is then repeated with deeper holes and higher pump pressure. For this method polyurethane is superior to the other materials, as it generates carbon dioxide bubbles which build up further pressure, forcing the material into minute rock cracks. The pipes through which the chemicals are injected into the rock are often left in the holes as spiling rods to offer additional reinforcement.

Experience dictates that time is of the essence in longwall face recovery. There is an old mining adage with a great deal of truth in it: 'If a face cannot be recovered in an hour, it will take a day. If it cannot be done in a day, it will take a week. If it cannot be done in a week, you are in serious trouble.'

The general modus operandi in face recovery is to start from a stable base and work toward the collapse,
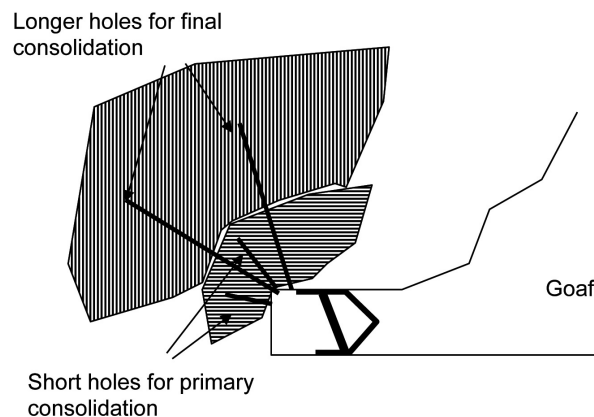
Figure 16. Method of stabilizing rock by chemical injection

Figure 15. The light coloured material oozing out of the face is polyurethane that was used to stabilize a standing face to prevent a possible face break. The fractures can be seen in the top left corner of the photograph. The timbers on the right-hand side of the photograph were installed under the shield tips, another precaution

Figure 17. This face has been stabilized by installing wooden dowels in the hitherto sound area close to the face break in the background

stabilizing the area all along. Even in 'good' areas close to the collapse, additional support should be installed. The first priority is to contain and isolate the collapse to prevent it growing worse, which it will invariably do if not contained. The face should be strengthened by wooden dowels, as shown in Figure 17.

It is also good practice to have a 'first aid kit' for face breaks handy. This kit, consisting of emergency equipment, can be kept in a car and moved with the face. It should contain items such as rock drills, drill rods, roof bolts, dowels, resin, cement, wiremesh, steel girders, etc.

Figure 18. Common layout for a face move in good ground

Figure 19. Method of shield extraction, making use of the protection of the remaining shields and replacing shields with timber packs

Face moves

The overall success of longwalling on a mine depends largely on the rate at which a face installation can be extracted from a completed face, transported and reinstalled in the next panel. During the face move, there is zero production, and on mines that rely on other methods in addition to longwalling, a face move invariably requires assistance from other crews as well, with a negative impact on production overall. Face moves therefore have to be well planned.

There are several methods of extracting a face, mainly dictated by ground conditions. A common layout in good ground conditions is shown in Figure 18. With the centre gate in place, the extraction of equipment can be done from three points. It is common practice for the shields to be left back from the face prior to extraction. After the face conveyor and other equipment have been removed, the shields are extracted from the furthest point under cover of the remaining shields closer to the exit point, shown in Figure 19. This is done using LHDs or tailor-made vehicles. The extracted shields are sometimes replaced by timber packs, depending on ground conditions. If a centre gate is used, good traffic control is necessary to avoid congestion at the point where all the extracted equipment converges.

In weak roof situations, it is necessary to extract the shields under cover of wiremesh. The mesh is installed in the roof in strips parallel to the face during the last number of face cuts. Each strip of mesh is linked to the previous strip with light rope lacing. The process
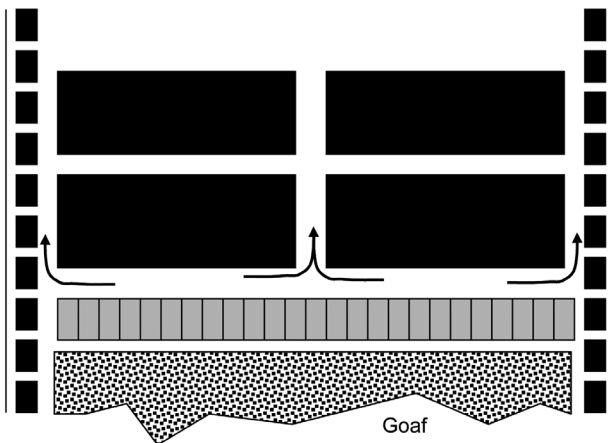

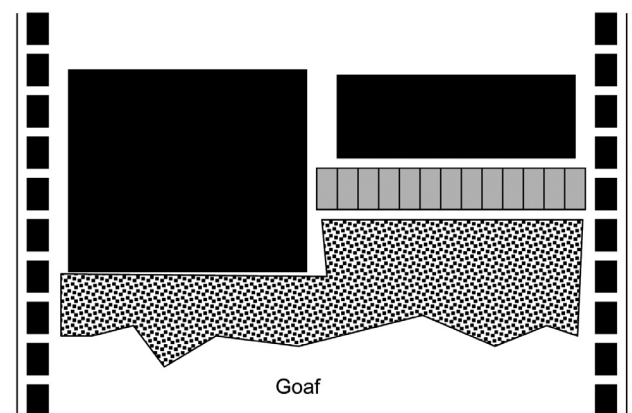**Figure 20. Multi phase face extraction. The left-hand side of the face has already been extracted. The distance between the stopping positions for the successive phases should not be less than 30 m**

ROCK ENGINEERING FOR UNDERGROUND COAL MINING

continues until the wiremesh behind the shields is trapped by the goaf. This is a time consuming process, which is in itself detrimental, as the slower the rate of advance, the worse the roof conditions usually become.

It has therefore been found necessary in severe cases to move a face in two or even three stages, using multiple extraction roads, as shown in Figure 20. The face is shortened from the tailgate. This method has the advantage that the face does not remain standing in any particular position for too long a period, although it increases the overall time for a face move considerably. If this has to be done, it is good practice to use the face move as an opportunity for equipment overhauls. It also assists the workshops, which are not flooded with all the equipment at the same time.

There have been attempts to decrease the time taken for longwall moves by mining out into a predeveloped and well-supported roadway, thereby saving the time lost to install wiremesh prior to the move. This should be approached with extreme caution. There are at least three possible modes of failure, all of which have occurred in practice in South Africa. However, there are also several examples worldwide where this has been done successfully.
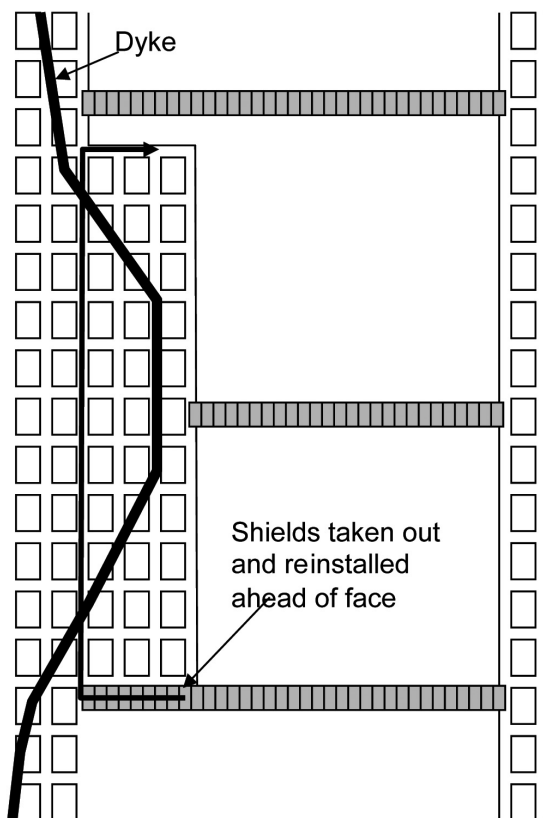

Figure 21. Lengthening and shortening a face to suit the geometry of the available ground

The first is crushing of the ever diminishing pillar ahead of the face as it approaches the predeveloped tunnel. The second is failure of the roof in the predeveloped tunnel as the longwall approaches. The third, which serves as an example in Chapter 9: Modelling, is that the final pillar may punch into the floor.

Negotiating dykes

The best way to handle dykes in a longwall panel is to avoid them. In areas where dykes are commonly present, this requires a good system of geological prediction, such as using horizontal drilling. However, avoidance is not always possible and very often a mine's infrastructure simply does not allow mining in dyke-free areas at the required time.

There are a number of methods of dealing with dykes in panels that have to be mined. Where dykes are very thin, they are simply cut (or rather, broken out) with the shearer. Blasting the dyke is sometimes done where the dyke is too thick or hard to cut, but this is a slow and arduous process and very often results in blasting damage to the shields, no matter how carefully the blasting is done. Old conveyor belt strips are used to protect the equipment during blasting and stringent methane precautions are taken.

In areas where dykes cross, breaking the available ground up into blocks that are too short for economical longwalling, faces have been lengthened to improve the volume of coal that is mined by a longwall. However, this requires that the mechanical elements of the longwall (i.e. the face conveyor, gearboxes, drive capacity, etc.) are able to handle the longer face. In other cases, faces have been lengthened and shortened to suit the geometry of the available ground, as is shown in Figure 21.

Another method that has met with some success in situations where a dyke cuts across a potential longwall panel is to pre-mine the dyke ahead of longwalling operations. The excavation so created has been supported by timber packs, or backfilled.

The timber packs did not work as well as the backfilling, mainly because the timber was surprisingly difficult to cut with the shearer and because the timber supports were too soft. Roof collapses took place, although on no occasion was a face ever lost or severely damaged.

For backfilling, it is important to use a fill material that has cutting properties that are compatible with coal and to have positive roof contact between the fill and

the roof. One face experienced a severe break where the fill material did not reach the roof, this in spite of a final round of topping up filling under pressure after the bulk filling had hardened.

A number of fill materials have been used successfully. Fine ash with cement and a fluidizer to reduce the amount of water in the mix worked well. The mix was designed to have a uniaxial compressive strength of 7 MPa. The best fill, however, was fine coal that was collected from the surface dump, with a small amount of cement added as a binder.

For positive roof contact, the best method—according to experience—is to install timbers on top of the fill mix. The method is to divide the tunnel into lateral sections by means of paddocks and then to fill each paddock to about a metre from the roof. After this first stage fill has hardened, the timbers are installed. The final stage of filling is then done. This is shown in Figures 22 and 23. Figure 24 is an illustration of an occasion where the second stage fill was not done properly due to a fall of roof in the tunnel that restricted the flow of the fill material. In spite of that, mining was done successfully due to the timber supports on top of the fill.

The best filling method was found to be direct filling through surface boreholes into paddocks. Where the boreholes became expensive due to mining depth, filling from surface into an underground container has also been done. The ash mix in that case was pumped from the container with a positive displacement compressed air pump. In all cases, however, provision has to be made to get rid of the run-off water.

Face length

As explained previously, the status of the overburden

Figure 23. Second stage filling flowing into the excavation after the timbers had been installed. The timbers are installed on foot boards to prevent them punching into the fill

Figure 24. Mining through the filled excavation in an area where the second stage filling was not done successfully. If the timbers had not been installed, roof falls would probably have occurred

dominates the stress regime in which a longwall operates. It is determined by uncontrollable parameters such as the mining depth and the composition of the overburden as well as the single controllable parameter, the panel width or face length. The overburden can be allowed to fail by increasing the face length, as explained in Chapter 10: Subsidence.

The decision as to whether the overburden should be allowed to fail or remain intact depends on a great number of variables. The first variable is cost: the longer the face, the higher the required capital expenditure. Increasing face length is more than just a matter of adding shields and conveyor pans. The face conveyor motors, gear boxes, and all the ancillary equipment must be in harmony.

At shallow depth, the high stresses accompanying an

Figure 22. Direct filling from surface through boreholes into the excavated dyke

intact overburden aid production because they assist in fracturing the face. At greater depth, they could have a detrimental effect if the induced stress levels are too high, resulting in severe spalling or even face breaks.

The stress is not uniform along a longwall face. It is higher in the centre than at the edges, even if the overburden fails completely. A short face with an intact overburden will be subjected to higher stresses than a slightly longer face with a failed overburden. However, a much longer face with a failed overburden will be subjected to higher stresses than a shorter face also with a failed overburden. The exact dimensions at which these changes occur, and the magnitudes of the stresses, are site dependent.

Another important consideration is water. In South Africa, the groundwater is usually contained above the dolerite sill. Breaking the sill results in more water having to be handled underground and has an adverse environmental impact. For mining purposes, this consideration becomes very important if mining has to progress down dip, as water will then accumulate on the face.

If the overburden is to remain intact, there will be a significantly higher load on the inter panel pillars. They then have to be wider than if the overburden is allowed to fail. The width should be determined by numerical modelling of the real situation.

Especially in the case where the overburden remains intact due to the presence of a dolerite sill, it has to be borne in mind that the sill may fail at a later stage, as has been seen in practice. It is therefore questionable to protect surface structures by mining a short face in the hope that subsidence will be restricted. However, subsequent dolerite failure is a rare occurrence.

Determining the face length is a very important aspect of longwall design. It can be used to manipulate the stress environment, which has an impact on productivity. For instance, higher stresses fracture the coal ahead of the face, aiding the mechanical cutting process.

Goafing

Where strong layers exist in the immediate roof, the collapse of the goaf can be traumatic. In the absence of a strong layer, the roof breaks up in small portions and the collapse process is a gradual one. However, when it hangs up for long distances, it tends to fail in a single mass. It then acts as a piston, displacing air at sufficiently high velocities to result in damage to ventilation stoppings and conveyor belts and possible injury to people.

The severity of the windblast is a function of the area that collapses and of the collapse area as a proportion of the total exposed area. The closer the collapse area is to the total available area, the more severe the blast. As damaging as the first wind blast, is the secondary suction that has sufficient force to draw people into the goaf. The turbulence is also more than sufficient to mix and displace methane gas from the goaf into the active workings.

If the strong layer that hangs up occurs higher up into the succession, with softer layers between it and the coal, the effects are masked. This is commonly the case with the dolerite sill in South Africa, where dolerite failure occurs almost unnoticed if there already is a mass of broken rock below the dolerite. The broken rock acts as a cushion, absorbing sufficient energy not to cause damage to the workings.

Early warning of goafing is a serious challenge to rock engineers. Recently, significant advances have been made with seismic monitoring of the overburden. On at least one mine in Australia, Moonee Colliery, it is done on a routine basis, as shown in Figure 25. An increase in the number of seismic events has been shown to precede the collapse of the overburden.

Micro seismic monitoring is done using portable monitoring stations that are leapfrogged as the face is mined. This is done to ensure good cover at all times. It was initially believed that additional geophones would have to be installed at different heights in the overburden to generate sufficient information, but it now appears that monitoring on the plane of the coal seam only is sufficient.

A disadvantage of the current system, which is barely beyond the experimental phase, is that it is manual. It requires a human observer using his judgement as to
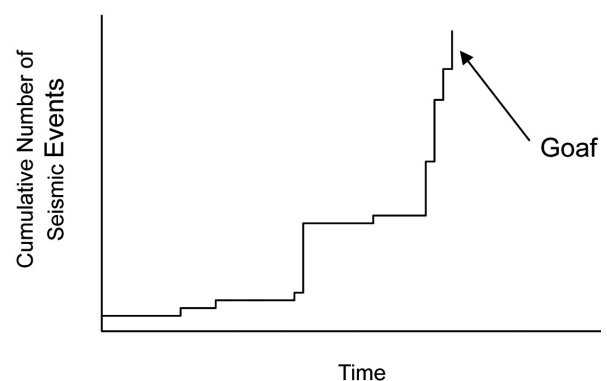

Figure 25. The steep increase in the cumulative number of seismic events has been seen to be a precursor to goaf collapse

when a dangerous situation is developing. Nonetheless, more than 80% of all goaf collapses have been successfully predicted with the system.

There are also other indicators of an impending goaf collapse. These include increased shield leg pressure and increased power consumption by the shearer. Efforts are currently underway to include these into the seismic monitoring system. Eventually, it is hoped to develop a method that will take cognizance of all the warning signs and integrate them into a single hazard evaluation system. It is hoped that the system can eventually be automated to the extent that an electronic signature of a dangerous situation will be developed, which will take the human observer out of the system.

Multiple seam longwalling

Depending on the seam height and the middling between seams, it is generally desirable to longwall on multiple seams in descending order. The exceptions are the areas where the seams are thin relative to the middlings (i.e. where the broken goaf of one seam is thinner than the middling between that seam and the upper one), as in the KwaZulu-Natal province. There, longwalling has been successfully done in almost any order. However, as long as one seam is within the goaf zone of another, the order of mining has to be from the top down.

If panels are to be superimposed, the inter panel pillars have to be progressively wider as the depth increases. This has the effect that the overall extraction ratio decreases with increasing depth.

The alternative is to stagger the deeper panels with respect to the shallower ones. This has the benefit that the lower inter panel pillars can be sited in destressed ground, which implies that they can be significantly smaller. The exact configuration should be determined by numerical modelling, taking care to situate the bottom inter panel pillars outside the zone of increased shear stress due to the pillars on the upper seam.

There is another perceived benefit of staggering the panels, namely that the resulting post subsidence surface topography will be less severe. This is not necessarily the case. While the resulting topography may be described as 'better' as compared to the case with superimposed panels, it will still be severe.

The previous remarks are of a generic nature. In practice, the decision whether to superimpose or stagger overlying longwall seams can only be taken by in-depth consideration of local conditions.

A case in point is the situation where two seams are separated by a strong sandstone parting.

In the ideal single seam situation, the overburden tends to break off very close to the shields at an angle overlying the goaf. The overburden over the shields themselves remain solid and to some extent at least, self-supporting. A certain amount of deflection takes place and this loads the shields, see Figure 26 for a conceptual explanation.

In the double seam situation with a strong layer between the two coal seams, the strong layer forms a cantilever which is loaded by the dead weight of the goaf created by the upper seam, see Figure 27. This beam can hang over for a certain distance until it fails, either in tension or in shear.

Tensile failure mode

The generic equation for tensile stress generated in a cantilever is

$$\sigma_t = \frac{3qL^2}{t^2} \qquad [1]$$

from which it follows that the maximum overhang distance for a given tensile strength is:
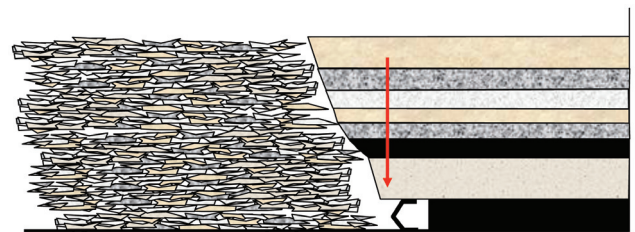
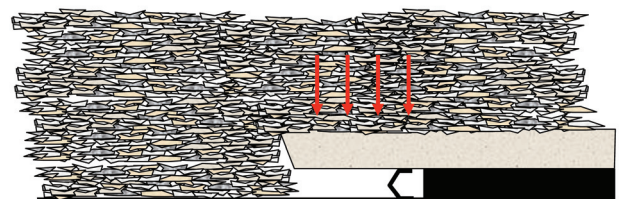$$L = \sqrt{\frac{\sigma t^2}{3q}} \qquad [2]$$

Figure 26.

Figure 27.

where $L =$ maximum overhang
$t =$ thickness of strong layer
$q =$ loading on beam, including the weight of the beam
$\sigma =$ tensile strength.

The loading, q, under the conditions of multiple seam mining, is the total weight of the overburden. In normal single seam operations, the overburden would have some strength at least, but here it is not the case, as shown by the subsidence cracks that occur beyond the mining perimeter.

Shear failure mode

Shear failure will occur if the shear stress exerted on the rock at the face exceeds the shear strength, or when

$$\tau t = Lq \qquad [3]$$

from which it follows that the maximum tolerable overhang distance for shear failure is:

$$L = \frac{\tau t}{q} \qquad [4]$$

where τ is the shear strength of the layer.

Comparison of shear and tensile failure modes

The maximum tolerable overhang lengths for the two possible failure modes were compared using the equations above. The shear strength of the sandstone was taken as 8 MPa and the tensile strength as 5 MPa. Figure 28 shows the comparison for different thicknesses of the beam, varying between 4 m and 13 m.

It is seen from the figure that the tensile failure mode is more likely to occur, as the maximum tolerable overhang length is less than for the shear failure mode.
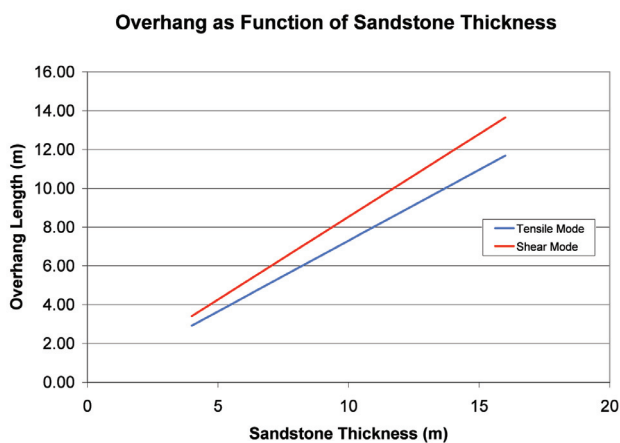

Figure 28. Overhang as function of sandstone thickness

Load on shields

The load on the shields, F_s, is determined by the length of the overhang, the position of the shields relative to the length of overhang and the height of the goaf on the upper seam. Simply, the fundamental equation for the load on the shields (transformed from beam fundamentals) is:

$$F_s = \frac{Lw\rho g\left[\dfrac{h}{f_b} + t\right]}{2d}\left[\frac{3L}{2} - d\right] \qquad [5]$$

where $L =$ length of overhang
$w =$ width of shield
$h =$ height of goaf on upper seam
$f_b =$ bulking factor
$t =$ thickness of overhanging beam
$d =$ distance of shields to face

Inspection of Equation [5] indicates that the longer the overhang, the thicker the beam, the higher the goaf on the upper seam and (ironically) the closer the shields to the face, the higher the load on the shields.

To quote numbers, a 10 m thick sandstone hanging up for 7 m will result in a load of 11 500 tonnes on the shields placed 2 m from the face. If, under the same conditions, the shields are 3 m from the face, the load will decrease to 10 200 tonnes. The irony is that good practice requires the shields to be close to the face.

If panels are to be staggered under these conditions, the situation will be aggravated because the upper seam's inter panel pillars will be situated over the face of the longwall on the lower seam. As there is no goaf over the inter panel pillars, the 'beam' will be of maximum thickness and thus maximum overhang length. Superimposition then is probably a better option.

By contrast, where the parting consists of weaker rock or thinner individual beams, the parting will fail sooner and the stress build-up on the face will be less severe.

Two practical examples illustrate the point. At Sigma Colliery, where the parting consisted predominantly of mudstone and thinner layers of siltstone, staggered longwalls were operated very successfully. By contrast, under very similar conditions of depth and parting thickness at Matla Colliery, staggered longwalls were plagued by face breaks. The parting at Matla consisted of a massive sandstone. Both mines were in the region of 100 to 140 m deep and the parting thickness was of the order of 10 m to 15 m.

Multiple seam mining

Introduction

Many collieries in South Africa have more than one economically recoverable seam. Where the seams are in close proximity the mining of one seam may influence the subsequent mining of other seams due to factors such as subsidence and stress concentrations. This may result in difficult mining conditions.

From a strata control point of view, the ideal sequence of mining is in a descending order, but due to marketing and coal quality constraints, this has often been difficult to achieve.

In the Witbank area, multi-seam bord-and-pillar mining is common. In KwaZulu-Natal, as many as four or five superincumbent seams have been exploited. Since the area produces high-grade anthracite and coking coal, there is a long history of applying high extraction methods. The unavailability of high quality virgin reserve areas has led to many examples of extraction taking place in areas that have been previously under or overmined.

Several combinations of mining multiple seams have been tried. Table I shows the potential safety hazards associated with various combinations of multi-seam mining sequences and extraction methods.

Factors influencing interaction

In multi-seam mining, several factors contribute to interaction between the seams. These are:

- Parting thickness
- Parting characteristics
- Mining method
- Relative location of layouts
- Percentage recovery of the coal seams
- Seam thickness
- Time difference following mining previous seam
- Depth
- *In situ* stress.

For bord-and-pillar mining in two seams, interaction may only depend on parting thickness, parting characteristics and relative position of the pillars. Where high extraction methods are used, the interaction may depend on all of the above factors.

Parting thickness

The greater the parting thickness, the lower the interaction.

Strata

The dominant rock types in the South African coalfields are sandstones and shales, each of which can have a different influence in a multi-seam situation. Relatively massive fine-grained sandstone layers can span much wider panels than thinly laminated shales. Therefore, the presence of sandstone in the parting tends to dampen the effect of stress transfer from one seam to another, because of the stiffness of the sandstone. In this case, the stress may be transferred to the barriers, relieving the lower seam in-panel pillars.

Sandstones have different bulking properties on failure compared to shales. Sandstones break into

Table I
Potential safety hazards in multi-seam mining layouts

Method of mining		Safety hazard
Upper seam	Lower seam	
B&P	B&P	Spalling of pillars and parting collapse if *P* is thin and no superimposition
PE (2)	B&P (1)	Roof falls in lower seam, parting collapses if *P* is thin
B&P (2)	PE (1)	Tensile zones and spalling in upper seam when mining over goaf/solid boundary, floor collapse over incomplete goafs, high safety risk if P/h ratio low
Remnant	B&P (2)	Intersection collapse in lower seam pillar (1) when mining under remnant. Sidewall spalling
PE (1)	PE (1)	Intersection collapse in lower seam when mining under remnant. Sidewall spalling
PE (1)	PE (2)	Intersection collapse in lower seam when mining under remnant. Sidewall spalling

In Table I, the following abbreviations are used:
- B&P = Bord and Pillar
- PE (1) = Pillar Extraction, (1) mined first
- P = Parting distance between two seams
- h = mining height

large blocks resulting in higher bulking factors than shales, which tend to fail in thin slabs. The type of strata determines the caving characteristics when high extraction methods are used. Two types of caving have been recognised, namely Bulking Factor and Parting Plane Controlled Caving, see Figure 1.

- *Bulking factor controlled caving*—the caving height is determined mainly by the bulking factor of the caved material. The height of caving H_c can be determined from:

$$H_c = \frac{h}{(bf - 1)} \qquad [1]$$

Where H_c = Height of caving
h = extraction height
bf = bulking factor.

Bulking factor controlled caving is typical of conditions where the strata consists of shales and mudstones and is therefore relatively weak.

- *Parting plane controlled caving*—the caving height is determined by the location of dominant parting planes or massive sandstone beds within the roof strata. A void will occur between the caved waste and the overlying strata. The height of the void, v, can be calculated from:

$$v = h - P(bf - 1) \qquad [2]$$

where P = height of the parting plane above the top of the extraction section.

Above the caved zone the strata will converge until it makes contact with the caved rock. Parting plane controlled caving is typical of conditions of alternating layers of different strengths. Where thick sandstone layers exist, incomplete caving can occur and voids can be expected.
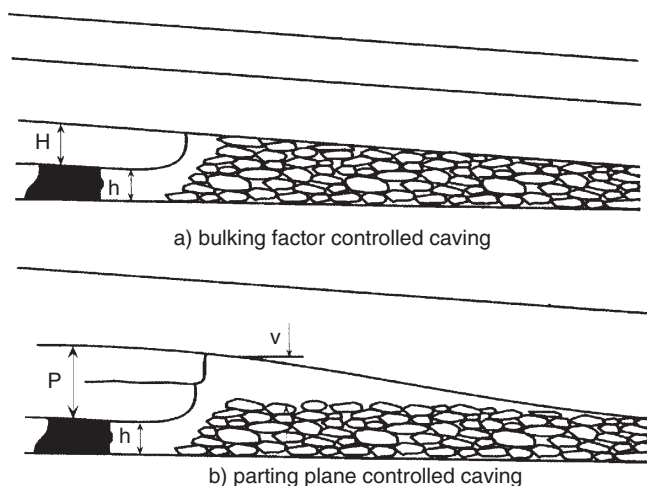

a) bulking factor controlled caving

b) parting plane controlled caving

Figure 1. Bulking factor and parting plane controlled caving

Mining method

High extraction mining methods have greater influence on other seams than do bord-and-pillar layouts.

Relative location of layouts

In bord-and-pillar workings, pillar and roadway stability depends on whether or not pillars and roadways are superimposed, if the seams are in close proximity. In high extraction layouts, especially longwalls, the location of the gate roads is important. They are often located below an upper seam goaf.

Percentage recovery

Should high extraction be practised in the upper seam, the higher the percentage recovery the better the conditions will be in the lower seams. Remnant pillars can cause stress transfer over large vertical distances.

Seam thickness

When mining over goafs, the seam thickness is of importance since it, together with the bulking factor of the intervening strata, determines the amount of subsidence in the strata.

Time difference

Where high extraction methods are carried out, caving and subsidence continue to take place over a period of time after mining. In the majority of cases more than 90% of the surface displacements occur within a period of less than three months after undermining. Full subsidence and the re-establishment of near virgin stress conditions may take many years.

Bord-and-pillar mining

Safety hazards may occur in multi-seam bord-and-pillar layouts if the seams are in close proximity and non-superimposed. Guidelines for multi-seam bord-and-pillar layouts were developed by Salamon and Oravecz in 1976. Whether pillars are superimposed or not, depends on the parting distance, P, in relation to the pillar Centre Distance, C, and the bord width B.

The general guideline is that if the parting distance is less than 0.75 times the pillar Centre Distance then the pillars should be superimposed. These guidelines were formulated from numerical modelling after determining the distance at which the alternating influence of bord-and-pillars is negligibly small, see Figure 2. This distance was determined as 0.75 to 1.0 C.

In the mid-1980s, Khutala Colliery, see Bradbury and Hill (1986), carried out a specific investigation for workings in the No. 2 and No. 4 Seams. The guidelines indicated that superimposition was necessary. However, the investigation showed that the limiting distance at which stresses above or below

bord-and-pillar workings return to near primitive stress values decreases with depth and also with increasing pillar size. If it is not clear whether superimposition should be carried out, a relatively quick analysis by numerical modelling can be used.

The guidelines recommend that, where superimposition is necessary, the Safety Factors should be at least 1.7. This is important where superimposing over pillars with irregular size.

When overmining old pillars with suspect stability because of jointing, a point to bear in mind is that overmining with superimposed bord-and-pillar workings will result in slight stress reduction of the bottom pillars. The reason is that the solid overburden loading the bottom seam pillars, is replaced by compressible pillars. The analogy is that the stiff overburden is replaced by springs.

The load reduction is not significant from a pillar loading point of view, but in marginal cases, it may just be sufficient to reduce the clamping forces on joints in the pillars and cause blocks to slide out.

Barrier pillars

The guidelines developed in 1976 suggested that the influence of barrier pillars will be considerably greater than panel pillars, but did not quantify their influence. A general guideline that has been used is to superimpose barrier pillars if the parting distance between two seams is less than 1.5 times the pillar centre distance.
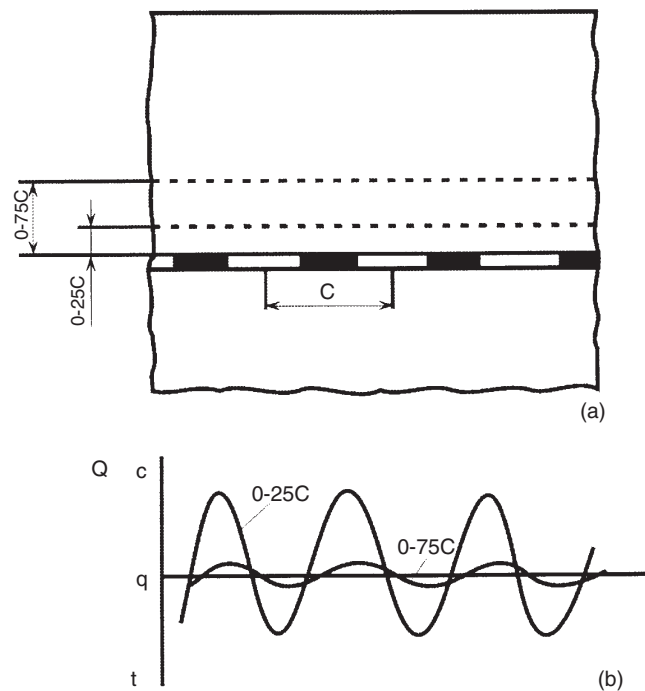
In the case of panel pillar design, full cover load is assumed to be acting on the pillars, and this is usually the case if the panel width-to-depth ratio is high. The effect of the barrier pillar on the panel pillars is ignored.

The barrier pillar, however, due to its greater stiffness, carries a disproportionate amount of the cover load. When examining the vertical influence of barrier pillars on other workings, the geometry and layout of the panel cannot be ignored. Table II shows the limiting distance of barrier pillars for various panel geometries.

From Table II it is seen that the limiting distance of the barrier pillar as a ratio of the pillar centre distance varies from 0.77 to 2.43 C, depending on the ratio of the barrier to panel pillar width.

For barrier pillars of the same width as the panel pillars ($Wb/Wp = 1$) the limiting distance is between 0.77 and 0.83 C for the examples shown. If the parting is greater than 0.9 or 1.0 C it will, therefore, not be necessary to superimpose barrier pillars.

Normally, if only bord-and-pillar mining is carried out, it does not matter whether the upper or lower seam is mined first, apart from where the parting thickness is thin and the parting composition is weak. An exception occurs when the strata surrounding the upper of two seams is weak (especially the roof), when it will be safer to expose these strata to the high strains in the constrained state, that is, before the constraint is removed by mining. In these situations, it will be preferable to mine the lower of the two seams

Figure 2. Stresses around bord and pillar workings, after Salamon and Oravecz (1976)

Table II
Limiting distance of barrier pillars for different panel geometries

W/H	Wb	Wp	Wb/Wp	LD	LD/C	LD/Wb
0.4	12	12	1.0	14	0.77	1.16
0.8	12	12	1.0	15	0.83	1.25
1.0	12	12	1.0	16	0.88	1.33
2.0	12	12	1.0	13	0.72	1.08
0.5	24	12	2.0	28	1.55	1.16
0.8	24	12	2.0	24	1.33	1.00
1.0	24	12	2.0	26	1.44	1.08
1.4	24	12	2.0	27	1.55	1.12
0.5	48	12	4.0	38	2.11	0.79
1.0	48	12	4.0	39	2.43	0.81
1.4	48	12	4.0	32	1.77	0.67
2.0	48	12	4.0	33	1.83	0.68

Where W/H = ratio of the width-to-depth of the panel
    Wp = width of the panel pillar
    Wb = width of the barrier pillar,
    LD = limited distance below barrier pillar where stress returns to
         5% of virgin stress
    C = pillar centre distance.

first. However, with thin partings of about 5.0 m of weak material and about 2.0 m for competent sandstone, it may well be necessary to mine the upper seam first to prevent parting failures due to tramming. In these cases, a detailed investigation into parting stability is required.

Parting stability

Where partings become thin in bord-and-pillar workings there exists the possibility of a parting collapse. For partings where the thickness is less than 0.2 of the bord width the tensile strength of the strata can be exceeded and failure can occur.

The thickness of a self-supporting beam, t, can be determined from the following equation:

$$t = f_p \rho g\, B^2 / 2\sigma \qquad [3]$$

where ρ = density of strata comprising beam
   γ = gravitational acceleration
   B = bord width
   σ = laboratory tensile strength of the parting
   f_p = suitable safety factor.

The minimum thickness required for a self-supporting span derived from the above Equation, is based on laboratory results, and assumes no discontinuities in the parting.

In the Witbank area, parting thickness of 1.0 m has been self-supporting between the No. 1 and No. 2 Seams at some collieries. The tramming of heavy machinery causes increased risk of parting collapse where the parting is thin. A 2.0 m parting of competent sandstone between the No. 1 and No. 2 Seams has been shown to be stable when trammed over by a continuous miner. By contrast, a weak 2.0 m thick mudstone/shale parting, at Sigma Colliery, failed under similar circumstances. The continuous miner made an unexpected appearance in the bottom seam workings and was only extracted with considerable effort. Examples of stable and failed partings are shown in Figures 3 and 4 respectively.

Parting stability is also dependent on the degree of superimposition of the pillars. Figure 5 shows a plan of bord-and-pillar workings where the workings were to be superimposed but have become partially offset. Should pillar extraction in the top seam have been carried out instability of the lower seam could be expected. Where thin partings exist, and there is the possibility of parting failure, the guidelines recommend that the safety factor in each seam should be 1.8. Also, the safety factor of hypothetical pillars having a height equal to the combined seam heights at the floor depth of the bottom seam should not be less than 1.4.

Figure 3. Example of a stable 2 m thick parting in sandstone

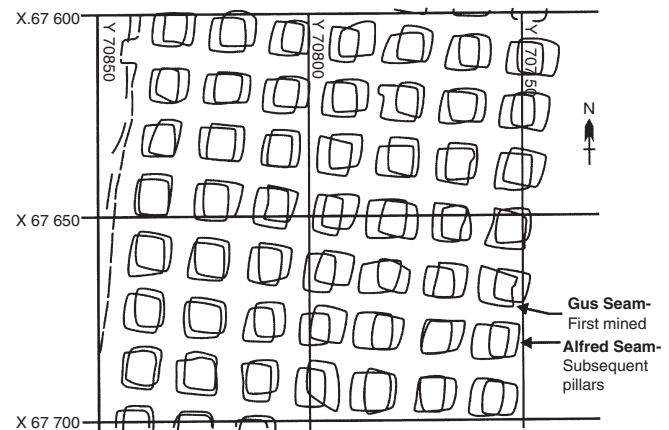**Figure 4. Example of a failed parting**

Figure 5. Pillars becoming non-superimposed due to a shift in the geometry

High extraction over bord-and-pillar workings

Any high extraction method will produce abutment stresses around the extraction panel. These abutment stresses extend above and below the plane of the workings into the surrounding strata. Bord-and-pillar

workings in a lower seam may deteriorate as a result of these stresses, jeopardizing their use as a long-life development or future pillar extraction of the lower seam.

The stress distribution on the lower seam workings will be changed as a result of overmining. As the abutment passes over, the pillars will experience an increase in load followed by considerable destressing, see Figure 6. As goafing and settlement continues in the top seam, the lower seam pillars will be reloaded.

The main factors affecting lower seam stability are:

- Parting distance
- The caving mechanism above the upper seam extraction area
- Upper seam mining method
- Upper seam mining layout
- Upper seam percentage extraction
- The presence or absence of remnant pillars and large snooks
- Depth
- Lower seam mining layout relative to that of the upper seam.

With increasing depth below the upper seam, stress conditions will tend towards the virgin stress state. As a consequence, the change in pillar load on the lower seam pillars will reduce with increasing parting distance because the abutment load will be distributed over more pillars.

The caving mechanism taking place in the top seam will have a considerable influence on the magnitude of the abutment stress and, therefore, the stress transferred to the lower seam pillars and parting. Parting plane controlled caving will produce higher abutment stresses than bulking factor controlled caving.

The stress distribution in the parting undergoes considerable change. Table III summarizes five case histories where total extraction has taken place over bord-and-pillar workings.
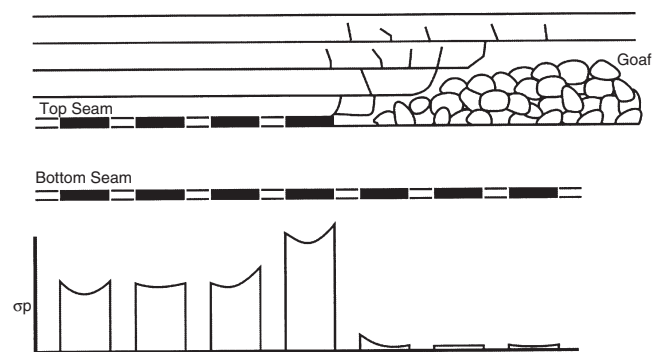

Figure 6. Pillar stress profiles in lower seam due to upper seam pillar extraction

Table III
Summary of conditions in lower seam bord-and-pillar workings where high extraction has taken place in upper seam

Mine	Upper seam		P	Lower seam			Comments
	Name	H (m)	(m)	Name	h (m)	H (m)	
A1	B	1.4	3.6–6.7	C	1.8	113	4 roof falls 1 parting collapse when P < 4.0 m
A2	Gus	0.98	15	Dundas	1.3	195	Remnants left in Gus, roof falls in Dundas
A3	Gus	1.1	15.4	Dundas	1.2	167	Spalling, roof falls and floor creep in Dundas
A4	Alfred	3.0	4.0	Gus	2.0	50	Large roof falls in Gus
A5	No. 5	1.9	38	No. 2	3.0	60	No effect on No. 2 seam workings

Since dynamic changes take place, any roof support installed should be compatible with the expected change in stress.

Longwalling underneath longwalling

Where longwalling is to be done underneath an existing longwall, the two major considerations are the design and placement of the inter-panel pillars of the bottom longwall, and the ingress of water from the upper seam goaf.

Placement and width of inter-panel pillar

If the pillars (thus the panels) are to be superimposed, the bottom seam inter-panel pillar (Barrier) has to be wider than the upper seam inter-panel pillar to compensate for the additional load transfer from the highly stressed upper seam inter-panel pillar. This is especially the case where the overburden has not failed completely. This means that the bottom seam panel will have to be narrower than the upper seam panel.

It also implies that the surface subsidence profile will be severe, as the mining of the second panel results in significantly more subsidence than the first panel. The reason for this is that in mining the second panel, the previous goaf is merely lowered and the process of goaf formation and subsequent recompaction, does not take place.

If the panels are staggered it is not necessary to widen the bottom seam inter-panel pillar as it is then placed in the destressed zone from the upper seam mining. However, it means that the stress effects of the upper seam inter-panel pillar will now be manifested on the bottom seam longwall face which, in severe cases, may result in face breaks.

At Sigma Colliery, longwalls were staggered successfully at a depth of 130 m with a parting thickness of 12 m. The position of the upper seam inter-panel pillar was noticeable on the bottom seam, indicated by additional scaling of the face, but no production problems were encountered. In that case, bottom seam production was actually enhanced by the additional scaling of the face.

There are no easy rules of thumb for the design and placement of the pillars in multiple seam longwalling. This type of design should be done with the aid of numerical modelling.

Water from the upper seam goaf

At Sigma Colliery, the immediate roof of the upper seam consisted of shale/mudstone, which turned into mud in the goaf. De-watering holes were drilled from the bottom seam gate roads into the upper seam goaf, but only small amounts of water were extracted. The mud tended to block the boreholes. The best policy is to mine the panels uphill so that water accumulates in the goaf and not on the face.

Longwalling underneath stooping

In the ideal situation where stooping was done successfully, and there are no unmined pillars or unfailed snooks in the upper seam, there is no difference between mining under a stooped panel and mining underneath a longwall. In reality, this will seldom be the case. There will invariably be snooks and other surprises coming from the upper seam.

Stooping remnants are usually highly stressed, transferring even more stress to the bottom seam than inter-panel pillars, see Figure 7. The major difficulty is that the positions of these remnants are usually not known. Stooping would invariably have been done by a crew other than the longwall crew and there will be no personal knowledge of the positions of these remnants. The positions will seldom be indicated on the mine plans.

The best policy in this situation is to be prepared for the unexpected. An emergency face break procedure must be in place and a 'first aid kit' consisting of emergency materials like rockdrills, hoses, long bolts, wiremesh, etc. must be kept close to the face.

Mining over goaf

Upper seam reserves have been written off in the past by operators assuming them to have been destroyed by high extraction mining on a lower seam. Several collieries in KwaZulu-Natal have successfully mined seams that have been undermined.

Figure 8 shows a typical situation where mining has

taken place below two upper unmined seams.

There are four characteristics of this type of mining:

- Caving of the upper strata creates fracturing due to subsidence
- Remnant pillars in the lower seam causes differential subsidence to occur. This creates areas of instability due to tensile zones over the pillar-goaf boundary
- Remnant pillars cause stress concentrations, which will be transferred to the upper, seam workings. This may cause pillar spalling or floor heave
- Areas within an incomplete parting plane controlled goaf may be destressed.

The significance of the caving mechanism in upper seam stability is shown in Figure 9, which illustrates the four different situations that can occur.

Where the ratio of the parting thickness to lower seam height is high, and bulking factor controlled caving has taken place, the anticipated problems

Figure 7. The contrast in the face conditions shown in these two photographs illustrate the effects of a remnant in the upper seam on longwalling on the lower seam
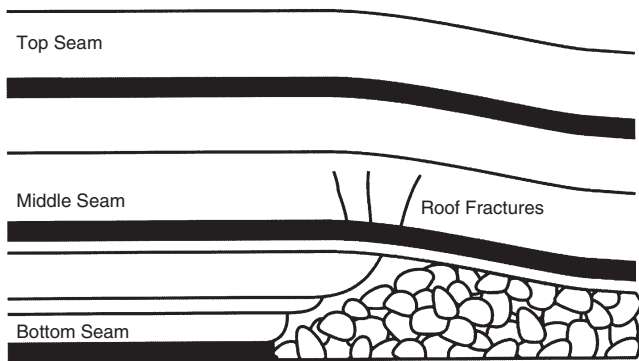
ROCK ENGINEERING FOR UNDERGROUND COAL MINING

Figure 8. Effect of caving and settlement of strata around two upper seams after mining the lower seam

a) Complete caving
Thick parting

b) Incomplete caving
Thick parting

a) Complete caving
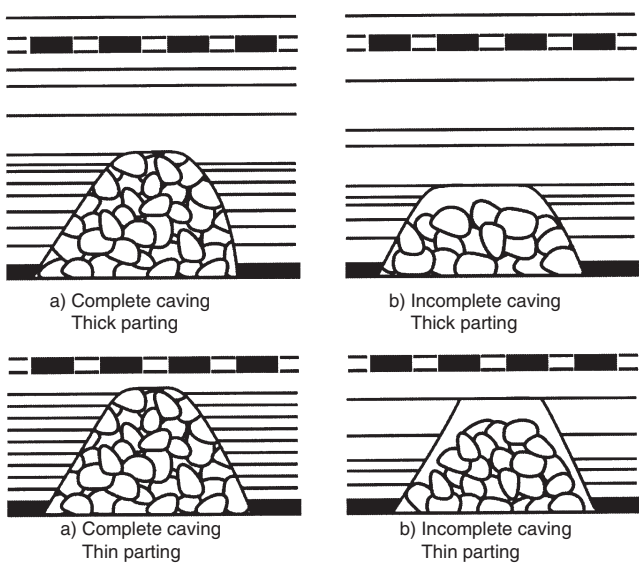Thin parting

b) Incomplete caving
Thin parting

Figure 9. Effect of caving mechanism from lower seam mining on upper seam stability

would be minimal. If the ratio of parting thickness to lower seam height is low and parting plane controlled caving has occurred, there is the possibility of mining over incomplete goafing or voids.

The potential for parting collapse will depend on:

• The thickness and properties of strata between the upper seam floor and the base of the bridging strata
• The length of unsupported bridging strata
• The upper seam layout
• Stress on the upper seam pillars.

Table IV summarizes the main parameters in each of the cases where mining has been carried out over goafs in KwaZulu-Natal. The case studies can be broadly divided into two groups.

Group 1 consisted of collieries B1, B2, B3, and B4. The P/h ratio was high (>9) and only minor roof control problems were experienced. The partings were all sandstones of thickness 14 m to 17 m. Pillar extraction was carried out safely at collieries B1 and B2, while bord-and-pillar workings were conducted in collieries B3 and B4.

Group 2 consisted of collieries B5, B6, and B7 where the P/h ratio was less than 6.0 and roof and floor stability problems existed. The low P/h ratio for colliery B7 necessitated a change to a more accommodating and safer mining method. Conditions in the upper seam can rapidly deteriorate when mining over two goafs, as at colliery B6, where floor failure occurred.

Simultaneous mining

Simultaneous mining is the mining of two (or more) seams in the same area, at the same time with the

Table IV
Mining over goafs case history details

Mine	Upper seam				Lower seam			P	Time	P/h
	Name	h (m)	H (m)	Mining	Name	h (m)	Mining		months	
B1	Alfred	0.8	160	*BP&PE*	Gus	0.99	*BP&PE*	15–17	18	15.1–17.1
B2	Gus	0.9	0–80	*BP&PE*	Dundas	1.4	*BP&PE*	17	2	12,4
B3	Gus	0.97	30–40	*BP*	Dundas	1.3–1.6	*BP&PE*	17	30–40	11
B4	Alfred	1.7	180–200	*BP*	Gus	1.5	*BP&PE*	14	20	9.33
B5	Alfred	2.43	100	*BP*	Dundas	2,6	*BP&PE*	15	50	5.65
B6	Alfred	1.82	90–100	*BP*	Gus & Dundas	0.91–2.13	*BP&PE*	8.3 and 7.0	30	5.0
B7	Middle	1.3	80	*HGLW*	Bottom	1.3–1.5	*BP&PE*	2.0–3.0	22	1.33–2.33

Where *BP* = Bord-and-pillar mining only
    BP&PE = Bord-and-pillar mining followed by pillar extraction
    HGLW = Hand-got longwall
    P/h = Parting thickness/lower seam height ratio.

Figure 10. Simultaneous stooping of two seams

same areal extraction rate. The horizontal distance between the two face lines in each seam is kept constant.

This type of mining has been carried out in KwaZulu-Natal in the past, especially where it has been difficult to keep lower seam roadways open for complete development under a goaf. It is normal for the coal to be transported out through one seam only.

Two methods have been employed

• *Simultaneous stooping in both seams*—Superimposed pillars are developed in both seams, see Figure 10. Stooping takes place simultaneously in both seams with the top seam extraction line being about half a pillar ahead of the bottom seam extraction line. Problems can be experienced if goafing is not consistent. Some collieries spent many years experimenting with different top seam leads over the lower seam extraction line to find the optimum distance. Simultaneous stooping of two seams is not currently practised.

• *Mining one seam*—The bottom seam is first developed on a bord-and-pillar layout. The pillars are extracted on a splitting system. As splits are developed, the parting is dropped by drilling and blasting. The top seam is recovered by top coaling from the top of the parting. Simultaneous mining has had mixed success, probably due to its reliance on good caving of the parting between the two seams.

Design flowchart

To assist with the design of multiple seam workings, a design flowchart is provided as Figure 11. The following example illustrates its use.

Example

The Main Development of a 3.0 m seam mined at 95 m depth below surface requires a pillar Centre Distance of 18 m, pillar width 12 m and bord width 6.0 m. Pillar extraction is planned in the secondary panels planned at right angles to the Main Development. A barrier of 24 m has been selected as a barrier between the secondary panels and the Main Development.

20 m below the seam is a 1.75 m seam. Using the multi-seam design flow chart, Figure 11, the parting is not greater than 1.5 times the Centre Distance: $C = 18 \times 1.5 = 27$ m. Therefore, the superimposition of the barriers is suggested by the flow chart. Applying the Limiting Distance Criteria, see Table II, the Limiting Distance for a 24 m barrier pillar is about 24–28 m, depending on the panel width-to-depth ratio. As the actual distance is 20 m the barriers pillar would have to be superimposed.

The panel pillars in the Main Development have 18 m centres. Applying the factor of $0.75 \times C$ the distance of 13,5 m implies that the panel pillars do not have to be superimposed. As the panel width of the upper panel is fixed in this case, the same pillar centres would be applied to the lower Main Development.

The barrier pillar width of 24 m was selected due to the requirement of a high pillar width-to-height ratio to protect the main development when pillar extraction operations commence. Experience has shown that, while extraction of one side of the Main Development is acceptable, both sides of the main development should not be extracted until there is no further need for the Main Development. This is particularly true when a thick dolerite sill overlies the workings.

Barriers between the secondary panels could be designed to less stringent requirements if the panels have a limited life. If a 12 m barrier is left between the panels the Limiting Distance, Table II, reduces to about 15 m. In this case the barrier and panel pillars would not require superimposition.
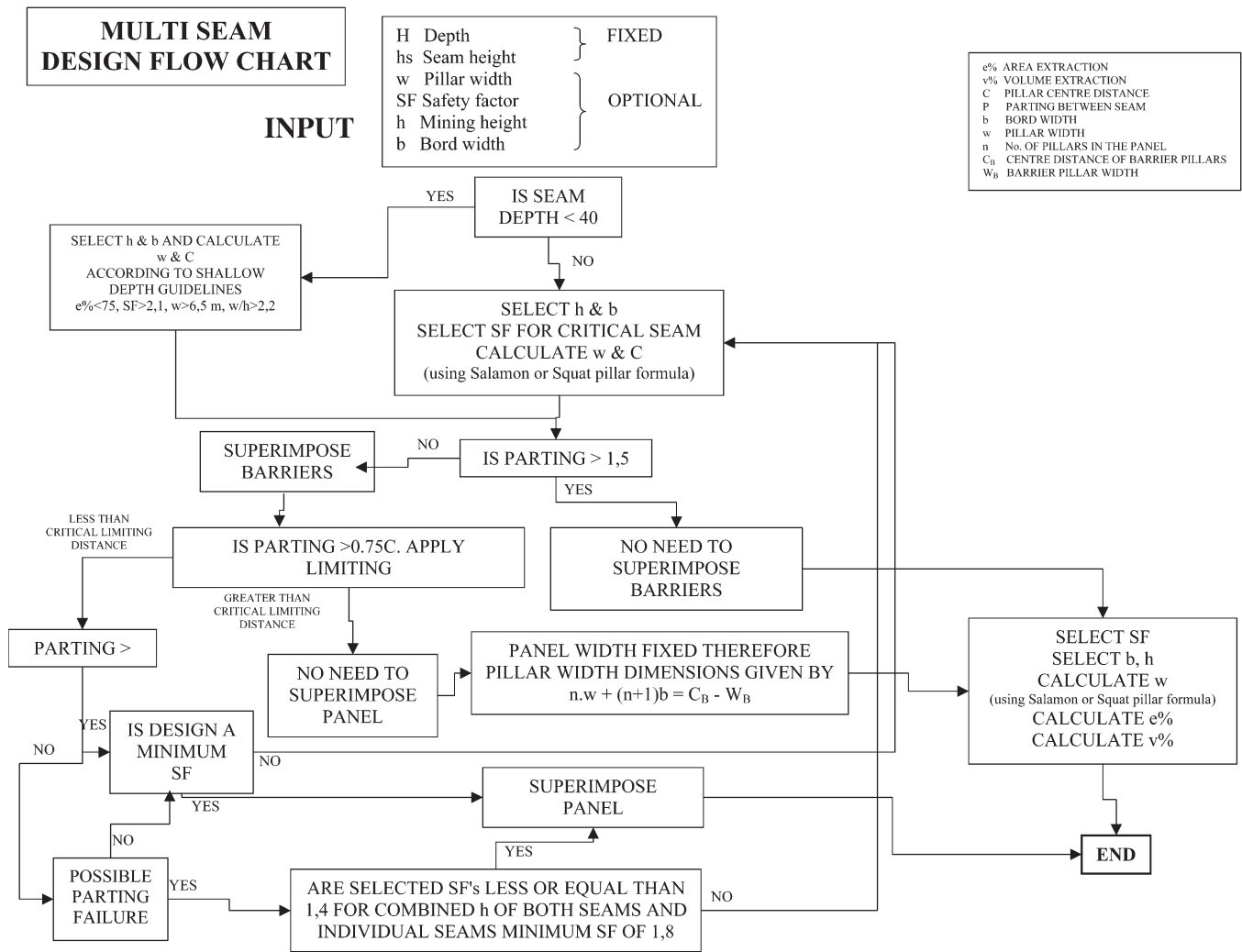
Figure 11. Multiple seam design flowchart

ROCK ENGINEERING FOR UNDERGROUND COAL MINING

Chapter 8

Shallow workings

Introduction

The shallower the mining depth, the lower the field stresses in which mining operations are conducted. It has been seen that at depth less than around 40 m below surface, the stress environment is sufficiently low to warrant special consideration. The most important differences between shallow and deeper mining are that the clamping forces in the roof are reduced, which can result in more roof collapses, weathering can weaken the strata and, in the case of high extraction mining, the tensile zone can extend all the way to the surface.

The coal-seams exploited in South Africa are predominately close to surface with approximately 40 per cent mined by surface mining methods. The economics of the operation will determine the depth that the opencast mining can operate. This also depends on the number of coal- seams that can be exploited, the quality of the coal-seams, the yield of each seam, the thickness of the coal-seams and the amount of 'softs', material (usually weathered) that can be removed by non-blasting methods, and the thickness of the 'hards'

strata that requires blasting. The capital employed will also determine the limitation of opencast mining from 10 m to 15 m in a thin seam with minimal capital to over 75 to 100 m using large dragline material handling methods.

Once the economic limit for surface mining methods has been reached, it is not uncommon for mining to continue underground by means of portals developed into the highwall. Some consideration of highwall stability is therefore warranted. Note that this is a specialist aspect, not dealt with in great detail here. The design methodology for surface mines is covered in detail in publications such as Stacey (2001) and Stacey and Swart (2002).

Underground mining from a highwall

Each cubic metre of material removed adds cost to the operation, and the operator aims to reduce the amount of material to be moved to a minimum. This can result in instability of both the 'softs' soil and weathered material, Figure 1, where no bench has been left between the 'softs' and the 'hards'. After the coal has

Figure 1. Collapse of 'softs' material extending to the pit floor because no bench between the 'softs' and 'hards' material was provided

been exposed and removed, the material overlying the coal-seam is removed by scraping the soil or blasting the rock and this material is 'cast' during the blasting of the overburden into the area where the coal has been removed or transported by truck and dumps into the void forming a 'lowwall'. Placing weathered material, particularly clayey soils, on the 'lowwall' and placing harder strata from the overburden blast over the clayey material can result in the reduction of the stable slope angle due to failure along the lower cohesion plane that the clayey material forms. Water, rain or groundwater, if not controlled away from the opencast area can aggravate the potential for slumping by reducing the cohesion on the failure plane.

Management has two opposing criteria when deciding on the profile of the opencast face: between reducing costs by having steep bench faces and minimal bench widths and having the potential for bench failure; and incurring additional costs by reducing the profile angles by reducing the angle of the slopes and increasing the stability of the bench slopes. Failure of the highwall (face) benches is acceptable provided the failure is not unexpected and does not endanger equipment, personnel or the viability of the operation

General guidelines for opencast workings should include that soil and weathered material should be battered to an angle of 35° with a 5.0 to 10 m wide bench. Drains should be placed at the base of the bench and a berm placed on top of the soft material to indicate the slope face and prevent personnel or machinery from inadvertently falling over the slope edge. Weathered strata should be battered at an angle of 45° with a 5.0 m wide bench. Individual face height should be limited to a maximum of about 25 m vertical height. Faces greater than 25 m would have a bench between 3.0 to 5.0 m that would restrict the face height.

Leaving soil and weathered material on a steep angle next to the highwall bench, as well as leaving loose blocks as a result of blast damage to the strata on the highwall crest edge, increases the likelihood of failure and damage or injury.

Underground mining from a highwall

When the economic limit of the opencast operation is reached and the coal reserves continue within the mining area, the option to continue exploiting the reserves using underground mining methods becomes available. Mining from the opencast highwall has been practised from many years. Selection of the location of the portals to the underground should be based on the stability of the rock mass in the highwall, including the presence and orientation of jointing.

Rockfalls from highwalls, while not common, can result in a significant volume of material failing, with the potential for damage to equipment and injury to personnel. Highwall classification systems for use in coal mines have been developed by Latilla (2002) and Canbulat *et al.* (2004). These classification systems can be used to classify the highwall bench face and select the most appropriate location for a portal to access the underground reserves.

Where the coal reserves are known to occur and an existing highwall has not been developed, geotechnical boreholes can be used to gain an indication of the rock mass using index tests such as impact splitting on borehole core and rockmass classification systems such as RMR, MRMR, and Q. However, the jointing in the rock mass cannot be determined by vertical boreholes and angles boreholes are rarely used. Typically the area is determined by mining considerations and the geotechnical engineer has to adjust to the rock mass conditions by using benches or support to stabilize the rock mass in the highwall. Blast lengths up to 20 m are not uncommon where a boxcut or highwall is to be formed. Whereas the strength of the rock mass can be

Figure 2. Joints oriented sub-parallel to the highwall face line, resulting in instability

predetermined by geotechnical drilling, joint location and orientation are usually found only after excavation of the blasted rock. Figure 2 shows joints orientated sub-parallel to the final highwall face and dipping into the excavation. Removal of the potential unstable blocks or supporting the blocks by cable anchors, mesh and bolts are options to prevent the blocks dislodging and causing damage or injury.

Where thick layers of soil and clay occur together with weak strata in the overburden, more sophisticated techniques such as numerical modelling are required to assess the stability of the overall slope profile.

The strata at the brow of the portal to the underground workings are usually affected by blasting during the formation of the highwall or boxcut. The brow should be supported after the first 3.0 m has been excavated by full column roofbolts and cable anchors. A double row of three cable anchors with full column grouting is commonly installed at the brow. Depending on the competency of the strata and the jointing in the immediate roof layer, mesh, cable anchors and reinforced shotcrete could be required to form a stable brow. Cable anchors can be installed in the highwall and the exposed roof of the underground workings and

Figure 3. Example of a sinkhole

wrapped over the mesh and tensioned to 10 tons. In very poor ground cable anchors can be installed prior to forming the portal brow.

Sinkhole formation

Where bord and pillar mining was done at shallow depth, it is not uncommon for sinkholes to develop, sometimes much later. Figure 3 is an example of a sinkhole in the Witbank area.

Salamon and Oravecz (1976) formulated a general guideline that when the depth is less than 4 to 5 times the bord width, typically 24 m to 30 m depth, roof instability can occur. Hill (1996) investigated sinkhole development in the Springs and Witbank-Highveld coalfields and determined that the main factors influencing sinkhole development are:

- Sinkholes are unlikely to occur when the depth exceeds 40 m
- Failure occurs where sandstone layers account for less than 30% of the overburden
- Large spans at intersections result in failure
- Extraction height determines the height of caving before bulking arrests upward migration
- Sinkhole development may occur decades after mining
- Blast vibration, especially large overburden opencast blasts, may cause failures.

Canbulat *et al.* (2002) in their investigation into the prediction of surface subsidence, examined sinkhole formation using beam theory (tensile and shear stresses) and bulking factor analysis. Sinkhole development will be initiated by the failure of the immediate roof layer, and this failure will be either tensile or shear. If the tensile strength of the initial material is not high enough, it will fail and initiate the sinkhole, and the broken material will spill into the bords. The amount of material will be determined by the bulking factor, mining height, and bord width.

Sinkhole development may be arrested by the presence of a strong layer in the overburden (Figure 4) or merely by the bulked roof collapse material choking the cavity; see Figure 5.

Determination of mineable depth

Due to the weathered nature of the overburden at shallow depth, it is also important to determine the stability of the overburden. This aspect was investigated by Canbulat *et al.* (2002). While competent layers can sustain more load, incompetent
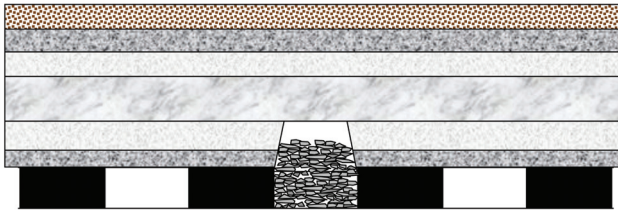
Figure 4. Sinkhole development arrested by a strong layer in the overburden
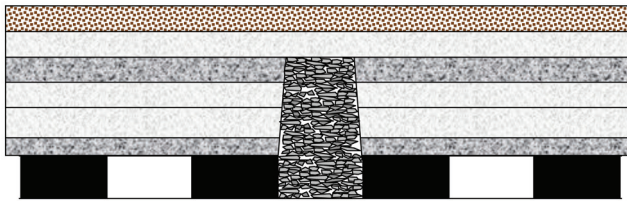

Figure 5. Sinkhole development arrested by collapsed and bulked material choking the cavity

layers can fail suddenly (Figure 6). The load-carrying capabilities of competent layers in the overburden should therefore be determined. This can be achieved by determining either the critical thicknesses or percentage of competent layers to total thickness in the overburden.

Tensile stress analysis

If the overburden pressure is high and the strata are solidly clamped at the sidewalls, the overburden strata are considered to behave like fixed beams. The maximum tensile and compressive stresses occur near to the ends of the beam. The procedure to predict failure is to ensure that the maximum tensile stresses are within the limits that competent material can

Figure 6. Sudden failure of incompetent layers at shallow depth

sustain.

$$\sigma_t = \gamma \frac{b^2}{2t} \qquad [1]$$

where
$\sigma_t =$ tensile stress (MPa)
$\gamma =$ unit weight (MN/m^3)
$b =$ span (m)
$t =$ beam thickness (m)

Consideration should be given to additional loading from thinner, incompetent overlying strata and also deadweight loading from totally weathered material.

The tensile stress due to additional deadweight loading can be calculated from:

$$\sigma_t = \frac{\gamma(t_s + t_u)b^2}{2t_s^2} \qquad [2]$$

where
$\gamma =$ density of sandstone and overburden (MN/m^3)
$t_s =$ total thickness of competent layer (m)
$t_u =$ total thickness of weathered material or depth (m)
$b =$ span (intersection diagonal width) (m)
$\sigma_t =$ tensile stress (MPa)

From the above equations the critical thickness of competent layer, t_s, can be solved as follows:

$$t_s = \frac{\gamma L^2 - \sqrt{(\gamma L^2)^2 - 4\sigma\gamma L^2 t_u}}{2\gamma L^2 t_u} \qquad [3]$$

It should be noted that total supported height (including additional load) should be subtracted from the total thickness of weathered material or depth below surface.

Figure 7 and Figure 8 show the critical competent layer thickness and required percentage of competent layer in the overburden for different tensile strength of layers at different depths, respectively.

In order to calculate the critical competent layer thicknesses, a series of Brazilian Tensile Strength (BTS) tests can be conducted on samples obtained from a borehole. The average tensile strength of competent layers is determined and this value is used to determine the critical thickness of competent layers at the shallow workings.

Note that the tensile strength value obtained from the laboratory tests should be downgraded for *in situ* rock mass strength.

Figure 9 shows the critical thickness and required percentage of competent layer in the overburden. This

ROCK ENGINEERING FOR UNDERGROUND COAL MINING

Figure indicates that although required thickness of competent layer increases as the depth increases, the required percentage of competent layer in overburden decreases. Using this figure, the mineable depth of shallow workings of the colliery can be calculated.

Bord and pillar mining at shallow depth

Several features make mining at very shallow depth different from mining at more common depths:

- The depth of weathering can reach to as much as 30 m below surface, will be a significant portion of the overburden, and may even extend into the workings.
- Large tensile zones will be present over the bords due to the low depth/span ratio.
- Vertical discontinuities, such as joints, may not be 'tight' and therefore allow vertical movement.
- Variations in surface atmospheric conditions, such as humidity are transferred to underground, therefore weathering can take place.

Figure 7. Critical thickness of competent layer for different tensile strength of competent material at different depths

Figure 8. Critical percentage of competent layer in the overburden for different tensile strength of competent material at different depths
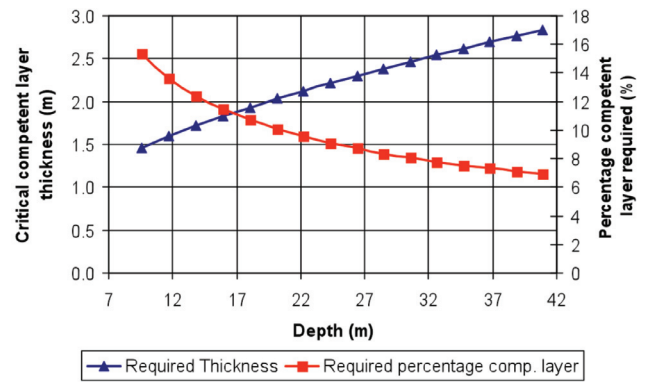

Figure 9. Critical thickness and required percentage of competent layer in the overburden (BTS=9.42 MPa, intersection diagonal length is 8.4 m, bord width is 6.0 m, unit weight is 0.025 MN/m³)

Pillar design at shallow depth

The pillar safety factor formula alone should not be used at shallow depth since other factors influence pillar stability.

In addition, the safety factor formula, which was developed for pillar stability, gives no indication of the stability of roadways. Bord failure at shallow depth can occur during mining or as much as 80 years or greater afterwards. Collapse of intersections can result in a sinkhole when the failure reaches the surface. Collapse of roadways between intersections can result in shallow troughs on surface. Sinkholes are common over many abandoned shallow bord and pillar workings in the South African coalfields, especially in the Witbank and Springs area (Figure 10).

Hill (1996) suggested that the following factors should be considered when mining at shallow depths (< 40 m):

- Use of the safety factor formula alone may be misleading since other factors also influence pillar stability.
- Floor failure may occur; although it is more likely to occur at depth as the load is greater. Floor failure has nevertheless occurred at shallow depths.
- Bords may fail to surface, forming sinkholes.
- Workings may be subjected to surface climatic changes.
- Shallow workings result in temporary or permanent changes in the groundwater table and this may lead to localized deepening of the influence of weathering.

The problems of shallow mining were also discussed by Madden and Hardman (1992) and the following design guidelines were established:
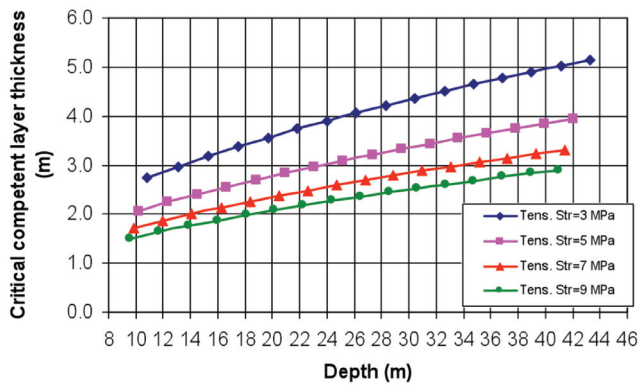
- Pillar width to mining height ratio should not be less than 2.0.
- Areal percentage extraction should not be greater than 75 per cent.
- The minimum pillar width should not be less than 5.0 m.
- A minimum safety factor of 1.6 should be used.

Canbulat and Madden (2004) after a review of pillar collapses suggested that the new shallow depth pillar design guidelines for Witbank Coalfield No. 1, 2, 4 and 5 Seams should be as follows:

- Pillar width to mining height ratio should not be less than 2.2.
- Areal percentage extraction should not be greater than 75 per cent (indicates a maximum bord width of 6.5 m).
- The minimum pillar width should not be less than 6.5 m.
- A minimum safety factor of 2.1 should be used.

Roof support design methodology at shallow depth

There are two important factors that have an addidtional impact on roof support design for shallow workings. Firstly, the roof material may be weaker than at greater depth due to weathering and, secondly, the lower magnitude of horizontal stress means that the clamping forces on vertical joints are lower. There are no special design methods for roof support at shallow workings, but it is clear that it should be approached with even more caution than at greater depth.

Special care should be taken to determine whether weathering has had an influence on rock material strength. The tensile strength is especially important. Instead of embarking on a time consuming and expensve programme of laboratory testing, it is often sufficient to obtain borehole core and then to perform impact splitting tests (see Chapter 2).

Figure 11 shows the relationship between the impact split tests and Brazilian Tensile Strength tests, according to Canbulat and Madden (2005). As can be seen there is a good correlation between the test results (R^2=0.903).

The nature of roof collapses are different in the sense that larger blocks, delineated by joints, are likely to fall. Joint support is therefore crucial.

High extraction mining at shallow depth

At shallow depth, the stress disturbance caused by mining follows a different pattern than at greater depth. It is more likely for the tensile zone above the high extraction mining area to extend to the surface, the reason simply being that the magnitudes of the *in situ* compressive stresses are lower. This is illustrated in Figure 12, a plot obtained with the Examine2D software (Rocscience, 2003).

The main implication of the greater extent of the tensile zone is that more extensive goafing can be expected and that the goaf will occur more quickly than at greater depth. The rock blocks inside the goaf are usually also larger as a consequence of the greater tensile zone. In general, it can be stated that the entire mining environment is 'looser'.

Due to the lower vertical stress magnitude, less scaling on the abutments will be observed, and it is more important to be aware of joints opening in the roof than excessive pillar scaling. While it is still important to monitor pillar scaling behind the line of pillars being extracted, it is also important to visually inspect the roof in roadways behind the extraction line.
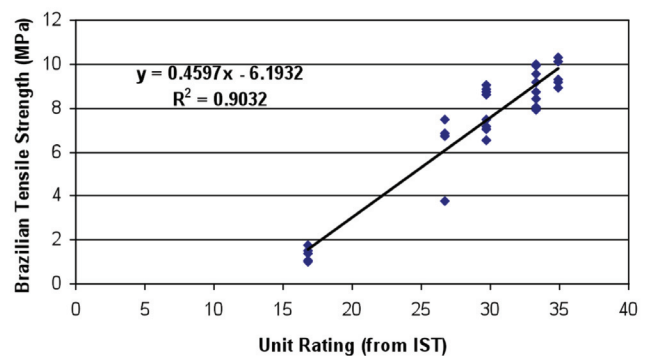

Figure 10. Intersection collapse at shallow depth

Figure 11. Relationship between the IST and BST

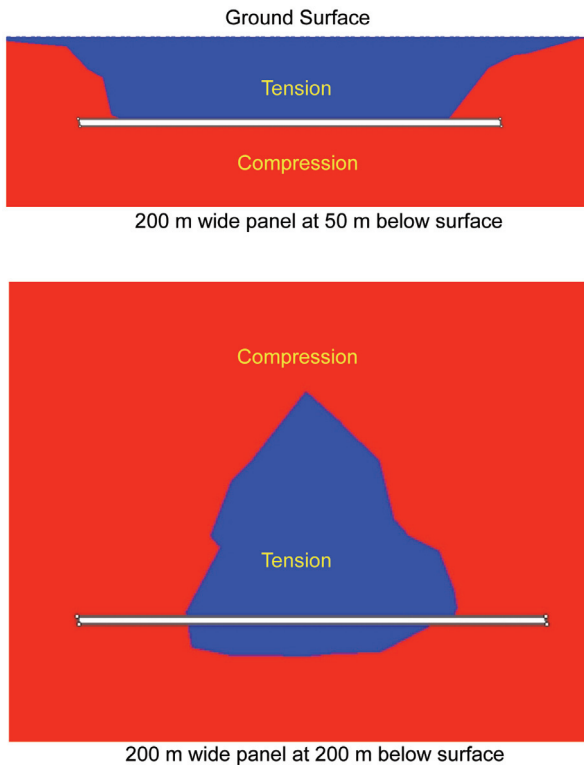ROCK ENGINEERING FOR UNDERGROUND COAL MINING

Figure 12. Model of a cross-section showing the larger extent of the tensile zone above a high extraction panel at shallower depth

Shallow longwalling

A recent experience with longwalling at shallow depth—30 m to 50 m below surface in this case—in the Highveld coalfield illustrates the impact of unravelling due to the lower general stress regime.

Frequent face breaks occurred and in one case so much material had to be loaded out to free the shields that a sinkhole developed on the surface, allowing sunlight to filter down to the underground workings, see Figure 13. The situation was aggravated by a period of heavy rain. The sinkhole afforded direct access for water to the underground workings and, on top of everything, flooding occurred.

Shallow pillar extraction

Due to the depletion of coal reserves in the Witbank coalfield, attention is more and more being turned to the extraction of old pillars that were not designed for secondary mining. As the depth was shallow, these pillars are small even though the safety factors are not necessarily low.

The small size of the pillars means that the more conventional methods of larger pillar extraction (i.e. cutting the pillar in half to create two fenders that are extracted in sequence or the typical NEVID layout)

cannot be used. Some pillars are even so small that the only way in which they can be mined is by means of a diagonal cut through the centre.

This is not considered good practice at depth due to the large intersection that is created. At shallow depth, however, it may be tolerated as a last resort if roof conditions allow. Extra care is still required to prevent accidents due to roof collapse, which is the higher risk. Proper awareness training is required and operators should always be on the lookout for joints that could open during the extraction process. Remote controlled continuous miners are recommended to ensure that the miner does not enter the large intersection that is created.

It is also necessary to evaluate pillar safety factors, preferably by means of modelling. The possibility of pillar runs should receive special attention.

Due to the unstressed nature of the roof, it will almost always be required to leave snooks in place. This is particularly challenging at shallow depth, as the lack of stress may mean that the snooks do not crush when they should. This could in turn result in large areas hanging up, with the subsequent danger of stress build-up on the remaining pillars and the possibility of a pillar run.

For pillars to collapse, they have to be stressed beyond their ultimate strength and the overburden also has to fail. It is distictly possible for pillars to be destroyed from a load bearing point of view and yet to remain standing because the overburden has not failed.

Consider the following example, where a 20 m thick sandstone occurs in the overburden and pillars are extracted in an 80 m wide panel underneath it.

Figure 13. Unique view of longwall shields underground illuminated by sunlight. Photo courtesy of Exarro Coal

It is known from fundamental elastic considerations, that the deflection of a self-loaded clamped beam is given by:

$$\eta = \frac{\rho g t L^4}{32 E t^2} \qquad [4]$$

where $t =$ thickness of layer
  $L =$ span of beam
  $E =$ modulus of elasticity (13 GPa for sandstone).

Using Equation [4], it is apparent that the beam can deflect by 123 mm in its centre without failing.

The ultimate strength of a snook (van der Merwe 2003) is:

$$\sigma = 3.5 \frac{w_e}{h} \qquad [5]$$

where $w_e =$ equivalent pillar width
  $h =$ pillar height.

The ultimate strength of a snook with equivalent width 3 m and mining height 3 m is 3.5 Mpa.

Pillar strain is given by:

$$\varepsilon = \frac{\sigma}{E_c} \qquad [6]$$

where E_c is the elastic modulus of coal (4 GPa).

It is then found that the strain of the pillar at the point of failure is 0.000875.

Pillar compression is simply

$$d = \varepsilon h \qquad [7]$$

which means that the pillar in the example will be compressed by 2.6 mm at the point of failure. This shows that for the stated conditions, it is possible for the pillars to be stressed to beyond the point where they offer support, but because the roof beam has not failed, no collapse is apparent. Figure 14 is an example showing very small pillar snooks that have not failed.

When this happens, the obvious, but not necessarily correct, conclusion could be that the snooks are too strong, and the follow-on reaction to that will be to mine more of the pillars, thereby increasing the risk of roof collapse but not addressing the root problem, which could be that the panel is simply not wide enough to allow the overburden to collapse.

The purpose of the example is to indicate the importance of also taking cognizance of the overburden composition and to consider the minimum mining span that will be required to cause collapse to occur in a controlled manner.

Figure 14. Small pillar snooks showing no signs of load

While pillar extraction at shallow depth is not necessarily bad practice, it needs to be approached with caution and proper investigation.

The following sequence of primary desk-top investigation is recommended:
Step 1: Conduct detailed underground inspection to evaluate roof conditions and to determine the extent of pillar scaling.
Step 2: Inspect geological records and identify strong layers in the roof. Be aware that especially old borehole logs were possibly not recorded with the same care as more recent ones. Redrill if necessary.
Step 3: Calculate minimum span to result in overburden failure.
Step 4: Embark on numerical modelling using actual (not as mined) pillar dimensions. Use the model to determine snook sizes, positions and extent of stopper lines if required and the possibility of pillar overruns.

Note: Chapter 9, Numerical Modelling, contains guidelines on the LAMODEL input for this purpose.

Practical considerations

The immediate strata type will also influence the mode of goafing. For example, in Figure 15 the competent sandstone layer has goafed along the edge of the pillars and did not intrude into the heading. However, the shale layers in Figure 16 slid into the heading due to their shape, which caused sliding of the shale blocks into the heading. This can influence the extraction of the pillar as the angle of the continuous miner is restricted by the material in the heading.

In both cases the roofbolt breakerlines were effective in limiting the strata to the edge of the pillar. Timber prop breakerlines have been replaced by roofbolt breakerlines due to the advantage that they can be installed outside the mining cycle of extraction. In addition, the timberline breakerlines can be knocked out by the goaf material, as could have been the case in Figure 16, which could have resulted in the roof of the

heading failing and extending into the pillar. Fatalities have occurred in the past where the roof overbreak extended to the intersection where personnel were standing. The roofbolt breakerlines have reduced the extension of the goaf into the heading.

Conducting pillar extraction by drill and blast methods is currently not acceptable by the authors due to the high risk of exposing personnel in the area where extraction is taking place. Pillar extraction using a continuous miner can be considered after an investigation into the pillar dimensions and geological conditions.

The rock engineering assessment of the panel should be undertaken and should include:

- The location of enlarged intersections
- Odd sized pillars, particularly smaller pillars than designed
- Geotechnical mapping of the section; the panel to be extracted must be mapped and the 'weak' side of all discontinuities noted
- Location of rolls in the seam
- Assessment of the condition of the initial support installed
- Location and extent of falls of ground
- The sequence of extraction must take into consideration the places where personnel will stand in relation to the geological features
- Calculation of the current safety factor and pillar width to mining height ratio, ideally a minimum of 1.8 for the safety factor and 2.0 for the width to height ratio is required, although a lower safety factor may be acceptable if the pillar width to mining height ratio is higher and if the overburden is expected to cave easily. Numerical modelling should be used in this part of the investigation.

The rock engineering report on the initial assessment of the area to be extracted should indicate the feasibility of the conducting pillar extraction and highlight potential problems that will require further investigation.

Issues to be addressed

Prior to starting extraction, a number of issues must be addressed including:

- Risk assessment: an in depth risk assessment must be conducted for the operation. The procedure for extracting the continuous miner from a burial should be in place as one of the mitigating measures and a 'tooth extractor' available in the section at all times during extraction operations.
- Sequence of extraction: a plan of the panel with each pillar numbered (numbers should be marked on each pillar in the section as well), and the cutting sequence for each pillar determined, taking into account the geotechnical mapping, enlarged intersections, and all pillar sizes. Pillars should be extracted against the ventilation to prevent personnel exposure to dust
- Roofbolt breakerlines: a double row of 1.8 m bolts will be required to be installed prior to extraction. The breakerlines should be installed at least two rows ahead of the pillar being extracted. The first row should be installed 0.5 m inbye of the solid pillar and the second row 1.0 m further inbye. The primary support installed could be utilized if the bolts installed were 1.8 m full column resin anchored.
- Training should be given to all personnel prior to

Figure 15. Competent sandstone layer goafing on pillar edge

Figure 16. Shale layers sliding into heading, note timber 'policeman' knocked out

the start of the extraction sequence. No person should be allowed inbye of the solid pillars unless under a protective canopy.

- Numerical Modelling; should be conducted to assess the increase in stress over the barrier pillars and the remnant pillars. The modelling could assist in determining if compartments are required within the panel being extracted.

Extraction sequence

Having confirmed that the panel is suitable for pillar extraction the sequence of extraction must be decided
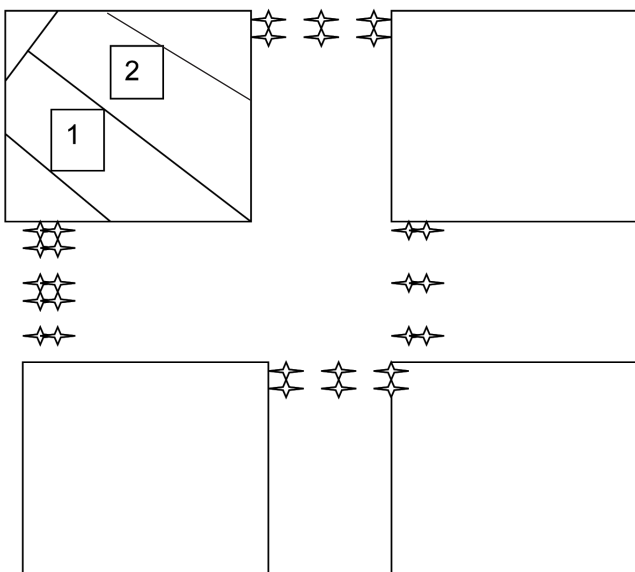

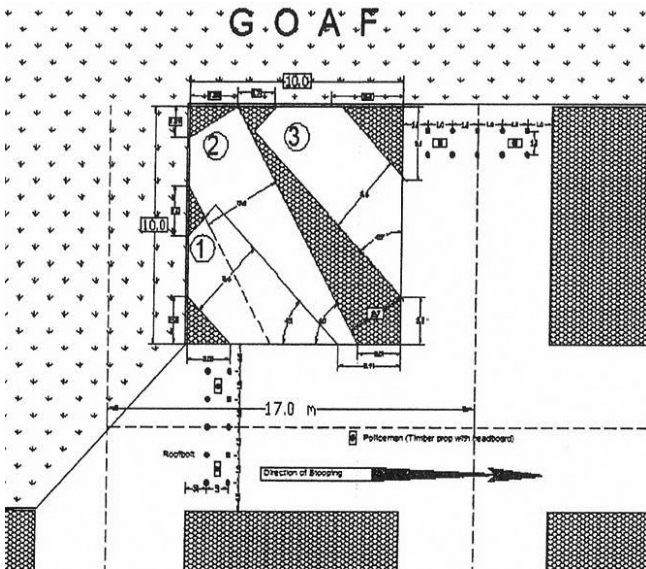**Figure 17. Sequence of cutting a 8 m wide pillar**

Figure 18. Sequence of cutting a 10 m wide pillar

upon. Small pillars with pillar widths of about 8.0 m are typically extracted using a double diagonal cut, Figure 17. Whether the cutting sequence is taken as shown or reversed is not important as both sequences mine toward a solid pillar. As the pillar size increases a third cut will be necessary. Figure 18 shows the cutting sequence for a 10 m pillar, the roofbolt breakerlines are installed and two timber 'policemen' have been installed between the roofbolt breakerline rows. Installing timber 'policemen' after the cutting sequence has begun is not suggested as that would involve personnel going inbye of solid pillars.

The angle of each cutting sequence is important, firstly to ensure that the maximum extraction of the pillar occurs and secondly to ensure that the planned snook on the intersection is of sufficient dimension to provide temporary support during the third cut. Painting the required angle of each cut on the roof and pillar assists the continuous miner operator in maintaining the cutting sequence. Experience has shown that reduced burial of continuous miner is achieved when mining a thick coal roof, for example the No. 2 and No. 4 Seams of the Witbank Coalfield, by limiting the distance of the third cut to approximately the diagonal line between the solid pillar corners, Figure 19. While some coal is left in the unmined portion which reduces the overall extraction, the cutting sequence is not disrupted by delays in extracting the buried continuous miner.

The timber 'policemen' can provide warning of an impending goaf, as shown by the bending of the timber 'policemen' in Figure 20. However, this is not always the case at shallow depth, where there is very little indication of roof convergence and where sudden failure can occur without warning. That is why it is
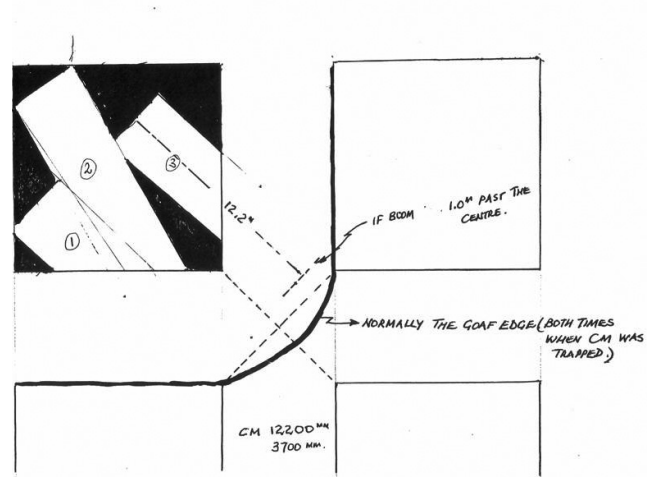

Figure 19. Limiting the distance of the third cut

ROCK ENGINEERING FOR UNDERGROUND COAL MINING

important to follow the planned sequence of extraction and cutting sequence. Extracting the first two rows of pillars at the start of a panel has been practised to assist in the first goaf. This includes the removal of all snooks.

Air blast

It is possible for goafs to hang up for long distances where shallow pillar extraction is done, especially in those cases where the overburden collapse is governed by the presence of a strong layer in the overburden that requires relatively long advance before it fails. When the overburden eventually collapses, it is invariably accompanied by an air blast.

Cutting into the adjacent panels has been conducted to increase the number of roads for the air to escape into, to dampen the effect of the air blast. When that is done, the adjacent panels must be inspected for accumulation of gas and water, and this should be conducted as part of the investigation prior to starting extraction. In addition, all repairs and routine maintenance should be conducted between the splits and not in the headings to reduce the risk to personnel from possible air blasts.

Taking the barrier pillar as part of the extraction sequence will assist in increased extraction and result in a smoother surface subsidence profile. A competent layer in the immediate roof can be beneficial in that the extraction of the pillar can be achieved without caving during the extraction process. However, if the roof strata are too competent goaf hang-up can occur whereby by load from the roof is transferred to the pillar being extracted. The increased load can result in premature failure of the ribs being extracted, especially

the snook left at the intersection as a temporary support to enable the extraction of the final cut into the pillar.

Working plan

A 'working plan' should be developed for each panel. The working plan should include the sequence of pillars to be extracted with each pillar numbered both on the plan and on the pillar sidewall. Slips and discontinuities should be marked on the plan with the 'weak' side indicated, marked by the direction of an arrow head towards the 'weak' side. Paint should be used to mark the slips underground with an arrow painted towards the 'weak' side of the slip. Should two arrows point towards each other, this is an indication that a wedge failure could occur, Figure 21, and this can be particularly dangerous as the wedge height could extend into the roof to a distance greater than the roofbolt support. Careful examination of potential wedges is necessary as additional support, such as cable anchors, may be required.

Figure 22 shows a typical section plan for shallow pillar extraction. Included on the plan are the numbered sequence of extraction, slips with the arrows indicating the weak side of the slip, seam height, and surveyed subsidence measurements. In addition, the planned sequence of extraction for pillars affected by the slips has been indicated. Planned exclusions of the cutting sequence within individual pillars are shown, detailed information would be shown on the working plan which may contain between four and two rows of pillars, depending on the volume of coal in the pillars. Deliberately leaving coal within a pillar has the consequence of delaying the goafing process. However, the attempt to extract beneath the 'weak' side of a slip could result in the burial of the continuous miner as the pillar supporting the roof is reduced to the point where

Figure 20. A timber 'policeman' providing indication of a sagging roof. This method is not always effective at shallow depth

Figure 21. Example of a wedge formed by joints

the slip would cause a local fall of ground, which could result in the burial of the continuous miner.

The 'two-edged sword' of taking all the planned cuts within a pillar (and risk a continuous miner burial) or leaving a particular sequence uncut to support the 'weak' side of a slip (and having the goaf hang-up), must be weighed up as to the consequences of each event. Considering the delay in removing a continuous miner beneath a goaf, together with the risks involved in the extraction process, the planned leaving of coal to protect the continuous miner is the preferred option.

On-board vs remote controlled continuous miner

There is debate whether it is preferable to have a remote controlled continuous miner or to have an 'on-board' continuous miner operator. The 'on-board' operator is stated to be able to 'feel' the cutting and can judge the load on the pillar by the ease of cutting. In addition, it is stated that the operator has better judgement of an impending goaf and can reverse to a safer place prior to the goaf occurring. The disadvantage of the 'on-board' operation is that should a burial occur, there is a tendency to rush to the aid of the trapped operator, which may result in injury to the well intentioned personnel who may not adhere to the correct procedures for the removal of a buried continuous miner. Also 'on-board' operators have tried to exit the cab in anticipation of a pending goaf and have been caught in a roof fall. Some companies have locked the 'on-board' operator into the cab to prevent the operator from an unplanned exit. While it is known

to be safer to stay in the cab, the prospect of being buried, perhaps for several hours, is a difficult choice to make when 'safety' is only some metres away. However, the risk in leaving the cab when an impending goaf is about to occur is high risk and has resulted in fatalities in the past.

The remote controlled continuous miner operator has the advantage of working within the solid pillars and has a better overall view of the working area, including timber 'policemen'. A burial of the continuous miner can be approached without the concern of one's co-worker and the correct recovery procedures can be undertaken, adhering to all safety standards. The removal of a continuous miner must be planned for as an event that can occur. A risk assessment and work procedures must be in place before the start of the continuous miner extraction process.

In addition, the correct equipment and temporary support units must be available and in working order within the section. Figure 23 shows a 'tooth extractor' used to remove a buried continuous miner. Some companies have developed special techniques for the removal of the continuous miner, including drilling into the goaf and support units to be installed when 'digging' for the continuous miner. While no-one aims to bury a continuous miner, recovering from this unplanned event must be planned for and the crew trained in their role in the extraction of the continuous miner so that this can be conducted in a safe manner in the minimum time.

Pillars not designed for extraction

The disadvantages of extracting pillars that were not designed for pillar extraction is that the pillar sizes may
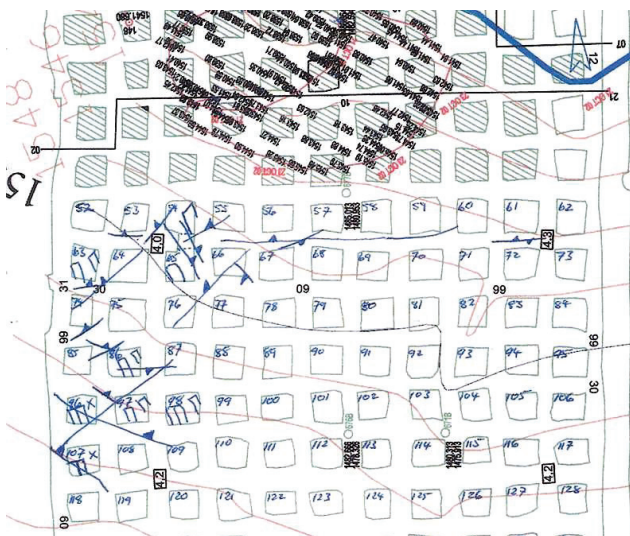

Figure 22. A typical section plan for shallow pillar extraction

Figure 23. 'Tooth extractor' used to extract continuous miner from goaf

ROCK ENGINEERING FOR UNDERGROUND COAL MINING

not suit the available equipment, resulting in less efficient extraction of the pillar or having to leave coal within a pillar, as mining the small remnant may be not be productive. In addition, the cost of resupporting the roof and construction of the infrastructure, belts, water and power, all have a cost that must be paid before extraction can begin. An additional disadvantage, particularly with small pillars and a low mining height, is that the rate of retreat is rapid, requiring frequent belt retractions, some times daily.

The decision to conduct pillar extraction must be carefully investigated and all the advantages and disadvantages weighed up before mining is done.

These include the full rock engineering investigations, risk assessment to identify problem areas, work procedures for all events, training of personnel in hazard identification and Awareness, including all work procedures, development of the working plan and systems to ensure compliance.

As the available coal reserves of the Witbank and Highveld coalfields are being depleted, the coal left in pillars that were not designed for pillar extraction become more attractive to exploit. The mining of these pillars can be conducted in a safe and efficient manner if the correct investigation into the mining of the pillars is conducted.

ROCK ENGINEERING FOR UNDERGROUND COAL MINING

Numerical modelling

Introduction

A model is an attempted simulation of reality. The characteristics of the model can be changed under the direct control of the modeller. It may be used for a number of purposes, from prediction to fundamental understanding. Its most important benefit is that, with a model, it is possible to simulate reality and the potential outcome of different ways of mining in harmless ways.

Subjective modelling is used by most people without their being conscious of it. For instance, when being approached by a car on the wrong side of the road when driving, one takes evasive action immediately. The subconscious model plays out the scenario of what will happen if nothing changes, and the reaction is to change course to avoid an unpleasant outcome. It does not matter if the precise velocities and masses of the cars are not known.

Most people use models on a regular basis. Reality can be simulated in many different ways. For the purposes of communicating to others, highly visual physical models are often used, but they can be misleading if the real material properties are not scaled correctly.

The advent of the computer has opened the way for, potentially, the most powerful type of model of all, namely the numerical model, to simulate a variety of complex geometries and laws of interaction between different parts of the model. The term 'numerical model' merely means that a great number of mathematical iterations are done to calculate the interaction between different parts of the model, using well established laws of physics. At the very basis of any model one invariably finds the basic laws of Sir Isaac Newton and others. The complications are brought about by the complexities of the models, which can consist of thousands or even millions of elements in different modes of contact with one another instead of just one object striking another and transferring energy.

In this chapter, some aspects of modelling will be discussed to enable the end user of the products of a model to judge the likely accuracy of the prediction and to know what pitfalls to avoid. It is not a modelling handbook – there are other excellent publications that cover that field in detail (see the list of recommended reading).

The 'NINO' principle

The success of the outcome of a model calculation is determined by two main parameters, namely, the quality of the input and the type of model that was used. The 'nonsense in, nonsense out' (NINO) principle holds true. However, this does not mean that models should not be used until all input parameters can be exactly quantified. It merely means that one should be aware of the limitations to the output accuracy. In any event, a model merely results in a quantified answer to a question about loads or displacements. Most of the time, judgement is still required to predict whether or not failure will occur in reality.

Failure criteria can be built into a number of programs, but the modeller should approach these with caution. As long as he or she is aware of the nature of the failure criteria that are used, he or she can exercise correct judgement. No modeller should expect a numerical model to replace the burden of engineering judgement.

One of the main characteristics of rock engineering is that there is no choice of construction material as, for instance, in building construction. Nature provides the material. It is also highly variable in quality, having been subjected to the ravages of nature over millions of years. Small rock specimens may be tested to any degree of accuracy, but the rock quality a few metres away from where the sample was taken may be different. The modeller will never have precise knowledge of the characteristics of the material he or she wishes to simulate in a model.

Yet, models have been, and are, used very successfully in several applications. There are hardly any civil engineering constructions like tunnels or dams—also in real rock—that are not modelled prior to construction. The modelling is followed by detailed monitoring and feedback into the model in a continuous process during construction.

It may be argued that mining applications are different, in the sense that the rate of excavation greatly exceeds that in civil excavations and there is little opportunity to attend to a single excavation at the same level of intensity. There is also limited opportunity to do the same number of rock tests to refine the input.

However, there is ample opportunity in mining rock engineering to refine models and rock characteristics based on the great number of excavations and the sheer volume of mining that takes place. The rate of mining also creates a large volume of data in a short period of time, which should enable the modeller to build up a database for back analysis very quickly.

Modelling input in the mining situation should be based on back analysis. The first few models should not be relied on absolutely, although a comparison between a number of different models would still yield enough information to make a good choice between a number of different mining layouts.

It all revolves around the degree of accuracy that is required. Coal mining takes place in a sedimentary environment, and for most model simulations, it is usually sufficient to start the model with average rock mass characteristics.

Choice of model

There are several different types of numerical models available and more are being created at an impressive rate. As computers become faster and more powerful, increasingly intricate calculation procedures can be performed quickly and easily. In this section, some of the basic types of models will be discussed against the background of the coal mining environment. Commercial brand names of the models will not be used, with the exception of one that is in the public domain.

All models are made up of elements that are linked to form a simulated geometry. There are two basic methods to achieve this. The first is to model the rock in which the mining takes place, and to leave openings for the mining excavations. These are the 'finite element' types of models. The second philosophy is to model the outline of the excavations, and let the body in between represent the rock environment—these are the 'boundary element' models.

The advantage of the finite element models is that different characteristics can be assigned to the rock mass at virtually any position. However, the calculation time is long compared to the boundary element models. For many years, mainframe computers were required to run finite element models.

The main attraction of boundary element models is the relative ease of setting up the models and the speed of execution. The solutions are not always as accurate as with finite element models, but it is a matter of the degree of accuracy that is required. For most mining applications, boundary elements are sufficiently accurate.

The other type of model, which can almost be seen as a compromise, is the discrete element model. These models approach the rock mass as a collection of discrete blocks of any geometry. Each block is a mini boundary element, bound to its neighbours by friction and cohesion, as specified by the user. The discrete element models come close to modelling the rock mass as a real mass of broken material. In the other models, joints or faults are simulated by softening the rock mass.

There are also hybrid models, which are essentially boundary and finite element models rolled into one. These combine the advantages of the different types of models, but are not as easy to use by non-professional modellers.

The creators of numerical models often miss the point that on a mine, the rock engineering personnel are not employed to run models, but to solve problems. Simplicity of use is thus one of the prime requirements, and for that reason, boundary element models are usually the preferred types.

The choice of model is largely governed by the reason for modelling. If the aim is merely to compare different mining methods or layouts to find the one that suits a specific requirement (e.g. load on a barrier pillar) the best, a simple boundary element model is usually sufficient. However, if it is to increase fundamental understanding of rock behaviour, a more sophisticated model is usually necessary.

Two-dimensional analysis

Two-dimensional boundary element models are fine for limited applications, for instance, to determine the load

on a solid inter panel pillar with different types of mining on either side. A two-dimensional model performs calculations on the basic assumption that whatever is modelled extends in the third direction for a very long distance, shown in Figure 1.

It is important, therefore, that two-dimensional models are used to model only situations that approximate to a two-dimensional problem, i.e. elements of the model in one direction must be 'very long' in relation to the other two directions.

In practice, given the limitations to input accuracy, the 'very long distance' requirement is usually met if, for instance, a cross-section of a roadway is modelled and the length of the roadway is more than twice its width. Intersections cannot be modelled in two dimensions.

Two-dimensional analyses are often useful to gain a first order approximation to a solution—the so-called 'quick and dirty' approach. An example of this is the approximation of pillar loads in stooping for different conditions, say an intact vs. a failed dolerite sill in the overburden. In this example, a two-dimensional boundary element model is used.

A sketch of the real geometry is shown in Figure 2. To allow two-dimensional analysis, certain simplifications have to be introduced. Firstly, a

separate calculation has to be done to determine the span at which the sill is likely to fail. In the model with the intact sill, the mined out span must then be restricted to the same dimension as the width at which the sill is expected to fail, irrespective of the real distance that mining has progressed, see Figure 3. For the model with the failed sill, the real mining span is even less important.

The input usually consists of geometrical input (of the model, not the real geometry) and certain basic rock characteristics such as the Modulus of Elasticity and the Poisson's ratio. Note that in this example, the goaf is simulated as a void. To balance the model, the floor of the goaf has to be loaded with a load that is equivalent to the load of the broken goaf material.

Boundary element models usually make use of two types of elements with which the model is constructed. There are the fictitious stress elements that are used to describe the outlines of excavations and then several types of displacement discontinuity elements. Differences in stiffness and other characteristics can be assigned to displacement discontinuity elements. They are usually used to simulate the coal seam.

In Figure 3, the symbols and dimensions have the following meanings:

Line A is a line of mined displacement discontinuity elements, representing the surface. This line should overlap the area of interest by at least the mining depth (H) on both sides.

Zone B is a closed loop of fictitious stress elements. The bottom elements are loaded by a normal load, G, equal to the loading of the goaf material. The height of the cavity, H_G, is the distance between the coal seam and the base of the dolerite sill.

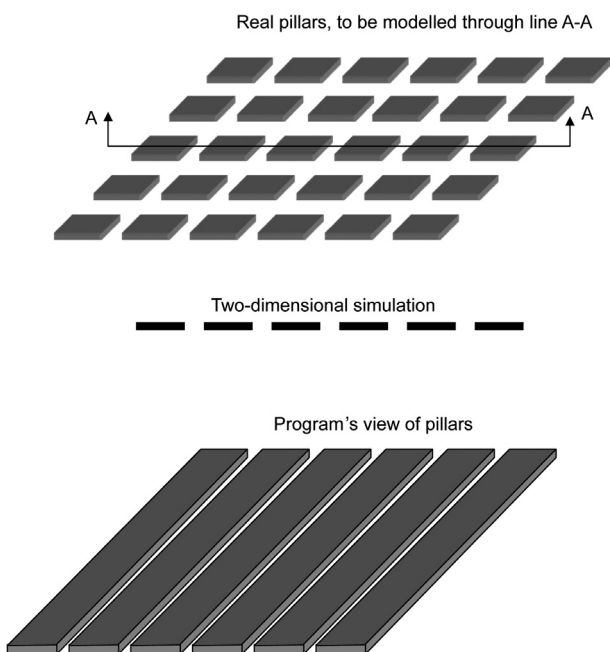Line C consists of alternating mined and unmined

Figure 1. Two-dimensional program's transformation of pillars. If real pillars are to be modelled two-dimensionally, conversions have to be made
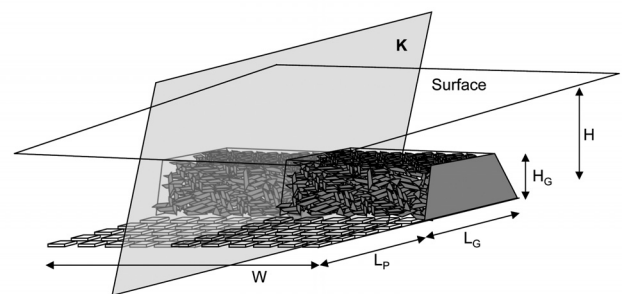

Figure 2. Sketch of a stooping panel with intact pillars in the foreground and a goaf at the back of the panel. The plane *K* through the panel is the plane at which a cross-section is to be modelled
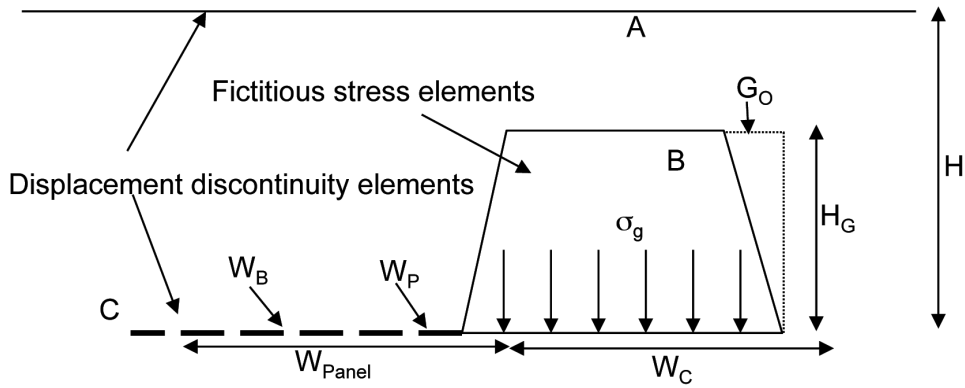
Figure 3. Model geometry obtained from the real situation

displacement discontinuity elements, representing the coal seam with bords and pillars.

$$_G = 0.025 H_G \text{ MPa} \qquad [1]$$

The goaf overhang, G_O, is:

$$G_O = H_G tan \quad , \qquad [2]$$

where ϕ is the goaf angle measured off the vertical.

The real bord and pillar widths are simulated. However, the modulus of elasticity, E_{2D}, as used in the model should be decreased, as follows:

$$E_{2D} = E_{3D}\left(1 - e_p\right), \text{ MPa} \qquad [3]$$

where E_{3D} is the real modulus of elasticity and e_p is the ratio of pillar length to pillar centre distance in the length direction.

W_C is the critical width, at which dolerite failure can be expected, see Chapter 10: Subsidence.

After the model has run, the pillar loads in the output file should be adjusted according to the real and modelled extraction ratios to compensate for the two-dimensional nature of the model. Simply:

$$Load_{real} = Load_{Model} \frac{e_{\text{mod} el}}{e_{\text{Re} al}} \qquad [4]$$

This model will yield the maximum pillar loads in a stooping panel, taking account of the dolerite sill in the overburden. Although crude, it is a quick and easy model to run in two dimensions and is superior to any manuel calculation for the given situation. This very basic model has been used successfully for many years.

Care should be taken to ensure that consistent units are used. The easiest way of doing this, is to develop a habit of using scientific notation for all inputs;
- KPa = 10^3 Pa
- MPa = 10^6 Pa
- GPa = 10^9 Pa

However, this sometimes creates problems in the output files, especially with the older codes with fixed column widths for the output numbers. If the numbers are large, they sometimes overlap. If large numbers are expected in the output, it is often better to provide all the stress input in MPa, making sure that all the stresses, stiffnesses, etc. are also converted to MPa. The output will also then be in MPa.

There are two methods of ensuring that all the input is correct. One is to run the model and then fix errors if it does not run or if the output looks unrealistic. The preferred method is to check the input before running the model.

Two-dimensional discrete element modelling

Rock behaviour in coal mining at shallow depth is characterized by the dominance of faults and jointing. At greater depth where the higher stress levels have a more pronounced clamping effect on discontinuities, the assumption that the rock mass is continuous is more attractive. Although the continuous type of models have been shown to yield acceptable results at shallow depth, the use of discrete element models is closer to the real rock situation.

Simulations that are more realistic can thus be created with the discrete element models. On the negative side, the codes tend to be more expensive and are invariably more difficult and cumbersome to handle. This is especially true for the three-dimensional discrete element codes.

The two-dimensional discrete element codes have been found handy for a number of applications, of which two examples are presented here. The first
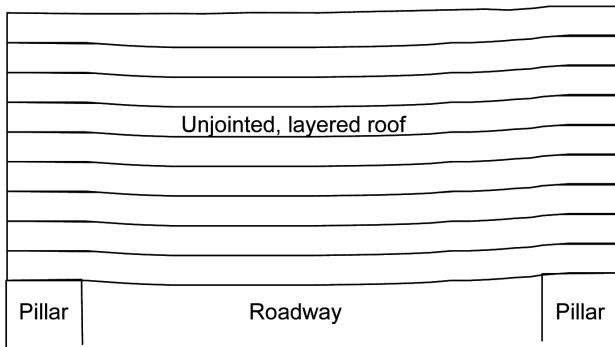
Figure 4. Example of a discrete element program output. This is a cross-section through a layered, unjointed roof. Some deflection is visible
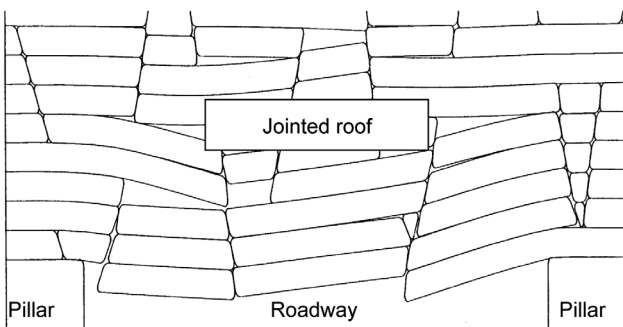

Figure 5. The same cross-section as in Figure 4, with joints added to the roof layers. Although the horizontal stress in this example was half of that in the previous example, significantly more roof deflection is evident
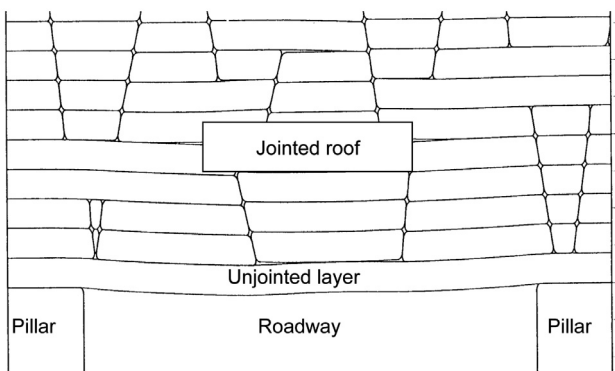

Figure 6. When an unjointed layer is added to the bottom of the jointed roof mass, the deflection is again reduced. In practice, the unjointed layer may, for instance, represent a layer of coal left in the roof, or an artificial beam that was created by bolting

example was an investigation of the effects of jointing under the conditions of high and low horizontal stress in a coal mine roof, and the other was to investigate a failed attempt to mine a longwall out into a pre-supported roadway.

In the first example, the jointed roof, a number of comparative simulations were modelled. First, there was an unjointed roof with low and higher horizontal stress. This was followed by a roof with random joints, again with low and higher horizontal stress. In this context, 'low' horizontal stress meant a k-ratio of 1.0 and 'higher' horizontal stress a k-ratio of 2.0. The horizontal stress magnitudes were respectively 2.5 MPa and 5 MPa. Finally, a jointed roof was simulated with a thin, unjointed layer underneath. The unjointed layer could be seen as representative of a layer of coal left in the roof or an artificial beam created by roof bolting.

The results of the investigation are shown in Figures 4 through 6. The major advantage of this type of analysis is immediately apparent. The results are highly visual, leading to enhanced understanding of the process of roof failure. What this example showed was that the major factor influencing roof deflection in this particular case was jointing, and that a roof with joints and a low horizontal stress deflected much more than an unjointed roof with higher horizontal stress.

The situation that was modelled for the second example was that of an attempt to reduce the time taken for a longwall move by mining out into a presupported roadway, as shown in Figure 7. Two dimensional boundary element modelling—see Figure 8—indicated that when the remaining pillar between the longwall face and the roadway was 3 m wide, the stress on the pillar could cause it to fail. That pillar was therefore reinforced with a dense pattern of wooden dowels.

The experiment was a failure. The remnant pillar punched into the floor, which lifted on both sides of the pillar. The longwall shearer was trapped against the roof and the face was inoperative for a long time. This effect was not predicted from the first model.

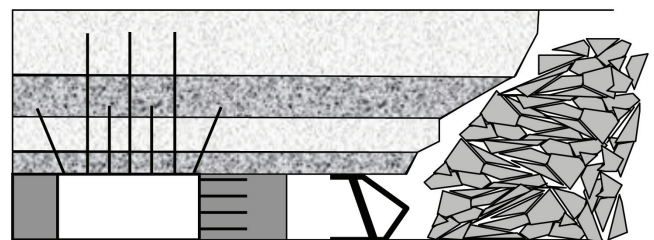Subsequent investigation indicated that a water

Figure 7. Cross-section view of the longwall approaching the presupported roadway

bearing joint was present in the pillar. The floor was a micaceous sandstone, which, when wet, turned into a material exhibiting plastic behaviour, much like modelling clay. This situation was then modelled again, this time with a discrete element model that could simulate both the jointed overburden and the plastic material in the floor. The result is shown in Figure 9. This time, the model simulated reality almost exactly.

This example indicates two very important prerequisites of numerical modelling. Firstly, it is important to use the correct model and secondly, if the input does not simulate reality, neither will the output. The first model assumed that there was a continuous overburden and the differential movement of the roof blocks on top of the pillar could not be simulated. Therefore, even if the soft, plastic floor material had been simulated, the pillar would not have been shown to punch into the floor.
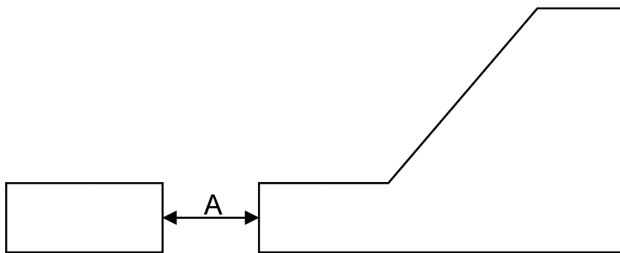

Figure 8. The two-dimensional boundary element model that was set up to simulate the cross-section in Figure 7. Fictitious stress elements were used to create the cavities. The dimension A was systematically reduced in a number of runs of the program to simulate the decreasing size of the remnant pillar between the longwall and the roadway. The stresses on the pillar were recorded
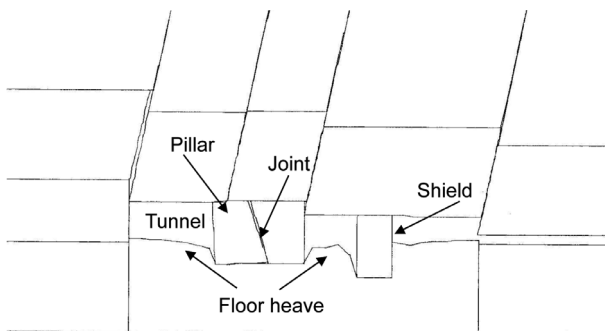

Figure 9. Output of the two-dimensional discrete element model, showing the pillar punching into the floor

Modelling of the subsidence process

There have been several attempts at the analytical prediction of subsidence, none of them really successful for shallow mining, such as coal mining in South Africa. By manipulating the overburden stiffness, continuous type models can simulate either the shape of the subsidence trough or the magnitude of subsidence satisfactorily, but not both at the same time. The reason for this should be obvious. It is shown in Chapter 10: Subsidence that the subsidence process is by nature discontinuous, characterized by friction controlled sliding of discrete blocks of rock. Continuous-type models cannot simulate this process.

The subsidence process is not only influenced by jointing in the rock mass; it is governed by it. Intuitively, discrete element models should be able to simulate the process well. It has been found that in order to be successful, the model should be set up with a soft goaf already in place. Subsidence then takes place by the compression of the goaf. When that is done, discrete element models have been seen to simulate subsidence significantly better than continuous type models.

Three-dimensional analysis of layouts

For the estimation of pillar loads in cases where more accuracy is required, pseudo three-dimensional codes have been developed. These are usually even easier to
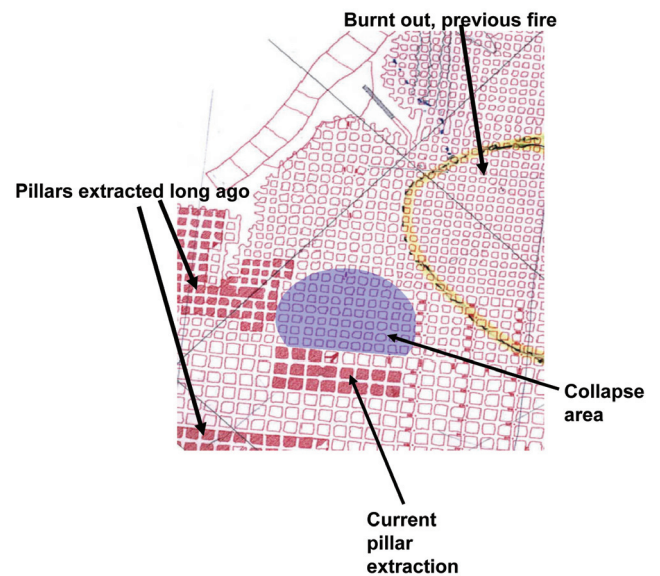

Figure 10. Layout of a stooping area where pillar failure occurred. The surrounding mining configuration was too complex to allow reasonable simulation with a two-dimensional model

ROCK ENGINEERING FOR UNDERGROUND COAL MINING

use than the two-dimensional ones, mainly because they were developed later and are accompanied by graphic user interfaces that make data input and output analysis much simpler.

One popular model is called LAMODEL. It was developed by the NIOSH Laboratory in Pittsburgh, PA, USA, and is in the public domain. LAMODEL can simulate an overburden consisting of several different layers, multiple seams, and an irregular surface topography. It has been used successfully for longwall inter panel pillar design in multiple seam situations, stooping of non-superimposed multiple seams, to explain pillar failure, etc.

Figure 10 is an example of a layout that was analysed with LAMODEL to determine pillar loads in a stooping situation. There was also mining underneath this area, shown separately in Figure 11. In this case, the surrounding mining was too complex to allow a reasonable estimation with a two-dimensional model. The reason for doing the analysis was that some of the pillars had failed and there were several possible reasons for the failure. The model was used to determine the loads on the failed pillars, which was the most probable reason for the failures.

The output of the analysis consists of several parameters; it is for the user to decide which is the important one for the particular problem. In this case, the pillar loads were the important parameters. An example of the output that can be obtained is shown in Figure 12. The pillars are shown in varying shades of grey—the darker the colour, the higher the stress. Note the size of the low stress circle inside each pillar. The higher the average stress on the pillar, the smaller the low stress zone.

The small pillars right next to the goaf have the highest stress and thus the smallest low stress zones. The further the pillars are from the new goaf, the lower the pillar stress and the larger the low stress zones in the pillars. The larger pillars next to the goaf also exhibit larger low stress zones.

In this particular example, the modelling was only one part of the investigation. It showed that the pillar stresses were not high enough to result in failure of pillars, with a strength that was in the expected range. Attention was then turned elsewhere, and it was found that the pillar strength had been significantly reduced over the long period—more than twenty years—that the pillars had been left standing before being stooped. In this case, modelling could not show the cause of the failure, but it could be used to eliminate one of the possibilities.

This is a typical example of the use of modelling in an investigation. It is very seldom that all the answers will be obtained by modelling, but as a supplementary aid, it is often invaluable.
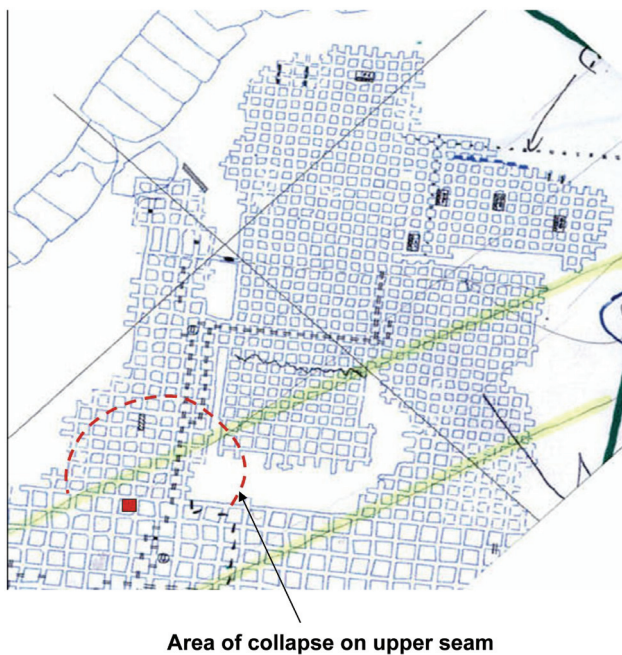

Figure 11. Mining layout on the seam underneath the mining shown in Figure 10. The outline of the failed pillar area on the upper seam is shown as reference
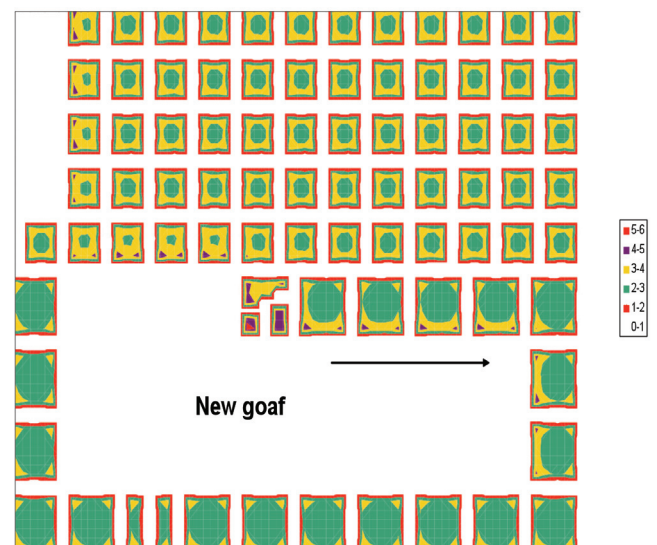

Figure 12. Graphical presentation of LAMODEL output showing the loads on the pillars that had collapsed

Detailed modelling in three dimensions

There are situations that can be modelled neither in two dimensions nor with the pseudo three-dimensional models like LAMODEL. These include special excavations such as underground surge bins, roadway intersections, advancing roadways, etc. For these problems, proper three-dimensional models are required. A number of such models are commercially available, each with unique features and options including the capability to model large strains, discrete elements, finite elements, boundary elements, etc.

Consider the following example, shown in Figure 13, where the deflection of the roof with an advancing face was modelled, Canbulat and van der Merwe (2000). This type of model can be used to assist in the determination of a safe cut-out distance for any given road width and roof composition. In this model, a number of consecutive runs, with an advancing face were executed with a fixed roadway width. Consecutive runs were done, varying the magnitude of the horizontal stress, the road widths, the thickness of the immediate roof layer and the stiffness of the roof layer. The deflection of the roof was recorded on each occasion, resulting in the graphs shown in Figures 14 to 17.

The conclusion drawn from this investigation was that roof deflection is primarily affected by road width and to a lesser extent by the magnitude of horizontal stress, the thickness of the immediate roof layer, and the stiffness of the immediate roof.

This example is a further illustration of an important use of numerical modelling. It is possible to investigate the effects of varying a great number of parameters quickly and easily. In this way, trends and sensitivities are easily identified for more focused underground investigation. The magnitudes of the displacements resulting from this investigation are in line with numerous measurements in South African coal mines.
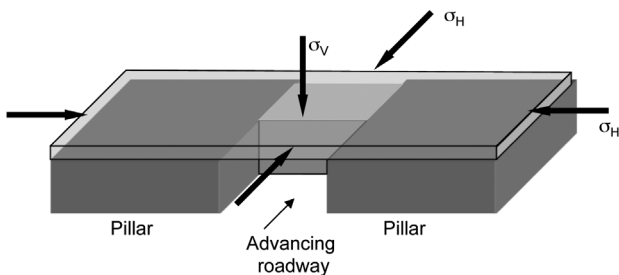
Figure 13. Basic model that was used for the analysis of roof deflection with increasing face advance

Estimating input parameters

There are essentially three methods by which input parameters for numerical modelling can be obtained. The first one, guessing, should be discarded outright – if one is to guess input for a sophisticated model, it is easier to just guess the output. The second is detailed laboratory testing, which is costly, time consuming and, seen against the background of the variability of rock qualities, not accurate in terms of the overall rock mass behaviour. If no prior experience or knowledge is available, laboratory testing is the only way to—at least—get an estimate.

The preferred method is by means of back analysis. The procedure to be followed is to first do a number of simulations in order to obtain a sensitivity analysis. These simulations should be done based on a known

Figure 14. Effect of road width on the roof deflection with advancing face position. The curves indicate that for any road width, the deflection increases rapidly with face advance until the advance equals approximately twice the bord width, where after it stabilizes

Figure 15. Effect of the thickness of the immediate roof layer on roof deflection with increasing face advance

ROCK ENGINEERING FOR UNDERGROUND COAL MINING

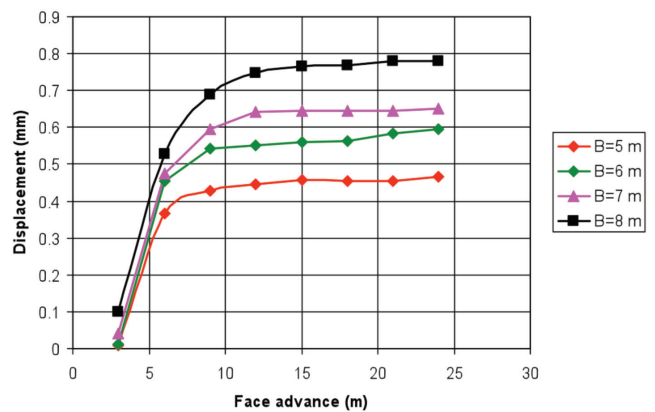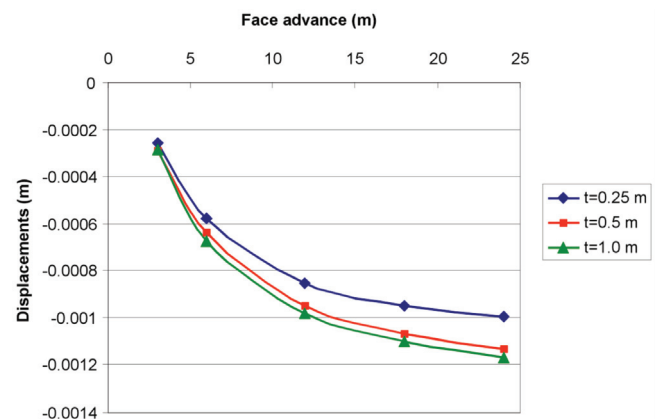case or cases where the geometry and the final results are available. In this context, the results can also have been obtained by visual observation if no measurements are available. The program that is to be used for the simulation should also be used for the sensitivity analysis.

Once the important parameters are known, they should be varied in the model until there is close correlation between the observed case and the model output. This should be an ongoing process, whereby the input parameters are continually refined. Cases that are modelled should be followed up by monitoring, for feedback into the back analysis loop. The more accurate the monitoring, the better the feedback, the more accurate the next round of input and the more reliable the results will be.

In the absence of any better information, the following can be considered for first round of input into numerical models:

Figure 16. Effect of the stiffness of the immediate roof layer on roof deflection with increasing face advance

Figure 17. Effect of the k-ratio on roof deflection with increasing face advance

Coal modulus of elasticity: 4 GPa
Shale, sandstone modulus of elasticity: 15 GPa
Mudstone modulus of elasticity: 5 GPa
Dolerite modulus of elasticity: 80 GPa
Goaf modulus of elasticity: 50 MPa
Sedimentary rock Poisson's ratio: 0.25
Coal Poisson's ratio: 0.3
Dolerite Poisson's ratio: 0.2
k-ratio: 2.0
Goaf angle, stabilised goaf: 15°
Goaf angle, advancing face: 30° – 45°

Input for LAMODEL models

Due to the ease of use, proven applicability and low cost (just the cost of downloading from the NIOSH website) of LAMODEL, it is recommended as a standard coal mining rock engineering tool. Depending on the purpose of running a model, there are several ways of approaching the type of elements and the input required.

For instance, if there is a need to determine pillar loads in a situation where the pillar stability is not suspect, but there are different pillar sizes in a panel (which places doubt on the validity of the Tributary Area Method), it may be sufficient to just use simple linear elastic elements without any yielding capability. However, if for instance the stooping of old, small pillars is considered, it is necessary to elevate the level of accuracy and hence the level of sophistication of the model.

It is not the purpose of this book to provide detailed information on the use of any particular model as that need is better served by detailed expert courses. However, it is felt that due to the frequency of use of LAMODEL, it would be of benefit to provide some guidance on the modelling of fairly common situations.

The following paragraphs describe the required input in the order they are required by the LAMODEL preprocessor, LAMPRE.

General model information

Provide a brief description of the model, number of seams, etc.

Number of in-seam materials

There should be a material type for each type of expected pillar behaviour. For instance, if no pillar failure is expected, one in-seam material (a linear elastic type) is sufficient.
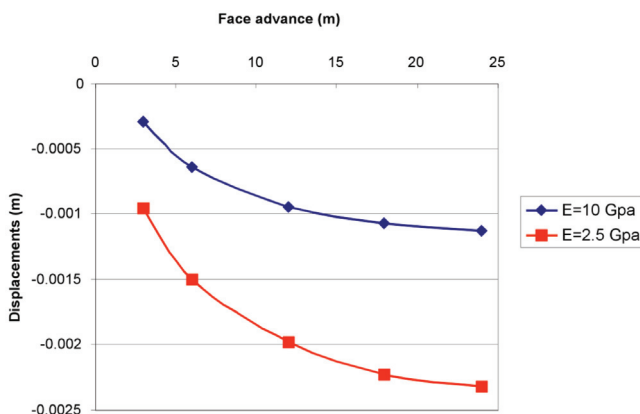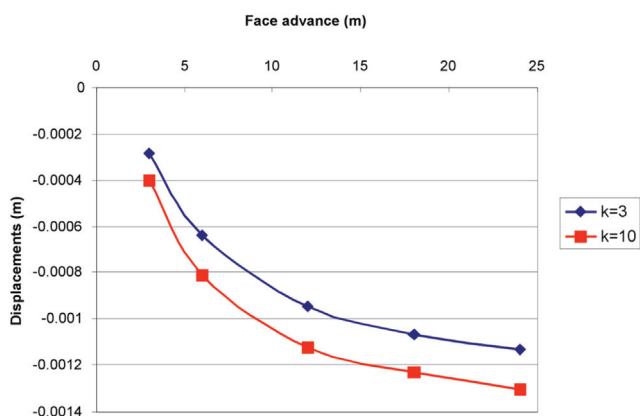
Where failure could occur, a separate material is required for each typical snook size that is in the model. Material types are denoted by letters. Pillars that could fail are best modelled as strain-softening elements.

Also select the units (m and MPa) and model type (LAMODEL).

Rock mass parameters

A Poisson's ratio of 0.25 and stiffness of 15 to 20 GPa is usually fine as input.

Note: LAMODEL requires consistent units—if MPA and m are selected, remember to input stiffness as 15 000 MPa.

Select the lamination thickness such that about 10 layers are present—this does not have to fit in precisely with the depth below surface. For instance, if the depth below surface is 97 m, specifying 10 m lamination thickness is fine; it does not have to be 9.7 m.

The stress gradient should be 0.025 MPa/m.

Seam geometry and boundary conditions

Size of element and number of elements

The size of the element and the number of elements are related—the smaller the chosen element size, the more elements are required to cover the same area. There will always be a trade-off between the size of element and the accuracy of the representation. This is a matter of judgement.

Due to the width of the cutting drum on a continuous miner, coal mining dimensions are often multiples of 3 m. Roadways are often 6 m wide and pillars often 9 m, 12 m, 15 m, etc. For standard bord and pillar layouts, 3 m or 3.5 m wide elements are often sufficient. The ideal element size is the largest common denominator between the road width and pillar width, although life is seldom as simple as that and some compromise will invariably have to be found.

When stooping is modelled, it usually means that different snook sizes need to be considered, and then 1 m or even 0.5 m elements will be required.

The number of elements is found by dividing the size of the area to be modelled by the element size. The size of area to be modelled should be determined by the complexity of the situation— for regular layouts, it should be at least equal to the depth below surface as a general guideline. Very often, this can be achieved

without creating a huge model by imposing symmetry on the boundaries.

Note: In LAMODEL, the number of elements has to be multiples of 10.

Boundary conditions

It is possible to select symmetry on all four boundaries, in which case the model will see an infinite repetition of the grid in all directions. Using symmetry is handy to simulate a huge area without building too large a grid if the layout is reasonably regular.

Also input the seam coordinates. It is usually simpler to work in local coordinates, i.e. specify the origin coordinates as 0, 0. If a large area is to be modelled with separate models, it is better to specify the origin coordinates using real mine coordinates to avoid confusing the results later.

If more than one seam is specified, the depth of each seam has to be input separately.

Wizard for defining in-seam material models

Ignore this input page.

Program control parameters

This set of input controls how the program will execute.

It is recommended not to change the Over Relaxtion Factor—rather keep the default value of 1.35. The same goes for the Displacement Convergence Level, which controls the accuracy of the solution – keep this at 1×10^{-7}.

The Maximum Number of Iterations controls the maximum number of cycles the program will execute—if it reaches the accuracy limits specified in the Over Relaxation Factor and the Displacement Convergence Level before it reaches the maximum number of iterations, it will stop execution and create the output files.

If the accuracy levels are not reached within the maximum number of iterations, it will also stop execution but without coming to a solution. This can happen with a large number of elements, especially if different material models are used.

To rectify this problem, rather increase the Maximum Number of iterations than decrease the level of accuracy.

Material models

The input for Linear Elastic Material is simple, being merely the Elastic Modulus and Poisson's ratio of coal, typically 4 000 MPa and 0.3. However, some calculation is required to derive the input for the Strain Softening Material.

Figure 18 shows the conceptual strain softening model.

Peak stress and peak strain (point B in Figure 18)

The peak stress is the pillar stress at the point of failure, and is found by

$$\sigma_p = 3.5 \frac{w_e}{h} \qquad [5]$$

where w_e = equivalent pillar width
(4.Area/Circumference)
h = mining height

The peak strain is the strain at the point of failure, simply:

$$\varepsilon_p = \frac{\sigma_p}{E} \qquad [6]$$

Residual stress and residual strain (point C in Figure 18)

Select a low stress value as the residual stress, say 0.1 MPa.

The residual strain is then found by applying the post failure modulus of the snook to the line connecting points B and C in Figure 18. This is given by Equation D.27, Appendix D, as follows:

$$E_{cp} = \frac{0.562 w_e}{h} - 2.293 \qquad [7]$$

The incremental strain, e_{ri}, is then:

$$\varepsilon_{ri} = \frac{\sigma_p}{E_{cp}} \qquad [8]$$

Finally, the residual strain is simply

$$\varepsilon_r = \varepsilon_p + \varepsilon_{ri} \qquad [9]$$

The calculations using Equations [5]–[9] should be repeated for each material model; the characteristics will be different as they are in fact controlled by the snook size.
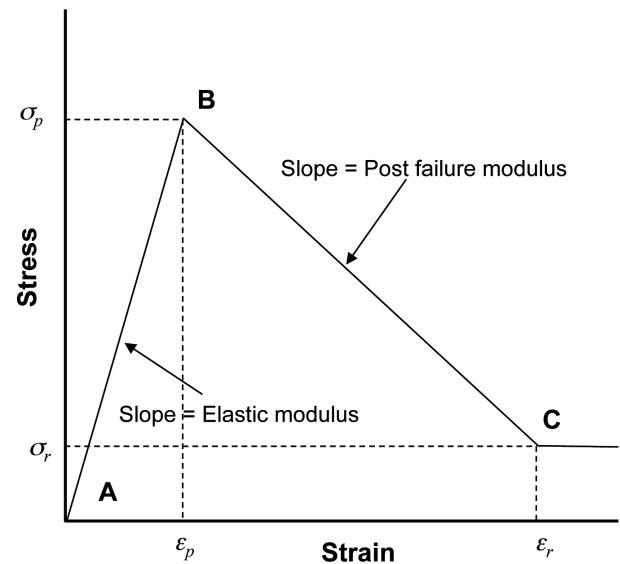
Figure 18. Conceptual strain softening model

General hints for creating grids

Once the input has been specified, the final step is setting up the grid. The following hints may come in handy:

- For a start, click on the top left corner outside the grid area and set the entire page to Material A, the linear elastic material.
- Then, select rows or columns by clicking on the numbered blocks just outside the grid to create roadways by inserting material 1 (i.e. mined elements) in the selected rows or columns.
- Once the unstooped pillars have been created, take one pillar and make it up to consist of the correct chosen material types.
- Copy that pillar by dragging across it, press Ctrl C and paste it into the correct position next to the pillar that has just been made up by pressing Ctrl V.
- Continue copying and pasting ever increasing areas to complete the grid.
- Save the grid regularly—under the 'File' drop-down box, simply click on 'Save'— LAMODEL will link the grid to the input parameters.
- When copying an area, always drag from the top left corner of the selected area to the bottom right corner.
- When pasting, select either the same size area as the copied area or a larger area. If you select a smaller area, LAMODEL will paste only in the smaller area.
- You can add or delete rows or columns, but always end up with rows and columns in multiples of 10.

Executing the program

Open LAMODEL, then open the input file using the drop-down box. LAMODEL will inform you that the file has been correctly read and then select 'Run'. The program will execute and store the solution in output files.

Evaluating the output

The output can be viewed using the post- processor, LAMPLT.

LAMPLT has the options to view various components of convergence or vertical stress.

While it is a handy facility, it has limitations and it is often better to save the output files in ASCII or DXF format, to view and manipulate further using standard CAD programs. LAMPLT provides the options to save files in these other formats.

General remarks

Numerical modelling is an invaluable aid to the rock engineer whose function is to advise management on safe and productive mining. There are a number of different types of models available, and within each broad category, there are several variations.

Two-dimensional boundary element models are handy tools for a quick analysis to get a basic feel for the subject, but are limited in their capacity to supply total solutions. Two-dimensional models in general can be used for excavations and layouts that have extended dimensions in one direction. For other applications, some form of adaptation has to be made. Depending on the exact circumstances, this may compromise the quality of the solution.

For more realistic simulations of real rock in two dimensions, discrete element models should be used. As the models are more realistic, a firmer grasp on the input variables is required.

Pseudo three-dimensional models are available with which mining layouts can be simulated. The latest generation of these types of model can cater for multiple seams, layered overburden, goafs, and uneven topography.

For the accurate modelling of openings of any shape, three-dimensional models are available with a variety of characteristics. These are especially useful to improve fundamental understanding of rock behaviour, but are also good for operational problem solving and predictions of rock mass behaviour. However, they are more expensive and difficult to use than the simpler two-dimensional models.

An important requirement for the use of any model is an understanding of the expected rock behaviour, without which an inappropriate model could be chosen for analysis. It is also important to understand that no matter how sophisticated, a model is only a simulation of reality. The quality of the solution is a function of the realism of the input.

The most appropriate method of determining input parameters is by back analysis. Modelling, monitoring and feedback into the system is an integrated loop. If one of the elements of this loop is absent, good quality input and consequently reliable results cannot be achieved.

Recommended reading

It is not the intention of this book to supply comprehensive information on numerical modelling. For that, the reader is referred to a number of specialist references on the subject below. The SIMRAC publication is an excellent comprehensive practical guide on a number of available codes.

1. SIMRAC. *Numerical Modelling Of Mine Workings*, vol 1 and 2. Dept of Minerals and Energy, Johannesburg, South Africa. 1999.

2. MINE MODELLING LTD. Map3D Version 36 User's Manual, Mine modelling Ltd, Mt Eliza, Victoria, Australia. 1996.

3. MINING STRESS SYSTEMS. 3D_BESOL: Three-Dimensional Boundary Element Solutions for Rock Mechanics: User's Guide For Multiple Seam Program BESOL_MS For Microsoft Windows Operating System, Version 3.4, Mining Stress Systems (Pty) Ltd,. Johannesburg, South Africa. 1997.

4. COETZEE, M.J., HART, R.D., VARONA, P.M. and CUNDALL, P.A. FLAC Basics – An Introduction To FLAC And A Guide To Its Practical Application, *Geotechnical Engineering*, 2nd Edition, ITASCA Consulting Group Inc, Minneapolis, MN, USA. 1998.

5. ITASCA CONSULTING GROUP. UDEC Users Guide. ITASCA Consulting Group Inc, Minneapolis, MN, USA. 1997.

6. MINING STRESS SYSTEMS. BESOL: Boundary ELement SOLutions for Rock Mechanics: User's Guide, Mining Stress Systems (Pty) Ltd,. Johannesburg, South Africa. 1997.

7. NIOSH. User's Guide For LAMODEL. NIOSH Pittsburgh Research Laboratories, Pittsburgh, PA, USA. 1998.

Chapter 10

Subsidence

Introduction

Only in isolated cases will subsidence have a direct effect on mining operations. More commonly, the effect is indirect from the mine's point of view, affecting the economics of mining by requiring mitigation of damages or sterilizing reserves in areas where subsidence cannot be allowed. The Environmental Management Programme Report (EMPR) usually contains a section on subsidence and how the mine intends dealing with it. Furthermore, before mining is permitted, the Environmental Impact Assessment (EIA) has to address the subsidence issue.

It should be stated at the outset that very few of the effects of mining on groundwater can be generalized, and even then only in the broadest of terms. They should form the subject of detailed, site specific investigations. By contrast, the mechanical effects of mining on the surface are easier to quantify and will be dealt with in detail in this chapter.

Given sufficient time, any act of removing material from underneath the surface of the Earth will result in subsidence. For instance, the extraction of oil in California has resulted in subsidence of more than six metres in the Long Beach area and the Ravenna district in north-eastern Italy was in danger of being submerged by the ocean due to water extraction. Whether or not the subsidence will be *noticed* depends on factors such as the amount of material removed, the depth at which it was done and the time at which the subsidence occurs.

In very broad terms, the magnitude of the subsidence itself is not an important parameter as far as resultant damage to surface structures is concerned. The accompanying effects such as the induced tilts and strains are far more important. Again in broad terms, those effects tend to diminish as the depth of mining increases although the magnitude of the subsidence may increase.

Typical deep South African gold mining, for instance, results in surface subsidence which is close to the mining height in magnitude, yet it is seldom noticed and for all practical purposes does not have any effect on surface structures. This is because the induced tilts and strains are below the damage threshold for any common type of structure.

Typical coal mining, on the other hand, by virtue of being carried out at relatively shallow depth, does result in damage in the majority of cases and consequently has to be managed. It cannot be ignored.

The other popular misconception is that it is only high extraction coal mining that is of any concern. Over the long term, the converse is true—all pillar mining will eventually result in subsidence and, due to the unknown time of occurrence, this subsidence is in fact more difficult to deal with than the almost immediate high extraction subsidence. It is only the mechanism of pillar failure and time of subsidence that will differ. As discussed in Chapter 4: Pillar design, there are several mechanisms of long-term pillar failure. The only certainty is that the pillar systems will fail; the main uncertainty is when it will happen.

Bord-and-pillar mining, unless artificially stabilized, will result in subsidence over the long term. In this context, 'long term' means long enough not to endanger the people working in that particular section. The actual time span can be anything from mere months to several millennia. Also, as shown in Chapter 4: Pillar design, it is a misconception that a high pillar safety factor will necessarily afford protection against pillar failure in the long term.

It is not possible to design a mining system without backfill that can be proven to be subsidence-proof. We have to accept that it will occur eventually. The challenge is to limit the effects to below the level that will cause more damage than the positive results of providing essential minerals to the community by the act of mining.

In this chapter, the focus will be on the broader subsidence issues; such as descriptions of the mechanisms to enhance understanding and on proven methods to manage the effects of subsidence. The technical details that will enable the reader to predict the magnitudes of the various subsidence elements are contained in Appendix E.
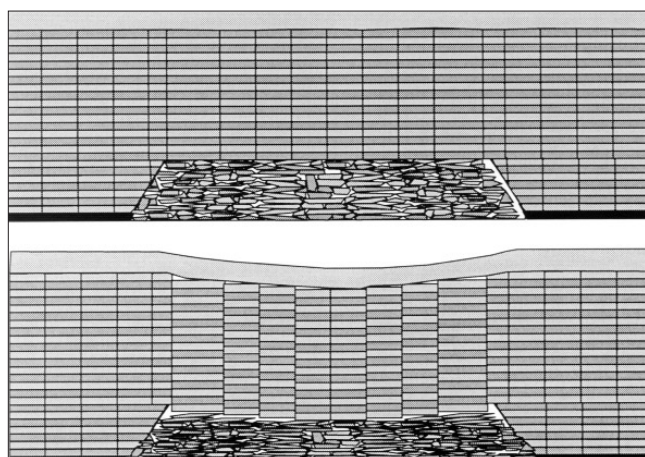
Figure 1. Simplified illustration of the subsidence process. In the upper diagram, an unconsolidated goaf has formed and there is no subsidence. In the lower diagram, the goaf has been compressed by the weight of the overlying strata and the surface has subsided

Mechanisms of subsidence

The subsidence caused by high extraction mining has a different mechanism than that caused by pillar system failure. This results in differences in the magnitudes and rates of subsidence. They will be discussed separately.

Mechanism of subsidence resulting from high extraction mining

Whether the mining method be longwalling or pillar extraction, the essential facts are that the back areas are left unsupported and that the roof is allowed to collapse. The collapsed area extends vertically, and the collapsed material occupies a larger volume than it did before it collapsed due to the presence of voids in the goaf. Eventually a stage is reached where the collapsed material makes contact with the overlying uncollapsed rock. Figure 1 illustrates the principle of subsidence.

At the stage where contact is made between the goaf and the overlying rock mass, the uncontrolled roof collapse ceases. If the rock material had been a continuous, unjointed mass, further subsidence would have been caused by bending of the overlying plate. However, it is known that the overlying rock mass is jointed. Under the influence of gravity, large blocks measuring several metres in all directions now slide down along pre-existing joint planes, compressing the voided goaf underneath. The more the goaf is compressed, the more resistance to further compression it offers. The process continues until the resistance offered by the goaf balances the weight of the overlying material.

This process explains two very important characteristics of high extraction subsidence. Firstly, the total magnitude of subsidence is significantly less than the original mining height; in the majority of typical South African cases, it is slightly less than half of the mining height.

The reason that the full mining height is not manifested as subsidence is that the weight of the overlying material is insufficient to recompress the goaf material to the solid state. This of course implies that the nether goaf region will always be voided, with the accompanying implications for long-term ground water considerations.

Secondly, the rate of subsidence is relatively slow. It takes roughly six weeks for more than ninety per cent of the full subsidence to occur, the rest occurring over a period of several years. The subsidence is not caused by free gravity induced fall of the overburden. The rate of subsidence is governed by the rate at which the goaf can be compressed. Furthermore, the process is governed by frictional sliding of the discrete overburden blocks of rock. It is not free bending of

Figure 2. Photograph taken of the sidewall of a sinkhole that occurred at the face end of a subsidence trough. The sinkhole was caused by a face break underground that required loading out a substantial amount of rock. Inside the circled area it can clearly be seen that discrete blocks of rock are displaced relative to one another and that the blocks undergo tilting relative to one another
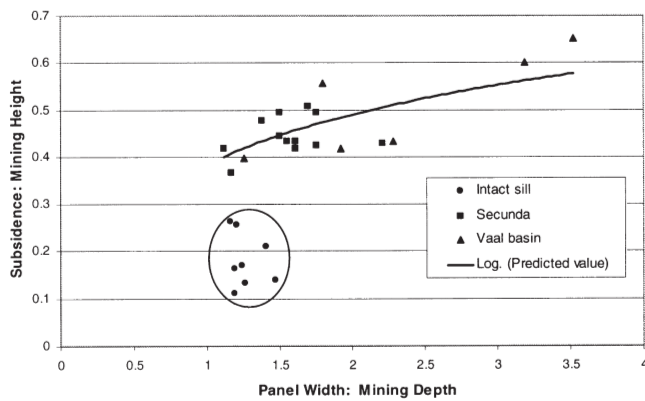
Figure 3. Relationship between the ratio of maximum subsidence to the ratio of panel width to mining depth

the overburden plate. Figure 2 is an illustration of the rock behaviour at the surface, where it can be seen clearly that subsidence is caused by the relative displacement of discrete blocks of rock.

The expected magnitude of vertical subsidence as a function of the panel width to mining depth ratio, was found empirically by Van der Merwe (1991) and is shown in Figure 3. The curve in Figure 3 can be mathematically expressed as

$$S_m = 0.39h\left(\frac{W}{H}\right)^{0.32} \qquad [1]$$

where h = mining height
H = mining depth
W = panel width
S_m = maximum vertical subsidence.

Mechanism of subsidence caused by pillar system failure

In contrast to high extraction mining, the areas where failure occurs in the case of pillar system mining are not totally devoid of support. Consequently, there is sufficient resistance to free collapse of the overlying rock mass to prevent a rubbly goaf from forming. Instead, the entire rock mass sits down on the failing pillars, as is shown schematically in Figure 4.

This difference in mechanisms explains the major differences between high extraction subsidence and that caused by pillar system collapse, be it due to pillar failure or foundation failure. Firstly, as there is no goaf to compress, the rate of subsidence is governed by the rate at which the pillars fail and the rate at which the sliding between the jointed blocks can occur. This is significantly greater than the rate of goaf compression. The meaningful amount of subsidence thus often occurs almost immediately, certainly within less than 24 hours. It has never been measured because it is not possible to know exactly where and when it will occur, but it is known that subsidence troughs may appear overnight.
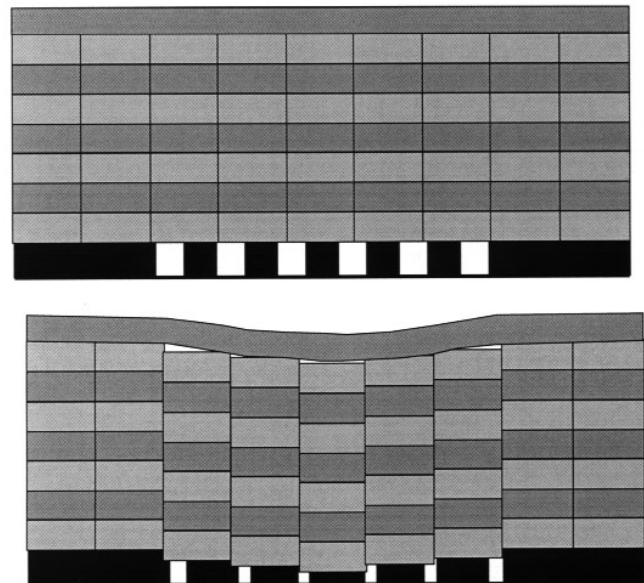
Figure 4. Simplified schematic drawing illustrating the basics of the subsidence mechanism in case of pillar failure. Note that there is no goaf, in contrast to subsidence caused by high extraction mining

Secondly, also due to the absence of a voided goaf, the total volume of subsidence is very close to the total volume of mining underground, if the mining depth is less than about eighty metres. The magnitude of subsidence is within eighty per cent of the effective mining height; which is the true mining height multiplied by the extraction ratio, i.e. if the mining height is 3 m and the extraction is 70 per cent, the effective mining height is 2.1 m.

At greater depth, the amount of subsidence is significantly less, as shown in Figure 5. The reason for this arrested subsidence is not clearly understood, but is believed to be due to the effects of frictional resistance to sliding of the overburden blocks, as the ratio of the weight of the overburden to the magnitude of the confining horizontal stress decreases with increasing depth.

The maximum expected subsidence in the case of pillar system failure could be estimated by

$$S_m = 0.8h_e \text{ for mining depth less than 80 m and by} \qquad [2]$$

$$S_m = 0.5h_e \text{ to } 0.1\,h_e \text{ for mining depth greater than 80 m,} \qquad [3]$$

where $h_e = eh$ and e is the extraction ratio. $\qquad [4]$

Influence of subsidence resistant layers in the overburden

In several coal mining districts of South Africa, the overburden contains either a dolerite sill or a thick, competent sandstone layer. Where this is the case, the subsidence may be partially delayed. In this context, the term 'partial delay' means that initially, the total

Figure 5. The relationship between the ratio of maximum subsidence to mining height and the mining depth, indicate that at shallow depth the subsidence factor is greater in the c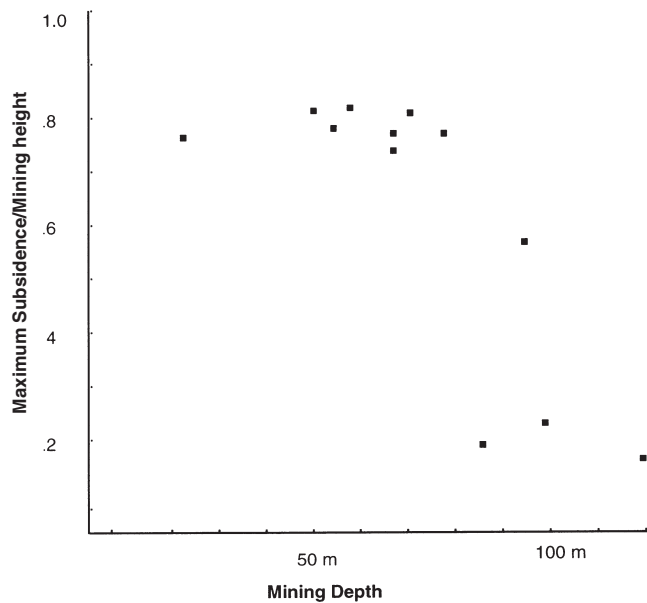ase of pillar failure than high extraction mining and also that there is a marked decrease in subsidence for mining depths in excess of 70 to 80 m

Figure 6. Representative subsidence half-profile for South African cases

amount of subsidence is significantly less than expected.

It was previously believed that dolerite sills, where thick enough, could be used to prevent subsidence altogether. However, there are known cases where mining underneath a forty metre thick dolerite sill initially resulted in less than half a metre of subsidence, only for the sill to fail after a period of about ten years. Where the combination of dolerite thickness, position and mining geometry is such that initially the dolerite sill does not fail, it should be realized that at an unknown time in the future, it may fail. This is especially important in cases where public utilities such as roads are undermined, or where utilities are provided over previously mined ground.

If at all possible, it is better from a subsidence control viewpoint to mine panels wide enough to ensure dolerite sill failure. In this way, whatever subsidence damage occurs can be repaired in a planned fashion.

Note that the remarks made here with regard to dolerite sills are equally valid for cases where a thick, strong sandstone is present in the overburden.

Related elements of subsidence

As remarked in the introduction to this chapter, it is not so much the amount of vertical subsidence, as the effects accompanying the subsidence that is the cause of damage or inconvenience. Nonetheless, these

effects are related to the vertical subsidence and consequently, the amount of subsidence as a single parameter can serve to indicate the severity of the other elements. For instance, for the same mining method in the same locality, more subsidence will result in higher magnitudes of strain and tilt. This section will demonstrate the link between the elements and to indicate how these elements can affect structures on the surface.

Figure 6 is an illustration of a subsidence profile that is valid for South Africa and the majority of cases in Australia and the USA. It is significantly different from the prediction curve that is usually applied in the UK, the main difference being that in South Africa, the USA and Australia the meaningful subsidence is usually contained within the perimeter of the underground mining. In the UK, half of the maximum subsidence usually occurs over the edges of the underground panel. In South Africa, only about 4% of the maximum subsidence usually occurs directly over the panel edges. There is a widespread misconception that no subsidence occurs over the ribside—this is possibly caused by the fact that the surface cracks usually occur inside the panel edges, but there is invariably some subsidence beyond the positions of the first cracks.

At the location where half of the maximum subsidence occurs, the shape of the curve changes from concave to convex. At this point, called the Point of Inflexion, which can be regarded as the anchor

point of the curve, the induced tilt is at a maximum and the induced strain is zero, as it changes from tensile to compressive.

It is important to note that the curve shown in Figure 6 is highly idealized; the author, for instance, has never come across a truly symmetrical subsidence profile. Also, the curve shown is only valid for the so-called 'sub-critical' case, characterized by the absence of a flat portion in the centre of the profile. It would appear that virtually all South African subsidence profiles fall in the sub-critical class. The flat portion in the centre has only been observed in those isolated cases where the *W/H* ratio was greater than 2.5.

Condition of the subsidence profile

Depending on the ratio of the maximum subsidence to the mining depth, the subsidence profile can be smooth and continuous to stepped with almost vertical sides. The classification presented in Table I can be used to gain some insight into what to expect. Figure 7 demonstrates examples of the different classes of subsidence.

Horizontal displacement

In the consideration of possible damage arising from subsidence, horizontal displacement is often overlooked. Vertical subsidence is almost invariably accompanied by horizontal displacement of a magnitude of up to one-third of the vertical subsidence. The horizontal displacement may be smooth or discontinuous, as shown in Figure 8. An interesting characteristic of horizontal displacement is that a point on the surface does not follow a straight line to its final position. Several types of movement have been observed, the most common ones are shown in Figure 9. Almost invariably, however, the final position is directed towards the centre of the panel.

Table I
Classification of subsidence profiles

Class	*Sm/H* ratio	Description
A	<0.001	Barely noticeable, smooth, continuous profile, hair-line cracks
B	0.00–0.005	Difficult to notice, smooth profile, cracks 1–2 cm wide
C	0.005–0.02	Noticeable in flat terrain, smooth, cracks 2–10 cm wide, compression ridges 1 to 5 cm high
D	0.02–0.05	Noticeable in most terrains, visible vertical displacements across cracks, cracks 10 to 50 cm wide, compression ridges 5 to 50 cm high
E	>0.05	Severe profile, almost vertical sides, cracks wider than 50 cm, compression ridges higher than 50 cm

Class B
$0.001 < S_m/H < 0.005$

Class C
$0.005 < S_m/H < 0.02$

Class D
$0.02 < S_m/H < 0.05$
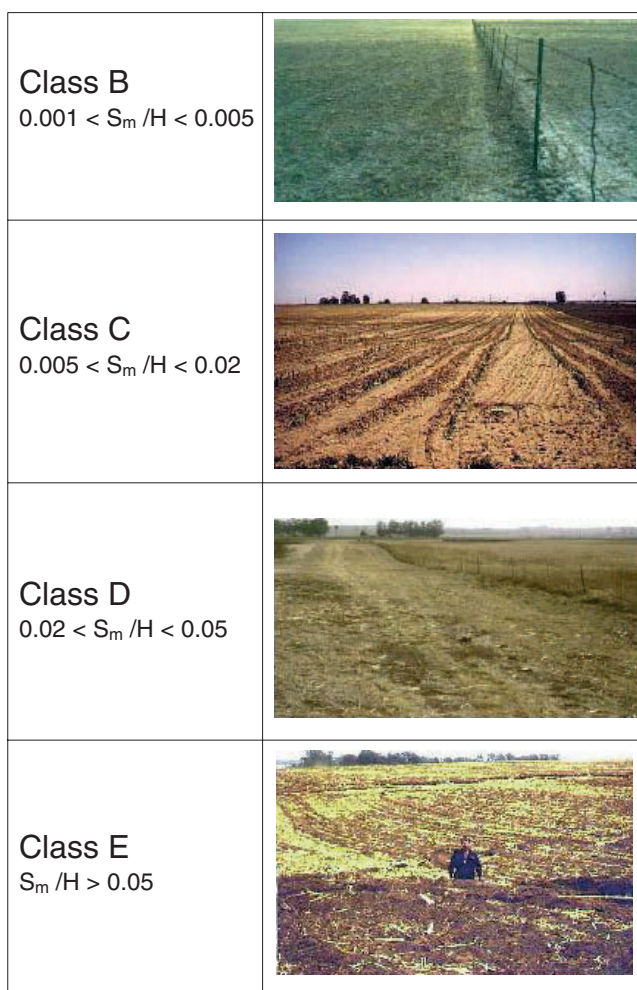
Class E
$S_m/H > 0.05$

Figure 7. Examples of different subsidence classes

Tilt

Whether the pre-mining surface is flat or undulating, subsidence will induce tilt of the surface. Tilt is the one parameter that determines the visibility of a subsidence trough with the naked eye. In the majority of cases in South Africa (as well as Australia and the USA), the subsidence troughs are not easily noticeable because the magnitudes of tilt are in the same range as naturally occurring tilts. Reference to Figure 7 will indicate that the major visible difference between the different classes of subsidence is the induced tilt.

The magnitude of the tilt is a function of the panel width, mining depth and the amount of vertical subsidence. In general terms, all else being equal, greater magnitudes of subsidence will result in greater magnitudes of tilt. In the classical literature, tilt is usually related to the ratio of mining depth to panel width. However, as subsidence is already related to that ratio, it is simpler to relate induced tilt to the magnitude of subsidence, as follows—Van der Merwe (1991):
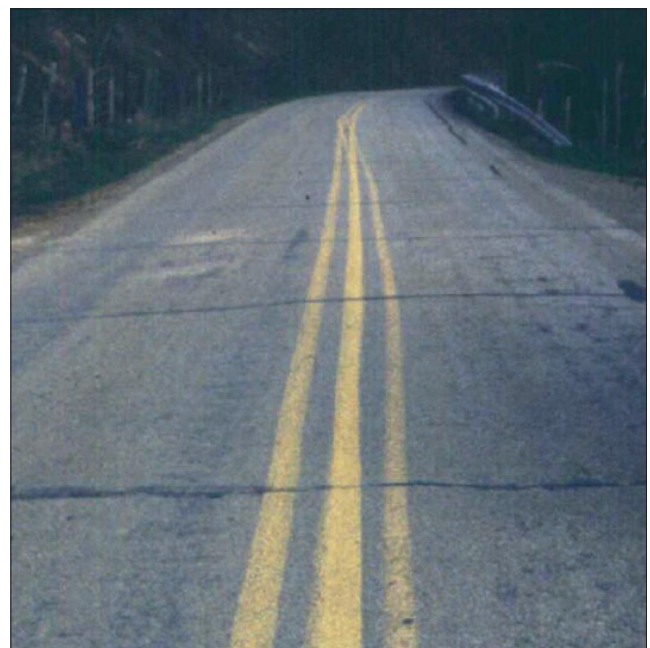
Figure 8. Examples of discontinuous (on the left) and continuous (on the right) horizontal displacement. The slightly curved centre line on the road in the right-hand photograph is the original centre line, which was repainted after the road had subsided
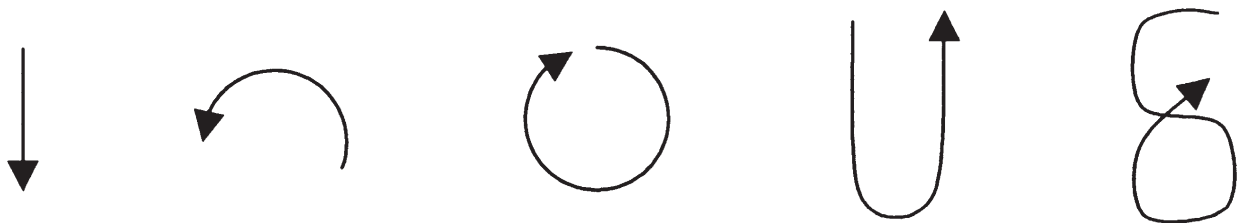
Figure 9. Some patterns of horizontal displacement that have been observed. When considering the damage that may be done by induced strain, it is necessary to take cognisance of the displacement route, in addition to the final position of a point on surface

$$T_m = 21.6S_m + 7 \text{ mm/m} \qquad [5]$$

where T_m = maximum tilt, **in mm/m**
S_m = maximum subsidence, **in m.**

The effect of the induced tilts, logically, is to tilt whatever structure is present on the surface.

Strain

Strain was defined in Chapter 1 as a change in length relative to the original length. In its pure sense, the definition is only valid for very small changes in length of a continuous object. In subsidence, this is not always the case and the correct term to use would be 'deformation'. However, as the term 'strain' in relation to subsidence is firmly embedded, the nomenclature will be retained.

Strain in subsidence areas is caused by a combination of factors. One is the deformation resulting from the bending of the surface, as if it were a beam. Several strain prediction methods erroneously rely on this phenomenon only. The displacement and tilting of discrete blocks, shown in Figure 2, contribute more towards the total strain experienced by the surface. As seen in Figure 6, the strain around the edges of a subsidence profile can be expected to be tensile, changing to compressive towards the centre of the panel.

In reality, this is an over-simplification of a complex matter. In most cases, the surface behaves like a plate and there are usually two principal strains at any point on surface. In some cases, both can be tensile, in other cases both can be compressive, or one can be tensile and the other compressive. Figure 10 shows an example where one strain was compressive and the other tensile. The most that can be said about the distribution of strains in a subsidence trough, is that the majority of strains will be tensile closer to the edges while the majority will be compressive closer to the centres of the panels.

Figure 10. The compression ridge in the foreground is crossed at right-angles by an open tension crack. This is an illustration of a case where the one principal strain was compressive and the other one tensile. This shows that it may be an over simplification to approach subsidence problems two-dimensionally; it is often necessary to consider the full three-dimensional impact of subsidence. (Photograph courtesy of EHR Schümann)

Figure 11. Illustrations of cracks caused by tensile strain. The crack on the left is about 2 cm wide and would correspond to Subsidence Class B. The 50 cm wide one on the right corresponds with Class D or E

Figure 12. Examples of compression ridges. The large one would correspond to Subsidence Class D or E and the small one in the inset with Class B

According to Van der Merwe (1991), the magnitude of maximum tensile strain can be approximated by,

$$\varepsilon_{m+} = 4.2S_m + 1.7 \text{ mm/m} \qquad [6]$$

and the magnitude of maximum compressive strain by,

$$\varepsilon_{m-} = -9.1S_m - 2.8 \text{ mm/m} \qquad [7]$$

where S_m in both cases is in m and ε in mm/m.

According to Equations [6] and [7], the absolute magnitude of the compressive strain will always be greater than that of the tensile strain; this is another characteristic of sub-critical panels.

Tensile strains will cause the surface to stretch and, if of sufficient magnitude, to crack. It is interesting to note that longwalling usually results in three roughly parallel cracks about a metre apart, while pillar extraction is usually characterized by more cracks with smaller apertures. Compressive strains will cause the surface to compress and if the surface material is not sufficiently soft, to buckle and form compression ridges. Figure 11 illustrates surface cracks caused by tensile strain and Figure 12 shows compression ridges caused by compressive strain.

Long-term after-effects of subsidence

Once the initial subsidence has occurred, the rate of subsidence decreases to a barely measurable level. It would be incorrect to state that after the initial six-weeks, period, subsidence ceases altogether. However, the amount of subsidence after that period is within the limits of seasonal changes in ground elevation and to discern mining-induced subsidence then becomes a matter of speculation rather than measurement. For engineering purposes, it is sufficient to state that subsidence ceases after approximately six weeks.

However, there remains one post-subsidence phenomenon that is cause for concern, that being sub-surface erosion. This phenomenon has not previously been described in detail, perhaps because it has not previously been linked to mining and because it does not occur under all conditions. It has been seen in most mining areas of South Africa, also in the USA and the UK and has been reported in connection with subsidence caused by oil extraction.

Mechanism of sub-surface erosion

Concurrent with subsidence, cracks commonly appear on the surface. After one rainy season, these cracks are usually filled in with soil, leaving only a scar. However, the cracks are not confined to the soil but extend down into the upper rock layers. These cracks in the rock act as reservoirs for soil that is slowly eroded into the cracks from the contact between the soil and the rock. Eventually a subterranean cavity forms at this contact position. Later, when it has grown to its critical size, it collapses, resulting in a pothole on the surface. The mechanism is illustrated in Figure 13.

These are usually of the order of 30 to 50 cm in diameter, but can also measure metres in diameter, by several metres deep, in deep, sandy soils. Figure 14 shows examples of the normal types of potholes and of the more severe occurrences. Figure 15 is an

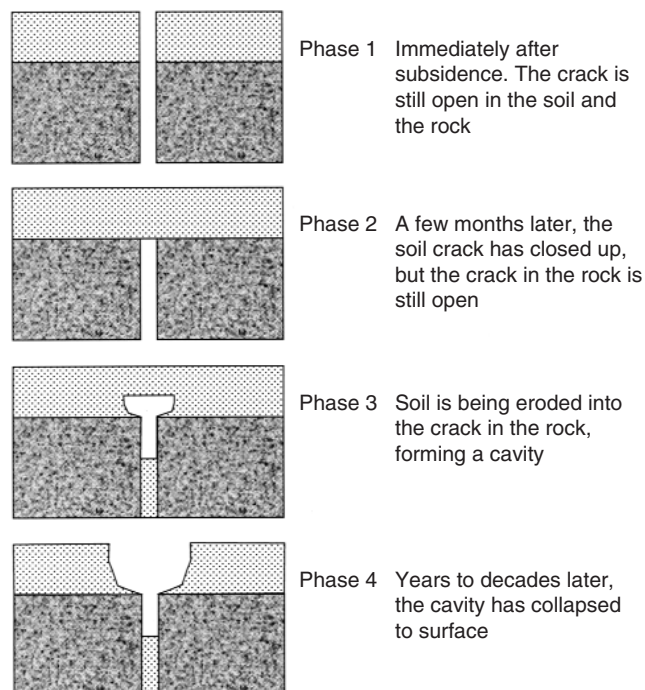|	
Phase 1	Immediately after subsidence. The crack is still open in the soil and the rock
Phase 2	A few months later, the soil crack has closed up, but the crack in the rock is still open
Phase 3	Soil is being eroded into the crack in the rock, forming a cavity
Phase 4	Years to decades later, the cavity has collapsed to surface

Figure 13. Diagrammatic vertical section, explaining the process of sub-surface erosion. Depending on the width of the crack in the rock, the type of soil, rainfall, etc., the process may take months to decades before it results in potholes on the surface

ROCK ENGINEERING FOR UNDERGROUND COAL MINING

Figure 14. Examples of early (on the left) and mature (on the right) sub-surface erosion potholes

example of a trench that was constructed at right-angles to a healed surface crack several years after mining had been completed. It shows a crack in the rock with the soil infilling and the resultant cavity underneath the surface.

Time of occurrence of potholes

Sub-surface erosion is a time dependent process, the rate of development being governed by the rate at which erosion occurs. Therefore, the availability of water to drive the process, the transportability of the soil and the width of cracks in the rock are the main controlling parameters. In sandy areas with rock cracks of about 50 mm wide and soil thickness of about 6 metres, the process has been seen to result in potholes some eight years after mining. In areas where the soil is predominantly clay of about a metre thickness, the same crack widths have resulted in potholes after about six years.

In other areas where mining was carried out at much greater depths—in the region of 1 000 m—the potholes only appeared some eighty years after mining had ceased. It is postulated that the delay in

the latter case was due to thinner cracks, requiring the eroded soil to penetrate deeper into the cracks before a cavity large enough to collapse was formed.

Detection of potholes

One of the serious aspects of sub-surface erosion is the absence of visual warning before collapse occurs, as illustrated in Figure 16. Of all the available geophysical techniques that are available, only one has proven to be successful and practical to apply, and that is Ground Penetrating Radar (GPR). However, even with GPR it was found that the success rate depended largely extent on the expertise of the operator. It was found with several trials under varying conditions of soil types and cavity sizes that the successful operators were consistently successful, while the unsuccessful ones were consistently unsuccessful.

The definition of success in this context is that the cavities should be located, but that the false alarms should be minimized. The latter can never be ruled out altogether as buried bits of foreign matter, small openings in the rock and buried pipes often have the
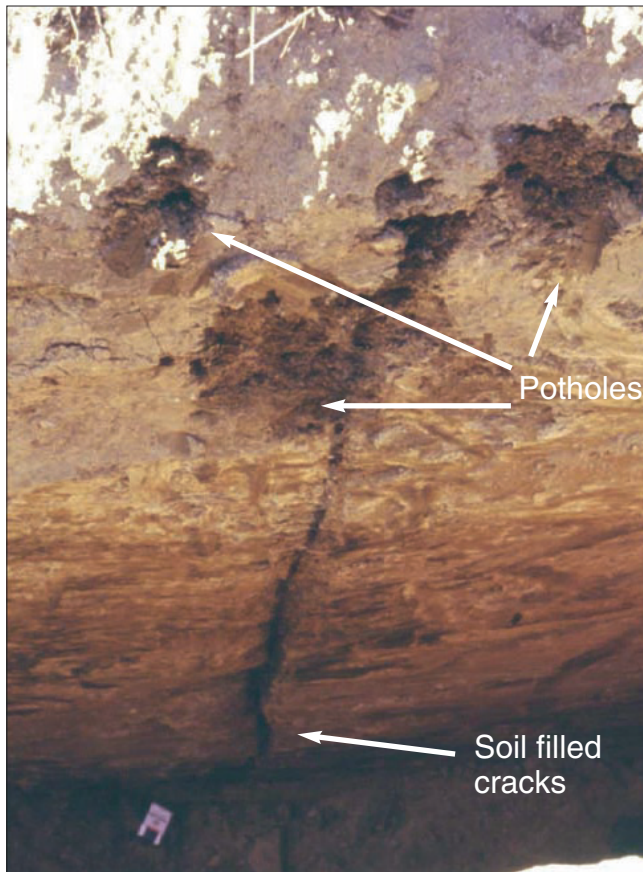
Figure 15. Photograph of the side of a trench that was excavated through sub-surface erosion potholes, showing the soil filled reservoir crack in the rock and the resultant cavities in the overlying soil

same radar signature as a sub-surface erosion cavity. Figure 17 is an example of a 'radar signature' of a sub-surface erosion cavity.

The first step in locating cavities is to conduct a visual search. The areas to concentrate on are those areas where subsidence cracks existed at the time of mining. If those positions were not recorded, it is best to traverse the area overlying the mined panel on a grid pattern. The zone between 10 m to 30 m inside the panel edge should receive special attention, but the interior areas of the panel should not be neglected. Cracks inside the panel tend to close up during the mining process, but they seldom close up completely. Although rare, potholes of significant size have been found inside the panels, away from the panel edges.

The best time to conduct the visual search is towards the end of winter, when the grass has not yet started growing. In the summer months one has to walk a very dense pattern to locate the holes. The best time of day to find scars of old cracks is during the first and last two hours of sunlight, when the light comes in at a shallow angle. Care should be taken to distinguish animal dwellings from potholes; the former are usually recognised by an inclined entrance to the hole and evidence of dug out soil around the edges. Collapsed ant colonies often have an appearance very much like sub-surface erosion potholes, but they are easily discernable.

Figure 16. There are no visible signs on the surface of the sub-surface cavity on top of which the man in the pictures is standing. The 1.8 m long steel rod has all but disappeared into the hole

ROCK ENGINEERING FOR UNDERGROUND COAL MINING

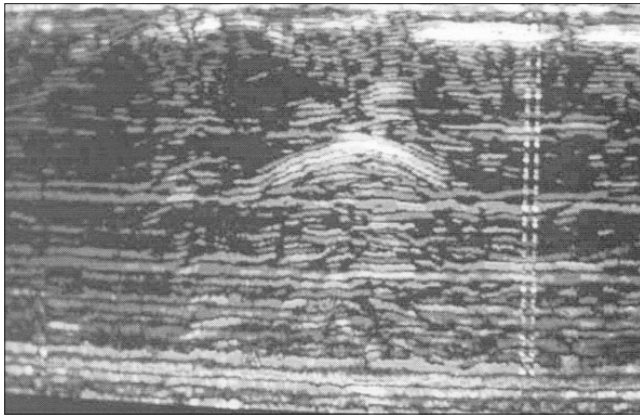Figure 17. Radar view of the sub-surface. The hyperbola in the centre is a strong indicator of the presence of a cavity

Figure 18. A freshly collapsed sub-surface erosion pothole, ballooning out below the surface. The diameter of the hole on the surface is about 50 cm

Young sub-surface erosion potholes have a circular opening at the top, ballooning out underneath the surface, as shown in Figure 18. It is good practice to use a stick to check whether the hole is wider further down rather than to stick one's hand inside. Animal holes often supply leads to the existence of sub-surface erosion. When three or more occur in a line, rather than a cluster, one can start looking out very carefully. Animals probably find it easier to dig in the ground that has already been disturbed.

In the veld, care should be taken against natural hazards. Always wear boots that cover the ankles, as the majority of snake bites are around the ankles. Insect repellant also comes in handy.

Estimating the sizes of potholes

The sizes of potholes are governed by an inter-relationship between the soil type and thickness, the size of the reservoir (or crack in the rock) and the strength of the upper soil layer. The finer the soil grains in relation to the width of the crack, the easier the soil will be eroded into the cracks. Dry clay is less transportable than dry sand, but wet clay becomes fluid very quickly. Potholes have been found in strong, black clay as well as loose sand. The thicker the soil layer, the larger the holes can be. Based on very limited data, it appears that the maximum hole width is about half of the thickness of the soil layer.

The upper soil layers are usually strengthened by grass and plant roots, and compacted by the passage of animals and humans. The stronger the upper layer, the wider the hole can grow underneath before it collapses. This has special bearing in cases where roads were undermined. While the strong road foundation will cover potential holes for a longer period, the holes will be larger when collapse eventually does occur. In all cases where roads were subjected to subsidence, annual inspections are essential. This should be done both visually and with GPR.

The majority of the holes are around 30 to 50 cm in diameter, but exceptions do occur. Holes with diameters of more than three metres and depths of five metres have also been seen. The first holes are circular in shape and occur along the lines of old cracks. As they mature, the holes link up to form long trenches, and can become as long as the original cracks. An example of such a mature sub surface erosion cluster is shown in Figure 19. The Figure shows the outward appearance of the potholes and the subterranean tunnel connecting the holes. The tunnel runs along the position of the original crack that was associated with the subsidence.

Prevention and treatment of existing potholes

Merely filling the holes with soil is not effective. Firstly, the soil has to be robbed from somewhere else and, secondly, it has been seen that soil-filled holes tend to reopen much more quickly than they took to develop in the first place. Filling with concrete is not effective either, as this tends to result in two new holes on either side of the original one. The only effective treatment is one that allows water to drain through the crack while retaining the soil.

Geomembranes would be effective but they are relatively expensive and difficult to place because they will require the upper rock layer to be exposed first. The best filter found to date was ash. The sifted minus 10 mm fraction was found to be optimal. Fly-ash tends to either solidify or be transported down the crack itself. Holes treated with ash have so far remained closed for more than ten years.

An effective prevention method is to fill the subsidence cracks with ash to about a metre from the top and then to fill the remainder of the crack with soil. Care should be taken to work the ash as deeply as possible down the crack.

**Figure 19. Mature sub-surface erosion, showing the surface
holes and details of the connecting tunnel between the individual holes. In time, the holes will join to form a long trench**

Sinkholes resulting from shallow workings

Another potential long-term effect of mining where bord-and-pillar mining has been conducted at shallow depth, is the appearance of sinkholes due to bord—mainly intersection—collapse underground. In contrast to sub surface erosion, these sinkholes are wide and deep. The width is usually approximately the same as the size of the intersection underground, i.e. six metres in diameter, by several metres deep.

This phenomenon is also better documented than sub-surface erosion. It is a recognized problem in several countries of the world. In South Africa it is known to occur in the Witbank area and certain old mining areas of the East Rand, notably east of Springs and in the Brakpan area. Figure 20 illustrates a cluster of old sinkholes in the Witbank area and Figure 21 a more recent one at the municipal golf course in Brakpan.

**Figure 20. Aerial photograph of a cluster of sinkholes in the
Witbank area**

**Figure 21. A recent sinkhole on a golf course. The hole was
approximately 4 m deep**

ROCK ENGINEERING FOR UNDERGROUND COAL MINING

It appears that the formation of sinkholes is especially prevalent at mining depths of less than approximately 50 metres. It is rare for sinkholes and pillar collapse to occur in the same area, as the effect of sinkholes is to decrease the load acting on the pillars. However, the two phenomena may be linked by underground fires. When sinkholes first appear, they let fresh air into the underground workings and this may supply the necessary oxygen for underground fires which will then result in pillar failure. In the Witbank area the two are linked, as illustrated in Figure 22.

Early detection of sinkholes is even more difficult than sub-surface erosion. Because the diameters of the holes are greater, the thickness of the final lids prior to collapse is also greater and it is necessary to penetrate deeper, which can be a problem with GPR. The best approach is to regard all shallow mined areas with suspicion.

The areas in danger of collapse now are invariably linked with very old mines and the accuracy of the mine plans can be questioned. Experience has shown, however, that the plans are surprisingly accurate once the links between surface and the underground have been fixed. The plans are sometimes incomplete, as has been found in some cases around Witbank. Areas that were shown to be unmined on the plans were found by drilling to have been mined. It is also conceivable that there may be areas that were mined of which the plans have been lost, or were never even maintained in the first place.

The circular shape of the sinkholes indicates that the failure mechanism is shear. The shear strength of most in situ rock types exceeds the shear stress exerted by the plug which has to fail in order for a sinkhole to appear. This is one reason why sinkholes are only

Figure 22. The depression on the right-hand side of the photograph was caused by the underground fire, indicated by the smoke coming out of the sinkhole

common where the mining depth was shallow, i.e. where the rock has been weakened by weathering. Also, if the soil cover overlying the rock is thick in comparison to the rock interburden, failure is more likely because the soil supplies additional loading to the rock layer without contributing to the strength.

The effects of subsidence on structures

The negative impact that subsidence will have on the surface is a function of two main parameters, namely, the nature of use of the surface and the severity of the induced subsidence. Very seldom will mining have no effect on the surface; even less seldom will it have catastrophic effects. It has been shown that most types of surface structures, even though not designed to accommodate the effects of subsidence, can withstand those effects with minimal precautionary measures.

This section will deal with various classes of surface use and types of structure. In each case, a generalized description of expected effects will be discussed together with proven methods of damage mitigation and prevention.

Surface structures will be sub-divided into various classes, i.e. linear structures, such as roads, pipelines and conveyor belts, tower structures such as power pylons and block structures such as houses. Agriculture will be briefly considered as a separate issue.

Linear structures

It was previously shown that the various elements of subsidence reach different values at different positions of the subsidence trough. Linear structures will encounter the full range and it is usually impossible to avoid damage by positioning of the mining panel relative to the position of the structure.

Conveyor belts

Conveyor belts can be affected as follows, by the different subsidence elements.

- *Tilt*:If the total inclination of the belt exceeds 18°, the coal may slip back on the belt. In general, the subsidence-induced tilts seldom exceed 3° to 4°, so induced tilt is unlikely to cause a serious problem unless the belt is constructed on undulating terrain, with pre-subsidence tilts close to the limit. However, isolated spots of greater tilt may develop, especially in shallow mining cases.

- *Horizontal displacement*: Horizontal displacement is potentially the most serious problem for the continued operation of a subsided conveyor belt, as shown in Figure 23. Conveyor belts should be straight, except for the specially constructed

curved ones. Whether the belt be straight or curved, deviations from the designed alignment are always serious as this will invariably result in the belt not running true on the rollers, leading to coal spillage, etc.

- *Strain*: Compressive strain could result in buckling of the conveyor's cover plates while excessive tensile strain may cause structural damage. However, there is usually sufficient inherent flexibility in conveyor belt constructions to prevent serious structural damage.

Precautions

It has been found that while conveyor belts in general are flexible enough to prevent strain-induced damage, they are yet rigid enough to maintain themselves in a straight line provided they are detached from the surface. Where conveyor belts are to be undermined, it is essential to cut the bolts attaching the legs to the foundation blocks.

Pipelines

Pipelines made of a flexible material can usually be undermined with simple precautions. However, pipes made of rigid materials such as asbestos, cement or ceramics will fail even with little subsidence.

- *Tilt*: Differential tilt (or curvature) can cause a pipe to pinch, disrupting the service, even if the pipe material does not suffer any damage. As this is an engineering consideration, being a function of the pipe wall thickness, diameter and type of material used, broad guidelines cannot be given. The subsidence engineer should predict the subsided profile of the pipe route and make this information available to the pipe design engineers for evaluation.

- *Horizontal displacement*: If a pipe is buried during the process of subsidence, the horizontal displacement can shear the pipe insulating material, causing the material to tear as shown in the example in Figure 24.

Precautions

Experience indicates that a buried pipe should be uncovered prior to undermining. Very little additional work is required, apart from regular inspections and keeping an emergency length of pipe available in case the unexpected happens. If very good reasons exist why the pipe should not be left open for the duration of subsidence, it can be covered with a cohesionless material such as washed river sand. If large magnitudes of subsidence are expected, a by-pass consisting of a snaked section of pipe to compensate for the increased length can be provided.

In a situation where a pipe is subjected to unexpected subsidence and it has to be uncovered

Figure 24. Even though the insulation material around the pipe was torn by the friction caused by horizontal displacement, the steel material of the pipe was not damaged

Figure 23. Horizontal displacement of the ground surface is the most important subsidence element that could affect the operation of a conveyor belt. The bolt, holding the leg of the structure to the foundation block, should be cut to allow the belt to maintain itself in a straight line

Figure 25. This pipe lifted clear off the ground surface after being uncovered

ROCK ENGINEERING FOR UNDERGROUND COAL MINING

after the event, there are a number of precautions that need to be implemented. Firstly, bear in mind that pipe positions do not always coincide with the surface markers. It is best to dig by hand to locate the pipe at 20 m intervals before mechanical equipment is used. Even then, the mechanical equipment should be used with the utmost care in order not to do more damage than the subsidence. Also, it is best to uncover the pipe in the centre of the subsided area and then to work toward the edges. The reason for this is that in several cases, the physical pipe will be shorter than its new profile route   and the pipe will tend to lift once it is uncovered, as shown in Figure 25. By working toward the deepest area of subsidence in the centre, the pipe will be clamped by the final island of soil cover and may then jump up suddenly.

Tarred roads

From an emotional point of view, roads are amongst the most sensitive structures of all to undermine. This is not without reason: a mishap on a road can all too easily result in a serious accident and thus subsidence to roads represents a potential danger to the public, while damage to most other structures will often cause nothing more than inconvenience.

Tarred roads usually have more rigid foundations than the underlying soils and will in most cases show visible damage after subsidence. In most cases a deviation of some sort should be provided during the period of active subsidence. However, except in the most severe cases, there is little justification to construct a costly by-pass, as a gravel by-pass in the road reserve is usually sufficient.

- *Tensile strain*–Tarred roads are very sensitive to tensile strain. Strain magnitudes as low as 0,5 mm/m will manifest as a small crack in the road. The greater the strain, the wider the crack. Cracks as wide as 50 mm are not uncommon under most situations, as shown in Figure 26.

Figure 26. Cracks on the road surface caused by tensile strain. Note that in this case, both of the principal strains were tensile

Figure 27. Example of smaller, dispersed compression ridges

- *Compressive strain*: Due to the rigid nature of road foundations, compressive strains will almost invariably result in ridges on road surfaces, like the one shown in Figure 10. These tend to develop suddenly (within less than an hour) as the road foundation fails. This is the main motivation for providing a by-pass, for even though the ridges are flattened easily, the first motorist being confronted by an unexpected ridge is likely to take emergency evasive action.

  Compressive strains sometimes result in a number of smaller, dispersed ridges rather than a single large one. An example is shown in Figure 27.

- *Tilt*: Induced tilts may impair the sight distance on the road surface. It may also affect the road's drainage system, resulting in accumulations of water on the road surface.

- *Horizontal displacement*: Horizontal displacements cannot be prevented, but are not considered serious. Figure 8 is an example of a case where a road in the USA which had subsided by about a metre, had its centre line repainted to compensate for the horizontal shift. Similar horizontal displacements are encountered in South Africa, although they tend to be less smooth and blocky in nature.

Gravel roads

An important difference between gravel and tarred roads is that gravel roads are usually more flexible in construction. For this reason, they are less susceptible to damage. Although cracks and ridges do appear, they are usually smaller and less important. This was found in the Secunda district, where tarred and gravel roads were allowed to subside next to one another for comparative purposes.

The ridges were folded over and did not pose any significant hazard to traffic. The cracks were also smaller and disappeared very quickly. It was on this basis that the conclusion was reached that instead of a costly deviation which usually involves at least some disruption and inconvience to surface owners, it would be sufficient to construct a simple gravel by-pass inside the road reserve for use during the six weeks period of active subsidence. This should not be seen as a blanket recommendation. It is still necessary to investigate the subsidence thoroughly before the event to predict the new road profile. This is especially true in the case of shallow mining, where steep subsidence edges will still necessitate a deviation beyond the mining area.

Precautions

In the case of road undermining, it is essential for a detailed prediction of the expected subsidence to be made using the procedures described in the appendix. The following descriptions are general and the exact nature of the precautions should follow a detailed investigation.

In most cases very little action will be needed for the undermining of a gravel road. During the period of active subsidence, the road should be patrolled on a regular basis—more than once per day. A heavy roller should be available to flatten any compressive ridges. It will seldom be necessary to construct a by-pass.

For tarred roads, a by-pass should be provided in most cases. However, it will usually be sufficient to construct a gravel by-pass within the road reserve, instead of a tarred one beyond the area of subsidence.

Traffic should be diverted onto the by-pass from the time that the mining is being carried out directly underneath the road, and should continue until subsidence surveys indicate that the subsidence has practically stabilized. This will usually be approximately six weeks after mining has passed underneath the road.

To reduce damage to the road foundation, slots may be cut to absorb the compressive strains. This prevents the formation of the compressive ridges, as shown in Figure 28.

Tower structures

Power pylons

The most common tower structures are power pylons. They are usually most severely affected by induced tilt and to some extent by horizontal strains and by subsidence.

The most severe consequence of induced tilt is that, as the pylon tilts, the fixed conductors tend to hold the structure back. This could induce severe stresses in the pylon, resulting in damage as shown in Figure 29.

Figure 28. The slot in the photograph was originally 30 cm wide. Compressive strain caused by undermining reduced the width to 10 cm. Note the ridge on the road shoulder in the background, where no slot was provided. If the slot had not been cut in the road, a ridge of the same height would have developed on the road
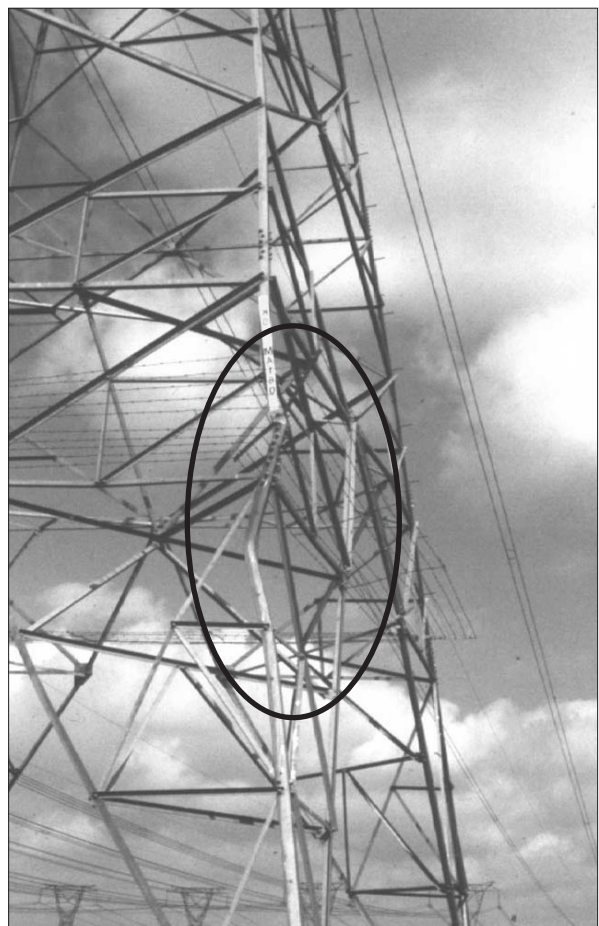

Figure 29. Structural damage to a power pylon that was not protected during subsidence

Figure 30. Temporarily suspending the conductors on rollers instead of the normal fixed fittings frees the pylon to move without damaging the structure

Horizontal strains, in severe cases, can tend to expand or reduce the base area of the legs of the pylon. In practice, however, this has not been found to cause significant problems.

Another problem is that of earth leakages, which can occur as a result of the clearance between the conductors and the ground being reduced. This is especially the case where a line of pylons is undermined by a series of high extraction panels, with the pylons situated in the centres of the panels.

Precautions

In most cases damage can be prevented by replacing the fixed fittings of the conductors to the pylons with rollers during the subsidence period, as shown in Figure 30. This has the effect of freeing the pylon to move horizontally. After the subsidence has ceased, the rollers can be replaced by the normal fittings.

Where the pylons are situated on the permanently sloping edge of a panel, it will sometimes be necessary to jack up the down dip legs of the pylon and to place elevated concrete foundations underneath them.

Floodlights

Floodlights are usually mounted on narrow hollow stems with concrete foundations. They are mostly affected by tilt.

Precautions

The maximum tilt should be predicted, and if that is less than the maximum that the structure can tolerate, it is often best to let the subsidence occur without any pre-emptive measures. Once the subsidence has ceased, the verticality of the floodlight can be restored by adjusting the holding nuts on the foundation.

Block structures

The most common types of block structures are houses and other buildings. In South Africa, houses are not often undermined, mainly because coal is mined in the more sparsely populated parts of the country. It is often possible to plan mining such that the undermining of houses can be prevented.

Buildings are primarily affected by tilt, strain and horizontal displacement. Although they occupy a small area compared to the total area of a panel, it is necessary to do a detailed prediction of the subsidence elements over that small area. Only in exceptional cases will it be possible to allow an occupied house to subside without careful precautions. The severity of the damage and the position of the building in the panel will determine whether or not repairs and re-habitation of a house will be possible.

- *Tilt: If a building is situated in the centre of a panel, the tilts will be of a transient nature and once the area has stabilized, walls, etc. will return to the vertical. During active subsidence, differential tilts may cause buckling of the building. Windows may crack and doors may be stuck.*

- *Strain*: Tensile strains may cause walls to crack and compressive strains may cause plaster and floors to buckle.

- *Horizontal displacement*: Services to buildings may be cut off by horizontal displacement.

Precautions

There is limited experience in South Africa of house underminings. In all the known cases, houses were vacated during the undermining. Most were demolished after mining, because typically they were old farm houses, situated on the permanently sloping edges of the panels. The repair costs in these circumstances would have exceeded the cost of building a new house. One notable exception occurred when the Sasol company undermined a house that was situated in the centre of a panel. After stabilization, the house was repaired and now houses the Sasol Centre for Ground Conservation. The house is shown in Figure 31. In the USA, timber constructions have been supported on steel beams and continuously re-levelled during the period of subsidence. The permanent service fittings are temporarily replaced by flexible ones as shown in Figure 32.

Another novel method, although it could prove too costly, is to physically move a house away from the area of influence. After mining, it is then transported back to its original setting and the services are reconnected. One such example is shown in Figure 33.

Figure 31. The Sasol Centre for Ground Conservation in Secunda, South Africa. The white markings on the walls indicate the floor elevation of the house before subsidence

Figure 32. Steel beam underneath a timber house during undermining in the USA

Figure 33. A house in the USA being removed to a stable position prior to undermining (Photograph courtesy of Robert A Bauer)

The effects of subsidence on agriculture

Coal mining in South Africa is most often carried out in sparsely populated farming areas, so the activity most commonly affected by subsidence is agriculture. The degree to which farming is affected by subsidence depends on the extent of mining, the characteristics of the subsidence and the nature of the agricultural activity. In general, it can be stated that the effects of surface subsidence on farming are not disastrous, but if a particular farm happens to be marginally economic, even a small detrimental effect can have serious consequences to the individual farmer.

Another aspect that deserves attention is the emotional impact of subsidence. This is especially true in cases where family farms have been in the possession of the same family for several generations. What appears to be inconsequential, minor deformation of the surface to a mine operator is serious disfigurement of a family heirloom in the eyes of the farmer. The mine often does nothing more than

to exercise its right to mine the coal it purchased from the farmer, a right that the farmer has been compensated for to an extent that satisfied him at the time of selling his mineral rights.

However, mining is often carried out a long time after purchase of the mineral rights and several farmers experience the inconvenience of subsidence at a time when the income from the mineral rights has already been forgotten. In retrospect, the amount of compensation may appear insufficient to the farmer at the time when mining eventually takes place. In reality, what may have been fair compensation at the time of purchase of the mineral rights may be inadequate at the time of mining. In some cases, the compensation was even paid to previous generations.

Mine managers cannot ignore these emotional impacts. They are real and often lead to claims of damage. The situation must be approached with the same care as the physical changes that take place; in fact, the emotional issues are very often the most difficult ones to deal with.

The most serious effects of subsidence relate to water. Induced tilts will invariably result in changed drainage patterns of surface water that may, in turn, result in soil erosion.

The most obvious visible effect of mining is ponding of surface water, such as the example shown in Figure 34. Ponding is not common, affecting between 5% and 7% of the total area undermined by high extraction methods. The flatter the pre-mining surface, the more likely ponding is to result.

There are several ways of dealing with ponding and local circumstances will dictate which is the better approach to adopt. Trenching to de-water a pond is common practice and is usually successful in cases where the surface is slightly undulating. If the surface

Figure 34. Severe case of ponding caused by deep subsidence troughs in very flat terrain

is very flat, it may not be the correct solution as the trenches could be too long. There are agricultural guidelines that govern the slopes of the trench and the provision of water breaks to decelerate water to prevent undue soil erosion. The Department of Agriculture is usually very helpful with regard to advising how a trench should be constructed.

Pumping has been resorted to in exceptional cases but it has several disadvantages, for instance, the maintenance of pumps and the provision of electricity. Filling a pond is usually not a good solution as the soil required has to be obtained elsewhere—this comes down to robbing Peter to pay Paul.

It is a popular misconception that a pond in grazing land has no consequences at all and may, in fact, be to the farmer's advantage. Several farmers argue that such ponds are breeding areas for parasites and insist that they be fenced off. Others seem not to be too concerned. In the majority of cases, farmers are satisfied with no action being taken, provided an amount of compensation is paid for the loss of income resulting from the pond.

Other effects like the appearance of surface cracks and compression ridges are easier to deal with, as time tends to heal them fairly quickly. The majority of cracks disappear after one rain season. Wide cracks need to be filled in to prevent injury to farm animals. It is a wise precaution to fill cracks with sifted ash to prevent the formation of sub surface erosion pot holes in later years—referred to earlier in this chapter.

The most important issue is to keep farmers informed of what is happening and what is likely to happen on their farms in time to come. The dialogue should begin before mining commences and remedial action should always be taken in consultation with the farmer.

Potentially the most serious effect of high extraction mining is on groundwater. It is to be expected that boreholes in the vicinity of high extraction panels will dry up, although notable exceptions have been observed in South Africa. There have been cases where boreholes in the centres of high extraction panels retained pre-mining water levels. In most cases, however, boreholes inside the perimeter of high extraction panels, and often ones located outside the panels, dry up.

In the Appalachian regions of the USA, it has been found that the drying up of shallow boreholes is temporary and that water levels are restored within a few months of mining, where the bore holes were not deep enough to penetrate into the goaf. It has also been found that the quality of groundwater is not affected, as the contaminated water at the coal horizon tends to stratify and remain at the bottom. The clean water extraction and replenishment cycle appears to be a shallow phenomenon.

The groundwater issue is a very important one, especially in South Africa with relatively limited water resources. It is currently the subject of much research and, hopefully, more will be known in the near future.

It is common practice in South Africa to provide alternative boreholes prior to mining and to accept that holes in the immediate vicinity of mining will dry up. This is often a demonstration of goodwill from the mines' side. In other cases, mines have been known to replace boreholes with piped water from elsewhere, although the long-term sustainability of this measure is questionable.

There are a number of other, lesser effects that have to be dealt with during the mining process. These include repairing or replacing fences that break in the tensile zones and tend to slack in the compressive zones of subsidence troughs. Farm roads often suffer minor damage and have to be maintained.

Handling of subsidence in general

Before high extraction mining commences, it is essential to determine which structures may be affected by subsidence. The first step is to conduct a survey of existing structures and farming activities. This should not be confined to a plan study—the surface areas have to be inspected *in loco*. Although the regulations prohibit the erection of structures without the consent of the mineral rights holder, all structures are protected by law, whether they were erected legally or not.

The next step is to communicate with the owners or custodians of the surface and the structures. Permission for the undermining of structures has to be obtained from the Department of Mineral Resources (DME), who will invariably insist on an agreement with the owner of the structure before they will consider the case. Agreement with the owner will not guarantee that permission will be given, as the authorities have to be convinced that there will be no resultant danger to the public.

This implies that a prediction of the subsidence elements will have to be provided and that monitoring will have to be carried out. Action plans in the case of unexpected magnitudes of subsidence will have to be provided, as will methods of repair to damage. The provisions with regard to structures remain valid even in the case where the mine is the owner of the structures.

Where there are no artificial structures and the only activity is agriculture, prior permission from the DMR is not required but it is still wise to communicate with the farmer. In any event, it is a requirement to carry out subsidence monitoring and to notify the DMR of surface depressions. This requirement is usually satisfied by indicating the depressions on the statutory plans that have to be submitted to the DMR quarterly. Dangerous depressions have to be fenced off and reported individually.

In general, mine managers should be prepared for the emotional resistance to subsidence in addition to the physical effects. Open communication with all stake-holders is essential, aiding in the building of healthy relationships.

Monitoring

Introduction

Monitoring should form an integral part of the overall mining operation. It is to be carried out on three levels, namely operational monitoring to yield ongoing information on the stability of an excavation, research-related monitoring to supply scientific information and quality control monitoring of the support materials and installations.

Three monitoring subjects will be covered in this chapter: roof, pillar and subsidence monitoring. The emphasis will be on practical monitoring, concentrating on the operational aspects.

Roof monitoring

From an operational safety point of view, roof monitoring is by far the most important aspect. The subject of roof monitoring is covered by a number of different factors. Visual monitoring is the least sophisticated, but the simplest, yielding a vast amount of information. The next level is simple instrumentation and elementary tests, followed by detailed instrumentation with accurate instruments.

Visual monitoring

Visual monitoring does not supply quantifiable information and is often subjective. This means that it is of limited scientific use, but that is not its primary intention. The main aim is to have ongoing information and to make the observer aware of unusual situations. It is often done intuitively by experienced underground operators who link observation and result through experience.

Indications of sub-optimal support systems

If a roof support system is optimally or over designed, there will be little to observe. On the other hand, sub-optimal systems will result in visible damage in the form of cracks or falls of roof. The shape and size of falls of roof supply valuable information to the trained observer. In the next paragraphs, the most common indicators are described, followed by their causes and quick remedies if they are available.

Open crack in centre of roadway

These cracks are seldom perfectly straight or exactly in the centre of a roadway. They tend to follow small joints in the central areas of roadways. Figure 1 is an illustration of a typical open tension crack in a roadway.

An open crack in a roadway is an indication of excessive horizontal tension. The tension may be due to one or more of three causes:

- Excessive road width, resulting in excessive induced tension in the bottom centre of the roof beam.
- Lack of horizontal compression—although not common, this is sometimes seen at the bottoms of troughs underground.
- Excessive horizontal compression that caused over-thrusting higher up in the roof, pushing the lower layers down.

Remedy

As with several other causes of roof instability, the immediate reaction should be to decrease the road width. If this does not solve the problem, long anchor support is often required. A specialist should investigate the problem.

Over-thrusting

Shown in Figure 2, over-thrusting is caused by horizontal stress. It is seen more commonly in the USA and Australia than in South Africa. It often occurs near dykes and at the crests of rolls in the seam.

Remedy

If practicable, the section should be turned to be oriented at 45° to the direction of the stress. In addition, the support system should be stiffened by using full column pre-tensioned resin bolts. A dual speed resin should be used to achieve pre-tension and the annulus between the bolt and the hole should be as small as possible.

Thin falls between bolts

This is most often caused by a lack of tension on the bolts, aggravated by excessive bolt spacing and is often seen where mechanical anchor bolts have been used. If there are no small sections of rock left between the washer plates and the intact roof, as shown in Figure 3, the cause is almost certainly a lack of pre-tension.

Figure 1. Example of a tension crack in the roof over a roadway

Figure 2. Over-thrusting in the roof caused by high horizontal stress

If, on the other hand, there are rock remnants caught between the washer plates and the roof, as shown in Figure 4, it indicates that while there was sufficient pre-tension on the bolts, the bolt spacing was simply too wide.

Remedy

The simple remedy is to decrease the bolt spacing and to check the bolt installations to ensure that proper pre-tension is applied.

ROCK ENGINEERING FOR UNDERGROUND COAL MINING

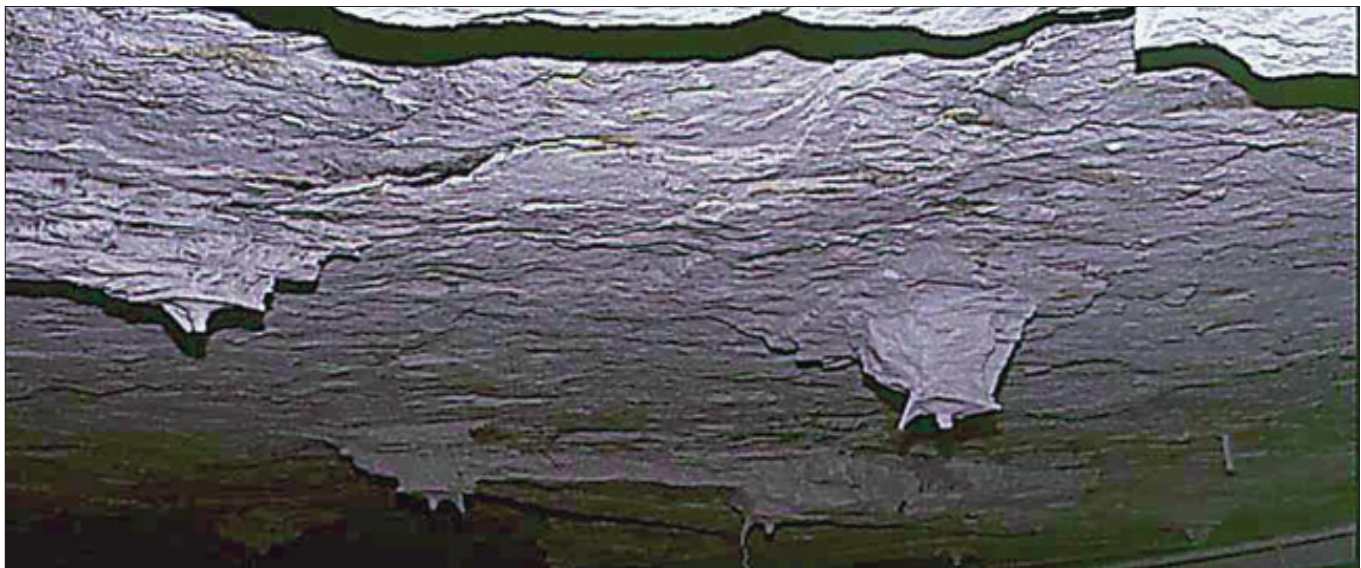**Figure 3. Illustration of a typical fall indicating a lack of pre-tension on the bolts and excessive spacing**

Figure 4. The small rock remnants on top of the washer plates indicate that the bolt spacing was too wide, although the pre-tension was sufficient

Roof falls higher than bolt length

If the roof falls out higher than the length of the bolts, it indicates that the bolts are too short, or that the bolt density or pre-tension is insufficient to create a beam that is capable of carrying the overlying strata. An example of this is shown in Figure 5. In this particular instance, the bolt lengths were 1.5 m and the fall height was 1.6 m.

Remedy

Increase the length of the bolts, alternatively increase the density and the pre-tension (use dual speed resin) to create a stronger beam.

Roof falls up to anchor position of mechanical anchor bolts

This is not a common occurrence, but is included because it indicates how the wrong choice of support elements can create a dangerous situation. In this case, mechanical anchors were used in a shale roof. By virtue of their mechanism, mechanical anchors exert horizontal compression on the roof rock in the immediate vicinity of the anchor. In this case, the bolt spacing was small and the pre-tension was high, creating a highly stressed horizon in the roof, forming a thin separation. Over time, water seeped in and corroded the anchors.

Figure 5. Example of a roof that fell out higher than the length of the bolts. The roof under which the people are seen, was re-supported even though the bolts cannot be clearly seen in the photograph

Figure 6 shows the 'saucers' of rust in the roof at the anchor positions, with the anchors still in place.

Remedy

Where the roof rocks are weak, resin anchors should be used instead of mechanical anchors.

Indications of incorrect bolt installations

There is no definitive test that can be done to check on the correctness of the installation of resin bolts. The adherence to the required pattern can be measured, but the quality of the anchor can only be deduced. Pull tests can be done to test for major deviations on full column installations, but not to determine the full anchor resistance of the bolt.

The reason for this is that a pull test is performed on the protruding end of the bolt and consequently the load that is obtained in the test is the full frictional resistance over the entire length of the bolt. Even if the resin bond is inferior, it is possible for the full load to exceed the breaking strength of the steel. For instance, the unit frictional resistance between the resin and the rock is in the range of 2000 kPa to 3000 kPa for most rock types. If something went wrong during the installation, that resistance will be reduced.

Say it is reduced to 1500 kPa, approximately half of the required resistance, then the total load in a pull out test for a 1.8 m long bolt in a 28 mm hole will be 237 kN, which is in excess of the strength of most 20 mm bolts. Thus, even with only 50% of the required resistance, the bolt could pass during the test. Moreover, it will seldom be possible in practice to obtain loads equal to the steel material strength, as the pull test will invariably be done on the threads, which will fail at lower loads in most cases.

As a quick reference, the visual appearance of installations can be used to supply some guidance even if the resistance cannot be quantified. A bolt that passes the visual test, may still be sub-standard in terms of actual resistance, but the probability of that happening is much less than that of a visibly poorly installed bolt being sub-standard.

The most common errors during installation are incorrect hole lengths and incorrect resin mixing. The materials are also sometimes defective; washer plates may be too thin and crimps on the crimp nuts may be too weak or too strong. Torque settings on roof bolters may be too high or too low and sometimes the spinning adapters are worn.

The visual appearance of a correctly installed bolt is shown in Figure 7. This can be used as a reference when viewing the most common deviations shown in Figure 8. For ease of use, Figure 8 also contains descriptions of the possible causes of the deviations and the rectifying steps.

Before coming to any conclusions regarding the quality of installations, it is necessary to investigate the combinations and patterns that often occur in observed deviations. For instance, if washer plates are loose and there is little or no thread visible, it is

Figure 6. The rust rings are clearly visible at the anchor positions of the holes

almost certain that the crimps are too strong. If consistent deviations occur in batches alternating with correct installations, it probably indicates that the bolting crew on one of the shifts is indifferent or in need of training.

The best way to ensure correct bolting installations is proper training and discipline on the face.

Instrument-aided roof monitoring

The next level of roof monitoring involves the use of instruments. This may be of a visual nature, like petroscopes, or one of several forms of extensometery that is aimed at measuring deformations that take place in the roof beyond the range of unaided visual observation. The objective may be to gain scientific information, to monitor the efficiency of the support system or to be aware of changes that occur in the roof.

Petroscope observations

A petroscope, illustrated in Figure 9, is inserted into a drill hole in the rock (roof or pillar) to observe the sides of the hole. It is primarily used to find bed separation in the roof and dog-earing in a drill hole. The most common types consist of a light source and a single angled mirror to observe the sides of the hole. More sophisticated models are available, but none are more simple to use than the basic model.

The popular basic model fits into a 35 mm diameter drill hole that is easily drilled with the available roof bolting machines in use underground. The ability to fit into a thin hole enhances its practical applicability, but it has a disadvantage in that the sighting mirror is small.

An obvious disadvantage of this instrument is the limited sighting distance. This is user dependent, but an effective sighting distance seldom exceeds 1.5 m. One attempt at an improvement was the optical cable model, but it could not quite compare with the visual clarity of the basic model. Digital recording models are available, but are not yet in common use.

Petroscopes are relatively cheap, easy to use and supply direct evidence of the exact position of bed separations in the roof. They require neither special installation techniques nor intensive training to use. The basic models in use are also intrinsically safe.
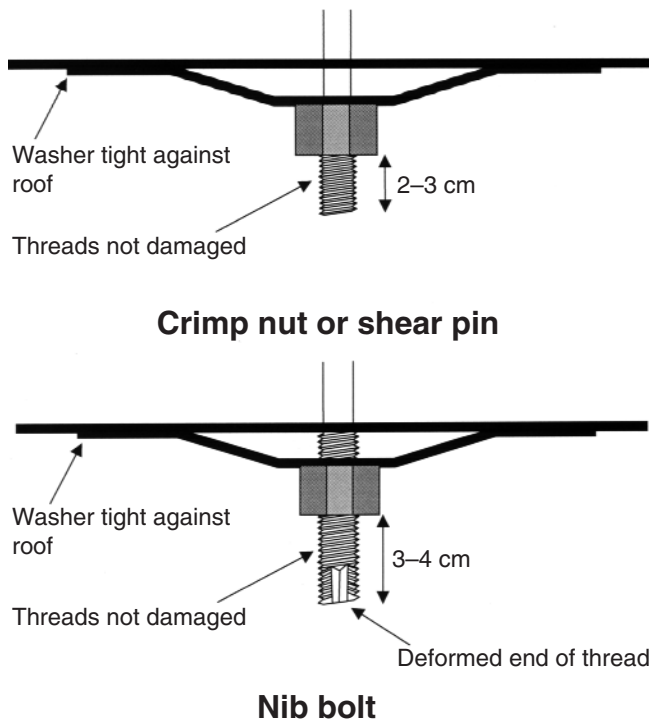
Washer tight against roof

Threads not damaged

2–3 cm

Crimp nut or shear pin

Washer tight against roof

Threads not damaged

3–4 cm

Deformed end of thread

Nib bolt

Figure 7. Visual appearances of correctly installed crimp nut and nib bolts

Appearance	Cause	Remedy
Too much thread protruding	● Hole may have been drilled too short or too long ● Anchorage may be below standard, causing bolt to be pulled out during tensioning	● Correct hole length ● Check resin, check spinning and holding times
Too little thread protruding	● Crimp may be too strong ● Roofbolter torque setting may be too low ● Hole may have been drilled too long	● Check crimps ● Check torque setting ● Check hole length
Deformed washer plate	● Washer plate may be too thin ● Roofbolter torque setting may be too high ● Secondary movement may have occurred in roof	● Check washers ● Check torque setting ● Not abnormal in pillar extraction, otherwise call expert
Loose washer plate	● Roofbolter torque setting may be too low ● Bolt or nut threads may be uneven ● Roof may have frittered away	● Correct torque setting ● Check threads ● Retighten bolts
Rounded nut	● Spinning adapter may be worn ● Crimp may be too strong ● Threads may be uneven	● Check adapter ● Check crimps ● Check threads

Figure 8. Some of the most common visual indications of sub-standard bolt installations

Light source and battery pack

45 degree mirror

Extendable rod

Figure 9. Schematic illustration of the use of the basic petroscope

Extensometers

As the name implies, extensometers measure the extension of rock. When installed in the roof, they supply information about the extension of the roof relative to a fixed point. They have been in use in one form or another for several decades and their use is increasing.

In essence, the operational safety-monitoring model consists of a single stem that is anchored in the rock beyond the position at which bed separation is expected. The basic principle is illustrated in Figure 10.

There are several commercially available variations on the basic theme. The anchor can be a very short portion of a resin capsule, a spring anchor or a mechanical expansion anchor. Measurement at the mouth of the hole can either be done directly or an indicator can be fitted that supplies visual information. The protruding end can have bands of different colours to indicate movement or be fitted with a dial gauge. The stem can be either a thin rod or a flexible cable, depending on whether horizontal displacement is expected inside the hole.

Which model to use is determined by the practical situation. For instance, at low mining heights the dial gauge is more difficult to read than the protruding ends with different colours. At high mining heights,
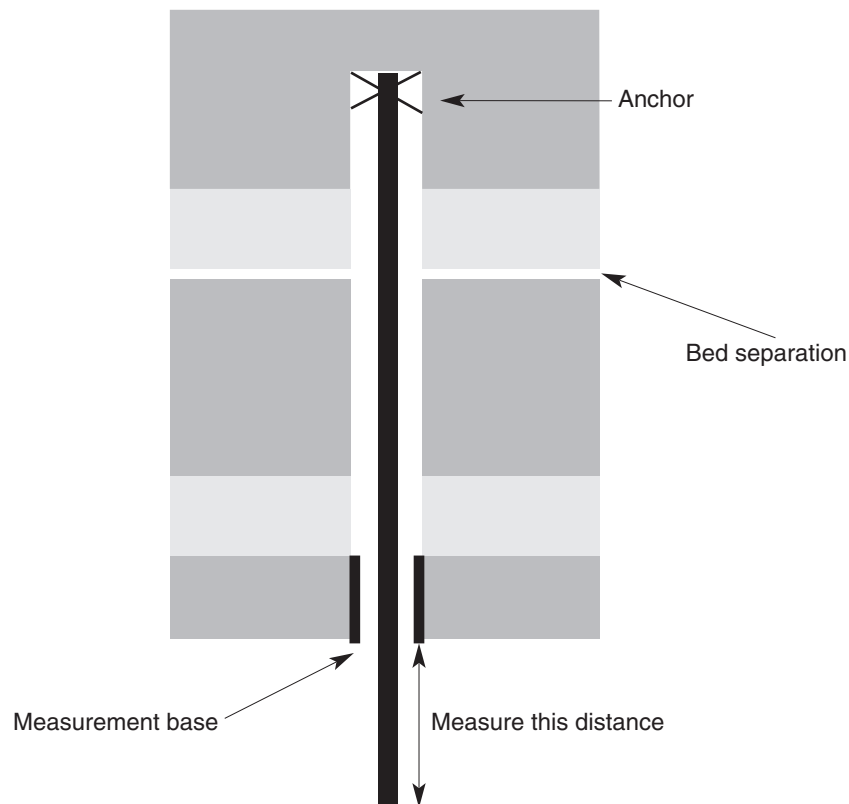
ROCK ENGINEERING FOR UNDERGROUND COAL MINING

Figure 10. Basic principle of the single point extensometer

the direct measurement option is not practical and the dial gauge becomes more attractive. The important point is that monitoring should be done, and the system to be used is the one that makes it easiest under the circumstances.

Elements to be considered prior to installing extensometers

Length

One of the important points to consider when installing extensometers is the correct length that is to be used. It is important for the anchor to be situated beyond the position at which bed separation is expected.

That position is variable, depending mainly on the composition of the roof, the horizontal stress situation and the road width. The best method to determine the correct length is to first embark on a series of accurate measurements with multi-point extensometers to determine the characteristic roof behaviour.

In the past, multi-point extensometers consisted of a number of anchors in a single borehole, each equipped with a thin rod or cable. The distances between the end points were then measured to gain insight into the relative displacements between the anchors. This system was difficult to install and it was not

uncommon for wires to be damaged or entangled inside the holes.

The improved system that is in common use is the sonic probe extensometer. Circular magnetic anchors are fitted at various positions in the hole, the distance between anchors being a function of the desired accuracy. A probe is then passed through the anchors to the back of the hole and the distance between the anchors is determined electronically to within fractions of a millimetre. The elements of the system are schematically shown in Figure 11.

The multi-point extensometer usually indicates a typical zone within which roof movement occurs. Once this is known, the length of the operational monitors can be chosen such that the anchor is beyond this zone. A typical plot of a sonic probe extensometer measurement is shown in Figure 12.

It is prudent to back up the operational monitors, like tell-tales, with permanent multi-point extensometer stations. The more variable the roof conditions, the closer the permanent multi-point extensometer stations should be sited to each other. Under stable conditions, these stations can be far apart, but where either the roof composition or the stress conditions are more variable, this distance can be decreased to a few tens of metres.
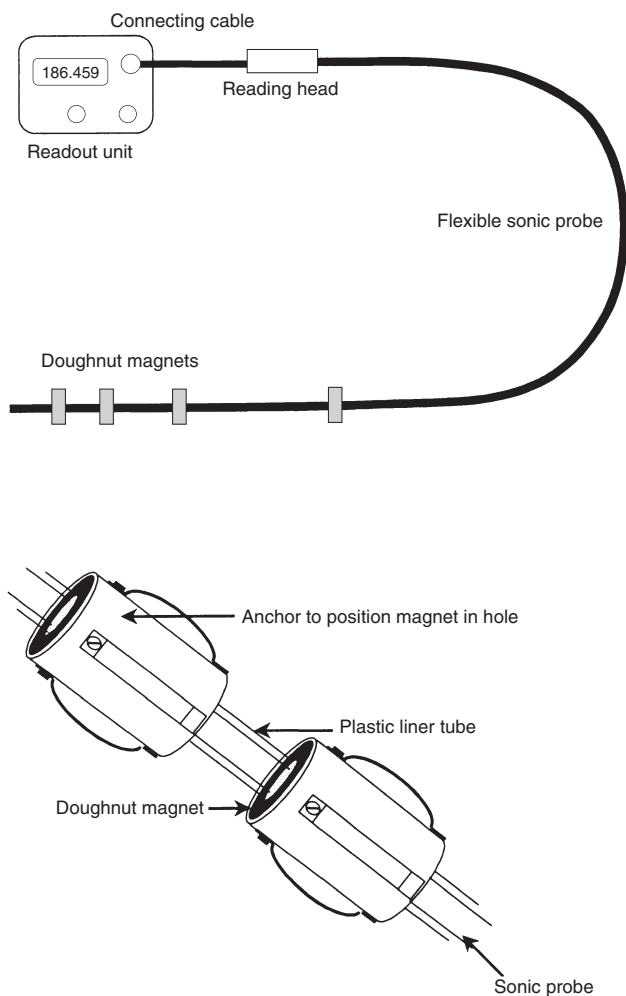
Connecting cable

186.459

Reading head

Readout unit

Flexible sonic probe

Doughnut magnets

Anchor to position magnet in hole

Plastic liner tube

Doughnut magnet

Sonic probe

Figure 11. Elements of the sonic probe (After Rock Mechanics Technology)

DISTANCE INTO THE ROOF (m)

A

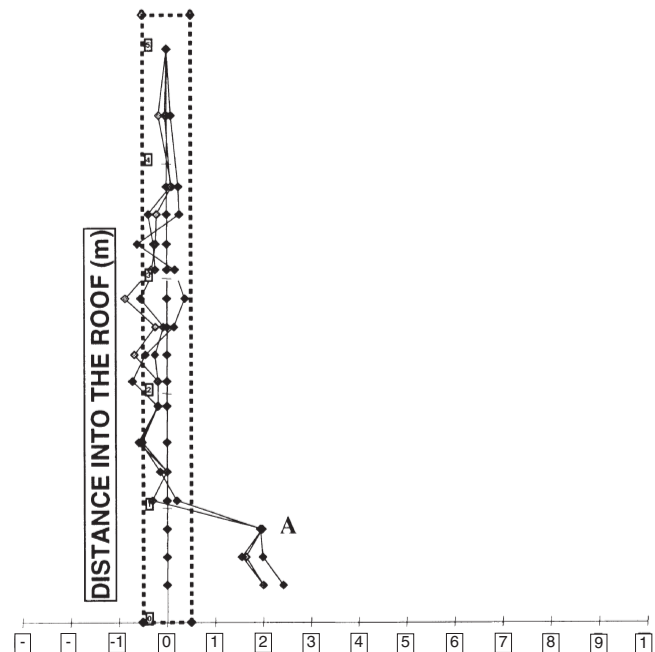- - -1 0 1 2 3 4 5 6 7 8 9 1

Figure 12. Example of a sonic probe output. The different lines represent measurements taken at different times. The displacement between anchors is shown on the horizontal scale while the positions of the anchors into the roof are shown on the vertical. This example indicates bed separation of 2 mm between anchors 3 and 4. The accuracy of the instrument is ± 0.5 mm

Interpretation of extensometer results

The very basic use underground of the popular operational monitoring extensometers ('tell-tales') is to see whether movement in excess of predetermined limits has occurred in the roof. Any change that is observed requires investigation. The first step is to check the integrity of the instrument—it may have been bumped or the anchor may have slipped.

Usually, the protruding end of the extensometer will have shortened, indicating separation in the roof somewhere between the skin of the roof and the anchor position. If the extensometer stem is a cable, horizontal displacement in the roof will also be indicated by shortening of the protruding end. Further investigation should include checking the neighbouring extensometers, searching for cracks in the roof, guttering, etc. Expert assistance should be obtained if the cause of the movement cannot be established.

The protruding end can also lengthen, indicating compression of the roof. This may happen, for instance, if openings that existed prior to installation of the extensometer are closed by re-support or re-tensioning of bolts. It may also simply indicate that the anchor is slipping.

If the protruding length of the extensometer is measured, and records are kept, more information may be obtained from the instrument. By plotting the length against time, it is possible to identify imminent instability. This is indicated by an acceleration of the shortening of the protruding end, indicating an acceleration of the roof dilation. Examples of possible characteristic behaviours are shown in Figure 13.

Another use of the records is to compare the displacement with the maximum tolerable displacement. In Chapter 3: Roof and sidewall stability, it is shown that any roof beam can only deflect a certain amount before it fails. The maximum deflection depends on the road width, characteristics of the roof material, thickness of the layers, etc. Figures 14 and 15 can be used to obtain the maximum tolerable deflections for two roof types, a softer mudstone or coal roof and a relatively stiff and strong sandstone. Note that these curves should only be used if no other information is available; the correct method is to determine the *in situ* characteristics by detailed and careful monitoring.
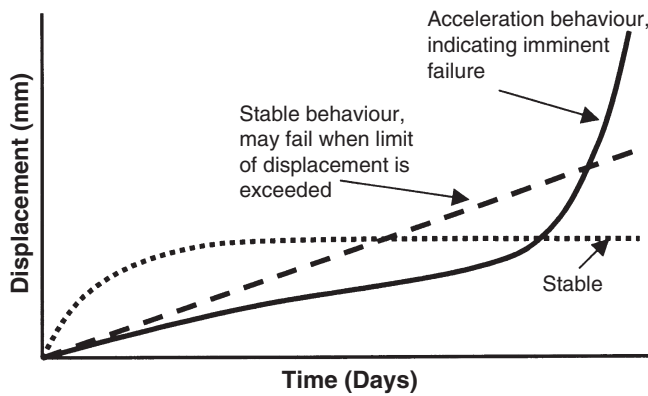
ROCK ENGINEERING FOR UNDERGROUND COAL MINING

Figure 13. Examples of different types of characteristic roof deflection behaviour

Figure 14. Maximum displacement before failure for a mudstone or coal roof, for various road widths and layer thickness. The numbers next to the curves indicate road widths, in metres

Figures 14 and 15 also indicate the need for instrumented monitoring of coal mine roofs. The maximum tolerable displacements are small and difficult to see with the naked eye. Even with a basic type of extensometer, some of the maximum tolerable displacements are still very small and it indicates that some form of movement magnifying arrangement is required on the extensometers.

The Figures also explain why many miners feel safer under a mudstone roof than sandstone—the mudstone roof displays more visible movement prior to failure, the sandstone failing with less visual warning.

Load measurement on bolts

In order to optimize bolting systems and to gain insight into the forces acting in the roof, bolts are sometimes instrumented with strain gauges from which the loads that develop on the bolts can be measured at different positions along the bolts.

This yields information on the performance of the bolting system and is an aid to scientific design of bolting systems, including bolt length, required strength and positioning of bolts.

Pillar monitoring

Since the introduction of the Salamon and Munro (1967) formula for safety factors in South Africa, not one disaster in terms of loss of life because of pillar failure has occurred. However, there have been a number of near misses in pillar extraction and in areas where the coal is weaker than in most other areas, notably the Vaal Basin in South Africa.

There are three basic modes of pillar system failure, namely progressive pillar scaling, foundation failure and fire. Only the first two modes will be discussed in this chapter.
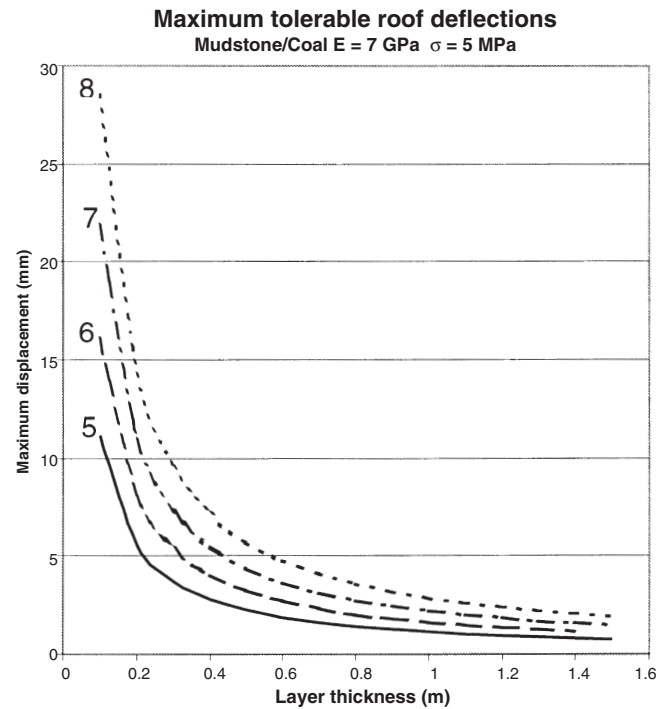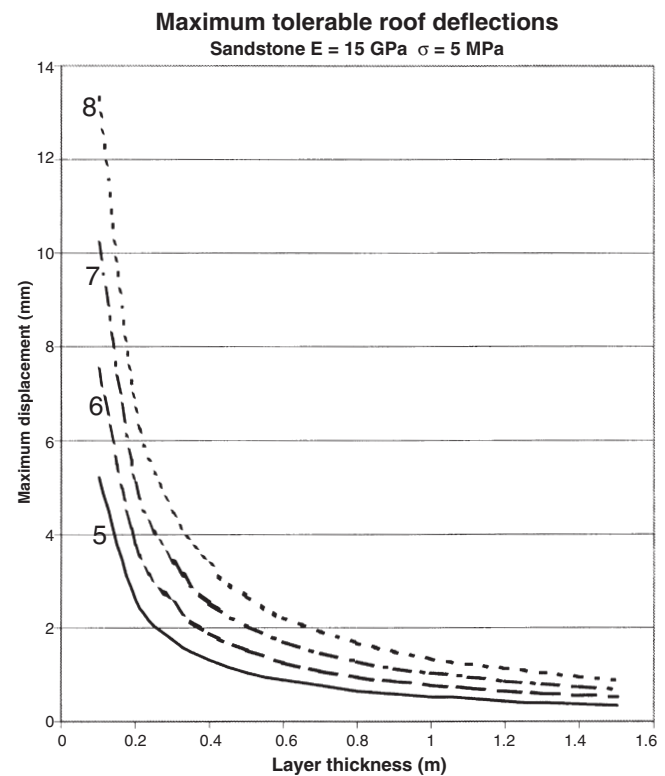

Figure 15. Maximum displacement before failure for a sandstone roof, for various road widths and layer thickness. The numbers next to the curves indicate road widths, in metres

Progressive scaling

Due to the limited number of pillar failures, and the absence of these in populated areas, not much is known about the visual appearance of pillars immediately prior to failure. However, it has been seen on two occasions in the Vaal Basin where pillars failed progressively and gradually, that the nature of the fractures changed when the pillars were on the point of collapse.

Normally, the orientation of the fractures are such as to result in a concave shaped pillar, such as those in the example in Figure 16. Immediately prior to collapse, the fractures change direction at the top contact between the ribside and the roof, running into the pillar. This is shown in Figure 17, based on personal observation in an area where pillars were failing at a rate that was slow enough to permit observation.

One possible explanation for the phenomenon may be in the fundamental consideration of stress concentration caused by the creation of an opening in rock, as explained in Chapter 3: Roof and sidewall stability. This is a classical case of a k-ratio of less than one (i.e. vertical stress greater than horizontal), resulting in guttering in the ribside, as opposed to in the roof. Another example is shown in Figure 18, which is a snook in the process of being extracted. The snook is subjected to elevated levels of vertical stress, in this case obviously greater than the horizontal stress.

The most practical monitoring instrument, for cases where pillar failure is a possibility, is a simple convergence meter. These can be made on the mine, such as the example shown in Figure 19. Alternatively, more accurate (and expensive) instruments can be purchased. The preferred method is to use a great number of convergence meters, even if they are slightly less accurate, rather than a small number of more accurate instruments. The basic model shown in Figure 19 cannot distinguish between roof dilation, floor heave and pillar compression, but is still useful to trigger further investigation.

Convergence meters should, ideally, be coupled with a simple pillar compression instrument (shown in Figure 20) and roof extensometers, to be able to distinguish between roof and floor movement and pure pillar compression. If pillar compression only is of concern, then the pillar compression monitor will suffice on its own. Note that the example shown in Figure 20 is only practical in situations where significant pillar compression is expected. In more common situations, where compression of only a few millimetres is expected, the measuring rod should be replaced by a more accurate device, such as an infra-red or laser instrument.

Convergence meters should, ideally, be installed as close to the pillars as possible, to minimize dilution of the measurements by roof movement, but in that position they are more susceptible to damage from the scaling debris.

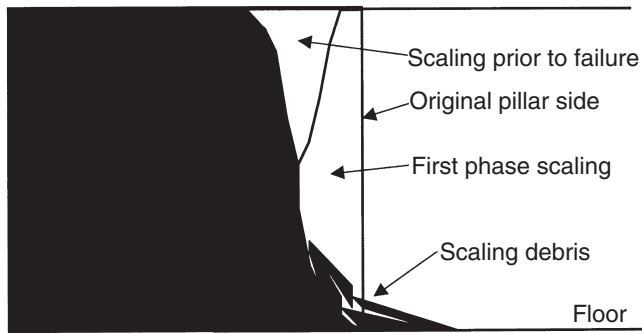Figure 16. Severe pillar scaling, resulting in a concave-shaped pillar

ROCK ENGINEERING FOR UNDERGROUND COAL MINING

Figure 17. Nature of scaling observed immediately prior to pillar failure

Example of use of combination of convergence meter, roof extensometer and pillar compression monitor

Say the following readings were obtained:

Convergence meter	30 mm compression
Roof extensometer	10 mm downward
Pillar compression meter	15 mm compression

Then,

Pillar compression plus floor heave	= convergence meter minus roof extensometer
	= 20 mm
Floor heave	= 20 mm minus pillar compression
	= 5 mm upward

Thus, the following has happened:

Roof deflection	= 10 mm downward
Floor heave	= 5 mm upward
Pillar compression	= 15 mm compression.

Foundation failure

Foundation failure includes roof and floor failure, and is possible under the conditions of soft and weak roof and/or floor. Roof failure results in increased height of pillars, with a possible accompanying weakening effect. Roof failure and monitoring are extensively covered elsewhere in this book, and will not be dealt with further.

The mechanism of floor failure where the floor is very soft deserves special attention. The floor may be displaced laterally from underneath the pillars, and the resultant shear action may then tear the pillars apart. The mechanism is shown conceptually in Figure 21. The same could happen in the roof, especially when the immediate roof material consists of a soft, almost plastic material like torbanite.

Figure 22 shows an open tension crack running into a pillar, in a case where pillar punching occurred.

Where pillars punch into the floor, one of the side effects will invariably be floor heave. The combined instrumentation layout described in the preceding sections on pillar monitoring also covers floor heave. Floor heave is indicative of either high horizontal stress, pillar punching or weakened floor rocks.

Where floor heave is apparent all around the pillar, the likely cause is pillar punching, swelling or weakening of the floor rock due to weathering. If it occurs in a single direction, i.e. on two sides of the pillars only or crossing intersections, the most likely cause is horizontal stress.

Stress monitoring

Previous discussions centred on situations where the

Figure 18. Sidewall guttering, indicating that the vertical stress on the pillar exceeds the horizontal stress
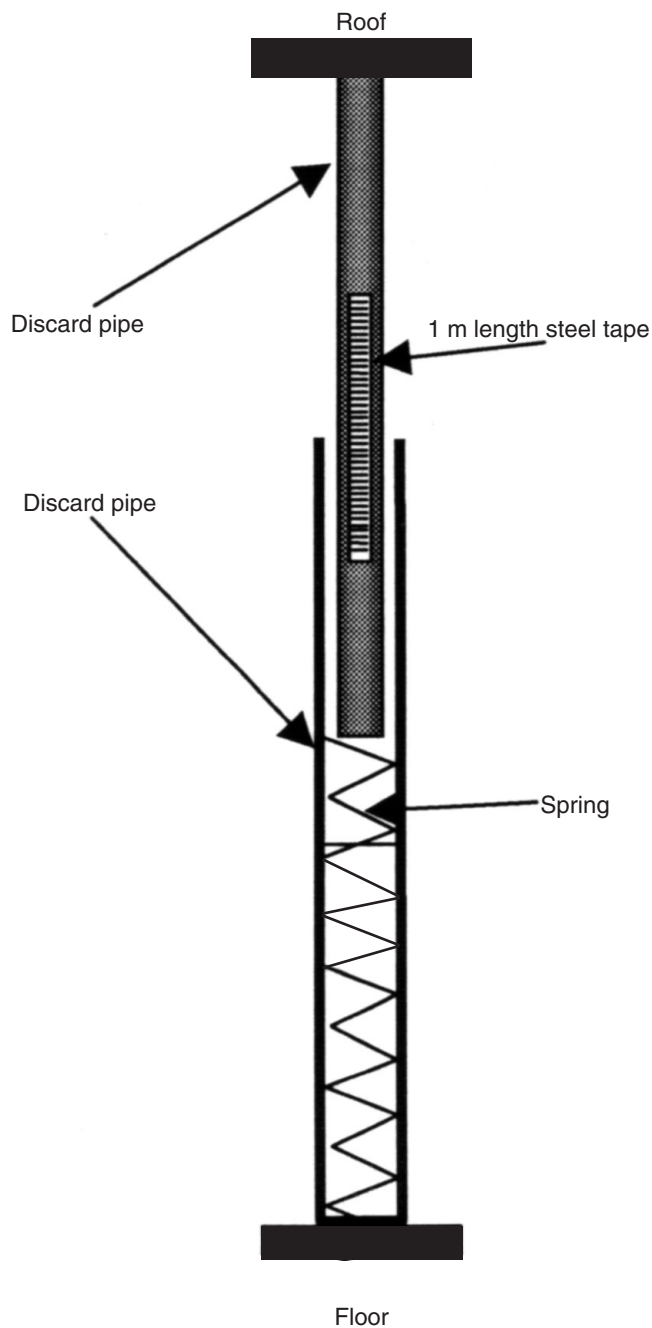
Figure 19. Drawing of a simple convergence meter that can be made on the mine from second-hand materials

Figure 20. Drawing of a simple pillar compression monitor that can be made on the mine and installed without expert assistance

Figure 21. Exaggerated sketch of pillar punching resulting in lateral floor material displacement, causing tensile stress damage to the pillar

Absolute stress magnitude

The virgin stress regime at shallow depth is highly variable, as indicated by Figure 23, a compilation of k-factor results from stress measurements gathered by Stacey and Wesseloo (1998). While the average is around 1.9, the range is from 0.5 to over 5 for typical South African coal mining depths of 50 m to 200 m.

It is clear that if it is necessary to know the magnitude of the stresses in the coal-mining environment, it should be measured.

Absolute stresses cannot be measured directly. All the methods rely on measurement of deformation and subsequent back calculation of the stress magnitude. Although the indirect nature of the methods, introduce a certain measure of uncertainty, they have become widely accepted. The basic premise of all the methods is to allow the rock to relax, measure the amount of relaxation and then back calculate the stress that was required to cause the deformation.

The methods are complicated and require expert involvement. Rather than discuss the intricacies of the methods, only the principles will be discussed here.

existing stress exceeded the strength of the material, be it the pillars, the roof or the floor. This resulted in failure, which is the final effect of an imbalance and in most situations, the most important consideration for rock engineers.

However, there are situations where it is important to know the magnitudes of the stress, which cannot be visually observed. In certain situations, it can be estimated indirectly, but those methods do not yield reliable results.
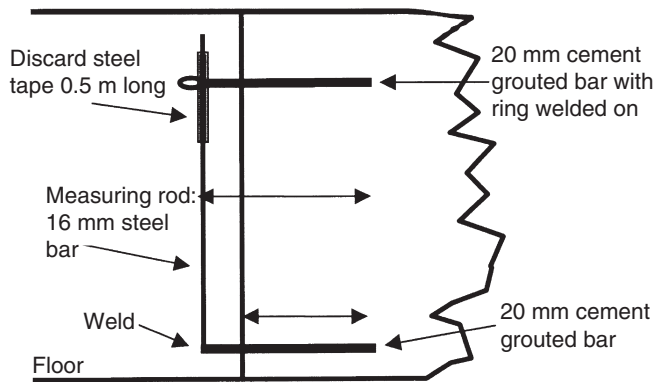
Figure 22. Example of an open crack running into a pillar.
In this case, there was floor heave all around the pillars and it was concluded that the pillars were being torn apart by floor material
flowing out from underneath the pillars. These pillars eventually failed

A hole is drilled and a very accurate deformation measuring device—-a strain cell—is glued to the end of the hole. The hole with the strain cell is th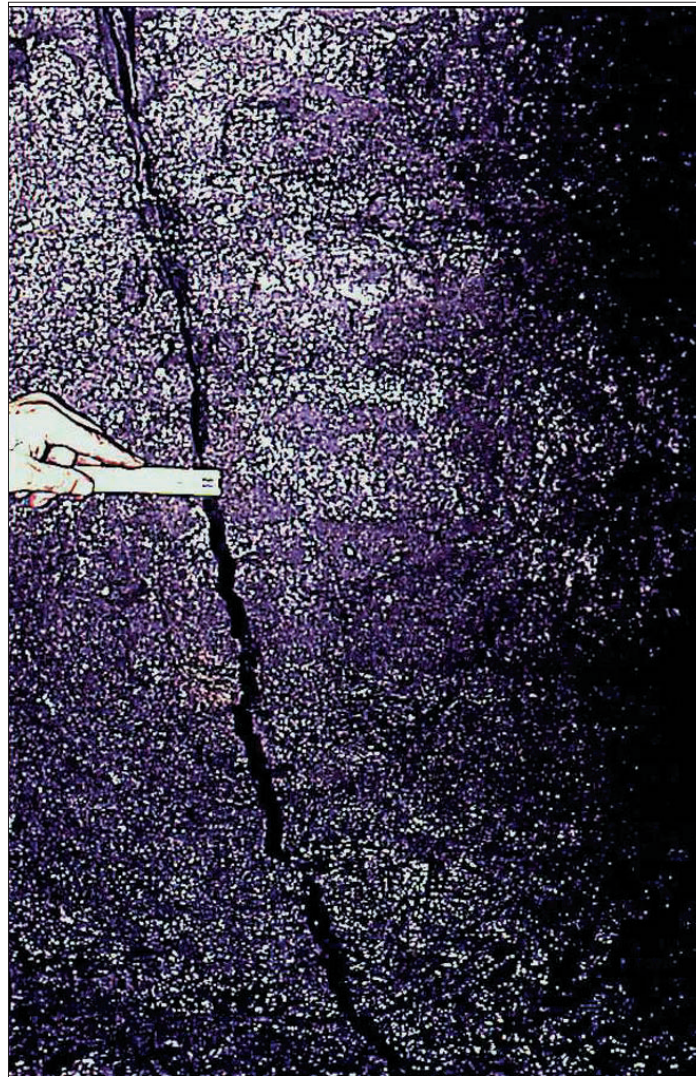en overcored and the core is broken free of the hole. Once free from the stressed environment, the core expands. The expansion is measured and the stress that was required to compress it in the first place is calculated.

Inaccuracies could arise due to the imperfections of the surface on which the strain gauge is mounted and the characteristics of the glue that is used in the process.

Another method is to cut a slot in the rock and to measure the change in distance between points on either side of the slot. A hydraulic cell is then placed into the slot and pressurized. The pressure, at which the change in distance between the measurement points is cancelled, is equal to the stress in the rock.

Stress change

By comparison, measuring changes in stress is simpler than measuring the absolute magnitude. In principle, this is accomplished by inserting a direct measurement cell in a hole at the position where the stress is to be measured. The stress measurement device is usually a hydraulic cell consisting of a thin metal container, filled with oil, that is grouted into the hole or a strain cell. The pressure in the cell is then measured directly at various times, as the stress changes.

The construction of the cell and especially the characteristics of the grout that is used are very important.

All the stress measurement methods can only measure stress at a point in the rock mass. In order to gain insight into the stress distribution—which is known to be variable—a great number of
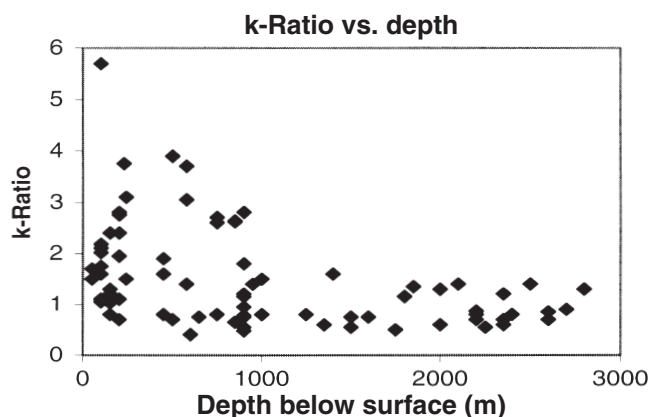
k-Ratio vs. depth

Figure 23. Variation of k-ratio at shallow depth, after information in Stacey and Wesseloo (1998)

measurements are required. In view of the high costs involved in stress measurement, it is usually only done in exceptional circumstances.

Stress direction

The direction of the maximum stress can be obtained by relatively simple stress mapping in the section, a mainly visual technique. Figure 24 illustrates the most important effects to be observed. This technique has been used with success in several collieries.

Subsidence monitoring

Subsidence monitoring may be done for three purposes, namely to check whether goafing is progressing satisfactorily, to satisfy statutory requirements or for research. In the latter two cases, proper survey measurements are taken on stations installed prior to mining.

For statutory requirements, it is sufficient to determine the amount of subsidence to centimetre accuracies and a small number of measurement stations are usually sufficient. For research purposes, a higher level of precision is required, as it is important to determine both the vertical and horizontal displacements at an accuracy of millimetres or better. A single line of stations is sufficient for statutory requirements, for research at least a double line is necessary. The Appendix on Subsidence contains details of the analysis and measurement procedures.

It is sometimes necessary to determine whether subsidence has occurred in situations where no measurements were done prior to mining, for instance, in the case of unexpected pillar failure and situations where subsidence may have occurred before it was necessary to record subsidence. The observer then has to rely on indirect observations. The rest of this chapter is devoted to the indirect indicators of subsidence.

Fences, conveyor belts, electricity and telephone lines

In the natural veld, it is virtually impossible to detect subsidence of the order of one to two metres over widths of 150 to 200 m with the naked eye. The natural inclination of even a 'level' surface is of the order of 6 to 10 degrees. This is less than the inclinations induced by subsidence, which are of the order of two to four degrees for mining at depths of 100 m or more. The obvious exceptions are the cases where mining was done at shallow depth, where visual detection is relatively easy due to the high magnitudes of induced tilt plus open tension cracks and clear compression ridges.

However, where fences (or electricity and telephone lines) were erected prior to mining, it becomes easier. Firstly, it is easier for the naked eye to observe dips in elevation when looking along a familiar type of structure. Secondly, fences are good indicators of zones of horizontal tension and compression, as shown in Figure 25. Where lines are tight (or even broken) in two separate areas and slack in the area between the tight zones, it is a strong indicator of subsidence.

Cracks and crack scars

Fresh cracks, such as the examples shown in Chapter 10: Subsidence, are easy to detect, especially in the
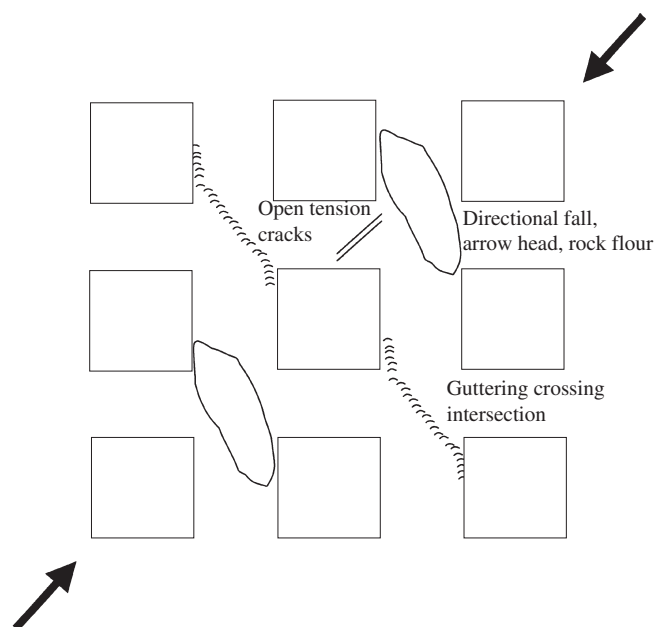
Figure 24. Illustration of some of the more important effects that indicate the presence of high horizontal stress. Note that guttering *per se* is not necessarily an indication—however, when it crosses intersections, it usually is. Similarly, displacement in vertical holes could be caused by bending of the roof beams as well as horizontal stress, but dog-earing in such holes can only be caused by horizontal stress

ROCK ENGINEERING FOR UNDERGROUND COAL MINING

early summer or late spring before the grass has grown high. Older cracks normally fill up after up one or two rain seasons and only the scars are left, as shown in Figure 26. They are easier to find when the sun is low on the horizon, i.e. during the first and last two hours of sunlight. Very often, weeds grow in the crack scars, and various field animals like mice and porcupines find it easier to burrow in the disturbed ground. When animal holes are found in lines instead of clusters, it is often a good indicator of old cracks.

On a field investigation, it is a good idea to have a pair of binoculars and a compass handy. Positions can be estimated from major landmarks and structures such as roads, power lines, etc., that are likely to appear on mine maps, or a GPS instrument can be used.

Estimating the depth of subsidence without instruments

A bottle half filled with water can be used as a level to estimate the depth of subsidence. The method is simple: proceed to the estimated position of the deepest point of the subsidence and view the estimated edge of the subsidence in four or more directions over the 'level'. Measure the height of the water bottle on each occasion and calculate an average. Figure 27 may assist in clarifying the method. The water bottle may be replaced by a building level, but it is not as easy to use as the bottle.

Estimating the height of the goaf in a borehole

A short steel rod with a hole drilled in an off-centre position can be gently lowered down the hole on a thin fishing line in one metre increments, see Figure 28.

The rod should be longer than the hole diameter. At the top of the goaf, the rod will swing over, jerking the line. By alternately gently lowering and lifting the fishing line, the positions of dislocations in the hole can also be determined, as the rod will stick at the positions of dislocations. The height of the cavity on top of the goaf—if any—can be estimated by lifting the rod until it sticks at the top of the cavity and then gently lowering it until the line goes slack.

With some practise, it will be possible to retrieve the rod, by dropping and jerking the line with short, sharp movements to let it swing at the bottom. Once swinging, the line should be gently lifted and lowered —at the right moment, it will enter the hole and can be pulled all the way up. Alternatively, the line can merely be broken and the rod discarded.

The water level in a borehole can be estimated by dropping a small pebble and counting seconds until it hits the water. Allow approximately 5 m for every second. A mirror can also be used to reflect light down into a borehole.

The following field items are handy for subsidence observations:

- Small mirror
- Compass
- Thin fishing line
- Rod with off-centre hole
- Binoculars
- Transparent water bottle
- Measuring tape
- Notebook
- Camera
- Mine plan showing surface structures superimposed on the underground workings.

Figure 25. The slack in the fence is a good indication of the position of the compressive zone in a subsidence trough

Figure 26. Example of scars of subsidence cracks. The dotted lines are drawn in next to the scars

With these at hand, the observer can gather a surprising amount of information without sophisticated instruments. This is especially useful for situations where properly measured information is less important, usually as a precursor to more accurate work.

General discussion

Monitoring is an essential element of the design process, feeding information back into the system for refinement, adaptation or merely confirmation. Without monitoring, change will only take place after damage has occurred. With monitoring, pre-emptive action can be taken.

What has been presented in this chapter concentrated on operational as opposed to scientific monitoring. This does not mean that more accurate, instrumented monitoring is less important. The objective was to supplement the more accurate work-that usually requires expert assistance—with simple monitoring that can be done on an operational level. Where deviations are found by the simple methods presented here, experts should be called in to embark in more detailed investigation.

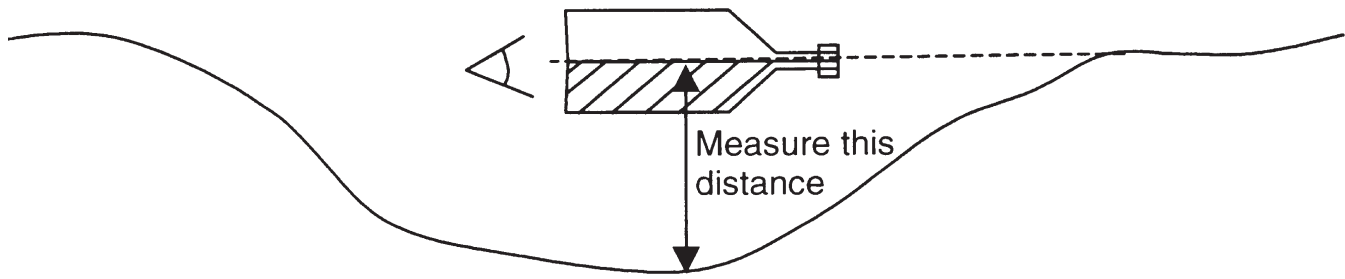ROCK ENGINEERING FOR UNDERGROUND COAL MINING

Figure 27. Method to estimate the depth of subsidence using a water bottle

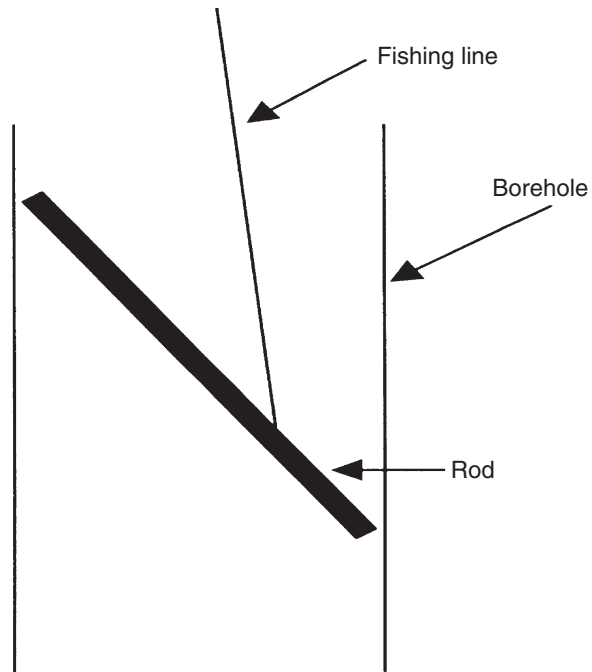**Figure 28. Simple method to detect cavities at the top of a goaf, using a thin fishing line and a short steel rod**

ROCK ENGINEERING FOR UNDERGROUND COAL MINING

Fundamentals

Introduction

Rock engineering is based firmly on the principles of solid mechanics. Solid mechanics deals with the relationship between stress and strain in elastic and plastic materials. Furthermore, it considers how stress and strain can cause damage to such materials, ultimately leading to failure. In order to understand rock engineering, it is necessary to have a good understanding of both stress and strain. It is also necessary to understand what is meant by elastic and plastic materials. Knowledge of how solid materials can, in general, fail, when subjected to admissible stresses and strains, is also essential.

Before considering material behaviour it is necessary to be able to define the material geometry in space. This is achieved by prescribing a relevant co-ordinate system. In general, in rock engineering, one of two types of co-ordinate systems is used, either the Cartesian system or the polar system. In the case of the Cartesian co-ordinate system both right-handed and left-handed systems are in common use in the South African mining industry. A common mistake is the selection of the incorrect co-ordinate system for the specific case study. This error can result in highly confusing output from, for instance, numerical models (e.g. tensile stresses when the stresses should be compressive).

This appendix provides a minimum of necessary information for the rock engineering practitioner to understand the medium being dealt with. Although this appendix may appear daunting to many, every effort has been made to ensure all the mathematical equations are explicit in nature; it is always possible to insert values into the right-hand side to produce a result on the left-hand side. Formulations have only been left in matrix form in the few circumstances where it would be tedious for both the authors and the reader to provide the individual equations. Furthermore, the topics of discussion in this appendix are limited to isotropic, homogeneous media. A material is **isotropic** when its elastic properties remain the same in all directions. A **homogeneous** material is one that has the same mechanical properties throughout.

In addition to providing an understanding of the physical principles involved, this appendix also provides a self-contained reference to the mathematical formulae most commonly required by the rock-engineering practitioner.

Co-ordinate systems

The most commonly used co-ordinate system in rock engineering is the **rectilinear Cartesian co-ordinate system**. According to this system, three mutually perpendicular spatial axes are defined. These three axes are commonly referred to as the x, y and z-axes. The system is considered to be linear as distance increases in equal increments along the straight line axes. A Cartesian co-ordinate system in three dimensions can be either left- or right-handed, depending on the relationship between the axes, as shown in Figure 1(a) and (b), respectively.

Stress, strain and Poisson's ratio

Strain

The deformation of a body due to an applied external load is termed **strain**. Consider a cylinder that is subjected to an external compressive force acting in the direction of the length of the cylinder (i.e. axially), its length will decrease (see Figure 2). Quantitatively strain, ε, is defined as the change in unit length of the material in the direction of the applied external force and is given by the following equation:
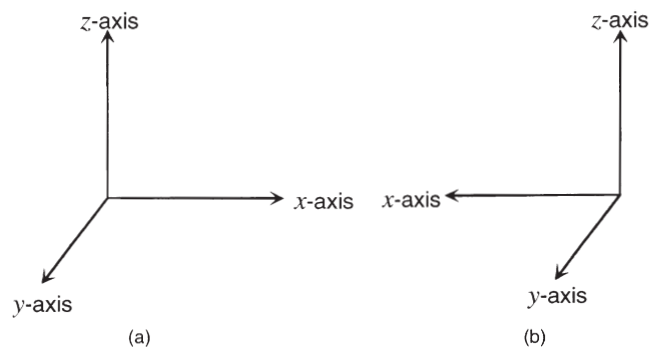

Figure 1. Co-ordinate systems most commonly used in rock mechanics (a) Left-handed three-dimensional Cartesian system and (b) right-handed three-dimensional Cartesian system
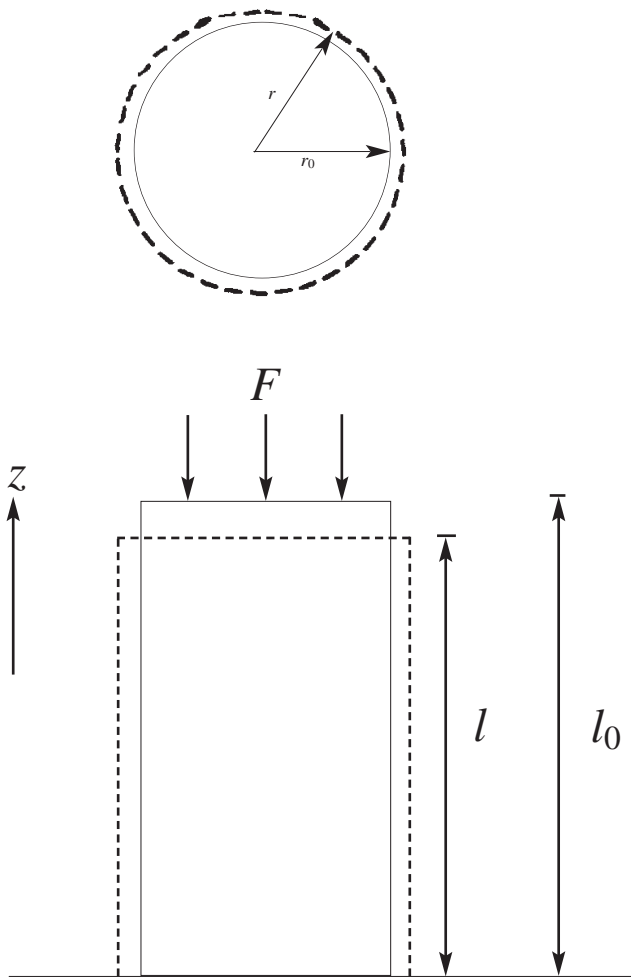
Figure 2. Deformation of an unconfined cylindrical specimen due to an external force (F) acting on the cylinder in a uniaxial direction. l_0 and r_0 are the initial length and radius of the cylinder, and l and r are the final length and radius of the cylinder

$$\varepsilon = \frac{l_0 - l}{l_0} \qquad [1]$$

The parameter l_0 is the original length of the cylinder, l the final length, and $l-l_0$ the change in axial length. By definition, strain is a dimensionless quantity, but it is customarily expressed in units of %, or in mm^{-1}, or commonly in rock mechanics as **millistrains** (mm/m). The convention in geomechanics is for strain to be positive when it signifies shortening (**compressive strain**) and negative when lengthening occurs (**tensile strain**). This convention is converse to general engineering conventions, but makes sense in the rock engineering context, where most strains encountered are compressive.

Poisson's ratio

When an elastic material is compressed in one direction, say the z, or axial direction, it will extend in the other directions, the x and y, or the radial direction. This phenomenon is known as the Poisson effect and has been depicted in Figure 2. **Poisson's ratio**, v, is the ratio of the radial to axial strain for the deformation of a cylindrical sample subjected to uniaxial loading and is given by:

$$v = -\left(\frac{r_0 - r}{r_0} / \frac{l_0 - l}{l_0} \right) \qquad [2]$$

From Equation [2] it can be seen that Poisson's ratio is a dimensionless quantity. Mathematically, Poisson's ratio can range in value between 0.5 and –1.0. In the case of physical materials, however, the lower limit is considered to be zero. A value of zero corresponds to a material where the **radial dimension** does not change when a sample is strained axially, for example cork. If the **volume** of a material sample remains unchanged when strained, then the value of Poisson's ratio will tend towards 0.5. However, a Poisson's ratio of 0.5 can never actually be achieved since a material must maintain a positive definite value of strain energy density. Materials having a Poisson's ratio between –1 and zero are physically implausible. A negative Poisson's ratio implies that a cylindrical specimen of the material would be **reduced** in radius when subjected to axial **compression**.

Stress

Having defined strain it is necessary to consider the cause of this deformation. Strain is the result of a stress acting on the material. **Stress**, σ, is the force per unit area acting on the surface of a body. If a cylindrical, homogeneous solid of cross-sectional area A is compressed vertically (in the z direction) by a uniformly distributed force F (as shown in Figure 2), the vertical stress, σ_z acting on and inside the cylinder, is given by:

$$\sigma_z = \frac{F}{A} \qquad [3]$$

Stress is a tensor, thus in addition to magnitude, it contains directional information. The concept of tensors is discussed in a later section. The SI unit of

Table I
Young's modulus and the shear modulus for a few commonly encountered materials

Material	Young's modulus (Pa)	Shear modulus (Pa)
Aluminium	70×10^9	24×10^9
Steel	200×10^9	84×10^9
Glass	70×10^9	23×10^9
Hardwood	10×10^9	10×10^9
Rubber	1×10^6	
A typical rock	30×10^9	21×10^9

stress is the pascal (Pa). In rock engineering, more common units are kPa, MPa, or GPa.

Both stress and strain can be described as normal, shear, or a combination of the two, depending on their directional orientations relative to the surface of the body. If a force acting on a plane is perpendicular to the plane at the point of application, then a **normal stress** is acting on the plane. The resultant displacement of the plane in the direction of the applied force is **normal strain** (as shown in Figure 2). If, however, the force is parallel to the plane at the point of application, a **shear stress** results and produces shear strain. Unlike normal strain, **shear strain** does not necessarily represent a change in volume of the body.

Relationship between stress and strain

Stress and strain can be related to one another via the following empirical relationship:

$$\sigma = f(\varepsilon) \tag{4}$$

The function f is the **constitutive law**, or **constitutive relationship**, describing the mechanical behaviour of the material. Constitutive laws are determined from experimental and/or observational data.

Elasticity

Any material sample that is loaded and then subsequently unloaded, and returns to its original shape and size, is said to behave **elastically**. That is, any deformation incurred on loading is fully recoverable. Furthermore, elasticity of a substance signifies that, if the material is loaded and subsequently unloaded, the same path is traversed on the **stress-strain curve** (see Figure 3). The stress-strain curve can be either linear (a straight line) or non-linear (a curved line). Using the stress-strain curve, stress can always be uniquely defined from strain, however, the inverse does not necessarily hold for non-linear elastic materials. If a material is elastic, it is said to be path-independent and the material has no 'memory' of its loading history. In other words, from a numerical modelling point of view, a rock mass behaving elastically does not 'see' a difference between many small mining steps and one large mining step, assuming the latter is the sum of all the smaller mining steps.

Linear elasticity; Young's modulus and Hooke's law

An elastic material is either linearly elastic or non-linearly elastic. If a material is **linearly elastic** (Figure 3(a)), the applied stress and resultant strain are
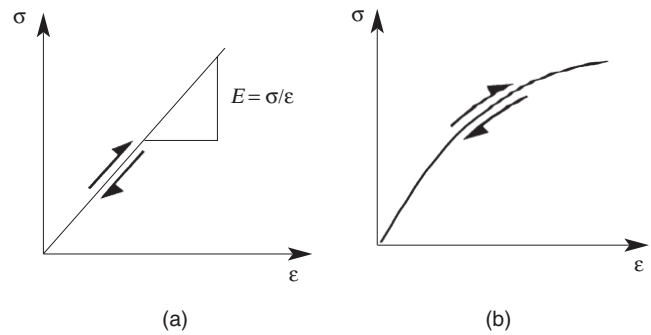
Figure 3. Stress-strain curves for (a) linearly and (b) non-linearly elastic materials

directly proportional, i.e. the stress-strain curve describes a straight line. The proportionality constant, E, is referred to as **Young's modulus**, the elastic modulus, or the modulus of elasticity, and is defined as:

$$E = \frac{\sigma}{\varepsilon} \tag{5}$$

The unit of E is the pascal.

In the South African mining industry, Young's modulus is usually determined by performing uniaxial tests on cylindrical rock samples. In practice, the stress-strain curve derived from a laboratory test is not a straight line, but is curved as shown in Figure 4. In practice, the axial Young's modulus of a specimen varies throughout the loading history, i.e. Young's modulus is not a uniquely determined constant for any given rock sample. The most common ways of defining the elastic modulus are:

- *Tangent Young's modulus*—E_t is the slope of the axial stress–axial strain curve at some fixed percentage, generally 50%, of the peak strength.
- *Average Young's modulus*—E_{av}, is the average slope of the more-or-less straight line portion of the axial stress-axial strain curve. In Figure 4, $E_{av} = E_t$.
- *Secant Young's modulus*, E_s,—is the slope of a straight line joining the origin of the axial stress-strain curve to a point on the curve at some fixed percentage of the peak strength. (In Figure 4 this is 100%.)

Corresponding to any value of Young's modulus, a value of Poisson's ratio may be calculated as:

$$v = -\frac{\left(\Delta\sigma_a / \Delta\varepsilon_a\right)}{\left(\Delta\sigma_a / \Delta\varepsilon_r\right)} \tag{6}$$

Through rearranging Equation [5], the constitutive law that is commonly referred to as **Hooke's Law** in one dimension, Equation [7], can be derived.

$$\sigma = E\varepsilon \tag{7}$$

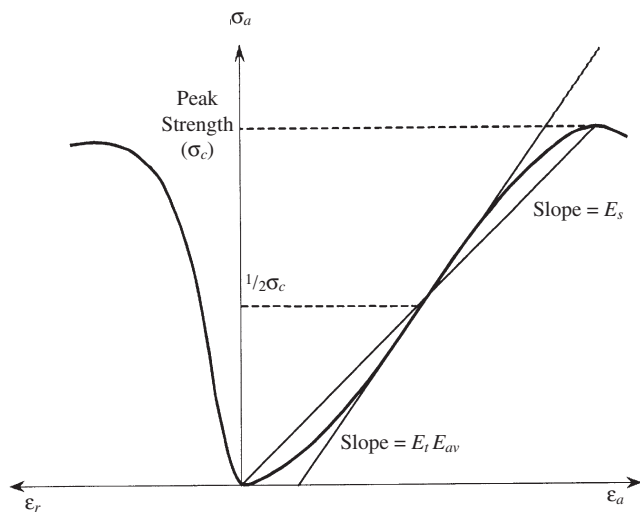**Figure 4. Schematic of the results obtained in a uniaxial compression test on rock. The average axial stress, σ_a, is shown plotted against overall axial strain, ε_a, and against radial strain, ε_r. The calculation of tangent, average and secant Young's moduli are shown (after Brady and Brown, 1985)**

<div style="text-align:center">

Table II
Summary of the important aspects of three moduli

</div>

Summary of the three moduli of elasticity		
Young's modulus, E (Common units: GPa)	Shear modulus, G (Common units: GPa)	Bulk modulus, K (Common units: GPa)
Alternative terminology: modulus of elasticity, elastic modulus	shear stiffness, modulus of rigidity	normal stiffness
Definition: $\dfrac{\text{stress}}{\text{strain}}$	$\dfrac{\text{shear stress}}{\text{shear strain}}$	$\dfrac{\text{pressure change}}{\text{volume change}}$
Relates to change in: **length** ('tensile')	**shape** ('shear')	**volume** ('bulk')
Applies to: only solids	solids and liquids	all materials, with a low value for gases
$E = \dfrac{F/A}{e/l}$	$G = \dfrac{F/A}{\alpha}$	$K = \dfrac{\Delta p}{-\Delta V/V}$

Bulk modulus and shear modulus

Having defined both Young's modulus and Poisson's ratio it is now possible to define the bulk modulus and the shear modulus of a material.

The **bulk modulus**, K, is a measure of volumetric stiffness under normal loading conditions and is given by:

$$K = \frac{E}{3(1 - 2v)} \tag{8}$$

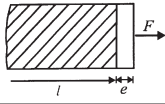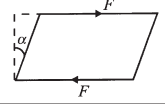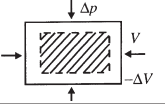The bulk modulus is sometimes referred to as the normal stiffness of a material.

The **shear modulus**, $G,$ which is also known as the shear stiffness or the modulus of rigidity, is the shear stress (the shear force per unit area) divided by the shear strain. It is calculated using the following equation:

$$G = \frac{E}{2(1 + v)} \tag{9}$$

The unit of both bulk modulus and shear modulus is the pascal (Pa).

All materials have a finite bulk modulus. In the case of gases the bulk modulus is low, but in fluids and solids it is often quite high. Rubber, however, is an example of a material with a relatively low bulk modulus. All solids have a finite elastic shear modulus, while fluids have a zero elastic shear modulus; that is, they do not resist shear. Table I gives examples of Young's modulus and the shear modulus of a few commonly encountered materials. Table II summarizes the important aspects of the three moduli discussed in this Appendix.

Non-linear elasticity

The fundamental difference between a linearly elastic and a non-linearly elastic material is that the stress-strain curve characterizing **non-linear elastic** behaviour (see Figure 3.(b)) does not describe a straight line. That is, the constitutive law given in Equation [4], describing the behaviour of the material, is not a linear equation. When modelling, non-linear elastic materials are generally referred to as user defined materials, and, the stress-strain response of the material is approximated using corresponding pairs of stress-strain values obtained from physical measurements.

Hooke's law in 1 dimension

The simplest way of illustrating Hooke's law is to consider a spring with a force, F, acting on it, as shown in Figure 5. F will cause the spring to extend or contract, depending upon whether it is pulling or pushing the spring. That is, the spring is subjected to a tensile or a compressive force. Plotting a force-displacement curve (which is equivalent to a stress-strain curve) will produce a straight line, characteristic of linear elastic behaviour, with the spring stiffness, k, being the constant of proportionality. In this case, the spring stiffness is equivalent to Young's modulus, E. The constitutive relationship describing the behaviour of the spring is that given by Equation [5].

Uniaxial stress

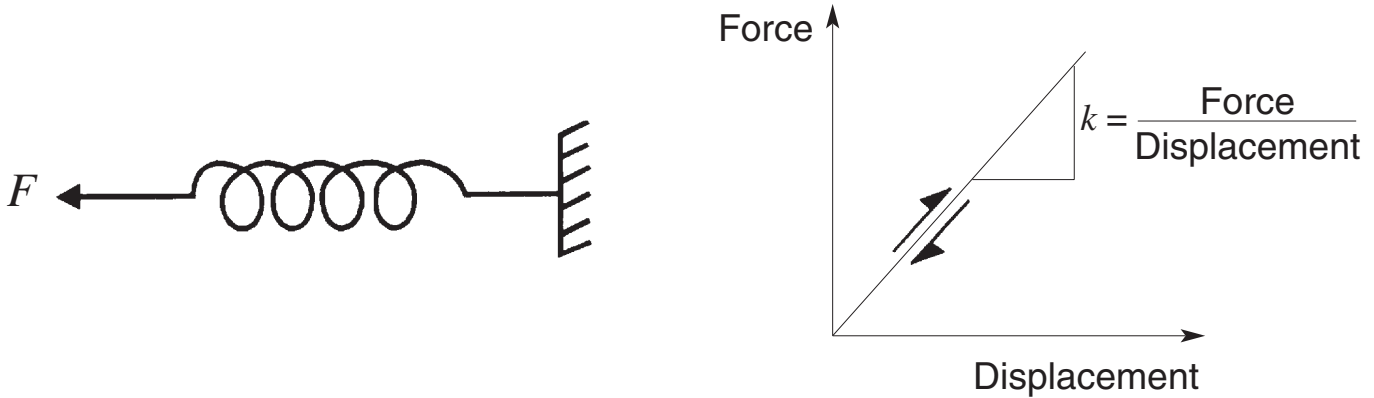Extending this idea further, suppose a material sample

Figure 5. Spring used to illustrate Hooke's law in one dimension

is subjected to a force, *F*, acting in one direction, and it is unconfined (not stressed) in the remaining two directions, then it is said to be in a state of **uniaxial stress**. This is the situation depicted in Figure 2. Not only will this stress, σ_z, produce a corresponding strain, ε_z, but it changes the linear dimensions of elements aligned perpendicular to the axis of stress. If $v > 0$, and, if the stress is compressive, the sample will contract in the *z* direction and expand in the *x* and *y* directions, and vice versa if the stress is tensile.

Uniaxial strain

As with stress, it is possible for a material to experience uniaxial strain. The state of **uniaxial strain** corresponds to a change in volume of a material sample in one direction only, say ε_z. In order to achieve this the sample not only needs to be subjected to a stress σ_z, but it also needs to be confined in the directions perpendicular to the *z* axis. An example of uniaxial strain pertinent to the mining industry, is that of the undisturbed vertical stress in a homogeneous rock as depicted in Figure 6. At a depth *z*, the vertical stress, σ_z, due to the weight of the overlying strata, is:

Figure 6. A material sample subjected to uniaxial strain (after Turcotte and Schubert, 1982)

$$\sigma_z = \rho g z \qquad [10]$$

Where ρ is the average density of the overlying strata and *g* is acceleration due to the force of gravity.

Hooke's law in 2 dimensions

Stress in 2 dimensions

The concepts discussed in the preceding section can be extended to include geometry in two dimensions. Imagine a body in equilibrium under the action of an external force, *F*, as shown in Figure 7(a). If the body is divided in half, along an imaginary plane that has area *A*, both halves will be in equilibrium, with the internal forces continuously distributed throughout the body. If the imaginary plane is inclined, as shown in Figure 7(b), a stress will act on the plane. This stress can be represented by two components as shown in Figure 7(c), the normal stress (σ_{normal}), which is orientated perpendicular to the imaginary plane, and the shear stress (σ_{shear}), which lies parallel to the plane.

If the stress vectors all lie in a single plane, determining the state of stress at a point in a body is greatly simplified. If this condition is satisfied at every point in the body then a two-dimensional stress, or a state of **plane stress**, prevails. As will be seen in the next section, which discusses Hooke's law in three dimensions, plane stress is a special case of the more general three-dimensional situation. (In this later section a more complete derivation of stresses, in terms of the traction vectors acting on an element, is presented.)

When considering a two-dimensional state of stress, all the external forces are assumed to be acting in the (*x*, *y*) plane. That is, the stresses in the *z* direction are all zero, making this a special case of the three-dimensional situation. A small element in a two-dimensional body will be subjected to the normal
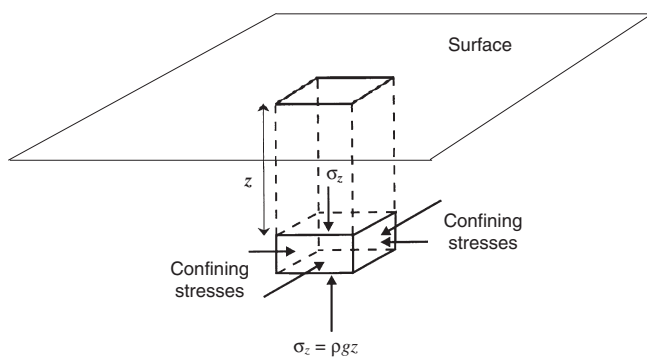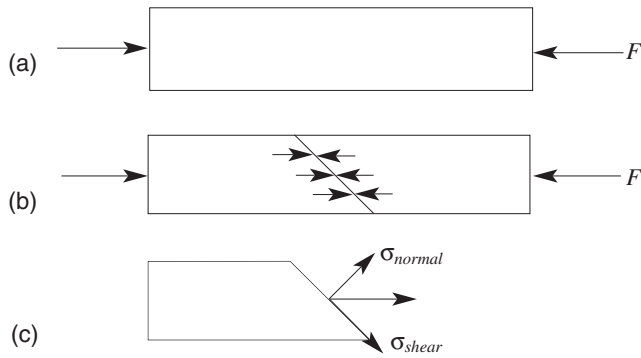
Figure 7. Forces creating stresses in a two-dimensional body.
(a) The body is in equilibrium under the action of external forces.
(b) Stresses acting on an imaginary inclined plane in the body.
(c) The stress, σ = F/A, represented by a normal stress (σ$_{normal}$) and a shear stress (σ$_{shear}$).

components of stress, σ_{xx} and σ_{yy}, together with the shearing components of stress, σ_{xy} and σ_{yx}, as shown in Figure 8. In order to maintain equilibrium in a solid continuum σ_{xy} must equal σ_{yx}. Consequently, in a two-dimensional situation, the state of stress can be fully described using three components of stress, σ_{xx}, σ_{yy} and σ_{xy}.

Principal stresses in 2 dimensions

A concept of fundamental importance to rock mechanics is that of principal stresses. It is always possible to find an orientation such that there are no shear stresses acting on the faces of a material element. Under this condition the applied normal stresses are referred to as the **principal stresses**. In a two-dimensional situation the principal stresses are

referred to as σ_1 and σ_2, where $\sigma_1 \geq \sigma_2$ and they act at 90° to one another. The following equations can be used to calculate the magnitudes of σ_1 and σ_2 from given x and y stress components:

$$\sigma_1 = \tfrac{1}{2}\left(\sigma_{xx} + \sigma_{yy}\right) + \tfrac{1}{2}\sqrt{\left(\sigma_{xx} - \sigma_{yy}\right)^2 + 4\sigma_{xy}^2} \qquad [11]$$

$$\sigma_2 = \tfrac{1}{2}\left(\sigma_{xx} + \sigma_{yy}\right) - \tfrac{1}{2}\sqrt{\left(\sigma_{xx} - \sigma_{yy}\right)^2 + 4\sigma_{xy}^2} \qquad [12]$$

Furthermore:

$$\sigma_1 + \sigma_2 = \sigma_{xx} + \sigma_{yy}. \qquad [13]$$

In general, principal stresses do not act in the same directions as σ_{xx} and σ_{yy}. (If this was the case, shear stresses would be present and, consequently, the normal stresses would no longer be the principal stresses.) The angle of orientation, θ, of σ_1 is calculated using Equation [14]. θ is measured in a direction counter-clockwise from the positive x axis as depicted in Figure 9.

$$\theta = \tfrac{1}{2}\arctan\left(\frac{2\sigma_{xy}}{\sigma_x - \sigma_y}\right) \qquad [14]$$

The angle of orientation of σ_2 is obtained by either adding or subtracting 90° from θ such that σ_1 and σ_2 lie in quadrants I and II (see Figure 9).

It is also possible to calculate the maximum shear stress, $\sigma_{xy(max)}$, acting on an element in terms of σ_{xx} and σ_{yy} or in terms of the principal stresses using the following equations:

$$\sigma_{xy(max)} = \tfrac{1}{2}\left(\sqrt{(\sigma_{xx} - \sigma_{yy})^2 + 4\sigma_{xy}^2}\right) \qquad [15]$$

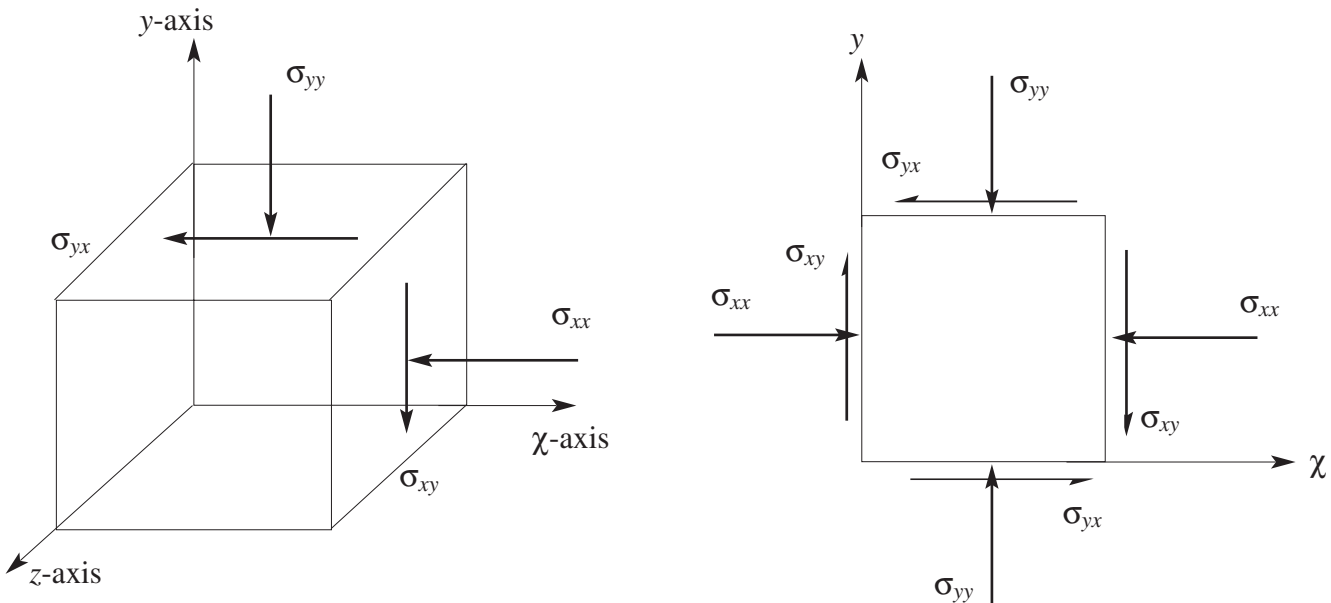$$\sigma_{xy(max)} = \tfrac{1}{2}(\sigma_1 - \sigma_2) \qquad [16]$$

Figure 8. State of plane stress or the general state of stress in two dimensions
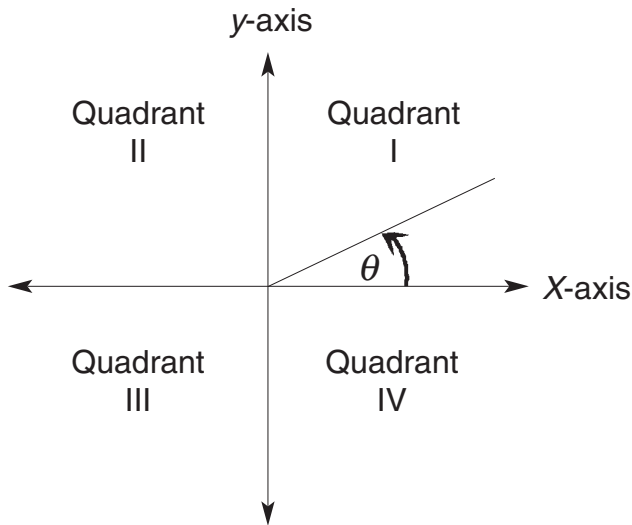
Figure 9. The Cartesian co-ordinate system in two dimensions; showing the measurement of angle θ as well as the four quadrants. (In the two-dimensional case the z axis is perpendicular to the plane of the page)

$\sigma_{xy(max)}$ is oriented in a direction that is at 45° to that of the principal stresses.

Strain in 2 dimensions

Having considered stresses in two dimensions, the resulting strains need to be investigated. A solid body, in equilibrium under the application of a system of external forces, will undergo deformation. Consequently, points in the body are displaced relative to their original positions, i.e. they are strained. As is the case with stress, strain can be either normal or shear.

Strain, as defined by Equation [1], and depicted in Figure 2, is referred to as normal strain. Normal strain along the x and y axes is indicated by ε_{xx} and ε_{yy}, respectively. Normal strain is taken to be positive when it signifies shortening (compressive strain) and negative when lengthening is implied (tensile strain).

Figure 10(a) shows an element that is subjected only to shearing stresses. During the induced deformation, side 0B undergoes a rotation, denoted by $^{1}/_{2}\gamma_{xy}$ (see Figure 10(b)). Therefore, $^{1}/_{2}\gamma_{xy}$ represents half the increase in the right angle between the two sides of the element that were initially perpendicular to one another. By considering the angular rotation of the element side 0A, the other half of the increase in the right angle A0B is obtained. The total increase in the right angle, γ_{xy}, is brought about by shearing only, and is thus referred to as shear strain. When γ_{xy} represents an increase in the right angle A0B, it is considered to be positive. Conversely, when this angle is decreased by γ_{xy}, it is negative. γ_{xy} is measured in radians, where $360° = 2\pi$ radians.

In summary, the sign convention used for both normal and shear strains in rock mechanics is that positive displacement represents movement towards the negative direction of the co-ordinate axes. Conversely, negative displacement represents movement towards the positive direction of the co-ordinate axes.

Principal strains in 2 dimensions

In the same way that there are principal stresses, there are principal strains. It is always possible to find two mutually perpendicular directions about a point in which the component of shear strain is zero. These directions are referred to as the **principal strain directions** and the corresponding normal strains are **principal strains**, denoted by ε_1 and ε_2, where $\varepsilon_1 \geq \varepsilon_2$. The principal strains, and principal strain directions, can be calculated using the following equations:

$$\varepsilon_1 = \tfrac{1}{2}\left(\varepsilon_{xx} + \varepsilon_{yy}\right) + \tfrac{1}{2}\sqrt{\left(\varepsilon_{xx} - \varepsilon_{yy}\right)^2 + \gamma_{xy}^{2}} \qquad [17]$$

$$\varepsilon_2 = \tfrac{1}{2}\left(\varepsilon_{xx} + \varepsilon_{yy}\right) - \tfrac{1}{2}\sqrt{\left(\varepsilon_{xx} - \varepsilon_{yy}\right)^2 + \gamma_{xy}^{2}} \qquad [18]$$

$$\theta = \tfrac{1}{2}\arctan\left(\frac{\gamma_{xy}}{\varepsilon_{xx} - \varepsilon_{yy}}\right) \qquad [19]$$

Also:

$$\varepsilon_1 + \varepsilon_2 = \varepsilon_{xx} + \varepsilon_{yy} \qquad [20]$$

The maximum shear strain, $\gamma_{xy(max)}$, can be calculated using either the normal strains or the principal strains, as given below:

$$\gamma_{xy(max)} = \sqrt{\left(\varepsilon_{xx} - \varepsilon_{yy}\right)^2 + \gamma_{xy}^{2}} \qquad [21]$$

$$\gamma_{xy(max)} = \varepsilon_1 - \varepsilon_2 \qquad [22]$$

Stress-strain relationships in 2 dimensions

Since the material under consideration is assumed to behave in a linearly elastic fashion, the stresses and resulting strains can be related via Hooke's law. If an element is subjected to the actions of σ_{xx}, σ_{yy} and σ_{xy}, the mathematical expressions for the corresponding strains are:
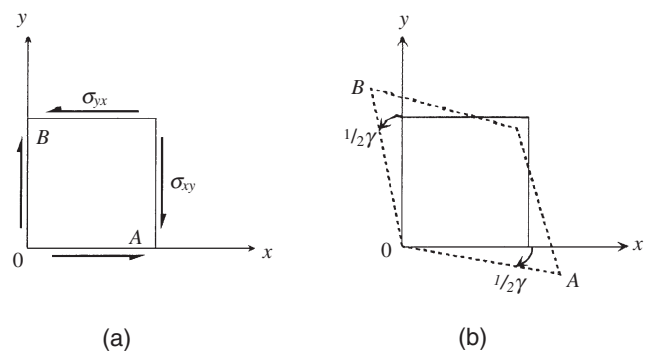

(a)	(b)

Figure 10. Deformation of an element under shearing stresses

$$\varepsilon_{xx} = \frac{1}{E}\left(\sigma_{xx} - v\sigma_{yy}\right) \qquad [23]$$

$$\varepsilon_{yy} = \frac{1}{E}\left(\sigma_{yy} - v\sigma_{xx}\right) \qquad [24]$$

$$\gamma_{xy} = \frac{1}{G}\sigma_{xy} \qquad [25]$$

Likewise, the stresses can be written in terms of the strains:

$$\sigma_{xx} = \frac{E}{1-v^2}\left(\varepsilon_{xx} + v\varepsilon_{yy}\right) \qquad [26]$$

$$\sigma_{yy} = \frac{E}{1-v^2}\left(\varepsilon_{yy} + v\varepsilon_{xx}\right) \qquad [27]$$

$$\sigma_{xy} = G\gamma_{xy} \qquad [28]$$

Similarly, the principal stresses and strains can be related using the following equations:

$$\sigma_1 = \frac{E}{1-v^2}\left(\varepsilon_1 + v\varepsilon_2\right) \qquad [29]$$

$$\sigma_2 = \frac{E}{1-v^2}\left(\varepsilon_2 + v\varepsilon_1\right) \qquad [30]$$

$$\varepsilon_1 = \frac{1}{E}\left(\sigma_1 - v\sigma_2\right) \qquad [31]$$

$$\varepsilon_2 = \frac{1}{E}\left(\sigma_2 - v\sigma_1\right) \qquad [32]$$

Hooke's law in 3 dimensions

State of stress in 3 dimensions

The state of stress and strain in both one and two dimensions, as discussed in the previous two sections, are special cases of a more general three-dimensional state of stress and strain.

When a force acts on the surface of a body and stresses it, the applied stress can be resolved into three mutually perpendicular components, t_x, t_y and t_z, directed parallel to the reference axes, x, y and z, respectively. The quantities t_x, t_y and t_z are the **traction components** acting on a surface at a point. Of these components, one is a normal component, that is perpendicular to the surface at the point of action, and two are shear components, that are parallel to the surface at the point of action. Supposing t_x is the normal component, then the three components defining the state of stress at the point of interest are:

$$\sigma_{xx} = t_x,\ \sigma_{xy} = t_y\ \text{and}\ \sigma_{xz} = t_z$$

where σ_{xx} is the normal component and, σ_{xy} and σ_{xz} are the two shear components. Similarly, if t_y or t_z is the normal stress, then the components defining the state of stress at the point are:

$$\sigma_{yx} = t_x,\ \sigma_{yy} = t_y\ \text{and}\ \sigma_{yz} = t_z$$

or

$$\sigma_{zx} = t_x,\ \sigma_{zy} = t_y\ \text{and}\ \sigma_{zz} = t_z$$

respectively, where σ_{yy} and σ_{zz} are the normal stresses and σ_{yx}, σ_{yz}, σ_{zx} and σ_{zy} are the shear stress components. From the above mathematical expressions it can be concluded that there are nine components of stress. The directions of action of the stress components, defined by these expressions, are shown on the visible faces of the cubic free body in Figure 11.

Conventionally, the nine stress components, defined above, comprise the **stress tensor** and are written in a matrix form. The stress tensor, $[\sigma]$, is given in Equation [33]:

$$[\sigma] = \begin{bmatrix} \sigma_{xx} & \sigma_{xy} & \sigma_{xz} \\ \sigma_{yx} & \sigma_{yy} & \sigma_{yz} \\ \sigma_{zx} & \sigma_{zy} & \sigma_{zz} \end{bmatrix} \qquad [33]$$

In order to maintain equilibrium in a solid continuum the following relationships need to hold:

$$\sigma_{yx} = \sigma_{xy},\ \sigma_{zy} = \sigma_{yz}\ \text{and}\ \sigma_{xz} = \sigma_{zx}$$

thus, Equation [33] can be written as:

$$[\sigma] = \begin{bmatrix} \sigma_{xx} & \sigma_{xy} & \sigma_{zx} \\ \sigma_{xy} & \sigma_{yy} & \sigma_{yz} \\ \sigma_{zx} & \sigma_{yz} & \sigma_{zz} \end{bmatrix} \qquad [34]$$

Hence, the state of stress at a point in a medium that is in equilibrium, can be specified in terms of only six independent stress components. The stress tensor is a **symmetric matrix** as it is symmetrical about the diagonal, running from the top left-hand corner to the bottom right-hand corner.
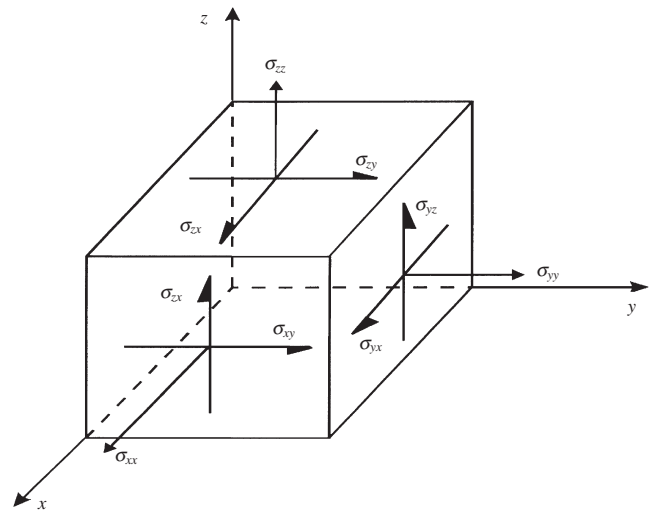

Figure 11. Three-dimensional state of stress

$$\begin{vmatrix} \sigma_{xx} - \sigma_p & \sigma_{xy} & \sigma_{zx} \\ \sigma_{xy} & \sigma_{yy} - \sigma_p & \sigma_{yz} \\ \sigma_{zx} & \sigma_{yz} & \sigma_{zz} - \sigma_p \end{vmatrix} = 0 \qquad [38]$$

The directions of the principal stresses are obtained by calculating the **directional cosines**, *l*, *m* and *n*, of the **transformation matrix**. The transformation matrix is not discussed in detail here, however; suffice it to say that it is obtained when changing the stresses from one local co-ordinate system to another.

By solving the following three simultaneous equations using each principal stress in turn, three sets of directional cosines can be obtained:

$$l(\sigma_{xx} - \sigma_p) + m\sigma_{xy} + n\sigma_{zx} = 0 \qquad [39]$$

$$l\sigma_{xy} + m(\sigma_{yy} - \sigma_p) + n\sigma_{yz} = 0 \qquad [40]$$

$$l\sigma_{zx} + m\sigma_{yz} + n(\sigma_{zz} - \sigma_p) = 0 \qquad [41]$$

Each set of directional cosines, corresponding to a given eigen value, is an **eigen vector** of the stress tensor, and represents the direction of the particular principal stress components in the co-ordinate system of the given components σ_{xx}, σ_{yy} and σ_{zz}.

Stress invariants

It has been mentioned that, since stress is a tensor, it is possible to calculate invariants. The **stress invariants**, denoted I_1, I_2 and I_3, are calculated using the following equations:

$$\begin{aligned} I_1 &= \sigma_{xx} + \sigma_{yy} + \sigma_{zz} \\ &= \sigma_1 + \sigma_2 + \sigma_3 \end{aligned} \qquad [42]$$

$$\begin{aligned} I_2 &= \sigma_{xx}\sigma_{yy} + \sigma_{yy}\sigma_{zz} + \sigma_{zz}\sigma_{xx} - (\sigma_{xy}^2 + \sigma_{yz}^2 + \sigma_{zx}^2) \\ &= \sigma_1\sigma_2 + \sigma_2\sigma_3 + \sigma_3\sigma_1 \end{aligned} \qquad [43]$$

$$\begin{aligned} I_3 &= \sigma_{xx}\sigma_{yy}\sigma_{zz} + 2\sigma_{xy}\sigma_{yz}\sigma_{zx} - (\sigma_{xx}\sigma_{yz}^2 + \sigma_{yy}\sigma_{zx}^2 + \sigma_{zz}\sigma_{xy}^2) \\ &= \sigma_1\sigma_2\sigma_3. \end{aligned} \qquad [44]$$

The stress invariants and the principal stresses satisfy the following equation:

$$\sigma_p^3 - I_1\sigma_p^2 - I_2\sigma_p - I_3 = 0. \qquad [45]$$

Spherical and deviatoric stresses

Another useful property of the stress matrix is that it can be split into two components. The first component is the **spherical stress** (or hydrostatic, or mean normal stress) component, $[\sigma_m]$, where *m* represents mean. The second component is the **deviatoric component**, $[\sigma_d]$. The complete stress tensor, as defined in Equation [34], is the sum of the spherical and deviatoric components as given in Equation [46]:

Tensors

A tensor is a matrix with specific attributes. A physical property can be represented by a tensor if the relationships or laws characterizing it remain valid, regardless of the system of co-ordinates used in specifying the quantities involved. In the case of stresses, the stress tensor is a set of quantities enabling calculation of the traction vector on a plane of any arbitrary orientation. One of the attributes of a tensor is that of invariants. An **invariant** is a physical quantity of the system that does not change, should the reference axes change (see the previous section). Any other quantity, derived from any of the invariants, is also invariant. Stress and strain are both tensors of the **second order** as each component has two directional indices, σ_{xy} for example. (A quantity such as ψ_{ijk} is a third order tensor.) Tensor analysis is critical to the fields of classical mechanics (the topic dealt with here), quantum mechanics and fluid mechanics, to name just a few. Much of the groundwork in this area was carried out by mathematicians such as Gauss, Riemann and Christoffel.

Principal stresses in 3 dimensions

The concept of principal stresses, as discussed in a previous section, can also be extended to the three-dimensional stress state. It is always possible to find three mutually perpendicular principal stress directions, with corresponding principal stresses, such that no shearing stresses act on the sides of the element. The principal stresses, σ_1, σ_2 and σ_3 are invariant since they can be calculated from the invariants of the stress tensor. More commonly, the principal stresses are referred to as:

σ_1 = major principal stress

σ_2 = intermediate principal stress

σ_3 = minor principal stress

where, $\sigma_1 \geq \sigma_2 \geq \sigma_3$. As with the two-dimensional case:

$$\sigma_1 + \sigma_2 + \sigma_3 = \sigma_{xx} + \sigma_{yy} + \sigma_{zz}. \qquad [35]$$

The magnitude of the principal stresses is equal to the **eigen values** of the stress tensor. The eigen values are obtained by solving:

$$\det([\sigma] - \sigma_p[\mathbf{I}]) = 0 \qquad [36]$$

where det indicates determinant, σ_p are the principal stresses and $[\mathbf{I}]$ is the identity matrix of order three as given in Equation [36].

$$[\mathbf{I}] = \begin{bmatrix} 1 & 0 & 0 \\ 0 & 1 & 0 \\ 0 & 0 & 1 \end{bmatrix} \qquad [37]$$

Equation [36], a polynomial of order three, is the characteristic equation of the stress tensor. The three scalars σ_p that satisfy this equation are the eigen values, i.e. the magnitudes of the principal stresses. Equation [36] is more commonly written as:

$$[\sigma] = [\sigma_m] + [\sigma_d].$$ [46]

The spherical stress matrix is defined by:

$$[\sigma]_m = \begin{bmatrix} \sigma_m & 0 & 0 \\ 0 & \sigma_m & 0 \\ 0 & 0 & \sigma_m \end{bmatrix}$$ [47]

where:

$$\sigma_m = \frac{1}{3}\left(\sigma_{xx} + \sigma_{yy} + \sigma_{zz}\right)$$
$$= \frac{1}{3}\left(\sigma_1 + \sigma_2 + \sigma_3\right)$$ [48]

By rearranging Equation [46] and substituting in Equation [43], it can be seen that the deviator stress matrix is given by:

$$[\sigma_d] = \begin{bmatrix} \sigma_{xx} - \sigma_m & \sigma_{xy} & \sigma_{xz} \\ \sigma_{yx} & \sigma_{yy} - \sigma_m & \sigma_{yz} \\ \sigma_{zx} & \sigma_{zy} & \sigma_{zz} - \sigma_m \end{bmatrix}$$ [49]

The spherical stress is responsible for the change in **volume** of the body, as it involves only normal stresses. The deviator stress, which contains shear stresses, is responsible for **distortion** of the body.

Strains in 3 dimensions

In the discussion thus far it has been stated that, if a body is stressed as a result of the application of external forces, it will respond by deforming, or straining. The concept of strain presented so far now needs to be extended to enable the analysis of the deformation of a body in three-dimensional space. A complete derivation of strain in three dimensions can be found in Brady and Brown (1985). The following discussion is based on their presentation.

The application of a set of forces to a body changes the relative positions of points within it. The change in loading conditions from the initial state to the final state causes a displacement of each point relative to all other points. If the applied loads constitute a self-equilibrating set, the problem is to determine the equilibrium displacement field induced in the body by the loading. The displacements experienced by each element within a body arise from both deformation of the element, and rigid-body rotation of the element. Furthermore, the deformation of a body is made up of the elongation and distortion of the elements. Normal strain is responsible for any elongation or contraction the element experiences, while shear strain accounts for distortion. The total displacement components due to all modes of strain can be combined to produce the strain tensor, $[\varepsilon]$, which is given in Equation [50]:

$$[\varepsilon] = \begin{bmatrix} \varepsilon_{xx} & \frac{1}{2}\gamma_{xy} & \frac{1}{2}\gamma_{zx} \\ \frac{1}{2}\gamma_{xy} & \varepsilon_{yy} & \frac{1}{2}\gamma_{yz} \\ \frac{1}{2}\gamma_{zx} & \frac{1}{2}\gamma_{yz} & \varepsilon_{zz} \end{bmatrix}$$ [50]

From this equation it can be seen that the state of strain at a point in a body is completely defined by six independent components.

Principal strains and strain invariants

Since a state of strain is defined by a second order strain tensor, determination of the principal strains, and other manipulation of strain quantities, are completely analogous to the processes employed in the analysis of stress. Thus, principal strains and principal strain directions are determined as the eigen values and the associated eigen vectors of the strain matrix. Solving Equation [51] will yield the magnitudes of the principal strains ε_1, ε_2 and ε_3:

$$\begin{vmatrix} \varepsilon_{xx} - \varepsilon_p & \frac{1}{2}\gamma_{xy} & \frac{1}{2}\gamma_{zx} \\ \frac{1}{2}\gamma_{xy} & \varepsilon_{yy} - \varepsilon_p & \frac{1}{2}\gamma_{yz} \\ \frac{1}{2}\gamma_{zx} & \frac{1}{2}\gamma_{yz} & \varepsilon_{zz} - \varepsilon_p \end{vmatrix} = 0$$ [51]

The strain invariants are given by:

$$I_1 = \varepsilon_{xx} + \varepsilon_{yy} + \varepsilon_{zz}$$
$$= \varepsilon_1 + \varepsilon_2 + \varepsilon_3$$ [52]

$$I_2 = \varepsilon_{xx}\varepsilon_{yy} + \varepsilon_{yy}\varepsilon_{zz} + \varepsilon_{zz}\varepsilon_{xx} - \frac{1}{4}\left(\gamma_{xy}^2 + \gamma_{yz}^2 + \gamma_{zx}^2\right)$$
$$= \varepsilon_1\varepsilon_2 + \varepsilon_2\varepsilon_3 + \varepsilon_3\varepsilon_1$$ [53]

$$I_3 = \varepsilon_{xx}\varepsilon_{yy}\varepsilon_{zz} + \frac{1}{4}\gamma_{xy}\gamma_{yz}\gamma_{zx} - \frac{1}{4}\left(\varepsilon_{xx}\gamma_{yz}^2 + \varepsilon_{yy}\gamma_{zx}^2 + \varepsilon_{zz}\gamma_{xy}^2\right)$$
$$= \varepsilon_1\varepsilon_2\varepsilon_3.$$ [54]

The principal strains and the strain invariants satisfy the following equation:

$$\varepsilon_p^3 - I_1\varepsilon_p^2 - I_2\varepsilon_p - I_3 = 0.$$ [55]

Volumetric strain

The volumetric strain, Δ, is defined by:

$$\Delta = \varepsilon_{xx} + \varepsilon_{yy} + \varepsilon_{zz}.$$ [56]

Note that Δ is also the same as strain invariant I_1. The three-dimensional strain matrix can be subdivided into the non-deviatoric and deviatoric strain matrices; where the former describes the volume change and the latter the distortion.

$$[\varepsilon] = \begin{bmatrix} \frac{1}{3}\Delta & 0 & 0 \\ 0 & \frac{1}{3}\Delta & 0 \\ 0 & 0 & \frac{1}{3}\Delta \end{bmatrix} + \begin{bmatrix} \varepsilon_{xx} - \frac{1}{3}\Delta & \frac{1}{2}\gamma_{xy} & \frac{1}{2}\gamma_{zx} \\ \frac{1}{2}\gamma_{xy} & \varepsilon_{yy} - \frac{1}{3}\Delta & \frac{1}{2}\gamma_{yz} \\ \frac{1}{2}\gamma_{zx} & \frac{1}{2}\gamma_{yz} & \varepsilon_{zz} - \frac{1}{3}\Delta \end{bmatrix} \quad [57]$$

<div align="center">

Non - deviatoric   Deviatoric

</div>

Stress-strain relationships in 3 dimensions

When formulating the constitutive equations for stress and strain in three dimensions, it is useful to construct column vectors from the elements of the stress and strain tensors. These stress and strain vectors are defined, respectively, by:

$$[\sigma] = \begin{bmatrix} \sigma_{xx} \\ \sigma_{yy} \\ \sigma_{zz} \\ \sigma_{xy} \\ \sigma_{yz} \\ \sigma_{zx} \end{bmatrix} \quad \text{and} \quad [\varepsilon] = \begin{bmatrix} \varepsilon_{xx} \\ \varepsilon_{yy} \\ \varepsilon_{zz} \\ \gamma_{xy} \\ \gamma_{yz} \\ \gamma_{zx} \end{bmatrix}$$

The most general statement of linear elastic constitutive behaviour is a generalized form of Hooke's law, in which any strain component is a linear function of all the stress components. This is given in Equation [58]:

$$\begin{bmatrix} \sigma_{xx} \\ \sigma_{yy} \\ \sigma_{zz} \\ \sigma_{xy} \\ \sigma_{yz} \\ \sigma_{zx} \end{bmatrix} = \begin{bmatrix} D_{11} & D_{12} & D_{13} & D_{14} & D_{15} & D_{16} \\ D_{21} & D_{22} & D_{23} & D_{24} & D_{25} & D_{26} \\ D_{31} & D_{32} & D_{33} & D_{34} & D_{35} & D_{36} \\ D_{41} & D_{42} & D_{43} & D_{44} & D_{45} & D_{46} \\ D_{51} & D_{52} & D_{53} & D_{54} & D_{55} & D_{56} \\ D_{61} & D_{62} & D_{63} & D_{64} & D_{65} & D_{66} \end{bmatrix} \begin{bmatrix} \varepsilon_{xx} \\ \varepsilon_{yy} \\ \varepsilon_{zz} \\ \gamma_{xy} \\ \gamma_{yz} \\ \gamma_{zx} \end{bmatrix} \quad [58]$$

which is generally written as:

$$[\sigma] = [\mathbf{D}][\varepsilon] \quad [59]$$

The matrix $[\mathbf{D}]$ is the **elasticity matrix**, or the matrix of elastic stiffnesses, and is generally referred to as the stiffness matrix. This matrix is, however, a symmetric matrix and, thus, it contains only 21 independent stiffnesses for a general anisotropic material. By substituting in the stiffnesses for an isotropic elastic solid, Equation [58] can be written as:

$$\begin{bmatrix} \sigma_{xx} \\ \sigma_{yy} \\ \sigma_{zz} \\ \sigma_{xy} \\ \sigma_{yz} \\ \sigma_{zx} \end{bmatrix} = A \begin{bmatrix} 1 & \frac{v}{(1-v)} & \frac{v}{(1-v)} & 0 & 0 & 0 \\ \frac{v}{(1-v)} & 1 & \frac{v}{(1-v)} & 0 & 0 & 0 \\ \frac{v}{(1-v)} & \frac{v}{(1-v)} & 1 & 0 & 0 & 0 \\ 0 & 0 & 0 & \frac{1-2v}{2-2v} & 0 & 0 \\ 0 & 0 & 0 & 0 & \frac{1-2v}{2-2v} & 0 \\ 0 & 0 & 0 & 0 & 0 & \frac{1-2v}{2-2v} \end{bmatrix} \begin{bmatrix} \varepsilon_{xx} \\ \varepsilon_{yy} \\ \varepsilon_{zz} \\ \gamma_{xy} \\ \gamma_{yz} \\ \gamma_{zx} \end{bmatrix} \quad [60]$$

where $A = \dfrac{E(1-v)}{(1+v)(1-2v)}$.

In Equation [60], the majority of the entries in the off diagonals of the elasticity matrix are zero and,

hence, it is referred to as a sparse matrix. From a computational point of view, a sparse matrix means that the computation time is substantially reduced.

Instead of using matrix notation, the stress-strain relationships can be written out in longhand, as given below by Equations [61] to [69]:

$$\sigma_{xx} = \frac{2G}{1-2v}\left\{(1-v)\varepsilon_{xx} + v(\varepsilon_{yy} + \varepsilon_{zz})\right\} \quad [61]$$

$$\sigma_{yy} = \frac{2G}{1-2v}\left\{(1-v)\varepsilon_{yy} + v(\varepsilon_{xx} + \varepsilon_{zz})\right\} \quad [62]$$

$$\sigma_{zz} = \frac{2G}{1-2v}\left\{(1-v)\varepsilon_{zz} + v(\varepsilon_{xx} + \varepsilon_{yy})\right\} \quad [63]$$

$$\sigma_{xy} = G\gamma_{xy} \Rightarrow \gamma_{xy} = \frac{1}{G}\sigma_{xy} \quad [64]$$

$$\sigma_{yz} = G\gamma_{yz} \Rightarrow \gamma_{yz} = \frac{1}{G}\sigma_{yz} \quad [65]$$

$$\sigma_{zx} = G\gamma_{zx} \Rightarrow \gamma_{zx} = \frac{1}{G}\sigma_{zx} \quad [66]$$

$$\varepsilon_{xx} = \frac{1}{E}\left\{\sigma_{xx} - v(\sigma_{yy} + \sigma_{zz})\right\} \quad [67]$$

$$\varepsilon_{yy} = \frac{1}{E}\left\{\sigma_{yy} - v(\sigma_{xx} + \sigma_{zz})\right\} \quad [68]$$

$$\varepsilon_{zz} = \frac{1}{E}\left\{\sigma_{zz} - v(\sigma_{xx} + \sigma_{yy})\right\} \quad [69]$$

Special cases

Plane stress

When Hooke's law in two dimensions was discussed previously, it was mentioned that plane stress is a special case of the more general three-dimensional situation, where the **stresses acting in the z direction are zero**. The equations relating stress and strain in the (x, y) plane were given, however, the out-of-plane strain (the strain in the z direction) was omitted. Since the body is unconfined in the z direction, it will deform in this direction. The normal strain, ε_{zz}, is given by:

$$\varepsilon_{zz} = -\frac{v}{E}(\sigma_{xx} + \sigma_{yy}). \quad [70]$$

This equation can easily be obtained by setting $\sigma_{zz} = 0$ in Equation [69]. There is also a principal strain acting in the z direction, the magnitude of which can be calculated by solving:

$$\varepsilon_3 = -\frac{v}{E}(\sigma_1 + \sigma_2). \quad [71]$$

Plane strain

Plane strain is a further, commonly encountered, special case of the three-dimensional situation. In the case of **plane strain** a body is confined in one direction and allowed to strain in the remaining two directions, e.g. $\varepsilon_{zz} = \gamma_{zx} = \gamma_{yz} = 0$ but $\sigma_{zz} \neq 0$. Physically,

plane strain is associated with long structures or excavations with constant cross-section and acted on by loads in the plane of the cross-section, such as shaft barrels and tunnels, as depicted in Figure 12.

Pure shear

Pure shear occurs within a body when it is strained but there is no rotation of the principal directions of strain, with respect to the axes of the reference frame, and there is no change in volume of the body during the development of the strain.

In the case of plane stress, induced pure shear occurs when $\sigma_1 = -\sigma_2$ and $\sigma_3 = 0$, thus from Equation [71] $\varepsilon_3 = 0$. Also $\theta = 45°$ such that $\sigma_{xx} = \sigma_{yy} = 0$ and $\sigma_{xy} = |\sigma_1|$, as shown in Figure 13(a). Furthermore, $\varepsilon_{xx} = \varepsilon_{yy} = 0$ and $\gamma_{xy} = \varepsilon_1$. Although the Mohr circle diagram is introduced and discussed in later, for completeness the Mohr circle, for a plane stress pure shear situation, has been included in Figure 13(b). The radius of the Mohr circle can increase or decrease depending on the values of σ_1 and σ_2 but it will always be centred on the origin of the (σ_n, τ) axes.

Pure shear can also develop under plane strain circumstances. In this case, supposing that the (x, y) plane is the plane of deformation, the deformation could be a combination of pure extension in the x direction and pure compression in the y direction (Turner and Weiss, 1963).

Simple shear

Simple shear is similar to pure shear in that volume is preserved, however, the principal directions of strain can rotate, with respect to the co-ordinate reference frame. The deformation of a square subjected to simple shear is depicted in Figure 14. From this Figure it can be seen that the sides of the square parallel to the direction of shear do not rotate or change length. Although a sample is subjected to

simple shear, each point within the sample is subject to a state of pure shear. Simple shear is a simplified concept that is rarely satisfied in reality although it is often used as a descriptive tool in geology texts. Simple shear can, however, be associated with displacement in a shear zone, such as that associated with a strike-slip fault.

Stress transformations

In the foregoing two sections it was mentioned that the Cartesian co-ordinate system can be rotated through an arbitrary angle θ to obtain a new reference co-ordinate system. This rotation is known as a **co-ordinate transformation**. Since the choice of orientation of the reference axes in specifying a state of stress is arbitrary, situations arise in which a differently oriented set of reference axes can prove more convenient for solving the problem at hand. Co-ordinate rotation, or transformation, forms an integral part of the calculation of principal stress and strain directions.

Rotation matrix

Suppose x and y are a particular set of axes and that l and m are a second, or rotated set of axes, and β is the
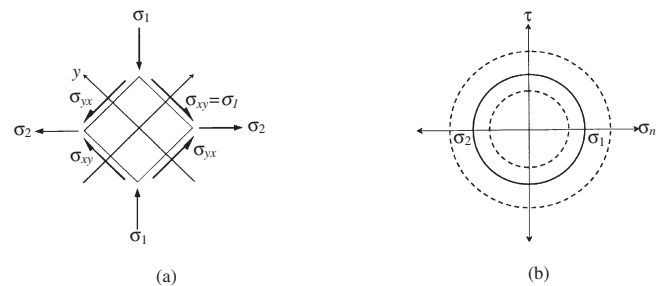
Figure 13. Diagrammatic representation of plane stress pure shear. (a) Body diagram showing the principal and shear stresses for pure shear. (b) The Mohr circle diagram for pure shear where τ represents the applied shear stress and σ_n represents the applied normal stress

Figure 14. Diagrammatic representation of simple shear showing the shear stresses and resultant deformation

Figure 12. Tunnel subject to plane strain

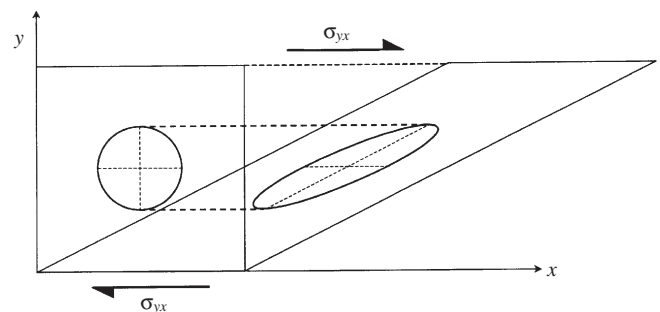angle of rotation, as shown in Figure 15. Included in this Figure is a point P that has the co-ordinates (U_x, U_y) in the old co-ordinate system and (U_l, U_m) in the new co-ordinate system. Using the geometric relations indicated in Figure 15, the following relationships can be obtained:

$$U_l = U_x \cos\beta + U_y \sin\beta \qquad [72]$$

$$U_m = -U_x \sin\beta + U_y \cos\beta. \qquad [73]$$

These equations can be written in matrix form as:

$$\begin{bmatrix} U_l \\ U_m \end{bmatrix} = \begin{bmatrix} \cos\beta & \sin\beta \\ -\sin\beta & \cos\beta \end{bmatrix} \begin{bmatrix} U_x \\ U_y \end{bmatrix} \qquad [74]$$

where:

$$\begin{bmatrix} \cos\beta & \sin\beta \\ -\sin\beta & \cos\beta \end{bmatrix} = [\mathbf{R}] \qquad [75]$$

is the **rotation matrix**. The individual components of this matrix are the directional cosines, and Equation [75] can be rewritten as:

$$[\mathbf{R}] = \begin{bmatrix} l_x & l_y \\ m_x & m_y \end{bmatrix}. \qquad [76]$$

The orientation of a particular axis, say the l axis, relative to the original x and y axes may be defined by a row vector (l_x, l_y) of direction cosines. In this vector, l_x represents the projection on the x axis of a unit vector orientated parallel to the l axis, with a similar definition for l_y. Likewise, the orientation of the m axis, relative to the original axes, is defined by the row vectors of directional cosines (m_x, m_y). A **unit vector** is a vector that has a length of one unit. An important property of the rotation matrix is that the inverse is equal to the transpose, that is:

$$[\mathbf{R}]^{-1} = [\mathbf{R}]^T = \begin{bmatrix} l_x & m_x \\ l_y & m_y \end{bmatrix}. \qquad [77]$$
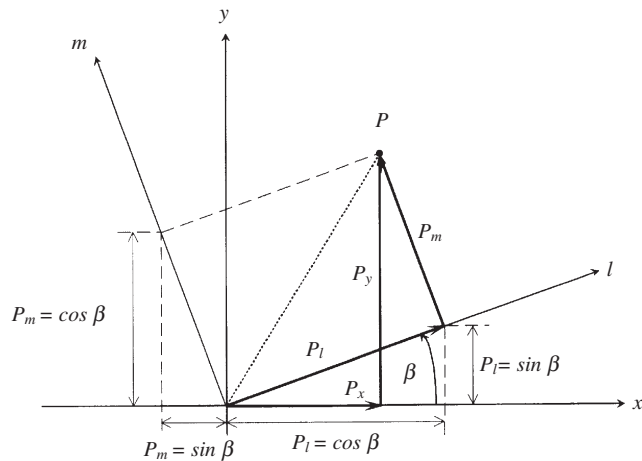

Figure 15. Rotation of a displacement from the (x, y) axes to the (l, m) axes

Stress transformation equations

Having derived the rotation matrix, it is now possible to define the general stress transformation equation that is given by:

$$[\sigma^*] = [\mathbf{R}][\sigma][\mathbf{R}]^T \qquad [78]$$

where $[\sigma]$ is the state of stress in the original co-ordinate system and $[\sigma^*]$ is the state of stress in the new co-ordinate system. Also, Equation [78] indicates that the state of stress at a point is transformed, under a rotation of axes, as a second order vector. Brady and Brown (1985) give the full derivation of this equation. For the two-dimensional case Equation [78], when expanded, becomes:

$$\begin{bmatrix} \sigma_{ll} & \sigma_{lm} \\ \sigma_{lm} & \sigma_{mm} \end{bmatrix} = \begin{bmatrix} l_x & l_y \\ m_x & m_y \end{bmatrix} \begin{bmatrix} \sigma_{xx} & \sigma_{xy} \\ \sigma_{xy} & \sigma_{yy} \end{bmatrix} \begin{bmatrix} l_x & m_x \\ l_y & m_y \end{bmatrix} \qquad [79]$$

In the three-dimensional case it is:

$$\begin{bmatrix} \sigma_{ll} & \sigma_{lm} & \sigma_{nl} \\ \sigma_{lm} & \sigma_{mm} & \sigma_{mn} \\ \sigma_{nl} & \sigma_{mn} & \sigma_{nn} \end{bmatrix} = \begin{bmatrix} l_x & l_y & l_z \\ m_x & m_y & m_z \\ n_x & n_y & n_z \end{bmatrix} \begin{bmatrix} \sigma_{xx} & \sigma_{xy} & \sigma_{xz} \\ \sigma_{xy} & \sigma_{yy} & \sigma_{yz} \\ \sigma_{zx} & \sigma_{zy} & \sigma_{zz} \end{bmatrix} \begin{bmatrix} l_x & m_x & n_x \\ l_y & m_y & n_y \\ l_z & m_z & n_z \end{bmatrix} \qquad [80]$$

Stress transformations in 2 dimensions

The stress transformations for determining the shear and normal components of stress acting on a plane oriented at angle α in an (x, y) stress space are given by Equations [81] and [82]:

$$\sigma_s = (\sigma_{xx} - \sigma_{yy})\sin\alpha\cos\alpha - \sigma_{xy}(\cos^2\alpha - \sin^2\alpha) \qquad [81]$$

$$\sigma_n = \sigma_{xx}\cos^2\alpha + 2\sigma_{xy}\sin\alpha\cos\alpha + \sigma_{yy}\sin^2\alpha \qquad [82]$$

The stress transformations from the (l, m) axes inclined at angle β to the (x, y) orientation are given by Equations [83] to [85].

$$\sigma_{xx} = \sigma_{ll}\cos^2\beta + 2\sigma_{lm}\sin\beta\cos\beta + \sigma_{mm}\sin^2\beta \qquad [83]$$

$$\sigma_{yy} = \sigma_{ll}\sin^2\beta + 2\sigma_{lm}\sin\beta\cos\beta + \sigma_{mm}\cos^2\beta \qquad [84]$$

$$\sigma_{xy} = \sigma_{yx} = (\sigma_{ll} - \sigma_{mm})\sin\beta\cos\beta + \sigma_{lm}(\cos^2\beta - \sin^2\beta) \qquad [85]$$

The inverse case of transforming from the (x, y) orientation into the (l, m) system oriented at angle β to the (x, y) system is given by Equations [86] to [88]:

$$\sigma_{ll} = \sigma_{xx}\cos^2\beta - 2\sigma_{xy}\sin\beta\cos\beta + \sigma_{yy}\sin^2\beta \qquad [86]$$

$$\sigma_{mm} = \sigma_{xx}\sin^2\beta + 2\sigma_{xy}\sin\beta\cos\beta + \sigma_{yy}\cos^2\beta \qquad [87]$$

$$\sigma_{lm} = \sigma_{ml} = (\sigma_{xx} - \sigma_{yy})\sin\beta\cos\beta + \sigma_{xy}(\cos^2\beta - \sin^2\beta) \qquad [88]$$

Friction

In rock mechanics the study of friction is of great importance as its effects are apparent on all scales:

- the microscopic scale in which friction is postulated between opposing surfaces of minute cracks
- a larger scale in which it occurs between individual grains or pieces of aggregate, and
- the friction of joint or fault surfaces in which the areas in question may vary from a few to many square metres.

To date, friction is a poorly understood phenomenon. In this section, however, the subject is reviewed in the simplest terms to afford the reader a physical understanding of the issues relevant to numerical modelling from a rock engineering point of view.

Amontons's Laws

Although the basic properties of friction have been common knowledge since ancient times, the first systematic understanding of friction was obtained during the fifteenth century by Leonardo da Vinci. Through careful experimentation he discovered the two main laws of friction and further observed that friction is less for smoother surfaces. Da Vinci's discoveries remained hidden in his codices and were rediscovered two centuries later by Amontons. In his paper of 1699, Amontons described the two main laws of friction:

- The frictional force is independent of the size of the surfaces in contact
- Friction is proportional to the normal load.

Coulomb friction

Friction between solid bodies provides the resistance to sliding when one body moves tangentially against another body. Frictional forces always develop in the direction to oppose the motion or impending motion. In the case where contact between bodies is along a pre-defined plane the friction is referred to as dry, contact or **Coulomb**, friction. The laws of solid friction are simple when they apply to two approximately flat surfaces; e.g. a fault, fracture or bedding plane as shown in Figure 16. The shear stress, τ, on a surface necessary to cause sliding, is linearly proportional to the normal stress, σ_n, acting on the surface. The coefficient of friction, μ_0, is a dimensionless proportionality constant relating the two aforementioned variables:

$$\mu_0 = \tau / \sigma_n. \tag{89}$$

A hundred years after Amontons formulated the laws of friction, Coulomb observed that the shear stress necessary to initiate sliding from a static condition is greater than that required to maintain sliding in the dynamic condition. That is, the coefficient of static friction, μ_0, is greater than the coefficient of dynamic, or mobile, friction, μ_m. Prior to slip occurring along the plane of contact the additional resistance to motion is the *cohesion* of the contact surface, S_0. As the relative velocity of the surfaces increases, the friction is also further reduced. Friction can be represented on a σ_n versus τ graph as shown in Figure 17. The function describing static friction is:

$$\tau = S_0 + \mu_0 \sigma_n \tag{90}$$

and that describing dynamic friction is:

$$\tau = \mu_m \sigma_n \tag{91}$$

In rock mechanics friction is generally measured in terms of the friction angle, ϕ_0. In the case of static friction:

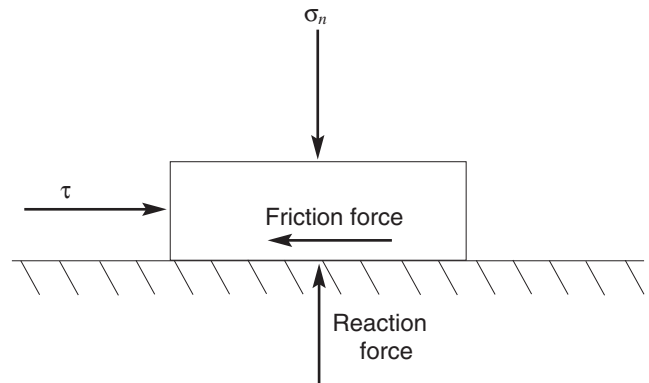$$\mu_0 = \tan \phi_0 \tag{92}$$

and in the dynamic case:

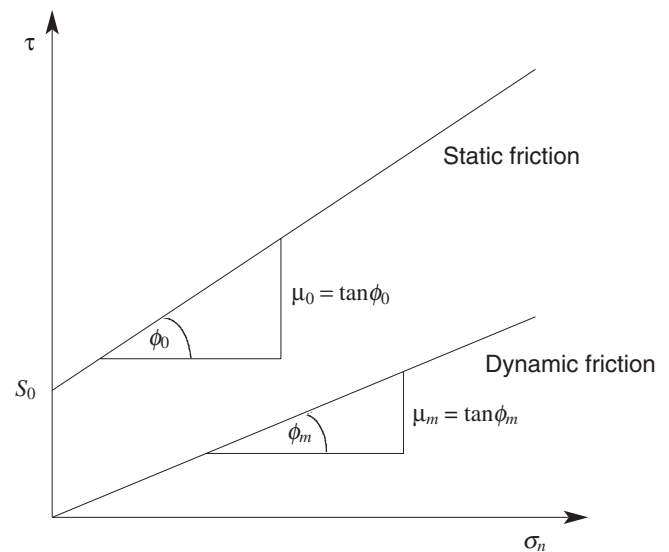**Figure 16. Coulomb frictional force generated between two surfaces**

Figure 17. Graphical representation of static and dynamic friction for a predefined plane of weakness

ROCK ENGINEERING FOR UNDERGROUND COAL MINING

$$\mu_m = \tan \phi_m \tag{93}$$

Since the coefficient of static friction is greater than or equal to the coefficient of dynamic friction, $\phi_0 \geq \phi_m$. This is also shown in Figure 17.

Internal friction

When an intact rock sample is subjected to external forces, friction is present. In this case friction is referred to as **internal friction**. The relationships governing Coulomb friction are also valid for internal friction. That is:

$$\tau = C + \mu\sigma_n \tag{94}$$

where C is the cohesion of the rock and μ is the internal coefficient of friction. (The cohesion of the rock mass is not to be confused with the uniaxial compressive strength of the rock, σ_c). Furthermore, the angle of internal friction, ϕ, is related to μ by:

$$\mu = \tan \phi \tag{95}$$

Internal friction, which is generally greater than contact friction, can be represented in Mohr stress space as shown in Figure 18.

Rock strength and failure criteria

Understanding the strength of a jointed rock mass is an area of major uncertainty for the mining engineer. The most common approach to the failure of materials is to postulate a mechanism of failure and then find the combination of physical stresses that cause failure by this mechanism. This can be done in two different ways. The first is to propose a fundamental concept and then examine it for correctness and fit. In this way both the reason and the criterion are developed and
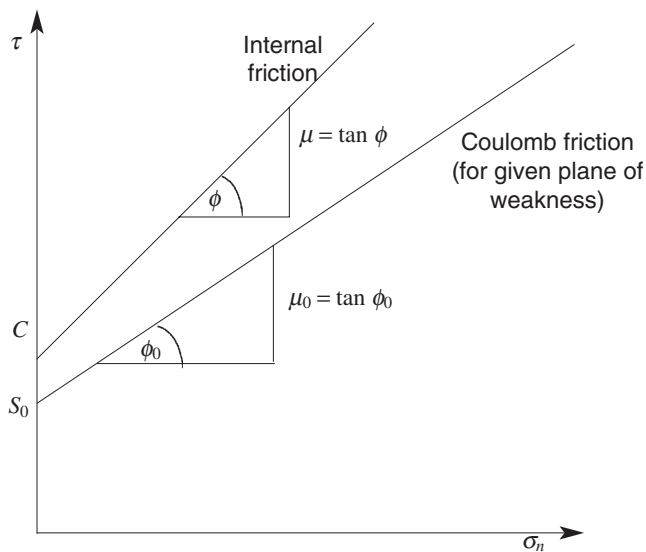

Figure 18. Comparison between Coulomb friction and internal friction in Mohr stress space

failure is fully explained. The second way is empirical and attempts to describe the stress environment at failure without necessarily explaining why failure takes place. The two failure criteria documented in the following sections fall into this second category. In this context, failure criteria are empirical equations that link the limiting combinations of stress components, separating acceptable from inadmissible conditions. Inadmissible stress conditions are those that a rock mass cannot sustain because it will yield or fail before they are reached.

Mohr-Coulomb failure criterion

Prior to investigating the Mohr-Coulomb failure criterion, it is necessary to review the Mohr circle diagram as it forms an integral part of this failure criterion.

Mohr circle diagram

The state of stress at a point in a two-dimensional body can be represented graphically using the **Mohr**

Adhesion theory of friction

The modern concept of friction is generally attributed to Bowden and Tabor's adhesion theory developed during the 1950s and 1960s (Scholtz, 1990). According to this theory all real surfaces have topography, so that when they are brought together they only touch at a few points, or asperities. The sum of all such contact areas, A_r, is generally much smaller than the apparent, or geometric, area (A) of the contacting surfaces. When the two surfaces are placed in contact yielding occurs at the contacting asperities until the contacting area is just sufficient to support the normal load N, thus

$$N = pA_r \tag{96}$$

where p is the penetration hardness, a measure of the strength of the material. They then supposed that, due to the very high compressive stress at the contact points, adhesion occurred, welding the surfaces together at these points. To accommodate slip, these welded points have to be sheared. Thus the friction force, F is the sum of the shear strengths of the welded points,

$$F = sA_r \tag{97}$$

where s is the shear strength of the material. Combining Equations [96] and [.97], friction can be described using a single parameter, the coefficient of friction, μ,

$$\mu \equiv F / N = s / p \tag{98}$$

These results are elegantly simple and Equation [96] satisfies both of Amonton's laws.

Although the adhesion theory of friction conceptualizes the physical essence of the frictional interaction, in most cases it does not predict the correct value for μ. This is because overcoming weld point adhesion is usually not the only work done in friction. Asperities often plough through the adjacent surface, or interlock, requiring additional deformation that is not specified in Equation [97]. (After Scholtz, 1990.)

circle diagram. In some texts the Mohr circle diagram is referred to as the Mohr stress circle. The Mohr circle is plotted on Cartesian axes where the x axis represents values of normal stress (σ_n), and the y axis represents values of shear stress (τ) with the positive axis directed downwards. The co-ordinates of each point on the Mohr circle represent, at a glance, the values of the normal and shear stress components acting across a plane at an arbitrary orientation.

Construction of the Mohr circle diagram is illustrated in Figure 19. The state of stress in a small element *abcd* is specified, relative to the (x, y) axes, by the known values of σ_{xx}, σ_{yy}, σ_{xy} as shown in Figure 19(a). The **diameter** of the Mohr circle is obtained by plotting the points (σ_{xx}, σ_{xy}) and (σ_{yy},$-\sigma_{xy}$), and joining them. The point where this line intersects the σ_n axis is the centre of the Mohr circle. With 0 as the origin of the (σ_n,$c\tau$) o-ordinate system, the following quantities of stress can be plotted as shown in Figure 19(b):

$$\overline{0C} = \tfrac{1}{2}\left(\sigma_{xx} + \sigma_{yy}\right) \qquad [99]$$

$$\overline{CD} = \tfrac{1}{2}\left(\sigma_{xx} - \sigma_{yy}\right) \qquad [100]$$

$$\overline{DF} = -\sigma_{xy} \qquad [101]$$

In the circle diagram construction, if σ_{xy} is positive, the point F plots above the σ_n axis. Construction of the line FDF′ returns values of $\tau = \sigma_{xy}$ and $\sigma_n = \sigma_{xx}$ which are the shear and normal stress components acting on the surface *cb* of the element. Suppose the surface *ed* in Figure 19(a) is inclined at an angle θ to the negative direction of the y axis. In the circle diagram, the line FG is constructed at an angle θ to FDF′, and the normal GH constructed. The distances 0H and HG represent the normal and shear stress components on the plane *ed*. A further useful application of the Mohr circle is that the distances 0S$_1$ and 0S$_2$ represent the magnitudes of the major and minor principal stresses, σ_1 and σ_2. The line FS$_1$

defines the orientation of the major principal plane, so FS$_2$, that is perpendicular to FS$_1$, represents the orientation of the major principal axis. Hence, the angle α_1 gives the orientation of σ_1. Finally, the maximum shear stress, $\sigma_{xy(max)}$, can be obtained by measuring the shear stress at the top of the circle (see Figure 19(b)).

Mohr circle diagrams can also be constructed to represent the strain at a particular point within a material. In this case the horizontal axis represents normal strain, ε_n, and the vertical axis represents shear strain, $\tfrac{1}{2}\gamma$. As a consequence of the correspondence principle relating stress and strain ($\sigma \Rightarrow \varepsilon$ and $\tau \Rightarrow \tfrac{1}{2}\gamma$), the construction of, and results obtained from, a Mohr strain circle are analogous to those for the Mohr stress circle. This theory however, does not match experimental data except under certain conditions.

In 1776 Coulomb postulated that the shear strengths of rock and soil are made up of two parts—a constant cohesion and a normal stress-dependent frictional component. That is, he postulated that failure will occur where the maximum shear stress reaches the constant cohesion, or inherent shear strength of the material (*C*). The internal shear strength of a material is not the same as the uniaxial compressive strength of a material (discussed earlier). (At the time, Coulomb presented his ideas in terms of forces since the concept of stress, as we know it, was only introduced in the 1820s by Cauchy.) The Mohr-Coulomb failure criterion is empirical and assumes that rock will fail in shear. This criterion is also known as the Navier-Coulomb failure criterion, because Navier modified Coulomb's theory by assuming that the normal stress across the plane of failure increases the shear resistance of the material by an amount proportional to the magnitude of the normal stress. The criterion consists of a line touching all the circles on a Mohr diagram, representing critical combinations of principal stresses as shown in Figure 20. This line is called the **Mohr**, or **Mohr-Coulomb**, **failure envelope** and is described by the following empirical relationship:

$$\tau = \sigma_n \tan\phi + C \qquad [102]$$

where *C* is the static or initial cohesive strength and ϕ is the angle of internal friction (it describes the rate of increase of peak strength with normal stress). Cohesive strength is usually quoted in megapascals (MPa) and the angle of friction in degrees. The true tensile strength of rock is usually less than the Coulomb tensile strength, the point where the Mohr-Coulomb failure envelope intersects the σ_n axis. Consequently, a tensile cut-off has been introduced as shown in Figure 20. According to the Mohr-Coulomb
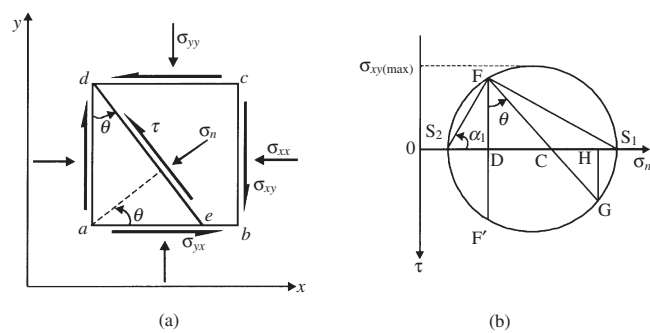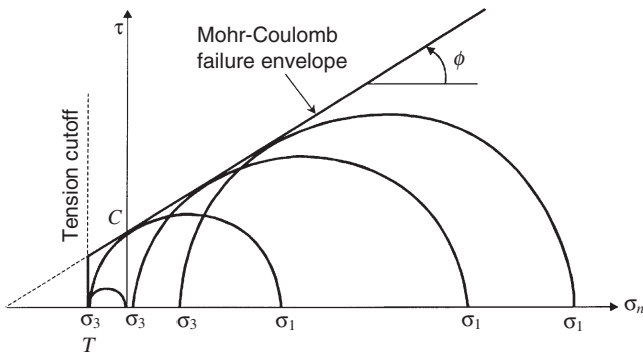

Figure 19. Construction of a Mohr circle diagram for an element (depicted in (a)) using the geomechanics convention of stresses

Figure 20. The Mohr-Coulomb failure criterion with a tension cut-off

Figure 21. The Mohr-Coulomb failure criterion showing (a) a Mohr circle that lies below the failure envelope and therefore represents a stable stress state, (b) a Mohr circle that intersects the failure envelope and thus represents an unstable or inadmissible stress state, and (c) a Mohr circle that is tangent to the failure envelope and represents the state of stress at the instant of failure

failure criterion, the strength of a rock material can be fully defined if, C, ϕ and the tensile strength cut-off T are known.

An advantage of this failure criterion is that it takes into account the increase in rock strength due to the presence of confining stresses.

The Mohr-Coulomb failure criterion can be used to compare calculated stress states with estimated rock strength. If the Mohr circle lies below the Mohr-Coulomb failure envelope (Figure 21(a)) then, according to its estimated strength, the rock will remain intact, but, if it crosses the failure envelope (Figure 21(b)) then the rock will fail. If the Mohr circle touches the failure envelope (Figure 21(c)), that is it is tangent to it, then the rock is at the transition between remaining intact and failing. At this point the potential for rock mass failure has a safety factor of one.

The Coulomb failure criterion can also be written in terms of the uniaxial compressive strength of the material, σ_c, and the principal stresses σ_1 and σ_3 as shown in Equation [103]:

$$\sigma_1 = \sigma_c + q\sigma_3 \qquad [103]$$

where

$$q = \frac{1 + \sin\phi}{1 - \sin\phi} \qquad [104]$$

and

$$\sigma_c = 2C\sqrt{q} \qquad [105]$$

Although widely used, Coulomb's criterion is not a particularly satisfactory peak strength criterion for rock material (Brady and Brown, 1985). The reasons for this are:

- It implies that a major shear fracture exists at peak strength. Observations show that this is not always the case
- It implies a direction of shear failure that does not

always agree with experimental observations
- Experimental peak strength envelopes are generally non-linear. They can be considered linear only over limited ranges of σ_n or σ_3.

For these reasons, other peak strength criteria are preferred for intact rock. The Coulomb criterion can, however, provide a good representation of residual strength conditions of fractured rock and the shear strengths of geological discontinuities in rock. This aspect of the Coulomb criterion is commonly used in the computation of excess shear stress on faults and dykes.

Hoek and Brown failure criterion

Using a method of experimentation, Hoek and Brown (1980a) derived an empirical failure criterion in terms of the major and minor principal stresses at failure. The empirical relationship derived is:

$$\sigma_1 = \sigma_3 + \sqrt{m\sigma_c\sigma_3 + s\sigma_c^2} \qquad [106]$$

where σ_1 and σ_3 are the major and minor principal

stresses at failure and σ_c is the uniaxial or unconfined compressive strength of the rock. The value of σ_c is obtained from laboratory tests carried out on prepared rock samples. The constants m and s are dimensionless empirical constants that have no fundamental relationship with any physical characteristics of the rock. The constant m always has a finite positive value that ranges from about 0.001 for highly disturbed rock masses, to about 25 for hard intact rock. The value of the constant s ranges from 0 for jointed masses, to 1 for intact rock material. As with the Mohr-Coulomb failure criterion, the Hoek and Brown failure envelope is also plotted using Cartesian co-ordinates but in this case σ_1 is plotted on the y axis and σ_3 on the x axis.

Substitution of $\sigma_3 = 0$ and $s = 1$ into Equation [106] gives the uniaxial compressive strength of a rock mass as:

$$\sigma_1 = \sigma_c \qquad [107]$$

Similarly, substituting $\sigma_1 = 1$ in Equation [107] and solving the resulting quadratic equation for σ_3 gives the uniaxial tensile strength of the rock mass as:

$$\sigma_3 = T = \tfrac{1}{2}\sigma_c(m - \sqrt{m^2 + 4s}) \qquad [108]$$

The physical significance of Equations [106], [107] and [108] is illustrated in Figure 22. It is possible to represent the Hoek and Brown failure envelope using Mohr circles (see Figure 23).

Beams and plates

Generally, when an opening is excavated in laminated rock, the roof forms at a plane of weakness that is relatively smooth and flat. Due to the weak bond between laminae, the immediate roof rock becomes detached from the overlying rock, forming a layer or number of layers that are loaded only by gravity. From a mechanical point of view, the detached roof rock acts as a beam or plate. Thus, an appreciation of the deflections and stresses associated with beams and plates is essential for the design of openings in, and the support of, a laminated rock mass.

A beam is a straight structural element with a length that is at least eight times its thickness. A plate is a straight, flat structural element with a width that is at least four times its thickness and with a length equal to, or greater than, its width. Also, by definition, a laminated rock is composed of a succession of parallel layers whose thickness is small compared with the span of openings therein. The layers comprising a laminated rock are either unbonded or the bond strength between them is small compared with the tensile strength of the rock. In this context, a layer is

defined by the nature of bonding with adjoining units rather than by the lithology.

Deflections and stresses on a clamped beam

Consider a beam of length L with clamped ends that is composed of a perfectly elastic material and loaded only by its own weight and the weight of the superincumbent rock mass. When such a beam is bent the top of the beam will be in compression, the bottom of the beam in tension, and the neutral plane will be unstrained (see Figure 24). Furthermore, at the ends of the beam both the deflection and the slope of the neutral plane are zero.

Suppose that the beam described above has a rectangular cross-section of width b and thickness t (see Figure 24), and that the distributed load results
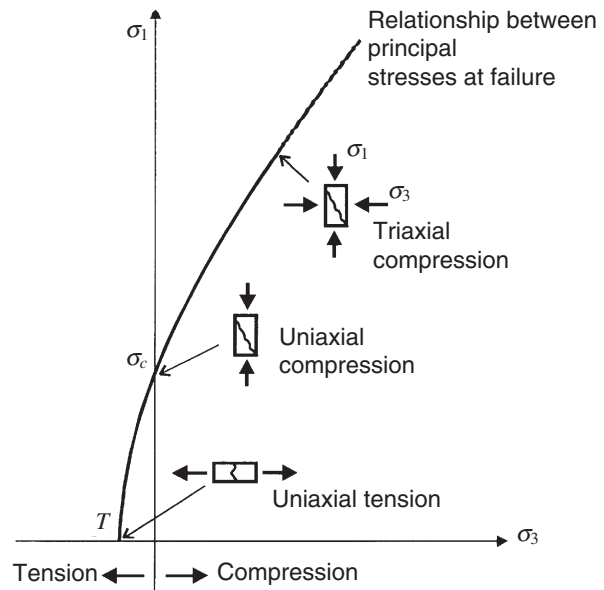

Figure 22. Graphical representation of stress conditions for failure of intact rock in (σ_1,σ_3) space (after Hoek and Brown, 1980)
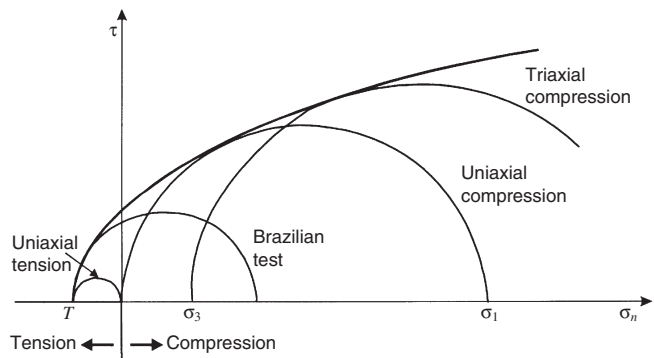

Figure 23. Representation of the stress conditions depicted in Figure 22 using a Mohr circle diagram (after Hoek and Brown, 1980)
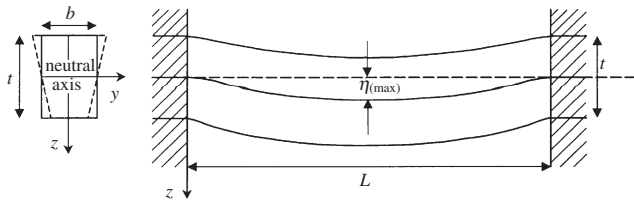
ROCK ENGINEERING FOR UNDERGROUND COAL MINING

Figure 24. Nomenclature for a clamped beam

only from the weight of the beam. Thus q, the load per unit length is:

$$q = \gamma bt \qquad [109]$$

where γ is the unit weight. In this case the use of the symbol γ must not be confused with shear strain. The maximum deflection at the centre of the beam, the maximum shear stress at the ends of the beam, and the maximum normal stress at the ends of the beam are given by Equations [110], [111] and [112] respectively:

$$\eta_{(max)} = \frac{\gamma L^4}{32Et^2} \text{ (Maximum Deflection)} \qquad [110]$$

$$\tau_{xz(max)} = \frac{3\gamma L}{4} \text{ (Maximum Shear Stress)} \qquad [111]$$

$$\sigma_{x(max)} = \frac{\gamma L^2}{2t} \text{ (Maximum Normal Stress)} \qquad [112]$$

where E is Young's modulus of the rock mass comprising the beam.

Multiple clamped beams

Consider an excavation in a layered rock mass where the roof comprises two beams of equal length and width, with their ends clamped together. Under these circumstances there are two cases to consider depending upon whether the beams remain in contact or not. If the beams do not remain in contact, as shown in Figure 25(a), then each beam acts independently and Equations [110] to [112] can be used to calculate the maximum deflection at the centre of the beam, the maximum shear stress and the maximum normal stress at the ends of the beam, respectively. If however, the beams do remain in contact, as depicted in Figure 25(b), the top beam will load the lower beam and conversely the lower beam will partially support the top beam.

In the case where the two beams remain in contact each beam has its own neutral plane, and cross-sections of each beam rotate about their own neutral axis, thus causing slippage on the plane between the beams (see Figure 25(b)). To calculate the additional load and/or support of the beams the following assumptions are made:

- the coefficient of friction between the two beams is zero
- the deflections of the two beams are equal
- the upper beam loads the lower beam with a uniform load per unit length of beam, and
- the lower beam supports the upper beam with an equal load per unit length.

Since the deflections of the two beams are equal, the additional load or support, Δq, to be added to the lower and subtracted from the upper beam is given by:

$$\Delta q = \frac{q_2 E_1 I_1 - q_1 E_2 I_2}{E_1 I_1 + E_2 I_2} \qquad [113]$$

where I is moment of inertia and the subscripts 1 and 2 stand for the lower and upper beam respectively. If the beams are rectangular of width b and thickness t, then the loads per unit length, q, and the moments of inertia of the cross-section, I, for each beam are:

$$q_1 = \gamma_1 bt_1 \qquad [114]$$

$$q_2 = \gamma_2 bt_2 \qquad [115]$$

$$I_1 = \frac{1}{12} bt_1^3 \qquad [116]$$

$$I_2 = \frac{1}{12} bt_2^3. \qquad [117]$$

When the upper beam loads the lower beam, the lower beam in turn supports the upper beam and each beam deflects as if its load per unit length is equal to the average load per unit length of the two beams. The weighted average unit weight of the two beams, $\overline{\gamma}$ weighted by the thickness of each beam is given by:

$$\overline{\gamma} = \frac{\gamma_1 t_1 + \gamma_2 t_2}{t_1 + t_2}. \qquad [118]$$

Also, the weighted average value of Et^2 for both beams, $\overline{Et^2}$, weighted by the thickness of the beams is calculated using the following equation:
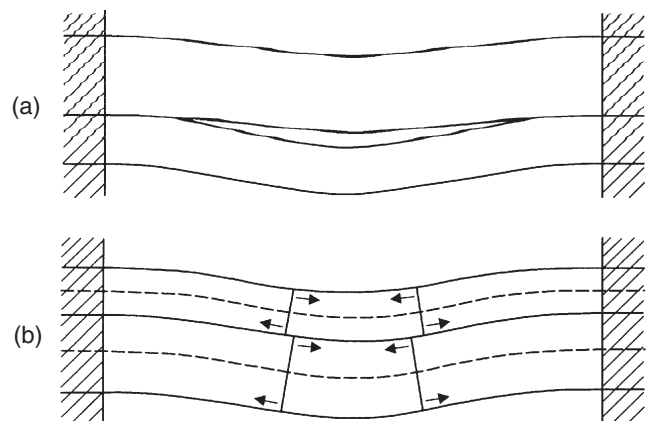

Figure 25. Multiple beams with built-in ends

$$\overline{Et^2} = \frac{E_1 t_1^3 + E_2 t_2^3}{t_1 + t_2} \qquad [119]$$

Equations [118] and [119] can be substituted into Equations [110], [111] and [112] enabling the calculation of the maximum deflection, the maximum shear stress and maximum normal stress for two gravity-loaded rectangular beams.

This procedure can be extended to any number of beams provided that each beam rests upon the beam below. The quantities $\overline{\gamma}$ and Et^2 for k beams are given by:

$$\overline{\gamma} = \frac{\sum_i^k y_i t_i}{\sum_i^k t_i} \qquad [120]$$

$$Et^2 = \frac{\sum_i^k E_i t_i^3}{\sum_i^k t_i}. \qquad [121]$$

Inertia and moment of inertia

The fact that a body stays at rest or retains its uniform linear motion in the absence of an applied force is known as Newton's first law of motion and is often called the law of inertia. **Inertia** is a passive property that does not enable a body to do anything except oppose active agents such as forces and torques. There are two numerical measures of the inertia of a body: its mass, which governs its resistance to the action of a force, and its moment of inertia about a specified axis, which measures its resistance to the action of a torque about the same axis.

Torque is the measure of the ability of a force to cause a body to rotate. A rigid body is in rotational equilibrium when there is no net torque acting on it.

The moment of inertia, or rotational inertia, is dependent on the shape and mass of the body as well as the position of its axis of rotation. The **moment of inertia** for a point mass is given by:

$$I = mr^2 \qquad [122]$$

To calculate the moment of inertia for a complex object, the object needs to be separated into N small pieces of mass $m_1, m_2, ..., m_N$ such that each piece is a distance $r_1, r_2, ..., r_N$ from its axis of rotation. The moment of inertia for the first piece is $m_1 r_1^2$ that for the second is $m_2 r_2^2$, and so on. The net moment of inertia is the sum of all such terms:

$$I = m_1 r_1^2 + m_2 r_2^2 + ... + m_N r_N^2$$
$$= \sum_1^N m_i r_i^2 \qquad [123]$$

In the limiting case the moment of inertia is calculated by taking the integral over the whole body;

$$I = \int r^2 dm. \qquad [124]$$

From Equation [123] or [124] it is clear that as the distance between the mass and the rotational axis increases so does the moment of inertia of the body.

Rectangular plates

A plate is essentially a beam where the width is equal to or greater than the length. As this is the case, the dimension of a beam referred to as the length is known as the width of a plate. Conversely, the width of a beam is referred to as the length of a plate.

Consider a thin rectangular plate of length b, width a, and thickness t with built-in edges on all sides supporting a uniformly distributed load. The maximum deflection occurs at the centre of the plate and is given by:

$$(\eta)_{max} = \alpha \frac{qa^4}{Et^3}. \qquad [125]$$

The maximum normal stress at the middle of the longer side is:

$$(\sigma_x)_{max} = 6\beta \frac{qa^2}{t^2}. \qquad [126]$$

In both these equations $q = \gamma t$ is the load per unit area of the plate and α and β are variables dependent upon the Poisson's ratio of the rock mass comprising the plate, see Table III.

For a gravity-loaded plate with built-in edges whose ratio of length-to-width is two or less (i.e. $b/a \leq 2$), Equations [125] and [126] should be used to calculate the maximum deflection and stress. However, if $b/a > 2$, Equations [110] to [112] for the simple beam may be used without introducing appreciable error.

State of stress in the rock mass

It is generally accepted that, prior to the excavation of underground openings, the rock mass is in equilibrium under the action of virgin stresses. When an unsupported excavation is made, the stresses on the surface of the opening are reduced to zero. The consequence of this change in stress condition is that the stresses within the rock mass are redistributed. A

Table III
Coefficients for Uniformly Loaded Plates, $v = 0.3$
(After Obert and Duvall, 1967)

b/a	1.00	1.25	1.50	1.75	2.00	>>>>
α	0.0138	0.0199	0.0240	0.0264	0.0277	0.0284
β	0.0513	0.0665	0.0757	0.0806	0.0829	0.0833

similar redistribution of the stresses takes place when an excavation is enlarged.

Virgin stress

The natural or undisturbed state of stress existing in a rock mass prior to the introduction of any mining excavations is termed the **virgin stress**. The virgin stress is the result of the weight of the overlying rock mass and any loading that may have been imposed as a result of geological processes.

In a homogeneous, geologically undisturbed, rock mass, the vertical component of the virgin stress (σ_{zz}) is the result of the depth (z) multiplied by the weight of the rock mass (ρg) i.e.:

$$s_{zz} = \rho g z$$

where ρ is the density of the rock mass and g is the acceleration due to gravity.

In an undisturbed rock mass, the horizontal components of stress are generally equal and are a direct function of the overburden thickness. The ratio of vertical stress to horizontal stress is termed the **k ratio**, such that:

$$\sigma_{xx} = \sigma_{yy} = k\sigma_{zz}. \tag{127}$$

The value of k is controlled by the Poisson's ratio of the rock mass; the amount of horizontal stress that can be developed in the rock is a function of the vertical compression and horizontal confinement:

$$k = \frac{v}{1-v}. \tag{128}$$

In solid mechanics, this is termed the **Poisson effect**. As the Poisson's ratio for most rocks lies between just under 0.2 and just over 0.33, the k ratio for linear elastic rock masses must lie between 0.25 and 0.5 in most cases. Due to geological factors, however, the k-ratio is generally >0.5 at shallow depth.

If the rock mass behaves in a plastic or visco-plastic manner, then the horizontal stresses tend to equalize to the vertical stresses. That is, k tends towards 1.0.

Induced and resultant stresses

Under natural circumstances the stress in a rock mass is in a state of equilibrium. If an excavation is to be made in the rock mass, then it is possible to consider that, immediately prior to the excavation, the rock in its interior provides support to the surrounding rock mass that maintains this equilibrium state (Figure 27(a)). In other words, the resultant force at the proposed excavation boundary must be zero.

Once the excavation has been made the stresses acting normal to its boundary are zero and the original equilibrium state is disturbed. The rock mass around the excavation boundary will displace as a result of

this disturbance and the stresses will be redistributed. Ultimately (instantaneously in the elastic case) the stresses will re-equilibrate and a new equilibrium state will occur. In this new equilibrium state there must be a new stress acting—that equals, but opposes—the stress that the original excavated rock mass imposed to support the surrounding rock mass: this is the induced stress. In other words, in order to maintain equilibrium in the excavated state the induced stress must be superimposed on the virgin stress (Figure 27(b)). In the new equilibrium state the final stress is called the resultant stress. Figure 26 illustrates the relationship between virgin stress, induced stress and resultant stress in Mohr stress space where τ represents the applied shear stress and σ_n the applied normal stress.

It is clear that the displacements associated with excavating rock are the result of the induced stress. As such, they are termed induced displacements. The induced displacements are responsible for induced stresses that act to stress or damage the rock mass.

Tectonic stress

In addition to the normal overburden or virgin stress found in unmined rock, there may exist tectonic and residual stresses. **Tectonic stresses** are the result of geological processes, such as faulting and the intrusion of dykes. Such occurrences are generally the result of crustal disturbance and may also involve crustal warping and folding.

Residual stress

Residual stress is the term commonly applied to stresses that remain in the rock mass after the cause has been removed. Residual stress is the result of a

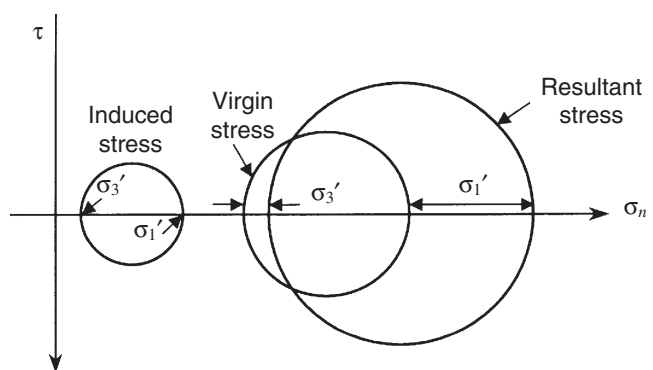**Figure 26. Mohr stress diagram illustrating the relationship between virgin stress, induced stress and resultant stress where τ represents the applied shear stress and σ_n the applied normal stress. The principal stresses, σ_1 and σ_3 used in the construction of the induced stress circle are the difference between the principal stresses for the resultant and virgin stresses as shown in the Figure**
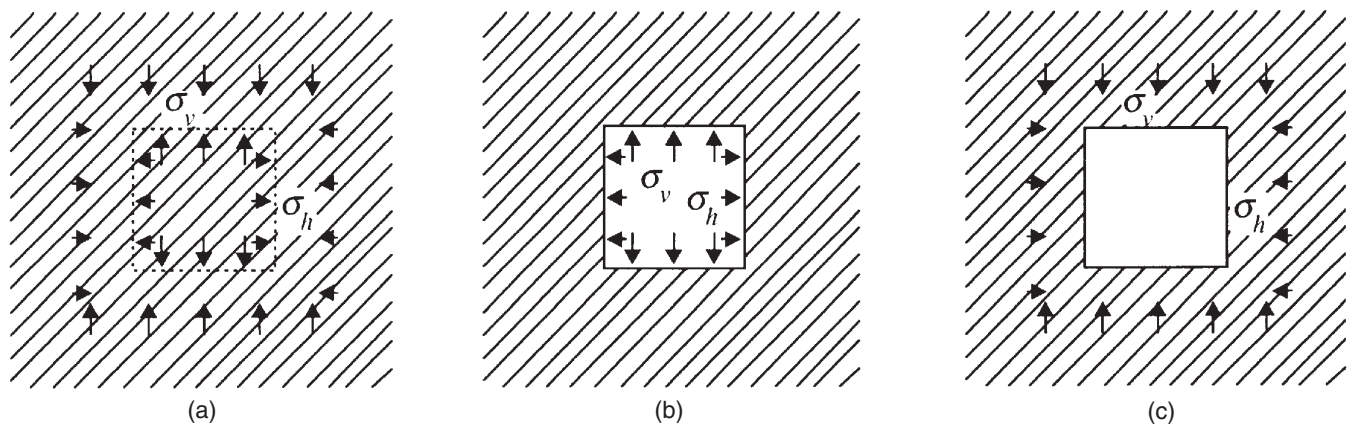
Figure 27. (a) Virgin, (b) induced and (c) field stresses for a rectangular opening (from Budavari, 1982)

previous loading history and the ability of rock mass granules to remain strained without undergoing a process of full relaxation. Budavari (1982) cites the example of residual stresses found in the North American plate. During the ice ages, the continent was covered by a thick layer of ice and snow. This added overburden resulted in an induced vertical stress that was greater than that resulting from the existing rock mass alone. At the close of the ice age the loading from the snow and ice was removed, however, the rock mass remained in a state of permanent strain. The effect of this locked-in stress is often encountered when making shallow to moderate depth excavations.

Field stress

The field stress is the sum of all the stresses discussed so far. In a mining area the **field stress** is the sum of the overburden, or virgin, stress, the tectonic stress, and the induced stress (Figure 27(c)). In general, the field stress is the state of stress with which the rock engineer is concerned. The **induced stress** is the amount by which the stress state is going to change as a result of any mining excavations. Tectonic stresses are difficult to compute theoretically; the only way to determine tectonic stresses is by field measurement.

Plasticity

Thus far, the concepts presented in this chapter have assumed that the rock mass behaves in an elastic manner. In reality, however, rock only exhibits elastic behaviour until a certain strain is reached, beyond which it ceases to behave elastically. The stress level at which this departure occurs is referred to as the **yield stress**, or **yield strength**, denoted by σ_0. Beyond this point the material is subjected to permanent or non-recoverable deformation, generally known as damage. Once the yield stress has been exceeded, a rock mass can deform in a number of different ways depending on both its physical properties and environmental conditions. It can either fail in a brittle manner or deform plastically (see the following Sections). At low confining pressures rock tends to behave as a brittle material. However, when the confining pressure approaches a rock's brittle strength, a transition from brittle or elastic behaviour to plastic behaviour occurs.

Brittle failure

Brittle failure is the process by which sudden loss of strength occurs across a plane following little or no permanent deformation. That is, it fractures suddenly; losing cohesion and can no longer support the stress (see Figure 28). The deformation resulting from brittle failure is irrecoverable.

Fracture is the formation of planes of separation in the rock material. It involves the breaking of bonds to form new surfaces. (The onset of fracture is not necessarily synonymous with failure or with the attainment of peak strength as will be seen later in this section.)

Plastic deformation

Prior to investigating the implications of plastic deformation, it is necessary to review the concept of plasticity. The word plastic is derived from a Greek word with the meaning 'to mould'.

A **perfectly plastic** substance is characterized by the assumption that the stress causing the permanent, non-recoverable strain must reach a certain value before any extension or contraction can take place. When the yield stress, σ_0 is reached the substance deforms permanently and continues to yield at this stress without fracture. The stress-strain curve for a perfectly plastic material sample is depicted in Figure 29.
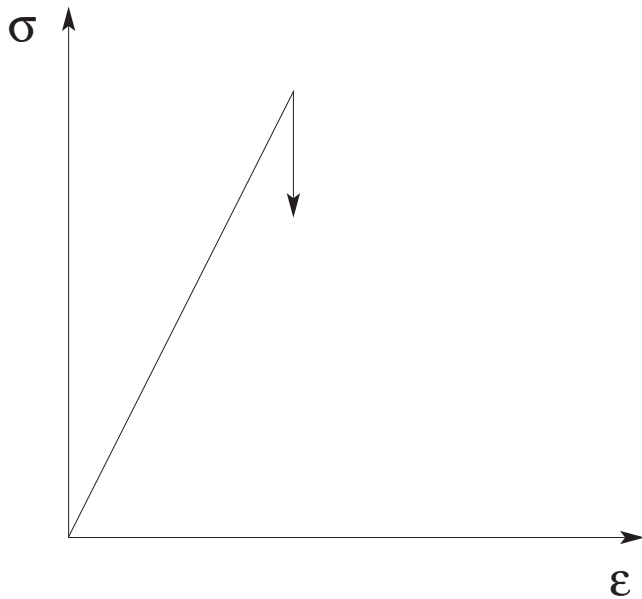
ROCK ENGINEERING FOR UNDERGROUND COAL MINING

Figure 28. Elastic deformation followed by brittle failure; note that failure is indicated by a sudden stress drop
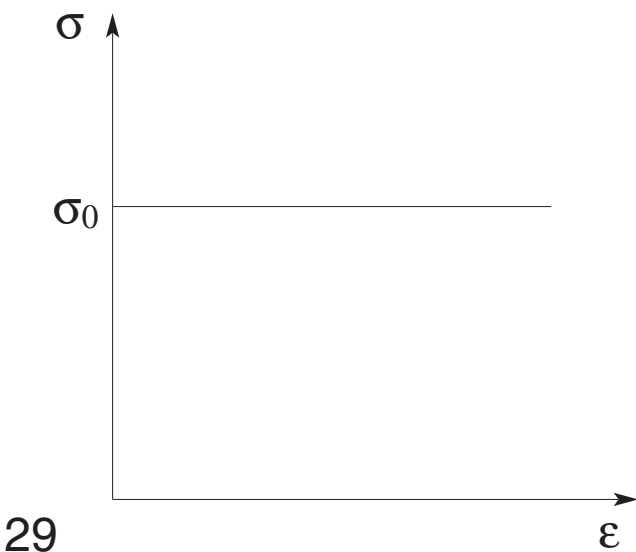

Figure 29. Stress-strain curve for a perfectly plastic material where σ_0 is the yield stress

There are three different modes of plastic deformation that a rock mass may exhibit; elastic perfectly-plastic, strain hardening, or strain softening, depending upon the slope of the stress-strain curve beyond the yield stress. If the curve still has a positive slope beyond σ_0, the rock is said to exhibit strain hardening during deformation. However, if the curve has a negative slope beyond σ_0, the rock exhibits strain softening.

Since rock tends to deform elastically, and then plastically, it can be said that rock exhibits composite behaviour. Using the properties of the two basic materials defined, those of an elastic material and a plastic material, a material with composite properties can be defined and its constitutive equations derived.

Elastic perfectly-plastic material behaviour

The simplest composite material is that which exhibits **elastic perfectly-plastic behaviour**. Such materials behave elastically for stresses less than the yield stress, then deform without limit at the yield stress. The stress-strain curve of an elastic perfectly-plastic material is shown in Figure 30. On loading, the material follows the stress-strain path ABC. Along the section AB the linear elastic relation $\sigma = E\varepsilon$ (Equation [5]) applies. On BC; $\sigma = \sigma_0$, and ε can be arbitrarily large. At this point the total strain is the sum of elastic strain (ε^E) and the plastic strain (ε^P), that is:

$$\varepsilon = \varepsilon^E + \varepsilon^P.$$ [129]

Upon unloading, the material behaves elastically in a manner unaffected by the plastic flow; that is, it follows path CD, which is parallel to AB. When the applied stress is reduced to zero, the elastic strain $\varepsilon^E = \sigma_0/E$ is recovered, but the plastic strain AD, which is equal to BC, is unrecoverable.

In a mining environment, rock does not behave in an elastic perfectly-plastic manner. However, rocks in the Earth's mantle, that are subjected to temperatures and confining pressures of the order of 800°C and 500 MPa, respectively, do tend to follow an elastic-perfectly plastic deformation curve.

Strain softening

The stress-strain curve for a sample undergoing strain softening is shown in Figure 31. When the rock has exceeded its elastic limit (the stress has exceeded σ_0), it yields by fracture without losing all cohesion. It then continues to yield until the strength or **peak strength** of the rock is reached as shown in Figure 31. This is the maximum stress that can be sustained by a rock before it begins to fail. Thereafter it is subjected to strain softening. During strain softening either the cohesion or internal friction angle, or both, are reduced, but the specimen still has some load carrying capacity. The minimum, or **residual strength**, is generally reached only after considerable post-peak deformation (see Figure 31).

Strain hardening

A material is subject to **strain hardening** if, once the yield stress has been exceeded, the slope of the stress-strain curve remains positive. Figure 32 shows the stress-strain curve for a material that has experienced strain hardening. Each portion of this curve is defined by its own Young's modulus as shown in the Figure.
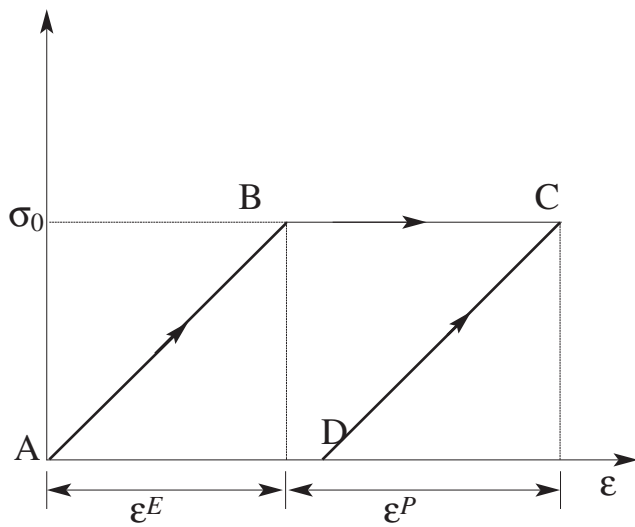
Figure 30. The stress-strain curve for an elastic perfectly-plastic material, where ε^E is the recoverable elastic strain and ε^P is the unrecoverable plastic strain

Figure 32. Stress-strain curve for a material sample subjected to strain hardening, where the first portion of the curve has a Young's modulus of E_1 and the second portion a Young's modulus of E_2
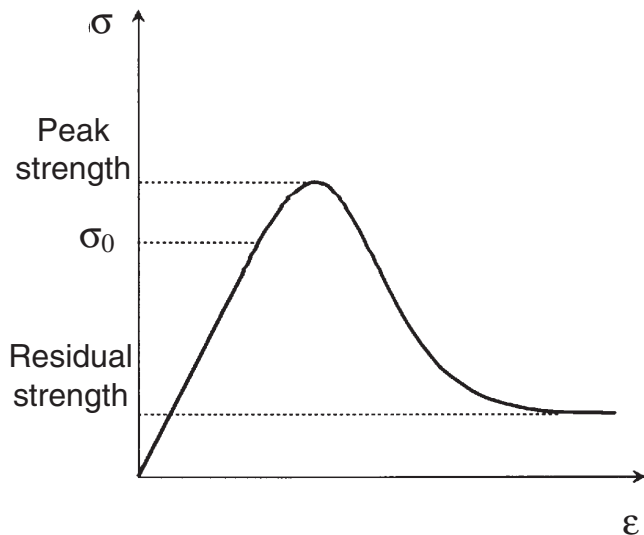

Figure 31. Stress-strain curve for a material sample subjected to strain softening with a residual strength

Ductile behaviour

Ductile deformation occurs in a material without loss of cohesion across a plane. A material is referred to as exhibiting ductile behaviour, if it is able to sustain a load while undergoing plastic failure. This is very rare in hard rock but is encountered in earthquake mechanics and, occasionally, in coal mining.

Continuum mechanics

Most descriptions of deformable solids are based on continuum theory. In **continuum theory**, the granular structure of the material is disregarded and is replaced by an equivalent continuum whose overall behaviour

is an approximation, in a mathematical sense, of the original material. As a consequence, the problems are solved in terms of the average displacement of points or elements in the material, rather than in terms of the displacement of the granules themselves. A continuous material body, thus, needs to be divided into a set of discrete volumes, areas, lines, or points, depending on the number of dimensions involved. This process of division is called **discretization**, and is a fundamental aspect of all numerical modelling methods. The continuum can be reconstructed by making each element infinitely small. The relevant constitutive equations are solved for each discrete entity, and not for the body as a whole. Through combining the effect of each discrete solution, the behaviour of the rock mass can be approximated and analysed.

In **finite element** numerical modelling codes, the continuum is approximated as a series of discrete elements connected to adjacent elements only at specific shared points called nodes (see Figure 33(a)). The behaviour of each element is then described individually using exact differential equations. The global behaviour of the material is modelled by combining all the individual elements.

In the case of a **finite difference** numerical technique, the material is considered to be a continuous medium, but the differential equations are approximated through the use of difference equations.

A discrete grid-point, or node, is allowed to displace as a result of applied forces. In general, the point or

(a)
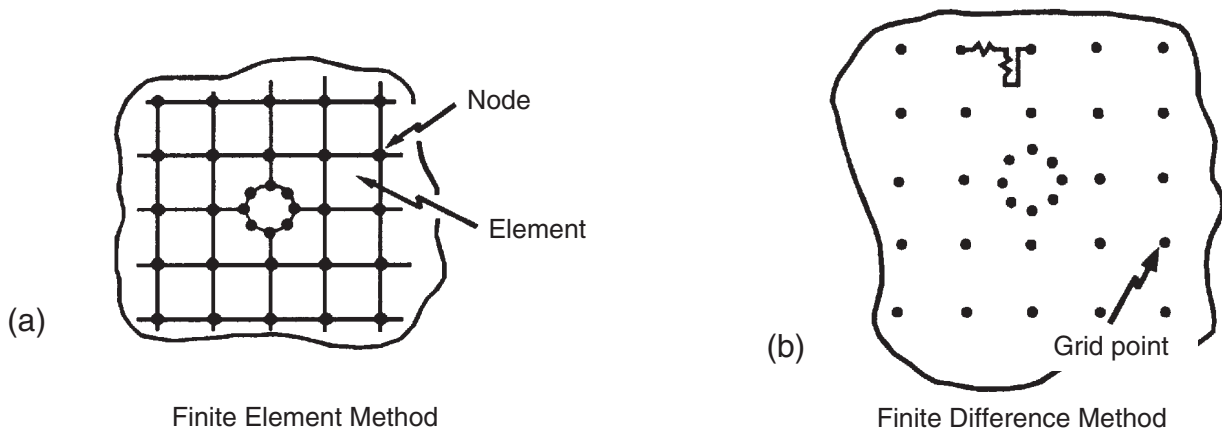
Finite Element Method

Approximate the continuum as a series of separate elements connected to adjacent elements only at their nodes.

(b)

Finite Difference Method

Approximate the differential equations as difference equations but maintain the continuity of the continuum.

Figure 33. Graphical representation of (a) the finite element and (b) the finite difference continuum analysis methods
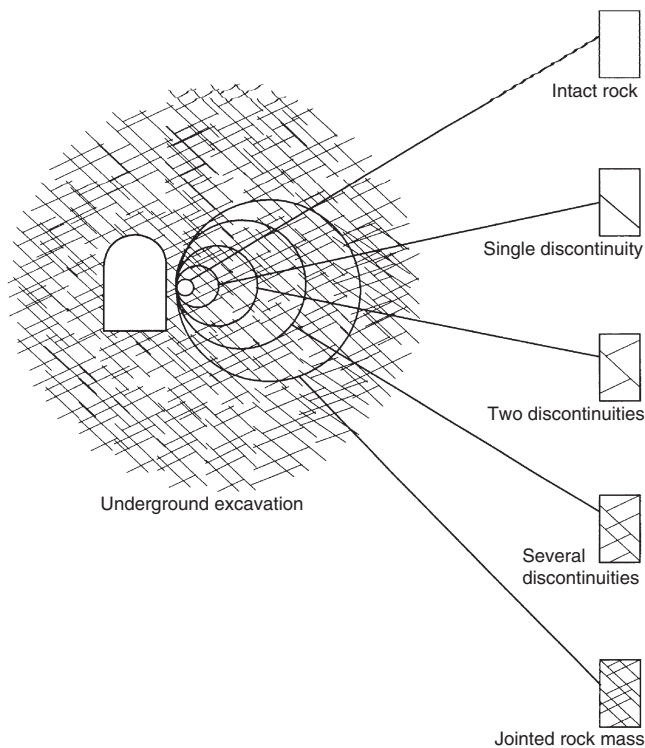
Figure 34. Idealized diagram showing the transition from intact rock to heavily jointed rock mass with increasing sample size (after Hoek and Brown, 1980)

node can only displace in a translational mode, but single points cannot rotate. In three dimensions, the translation can be along any of the three axes, x, y, or z. The three modes of translation are said to provide three degrees of freedom at that point. In two dimensions, the point can only translate in the x and y directions, and as such, is said to have two degrees of

freedom. The actual number of **degrees of freedom** in any discrete mesh is the product of the degrees of freedom at each point and the number of points. The more degrees of freedom a model has, the more flexible it is. Grid-points, or nodes, can be constrained in one or more degrees of freedom in order to prescribe, or control, specific behaviour.

Discontinuum mechanics

The discussion so far has concentrated on solid or continuum mechanics. In general, any large-scale discontinuities are ignored and the material between such features is treated as being completely continuous. In practice, however, this material is often fractured and jointed, and hence it is not truly a continuum at all. Brown (1987) describes a useful rock mass representation that incorporates scale to represent the effect of these fractures and joints (Figure 34). At one end of the scale (micro) the rock is truly intact and on such a scale can be represented as a continuum. At the other end of the scale (macro) the rock is so heavily jointed that it can be considered as a continuum that is governed by some non-linear, inelastic constitutive law to define its macro behaviour. Between the two extremes of the scale, however, the rock is fractured and jointed to varying degrees and cannot be described as either truly solid, or by some constitutive model. In the region between the extremes, the rock mass must be considered as a discontinuum.

Discontinuum mechanics is a field that lies beyond the scope of this text. Suffice it to say that, there are times when the discontinuous nature of the rock mass cannot be ignored, and to treat it as some form of

continuum misses the true governing processes controlling the behaviour of that rock mass. Such is the case when considering the stope-skin and support interaction in a deep-level excavation, where the rock mass is highly fractured, but forms discrete blocks on the same scale as the support itself. Attempting to model this jointed rock mass as a continuum could lead to misleading results.

Recommended further reading

BRADY, B.H.G and BROWN, E.T. *Rock Mechanics for Underground Mining*, George Allen and Unwin, London. 1985.

BROWN, E.T. (Ed.) *Analytical and Computational Methods in Engineering Rock Mechanics*, George Allen and Unwin, London. 1987.

BUDAVARI, S. (Ed.) *Rock Mechanics in Mining Practice*, Monograph Series M5, S. Afr. Inst. Min. Metall., Johannesburg. 1982.

GOODMAN, R.E. *Introduction to Rock Mechanics*, 2nd Edition, John Wiley & Sons, New York. 1989.

HEGERT, G. *Stresses in Rock*, A.A. Balkema, Rotterdam, Netherlands. 1988.

HOEK, E. and BROWN, E.T. *Underground Excavations in Rock*, The Institution of Mining and Metallurgy, London. 1980.

OBERT, L. and DUVALL, W.I. *Rock Mechanics and the Design of Structures in Rock*, John Wiley & Sons, Inc., New York. 1967.

Roof support

Introduction

The ideal process of supporting roof is to begin by determining the mode of roof failure in the specific circumstances; deciding how to prevent losses (i.e. accept rock failure but prevent the failed material from falling or prevent failure in the first place); designing a system; using the materials that will best perform the desired function; installing the system; and finally monitoring.

In this section, guidance will be given for the scientific design of support systems. Everything is based on simple, fundamental concepts that are sometimes slightly expanded. It is recognized that the rock is imperfect and highly variable in nature and that underground mining differs from desktop drawings. There is thus little point in, for instance, designing support spacing to the nearest millimetre.

The equations have been simplified as far as possible by inserting reasonable values for some of the constants. In this way, they are easier to handle, without distracting from their fundamental basis. While this argument justifies the simplified approach that is followed, it does not distract from the fact that all materials follow the basic laws of nature. It is therefore useful to perform some form of calculation, even in simplified form.

The suggested support design methods should be seen as first order methods, not final designs. The roof nature is too variable and the unknowns too many to even hope to deliver the correct and optimal design system with a desk calculation. The ideal design procedure is to investigate, gather the important information, design, implement, and then to monitor and adapt on a continuous basis. The loop is an iterative one: monitoring is part of the design process.

The terms 'competent beam' and 'competent layer' will often be used in this Appendix. In this context it refers to any rock layer or cemented sequence of laminated material that is comparable in strength and stiffness to a massive sandstone layer. Likewise, the term 'sandstone', should be understood to imply also any other rock layer with comparable qualities.

Throughout this section, some of the equations will be shown in simplified form, where some of the constants have been replaced by reasonable values, merely to reduce the level of intimidation of some of them. Where that has been done, the following constants were used:

σ_t = 5 MPa (Tensile strength)
F = 1.5 (Safety factor)
γ = 25 kN/m^3 (Unit weight of roof material)

The stress effects of creating a roadway

The first effect of creating an opening in the earth is to cause a redistribution of the stresses that are already there. This implies that in some areas, the stresses will be reduced while in others, they will be increased. These effects are well known and are repeated here only for continuity. The references in Appendix G should be consulted for more detailed discussion and information.

Figure 1 is a condensation of the stress concentration effects at the corners of a roadway. The diagrams indicate the following important points:

- The maximum value of the stress concentration factor in the corners is about 5 to 7, for common coal mine roadways with 'squarish' corners.
- As the ratio of horizontal to vertical stresses (the k-factor) increases or decreases, the stress concentration factor decreases although the absolute magnitude of the stress that is concentrated, may be greater.
- As the k-ratio increases, the area that is subjected to the highest stress concentration increases in the roof—as the k-ratio decreases, the area increases in the ribside.
- If the principal stress direction in the vertical plane is orientated off vertical/horizontal, the stress concentration becomes asymmetrical around the excavation.

The most important effect of the stress redistribution shown in Figure 1 is the phenomenon of guttering. In the corners, where the tangential stress is a maximum, the radial stress is zero. Consequently, the shear stress is a maximum and equal in magnitude to half of the tangential stress, which is a normal compressive stress. Rock is more than twice as strong in compression than
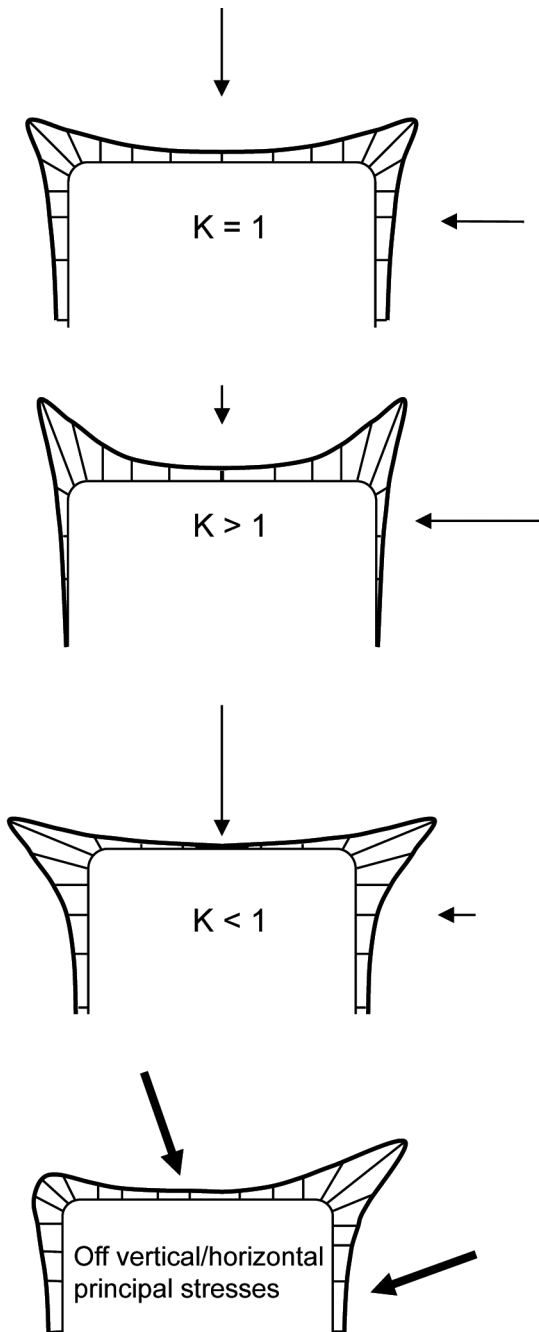

Figure 1. Illustration of the different nature of the tangential stress redistribution, depending on the pre-mining stress configuration. The distance of the stress line away from the edge of the excavation indicates the magnitude of the stress concentration factor of the tangential stress on the skin of the excavation

in shear. Consequently, the expected failure mode is shear, which is guttering.

Guttering is often mistaken as a definitive sign of very high horizontal stress; this is not necessarily the case. For instance, consider the case where the horizontal stress is 5 MPa, corresponding to a k-ratio of 2 at a depth of 100 m. Say the stress concentration factor is 5, resulting in a total stress of 25 MPa. Then, the shear stress is 12.5 MPa, which is greater than the shear strength of, for instance, coal or mudstone. Shear failure is then likely to occur in the corners, which is guttering. If the stress orientation is not truly vertical/horizontal, the guttering will be more likely to appear in one corner than in the other.

If guttering crosses intersections, it is more than likely an indication that the horizontal stress, without any amplification, is in excess of the compressive strength of the roof material. This usually calls for rather drastic support measures.

Shear-type flaking is sometimes observed in the upper portions of ribsides, especially in pillar extraction sections. That is an indication of the vertical stress component being greatly in excess of the horizontal. It corresponds with the diagram in which k<1 in Figure 1. Examples of the two types of guttering are shown in Figures 2(a) and (b).

Typical South African roof composition

In addition to the stress redistribution described in the previous section, there are additional disturbances that are caused by the layered nature of the roof. In general, the layered roof can be considered as consisting of a succession of plates. This can usually be simplified for analysis purposes to the behaviour of beams. If a roadway length is more than twice its width, the beam approximation leads to results that are within reasonable limits of accuracy.

At intersections, this is not the case and the only accurate reflection is obtained with the aid of numerical models. There is no simple analytical plate solution for the intersection geometry. The beam analogy can still be used, but the engineer should be aware that the stress results so obtained are exaggerated.

The magnitude of the stress disturbance caused by the beam effects is a function of, amongst other variables, the roof composition. The support philosophy will vary for the various conditions. Therefore, the beam effects will be discussed against the background of 'typical' roof compositions.

ROCK ENGINEERING FOR UNDERGROUND COAL MINING

Figure 2(a). An example of ribside guttering, indicating that the vertical stress is in excess of the horizontal, or the k-ratio is less than unity

Figure 2(b). An example of roof guttering, indicating that the horizontal stress is greater than the vertical, or that the k-ratio is greater than unity

There are essentially three broad classes of roof composition in South African collieries. Each has its own characteristics and requires unique support philosophies. There are no clear boundaries between these; the classes to follow should be seen as representing the midpoints of fairly broad ranges of roof types, schematically shown in Figure 3. They are presented in ascending order of difficulty to support.

In the following paragraphs, suggested design procedures are given for each 'typical' roof situation. They are to be applied where high horizontal stress is not deemed to be a significant problem.

Sandstone or other competent roof

A thick, continuous sandstone roof is relatively rare but does occur. In this context, the term 'thick' implies thick enough to be self-supporting over prevailing road widths and 'continuous' means containing joints and other discontinuities at spacings wider than prevailing road widths.

There are potential hazards associated with this roof type: thin coal bands left underneath the sandstone and unexpected changes in geology leading to thinning of the competent layer or an increase in jointing or cross bedding.

Thin coal layer

The coal layer in the roof usually varies in thickness due to varying operator proficiency and seam thickness. It is left to prevent premature blunting of continuous miner picks by cutting into sandstone and to prevent both possible methane ignitions by causing sparks and the even more serious thin, hot metal smear layer on the roof. The coal layer in the roof is best treated by barring it down, although most mines install roof bolts at wide spacings or employ spot bolting as support.

Increased jointing

Increased jointing, or a single joint in a roadway, is very often not detected until it is too late. The effect of a joint in a roadway, as shown in Figure 4, i.e. to increase the induced horizontal tension in the roof sixfold, is well known but is repeated here.

The tensile stress generated in a clamped beam loaded by its own weight is:

$$\sigma_{nj} = \frac{\gamma L^2}{2t} \qquad [1]$$

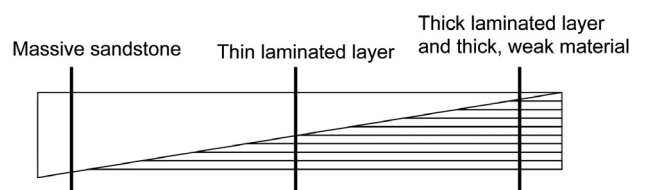and in the case of a cantilever it is:

$$\sigma_j = \frac{3\gamma L^2}{t} \qquad [2]$$

Figure 3. Graphic representation of roof types, indicating the gradual transition from one type to another

where :

σ_j = induced horizontal tension in jointed roof (i.e. cantilever)

σ_{nj} = induced horizontal tension in unjointed roof (i.e. clamped beam)

L = span (road width)

t = competent layer thickness

γ = unit weight of roof material (ρg)

Therefore, it can be seen that:

$$\frac{\sigma_j}{\sigma_{nj}} = 6 \qquad [3]$$

The spot bolting, which is intended to support the thin coal layer in the roof, will invariably not be able to support the competent beam if it is weakened by joints. Even increasing the bolt density will be ineffective if the bolts are shorter than the beam thickness. This is very often the case in practice.

The only effective support measures are to employ one of the common joint support techniques, such as installing inclined bolts to intersect the joint plane or installing short W-straps or conveyor belt strips across the joint. Note that one common joint support technique, installing short vertical bolts on either side of a steeply dipping joint, has no beneficial effect. Common joint support methods are discussed in Chapter 3: Roof stability.

In severe cases, e.g. a heavily jointed sandstone roof, long cable anchors, trusses or standing supports such as mine poles, cluster sticks or sets, are about the only successful roof supports.

The risk of roof falls can be minimized by adapting the mining layout to suit the geology. However, in
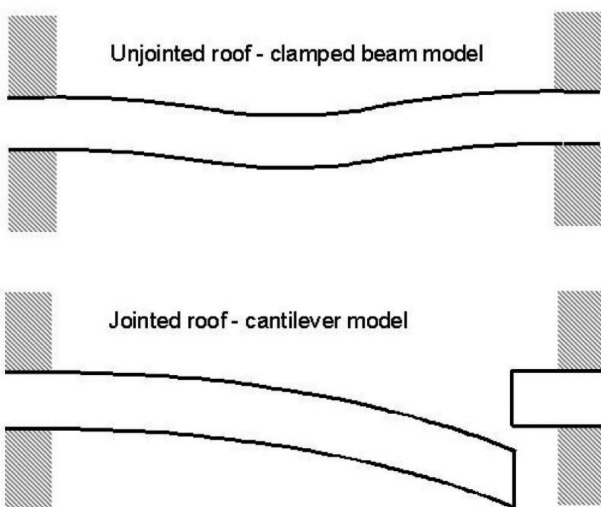
Figure 4. The effect of a joint in the roof is to change the basic behaviour from that of a clamped beam to a cantilever

most cases, this strategy has limited application because the zones of intensive jointing become known only after the mine has been established, and it is then impractical to change the directions of major development. What can still be done is to minimize the widths of roads running parallel to the major joint direction, or to stagger intersections in order to reduce the number of joints daylighting in roofs. Rectangular pillars with the long axis orientated perpendicularly to the joint direction can also be implemented, see Figure 5.

Thinning sandstone roof

The stability of a roof plate (here simplified to a clamped beam loaded only by its own weight) is dependent on its thickness and the road width, or because:

$$\sigma_t = \frac{\gamma L^2 F}{2t} \qquad [4]$$

It follows that the maximum span over which a given beam will be stable, is:

$$L = \sqrt{\frac{t 2 \sigma_t}{\gamma F}} \qquad [5]$$

which can be simplified to:

$$L = 16.3\sqrt{t} \qquad [6]$$

for a competent layer with 5 MPa tensile strength, $_t$, and safety factor, F, of 1.5.

Therefore, the minimum required thickness, t, of a competent beam must be:

$$t = \frac{L^2 \gamma F}{2 \sigma_t} \qquad [7]$$

or, in the simplified version,

$$t = \frac{L^2}{266} \qquad [7a]$$

In simplified terms, under these specific conditions, this means that for a 6.6 m wide roadway the minimum thickness of a self-supporting competent beam must be 16 cm.

The above is valid only for a competent unit that is overlain by another competent layer or another unit that is as thick or thicker and as stiff or stiffer than sandstone. This will seldom be the case.

More often, there will be alternating layers of stiff and softer material, i.e. sandstone and shale. In this

ROCK ENGINEERING FOR UNDERGROUND COAL MINING
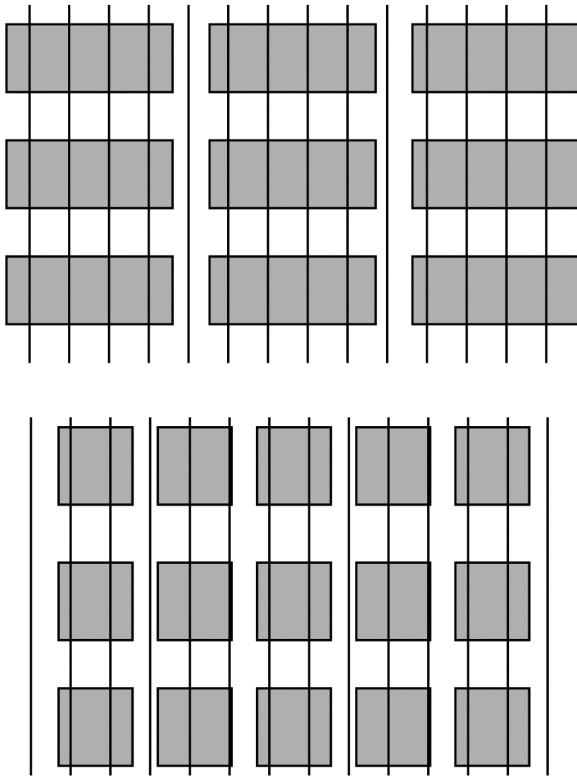
Figure 5. Road widths and pillar shapes can be adjusted to cater for areas of intensive jointing without changing the direction of sections

more common case where sandstone is overlain by, say, a shale layer, the shale will load the sandstone. Equations [4] to [6] should then be adapted to cater for the additional loading. The amount of load that is transferred to the bottom layer is a function of the relative thickness of the beams and their material stiffness. A simplified approach erring on the conservative side is followed here.

For instance, if the competent layer is overlain by a shale of the same thickness as the competent layer, the safe assumption that the competent layer is loaded by the full weight of the shale can be made. Therefore, the term γ in Equation [4] should be replaced by 2γ and Equations [4] to [7] then become:

$$\sigma_t = \frac{\cdot\gamma L^2}{t}F \qquad [8]$$

$$L = \sqrt{\frac{t\sigma_t}{\gamma F}} \qquad [9]$$

and

$$t = \frac{L^2\gamma F}{\sigma_t} \qquad [10]$$

simplified to:

$$L = 11.5\sqrt{t} \qquad [9a]$$

$$t = \frac{L^2}{133} \qquad [10a]$$

Under these circumstances the required minimum thickness of a self-supporting competent beam for a 6.6 m wide roadway is 33 cm.

In simplified generic terms, Equation [6] can be expressed as:

$$t = \frac{nL^2\gamma F}{2\sigma_t} \qquad [11]$$

simplified to

$$t = \frac{nL^2}{266} \qquad [12]$$

where

$$n = 1 + \frac{thickness\ of\ softer\,/\,thinner\ rock}{thickness\ of\ sandstone}$$

Suggested precautions

It has been shown that unexpected variations in geology can cause a dramatic change in the support requirements of a competent roof. Under very favourable conditions, barring with or without light bolt support is sufficient. The increased frequency of isolated joints will necessitate the installation of W-straps or similar types of supports at the joints, whereas dense jointing will require significantly longer bolts or cable anchors.

The key to the continued stability of a roof is in the geology and this is what monitoring should concentrate on. It is suggested that test holes should be drilled at intersections. Ideally the holes should be inspected with a petroscope, but observation of the drill chips during drilling by an experienced person could also be sufficient.

Competent layer underlain by thin layer of laminated material

This is a common situation in South African coal mines, and sometimes the least well supported one. The reason for this may be that the laminated layer, mostly consisting of alternating layers of stiff and soft material, may have a stiff and stable appearance. Its hazard is often underestimated because it is relatively thin.

What one tends to forget is that a 50 mm thick slab of rock measuring 2×2 m has a mass of 500 kg, more than enough to cause severe injury—or worse—when it falls.

The most common support philosophy for this type of situation is weight suspension. The support spacing required to prevent falls between the bolts is a very important element of the support system and should not be overlooked.

Design procedure

Note: the units used in this and following discussions are m, kN and kPa. The weight suspension design procedure is relatively simple: it requires that the bolt system's support capacity must exceed the weight of the laminated material; that the spacing of bolts is dense enough to prevent falls between bolts; and that the overlying competent beam must be thick enough to support itself plus any softer overlying layers and the laminated material suspended underneath. Figure 6 explains some of the symbols used in the following paragraphs.

In the following paragraphs, frequent mention is made of 'laminated layers'. This needs to be explained, as the term is not used in the strict lithological sense.

The required design procedure is as follows for resin anchors

Step 1: Check integrity of the competent layer

The required thickness in this case is

$$t = \frac{n_l L^2 \gamma F}{2\sigma_t} \qquad [13]$$

or

$$t = \frac{n_l L^2}{266} \qquad [13a]$$

where

$$t = \frac{n_l L^2}{266} \qquad [13b]$$

Step 2: Calculate bolt spacing

Calculate maximum bolt spacing by

$$S_b = \sqrt{\frac{2t_{ave}\sigma_t}{n_q \gamma F}} \qquad [14]$$

or, in the simplified version,

$$S_b = 16.3\sqrt{\frac{t_{ave}}{n_q}} \qquad [14a]$$

where

$$n_q = 1 + \frac{t_{soft}}{t_{stiff}} \qquad [15]$$

t_{lam} = combined thickness of layers in laminated zone

t_{stiff} = average thickness of stiff layers in laminated zone

t_{ave} = average thickness of all layers in laminated zone

t_{soft} = average thickness of soft layers in the laminated zone

(Note: the term n_q is introduced to take account of the loading imposed by the soft layers within the laminated zone on the stiffer layers. If there is no difference between the layers in the laminated zone, $n_q = 1$)

Step 3a: Bolt length (resin anchors)

Calculate bolt length, l_b, by:

$$l_b = t_{lam} + l_a \qquad [16]$$

where:

l_a = anchor length

Rudimentary experimental work is required to determine the anchor length. This consists of doing a number of pull tests on short resin capsules to determine the shear resistance, τ, of the resin/rock interface.
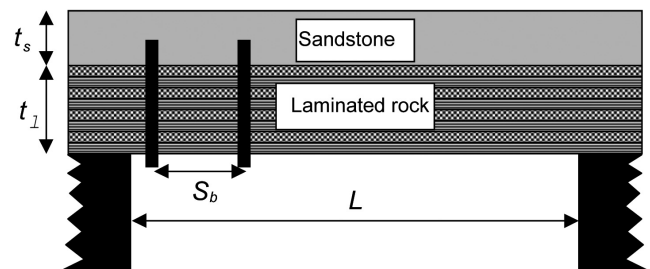
Per definition,

$$\tau = \frac{P}{\pi d \ell_r} \qquad [17]$$

Figure 6. Sketch explaining some of the symbols used in the following text

ROCK ENGINEERING FOR UNDERGROUND COAL MINING

Where P is the load at which the bolt pulls out, d is the hole diameter and l_r is the length of the resin/rock bond in the hole.

Then,

$$l_a = \frac{\gamma S_b^2 t_{lam}}{\pi d \tau} \qquad [18]$$

Equation [16] can then be written as:

$$l_b = t_{lam}\left[1 + \frac{\gamma S_b^2}{\pi d \tau}\right] \qquad [19]$$

simplified to:

$$l_b = t_{lam}\left[1 + \frac{8 S_b^2}{d \tau}\right] \qquad [19a]$$

In the case where mechanical anchors are used, the procedure is somewhat different because the anchor resistance is fixed (not dependent on anchor length).

Step 3b: (mechanical anchors)

The first two steps remain the same, but the anchor length is merely the thickness of the laminated layer plus, say, 150 mm to ensure that the anchorage is in a competent layer. Then follows a check to ensure that the spacing is such that the weight of the roof to be suspended does not exceed the anchor resistance.

Determine the maximum spacing S_m, to ensure that the anchors do not pull out.

$$S_m = \sqrt{\frac{P}{F \gamma t_{lam}}}, \qquad [20]$$

simplified to:

$$S_m = \sqrt{\frac{P}{37.5 t_{lam}}}, \qquad [20a]$$

where P is the anchor resistance.

The spacing to be used is the smaller of S_b determined with Equation [14] or S_m determined with Equation [20].

In general, bolt patterns in coal mines are specified by stating a number of bolts per row and the spacing of rows in the direction of face advance. The 'spacing' in the context of this paragraph is the maximum distance that two bolts are apart in any direction. Note also that this criterion cannot be satisfied by adjusting the pattern so that the area between bolts equals the square of the maximum spacing determined by Equations [14] and [20]. This will satisfy the weight criterion (thus anchors will not pull out) but could result in falls between the

bolts if any dimension exceeds the calculated maximum spacing.

Step 4: Check to ensure that the steel does not fail

The final step in this simple design procedure is to ensure that the load does not exceed the tensile strength of the steel body of the bolt. In the case of mechanical anchors, this will seldom be the case as anchors tend to slip at loads in the range of 50 to 60 kN while even an M16 bolt should have tensile strength in excess of 70 kN.

At equilibrium, the bolt strength should equal the load on the bolt. Simply, then,

$$F \gamma t_{lam} s_f^2 = \frac{\pi d_b^2}{4} \sigma_b \qquad [20b]$$

from which it follows that:

$$s_f = d_b \sqrt{\frac{\pi \sigma_b}{4 F \gamma t_{lam}}} \qquad [20c]$$

simplified to:

$$s_f = 0.15 d_b \sqrt{\frac{\sigma_b}{t_{lam}}} \qquad [20d]$$

where:

σ_b = yield strength of steel

s_f = maximum bolt spacing to ensure non failure of the steel body

d_b = bolt body diameter (usually 2 mm less than the thread diameter)

Worked example

The immediate roof in a coal mine with 7 m wide roadways consists of 0.5 m of weakly bonded laminated sandstone/mudstone layers, each 20 mm thick. This layer is overlain by a 0.6 m thick competent sandstone layer. Design a suitable support system for this situation, comparing two basic methods:

- A mechanical anchor system with 16 mm diameter stems
- A resin point anchor system comprising 20 mm bolts in 28 mm holes.

The shear resistance of the resin/contact plane is 2 MPa and the yield strength of the rebar used with the resin is 600 MPa. The steel used for the stem of the mechanical anchor has yield strength of 450 MPa and the anchors slip at at a load of 40 kN (0.04 MN).The

tensile strength of the sandstone is 6 MPa and that of the mudstone is 5 MPa. The unit weight of the roof material is 0.025 kN/m^3. Use a safety factor of 1.5.

Step 1: Check sandstone layer

$$n_l = 1 + \frac{0.5}{0.6} = 1.83 \quad \text{(Equation [13b])}$$

$$t = \frac{1.83 \times 7^2 \times 0.025 \times 1.5}{2 \times 6} = 0.28 \quad \text{(Equation [13])}$$

As the thickness of the sandstone layer is in excess of the required 0.28 m, the suspension principle can be used.

Step 2: Bolt spacing

$$n_q = 1 + \frac{0.02}{0.02} = 2 \quad \text{(Equation [15])}$$

$$S_b = \sqrt{\frac{2 \times 0.02 \times 5}{2 \times 0.025 \times 1.5}} = 1.63 \quad \text{(Equation [14])}$$

Step 3a: Bolt length (resin point anchor)

The required bolt length is

$$l_b = 0.5\left[1 + \frac{.025 \times 1.63^2}{\pi x .028 \times 2}\right] = 0.69 \text{ m} \quad \text{(Equation [19])}$$

Step 3b Mechanical anchors

The maximum spacing to prevent anchor slip is:

$$S_m = \sqrt{\frac{0.04}{1.5 \times 0.025 \times 0.5}} = 1.46 \text{ m} \quad \text{(Equation [20])}$$

Thus the maximum spacing to prevent anchor slip is less than the proposed spacing to prevent small falls between bolts. If mechanical anchors are to be used, the spacing will thus have to be decreased to maximum 1.46 m.

The length of the mechanical anchor bolts should be at least 0.2 m longer than the thickness of the laminated layer, thus 0.5 + 0.2 = 0.7 m.

Step 4: Check steel strength

The maximum tolerable spacing to prevent steel failure for the resin anchors should be:

$$s_f = (0.02 - 0.002)\sqrt{\frac{\pi \times 600}{4 \times 1.5 \times 0.025 \times 0.5}} = 2.85 \text{ m} \quad \text{(Equation [20c])}$$

The maximum tolerable spacing to prevent steel failure for the mechanical anchors should be:

$$s_f = (0.016 - 0.002)\sqrt{\frac{\pi \times 450}{4 \times 1.5 \times 0.025 \times 0.5}} = 1.92 \text{ m}$$

In both cases, the proposed spacings are less than the maximum spacings to prevent steel failure and therefore the steel should not fail.

The initial support designs are thus the following:
- Resin – 20 mm rebar in 28 mm holes, 0.7 m long at 1.63 m spacing.
- Mechanical anchor – 0.7 m long at 1.46 m spacing.

In practice, the spacings will be adapted—reduced—to fit production and equipment requirements. This will be a first order design, to be monitored and then finally adapted at the hand of practical experience.

One of the most often overlooked aspects is that of variability. As conditions change, so will the support requirements. Monitoring should thus not be confined to the performance of the support system, but has to include the rock parameters such as thickness of the various layers.

Thick laminated roof

Not all laminated roofs are prone to collapse. In some cases the cohesion and friction between layers are sufficient to allow the laminated zone to behave like a single beam. Where this is not known beyond doubt to be the case, it is better to assume that the laminations can move relative to one another and will act like a number of separate beams.

This type of roof can be supported by beam creation or suspension. Beam creation is the more sophisticated design procedure and often results in substantial savings because some of the rock properties (i.e. cohesion and friction between layers) are used to create a stable beam. However, there are a number of vitally important prerequisites that must be met before this design method can be used. If these prerequisites are not in place on a mine, then the weight suspension design method must be used.

Beam creation

The most important prerequisite is that the bolts have to be installed before the roof layers have started to sag or separate. Once sag has been initiated, the roof layers have already slid over one another and reduced

the frictional resistance. The second prerequisite is that the support materials used and the roofbolting equipment on the mine must allow the required amounts of pre-tension to be applied to the roof.

The amount of roof sag depends on the road width, advance before bolts are installed, horizontal stress, and the time lapse between exposing the roof and installing the bolts. The influence of each will be summarized in the following paragraphs.

Road width

The roof sag, η, of a gravity loaded beam is:

$$\eta = \frac{qL^4}{32Et_b^4} \qquad [21]$$

where E = Modulus of Elasticity of the roof material and t is the beam thickness.
t_b = thickness of the beam
q = uniform loading on the beam, or $\rho g t_f$, where t_f is the total thickness of roof the beam has to support.

Equation [21] shows that deflection is proportional to the fourth power of road width. Increasing the road width from 6,6 m to 7,8 m will thus double the amount of sag.

Cut-out distance

As in most other discussions about roof support, the theoretical aspects are simplified to those of a beam instead of a plate. The simplification is valid, provided that the length of the excavation is more than 1.4 times the width. Once that ratio has been exceeded, the roof behaviour is like that of a beam for all practical purposes.

The implication of this is that once the unsupported advance is more than 1.4 times the road width, further roof sag will be arrested. Therefore, for a 6.6 m wide roadway there is little point to restrict the face advance to a distance that is greater than 9.3 m because once the 9.3 m distance has been exceeded, the full sag for that particular road width will already have occurred. This also implies that the narrower a roadway, the further it can advance because the sag will be arrested sooner.

Time lapse between roof exposure and support

The stress redistribution following the creation of an excavation is immediate, but the failure process is time dependent.

The full roof sag does not manifest itself immediately as the roadway is driven. Exactly how long it takes is not yet known, but what is known is that the longer it takes before bolts are installed, the higher the probability of getting a roof fall. Rico *et al.* (1997) measured continuous movement of a mudstone roof for more than six months in Mexico.

By contrast, Canbulat and Jack (2000) found in South Africa that roof movement ceased within days of exposing the roof.

The failure process starts with the development of micro cracks that grow over time. Therefore, even if bolts are installed before the actual fall occurs, the roof has already been weakened and stress changes at a much later time may then result in an acceleration of the process, causing roof falls.

Restricting the cutting distance to 12 m does not have meaningful benefits for stabilization from a dimensional viewpoint, as mentioned in the previous section, but it does mean that the time lapse between exposure and support is reduced. This could be a substantial benefit.

Design procedure

Beam creation in a laminated roof is based on the principle that the individual layers are bound together to form a single unit that acquires strength by virtue of its thickness. The bounding process hinges on preventing the individual laminae slipping relative to one another. This is achieved by installing bolts that do two things, as described in the following paragraphs.

Firstly, they act as pins and, secondly, by tensioning them, they increase the normal stress on the layers to enhance the natural frictional resistance between the layers.

Step 1: Calculate the minimum thickness of the beam to be created

From

$$\sigma = \frac{qL^2}{2t^2} \qquad [22]$$

where q = uniform load on the beam (best determined from observation of previous roof falls) it follows that:

$$t_m = \sqrt{\frac{qL^2}{2\sigma_t}} \qquad [23]$$

where t_m = the minimum beam thickness

σ_t = the tensile strength of the beam material.

q = uniform loading on the beam, or $\rho g t_f$, where t_f is the total thickness of roof the beam has to support.

Step 2: Calculate maximum permissible sag in the centre of newly created beam

The artificial beam will be allowed to undergo a certain amount of deflection before it fails. This maximum deflection is:

$$\eta = \frac{qL^4}{32Et_m^4} \qquad [24]$$

Step 3: Determine position of bolt at edge

The relative displacement between laminations in a composite clamped beam is zero at the centre and reaches a maximum at the edges. Therefore, the closer to the edge, the more effective the bolt becomes. Due to practical limitations it is not always easy to install bolts right at the edge.

Most of the roofbolters used in South African collieries can drill only vertical holes, and often the closest that one can drill from the ribside is a distance equal to half of the roofbolter's width. This limitation can be overcome by turning the bolter so that it stands at 90° to the ribside, but then one has to be careful not to let the bolter assistant move in under unsupported roof. The required manoeuvring also slows down the support process.

Let the minimum practical distance be S_r.

Step 4: Calculate the maximum permissible inter layer displacement, $\Delta\ell_d$, see Figure 7

$$\Delta\ell_d = \theta t_{\ell i} \qquad [25]$$

where $t_{\ell i}$ is the average thickness of the individual laminae and:

$$\theta = \frac{\pi}{2} - \arctan\left(\frac{R-\eta}{L/2 - S_r}\right) \qquad [26]$$

The radius of curvature of the roof, R, is:

$$R = \frac{L/2}{Cos\beta} \qquad [27]$$

and:

$$\beta = \arctan\left(\frac{L/2}{\eta}\right) - \arctan\left(\frac{\eta}{L/2}\right) \qquad [28]$$

Step 5: Compare the maximum allowable displacement, $\Delta\ell_d$, with the possible displacement, $\Delta\ell_p$.

The possible displacement is the sum of two components, namely the resin shrinkage upon setting $\Delta\ell_{rs}$, and the resin compression, $\Delta\ell_{rc}$:

$$\Delta\ell_{rs} = F_v^{0.333}\left(d_h - d_b\right) \qquad [29]$$

where F_v = volumetric shrinkage factor of resin

d_h = hole diameter

d_b = bolt diameter

The resin compression is due to the shear stress generated in the beam, τ_b, see Figure 8. This becomes a compressive stress on the resin column,

$$\sigma_r = \frac{\tau_b S_b}{d_b} \qquad [30]$$

where S_b is a chosen 'seed' bolt spacing.

Then, the total resin compression due to the compressive stress is:

$$\Delta\ell_{rc} = \frac{\sigma_r\left(d_h - d_b\right)}{2E_r} \qquad [31]$$

where E_r is the resin's modulus of elasticity.

Finally:

$$\Delta\ell_p = \Delta\ell_{rc} + \Delta\ell_{rs} \qquad [32]$$

If $\Delta\ell_p < \Delta\ell_d$ the position of the edge bolt is confirmed. If not, one or more of the elements of the system has to change. It is noteworthy that one of the important elements of this system is the annulus. The greater the annulus, the more the resin can compress. Tadolini
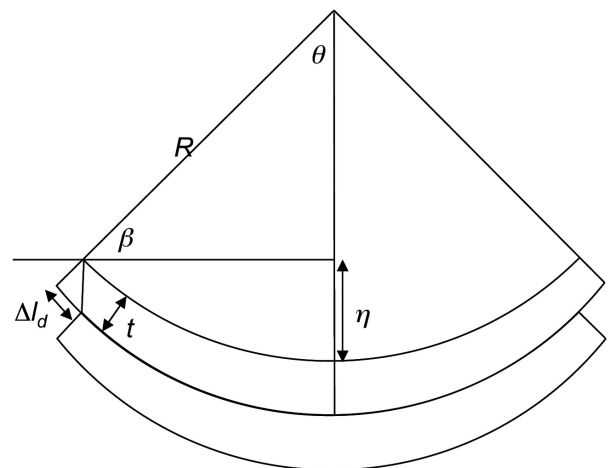
Figure 7. The simplified basis for the calculation of inter laminae slip in the roof

(1998) described the benefits of reducing the annulus in full column resin applications.

It is theoretically possible to create a stable beam with two side bolts per row only. However, due to variations in the efficiency of support installation and complexity of geological materials, it is required to add supplemental bolts. The suggested method to determine the spacing of the supplemental bolts is to use the procedure to prevent falls between bolts, as described earlier in this Appendix.

In beam creation, the edge bolt is the pivot around which the entire system is constructed. Note that if this design process is used, the bolt pretension is not considered – in fact, it is not required to pretension bolts.

In practice, however, this is a difficult design procedure as the resin shrinkage factor and Modulus of Elasticity are not always readily available and the layer thickness is not easy to estimate.

Another approach is to base the design on increasing the normal force across layers, in order to increase the frictional resistance to sliding. The following simpler procedure can therefore also be used:

Step 1: Determine minimum beam thickness, using Equation [23]

Step 2: Calculate required pretension in bolts

If slip between the roof layers is to be prevented, the frictional resistance must at least equal the disturbing forces. The maximum disturbing shear, τ_d, is:

$$\tau_d = \frac{3qLF}{4t_m} \qquad [33]$$

where F is the safety factor and q is the uniform load
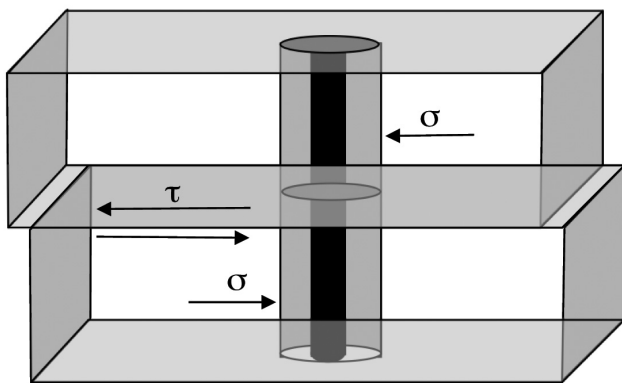
Figure 8. Shear displacement between roof layers causes a normal stress on the resin

on the beam.

The shear resistance, τ_r, is,

$$\tau_r = C + \sigma_e \tan\phi \qquad [34]$$

where C = cohesion between layers
   σ_e = effective stress applied by bolts
   ϕ = angle of friction of inter laminae contact plane.

The effective normal stress, σ_e, is the balance between gravity induced tension and the compression supplied by the bolt's pretension. With the simplifying assumption that the pretension load is distributed evenly over the supported area per bolt,

$$\sigma_e = \frac{F_b}{S_b^2} - q \qquad [35]$$

Where F_b is the pretension of the bolt and S_b is the bolt spacing. Note that 'q' has to be subtracted, as the weight of the material to be supported acts against the supplied pretension. If one then ignores the cohesion between layers (assumed to be destroyed by delamination caused by gravity), Equations [33], [34] and [35] can be combined to yield an expression for the required pre-tension:

$$F_b = S_b^2 \left[\frac{0.75qLF}{t_m \tan\phi} + q \right] \qquad [36]$$

At this point, it has to be realised that in practice, there will be an upper limit to the pretension that can be supplied, being a function of the torque setting on the roofbolter. If the maximum pretension is *Fm*, Equation [36] can then be used to determine the required area per bolt, A_b (with the necessary prerequisite that the pretension is less than the breaking strength of the bolt):

$$A_b = \frac{F_m}{\left[\dfrac{0.75qLF}{t_m \tan\phi} + q \right]} \qquad [37]$$

Step 3: Check for steel failure

The tensile stress generated in the steel body of the rebar, σ_s, is quite simply

$$\sigma_s = \frac{4F_b}{\pi d_s^2} \qquad [37a]$$

where d_s is the steel tendon diameter. If σ_s is less than the yield strength of the steel, the system is fine. If not, repeat the procedure with either thicker steel or reduced spacing.

Step 4: Calculate the required anchor length

The next step is to calculate the required length of anchor, ℓ_a, which will have the resistance to slip, with Equation [38]. Simply,

$$\ell_a = \frac{F_m}{\pi d_h \tau} \qquad [38]$$

where

l_a = required anchor length
τ = shear resistance of the resin/rock contact plane
d_h = hole diameter

The total bolt length is then the sum of the beam thickness and the anchor length, or

$$\ell_b = \ell_a + t_m \qquad [39]$$

Worked example

Design a support system for a thick, weak mudstone coal mine roof using the beam creation procedure. Previous observations indicated that the average height of roof falls was 1 m. The road width is 6 m and the tensile of the mudstone is 5 MPa. The angle of friction is 30° and the cohesion is negligible (or = 0). The bolt diameter is 20 mm and the hole diameter is 25 mm. The yield strength of the steel is 600 MPa and the shear strength of the resin/rock contact plane is 2 MPa. The maximum pretension the roofbolter can supply, is 100 kN. Use a safety factor of 1.5, the unit weight of the roof rock is 25 kN/m2.

Step 1. Required beam thickness (Equation [23])

The required beam thickness is

$$t_m = \sqrt{\frac{qL^2}{2\sigma_t}}$$

$$t_m = \sqrt{\frac{0.025 \times 1 \times 6^2}{2 \times 5}}$$

$$t_m = \sqrt{\frac{0.025 \times 3 \times 6^2}{2 \times 5}} = 0.3$$

Step 2: Calculate area per bolt (Equation [37])

$$A_b = \frac{F_m}{\left[\frac{0.75qLF}{t_m \tan\phi} + q \right]}$$

$$A_b = \frac{.1}{\left[\frac{0.75 \times .025 \times 6 \times 1.5}{.3 \times \tan 30^0} + .025 \times 1 \right]} = .1m^2$$

A bolt spacing of 0.3 m by 0.3 m will be necessary to result in an area per bolt of 0.1 m2. Note that this is the minimum spacing (highest density) of bolts required at the edge of the roadway, where the maximum shear stress occurs in the roof. The required spacing decreases with distance away from the edge of the roadway, so that in theory the only bolts required at the centre of the roadway are those that are necessary to counteract gravity.

The area required per bolt in the centre of the roadway is simply

$$A_b = \frac{F_m}{q}$$

or in this case,

$$A_b = \frac{.1}{.025 \times 1} = 4m^2$$

In the centre, a spacing of 2 m by 2 m will satisfy this requirement.

The theoretical requirement for bolt spacing will thus be to install bolts at 0.3 m at the edge of the roadway, increasing to 2 m at the centre of the roadway. This is clearly not a practical solution, so that the spacing to be adopted in practice will more likely be the average between 0.3 and 2.0 m, or a regular pattern of 1.1 m by 1.1 m.

One has to realise that this still means that the bolts are less dense than they should be at the position where they are most required, i.e. at the edge of the roadway. It is therefore suggested that an additional bolt be installed between the rows at the edge of the roadway. It remains vitally important that once a design like this has been implemented, it has to be checked by extensometer monitoring and the final design should be modified according to the observations.

Step 3: Calculate bolt length

Using Equation [38], and bearing in mind that the system is now optimised for steel strength, the required anchor length is

$$\ell_a = \frac{F_m}{\pi d_h \tau}$$

$$\ell_a = \frac{.1}{\pi \times .025 \times 2} = .6m$$

The bolt length is then 0.3 + 0.6 = 0.9 m

The system specification is then to use 0.9 m long 20 mm bolts in 25 mm holes, spaced at 1.1 m and pretensioned to 100 kN, with an additional bolt installed between rows at the edge of the roadway.

Optimization of resin capsule lengths

The creation of the beam requires that the pretension must be applied to the bolt while the resin is still fluid over the thickness of the beam, while the anchor portion must already have set. Therefore the anchor must be a fast resin, and the beam must have the slower resin.

$$\ell_{frc} = \frac{d_h^2 - d_s^2}{d_c^2} . \ell_a \qquad [40]$$

where l_{frc} is the length of fast resin capsule and d_c is the diameter of the resin capsule.

Similarly, the length of the slow resin capsule, l_{src}, is:

$$\ell_{src} = \frac{d_h^2 - d_s^2}{d_c^2} t_m \qquad [41]$$

One is unlikely to be able to purchase the exact length of capsule that is required and some practical compromise will inevitably be required. The effects of any such compromise must, however, be considered by calculation before installation proceeds.

Suspension of thick weak roof

It has already been stated that the ideal support philosophy for a thick, weak roof is beam creation. Unfortunately this is not always possible for a number of reasons, including excessive cutout distances, non-suitability of the available equipment or material, etc. The alternative, less sophisticated, but equally effective philosophy, is to accept that the roof will fail by whatever mechanism and to supply merely a basket in which the loose roof can be suspended without causing damage. The negative consequences materialize in practice only when the roof falls, not when it fails.

There are three subclasses in this division: standing supports, long cable anchors, and short inclined bolts or trusses.

Standing supports and long cable anchors

Standing supports include steel sets, arches and timber poles. These are no longer popular in South Africa (except in isolated bad spots like burnt coal, faulted zones, etc.) but their use should not be discarded outright. This is especially true for the lower spectrum of mining heights.

Long cable anchors are more common than standing supports, but the design procedure is often not very scientific. It is not a complex procedure, as shown in the following paragraphs.

Step 1. Determine the load on the system

This is most practically done by observing the height of existing roof falls—they are more often than not restricted by the presence of an even slightly stronger roof layer or merely by the width of the falls, h_f, reaching a stable dimension. In most cases the need for cable anchors will not be foreseen, as it is usually a reaction to increasing numbers of high roof falls, so that this information is usually available.

Then, the load, W, is

$W = \rho g F h_f$ MN per square metre, [42]

simplified to

$W = 37.5 h_f$ MN per square metre [42a]

Note that Equation [42a] is based on the conservative simplification that the falls are vertically sided. It also incorporates a safety factor 1,5.

Step 2. Determine the anchor spacing

Long cable anchors are usually secondary supports, and it is therefore easier to obtain even spatial distributions of the anchors. The required spacing, s_l, is

$$s_l = \sqrt{\frac{R}{W}} \text{ m} \qquad [43]$$

where R is the strength per cable.

Step 3. Determine cable length

The cable lengths are determined in the same way as the bolt lengths for suspension of thin layers, described earlier in this Appendix. The additional consideration is that the length must be sufficient to ensure that anchoring is obtained in a strong layer higher up in the roof, or it must be at least three times the height of the roof falls.

Although cables are often installed with resin

anchors, this is discouraged because the cable seldom mixes the resin properly. Mechanical anchors are easier to install, resulting in higher quality of support. Obtaining high anchorage loads with the mechanical anchors supplied, with cable anchors is easier than with the smaller anchors supplied with normal bolts. Following tensioning of the cables these should be cement grouted very soon after tensioning. Tensioning should always precede grouting. The pretension load should equal half of the breaking strength of the cables.

Step 4: Supply areal cover

This design method does not cater for the prevention of roof falls between supports by adjusting the support spacing, as that would be prohibitively expensive. Some form of areal cover is thus also necessary. This can range from W-straps, oslo-straps or other steel straps to wiremesh or wiremesh and lacing. The choice of material will be influenced by the nature of the immediate roof. A reasonable roof will not require more than strapping, while a friable roof should be meshed.

The application of wiremesh in coal mines is often negated by the method of application. The mesh has to be an integral part of the cable system. This can be achieved only by installing the cables through the mesh. Installing the cables first and then installing the mesh with separate short bolts is not sufficient as it will not transfer the load of the loose material to the cables. Once the mesh has been properly installed behind the cables, additional, shorter bolts can be used to fix the mesh close to the rock—this is good practice especially where shotcrete is also to be applied.

Short inclined bolts and trusses

Short inclined bolts supplemented by areal cover are essentially a way to provide the same effect as steel sets, without the legs. With long cable anchors, the anchorage is obtained above the weak zone. With inclined bolts, it is obtained beyond the edge, in the compressive zone just above the pillars. The concept is illustrated in Figure 9. Note that this is also the design method for support with roof trusses or cable trusses only.

The design procedure, as with all suspension problems, is simply a matter of balancing the weight of the falls by the support resistance of the bolt system. The main advantage of the inclined bolt system is that the same anchorage is obtained with

significantly shorter bolts as the full length of the bolt is used for anchoring; the 'dead' length traversing the weak zone does not exist.

Step 1. Determine the load on the system

Use the same method as for long cable anchors. For this application, however, the load per running metre of roadway is the central parameter, and therefore the load equation, for 25 kN/m³ unit weight of roof rock and 1.5 safety factor, becomes:

$$W = \gamma h_f FL \text{ kN/m} \qquad [44]$$

simplified to:

$$W = 37.5 h_f L \text{ kN per running metre} \qquad [44a]$$

Step 2: Choose bolt length, calculate spacing

The support resistance is determined by a combination of hole diameter, d_h, bolt length, l_b, and bolt spacing. It is recommended to use maximum hole diameters of 28 mm with 20 or 22 mm bolts for this application. The hole length is a practical consideration and the maximum can be considered as fixed for any given situation whereas the spacing is the parameter that can be adjusted most easily. Therefore it is suggested to fix the diameters and length and calculate only the spacing. In simplified form, the spacing, S_b, is then:

$$s_b = \frac{\pi d_h l_b \tau_{res}}{W} \qquad [45]$$

where

τ_{res} = shear strength of resin/rock interface.

Equations [43] and [44] can be combined to yield the single equation for determining bolt spacing as a function of fall height, bearing in mind that there are two bolts, one on either side of the roadway:
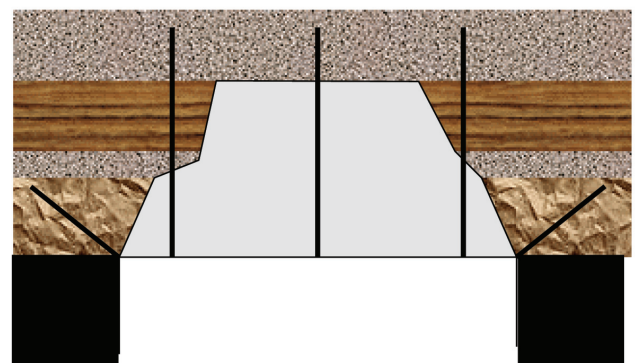

Figure 9. Bolts inclined over the pillars can result in the same anchorage as longer vertical bolts because they do not traverse the potential fall height

$$s_b = \frac{2\pi d_h l_b \tau_{res}}{\gamma F h_f L} \varsigma N \qquad [46]$$

simplified to

$$s_b = \frac{0.17 d_h l_b \tau_{res}}{h_f L} \ N \qquad [46a]$$

If this spacing is too dense, adjust the system by increasing the hole and bolt diameters or increasing the hole lengths.

Step 3: Check for steel strength

It is possible for the load per bolt to exceed the strength of the bolt if the equations are used without checking. The bolt strength, F_{sb}, should be greater than the bolt load, or:

$$F_{sb} > \frac{W}{2s_b} kN \qquad [47]$$

which can also be written as:

$$F_{sb} > \frac{\gamma F h_f L}{s_b} kN \qquad [48]$$

simplified to:

$$F_{sb} > \frac{18.75 h_f L}{s_b} \ kN \qquad [48a]$$

Step 4: Supply areal cover

This support method is reliant on areal cover, as the basic idea is to install no intermediate bolts. Therefore, if trusses are to be replaced by bolts, W-straps or something similar are essential, not preferable. The remarks about areal support in the previous section on long vertical cable anchors also apply to this section.

Effect of position of hole

The method described above is based on the assumption that the support holes are drilled in the corner of the roof. Additional benefit may be obtained if the inclined holes are drilled approximately 0.5 m from the corner, as shown in Figure 10. In doing that, the bolts penetrate the plane along which the fracture causing the roof falls will develop. They then also fulfil a preventative role as well as supporting the dead weight of potential falls.

However, an additional check is then necessary to ensure that the shear strength of the steel, F_{ssb}, is not

exceeded. Therefore, it is important to check that

$$F_{ssb} > \frac{\gamma F h_f L}{2s_b} \qquad [49]$$

simplified to:

$$F_{ssb} > \frac{18.75 h_f L}{s_b} \ kN \qquad [49a]$$

In most cases it will be easier to drill holes right in the corner with handheld equipment or light rigs, but there are significant benefits to installing the bolts about 0.5 m from the corner.

Concluding remarks on design methods in the absence of high horizontal stress

As stated in the introduction, the recommended design methods depend on a basic understanding of the roof type and consequently the expected failure mechanism. There is no such thing as the best design method—there are only effective methods for the prevailing conditions.

In the preceding descriptions three basic conditions were identified. They represent midpoints of 'sections' in an infinite variety of gradual changes. For instance, one question that was not answered was at what thickness of the laminated layer, underneath a competent layer, does one change over from a suspension philosophy to beam creation?

There is no technically correct answer to this question, but the user will be guided by practical matters such as the maximum bolt length that can be
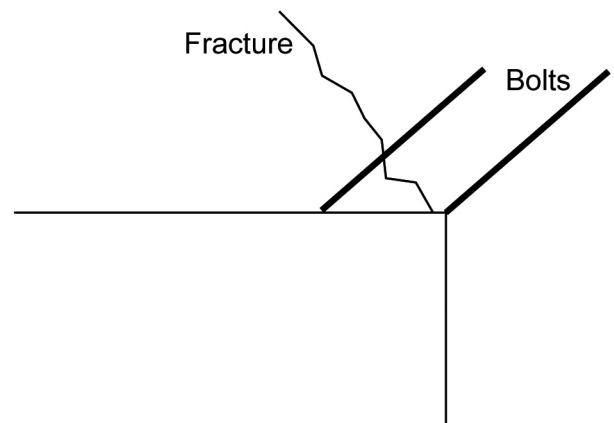

Figure 10. Cross-section of the corner of a roadway, showing how an inclined bolt, a short distance away from the ribside, penetrates the fracture plane

installed, whether it is at all possible to install bolts before the roof has deflected, etc. In the grey zone, it should eventually become a matter of economics, i.e. in choosing between two equally safe roof support methods, simply pick the cheapest one.

The greatest danger to avoid is wishful thinking — the roof is what it is, not what we wish it is. Roof beams cannot be created if the bolts are installed after deflection has occurred, or if the bolters cannot supply the required pretension.

The work is not complete once the system has been designed. Monitoring of the performance of the system will in most cases highlight design shortcomings and changes in roof composition that have to be catered for by adaptation. The monitoring/correction action, discussed in Chapter 11, should be seen as a continual process, not a one-off step.

The total stress state around a coal mine roadway (horizontal stress)

At shallow depth, coal mine roof stability tends to be dominated by geological features, as opposed to greater depth where the stresses dominate as disturbing features.

Basically, failure of any roof structure occurs when the loads exceed the strength of the roof material. At great depth, the stresses are often in excess of the strength of the surrounding rock, and a great deal of emphasis is placed on calculating and countering the stresses.

At shallow depth, the stresses are generally lower, and failure occurs when the surrounding rock loses strength due to joints, thinning of key layers, etc. However, there are cases where the stresses are high enough to result in serious stress related problems and therefore a brief discussion on the total stress state is pertinent.

For simplicity, the roof will be divided into two zones, namely the corners and the central zone.

The total stress around a coal mine roadway is the sum of three main components, being the re-distributed vertical and horizontal stresses, the induced beam stresses, and that caused by the moment due to the horizontal stress acting on the roof sag.

The effect of creating a roadway is to concentrate the field stresses in the corners by a factor, f, of 5 to 7. These are compressive normal stresses. In the roof, the horizontal stress, σ_{hr}, is concentrated while the vertical stress is concentrated in the ribside. Then,

$$\sigma_{hr} = \sigma_h f \qquad [50]$$

where σ_h = horizontal field stress
f = stress concentration factor.

Then, there is an additional compressive stress component due to bending of the roof beam in the corner close to the ribside. This stress is calculated with the aid of Equations [1] or [2], depending on whether or not a slip is present in the roof. They are repeated here, for ease of reference:

$$\sigma_{nj} = \frac{\gamma L^2}{2t} \text{ (no slip), and} \qquad [1]$$

$$\sigma_j = \frac{3\gamma L^2}{t} \text{ (slip present in roof).} \qquad [2]$$

The final component to be added is the fibre stress resulting from the moment caused by the horizontal stress and the roof deflection. This can be determined as follows:

The moment, M, is:
$$M = F_h \eta \qquad [51]$$

where F_h = horizontal force acting on beam
= roof deflection in centre of roadway.

$$F_h = \sigma_h t^2 \qquad [52]$$

where t = thickness of roof beam.

The generic equation for the fibre stress, σ_f, is

$$\sigma_f = \frac{Mz}{I} \qquad [53]$$

Then, with $z=t/2$ and $I=t^4/12$,

$$\sigma_f = \frac{6\sigma_h \eta}{t} \qquad [54]$$

The maximum deflection, η, is calculated with Equation [21], also repeated here:

$$\eta = \frac{\gamma L^4}{32 E t^2} \qquad [21]$$

The total horizontal compressive stress, $\sigma_{\tau\eta}$, in the corner of the roadway is the sum of the components, or

$$\sigma_{th} = \sigma_{hr} + \sigma_{nj} + \sigma_f \qquad [55]$$

if no slips are present in the roof, or

$$\sigma_{th} = \sigma_{hr} + \sigma_j + \sigma_f \qquad [56]$$

if there are slips.

On the skin of the excavation, the normal stress

perpendicular to the excavation is zero. Therefore, the magnitude of the shear stress in that position is half of that of the normal stress. In general, the shear strengths of sedimentary rocks are less than half of their compressive strengths. Therefore, the most likely failure mode in the corner is guttering.

Worked example

To illustrate the effects of the various stress components, consider the following example.

Assume a k-ratio of 2.0 at a mining depth of 100 m. Let the immediate roof consist of a mudstone layer 0.2 m thick, and say the roadway is 7 m wide. The shear strength of the sandstone is 15 MPa and the modulus of elasticity is 13 GPa. There are no joints in the roof.

σ_h = 5 MPa

Then,

σ_{hr} = 25 MPa (Equation [50])

σ_{nj} = 3,06 MPa (Equation [1])

η = 0,0036 m (Equation [21])

σ_f = 0,54 MPa (Equation [53])

The total normal stress in the corner is then σ_{hr} + σ_{nj}, or

σ_T = 28,6 MPa

The shear stress is then 14.3 MPa. As the shear strength of the sandstone is 15 MPa, guttering, or any other visible manifestation of stress, is unlikely to appear. However, if the roof is mudstone with shear strength of 8 MPa and modulus of elasticity of 7 MPa, the following will be the case:

σ_{hr} = 25 MPa

σ_{nj} = 3.06 MPa

η = 0.0067 m

σ_f = 1.01 MPa (Equation [53])

σ_T = 29.1 MPa

The shear stress is then slightly higher, being 14.5 MPa. However, this is almost twice as high as the shear strength of the mudstone and consequently guttering will appear in the corners. Note also that if a joint is present close to the ribside in the first example, the normal stress will increase to 43.9 MPa and the shear stress to 22 MPa. Also in this case, shear type failure will be apparent in the roof in the corner opposite to the joint.

High horizontal stress

Greatly elevated levels of horizontal stress—in excess of 6 times the vertical—have on occasion been measured in South Africa. Where these very high stresses exist in the roof, the situation described by the equations in the preceding paragraphs is much worse. Total horizontal stresses in excess of 100 MPa can then easily be generated. This is obviously greatly in excess of the strength of sedimentary rock types and severe conditions can be expected underground.

Severe guttering exists that is not confined to the corner regions of the roof. It is characteristic of the shear failure under these conditions to cross intersections, in a direction normal to the direction of the maximum horizontal stress. This direction is not always easy to determine, as the magnitudes of the maximum and minimum horizontal stresses are often very close. In cases like those, it is seldom an effective strategy to minimize the effects of the stress by orientating the panel at a direction 45° to the direction of the maximum stress. The only remaining strategy then is to rely on very good support.

The directions and magnitudes of the horizontal stresses should be determined by measurement. However, the current methods are cumbersome, time consuming and expensive. Stress mapping, relying mainly on visual observations, can also supply useful information.

The mapping should begin with regional observations of the directions of major dykes and faults. In this respect, readily available satellite photographs supply valuable information. Underground mapping should follow the regional observations. The most important effects to be observed are explained in Chapter 11: Monitoring.

Support strategy

As with several other causes of roof instability, there are two basic methods to deal with high horizontal stress. One, which is the least favoured albeit cheaper one, is to accept that roof failure will occur and to merely prevent the failed roof from falling and thus resulting in losses. This can be achieved in a number of ways, ranging from standing supports such as arches or timber sets to basket type roof support, explained in more detail earlier in this Appendix.

The preferred method is to provide sufficient confinement to the rock to prevent failure in the first place. It should be accepted that it is highly unlikely that, for instance, guttering can be prevented altogether. That will require high magnitudes of compressive stress to be supplied in the form of bolting.

If the guttering is to be prevented altogether, the required support resistance, σ_R, can be obtained from a Mohr diagram. Mathematically, it is:

$$\sigma_R = \sigma_{th} - 2\tau_R \qquad [57]$$

where τ_R = shear strength of the roof rock.

For example, if guttering is to be prevented by bolting in the second part of the previous example, the required support resistance is:

$$\sigma_R = 29.1 - 16 = 13.1 \text{ MPa.}$$

To achieve this magnitude of resistance, it implies that a force of 13.1 MN is to be supplied to the roof per square metre. With good installation, the best pre-tension that can be expected with a 25 mm bolt is about 0.2 MN—or, approximately 65 bolts per square metre will be required. This is clearly not possible.

However, the purpose of the support is not to prevent even minute guttering, but rather to prevent its unchecked progression into the roof. The magnitude of the tangential stresses decrease with increasing distance into the roof as the radial stresses increase. Therefore, the magnitudes of the shear stresses are decreased by a double mechanism, and consequently bolting becomes progressively more attractive as a preventative measure.

A first order design is best achieved by means of numerical modelling or by trial and error application underground. The error component of 'trial and error' should be minimized by monitoring in favour of haphazard improvisation. Therefore, for 'trial and error' read 'trial and monitoring'.

The general principles are relatively simple in concept, the main provision being that the support system should be as stiff as possible. This is achieved in practice by attending to all the aspects of roof support:

• The annulus should be as small as possible
• Steel bar with high shear and tensile moduli should be used
• Supports should be installed close to the face, to prevent the initial movement from taking place
• Resin with a high compressive modulus should be used
• Bolt spacing should be as dense as practicable
• Bolts should be pre-tensioned, implying that dual speed resin should be used
• W-straps or similar steel links between bolts should be used
• Bolts on the edges of the roadways should be doubled up.

In most practical situations, a bolting pattern of 6 or 7 bolts per row, spaced at 1.0 m has been seen to suffice.

The bolts should be 20 mm diameter high modulus (i.e. 600 MPa yield) installed in 25 mm diameter holes (or 25 mm bolts in 28 mm holes) pre-tensioned to at least 200 kN. The pre-tension can be reduced for bolts installed within less than a metre from the face.

Selection of components

There are several types and combinations of roof support components available. While most are effective for certain types of applications, they have different degrees of efficiency for different applications. Not all are equally effective for all conditions. The classification to be used for this selection guide, is to view the different systems under the groupings of the two basic types of applications, i.e. suspension and beam creation.

Suspension application

As the only requirement for suspension systems is a certain capacity for load bearing, virtually any type of bolt can be used.

Mechanical anchors

Mechanical anchors are sometimes acceptable, especially in hard sandstone where it is difficult to drill holes thinner than 32 mm diameter. The disadvantages are that in the absence of a grout filling, they are susceptible to corrosion; also, anchors may creep, and of course the anchor resistance is fixed at between 50 and 100 kN. What is not commonly appreciated is that once the bolt relaxes due to, for instance, frittering of the roof underneath the washer, the anchor itself may lose grip due to relaxation.

In cases where mechanical anchors are used, the bolt diameter needs to be only thick enough to be 1,5 times stronger than the required anchor resistance. In most cases a 16 mm bolt with a yield strength of 115 kN will be sufficient.

A very important element of any suspension system is the strength of the washer assembly, which includes the washer, nut and thread. The washer must be able to withstand 80% of the system's required resistance before it deforms and 100% before it fails, usually by the nut pulling through the washer. The nut and thread must be stronger than the bolt.

The recommended test procedure is the following:
• Design system, determine required resistance of bolt
• Install bolt underground in the chosen hole

diameter and perform pull test on anchor, using double nuts and a 25 mm thick steel washer at the protruding end of the bolt, as shown in Figure 11. Check whether the anchor offers the required resistance.

- Fit double nuts to the end of the bolts and a single nut of the type to be used underground, to the other end. Perform pull test in a workshop. The steel body must fail before the thread fails. This also tests the breaking strength of the steel.

- Fit the roof washer and nut to one end of the bolt. Insert a 25 mm thick steel washer—with a hole with diameter 1.5 times the diameter of holes to be drilled under-ground—on the inside of the roof washer and fit double nuts to the anchor end, as shown in Figure 12. Perform pull tests in workshop; check loads at which washer deforms and fails.

Point anchor resin bolts

Point anchor resin bolts are equally effective for suspension systems, with the major advantage that the anchor resistance can be adjusted by varying the length of the resin anchor. Also, the anchor does not lose grip when the bolt relaxes.

The major disadvantages of resin point anchors, as compared to mechanical anchors, is that the installation procedure is more complex, requires more discipline and that seasonal fluctuations in temperature may require adjustments to the installation procedure. It is also often necessary to use a thicker bolt than would be required from a strength point of view, merely to ensure proper mixing of the resin.

As with mechanical anchors, the anchor resistance depends on the rock type into which the anchors are installed. It is therefore necessary to do a number of pull-out tests on short anchors, in the actual rock where the support is to be installed, to determine the resistance. For this test, it is important that the test anchors be short enough to fail, as the actual failure loads have to be recorded.

The notes about the importance of the washer and nut assembly in the section on mechanical anchors are applicable to resin point anchor systems as well, as are points 2 to 4 on the recommended test procedure.

In order to optimize resin performance, it is important to allow proper mixing of the components. This is achieved by balancing the hole and bolt diameters—the bolt should be between 4 and 8 mm smaller in diameter than the hole for coarse resins.

Where resins with suitably fine filler is used, the annulus can be reduced to improve the stiffness of the system. This guide is based on practical experience. Commonly used systems are 16 mm bolts in 22 mm holes and 25 mm or 20 mm bolts in 28 mm holes. Some mines use 20 mm bolts in 25 mm holes, which has been seen to be effective support in high horizontal stress areas. The combination of 25 mm holes with 16 mm rebar is also in use on some mines but is discouraged because of inconsistent resin mixing.

In several situations, the system elements are determined by ease of drilling into the roof. It is paradoxical that in several suspension-type systems, where a relatively light load is to be supported, the overlying roof beam is a strong sandstone into which 28 mm holes are drilled because slimmer holes require
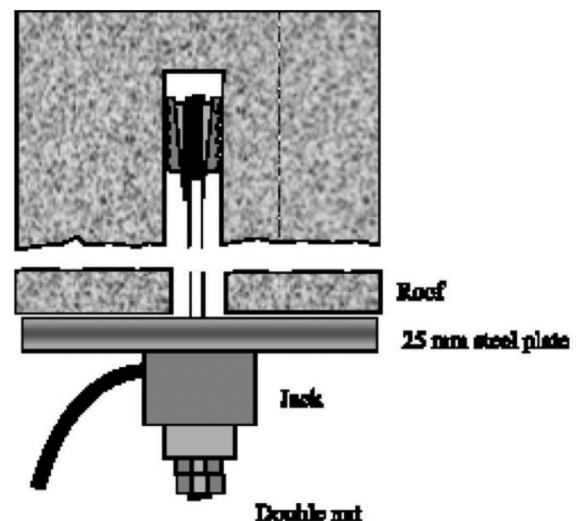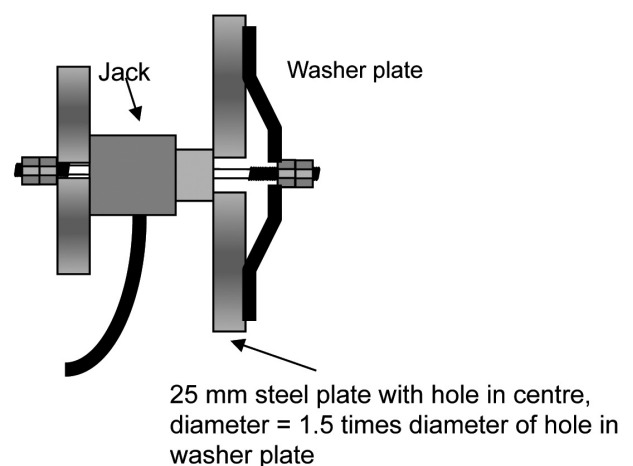

Figure 11. Pull test on a mechanical anchor

Figure 12. Pull test on a washer plate

thinner drill rods which cannot transmit the required thrust. Then, 20 mm steel bar has to be used to ensure resin mixing, when 16 mm would have been adequate from a suspension point of view.

From the foregoing discussion, it can be deduced that steel with circular cross-section can be replaced by other profiles—the important provision is satisfactory and consistent mixing of the resin. When alternative profiles with smaller cross-sectional area (like quad-bar) are used, it is important to check that the actual strength of the steel member conforms to the requirements. It is also important to ensure that the combination of profile and direction of spinning during mixing is such that the resin is not displaced down the hole.

Beam creation

It is only theoretically possible to achieve beam creation with point anchor elements. Provided the required amount of pre-tension can be supplied, the beam will be stable—but only for as long as the pre-tension is maintained. Pre-tension is usually lost shortly after installation, by anchor slippage and/or frittering of the roof strata underneath the washer plates.

When the pre-tension is lost, the normal stress on the lamination interfaces is also lost and the layers are free to slide. The inter laminae sliding will continue until the rock makes contact with the steel body of the bolts. This is after several millimetres of displacement (in the region of 6 to 16 mm relative displacement), and in several beam creation situations fractions of millimetres of displacement are sufficient to result in beam failure.

Full column dual speed resin systems are therefore recommended. With these, the pre-tension is locked in once the resin has set, and the void in the hole is filled by resin which restricts lateral inter laminae displacement. All the requirements mentioned in the section on point anchor resin systems are applicable, with the exception that there is now less emphasis on the washer assembly.

It will be prudent to place the same requirements on the washer assembly, but if significant savings can be achieved by using a washer assembly that is say 20% weaker, there is no real reason not to use the weaker washer. Theoretically, it is possible to create a stable beam without any washer at all, but because resin mixing is seldom perfect at the bottom end of the hole, practice dictates that there should be a washer of some description at least.

In beam creation, it is important to restrict the thickness of resin in the hole to the minimum. The thicker the resin, the more it can compress and consequently the greater the inter laminae slip will be.

The annulus must therefore be a minimum. So far, using commercially available products, it has been found difficult to achieve a smaller annulus than 5 mm—i.e. 20 mm rebar into a 25 mm hole, for any bolt longer than 1.2 m. Amongst other things, this is a function of the coarseness of the filler used in the resin. The coarser the filler, the more difficult it becomes to insert a bolt into a thin hole. There is a trade-off in this situation, because in general the coarser resins are both stronger and stiffer. Both coarse and fine resins are available in South Africa.

Care should be taken to ensure that all the system elements are in balance, especially when a small annulus is used. If the annulus is too small, there is a distinct danger that there will be 'dry spots' in the hole, where there is insufficient resin between the bolt and the sidewall of the hole. The resin has to be fine enough to be compatible with the small annulus. This can be determined only by *in situ* pull tests on short anchors.

The dual speed resins also suffer from the operational disadvantage that the order of resin capsule insertion into the holes must be correct, and that no matter what the length of the hole, at least two capsules are required. It is also not always possible to get the exact lengths of capsules that the system requires and consequently the anchor portions have to be longer than required. This has negative cost implications.

In countries such as Australia, single capsules with a fast resin at one end and the rest a slow resin, have been used for several years. These are now commercially available in South Africa as well.

Characteristics of resin

The resin used for roof support is supplied in a two component capsule, in which the resin (a polyunsaturated polyester) with a finely ground limestone filler is separated from the catalyst. The membrane is made of polyester material in which tears propagate easily once the material has been ruptured.

When the resin is mixed with the catalyst, it sets off a chemical reaction that causes the resin temperature to increase to approximately 80°C. At this elevated temperature, the short molecular chains join to form long chains and the resin's state changes from fluid to solid. During the joining up process, the links are

ROCK ENGINEERING FOR UNDERGROUND COAL MINING

weak and if broken, cannot recover.

It is therefore vitally important not to disturb the resin during the 'holding' period.

The second important point is that the resin setting process is temperature controlled. If the resin is cold, the linking up process takes longer and consequently the holding period should be increased. This is especially important in the winter months, and even more so for sections working close to intake shafts. Resin should be stored in the section for at least 24 hours before being used, to reach ambient temperature.

Even then, it is often necessary to increase the holding time in winter. Several mines have increased their holding times for the year round to the maximum holding time in winter, to avoid confusion. Figure 13 shows the effect of ambient temperature on the reaction time of the resin. The information from which the diagram was constructed was supplied by Fasloc Resins (Pty) Ltd.

The size of washers and the use of headboards

Whether to use flat washers, shaped washers, spherical seat washers, large or small diameter washers, steel or timber head boards, etc, depends on the function of the support, the nature of the immediate roof and the life expectancy of the excavation. Expensive spherical seat washers in a simple suspension application are wasted while using flat washers with inclined bolts in a beam creation system negates much of the effect of the system. Table I supplies general guidelines.

In Table I, a 'short' life means a few months only, i.e. typical bord and pillar production panels. Anything else is regarded as long life. A small washer means 100 mm square and a large washer means larger than 150 mm square.

In general, timber headboards play an important role in preventing falls of friable roof over the short term. They should not be used for any long-term application because as the timber decays or dries out it causes the bolts to lose tension, with negative consequences for the system as a whole. What is often neglected when timber headboards are used with resin anchors, is to shorten the holes to compensate for the thickness of the headboards, resulting in anchor loss.

Probabilistic design methods
(see also Chapter 3)

If the variabilities of the elements making up a support system are known, then the probability of failure can be quantified. The load on a support system can be described by a distribution, characterized by a mean and standard deviation— the smaller the standard deviation, the less the variability. The same can be done for the resistance to failure of the system. The area of overlap between the two distributions then represents the probability of failure because in the area of overlap, the load is greater than the resistance, see Figures 32 and 33, Chapter 3.

If the means and standard deviations of the two distributions are known, then the area of overlap of the distributions, is calculated as follows according to Harr (1987):

$$f = \frac{M_s - M_f}{\sqrt{S_s^2 + S_f^2}} \qquad [58]$$

where M_s = Mean of the distribution of the resistance of the system

M_f = Mean of the distribution of the load on the system

S_s = Standard deviation of the resistance of the system

S_f = Standard deviation of load on the system.

Then, for values of $f > 2.2$, the probability of failure P_f, is

$$P_f = \frac{1}{f}(2\pi)^{-0.5} \exp\left(\frac{-f^2}{2}\right) \qquad [59]$$

For values of $f \le 2.2$, the probability of failure is:

$$P_f = 0.5 - \psi(f) \qquad [60]$$

where $\psi(f)$ is found from statistical tables (Harr 1987, p.47).

Alternatively, the academically less correct but nonetheless evenly accurate method is to find $\psi(f)$ from the following best fit polynomial equation which is based on the values in the Harr table:

$$\psi(f) = .0006f^6 - .0096f^5 + .0563f^4 - .1379f^3 + .0423f^2 + .3893f + .0004 \qquad [61]$$

Note that Equation [61] is valid only for $f \le 2.2$.

Worked example

Consider the following example which demonstrates the power of the probabilistic process.

A weak layer, 0.5 m thick, needs to be supported. This results in a load density of 12.5 kN/m². It was found that a support system comprising of 0.7 m resin anchors at a spacing 1.63 m would be sufficient. The support density of the system is then 18.75 kN/m².

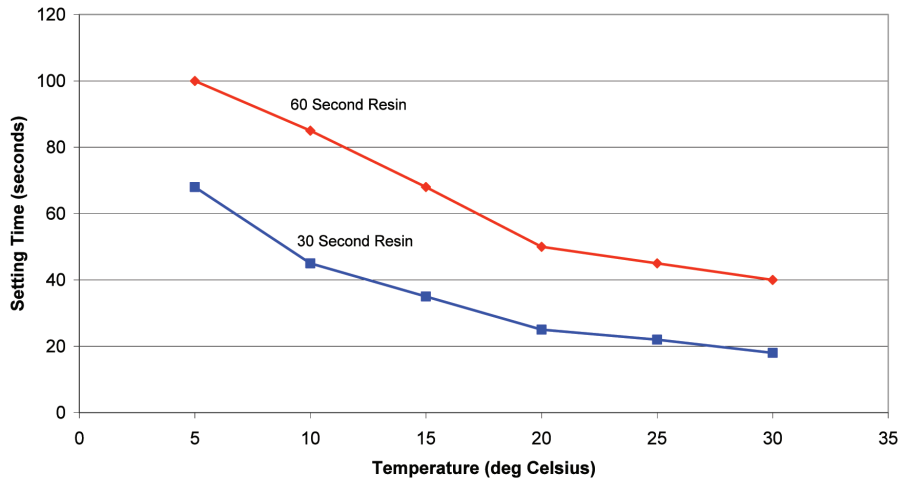However, it is known that both the load and the

Figure 13. The effect of temperature on the gel time of commonly used resins

Table I
General guidelines for washer types

Support method	Nature of roof	Life of excavation	Washer type
Suspension	Friable	Short	Timber headboard
Suspension	Friable	Long	Steel headboard or large flat washer
Suspension	Strong	Short	Small flat steel washer
Suspension	Strong	Long	Small domed steel washer
Beam creation	Friable	Short	Timber headboard
Beam creation	Friable	Long	Steel headboard with domed washer
Suspension, inclined bolts	Friable	Short	Large domed washer
Suspension, inclined bolts	Strong	Long	Large spherical seat washers
Beam creation, inclined bolts	Strong or weak	Long or short	Large spherical seat washers

support capacity are given to variability. Say the standard deviation of the thickness of the weak layer is 0.1 m (i.e. 85% of the weak layer is between 0.4 m and 0.6 m thick). This will translate directly to the load on the system, which will vary by the same percentage (20%). This means that the standard deviation of the load will be 2.5 kN/m².

Say further that only one of the variables making up the resistance, the shear strength of the resin bond, varies by 25% while all the other variables (hole length, steel diameter, etc.) remain constant. This means that the support resistance will also vary by 25%, i.e. the standard deviation will be 4.7 kN/m².

First find f from Equation [58]

$$f = \frac{18.75 - 12.5}{\sqrt{4.7 + 2.5}} = 1.174$$

As $f < 2.2$, the statistical tables have to be used to find $\psi(f)$, alternatively Equation [61] can be used.

Then, using Equation [61],

$\psi(f) = 0.0006(0.789)^6 - 0.0096(0.789)^5 +$
$0.0563(0.789)^4 - 0.1379(0.789)^3 +$
$0.0423(0.789)^2 + 0.3893(0.789) + 0.0004$
$= 0.380$

and from Equation [60]
$P_f = 0.5 - 0.380 = 0.120$

The probability of failure is thus 0.12, or 12%. Note that the safety factor of the system is 18.75/12.5 = 1.5.

If now the standard deviation of the resin can be reduced by half, say by applying more consistent installation or merely switching to a more consistent resin product, then the standard deviation of the support resistance will also reduce by 50% to 2.35 kN/m². It is then found by following the same process as outlined above that the probability of failure reduces to 3.4%, less than a third of the previous value.

This means that without increasing the safety factor, the probability of failure can be substantially reduced merely by reducing the variability of the shear resistance.

ROCK ENGINEERING FOR UNDERGROUND COAL MINING

Alternatively, if the resin shear strength cannot be made more consistent, it will be necessary to increase the safety factor to 1.8 to achieve the same probability of failure as with the more consistent shear strength. This will come at a cost.

Similar examples can be developed to demonstrate the impact of the other variables in the system. The numbers in the example are not totally out of the realistic range, and indicate that at the commonly accepted safety factor of 1.5, some failures are bound to occur. The failures are not due to inferior design, but due to variability.

The most important point to note, however, is that improvement can be achieved by limiting the variability inherent in the support elements without increasing the safety factor. This essentially comes down to tighter quality control, both over the quality of the product and the installation procedures.

Pillar design

In this Appendix, the pillar design procedures explained in Chapter 4: Pillar Design will be illustrated and expanded by means of examples.

Example 1: Mining underneath a hill, with increasing depth

The basic scenario is that a horizontal seam 4.0 m thick outcrops on a hillside where the depth to the floor increases from 0 to 250 m.

Management selects:

- The mining height, $h = 3$ m
- Bord width, $B = 6$ m and
- Required Safety Factor, *SF*:

  Main development   2.0

  Pillar extraction   1.8

  Production panel   1.6.

Section A: Mining depth = 40 m

COMRO Guidelines for Shallow Workings apply when depth to floor of seam is equal to or shallower than 40 m. These are:

- Pillar width 5.0 m minimum.
- Safety factor 1.6 minimum.
- Pillar width to mining height ratio 2.0 minimum and
- Maximum per cent extraction 75%.

Thus for a square pillar geometry the minimum pillar width of 6.0 m is required to fulfil the minimum pillar width to mining height ratio of 2.0

Safety factor

The safety factor is given by:

$$Safety\ factor = \frac{pillar\ strength}{pillar\ load} \qquad [1]$$

Salamon's pillar strength formula:

$$Strength = \frac{7.2w^{0.46}}{h^{0.66}} \ \ MPa \qquad [2]$$

Tributary area theory

Load is determined by the tributary area theory where individual pillars carry the overburden immediately above them, provided the panel width exceeds the depth to the workings and the pillars are uniform in size.

$$Load = \frac{25HC_1C_2}{w_1w_2} \ \ kPa \qquad [3]$$

Where w_1 is the pillar width in the split direction and w_2 is the pillar width in the direction of panel advance. C_1 is the centre distance in the split direction and is the sum of the pillar-and-bord width.

For the parameters $H = 40$ m, $B = 6.0$ m, $h = 3.0$ m the pillar strength and load can be calculated.

$$Strength = \frac{7.2w^{0.46}}{h^{0.66}} = \frac{7.2. \times 6^{0.46}}{3^{0.66}} = \frac{16.42}{2.06} = 7.97 \ \ MPa \quad [2]$$

$$Load = \frac{25HC^2}{w^2} = \frac{25 \times 40 \times 12 \times 12}{6 \times 6} = \frac{144000}{36} \qquad [3]$$

$$= 4000 \ \ kPa\ or\ 4\ MPa$$

$$SF = \frac{7.97}{4} = 1.99. \qquad [1]$$

Alternatively the safety factor could have been found using:

$$SF = \frac{288w^{2.46}}{Hh^{0.66}C^2}$$

$$SF = \frac{288w^{2.46}}{Hh^{0.66}C^2} = \frac{288 \times 6^{2.46}}{40 \times 3^{0.66} \times 12^2} = \qquad [4]$$

$$\frac{288 \times 82.08}{40 \times 2.06 \times 144} = \frac{23639.04}{11865.6} = 1.99$$

Areal percentage extraction

The percentage extraction is commonly quoted as the percentage per centre distance as per a section plan. For the parameters above where $w = 6.0$ m and $C = 12$ m the areal percentage extraction is:

$$e\% = 1 - \frac{w_1w_2}{C_1C_2}$$

$$e\% = 1 - \frac{w_1w_2}{C_1C_2} = 1 - \frac{6 \times 6}{12 \times 12} = 1 - \frac{36}{144} = \qquad [5]$$

$$1 - 0.25 = 0.75 \ or \ 75\%$$

For square pillars $e\% = 1 - \dfrac{w^2}{C^2}$

For rectangular pillars $e\% = 1 - \dfrac{w_1 w_2}{C_1 C_2}$ [6]

The average pillar load

The average pillar load can also be found assuming that the virgin stress, σ_v, is equal to 1 MPa per 40 m depth.

$$Average\ Pillar\ Load = \frac{\sigma_v}{1-e}$$

$$Average\ Pillar\ Load = \frac{\sigma_v}{1-e} = \frac{1}{1-0.75} = \frac{1}{0.25} = 4\ \text{MPa} \quad [7]$$

Overall areal percentage extraction, e_o

Assume that a nine road panel is to be mined and that the barrier pillar width, W_B, is 6 m.

$$e_o = \left[\frac{Panel\ width}{Panel\ width\ +\ Barrier\ width}\right]\left[1 - \frac{Panel\ area}{Centre\ area}\right] =$$
$$\left[\frac{(n-1)C + B}{(n-1)C + B + W_B}\right]\left[1 - \frac{(n-1)(w_1 w_2)}{[(nC_2) + B]C_1}\right] \quad [8]$$

$$e_o = \left[\frac{8 \times 12 + 6}{8 \times 12 + 6 + 6}\right]\left[1 - \frac{8 \times 6 \times 6}{(8 \times 12 + 6)12}\right] = \left[\frac{102}{108}\right]\left[1 - \frac{288}{1324}\right]$$
$$0.94(1 - 0.235) = 0.719 = 71.9\%$$

Volumetric percentage extraction

If only 3.0 m of the 4.0 m seam is mined the overall volumetric percentage extraction is:

$$V = \frac{h e_o}{h_s}$$
$$V = \frac{h e_o}{h_s} = \frac{3 \times 0.71}{4} = 0.53\ or\ 53\% \quad [9]$$

Where h is the mining height and h_s is the seam thickness, e_o is the areal percentage extraction.

Section B: Mining depth = 55 m

Rectangular pillars

Elongation of the pillars is used where an increase in pillar size is required but the roadways have to remain straight. In addition, where a variation in the mining height h and depth to the floor of the seam H occurs an option is to fix C_1, therefore the panel width remains constant.

For example, if one month's mining will result in a maximum depth of 55 m to maintain a safety factor of 2.0 the square pillar width required is 7.6 m (obtained from the design tables) for $h = 3.0$ m and $B = 6.0$ m.

The effective square pillar width of a rectangular pillar is given by:

$$w_{eff} = \frac{4 \times Pillar\ area}{Pillar\ perimeter}$$
$$w_{eff} = \frac{4 \times Pillar\ area}{Pillar\ perimeter} = \frac{4 \times w_1 w_2}{2(w_1 + w_2)} = \frac{2 w_1 w_2}{w_1 + w_2} \quad [10]$$

Therefore

$$w_2 = \frac{w_{eff} w_1}{(2 w_1 - w_{eff})} \quad [10]$$

For the example above the required elongation of the pillar to have an effective square width of 7,6 m is:

$$w_2 = \frac{w_{eff} w_1}{(2 w_1 - w_{eff})} = \frac{7.6 \times 6}{(2 \times 6 - 7.6)} = \frac{45.6}{4.4} = 10.36\ \text{m} \quad [11]$$

A 6.0 by 10.5 m pillar would give the required safety factor of 2.0 for the depth of 55 m and mining height of 3.0 m. The elongation of the pillar should only be applied where the length to width ratio is less than four.

Section C: Mining depth = 250 m

Squat pillars

In the example, the depth of the workings increases as mining continues, necessitating adjustments to the pillar size. At the depth of 125 m a pillar width of 15 m is required to maintain a safety factor of 2.0. The pillar width to mining height ratio is 5 (15/3=5). At the pillar width to mining height ratio of 5.0 the strengths of the Salamon/Munro and the squat pillar formulae are equal.

At a depth of 250 m; $h = 2.5$ m; $B = 6.0$ m a pillar width $w = 28.5$ m is required, using the Salamon/Munro strength formula, to maintain a safety factor of 2.0. The pillar width to mining height ratio, R, is = 11.4. At this ratio the Salamon/Munro pillar strength formula under-estimates the strength of 'squat' pillars. It should be noted that the use of the squat pillar formula is not depth dependent but related to the ratio of the pillar width divided by the mining height. Using the squat pillar strength formula, a pillar width of 22 m is required.

Comparing the two methods

$$Squat\ strength = k \frac{R_o^b}{V^a}\left\{\frac{b}{\varepsilon}\left[\left(\frac{R}{R_o}\right)^\varepsilon - 1\right] + 1\right\} \quad [12]$$

Where k = 7 176 kPa taken as 7.2 MPa
     R_o = critical pillar width to mining height ratio = 5
     ε = rate of strength increase = 2.5
     a = constant = 0.0667

b = constant = 0.5933

R = actual pillar width to mining height ratio. In this case = 22/2.5 = 8.8.

V = pillar volume, $w_1 w_2 h$. In this case = $(22 \times 22 \times 2.5) = 1\ 210$ m³.

$$Squat\ strength = 7.2 \frac{5^{0.5933}}{1210^{0.0667}} \left\{ \frac{0.5933}{2.5} \left[\left(\frac{8.8}{5} \right)^{2.5} - 1 \right] + 1 \right\}$$

$$= \frac{7.2 \times 2.6}{1.61} \left\{ 0.2373 \left[(1.76)^{2.5} - 1 \right] + 1 \right\}$$

$$= \frac{18.71}{1.61} \left\{ 0.2373[4.11 - 1] + 1 \right\}$$

$$= 11.66 \{ 0.2373[3.11] + 1 \}$$

$$= 11.66 \{ 0.74 + 1 \}$$

$$= \mathbf{20.29\ \ MPa}$$

Alternatively, for a quick hand calculation, the simplified formula could be used:

$$Strength = \frac{0.0786}{V^{0.0667}} \left\{ R^{2.5} + 181.6 \right\}$$

$$= \frac{0.0786}{1210^{0.0667}} \left\{ 8.8^{2.5} + 181.6 \right\}$$

$$= \frac{0.0786}{1.605} \{ 229.724 + 181.6 \}$$

$$= 20.14\ \ MPa.$$

The pillar load at 250 m depth, w = 22 and C = 28 ($w+b = 22 + 6 = 28$) is given by:

$$Load = \frac{25HC^2}{w^2} = \frac{25 \times 250 \times 28 \times 28}{22 \times 22} = \frac{4900000}{484} \quad [3]$$

$$= 10123.97\ \ kPa\ or\ 10.1\ \ MPa$$

Safety factor = strength divided by Load

$$Safety\ factor = \frac{20.29}{10.1} = 2.0$$

Comparing the squat strength to Salamon's strength, where H = 250 m, h = 2.5 m, B = 6.0 m, w = 28.5 m and C = 34.5 m:

$$Salamon\ strength = \frac{7.2w^{0.46}}{h^{0.66}} = \frac{7.2 \times 28.5^{0.46}}{2.5^{0.66}}$$

$$= \frac{7.2 \times 4.669}{1.83} = \frac{33.15}{1.83} = 18.1\ \ MPa$$

$$Load = \frac{25HC^2}{w^2} = \frac{25 \times 250 \times 34.5 \times 34.5}{28.5 \times 28.5}$$

$$= \frac{7439061.5}{812.25} = 9158\ kPa\ or\ 9.16\ MPa.$$

$$Safety\ factor = \frac{18.1}{9.16} = 1.96 (\text{The difference is due to rounding of the pillar dimension})$$

Differences in the calculations are: squat strength = 20.1 MPa for a 22 m pillar width compared to 18.1 MPa for a 28.5 m pillar using Salamon's formula. Using the squat formula thus results in higher extraction ratios.
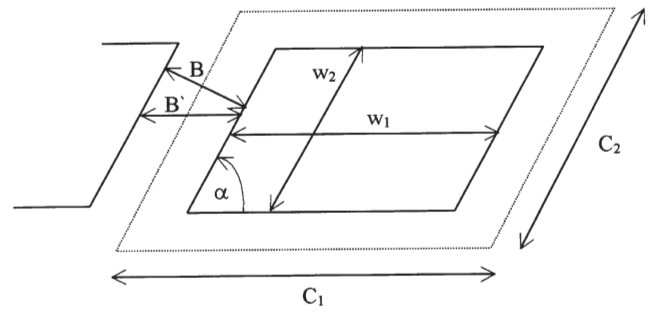
Figure 1. Rhomboidal pillar

Example 2: Herring-bone or Rhomboidal pillar

The herring bone layout has been applied to continuous miners and where continuous haulage systems are used. Assume that the pillar side lengths are 12.0 m and 15 m, bord width 6.0 m (i.e. the underground cutting width), mining height 3.0 m and the turn-off angle 70°.

Strength calculation

$$w_{ep} = \frac{2w_1 w_2 Sin\alpha}{w_1 w_2}$$

$$= \frac{2 \times 12 \times 15 \times 0.94}{12 + 15}$$

$$= \frac{338.4}{27}$$

$$= 12.53$$

$$Strength = 7.2 \frac{12.53^{0.46}}{3^{0.66}} = 7.2 \frac{3.2}{2.065} = 11.16\ MPa$$

Load calculation

$$C_1 = w_1 + \frac{B}{Sin\alpha} = 12 + \frac{6}{0.94} = 18.38$$

$$C_2 = w_2 + \frac{B}{Sin\alpha} = 15 + \frac{6}{0.94} = 21.38$$

$$Load = \frac{0.025HC_1 C_2}{w_1 w_2} = \frac{0.025 \times 120 \times 18.38 \times 21.38}{12 \times 15} =$$

$$\frac{1179}{180} = 6.55\ \ MPa$$

Safety factor

$$SF = \frac{Strength}{Load} = \frac{11.16}{6.55} = 1.7$$

Note that if the same dimensions had been used in a square lay-out, the safety factor would have been 1.82.

Example 3: Continuous miner adjustment

Note: *The continuous miner adjustment cannot be applied if the depth is greater than 175 m or the pillar width is less than 5.0 m.*

At a depth of 75 m, mining height 3.0 m, bord 6.0 m, the safety factor is 2.1 using Salamon's strength and tributary load. However, all cases used in Salamon's statistical analysis were pillars formed by drill-and-blast methods. The equivalent strength of pillars formed by continuous miner is given by:

$$\eta = \eta_o(1 + \frac{2\Delta w_o}{w})^{2.46} \quad [13]$$

where η = the equivalent continuous miner safety factor

η_o = Salamon's safety factor

Δw_o = The blast damage zone, taken as 0.25 to 0.3 m

w = the designed pillar width.

The equivalent continuous miner safety factor is:

$$\eta = \eta_o(1 + \frac{2\Delta w_o}{w})^{2.46} = 2.1(1 + \frac{2 \times 0.3}{10})^{2.46} =$$

$$2.1(1 + \frac{0.6}{10})^{2.46} = 2.1(1.06)^{2.46} = 2.1 \times 1.14 = 2.42$$

Thus the continuous miner formed pillar is stronger due to the absence of a blast damage zone.

There are two options when applying the continuous miner adjustment:

• Maintain the centre distance and reduce the pillar width by 0.6 m, the disadvantage of this is the stability of the increased bord width or
• Maintain the design bord width and reduce the pillar centre distance.

Option (a) Constant centre distance

In this example the bord increased from 6.0 m to 6.6 m and the pillar width reduced from 10 m to 9.4 m.

$C = 16$ m, $B = 6.5$ m, $w = 9.4$ m, $H = 75$.

$$SF_{cm} = \frac{288(w - 2\Delta w_o)^{2.46}}{H.h^{0.66}(b + w)^2}$$

$$SF_{cm} = \frac{288(w - 2\Delta w_o)^{2.46}}{H.h^{0.66}(b + w)^2} = \frac{288(10 - 0.6)^{2.46}}{75 \times 3^{0.66}(6 + 10)^2} = \quad [14]$$

$$\frac{288(9.4)^{2.46}}{75 \times 2.06 \times 16^2} = \frac{288 \times 247.68}{75 \times 2.06 \times 256} =$$

$$\frac{71331.84}{39552} = 1.8$$

Applying the continuous miner adjustment:

$$\eta = \eta_o(1 + \frac{2\Delta w_o}{w})^{2.46} = 1.8(1 + \frac{2 \times 0.3}{9.4})^{2.46} =$$

$$1.8(1 + \frac{0.6}{9.4})^{2.46} = 1.8(1.06)^{2.46} = 1.8 \times 1.164 = 2.1$$

Option (b) Constant bord width

An additional reduction in pillar width is possible due to the reduction in pillar centre distance. Therefore to balance the pillar strength and load calculations a reduction in pillar width 'X' is required. 'X' is found by iteration in this case 'X' is 1.0 m.

$$SF_b const = \frac{288(w - 2\Delta w_o - X)^{2.46}}{H.h^{0.66}(w + b - 2\Delta w_o - X)^2}$$

$$SF_b const = \frac{288(w - 2\Delta w_o - X)^{2.46}}{H.h^{0.66}(w + b - 2\Delta w_o - X)^2} =$$

$$\frac{288(10 - 0.6 - 1.0)^{2.46}}{75 \times 3^{0.66}(10 + 6 - 0.6 - 1.0)} = \quad [15]$$

$$\frac{288(8.4)^{2.46}}{75 \times 3^{0.66}(14.4)^2} = \frac{288 \times 187.81}{75 \times 206 \times 207.36} =$$

$$\frac{54089.28}{32037.12} = 1.69$$

Applying the continuous miner adjustment:

$$\eta = \eta_o(1 + \frac{2\Delta w_o}{w})^{2.46} = 1.69(1 + \frac{2 \times 0.3}{8.4})^{2.46} =$$

$$1.69(1 + \frac{0.6}{8.4})^{2.46} = 1.69(1.07)^{2.46} = 1.69 \times 1.18 = 2.0$$

Example 4: Design incorporating a weak floor

The pillar parameters are:

Depth to floor, $H = 50$ m

Centre distance, $C = 12$ m

Pillar width, $w = 6.0$ m

Mining height, $h = 2.4$ m

Weak floor thickness, $T_{sf} = 0.5$ m

$$Average\ Pillar\ Stress = \frac{\sigma_v}{(1 - e)} \quad [16]$$

σ_v is the virgin stress and e is the extraction ratio.

The virgin stress can be calculated as:

$\sigma_v = \rho\ g\ H$

Assuming the density as $\rho = 2\ 500$ kg/m^3 and gravity as $g = 10$ m/sec^2
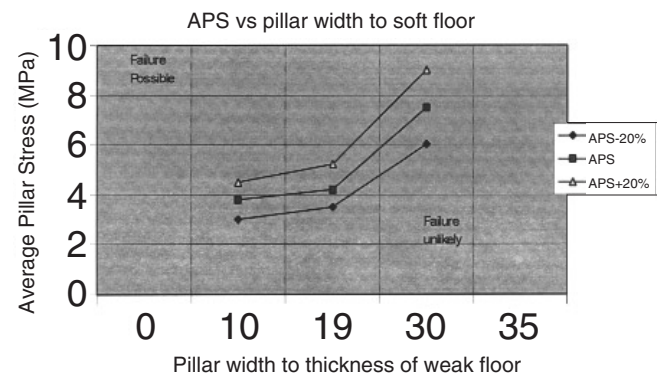
$\sigma_v = 0.025H$

or

Figure 2. Average pillar stress vs pillar width to thickness of weak floor

$$\sigma_v = \frac{H}{40}$$

Then, because

$$e = (1 - \frac{w^2}{C^2}), \qquad [4]$$

the average pillar stress can be calculated by:

$$Average\ pillar\ stress = \frac{\sigma_v}{(1-e)} = \frac{HC^2}{40\ w^2} \qquad [4c]$$

In the example the average pillar stress is 5.0 MPa. The ratio of pillar width to weak floor thickness is 6.0/0.5 = 12. This gives a plot on the possible failure side of the curve in Figure 2. In this case increasing the centre distance and reducing the bord width to 5.0 m will lower the average pillar stress into the Failure Unlikely region.

Example 5: Design for auger mining layouts

On occasions there is a zone between feasible opencast reserves and the underground operation which can be exploited by augering the highwall. The pattern of the auger holes will determine the percentage extraction. However, failure of the ribs between the auger hole has to be avoided to prevent loss of equipment and endangering the safety of the operating personnel. Therefore it is common to leave a larger rib after a series of closely spaced holes. In the design the rib between the holes is not taken into account as a support rib due to the low width-to-height aspect which could be affected by discontinuities or weak layers within the coal seam. Figure 3 shows a well laid out design from a highwall.

If the depth to the floor, H, is 30 m and the auger diameter 1.5 m the design could be as follows:
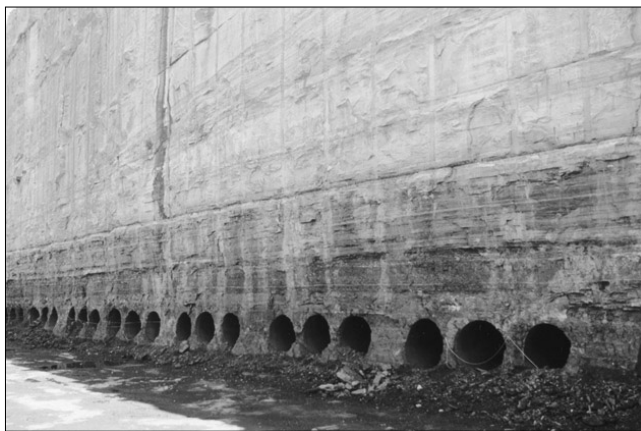
Figure 3. An example of a well designed auger extraction from a highwall

The spacing between the auger holes will be 0.2 m, and four auger holes will be mined before a 2 m rib is left. Thus the spacing between the larger ribs is 6.6 m. The larger rib, although continuous, has a width-to-height ratio of less than 2.0 and therefore the minimum width of 2.0 m will be used in the strength calculation instead of the effective width method which would have given an equivalent pillar width of twice the rib width.

The immediate strata above the auger holes and the presence of thick competent layers can influence the span between the larger ribs.

Depth to floor of the seam, H, = 30 m
Diameter of auger =1.5 m
Spacing between auger holes = 0.2 m
Rib size = 2.0 m
Number of auger hole sets between larger ribs = 4.

The strength calculation ignores the strength of 0.2 m ribs between auger holes and uses minimum rib width.

$$Strength = \frac{7.2w^{0.46}}{h^{0.66}} = \frac{7.2 \times 2^{0.46}}{1.5^{0.66}} = \frac{7.2 \times 1.38}{1.31} = 7.58\ \text{MPa} \quad [2]$$

The strength calculated is for a square pillar and has ignored the rib effect on strength.

The load is calculated assuming a two-dimensional aspect as the rib length is very large compared to the rib width. Therefore, a 2.0 m slice of the rib is used to calculate load, as the pillar strength was calculated for a 2.0 m square pillar.

$C_1 = [4\ \text{holes} + (3 \times 0.2)] + 2.0\ \text{m rib} = 8.6\ \text{m}.$

$$Load = \frac{0.025HC_1C_2}{w_1 w_2} = \frac{0.025 \times 30 \times 8.6 \times 2.0}{2.0 \times 2.0} = 3.22\ \text{MPa} \quad [3]$$

Therefore the safety factor for the design is:

$$Safety\ factor = \frac{strength}{load} = \frac{7.58}{3.22} = 2.35 \qquad [1]$$

Load acts in direction of gravity

Figure 4. Effect of gradient on pillar dimensions

To account for unforeseen circumstances such as discontinuities affecting the 2.0 m rib, mining off-line and weaknesses in the seam it is advisable to leave a wider rib say every fifth rib. In the example a 6.0 m rib with a width-to-height ratio of 4.0 could be left.
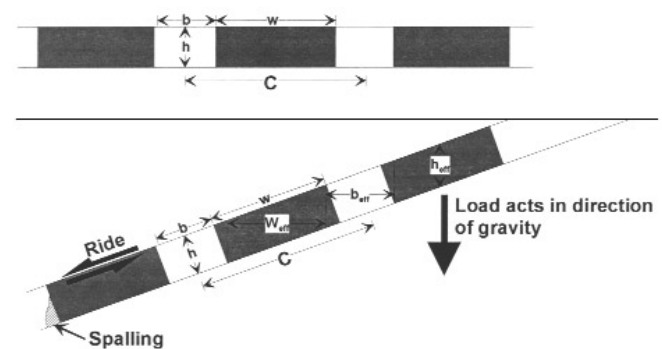
Example 6: Effect of gradient on pillar

Most of the coal seams currently mined in South Africa are approximately horizontal. However, the effect of dip on the strength of the pillar cannot be ignored once the dip exceeds about 6° or 1 in 10.

Dip affects pillar stability by:

(i)   A reduction in effective area of the pillar through which the pillars can transmit load to the floor
(ii) The down dip sides of the pillars may spall under the effects of gravity
(iii) The roof strata can 'ride' down dip inducing shear at the pillar contact planes and
(iv) Non-symmetrical stress distribution may result in higher load on the down dip side.

The magnitude of these effects is a function of the magnitude of the dip and the mining height impacts on effects (i) and (ii).

Resolution of pillar width and pillar centre distance into effective widths in the horizontal plane, shown in Figure 4, provides a first approximation to dealing with the problem.

In Figure 4:

• Effective pillar height, $h_{eff} = \dfrac{h}{\cos \theta}$,
• Effective pillar width along dip,
  $w_{eff} = (w - h \tan \theta) \cos \theta$
• Effective bord width along dip,
  $B_{eff} = (B + h \tan \theta) \cos \theta$
• Effective pillar centre distance along dip,
  $C_{eff} = (b + w) \cos \theta$
• Effective depth, $H_{eff} = H$ at pillar effective mid width ($w_{eff}/2$).

The above approach may be inadequate once the dip exceeds about 11° or 1 in 5 due to adverse effects of shear induced at the pillar contacts by ride and numerical techniques will have to be used to perform the design.

Consider, by way of an example, the situation where the bord width is 6 m, the mining height 3 m, pillar width 12 m and the depth of mining 120 m. If the seam is flat, the safety factor will be 1.6. However, if the seam dips at 10°, the following is the case:

$H_{eff} = 3.05$ m, $W_{eff} = 11.3$ m, $C_{eff} = 17.73$, and $B_{eff} = 6.43$

Then, the effective pillar width adjustment to compensate for the non-square pillar is:

$$w_e = \frac{2 \times 12 \times 11 \times 3}{12 + 11 \times 3} = 11 \times 6 \text{ MPa}$$

$$Strength = 7.2 \frac{11.6^{0.46}}{3.05^{0.66}} = 7.2 \frac{3.09}{2.09} = 10.65 \text{ MPa}$$

$$Load = \frac{0.025 \times 120 \times 18 \times 17.73}{11.3 \times 12} = \frac{957.4}{135.6} = 7.06 \text{ MPa}$$

$$SF = \frac{10.65}{7.06} = 1.51$$

Notes on pillar and overburden stiffness and yield pillars

Failure can occur in one of two ways, collapse can be sudden and violent as occurred in the Coalbrook disaster or it can be slow and controlled as recorded by Oldroyd and Buddery (1988). The stiffness of intact coal is a material property and has been found to be approximately 3.5 to 4.0 GPa. By contrast, the post-peak stiffness of a pillar is dependent on the pillar geometry. The mode of failure, violent or controlled, depends on the post-peak slope of the pillar's load/deformation characteristic and that of the system.

Pillar stiffness is obtained by:

Stiffness, λ, is the ratio of force to deformation (F/e),

$$E = \frac{stress}{strain} \qquad [17]$$

$$stress = \frac{force\ (F)}{Area\ (A)} \qquad [18]$$

$$strain = \frac{change\ in\ length\ (e)}{original\ length\ (h)} \qquad [19]$$

$$E = \frac{\dfrac{F}{A}}{\dfrac{e}{h}} = \frac{F\,h}{e\,A} \qquad [20]$$

$$\frac{EA}{h} = \frac{F}{e}$$

$$\lambda = \frac{EA}{h}$$

In the case of the post-peak stiffness the geometry of the pillar (w/h) influences the post-peak stiffness. The greater the w/h ratio, the greater the post-peak stiffness.

For stability $\lambda_m > \lambda_c < 0$, where λ_m is the post-peak failure slope of the pillars and λ_c is the critical system stiffness for a panel of pillars. The critical system stiffness reduces with the number of pillars in a panel.

Post-peak stiffness has been obtained by the back analysis of *in situ* coal pillar tests:

$$\lambda = 1.861 \left(\frac{w}{h} \right)^{-0.931} \text{ GPa after Van Heerden,} \qquad [21]$$
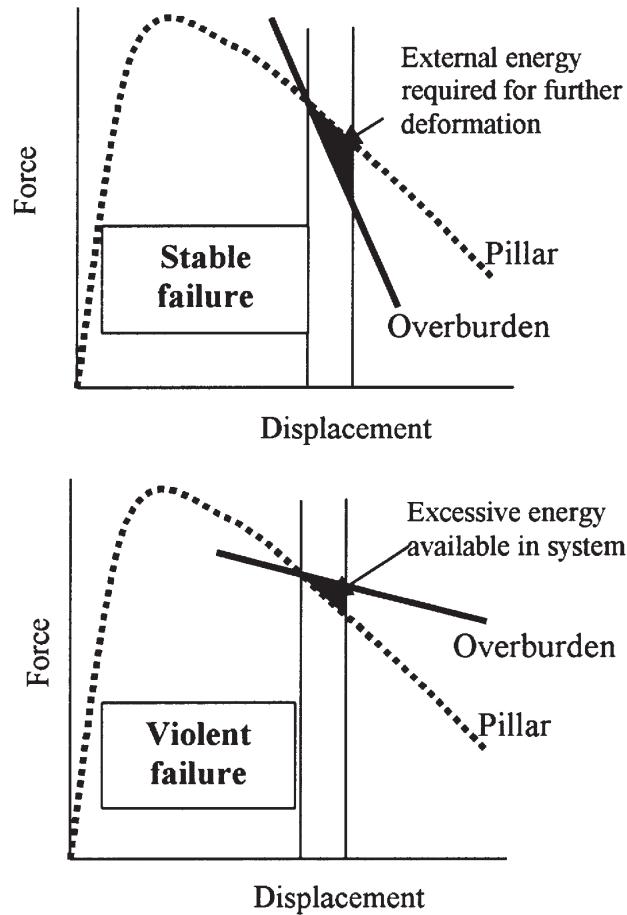
Figure 5. The concept of local system stiffness, after Salamon and Oravecz (1976)

$$\lambda = 1.033 \left(\frac{w}{h} \right)^{-1.159} \text{GPa after Wagner,} \qquad [22]$$

$$Ep = \frac{0.562w}{h} - 2.293 \text{ GPa from Van Heerden's} \qquad [23]$$

data after Van der Merwe (1998).

$$-\frac{Ep}{E} = 0.23 \left[\frac{5}{\left(\frac{w}{h} \right)} - 1 \right] \text{Normalized post-peak} \qquad [24]$$

modulus after Ryder and Ozbay (1990).

Where λ = post-peak stiffness, Ep = post-peak modulus, E = Young's modulus, w = pillar width and h = pillar height.

Based on the Salamon and Oravecz (1976) concept of local system stiffness, violent failure can occur if there is more energy released from the system than is required by the pillar for continued deformation. This condition is met if the system stiffness is greater (for clarity: smaller negative value of the force-deformation curve) than the post-peak stiffness of the pillar, see Figure 5. Conversely, to prevent violent failure, the pillar post-peak modulus has to be greater than the system stiffness.

In typical South African conditions of shallow depth with a relatively stiff overburden, the maximum elastic deflection of the overburden over a typical panel width of 130 m to 250 m is insufficient to allow typical pillars of 2.5 m to 5 m height pillars to fail.

For the destruction of the pillars, it is therefore a prerequisite that the overburden beams also have to fail. Under those conditions, the problem reduces to that of a dead weight resting on the pillars. In other words, the system stiffness reduces to zero.

This implies that in order for violent failure to be prevented, the post peak modulus of the pillars have to be positive. Therefore, from Equation [23]

$$E_p > 0$$

$$\frac{0.562\,w}{h} - 2.293 > 0.$$

This condition is met if the pre-failure ratio of w/h > 4.08. This corresponds with the suggestion of Ryder and Ozbay (1990) that pillars with a width to height ratio of 5.0 can only fail in a stable manner.

Pillar extraction

Introduction

This Appendix is aimed at the specialist rock engineer who needs quick and simple procedures to arrive at first order estimates of the additional load on interpanel pillars, in situations where the overburden remains intact due to the presence of a strong layer, such as a dolerite sill, and to evaluate the stability of partial pillar extraction methods.

NOTE: For simplicity, the presence of a strong layer, such as a dolerite sill, in the overburden will be referred to as a dolerite sill in the rest of this Appendix.

Estimating the effect of an intact overburden on interpanel pillars

The additional load on an interpanel pillar caused by non-failure of the overburden, because of the presence of a strong layer such as a dolerite sill, is a function of the mining depth, depth of the sill, panel width, and stiffness of the coal and surrounding strata. It is best determined using established numerical methods.

The following is presented as a method to do a first order estimate, in the absence of the facilities to carry out the more appropriate numerical modelling techniques.
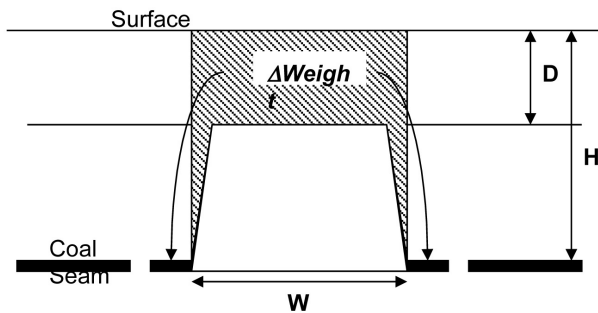
Figure 1. Cross-section explaining the additional loading on pillars in the event of an intact overburden over an isolated panel

Single panel (see Figure 1)

In the case of a single panel with unmined coal on either side, it is conservatively assumed that 80% of the additional load caused by the intact strata is borne by the barrier pillars. Each barrier then bears half of the total additional load.

The additional weight on the pillar per linear metre of pillar, *ΔWeight*, is:

$$\Delta Weight = 0.01(WD + p^2 \tan\phi) \qquad [1]$$

where:

W = panel width

p = parting between sill base and coal seam

D = depth of sill base

= goaf angle, measured off the vertical.

Therefore, the total pillar stress, σ_s, for a chain pillar with width w and road width B is:

$$\sigma_s = \frac{(0.025H)(w + B)^2 + \Delta Weight}{w^2} \qquad [2]$$

and for a continuous pillar, σ_{Sc}, is:

$$\sigma_{Sc} = \frac{(0.025H)(w + B) + \Delta Weight}{w} \qquad [3]$$

Multiple panels (see Figure 2)

In the case of multiple panels, all the additional load is borne by the inter panel pillars, then the additional pillar load per running metre, *ΔWeight_m*, is:

$$\Delta Weight_m = 0.025(LD + p^2 \tan\phi) \qquad [4]$$

and the total pillar stress, σ_m, for a chain pillar, is:

$$\sigma_m = \frac{(0,025H)(w + b)^2 + \Delta Weight}{w^2} \qquad [5]$$

whereas for a continuous pillar, σ_{mc}, it is:

$$\sigma_{mc} = \frac{(0.025H)(w + B) + \Delta Weight}{w} \qquad [6]$$

Interpanel pillar strength

If the interpanel pillars are chain pillars, the strength should be calculated by either using the slender pillar formula (Salamon and Munro), or the squat pillar formula.

In the case of a long, continuous pillar, the issue is less clear. There are essentially three approaches:

(a) Calculate the effective width using the 4A/C approach, in which case the effective width can be taken as twice the physical width

(b) Use one of the analytical approaches, i.e. Wilson's or Barron's, see Barron and Pen (1993)

(c) Use the Australian approach; i.e. use the actual pillar width.

Until more information becomes available, approach (a) is recommended, i.e. effective pillar width equals twice the physical width.

Strictly speaking, neither the Salamon-Munro (1967), nor the van der Merwe (1999), pillar strength equation is valid for this application as the conditions are beyond the statistical range that was used to derive those formulae. Therefore, it should not be used for design purposes. It can however, be used in a comparative sense to evaluate the effect of bridging strata on the interpanel pillars. Once the strength has been calculated, the comparative safety factor (CSF) is:

$$CSF = \frac{Strength}{\sigma_x} \qquad [7]$$

where $_x$ is $_s$, $_{sc}$, $_m$ or $_{mc}$.
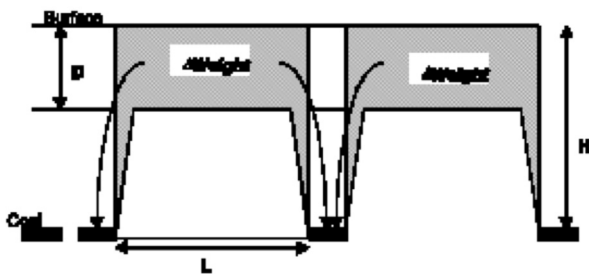
Figure 2. Cross-section showing the additional loading in the event of an intact overburden over multiple panels

Partial pillar extraction (PPE) and system stiffness

The success of PPE depends on three factors: the load bearing ability of the pillar remnants; the integrity of the overburden and the relative stiffness of both the overburden; loading system and the pillar remnants. Invariably, the remnants will be small, with safety factors in the region of unity. They will be in the zone of highest uncertainty about immediate failure.

Whether or not failure will occur immediately depends to a large extent on the ability of the overburden to bridge across the panel. This brings the panel width into play, in addition to the composition and characteristics of the over-burden. If failure does occur, the mode of failure (i.e. the degree of violence) depends on the ratio of the remnant stiffness to the overburden stiffness.

Stability of the pillar remnants

Pillar strength

The pillar strength is calculated with the Salamon-Munro formula:

$$\sigma_p = 7.2 \frac{w_e^{0.46}}{h^{0.66}} \text{ MPa} \qquad [8]$$

or the van der Merwe formula:

$$\sigma_p = 3.5 \frac{w_e}{h} \text{ MPa} \qquad [9]$$

where

w_e = equivalent pillar width
h = pillar height

Pillar load

Extensive numerical modelling was done to evaluate the applicability of the tributary area theory. It was found that, in addition to the relative stiffness of the overburden material to that of coal, and the ratio of panel width to mining depth, the percentage extraction also played an important role. The higher the extraction, the smaller the portion of the overburden load on the pillars (and the higher the load on the barriers). At lower extraction ratios the difference in loading is not significant, but in PPE the extraction ratios are high and a correction for the load is required.

The loads acting on these reduced pillar remnants can be estimated more accurately by the following:

ROCK ENGINEERING FOR UNDERGROUND COAL MINING

$$\sigma_L = \frac{F0.025H}{1-e} \qquad [10]$$

where

  F = load reduction factor
  H = mining depth
  e = extraction ratio

The load reduction factor, F, is:

$$F = 0.99(1-e^\alpha)\beta \qquad [11]$$

with,

$$\alpha = 2.2 + \frac{1.4L}{H} \qquad [12]$$

and

$$\beta = \frac{0.667}{1 + L/H} + 0.0067(4E_r/E_c - 1.5) \qquad [13]$$

where,

  L = panel width
  H = mining depth
  E_r = elasticity modulus of overburden
  E_c = elasticity modulus of coal

The pillar load calculated with this procedure, can be used to calculate the safety factors of the remnants, for as long as the overburden is continuous. The moment the overburden fails, the loading on the pillars is the full overburden load and $F=1$ in Equation [10].

Stability of the overburden

The maximum height of overburden that the pillars can support, H_m, is:

$$H_m = 40\sigma_p(1-e) \qquad [14]$$

If $H_m < H$, pillar failure is distinctly possible and the only condition under which it will not occur is where the overburden bridges across the panel.

A simple way of evaluating the stability of the overburden is to consider the tensile stresses generated by deflection in the overlying beams. The maximum compression of a pillar in the centre of the panel, dh, is:

$$dh = \frac{h\Delta\sigma_p}{E_C} \qquad [15]$$

where $\Delta\sigma_p$ is the load increase due to mining, i.e.

$$\Delta\sigma_p = \sigma_p - 0.025H \qquad [16]$$

Fundamentally, the maximum deflection of a beam is

$$\eta = \frac{\gamma L^4}{32Et^2} \qquad [17]$$

and the maximum tensile stress generated is,

$$\sigma_t = \frac{\gamma L^2}{2t} \qquad [18]$$

The tensile stress can then be expressed in terms of the deflection, as follows:

$$\sigma_t = \frac{16t\eta E_r}{L^2} \qquad [19]$$

or, substituting dh for η and H_m for t,

$$\sigma_{to} = \frac{16H_m h\Delta\sigma_p}{L^2} \bullet \frac{E_r}{E_c} \qquad [20]$$

Note that for a safety factor greater that unity, H_M should be replaced by H in Equation [20]. In reality, the calculation should be repeated for each of the successive overburden layers, replacing t with the thickness of the respective layers to test each layer for failure.

It is now possible to define an overburden stability factor, OSF, as follows :

$$OSF = \frac{\sigma_{tr} - \sigma_{to}}{\sigma_{tr}} \qquad [21]$$

where σ_{tr} is the tensile strength of the overburden material. One can then define the pillar stability factor, PSF, as follows

$$PSF = f_s - 1 \qquad [22]$$

where f_s is the safety factor calculated with the full overburden load. The system failure is thus governed by two factors, namely the OSF and PSF. These can be plotted in quadrants as shown in Figure 3.

The quadrants have the following meanings:
• Sector 1: Stable system. The pillars can support the full overburden and the overburden has not failed in tension.
• Sector 2: Possibly the most dangerous situation. The pillars cannot support the overburden, but may appear to be stable because the overburden has not yet failed. A single discontinuity may cause this overburden to fail without warning.
• Sector 3: This is a common stooping situation with small snooks which fail as mining progresses.

• Sector 4: This sector indicates failure over a long time period, governed by the time-related decay of pillar strength. The overburden has failed, resulting in full overburden load on the pillars, but they are (temporarily at least) strong enough to support the overburden.

Mode of failure

The relative violence of failure is the most important consideration in the situation where pillars fail. Violent failure can result in injury or loss of life and severe damage to equipment. In the discussion of the relative degree of violence, the most important paramenter is the ratio of system (or overburden) stiffness relative to pillar stiffness.

Pillar stiffness is obtained by:

Stiffness, , is the ratio of force to deformation (F/e),

$$E = \frac{stress}{strain} \qquad [23]$$

$$stress = \frac{force\ (F)}{Area\ (A)} \qquad [24]$$

$$strain = \frac{change\ in\ length\ (e)}{original\ length\ (h)} \qquad [25]$$

$$E = \frac{\dfrac{F}{A}}{\dfrac{e}{h}} = \frac{F \times h}{e \times A} \qquad [26]$$

$$\frac{EA}{h} = \frac{F}{e}$$

$$\lambda = \frac{EA}{h}$$

While the elastic modulus of the intact coal is remarkably consistent at around 4 GPa, its post failure modulus is a function of the pillar *w/h* ratio. Linear regression of data published by van Heerden (1975)—see Figure 4—yields the following formula for the post failure modulus of coal:

$$E_{cp} = \frac{0.562 w_e}{h} - 2.293 \text{ GPa} \qquad [27]$$

One requirement for the full destruction of pillars is that the overburden must be able to deflect fully. For this to happen, the overburden in most cases has to fail.

Transforming Equation [19] yields the following:

$$\eta = \frac{\sigma_t L^2}{16 t E_r} \qquad [28]$$

This equation can be used to calculate the maximum deflection that a beam can tolerate before the induced tensile stress exceeds its tensile strength. For instance, consider a 150 m wide panel overlain by a 20 m thick sandstone in the overburden. Assuming a modulus of elasticity of 30 GPa, and tensile strength of 5 MPa, the maximum elastic deflection of this beam is approximately 12 mm. This is also the amount of compression that is transferred to a pillar in the centre
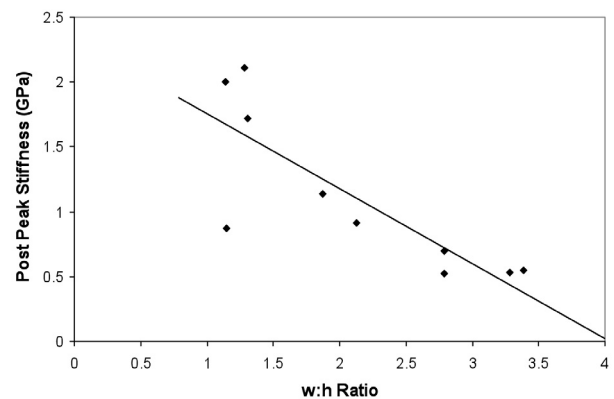

Figure 3. Quadrants with which the stability situation of PPE can be evaluated

Figure 4. Post peak modulus of coal as a function of the width-to-height ratio (after van Heerden, 1975)

ROCK ENGINEERING FOR UNDERGROUND COAL MINING

of the panel. If that pillar is 3 m high, the strain in the pillar is 0.004. With a modulus of elasticity of 4 GPa, the stress in the pillar is then 16 MPa. While this may be sufficient to cause severe damage to the pillar, it is unlikely to cause it to collapse. In any event, further downward movement of the roof is controlled by the sandstone beam, which cannot deflect more than 12 mm without failing. To deflect more, the beam has to fail.

Under these conditions, its stiffness is zero. Therefore, the only condition under which violent pillar failure can be avoided is for the post failure stiffness of the pillars to be positive. According to Equation [23], this requires the width to height ratio of the pillars to be greater that 4.08, say 5.0. In practice, this condition is most likely to be met by utilizing a system that entails the complete removal of selected pillars, leaving the others intact, as with chequerboard stooping.

Sizing of snooks

The size of snooks in pillar extraction is one of the most important elements in the design of a stooping layout. This should be the logical starting point—start with the size of the snook and then work back, taking cognizance of the equipment and operational considerations and the extraction safety factor to arrive at the initial pillar size.

In Chapter 5: Pillar extraction, a method to arrive at a first order design size of snooks is described. In this Appendix, that description is augmented with the following worked example, after van der Merwe (2005).

Stooping is done in a panel with 24 m pillar centres and 6 m road width at 3 m mining height, see Figure 5. Snooks are left on the four corners of the pillars. The last snook, i.e. the one closest to the next solid pillar, is the largest. The other snooks are significantly smaller.

The roof consists of a 3 m thick stiff, competent sandstone overlain by 17 m of softer mudstone. Find the size of snook that will be stable during the time that mining is done in its vicinity, but that will fail once the next line of pillars is extracted.

The following values can be assigned to the various parameters:

$b = 24$ m
$t = 3$ m
$T = 20$ m
a_h after the stooping of the first line = 24 m
a_h after the stooping of the second line = 48 m.

$a_x = 6$ m plus half of the snook size.
$\rho = 2\ 500$ kg/m³

The effect of the smaller snooks can be disregarded for the purposes of the example.

For convenience, the necessary equations are reproduced here from Chapter 5:

$$F_{xi} = \frac{3q}{2}\left(\frac{1}{2}\frac{a_h^2}{a_x} - \frac{1}{3}a_h + \frac{1}{12}a_x \right) \tag{29}$$

$$F_{xm} = 3.5\frac{w^3}{h} \tag{30}$$

$$\sigma_{si} = \frac{q}{3bt}\left[\frac{a_h^2}{2} + \frac{a_x^2}{4} - a_h a_x \right] \tag{31}$$

$$\sigma_{sf} = -\frac{3a_h^2 q}{bt} \tag{32}$$

The easiest way is to solve the different equations for a range of pillar sizes using a standard spreadsheet. This was done for pillars in the range 1 to 5 m wide. The results are summarized in Table I.

Using the results in Table I, Figure 6 was constructed, comparing the snooks' strength to their load for the two situations, i.e. after extraction of the first line of pillars and after the extraction of the second line of pillars.

The stabilizing role of the snooks is demonstrated by the 5th column in Table I. In the cases where the snooks have failed, a tensile stress is generated in the roof beam, indicating failure. In the cases where the snooks are intact, the stress situation remains compressive, indicating a stable roof and consequently
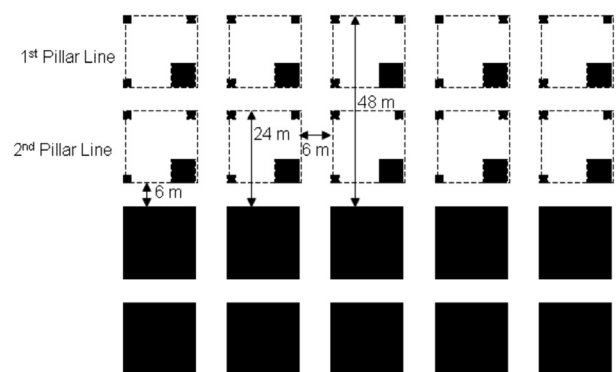

Figure 5. Layout of the pillar extraction exercise in the example

Table I
Results

Pillar width (m)	Pillar strength (MN) Equation [30]	Pillar load (MN) Equation [29]	Resistance R (MN)	Induced Tension* (MPa) Equation [31 and 32]
First pillar line mined (overhang = 24 m)				
1	1.17	23.50	0.00	-10.20
2	9.33	21.51	0.00	-10.20
3	31.50	19.78	19.78	2.16
4	74.67	18.28	18.28	1.99
5	145.83	16.96	16.96	1.81
Second pillar line mined (overhang = 48 m)				
1	1.17	103.14	0.00	-40.80
2	9.33	95.10	0.00	-40.80
3	31.50	88.13	0.00	-40.80
4	74.67	82.04	0.00	-40.80
5	145.83	76.66	76.66	13.50

* Tensile stresses are negative. A positive value indicates that the contribution of the snook results in a compressive stress at the edge of the overhang beam.

a safe working environment. This demonstrates the mutually dependent nature of snook and roof stability—the snooks are stable as long as the roof is intact, and vice versa.

Three zones are indicated in Figure 6. In the first zone, the load on the snooks less than 2.5 m wide, exceeds their strength even with mining of the first line of pillars. Those snooks will fail prematurely. At the other end, snook size greater than approximately 4.1 m, the snooks' strength exceed the load on them after mining of the second line of pillars, indicating that they will continue to be stable when they are in fact required to fail. The 'safe zone' is between these extremes, where the snooks' strength is greater than their load after mining of the first line of pillars, but less than their load after the extraction of the second line of pillars.

An alternative approach to the interpretation of the results would be to view the stability of the roof beam. Referring to the 5th column of Table I, it is indicated that after the mining of the first line of pillars, when roof stability is required, that the roof is in tension (thus failed) for snook sizes smaller than 3 m. The lower limit of snook size is thus between 2 and 3 m.

The upper limit is found by inspecting the roof beam
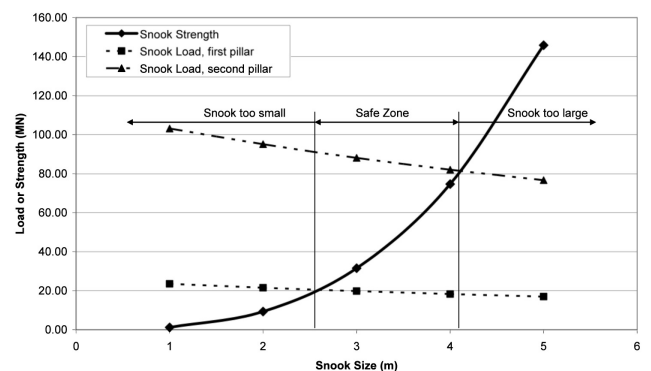
Figure 6. Comparison of the load on the snooks to their strength

condition after mining of the second line of pillars, when failure is required. It is seen that the roof beam is in tension—thus failed—only when the snooks are larger than 4 m. The upper limit is thus between 4 and 5 m.

Constructing a graph like the one shown in Figure 6 allows one to interpolate and thus draw the limits somewhat finer.

The optimum snook size for this example is thus in the range 2.5 m to 4 m.

Subsidence

Subsidence prediction

There are several methods of predicting subsidence, broadly classified as either analytical or empirical. The analytical methods invariably come down to calibrating (sometimes to the extent of 'fudging') one of the available continuum models to model the discontinuous nature of the process. It is rather surprising that the Distinct Element Methods have not yet come into their own in this field.

Empirical methods are by their nature restricted in use to the conditions for which they had been developed. This restriction is sometimes exaggerated, as different areas often have similar characteristics and as long as the characteristics are similar, there is no reason why the same empirical method should not be used. The empirical restrictions do not relate to geographical limits as much as they do to physical conditions. Rock is so variable in nature that there is sometimes a greater difference between profiles on the same mine than between two profiles in different countries. Given the variability of rock, arguing about a few millimetres here or there is rather academic.

Models developed in the USA and Australia do not deliver vastly different results from ones developed in South Africa. The one which is presented in this Appendix is rather simple and has been found suitable for both the Secunda and Sasolburg areas, and should therefore cater equally well for most South African, Australian and USA situations. It was derived empirically.

The conditions under which the development had been carried out, and thus the boundaries for application of the method, are the following:

- *Mining depth*—50 m to 200 m below surface
- *Mining height*—2.5 m to 4 m
- *Panel width*—130 m to 270 m
- *Mining method*—longwall and pillar extraction (note that for pillar extraction, the mining height should be linearly adjusted to compensate for incomplete coal extraction)
- *Overburden composition*—sedimentary rock types, predominantly shales and sandstones.

In this Appendix, some mention will be made of a dolerite sill in the overburden. It should be understood to also include any competent layer that is capable of bridging the mining excavation underground, thereby restricting the amount of subsidence.

The model requires the maximum subsidence to be calculated first, followed by the subsidence at regular intervals on the profile, then the tilts and finally the strains. The model is only valid for sub-critical panels (i.e. resulting in a subsidence profile that does not have a flat portion at the bottom) and where the dolerite is absent or had failed. In South Africa, it has been found that for a subsidence profile to be super-critical (i.e. with a flat portion at the bottom) the ratio of panel width to mining depth should be greater than 2.5.

Maximum subsidence

The maximum subsidence, S_m, is:

$$S_m = 0.39h\left(\frac{W}{H}\right)^{0.32}$$ [1]

where :
h = mining height
W = panel width
H = mining depth

Subsidence profile

The subsidence at a point x from the ribside, S_x—see Figure 1 is:
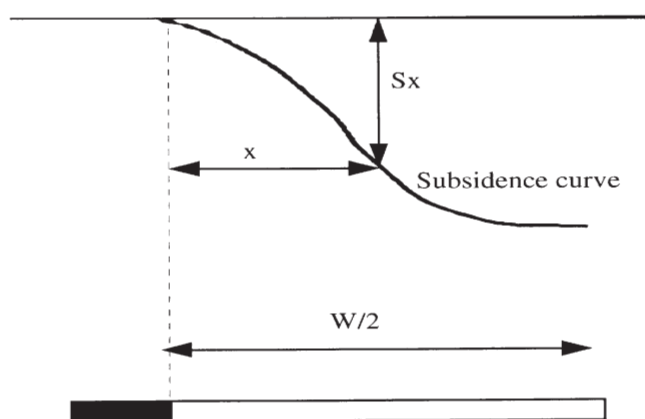

Figure 1. Exaggerated view of a subsidence half profile

$$S_x = 0.5 S_m \left[\tanh\left(\frac{7x}{W} - 1.645 \right) + 1 \right] \qquad [2]$$

Equation [2] should only be used to predict the half profile, i.e. $x \le W/2$, mirror imaging it to obtain the other half.

The tilt profile

The tilt between any two points on the profile is:

$$T = \frac{\Delta S}{d} \qquad [3]$$

where :

$$\Delta S = S_i - S_{i+1}$$
$$d = |x_i - x_{i+1}|$$

The strain profile

The strain at any point on the profile is:

$$\varepsilon = \frac{t_t \tan \alpha}{d} \text{ for the tensile zone} \qquad [4]$$

and

$$\varepsilon = \frac{-t_c \tan \alpha}{d} \text{ for the compressive zone} \qquad [5]$$

With

$$\alpha = \frac{\beta_1 - \beta_2}{2} \qquad [6]$$

$$\beta_1 = \arctan T_i^1 - \arctan T_{i+1}^1 \qquad [7]$$

$$\beta_2 = \arctan T_i - \arctan T_{i+1} \qquad [8]$$

T_i = tilt of section i along profile before subsidence

T_{i+1} = tilt of section $i+1$ along profile before subsidence

T_i^1 = tilt of section i along profile after subsidence

T_{i+1}^1 = tilt of section $i+1$ along profile after subsidence

t_t = tensile reactive depth

t_c = compressive reactive depth

d = distance between mid-points of sections i and $i+1$.

Notes

- The procedure requires that the actual pre-mining topography be used for strain prediction. If the surface is flat, $\beta_2 = 0$ and
  $\alpha = \frac{1}{2} (\arctan T_i^1 - \arctan T_{i+1}^1)$.
- The parameters t_t and t_c are rather complex, and should be determined empirically. It has been found that $t_t = 3.5$ m and $t_c = 4.7$ m give reasonable results and can be used if more accurate information is not available.
- The transition from tensile to compressive zones occurs at the position of maximum tilt. At that

point, the Point of Inflexion, $\varepsilon = 0$. It has been found that the Point of Inflexion occurs at $x = 0.23W$.

Figure 2 illustrates the subsidence-related subsidence elements.

Maximum tilt and strain in real profiles

As stated previously, the overburden rock is highly variable in nature—the variability is exposed by a study of subsidence profiles. The author, for instance, has never seen a truly symmetrical subsidence profile. Prediction models can only predict the best possible smooth fit for the subsidence curves. There will be unpredicted uneven areas in reality. This means that the outliers in tilt and strain, that accompany the uneven areas of real profiles, are lost when basing the predictions on smooth profiles.

The real maxima, which should be expected notwithstanding the predictions made by using Equations [1] to [8], were determined empirically. They are:

Maximum tilt $T_m = 21{,}6\, S_m + 7\ mm/m$ [9]

Maximum tensile strain $\varepsilon_{m+} = 4{,}2\, S_m + 1{,}7\ mm/m$ [10]

Maximum compressive strain
$\varepsilon_{m-} = -9{,}1\, S_m - 2{,}8\ mm/m$ [11]

Note that in Equations [9] to [11], units of m should be used for S_m.

Dolerite failure

As the dolerite condition (intact or failed) overrides all other considerations in subsidence prediction, it is relevant to this section.

The critical span for dolerite failure, L_c, is

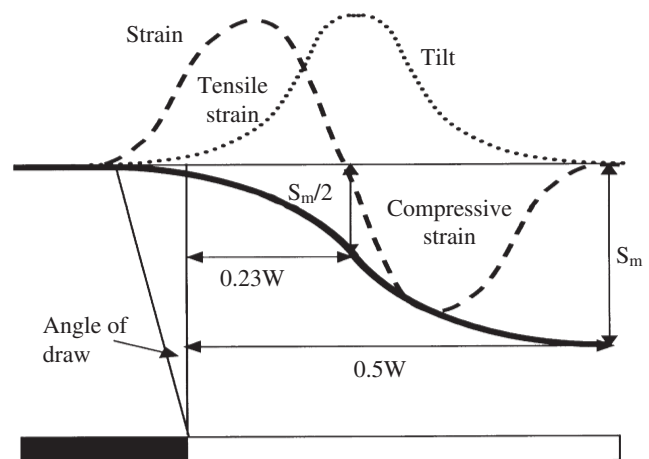$$L_c = 2T \sqrt{k + \frac{\beta}{D}} + 2(H - D)\tan\phi \qquad [12]$$

Figure 2. Subsidence half profile, showing the related elements

with,

$$\beta = \frac{c - b\gamma d}{\gamma_m \tan\varnothing} - \frac{k\lambda}{2} \qquad [13]$$

and,

$$\gamma_m = \gamma_s \frac{D - T}{D} + \gamma_d \frac{T}{D} \qquad [14]$$

where:

γ_s = unit weight of sedimentary rocks
γ_d = unit weight of dolerite
k = ratio of horizontal to vertical virgin stress
H = mining depth
D = depth of dolerite base
T = thickness of dolerite
ϕ = goaf angle (measured off the vertical)
$\varnothing$ = angle of friction of dolerite joint
b = spacing of vertical joints
c = cohesion of dolerite joint
λ = height of key block.

By substituting known values for the constants in Equations [13] and [14], they can be rewritten in simplified form as :

$$\beta = \frac{1.53}{\gamma_m} - 0.8 \qquad [15]$$

and

$$\gamma_m = 0.025 \frac{D - T}{D} + 0.03 \frac{T}{D}. \qquad [16]$$

Subsidence monitoring

Regarding subsidence as a two-dimensional problem by analysing a line across the trough is an over simplification. In reality, it is an areal problem and the proper analysis should be based on plates rather than lines. The plate approach (or Surface Element Approach—SEA) allows one to consider principal strains rather than mono-linear ones. It is shown in Chapter 9: Subsidence, that more often than not, two perpendicular strains exist in the same area. The most practical method of monitoring in practice has been found to be by means of double, as opposed to single, lines of observation. This is shown in Figure 3. Each set of four adjoining subsidence beacons then represents the corners of a plate on surface. The analysis procedure is briefly explained in the following paragraphs.

Note that in this procedure, the actual pre-mining topography is used as the basis for calculation, as opposed to the simplified method based on a flat and level surface that is often used. It has been found that several of the non-symmetries observed in practice can be explained by taking account of the real topography. Basing calculations on the assumption that the pre-mining topography is flat and level, can

lead to significant contradictions between visually observed effects and calculated results for strain as well as tilt.

Calculation procedure for the SEA

The equations presented in this section are only valid for the square Surface Element layout—see Figure 3.

Major tilt

First, calculate the two minor tilts, T_A and T_B, across the diagonals of the square before subsidence.
Then,

$$\alpha = \arctan\left(T_B / T_A\right) \qquad [17]$$

and

$$T_m = \frac{T_A}{Cos\alpha} \qquad [18]$$

where:

T_m = major tilt
α = direction of T_m relative to T_A.
Then,
calculate the tilts T_A^1 and T_B^1 after subsidence.

$$\alpha^1 = \arctan\left(T_B^1 / T_A^1\right) \qquad [19]$$

and

$$T_m^1 = \frac{T_A^1}{Cos(\alpha^1)}. \qquad [20]$$

The induced major tilt, T_{MI}, is:

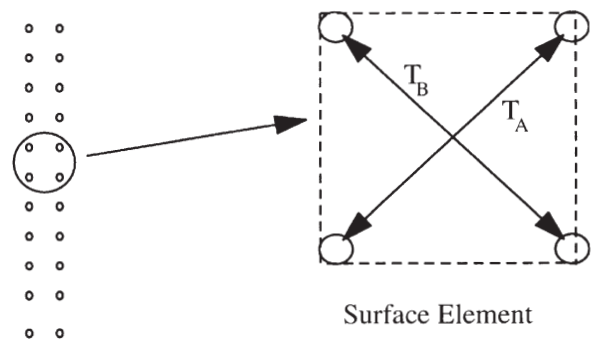$$T_{MI} = \sqrt{\left(T_M Cos\gamma - T_M^1\right)^2 + \left(T_M Sin\gamma\right)^2} \qquad [21]$$

where:

$$\gamma = \alpha^1 - \alpha$$

$$\alpha_1 = \arctan\left[\frac{T_M Sin\gamma}{T_M Cos\gamma - T_M^1}\right] \qquad [22]$$

α_I = direction of T_{MI} relative to T_M^1

Double line of
survey beacons

Figure 3. the square Surface Element formed by installing a double line of survey beacons
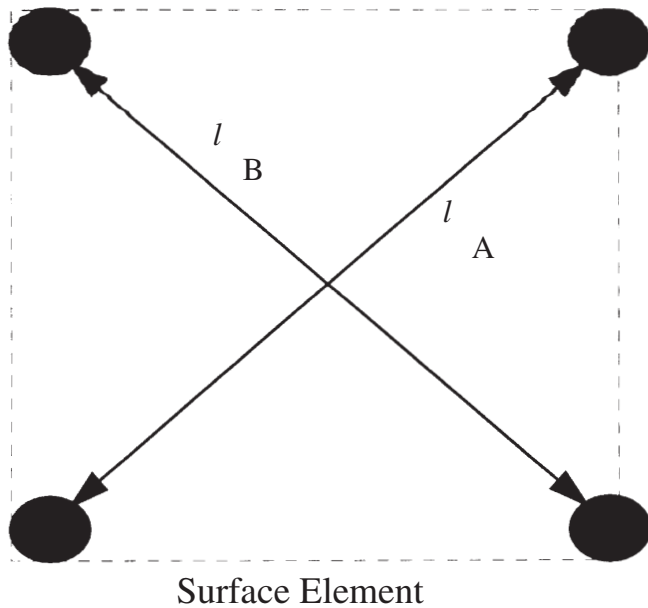
Surface Element

Figure 4. The basis of the calculation of Principal Strains, using the Surface Element Approach

Principal strains

First, calculate the diagonal distances across the corners of the Surface Element before and after subsidence, see Figure 4.

Then,

$$\varepsilon_A = \frac{l_A^1 - l_A}{l_A} \qquad [23]$$

and

$$\varepsilon_B = \frac{l_B^1 - l_B}{l_B} \qquad [24]$$

where:

l_A = distance across first diagonal before subsidence

l_A^1 = distance across first diagonal after subsidence

l_B = distance across second diagonal before subsidence

l_B^1 = distance across second diagonal after subsidence

$$\varepsilon_{1,2} = \frac{1}{2}(\varepsilon_A + \varepsilon_B) \pm \sqrt{\Gamma^2 + \frac{1}{4}(\varepsilon_A - \varepsilon_B)^2}$$

$$\Gamma = \frac{1}{2}\tan\phi \qquad [25]$$

ϕ = angular distortion

$\varepsilon_{1,2}$ = major and minor principal strains.

Also,

$$Tan2\theta = \frac{2\Gamma}{\varepsilon_A - \varepsilon_B} \qquad [26]$$

where :

θ = direction of ε_1 relative to direction of ε_A

Fitting an equation to the subsidence profile

Equation [2] is the best fit which could be obtained for a number of representative subsidence profiles in the Secunda and Sasolburg areas. Local conditions may require a slightly different form for the equation. What is presented here is a quick pragmatic method to obtain the equation, based on minimum information. The subsidence directly over the ribside (S_r), the maximum subsidence (Sm) and the position relative to the ribside where half of the maximum subsidence occurs, are the only parameters that must be known.

The basic hyperbolic tangent equation has been found to describe smoothed versions of subsidence profiles very well. One generic form of the equation (similar to Equation [2]) is:

$$S_x = 0.5 S_m \left[\tanh\left(\frac{c_s x}{W} - k_s\right) + 1 \right] \qquad [27]$$

Directly over the ribside, $x = 0$. If the subsidence at that point is known, k_s can easily be found. Let S_r be the subsidence directly over the ribside.

Then,

$$S_r = 0.5 S_m \left[\tanh(0 - k_s) + 1 \right] \qquad [28]$$

which can be transformed to

$$k_s = \text{arctanh}\left[1 - \frac{2 S_r}{S_m} \right] \qquad [29]$$

Then, let $\frac{1}{2} S_m$ occur at position x from the ribside:

$$0.5 S_m = 0.5 S_m \left[\tanh\left(\frac{c_s x}{W} - k_s\right) + 1 \right] \qquad [30]$$

which means that

$$\tanh\left(\frac{c_s x}{W} - k_s\right) = 0 \qquad [31]$$

or

$$c_s = \frac{k_s W}{x} \qquad [32]$$

In practice, it is very difficult to know beforehand exactly where $S_m/2$ is going to occur and to monitor that particular position. This difficulty can be overcome by monitoring say three or four positions spanning across 15 to 20 m and covering the position halfway between the panel edge and the panel centre line. The $S_m/2$ position should fall in that area, and can be determined by interpolation. Alternatively, pick any convenient spot about halfway between the panel edge and the centre line. Say the horizontal distance there is y from the panel edge, and the final subsidence at the spot is S_y.

Then,

$$S_y = 0.5 S_m \left[\tanh\left(\frac{c_s y}{W} - k_s\right) + 1 \right], \qquad [33]$$

from which it follows that;

$$c_s = \frac{W}{y}\left[\text{arctanh}\left(2\frac{S_y}{S_m}-1\right)+k_s\right] \qquad [34]$$

Alternatively, if the chosen position is exactly halfway between the panel edge and the centre line, Equation [34] can be simplified to:

$$c_s = 4\left[\text{arctanh}\left(\frac{2S_y}{S_m}-1\right)+k_s\right] \qquad [35]$$

This calculation process appears mathematically more complex (the equation only looks more intimidating) but it requires a much simpler monitoring procedure.

The equation will finally need a minor adjustment to predict S_m correctly for sub-critical profiles. The easiest way to do this is to calculate S_m with the equation, and then to adjust the 0.5 constant in the equation with the ratio S_{mr}/S_{mp}, with S_{mr} the measured maximum subsidence and S_{mp} the predicted value.

Example 1

Say a single profile over a 200 m wide panel was measured, and the following was found:

$S_m = 1.3$ m
$S_r = 0.05$ m
$x\ \ = 46$ m.

Then

$$k = \text{arctanh}\left[1-\left(\frac{2S_r}{S_m}\right)\right]$$
$$= \text{arctanh}(0.923)$$
$$= 1.609.$$

Further,

$$c_s = \frac{k_s W}{x}$$
$$= \frac{1.609 \times 200}{46}$$
$$= 6.996.$$

Then,

$$S_x = 0.5S_m\left[\tanh\left(\frac{6.996x}{W}-1.609\right)+1\right].$$

At $x = W/2$, S_x should equal S_m. With the equation, it is:

$$S_x = 0.5S_m\left[\tanh\left(\frac{6.996W}{2W}-1.609\right)+1\right]$$
$$= 0.5. \times 1.3[\tanh(1.889)+1]$$
$$= 1.297 \text{ m}.$$

Adjustment

$$\frac{S_{mp}}{S_{mr}} = \frac{1.3}{1.297} = 1.0023$$

Then

$$0.5 \times 1.0023 = 0.5012$$

The adjusted equation is:

$$S_x = 0.5012\left[\tanh\left(\frac{6.996x}{W}-1.609\right)+1\right].$$

Example 2

Alternatively, suppose the subsidence was measured at the centre of the panel, over the ribside and at a position halfway between the centre and the ribside. Say the following was found:

$S_m = 1.3$ m
$S_r\ = 0.05$ m
$S_y\ = 0.75$ m
$y\ \ = 50$ m.

Then,

$$k = \text{arctanh}\left[1-\frac{2S_r}{S_m}\right]$$
$$= \text{arctanh}(0.923)$$
$$= 1.609$$

Further,

$$c = 4\left[\text{arctanh}\left(\frac{2S_y}{S_m}-1\right)+k\right]$$
$$= 4[\text{arctanh}(1.1538-1)+1.609]$$
$$= 4[\text{arctanh}(0.1538)+1.609]$$

Therefore,

$$S_x = 0.5S_m\left[\tanh\left(\frac{7.056x}{W}-1.609\right)+1\right].$$

at $x = W/2$, S_m should equal 1.3 m.

With the formula, it is 1.273. The 0.5 factor should thus be adjusted to 0.511, and the final 'quick and dirty' formula is:

$$S_x = 0.511S_m\left[\tanh\left(\frac{7.056x}{W}-1.609\right)+1\right]$$

The same procedure, applied to the general Secunda/Sasolburg case (with $S_r/S_m = 0.04$, $x/W = 0.23$) would transform Equation [2] to the following:

$$S_x = 0.512\left[\tanh\left(\frac{6.91x}{W}-1.589\right)+1\right] \qquad [36]$$

In practice, there is only a negligible difference between profiles constructed with Equations [2] and [36]

Recommended reading

PENG, SYD S. *Surface Subsidence Engineering*. Society for Mining, Metallurgy and Exploration Inc. Littleton, Colorado. 1996.

KRATZSCH, H. *Mining Subsidence Engineering*. Springer-Verlag, Berlin.

BRAUNER, G. *Subsidence due to underground mining*. United States Bureau of Mines Information Circular IC 8571. 1971.

VAN DER MERWE, J.N. Subsidence caused by high extraction coal mining in the Sasolburg and Secunda Areas: Prediction thereof and the mitigation of its effects. Ph.D. thesis, University of the Witwatersrand. 1991.

VAN DER MERWE, J.N. Experiences with undermining by coal in South Africa. Proc Third Workshop on Surface Subsidence Due to Underground Mining. West Virginia University, Morgantown WV. 1993.

WAGNER, H. and SCHÜMANN, E.H.R. The effects of total coal seam extraction on the surface and surface structures. *Chamber of Mines of South Africa Research Organisation*. Research Report 20/85. 1985.

Anon. *Proc. Symp. Construction Over Mined Areas*. South African Institution of Civil Engineers. 1993.

Glossary of terms and definitions

This glossary of terms and definitions was taken from DME Guideline GMEI7/4/1 I 8-AB2, with additions by the Rock Engineering Department of BHP-Billiton Energy Coal South Africa, and the authors.

Accelerometer	A seismometer, which measures ground acceleration.
Adit	A horizontal opening, starting from a hillside (or opencast high wall) to reach an orebody.
Back	This is the orebody between a level and the surface, or between two levels.
Barrier line	A single line of 3 mine poles with barrier tape placed approximately 1.0 m above floor elevation between the extracted area and the working place, similar to a stooping breaker line but which is not required to control goaf.
Barrier pillar	A continuous pillar designed to separate or compartmentalize a series of panel pillars.
Barricade	A visible, temporary or permanent structure installed above floor level and across the width of a bord in order to prevent access to that portion of the bord ahead of the structure.
Bleeder hole	A hole, which is drilled vertically into the roof for the sole purpose of allowing an accumulation of water or gas to escape freely from the roof.
Bord	Roadway driven in orebody or seam and specifically defined as that area between two pillars, which is not included in the definition of an intersection.
Bottom coaling	Secondary extraction of the lower portion of a seam subsequent to developing the upper portion.
Breakerline	A row or rows of either timber poles or roofbolts installed across the width of a bord specifically to: • arrest the planned displacement of roof strata at that point • prevent roof failures from spreading • form a clear demarcation between the goaf and the working area.
Brow	An abrupt step in the roof horizon which is 200 mm or greater and which is continuous for a distance of 2.0 m or greater.
Burden	Distance between an explosive charge and the free surface in the direction of the throw.
Burnt coal	Coal, which has been burnt or devolatilized by dolerite intrusions.
Cables/cable anchors	A flexible steel cable of thickness and length as specified by a rock engineering practitioner anchored by means of a mechanical anchor or resin and tensioned with a locking device to a load of at least l50 kN. Cable anchors should be fully grouted with cement.
Canche	See Brow.
Chequer board extraction	Extraction of every alternate pillar in a row and a column such that the extracted pillar is surrounded by four solid pillars.
Cluster stick pack	A number of timber poles installed skin to skin in a group.

Coal ridge	Protruding coal left in the roof after cutting (e.g. as a result of missing pick boxes or poor roof trimming).
Compressive stress	Normal stress tending to shorten the body in the direction in which it acts.
Controlled blasting	All forms of blasting designed to preserve the integrity of the remaining rocks (e.g. smooth blasting, pre-splitting, post-splitting).
Convergence	Reduction in the distance between two basically parallel surfaces (usually the hangingwall and the footwall or roof and floor).
Creep	Time-dependeant deformation.
Cross-cut	A horizontal opening, like a tunnel, that cuts the rock formation at an angle to the strike in order to reach an orebody.
De-coupling	Ratio of the radius of a blast hole to the radius of the charge; this causes a reduction in the amplitude of the strain wave by increasing the space between the charge and the blast hole wall.
Deformation	A change in shape or size of a solid body.
Dilatancy	The property of volume increase under loading.
Dip	Angle at which stratum or other planar feature is inclined from the horizontal.
Discontinuity surface	Any surface across which some property of a rockmass is discontinuous (e.g. Bedding planes, fractures).
Drive	A horizontal opening, like a tunnel, lying in or near the orebody parallel to the strike.
Dyke	A sheet-like body of igneous rock, which cuts across the bedding planes of the surrounding rockmass.
Elasticity	Property of a material whereby it returns to its original form or condition after an applied force is removed.
End wall	The exposed face remaining after stripping and coal removal has occurred in the outer extremities of the open pit.
Extracted Area	Any area in which any form of extraction, including chequer-board extraction that has been carried out. This area should, for all intents and purposes, be treated the same a goaf area.
Face	The surface of an excavation being worked in the direction of mining.
Fault	A fracture in rock along which there has been a discernable amount of displacement.
Fence	See barricade.
Fender	Strip of a pillar that has been isolated from the main body of the pillar by mining during stooping operations and which is to be mined out in the immediate next mining phase.
Fingerline	A row of timber poles installed in the centre of a cut taken from a pillar.
Footwall/Floor	Mass of rock beneath a discontinuity surface (in tabular mining, the rock below the reef plane or seam).
Force	An action that tries to move an object from a stationary position, or to change its rate of movement or its direction of movement.
Fossilized tree impressions	An impression in the immediate roof overlying a coal seam resulting from the fossilization of trees or branches of trees.

Frozen coal	Coal, generally less than 10 cm thick, left in the roof of an excavation after cutting or blasting.
Full column	Where a roofbolt or cable is fully grouted in the hole either by resin or cementitious grout. The anchor is in contact with the strata over the full length of the bolt or cable.
Gate road	Roadways at either end of a longwall or shortwall.
Geological discontinuities	Any geological feature, i.e: slip, joint, fault, dyke, etc, which causes the property of a rockmass to become discontinuous.
Geophone	A seismometer that measures ground velocity.
Geotechnical area	A portion of a mine where similar geological conditions exist which give rise to a unique set of identifiable rock-related hazards for which a common set of strategies can be employed to minimize the risk resulting from mining.
Goaf	The planned collapse of roof strata, which normally occurs as a result of total extraction mining.
Grout	Resin or cementitious material filling the annulus between a roofbolt and the hole in which it has been installed.
Hangingwall/roof	Mass of rock above a discontinuity surface (in tabular mining, the rock above the reef plane or seam).
Headboard	A metal or wooden device, which is employed specifically to spread load or increase the surface bearing area of the support.
Heading	An excavation being created in a seam into which no other excavations have holed.
Hollow roof	Roof having a drummy sound when struck with a sounding stick. This indicates that parting planes have opened up within the lower ± 200 mm.
Highwall	A vertical or near-vertical surface on the advancing side of the open pit, formed generally by pre-splitting in solid rock prior to excavation.
Hypocentre	Location in 3 dimensions of the source of a seismic event. Also known as the focus (or source location).
Inelastic deformation	The portion of deformation under stress that is not annulled by the removal of the stress.
Intersection	The area where two roadways meet or cross one another.
Joint	A geological discontinuity along which no visible displacement or movement of the interface has occurred.
Level	All openings at a horizon from which the orebody is opened up and mining is started.
Longwall mining	A retreat mining method where a very large rectangular pillar (often 100–150 m wide and more than 2 km long) is totally extracted. The 100–150 m long face is supported by means of self-advancing powered support units known as chocks or shields.
Low wall	The mined out area on the spoilpile side of the open cut.
Main development	See Primary development.
Magnitude (seismic)	Measure of the size of a seismic event. May encompass energy, moment or both in its calculation.
Metalliferous mine	Includes all mines that are not diamond or coal mines.
Mine poles	Dry poles of a hard wood type installed vertically or close to vertically between roof and floor in a coal mine.

Normal force	Force directed normal (perpendicular) to the surface elements across which it acts.
Overbreak	The quantity of rock that is removed beyond the planned perimeter of the final excavation.
Overburden	Body of rock and soil overlying the top of the mineable horizon or seam.
Panel	Mined area between barrier or inter-panel pillars.
Parting	Thickness of rock between the roof of a lower mineable seam and the floor of an overlying mineable seam.
Peak particle velocity	Maximum velocity of the rockmass measured directly at a geophone or calculated from ground motion relations.
Permanent support	Rock or coal left in situ during the mining process or artificial support, e.g. bolts installed to support the local hangingwall, roof, or to provide stability to the mine or portion thereof.
Pillar extraction	Removal of pillars.
Plasticity	State in which material continues to deform indefinitely whilst sustaining a constant stress.
Point anchor	A roofbolt anchoring system where the anchor is in contact with the strata for a short, or relatively short, distance. A point anchor can be either mechanical or resin.
Poisson's ratio	Ratio of lengthening in the transverse direction to shortening in the direction of an applied force in a body under compression below the proportional limit.
Policeman pole	A timber pole/stick specifically placed in a position to provide an audible or visual warning of impending roof displacement or collapse.
Primary development	Bord-and-pillar developments from which other panels are mined, providing access for one or more panels. Main arterial infrastructure of a coal mine.
Primitive (virgin) stress	State of stress in a geological formation before it is disturbed by man-made operations.
Principal stress (or strain)	Stress (or strain) normal to one of three mutually perpendicular planes on which the shear stress (or strain) at the point in the body is zero.
P-wave	Primary or compressive wave emanating from the source of a seismic event. Consists of a train of compressions and dilations (like a spring). Moves at approximately 6 000 m/s through quartzite.
Rock Engineering Consultant	A Professional Engineer or a Professional Natural Scientist specializing in rock engineering and practicing, or a graduate possessing the Chamber of Mines Certificate in Advanced Rock Engineering who has sufficient experience of rock engineering practice in the mining industry that he is able to advise management on strategic decisions that affect the industry and has sufficient theoretical knowledge to be able to understand and implement new research findings within the industry.
Rock Engineering Practitioner	A person who is at least in possession of the Chamber of Mines Certificate in Rock Engineering (Coal).
Radiated seismic energy	Total elastic energy radiated from a seismic source. Describes the potential for damage to man-made structures better than seismic moment, and is based on the velocity of ground motion.
Raise	Any tunnel having an inclination above horizontal in the direction of the working of more than 5 degrees (but not included under the definition of a shaft).
Rebar	Reinforcing bar threaded on one end used as a roofbolting tendon.

Reef	A vein, bed or deposit (other than a surface alluvial deposit) that contains minerals, except in the case of coal or diamondiferous formations.
Regular review	Assessment of the conditions of an area through discussions, plan critique, planning meetings and/or underground visits.
Roadway	An excavation developed in a coal seam, which encompasses both a bord and an intersection.
Rock	Any naturally formed aggregate of mineral matter occurring in large masses or fragments.
Rockburst	Seismic event that causes damage to underground workings.
Rock Engineering Review	Carried out on an annual basis by suitably qualified Rock Engineering Practitioners to assess compliance with the Code of Practice and identify possible problem areas. The review report must be appraised by a Rock Engineering Consultant.
Rockfall (fall of ground)	Fall of a rock fragment or a portion of fractured rockmass without the simultaneous occurrence of a seismic event.
Rockmass	Rock as it occurs in situ, including its discontinuities.
Rockmass instability	A softening within a critical volume of rock indicated by accelerating deformation and a drop in stress.
Roofbolt	A steel tendon anchored chemically (resin) or mechanically complete with a nut and washer and meeting performance specifications.
Roofbrushing	Any area (typically along travelling roads in low seam workings) in which the roof has been blasted down above the normal seam roof horizon.
Roof roll	A geological feature, which results in a change to the roof profile from generally flat to undulating. It may be a singular or repetitive feature.
Secondary development	A bord-and-pillar development providing access to production panels off the main development
Secondary mining	Any form of mining carried out after initial bord-and-pillar development.
Seismometer	Device (transducer) that converts ground motion into an electric signal.
Seismic event	Transient earth motion caused by a sudden release of the strain energy stored in the rock.
Seismic moment (scalar)	Measure of the strength of an earthquake or of a seismic event and an indication of the amount of deformation (displacement) at a seismic source.
Seismic moment (tensor)	Describes completely the equivalent forces acting at a seismic source and is equivalent to the total seismic moment integrated over the source volume of a seismic event.
Seismic strain	Sum of all moment tensors of all events within a given volume of the rockmass.
Seismic strain rate	Seismic strain over a specified period of time.
Seismic stress	Seismic energy radiated by all events recorded within a volume during a specified period of time.
Service area	Any portion of the bord-and-pillar workings which is utilized on a permanent or semi-permanent basis for ancillary purposes, for example, but not limited to; storage areas, workshops, belt drives, underground offices and electrical sub-stations.
Service excavation	Any underground area significantly higher and wider than the normal mining dimensions, which is not included in the definition of a shaft. Bins, bunkers, crusher chambers and major belt drive areas are typical examples of service excavations.

Shaft	Any tunnel having a cross-sectional dimension of 3.7 m or over and • having an inclination to the horizontal of 15 degrees or over, or • having an inclination to the horizontal of less than 15 degrees but more than 10 degrees where the speed of traction exceeds 2 m/s.
Shallow workings	Workings having a depth to floor of less than 40 m.
Sill	A sheet-like mass of igneous rock whose contacts lie approximately parallel with the bedding planes of the surrounding rockmass.
Sliping	Deliberately increasing the width of an excavation beyond its planned dimension.
Slip	A joint with slickensided or polished surfaces.
Smooth bar	A smooth tendon threaded on both ends for use with mechanical anchors.
Snook	Remnant of a pillar left during stooping operations that will not be mined out.
Spalling	Longitudinal splitting in uniaxial compression, or the breaking-off of platelike pieces from a free rock surface.
Special areas	During the course of routine mining an increased risk of rockfalls (fall of ground) or rockbursts may develop. Such areas requiring additional attention and precautions must be designated as special areas.
Splitting	Violent ejection of splinters of rock from the surface of an excavation.
Split	An excavation (bord) usually developed perpendicular to the overall direction of mining.
Sloping brow	Where the roof gradient exceeds 1:3 and cuts across bedding planes.
Stiffness	Ratio of force versus displacement.
Stope	An underground excavation made in removal of any ground or mineral, other than coal, but does not apply to excavations made for engine rooms and pump chambers or for development purposes such as shafts, drives, winzes and raises.
Stooping	A secondary form of mining where the majority of every coal pillar is extracted. This mining method is carried out on the retreat.
Strain burst	Rockburst at the lower end of the spectrum of violent events occurring essentially at the surface of an excavation.
Straps	Steel plates which have holes drilled through to accommodate roofbolts or cables.
Strata control officer	A person who is at least in possession of the Chamber of Mines Certificate in Strata Control (coal).
Strength	The maximum stress that a material can resist without failing.
Stress	Force acting across a surface element divided by the area of the element.
Strike	Direction of the azimuth of a horizontal line in the plane of an inclined stratum (or other planar feature) within a rockmass.
Stringer	An igneous intrusion with a width <0.3 m whose contact planes may be parallel or perpendicular with those of the surrounding rockmass.
Subsidence	Downward movement of the surface lying above an underground excavation or adjoining a surface excavation.

Support	A structure or a structural feature built into or installed around an underground excavation to maintain its stability.
Supported roof	Where permanent or temporary support structures have been installed or where no systematic support of the roof is required, the roof has been inspected by a miner and declared safe by him.
S-wave	Secondary or shear wave emanated from the source of a seismic event. Consists of elastic movement perpendicular to the direction of travel. Approximately 3650 m/s through quartzite.
Swelling	Mineralogical nature of the rock by which water is absorbed, causing a measurable increase in volume; swelling can exert very large time-dependent forces on rock or support systems and reduce the size of excavations.
Tangent modulus	Slope of the tangent to the curve of stress versus strain at a given stress value (generally taken at a stress equal to half the compressive strength).
Temporary support	Support which will be removed.
Temporary support (mechanical)	A freestanding support jack, which must meet performance specification.
Temporary support (on board)	A hydraulic support jack which is physically mounted to the body of a roofbolting machine and which must meet performance specification.
Tensile stress	Normal stress tending to lengthen a body along the direction in which it acts.
Thickness	Perpendicular distance between bonding surfaces (e.g. Bedding planes.
Timber headboards	As per headboards but constructed from timber.
Top coaling	Secondary extraction of the upper portion of a seam subsequent to developing the lower portion.
Transverse (shear) wave	Wave in which the displacement at each point of the medium is parallel to the wavefront.
'W' strap	Steel plate with cross-section deformed to simulate a flattened 'W' which has holes drilled through to accommodate roofbolts or cables.
Weathering	Process of disintegration and decomposition as a consequence of exposure to the atmosphere, to chemical action, and to the action of frost, water or heat.
Wedge	A block of wood with one tapered edge.
Width-to-height ratio	The width of a pillar divided by the mining height.
Winze	Any tunnel having an inclination (below horizontal) in the direction of the workings of more than 5 degrees (but not included under the definition of a shaft).
Working place	The place where mine workers normally work or travel.

References

ANON. *Proc. Symp. Construction Over Mined Areas.* South African Institution of Civil Engineers. 1993.

BARRON, K. and PEN, Y. A revised model for coal pillars. *Proc. Workshop on Coal Pillar Mechanics and Design,* US Bureau of Mines IC 9315. 1993.

BARTON, N. and GRIMSTAD, E. The Q-system: following 20 years of application in NATM support selection. Felsbau 12/1994.

BELL, E.T. *Men of Mathematics*, A Touchstone Book published by Simon and Schuster, New York. 1937.

BEUKES, J.S. Stooping Practices in South African Collieries. Chamber of Mines Research Organization of South Africa, Reference Report No. 43/90. 1990.

BEUKES, J.S. Pillar and rib pillar extraction. Chamber of Mines of South Africa Research Organisation Reference Report 43/90.

BIENIAWSKI, Z.T. and MULLIGAN, D. *In Situ* Large Scale Tests on Square Coal Specimens Measuring 5ft in Width and up to 5ft in height. CSIR Report MEG 567, Pretoria, South Africa. 1967.

BIENIAWSKI, Z.T. and VAN HEERDEN, W.L. The Significance of *In Situ* Tests on Large Rock Specimens. *Int. J. Rock Mech, Min. Sci S Geomech.* Abstr. vol. 12. 1975.

BIENIAWSKI, Z.T. A method revisited: coal pillar strength formula based on field investigations. *Proc. Workshop on coal pillar mechanics and design.* US Bureau of Mines IC 9315. 1992.

BRADBURY, T.J. and HILL, R.W. Bord and Pillar Design Considerations at Khutala Colliery. *Proc. Symposium on Recent Advances in Underground Coal Mining in South Africa.* South African National Group on Rock Mechanics. September, 1989.

BRADY, B.H.G. and BROWN, E.T. *Rock Mechanics for Underground Mining*, George Allen and Unwin, London. 1985.

BROWN, E.T. (Ed.) *Analytical and Computational Methods in Engineering Rock Mechanics*, George Allen and Unwin, London. 1987.

BUDAVARI, S. (Ed.) *Rock Mechanics in Mining Practice,* Monograph Series M5, S. Afr. Inst. Min. Metall., Johannesburg. 1982.

BUDDERY, P.S. and OLDROYD, D.C. Development of a Roof and Floor Classification Applicable to Collieries. *Eurock '92.* Thomas Telford, London. 1992.

CANBULAT, I. and JACK, B.W. Review of current design methodologies to improve the safety of roof support systems, particularly in the face area, in collieries. SIMRAC Final Project Report, COL 328, December 1998.

CANBULAT, I., MUNSAMY, L. and MINNEY, D.A. Risk Assessment Tool for Open Cast Mining in South Africa. *23rd International Conference on Ground Control in Mining*, USA. 2004.

CANBULAT, I. and VAN DER MERWE, J.N. Extended cut out distances in continuous miner sections in South African collieriess. *19th International Conference on Ground Control in Mines,* Morgantown, WV 3–5 August 2000.

CANBULAT, I., VAN DER MERWE, J.N., VAN ZYL, M., WILKINSON, A., DAEHNKE, A., and RYDER, J. The Development of Techniques to Predict and Manager the Impact of Surface Subsidence. Task 6.9.1 Coaltech 2020. 2002.

CANBULAT, I. and VAN DER MERWE, J.N. Design of optimum roof support systems in South African collieries using a probabilistic design approach. *Journal of South African Inst. Min Metall.* vol. 109, pp. 71–88.

COETZEE, M.J., HART, R.D., VARONA, P.M., and CUNDALL, P.A. FLAC Basics—An Introduction To FLAC And A Guide To Its Practical Application. *Geotechnical Engineering*, 2nd Edition, ITASCA Consulting Group Inc., Minneapolis, MN, USA. 1998.

COMRO Workshop 'The Design and Extraction of Underground Reserves. Dr B. J. Madden (editor) Internal Note No. CO 1/92, 1991.

COOK, N.G.W., HODGSON, K., and HOJEM, J.P.M. A 100-MN Jacking System for Testing Coal Pillars Underground. *Journal of South African Inst. Min Metall.* 1971. pp. 215–224.

COOK, N.G.W., KLOKOW, J.W., and WHITE, A.J.A. *Practical Rock Mechanics for Gold Mining*, P.R.D. Series no. 167, Chamber of Mines of South Africa, Johannesburg. 1973.

CROUCH, S.L. and STARFIELD, A.M. *Boundary Element Methods in Solid Mechanics*, George Allen and Unwin, London. 1983.

ENCYCLOPAEDIA BRITANNICA 15th Edition, Encyclopædia Britannica Inc., Chicago. 1986.

ESTERHUIZEN, G.S. Theoretical Investigations into the Strength and Loading of Barrier Pillars. University of Pretoria, Project No. *286/89*. Pretoria, 1992.

ESTERHUIZEN, G.S. Modification of Coal Pillar Strength to Account for the Effect of Jointing. SIMRAC Project COL 223. 1997.

ESTERHUIZEN, G.S. Modification of Coal Pillar Strength to Account for the Effect of Jointing. SIMRAC Report No. COL 337. 1998.

FAUCONNIER, C.J. and KERSTEN, R.W.O. *Increased Underground Extraction of Coal.* The South African Institute of Mining and Metallurgy, Monograph Series No. 4. 1982.

GOODMAN, R.E. *Introduction to Rock Mechanics,* John Wiley & Sons, New York. 1989.

HALLIDAY, D. and RESNICK, R. *Fundamentals of Physics,* John Wiley & Sons, New York. 1981. References

HARR, M.E. Reliability-based design in Civil Engineering. McGraw-Hill Inc. 1987.

HEGERT, G. *Stresses in Rock*, A.A. Balkema, Rotterdam, Netherlands. 1988.

HILL, R.W. Multiseam Design Procedures, SIMRAC Final Project Report, CSIR Project No. Col 026 Feb. 1994.

HILL, R.W. Multiseam mining in South Africa. *Proc. Symposium on Recent Advances in Underground Coal Mining in South Africa.* South African National Group on Rock Mechanics. September, 1989.

HILL, R.W. Safety and environmental risks associated with shallow bord and pillar workings. Chamber of Mines Research Organisation. Final project report. Report No: CE 9401. 1996.

HOEK E. Technical note: Estimating Mohr-Coulomb friction and cohesion values from the Hoek-Brown failure criterion, *Int. J. Rock Mech. Min. Sci. & Geomech.*, Abstr., vol. 27, no. 3, 1990. pp. 227–229.

HOEK, E. First Report on the Testing of Large Scale Coal Specimens *In Situ*, CSIR Report MEG 452. 1966.

HOEK, E. and BROWN, E.T. *Underground Excavations in Rock*, The Institution of Mining and Metallurgy, London. 1980.

HOEK, E. and BROWN, E.T. Empirical strength criterion for rock masses, *J. Geotech. Eng.*, ASCE, vol. 106, 1980a. pp. 1013–1035.

HOEK, E. KAISER, P.K., and BAWDEN, W.F. *Support of Underground Excavations in Hard Rock.* A.A. Balkema/Rotterdam. 1997.

HOLTZ, R.D. and KOVACS, W.D. *An Introduction to Geotechnical Engineering*, Prentice-Hall Inc., Englewood Cliffs, New Jersey. 1981.

IANNACHIONI, A.T., DOLINAR, D.R., PROSSER, L.J. , MARSHALL, T.E., OYLER, D.C., and COMPTON, C.S. Controlling roof beam failures from high horizontal stresses in under-ground stone mines. *Proc. 17th International Conferences on Ground Control in Mining.* Morgantown, West Virginia, 1998.

INTERNATIONAL SOCIETY FOR ROCK MECHANICS. Commission on Terminology, Symbols and Graphic Representation, Final draft (prepared by the Commission on Terminology, Symbols and Graphic Representation, appointed in 1968), International Society for Rock Mechanics, Lisbon, Portugal. 1975.

ITASCA Consulting Group. UDEC Users Guide. ITASCA Consulting Group Inc, Minneapolis, MN, USA. 1997.

ITASCA Consulting Group, Inc. FLAC—Fast Lagrangian Analysis of Continua: Theory and Background, FLAC Version 3.4 User's Manual, Itasca Consulting Group, Inc., Minneapolis. 1998.

JAEGER, J.C. and COOK, N.G.W. *Fundamentals of Rock Mechanics*, 2nd Edition, Chapman and Hall, London. 1976.

JAFARI, A. Application of high pre-tension to full-column grouted bolts in roadway support in underground coal mines. Ph.D. thesis, University of New South Wales 1996.

JENKINS-JONES S. (Ed.). *The Hutchinson Dictionary of Scientists*, Helicon Publishing Ltd., Oxford, England. 1996.

KANE, J.W. and STERNHEIM, M.M. *Physics SI Version,* John Wiley & Sons, New York. 1980.

KAUFFMAN, P.W., HAWKINS, S.A., and THOMPSON, R.R. Room and pillar retreat mining. United States Bureau of Mines. Information Circular IC 8849.

LAMA, R.D. and VUTUKURI, V.S. *Handbook on Mechanical Properties of Rocks - Testing Techniques and Results,* vol. 3. Trans Tech Publications, Germany, 1978. pp. 209–320.

LATILLA, J.W. Highwall Monitoring To Combat Rockfall Accidents at Opencast Collieries. *Proceedings of the SANIRE Symposium, 'Re-defining the boundaries'*, Maccauvlei. 2002.

LATILLA, J., VAN WIJK, J.J., WEVELL, E., and NEAL, D. Evaluation of impact splitting technique used for predicting geotechnical conditions in underground coal mines. *Re-defining boundaries, SANIRE Symposium* Vereeniging, 6 September. 2002.

MacCOURT, L, MADDEN, B.J. and SCHÜMANN, E.H.R. Case studies of surface subsidence over collapsed bord and pillar working E. Proc. Symp. *The effect of underground mining on surface*, South African National Group on Rock Mechanics. 1986.

McCOSH, N.T., HEWITSON, K., and BUDDERY, P.S. Stooping with roofbolt breakerlines on the Alfred Seam, Savmore Colliery, SACMA Circular, No. 2/89, August 1989.

McNALLY, N. Geotechnical Application and Interpretation of Downhole Geophysical logs. ACIRL Report No. 08/0621. 1987.

MADDEN, B.J. A Re-assessment of Coal Pillar Design. *J. South Afr. Inst. Min. Metall.*, vol. 91, no. 1. January., 1991. pp. 27–37.

MADDEN, B.J. Coal Rock Mechanics Course Notes. 1995.

MADDEN, B.J. Re-assessment of Coal Pillar Design. *J. South Afr. Inst. Min. Metall.*, Colloquium 'The Utilization of Coal Resources', Witbank. November. 1989.

MADDEN, B.J. CANBULAT, I., and YORK, G. 'Current South African Coal Pillar Research'. *J. S. Afr. Inst. Min. Metall.*, vol. 98, no. 1, January, 1998. pp. 7–10.

MADDEN, B.J. and CANBULAT, I. Practical Design Considerations for Pillar Layouts in Coal Mines. SARES 1997 – Implementing Rock Engineering Knowledge, Johannesburg. 1997.

MADDEN, B.J. and CANBULAT, I. Practical Design Considerations for Pillar Layouts in Coal Mines. SARES 1997—Implementing Rock Engineering Knowledge. Johannesburg. 1997

MADDEN, B.J. and HARDMAN, D.R. Long term stability of bord and pillar workings. *COMA: Symposium on Construction Over Mined Areas*, Pretoria, May. 1992.

MARK, C. and CHASE, F. Preventing massive pillar collapses in coal mines. NIOSH Information Circular IC9446, 1997.

MARSHAK, S. and MITRA, G. *Basic Methods of Structural Geology*, Prentice Hall, Englewood Cliffs, New Jersey. 1988.

MERCER, D. *Chronicle of the World*, Longman Group UK Ltd and Chronicle Communications Ltd. London. 1989.

MINE MODELLING LTD. Map3D Version 36 User's Manual, Mine modelling Ltd, Mt Eliza, Victoria, Australia. 1996.

MINING STRESS SYSTEMS. 3D—BESOL: Three-Dimensional Boundary Element Solutions for Rock Mechanics: User's Guide For Multiple Seam Program BESOL—MS For Microsoft Windows Operating System, Version 3.4, Mining Stress Systems (Pty) Ltd. Johannesburg, South Africa. 1997.

MINING STRESS SYSTEMS. BESOL: Boundary ELement SOLutions for Rock Mechanics: User's Guide, Mining Stress Systems (Pty) Ltd. Johannesburg, South Africa. 1997.

MOLINDA, G.M. and MARK, C. Coal Mine Roof Rating (CMRR): A Practical Rock Mass Classification for Coal Mines. Bureau of Mines Information Circular, IC 9387. 1994.

NELKON, M. and PARKER, P. *Advanced Level Physics*, 4th Edition, Heinemann Educational Books, London. 1977.

NIOSH. User's Guide For LAMODEL. NIOSH Pittsburgh Research Laboratories, Pittsburgh, PA, USA. 1998.

OBERT, L. and DUVALL, W.I. *Rock Mechanics and the Design of Structures in Rock*, John Wiley & Sons, Inc., New York. 1967.

OLDROYD, D.C. Yielding Pillar Design in South African Collieries. M.Sc. dissertation. Faculty of Engineering, University of the Witwatersrand. 1997.

OLDROYD, D.C., LATILLA, J.W., and WEVELL, E. 'Three modes of floor failure'. Presentation to the Coal fields Branch, SANIRE. 1997.

OLDROYD, D.C. and BUDDERY, P.S. Two Cases of Progressive Pillar Failure at Collieries in Swaziland and KwaZulu-Natal: *ISRM International Symposium: Rock Mechanics in Africa*, Swaziland, November. 1988.

OLDROYD, D.C. and VAN ROOYEN, P.J. Partial Extraction at Ermelo Mines, the Birth Pangs of Yield Pillar Mining in Collieries? Presented at SACMA meeting. 1999.

OLDROYD, D.C. and LATILLA, J. Personal communication. 1998.

ORAVECZ, K.I. Loading of Coal Pillars in Bord and Pillar Workings. Ph.D. thesis, University of the Witwatersrand. 1973.

PENG, S.S. *Coal Mine Ground Control.* Wiley and Sons, New York.

PENG, S.S. and CHIANG, H.S. *Longwall Mining.* Wiley and Sons, New York.

PENG, S.S. *Coal mine ground control*, 2nd Edition, John Wiley & Sons, USA 1986.

ROCSCIENCE. Examine 2D software, www.rocscience.com. 2003.

RICO, G.H., OREA, R., MENDOZA, L., and TADOLINI, S.C. Implementation and evaluation of roof bolting in MICARE Mine II. *Proc 16th International Conference on Ground Control in Mines.* Morgantown, West Virginia, USA, 1997.

RYDER, J.A. Unpublished report to Sigma colliery. 1994.

RYDER, J.A. and OZBAY, M.U. A Methodology for Designing Pillar Layouts for Shallow Mining. *ISRM Symposium: Static and Dynamic Considerations in Rock Engineering*, Swaziland. 1990.

SALAMON, M.D.G. A Method of Designing Bord and Pillar Workings. *J. South Afr. Inst. Min. Metall.,* September vol. 68, no. 2. 1967. pp. 68–78.

SALAMON, M.D.G. Unpublished Report to Wankie Colliery. 1982.

SALAMON, M.D.G. and MUNRO, A.H. (1967) A Study of the Strength of Coal Pillars. *J. South Afr. Inst. Min. Metall.*, September, 1967. pp. 56–67.

SALAMON, M.D.G. and ORAVECZ, K.I. Rock Mechanics in Coal Mining. Chamber of Mines of South Africa. P. R. D. Series No. 198. 1976.

SALAMON, M.D.G. and WAGNER, H. Practical Experiences in the Design of Coal Pillars. Safety in Mines Research. *Proceedings of the 21st International Conference*. Sydney 21–25 October. 1985.

SCHOLTZ, C.H. *The Mechanics of Earthquakes and Faulting,* Cambridge University Press, New York. 1990.

SHERIFF, R.E. *Encyclopedic Dictionary of Exploration Geophysics*, 2nd Edition, Society of Exploration Geophysics, Tulsa, Oklahoma. 1984.

SIMRAC. *Numerical Modelling Of Mine Workings*, vol. 1 and 2. Dept of Minerals and Energy, Johannesburg, South Africa. 1999.

SOKOLNIKOFF, I.S. *Mathematical Theory of Elasticity*, McGraw-Hill Book Company Inc., USA. 1956.

STACEY, T.R. Best Practice Rock Engineering Handbook For 'Other' Mines. SIMRAC Project Number OTH 602. 2001.

STACEY, T.R. and SWART, A.H. Practical Rock Engineering Practice for Shallow and Opencast Mines. SIMRAC Project OTH602. 2001.

STACEY, T.R. and WESSELOO, J. *In situ* stresses in the mining areas in South Africa. *Jnl. S.A. Inst. Min. Metall.* vol. 98, no. 7. 1998. pp. 365–368.

STANKUS, J. and GUO, S. New design criteria for roofbolting systems. *Proc. 16th International Conference for Ground Control in Mines*. Morgantown, West Virginia, USA, 1997.

TADOLINI, S.C. The effects of reduced annulus in roof bolting performance. *Proc. 17th International Conference on Ground Control in Mines*. Morgantown, West Virginia, USA, 1998.

TURCOTTE, D.L. and SCHUBERT, G. *Geodynamics Applications of Continuum Physics to Geological Problems*, John Wiley & Sons, New York. 1982.

TURNER, F.J. and WEISS, L.E. *Structural Analysis of Metamorphic Tectonites*, McGraw-Hill Book Company, USA. 1963.

VAN DER MERWE, J.N. Coal pillar life prediction in the Vaal Basin, South Africa. *Proc. 17th International Conference on Ground Control in Mines*, Morgantown, West Virginia, USA. August 1998**a**.

VAN DER MERWE, J.N. Experiences with undermining by coal in South Africa. *Proc. Third Workshop on Surface Subsidence Due to Underground Mining*. West Virginia University, Morgantown WV. 1993**b**.

VAN DER MERWE, J.N. New strength formula for coal pillars in South Africa. *Proc. 2nd Intnl Workshop on Coal Pillar Mechanics and Design*, Vail, CO, USA. June 1999.

VAN DER MERWE, J.N. *Practical Coal Mining Strata Control,* Second Edition. ITASCA Africa (Pty) Ltd. 1998**b**.

VAN DER MERWE, J.N. Prediction of dolerite sill failure. *Proc. 8th Congress of the Intnl. Soc. for Rock Mechanics,* Tokyo. 1995.

VAN DER MERWE, J.N. Revised Strength Factor for Coal in the Vaal Basin. *J. S. Afr. Inst, Min. Metall*, vol. 93. 1993**a**. pp. 71–77.

VAN DER MERWE, J.N. Subsidence caused by high extraction coal mining in the Sasolburg and Secunda Areas: Prediction thereof and the mitigation of its effects. Ph.D. thesis, University of the Witwatersrand. 1991.

VAN DER MERWE, J.N. The extraction safety factor concept for high extraction coal mining. *Journal of South African Inst. Min Metall. School on the Utilisation of Coal Reserves*. Witbank, October 1989**a**.

VAN DER MERWE, J.N. The surface element approach to the analysis of surface subsidence. *Proc. Symp. Advances in rock mechanics in underground coal mining*. South African National Group on Rock Mechanics. 1989**b**.

VAN DER MERWE, J.N. and OLIVIER, F.T. The development of a crush pillar system for high extraction coal mining. In *MASSMIN* 92, *Journal of South African Inst. Min Metall.,* Symposium Series S12. 1992.

VAN DER MERWE, J.N. New pillar strength formula for South African coal. *J. S. Afr. Inst, Min. Metall.*, vol. 103, 2003. pp. 281–292.

VAN DER MERWE, J.N. South African coal pillar database. *J. S. Afr. Inst, Min. Metall.*, vol. 106, 2006.pp. 115–128.

VAN DER MERWE, J.N. Verification of pillar life prediction method. *J. S. Afr. Inst, Min. Metall*, vol. 93, 2004. pp. 71–77.

VAN HEERDEN, W.L. *In situ* complete stress-strain characteristics of large coal specimens. *J. S. Afr. Inst. Min. Metall*. March 1975.

WAGNER, H. and SCHÜMANN, E.H.R. The effects of total coal seam extraction on the surface and surface structures. Chamber of Mines of South Africa Research Organisation Research. Report 20/85.

WAGNER, H. Determination of the Complete Load- Deformation Characteristics of Coal Pillars. *Proceedings of the 3rd ISRM Congress*, December, 1974. pp. 1076–1081.

WAGNER, H. Pillar design in coal mines. *J. S Afr. Inst. Min. Metall.* January 1980.

WAGNER, H. and MADDEN, B.J. Fifteen Years Experience with the Design of Coal Pillars in Shallow South African Collieries: An Evaluation of the Performance of the Design Procedures and Recent Improvements. *Design and Performance of Underground Excavations*. ISRM/BGS, Cambridge 1984. pp. 391–399.

WAGNER, H. Rock Mechanics of total extraction. In: *Increased Underground extraction of coal.* (Eds.), C.J. Fauconnier and R.W.O. Kersten. The South African Institute of Mining and Metallurgy, Monograph series, No. 4. 1982.

WELLS, D. *The Penguin Book of Curious and Interesting Mathematics*, Penguin Books Ltd. London. 1997.

WHITTEN, D.G.A. and BROOKS, J.R.V. *The Penguin Dictionary of Geology*, Penguin Books Ltd. Harmondsworth, England. 1972.

Units and conversion factors

The metric units of the Système International (SI) are used in this book. Only the ones most commonly used in rock engineering are shown here. In this book, the decimal point (not comma) notation is used.

Multiples

Factor	Prefix	Symbol
10^9	Giga	G
10^6	Mega	M
10^3	kilo	k
10^{-3}	milli	m
10^{-6}	micro	μ

Basic units

Quantity	Unit	Symbol
Length	metre	m
Mass	gram	g
Time	second	s

Derived units

Quantity	Unit	Symbol	Derivation
Force	Newton	N	$kg\text{-}m/s^2$
Pressure, stress	Pascal	Pa	N/m^2
Work, energy	Joule	J	N-m

Conversions to Imperial Units

Quantity	SI Unit	Imperial Unit
Length	1 m	3.281 ft
Area	$1\ m^2$	$10.764\ ft^2$
Volume	$1\ m^3$	$35.315\ ft^3$
Mass	1 kg	2.205 lb
Density	$1\ kg/m^3$	$62.428.10^{-3}\ lb/ft^3$
Force	1 N	0.225 lbf
Pressure, stress	1 Pa	$0.145.10^{-3}$ psi
Energy, work	1 J	0.738 ft-lb